

# **Power System Grounding and Transients**

# ELECTRICAL ENGINEERING AND ELECTRONICS

*A Series of Reference Books and Textbooks*

## EXECUTIVE EDITORS

*Marlin O. Thurston*  
Department of  
Electrical Engineering  
The Ohio State University  
Columbus, Ohio

*William Middendorf*  
Department of  
Electrical and Computer Engineering  
University of Cincinnati  
Cincinnati, Ohio

## EDITORIAL BOARD

*Maurice Bellanger*  
Télécommunications, Radioélectriques, et  
Téléphoniques (TRT)  
Le Plessis-Robinson, France

*Lionel M. Levinson*  
General Electric Company  
Schenectady, New York

*J. Lewis Blackburn*  
Bothell, Washington

*V. Rajagopalan*  
Department of Engineering  
Université du Québec  
à Trois-Rivières  
Trois-Rivières, Quebec, Canada

*Sing T. Bow*  
Department of Electrical Engineering  
The Pennsylvania State University  
University Park, Pennsylvania

*Earl Swartzlander*  
TRW Defense Systems Group  
Redondo Beach, California

*Norman B. Fuqua*  
Reliability Analysis Center  
Griffiss Air Force Base, New York

*Spyros G. Tzafestas*  
Department of Electrical Engineering  
National Technical University  
of Athens  
Athens, Greece

*Charles A. Harper*  
Westinghouse Electric Corporation  
and Technology Seminars, Inc.  
Timonium, Maryland

*Sakae Yamamura*  
Central Research Institute of  
the Electric Power Industry  
Tokyo, Japan

*Naim A. Kheir*  
Department of Electrical and  
Systems Engineering  
Oakland University  
Rochester, Michigan

1. Rational Fault Analysis, edited by Richard Saeks and S. R. Liberty
2. Nonparametric Methods in Communications, edited by P. Papantoni-Kazakos and Dimitri Kazakos
3. Interactive Pattern Recognition, Yit-zui Chien
4. Solid-State Electronics, Lawrence E. Murr
5. Electronic, Magnetic, and Thermal Properties of Solid Materials, Klaus Schröder
6. Magnetic-Bubble Memory Technology, Hsu Chang
7. Transformer and Inductor Design Handbook, Colonel Wm. T. McLyman
8. Electromagnetics: Classical and Modern Theory and Applications, Samuel Seely and Alexander D. Poulikas
9. One-Dimensional Digital Signal Processing, Chi-Tsong Chen
10. Interconnected Dynamical Systems, Raymond A. DeCarlo and Richard Saeks
11. Modern Digital Control Systems, Raymond G. Jacquot
12. Hybrid Circuit Design and Manufacture, Roydn D. Jones
13. Magnetic Core Selection for Transformers and Inductors: A User's Guide to Practice and Specification, Colonel Wm. T. McLyman
14. Static and Rotating Electromagnetic Devices, Richard H. Engelmann
15. Energy-Efficient Electric Motors: Selection and Application, John C. Andreas
16. Electromagnetic Composability, Heinz M. Schlicke
17. Electronics: Models, Analysis, and Systems, James G. Gottling
18. Digital Filter Design Handbook, Fred J. Taylor
19. Multivariable Control: An Introduction, P. K. Sinha
20. Flexible Circuits: Design and Applications, Steve Gurley, with contributions by Carl A. Edstrom, Jr., Ray D. Greenway, and William P. Kelly
21. Circuit Interruption: Theory and Techniques, Thomas E. Browne, Jr.
22. Switch Mode Power Conversion: Basic Theory and Design, K. Kit Sum
23. Pattern Recognition: Applications to Large Data-Set Problems, Sing-Tze Bow
24. Custom-Specific Integrated Circuits: Design and Fabrication, Stanley L. Hurst
25. Digital Circuits: Logic and Design, Ronald C. Emery
26. Large-Scale Control Systems: Theories and Techniques, Magdi S. Mahmoud, Mohamed F. Hassan, and Mohamed G. Darwish
27. Microprocessor Software Project Management, Eli T. Fathi and Cedric V. W. Armstrong (Sponsored by Ontario Centre for Microelectronics)
28. Low Frequency Electromagnetic Design, Michael P. Perry
29. Multidimensional Systems: Techniques and Applications, edited by Spyros G. Tzafestas
30. AC Motors for High-Performance Applications: Analysis and Control, Sakae Yamamura

31. Ceramic Materials for Electronics: Processing, Properties, and Applications, *edited by Relva C. Buchanan*
32. Microcomputer Bus Structures and Bus Interface Design, *Arthur L. Dexter*
33. End User's Guide to Innovative Flexible Circuit Packaging, *Jay J. Miniet*
34. Reliability Engineering for Electronic Design, *Norman B. Fuqua*
35. Design Fundamentals for Low-Voltage Distribution and Control, *Frank W. Kussy and Jack L. Warren*
36. Encapsulation of Electronic Devices and Components, *Edward R. Salmon*
37. Protective Relaying: Principles and Applications, *J. Lewis Blackburn*
38. Testing Active and Passive Electronic Components, *Richard F. Powell*
39. Adaptive Control Systems: Techniques and Applications, *V. V. Chalam*
40. Computer-Aided Analysis of Power Electronic Systems, *Venkatachari Rajagopalan*
41. Integrated Circuit Quality and Reliability, *Eugene R. Hnatek*
42. Systolic Signal Processing Systems, *edited by Earl E. Swartzlander, Jr.*
43. Adaptive Digital Filters and Signal Analysis, *Maurice G. Bellanger*
44. Electronic Ceramics: Properties, Configuration, and Applications, *edited by Lionel M. Levinson*
45. Computer Systems Engineering Management, *Robert S. Alford*
46. Systems Modeling and Computer Simulation, *edited by Naim A. Kheir*
47. Rigid-Flex Printed Wiring Design for Production Readiness, *Walter S. Rigling*
48. Analog Methods for Computer-Aided Circuit Analysis and Diagnosis, *edited by Takao Ozawa*
49. Transformer and Inductor Design Handbook, Second Edition, Revised and Expanded, *Colonel Wm. T. McLyman*
50. Power System Grounding and Transients: An Introduction, *A. P. Sakis Meliopoulos*

*Additional Volumes in Preparation*

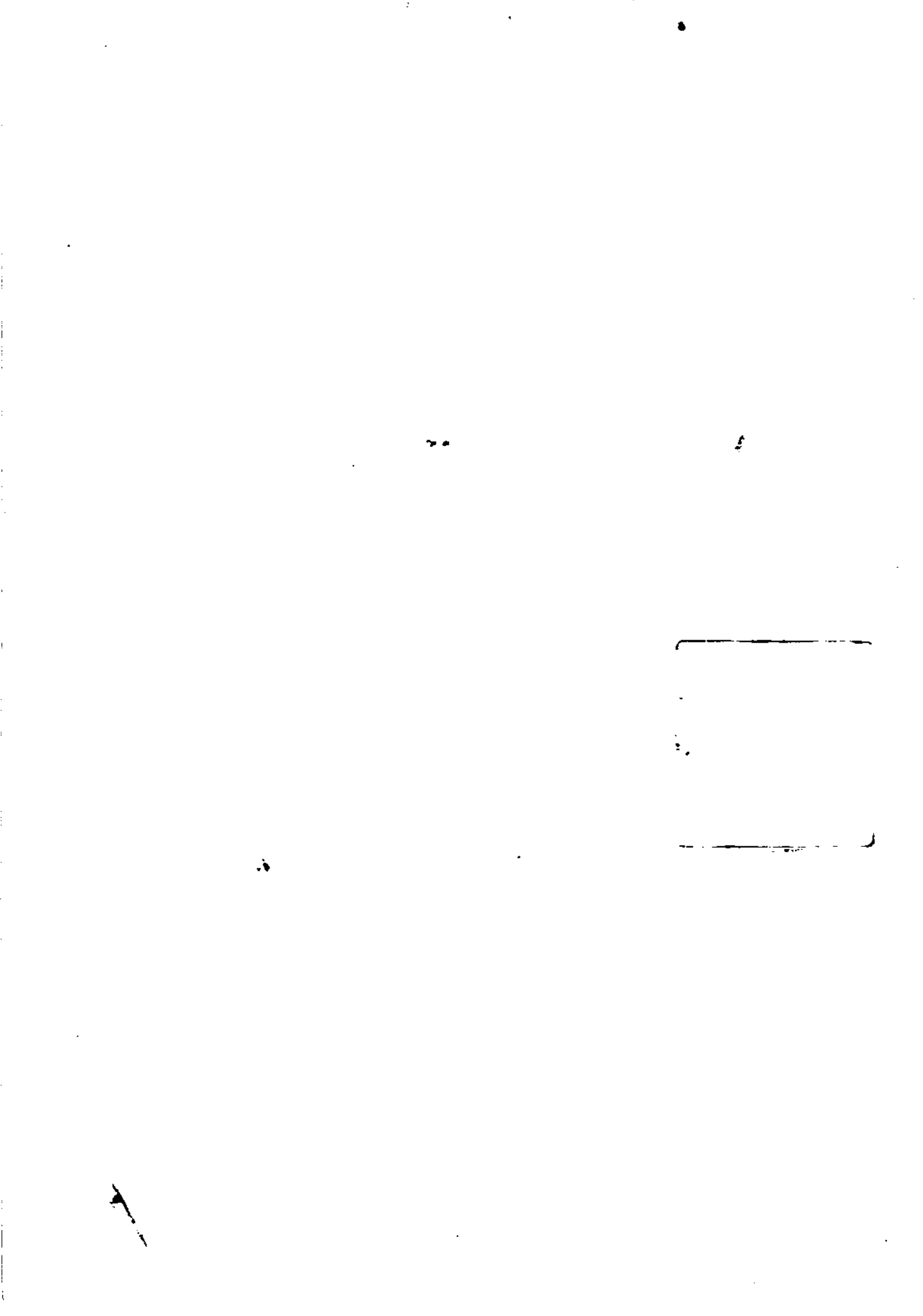
Signal Processing Handbook, *edited by C. H. Chen*

Dynamic Models and Discrete Event Simulation, *William Delaney and Erminia Vaccari*

Electronic Product Design for Automated Manufacturing, *H. Richard Stillwell*

## **Electrical Engineering-Electronics Software**

1. Transformer and Inductor Design Software for the IBM PC.  
*Colonel Wm. T. McLyman*
2. Transformer and Inductor Design Software for the Macintosh.  
*Colonel Wm. T. McLyman*
3. Digital Filter Design Software for the IBM PC.  
*Fred J. Taylor and Thanos Stouraitis*



# **Power System Grounding and Transients**

**AN INTRODUCTION**

**A. P. Sakis Meliopoulos**

School of Electrical Engineering  
Georgia Institute of Technology  
Atlanta, Georgia

Marcel Dekker, Inc.

New York and Basel

**Library of Congress Cataloging-in-Publication Data**

Meliopoulos, A. P. Sakis

Power system grounding and transients : an introduction / A.P. Meliopoulos.

p. cm. — (Electrical engineering and electronics ; 50)  
Includes index.

ISBN 0-8247-7908-8

1. Electric currents—Grounding. 2. Transients (Electricity)  
I. Title. II. Series.

TK3227.M45 1988

621.31'7--dc 19

88-10919

CIP

**Copyright © 1988 by MARCEL DEKKER, INC. All Rights Reserved**

Neither this book nor any part may be reproduced or transmitted in any form or by any means, electronic or mechanical, including photocopying, microfilming, and recording, or by any information storage and retrieval system, without permission in writing from the publisher.

**MARCEL DEKKER, INC.**

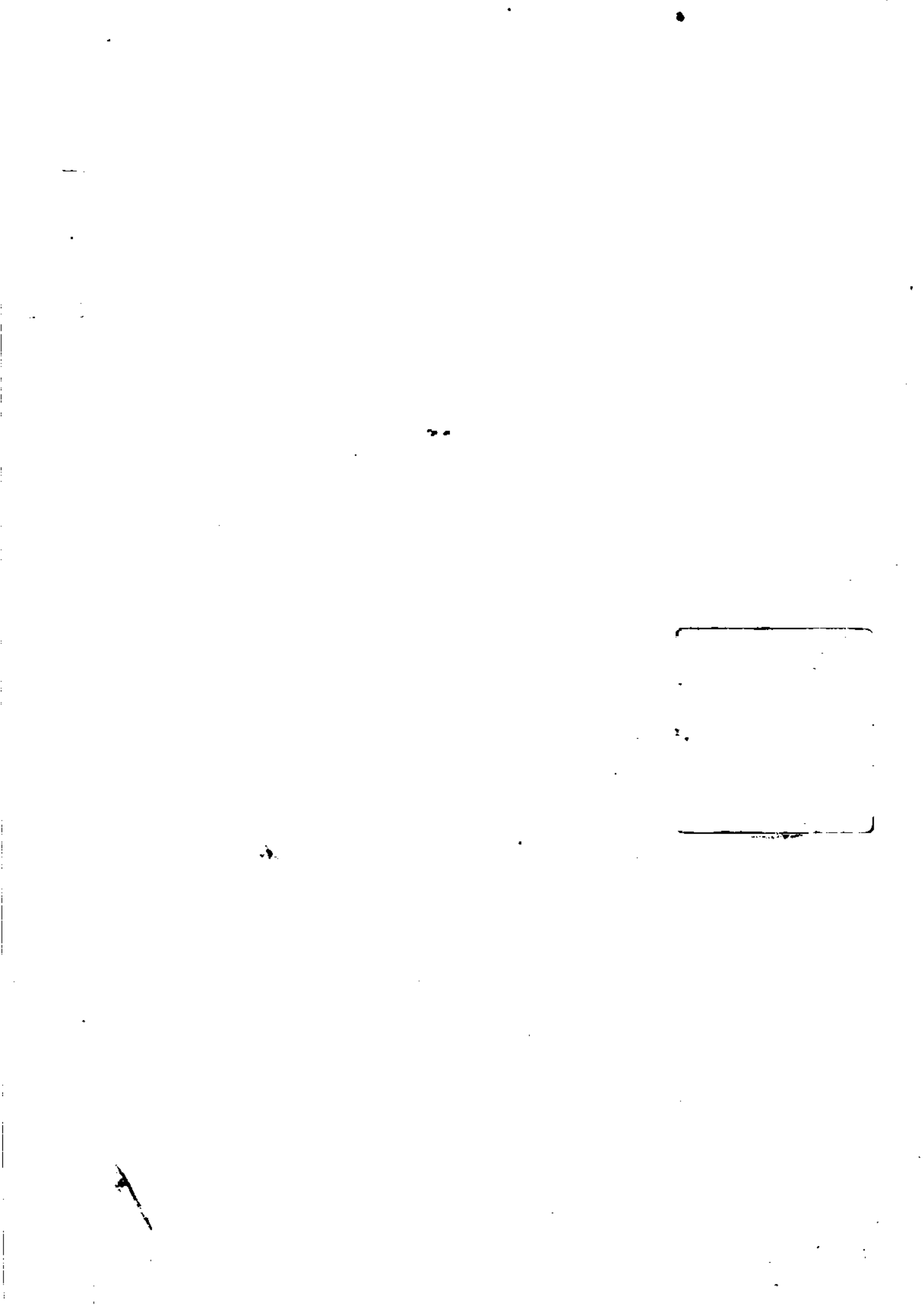
270 Madison Avenue, New York, New York 10016

**Current printing (last digit):**

10 9 8 7 6 5 4 3 2 1

**PRINTED IN THE UNITED STATES OF AMERICA**

*Dedicated to*  
*My daughters, Dee Anne and Victoria*  
*My wife, Kathy*  
*My parents, Victoria and Panagiotis*



# Preface

Since the installation of the first electric power transmission system a century ago, electricity has infiltrated our industrial and everyday life. As a result, the need for electric power transmission facilities has been increased amazingly. With it, numerous problems associated with the reliable and economic transmission of electric power have emerged. Through a century-long evolutionary process, the design of transmission equipment has been advanced to an amazing degree of sophistication, and the operating reliability of these systems is very high. As electric power systems grow larger and larger, the need for comprehensive analysis techniques, design, and optimization procedures has arisen. On the other hand, the availability of low-cost computing equipment resulted in the development of such techniques. Cost-conscious electric power designers and planners strive for optimal designs and highly reliable systems. The objective of this book is to provide coverage of modern analysis techniques employed in the design of electric power transmission systems. The book has been developed over a number of years of teaching undergraduate and graduate courses in electric power engineering and many years of research and consulting activities in related problems.

The first chapter is an overview of electric power transmission and defines the basic concepts and nomenclature. The next four chapters of the book are devoted to modeling of transmission systems. Simple, well-established models are presented together with the basic concepts underlying modern computer-based modeling techniques. The modeling in these chapters is approached from the electromagnetic fields point of view. The interrelationship between the simple

models and the rigorous computer models is emphasized. Modeling of grounding systems is addressed as an integral part of the transmission system.

Chapter 6 presents techniques that result in circuit models of transmission systems. This chapter provides the connecting bridge between the electromagnetic phenomena in transmission systems and the well-known circuit models of transmission systems. The impact of power system grounding on circuit parameters is emphasized with numerous actual system examples.

Chapter 7 presents the utilization of transmission system models to power system fault analysis. The conventional approach based on symmetrical components is presented. The limitations of this approach to specific applications, for example, design of power system grounding, are pointed out. Modern fault analysis methods are also presented, which explicitly represent power system grounds and asymmetries. These methods are suitable for the computation of a ground potential rise of grounding systems, which is the single most important parameter in the design of grounding systems and protection of communication systems.

Chapter 8 discusses the utilization of the models and analysis methods in the design of power grounding systems. A coordinated approach is presented by which the distributed grounds of a power system are utilized to meet safety objectives. The impact of various parameters affecting the design of grounding systems is discussed with many examples.

Chapter 9 presents analysis procedures for computing electrical transients in a power system. The analysis procedures utilize models presented in earlier chapters. Emphasis is placed on the selection of appropriate power system models for specific applications. Simple analysis methods are presented, as well as modern computer-based numerical methods for transient analysis. Emphasis is placed on the practical application of these methods to power system transients. The most commonly occurring electrical transients in a system are studied, such as switching and lighting transients, fault transients, transient recovery voltage, breaker restrike, and transformer inrush current. Models and methods for each of these transients are presented with a discussion of the effects of these transients on the design process. The chapter concludes with a discussion of overvoltage protection apparatus.

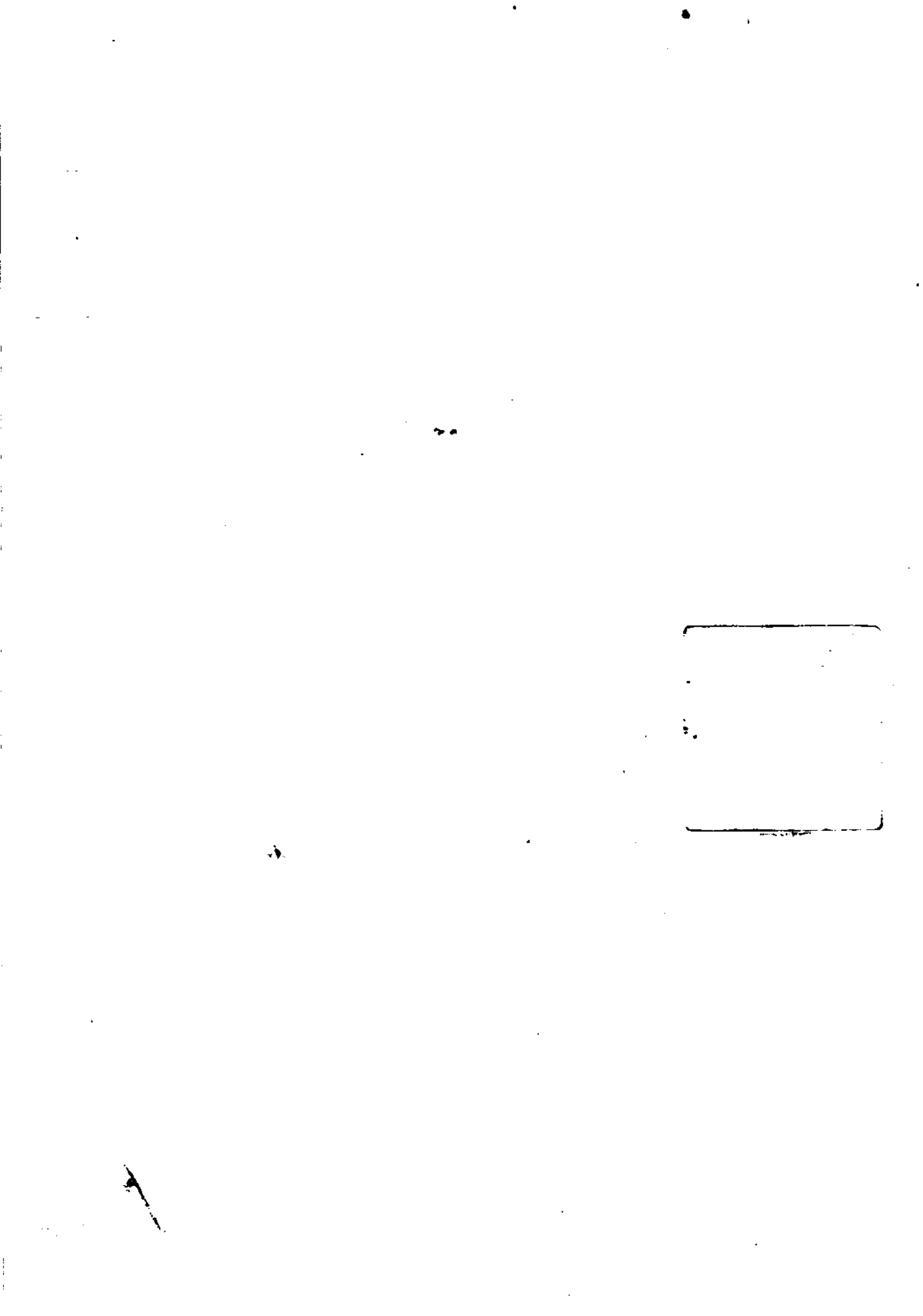
My intention in writing this book is to provide rigorous modeling procedures of power system components and their utilization in the design process. These procedures are essential for present-day design practices of grounding systems, transient analysis, and overvoltage protection. The material in this book is applicable to power system modeling for harmonic analysis. It is my hope that the book will help those engineers who are increasingly concerned about the injection of harmonics into the power system. The book should be

## Preface

useful for students and practicing engineers concerned with grounding systems, transient analysis, and harmonic analysis of power systems.

Many have contributed to the realization of this book. First, I would like to recognize my students, especially my doctoral students Dr. Feliachi, Dr. Cokkinides, Dr. Bakirtzis, and Dr. Paplexopoulos, for their contributions to the development of this book through their many stimulating questions and their suggestions for the improvement of the manuscript. The material in Chapters 5, 7, and 8 was inspired from a multiyear research program sponsored by the Electric Power Research Institute (EPRI). The success of the research program is due to John Dunlap of EPRI. His leadership and support are acknowledged as two of the primary forces in the realization of this book. In the early stages of the EPRI research program, the author worked with Professors Joy and Webb. This collaboration is also acknowledged. Recognition is due to the EPRI project advisors. I have benefited and learned from their practical experiences and suggestions. I was also fortunate to be a member of the IEEE working group on the revision of Standard 80. Our work resulted in the 1986 edition of the guide. My association and work with the working group influenced the structure of this book and, hopefully, increased its value to the industry. I would also like to thank Tony Ayoub and Shashi Patel of Georgia Power Company for providing many actual system data for the examples of the book and for sharing their experience with me. The permission of the Georgia Power Company to utilize these data is gratefully acknowledged. Last but not least, I would like to thank Peggy Knight for her patience in the many hours of typing and revising the manuscript.

A. P. Sakis Meliopoulos



# Contents

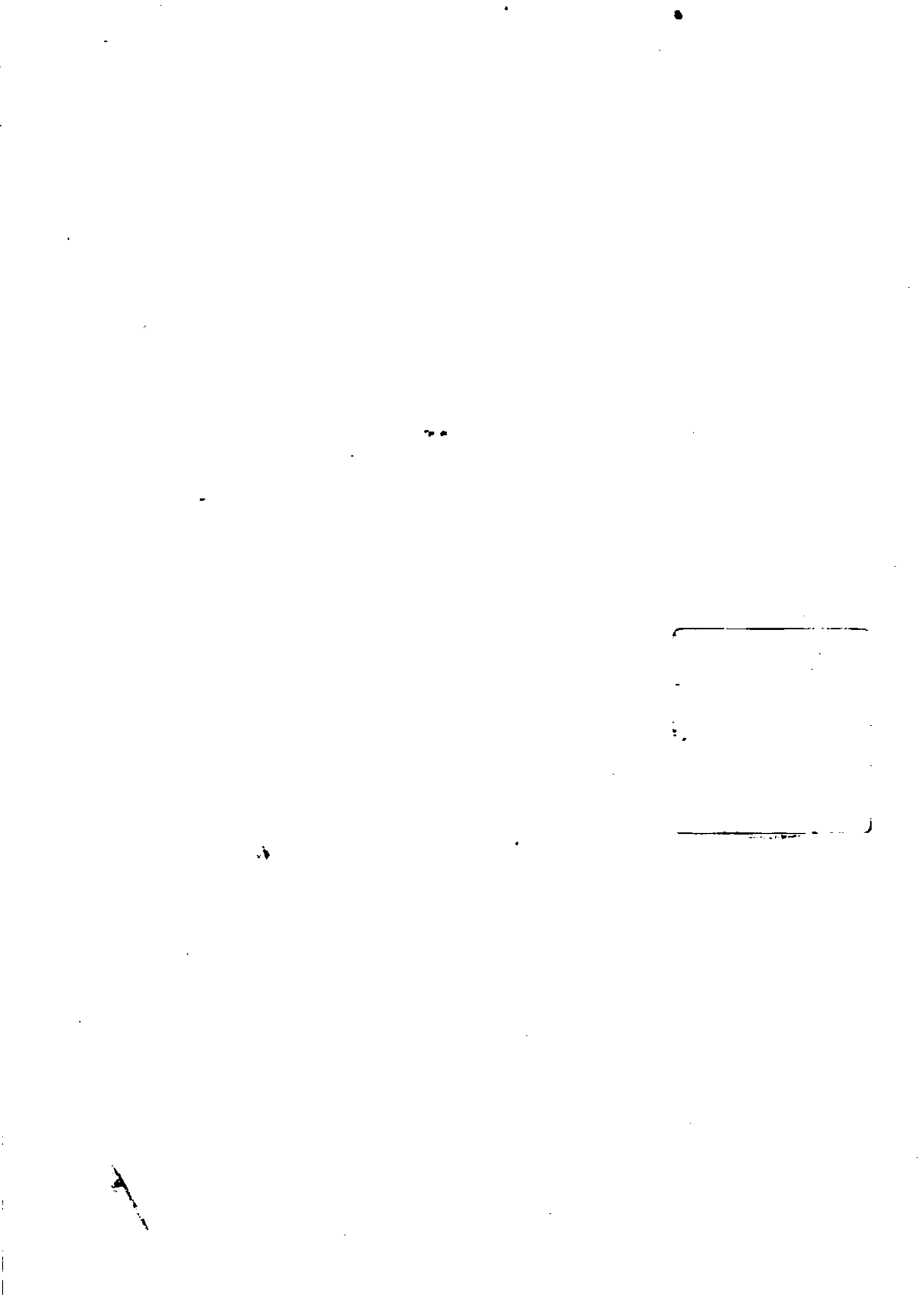
Preface	v
1. POWER TRANSMISSION SYSTEMS	1
1.1 Introduction	1
1.2 Basic Definitions and Nomenclature	1
1.3 Transmission Line Design	5
1.4 Distribution System Design	8
1.5 Power System Grounding	11
1.6 Power System Transients	11
1.7 Summary and Discussion	12
2. TRANSMISSION LINE MODELING: LINE INDUCTANCE	13
2.1 Introduction	13
2.2 Magnetic Field of an Infinitely Long Circular Conductor	14
2.3 Magnetic Field of Two Circular Infinitely Long Conductors	20
2.4 Interpretation of Inductive Reactance Components	23
2.5 Practical Considerations: Use of Tables	26
2.6 Inductive Reactance of Typical Line Configurations	27
2.7 Transposition	34
2.8 Method of Geometric Mean Distances	37
2.9 Applications of the Method of Geometric Mean Distances	40

2.10	Inductive Reactance of the Earth Path	47
2.11	Summary and Discussion	51
2.12	Problems	51
 3. TRANSMISSION LINE MODELING: LINE RESISTANCE		55
3.1	Introduction	55
3.2	Conductor Resistance to the Flow of DC Current	57
3.3	Skin Effect in Circular Conductors	58
3.4	Resistance and Geometric Mean Radius of Magnetic Conductors	76
3.5	Current Distribution in Earth	78
3.6	Summary and Discussion	90
3.7	Problems	90
 4. TRANSMISSION LINE MODELING: LINE CAPACITANCE		93
4.1	Introduction	93
4.2	Electric Field Around a Circular Infinitely Long Conductor	94
4.3	Electric Field of Two Parallel Infinitely Long Circular Conductors	96
4.4	Capacitance of a General n-Conductor Overhead Transmission Line	100
4.5	Practical Considerations: Use of Tables	104
4.6	Applications	105
4.7	Effects of Earth and Neutral/Ground Wires	110
4.8	Summary and Discussion	116
4.9	Problems	117
 5. POWER SYSTEM GROUNDING I: MODELING TECHNIQUES		119
5.1	Introduction	119
5.2	Analysis of Simple Grounding Systems	121
5.3	Body Currents Due to Touch and Step Voltages	128
5.4	Grounding System Safety Assessment	133
5.5	Numerical Analysis Techniques	135
5.6	Analysis of Spatially Small Grounding Systems	159
5.7	Simplified Equations	168
5.8	Equivalent-Circuit Representation of Grounding Systems	171
5.9	Parametric Analysis of Substation Ground Mats	178
5.10	Summary and Discussion	183
5.11	Problems	183

Contents	xi
<b>6. TRANSMISSION LINE ANALYSIS</b>	<b>187</b>
6.1 Introduction	187
6.2 The General Transmission Line Model	188
6.3 Transmission Line Models for Sinusoidal Steady State	195
6.4 Modal Decomposition	200
6.5 Equivalent Circuits	209
6.6 Computation of Sequence Parameters of Three-Phase Transmission Lines	214
6.7 Transmission Line Models Based on Admittance Matrix	226
6.8 Admittance Matrix Model of Mutually Coupled Transmission Lines	233
6.9 Computation of Transmission Line Sequence Parameters from the Admittance Matrix	236
6.10 Comparison of Transmission Line Models	240
6.11 Transmission Line Power Equations	245
6.12 Summary and Discussion	249
6.13 Problems	250
<b>7. POWER SYSTEM FAULT ANALYSIS</b>	<b>253</b>
7.1 Introduction	253
7.2 Review of the Theory of Symmetrical Components	255
7.3 Sequence Models of Three-Phase Apparatus	262
7.4 Fault Analysis Based on Sequence Models	266
7.5 Ground Potential Rise During Faults	277
7.6 Fault Current Distribution Based on Sequence Models	278
7.7 Direct Phase Analysis	291
7.8 Transfer Voltages During Faults	300
7.9 Summary and Discussion	305
7.10 Problems	305
<b>8. POWER SYSTEM GROUNDING II: DESIGN PROCEDURE</b>	<b>309</b>
8.1 Introduction	309
8.2 Basic Problems and Solutions	310
8.3 Determination of a Soil Model	312
8.4 Computation of Ground Resistances	317
8.5 Maximum Ground Potential Rise	319
8.6 Investigation of Touch and Step Voltages	324
8.7 Safety Assessment	330
8.8 Mitigation of Touch and Step Voltages	333
8.9 Design Examples	334
8.10 Summary and Discussion	338

9. POWER SYSTEM TRANSIENTS	339
9.1 Introduction	339
9.2 Models for Transient Analysis	341
9.3 The Ideal Distributed-Parameter Line	343
9.4 Graphical Techniques	347
9.5 Analytical Techniques	356
9.6 Numerical Techniques	369
9.7 Time-Domain Numerical Techniques	369
9.8 Transient Analysis of Three-Phase Systems	381
9.9 Simulation of Frequency-Dependent Models	391
9.10 Basic Power System Switching Transients	398
9.11 Transformer Inrush Currents	417
9.12 Lightning Overvoltages	421
9.13 Overvoltage Protection Devices	422
9.14 Summary and Discussion	427
9.15 Problems	427
References	433
Appendix	
Table A.1 Characteristics of Copper Conductors	440
Table A.2 Characteristics of ACSR Conductors	442
Table A.3 Characteristics of Copperweld Conductors	444
Table A.4 Electrical Characteristics of Alumoweld Ground Wires	445
Table A.5 Electrical Characteristics of Seven-wire Bethanized Steel Conductor	446
Index	447

# **Power System Grounding and Transients**



# 1

## Power Transmission Systems

### 1.1 INTRODUCTION

This book addresses the topics of power system grounding and transients. The two topics are as old as power engineering itself. Since the early days of power system engineering, the two topics were investigated experimentally and appropriate solutions were invented which resulted in established practices. As power systems grew in size and complexity, it became necessary to reevaluate present practices and to improve design procedures of grounding systems and protection against transient overvoltages. Recent technology advancements coupled with research efforts resulted in improved models for the analysis of grounding systems and analysis of transient phenomena in power systems. The improved analytical models are the cornerstone for better designs of power systems apparatus and installations.

Analytically, the two topics are closely interrelated. Specifically, the theoretical bases for building analytical models for the study of these phenomena are similar. In subsequent chapters we introduce the modeling procedures and examine specific applications, such as design of grounding systems, protection against electrical transients, and so on. In this chapter we introduce basic definitions and nomenclature and discuss the general characteristics of the systems and phenomena to be studied in this book.

### 1.2 BASIC DEFINITIONS AND NOMENCLATURE

In this section we introduce basic definitions and nomenclature that will be utilized throughout the book. First, instantaneous values of voltages and currents will be denoted by lowercase letters. For

example,  $v(t)$  and  $i(t)$  denote the instantaneous value of voltage and current, respectively, as a function of time.

Many power system analysis problems deal with the power system operating under steady-state conditions. The generating units of the system generate nearly sinusoidal voltages and currents. In this case the voltage or current at any point of the system is varying sinusoidally with time. In general, the sinusoidally varying voltage or current is expressed as follows:

$$v(t) = \sqrt{2} V \cos(\omega t + \phi) \quad (1.1a)$$

$$i(t) = \sqrt{2} I \cos(\omega t + \theta) \quad (1.1b)$$

where

$V$  or  $I$  = rms value of the voltage or current

$\omega$  = angular frequency

$\phi$ ,  $\theta$  = phase angles

The sinusoidal voltage or current of (1.1) can also be represented with phasors. The phasors are complex numbers and provide an alternative way for representing sinusoidal waveforms. The phasors will be denoted by uppercase letters with a "̃" above them. Thus the voltage and current phasors representing Eqs. (1.1) are denoted by  $\tilde{V}$  and  $\tilde{I}$ , respectively. The instantaneous values of the voltage or current is by definition

$$v(t) = \text{Re}\{\tilde{V}e^{j\omega t}\} \quad (1.2a)$$

$$i(t) = \text{Re}\{\tilde{I}e^{j\omega t}\} \quad (1.2b)$$

where  $\text{Re}\{Z\}$  means the real part of the complex number  $Z$ . By equating Eqs. (1.1) and (1.2), it is apparent that

$$\tilde{V} = V e^{j\phi} \quad (1.3a)$$

$$\tilde{I} = I e^{j\theta} \quad (1.3b)$$

The majority of power systems comprise three-phase arrangements. It is expedient to introduce terms and definitions that will be used extensively in describing these systems.

In general, a three-phase system is constructed with single elements that are connected in a three-phase arrangement. Examples are electric loads, transformers, and motors. The elements may be connected in a delta or a wye configuration or any combination of these two. The delta and wye connections are illustrated in Fig. 1.1. For the description of three-phase systems, the following definitions are introduced:

Definition 1.1: Balanced Set of Three-Phase Voltages. A set of three-phase voltages,  $v_a(t)$ ,  $v_b(t)$ ,  $v_c(t)$ , is called balanced if and only if:

The voltages vary sinusoidally with time.

The amplitudes of the voltages are equal.

There is a  $120^\circ$  phase difference between any two.

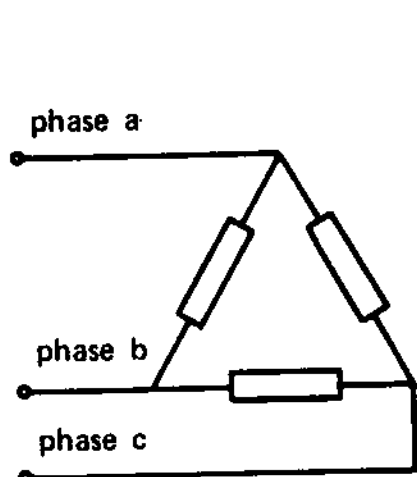
As an example, the following set of three-phase voltages is balanced:

$$v_a(t) = \sqrt{2} V \cos(\omega t + \phi) \quad (1.4a)$$

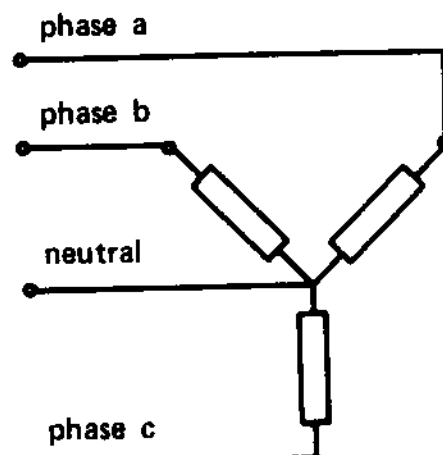
$$v_b(t) = \sqrt{2} V \cos(\omega t - 120^\circ + \phi) \quad (1.4b)$$

$$v_c(t) = \sqrt{2} V \cos(\omega t - 240^\circ + \phi) \quad (1.4c)$$

In Eqs. (1.4), the phase difference between the phase a voltage and the phase b voltage is  $120^\circ$  and positive. This phase relationship among the three phases will be called the positive phase sequence. A three-phase generator generates a set of three-phase voltages that are nearly balanced and of the positive phase sequence. It is expedient to introduce the concept of an ideal three-phase source, which is illustrated in Fig. 1.2. An ideal three-phase source generates a set of balanced three-phase voltages of the positive or negative phase sequence. It is apparent that a set of balanced three-phase voltages is completely described with the voltage magnitude  $V$ , the angular frequency  $\omega$ , the phase angle  $\phi$ , and the sequence. Alternatively, it can be completely defined with the phasor of the phase a voltage,  $\tilde{V}_a = V e^{j\phi}$ , and the sequence. Throughout the text, when



(a)



(b)

FIG. 1.1 Three elements forming a three-phase system. (a) Delta connection, (b) wye connection.

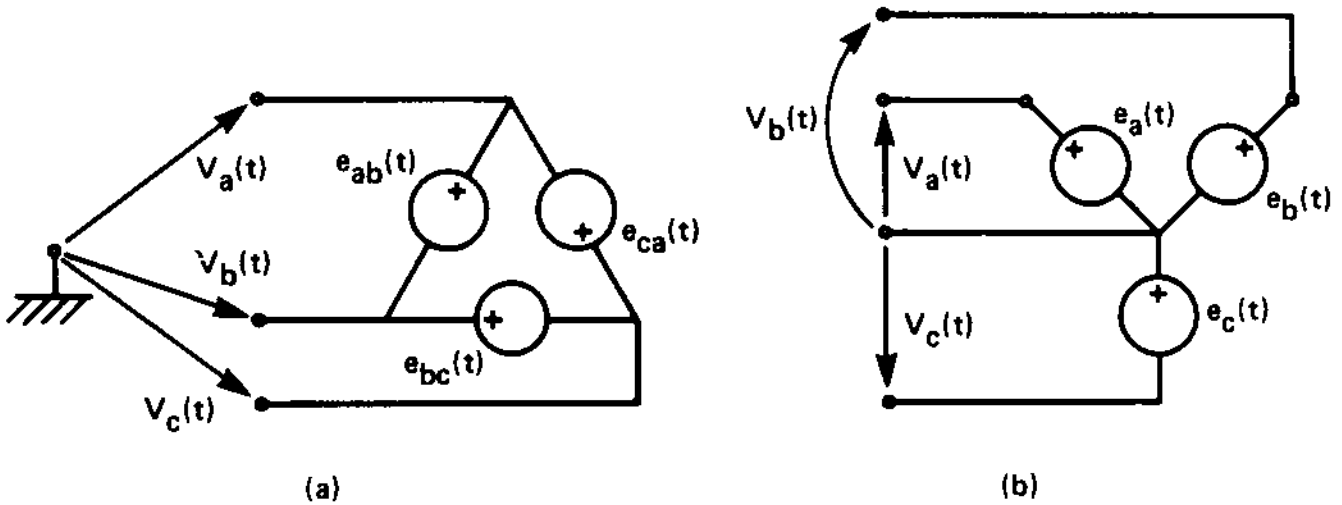


FIG. 1.2 Ideal three-phase voltage source. (a) Delta connected, (b) wye connected.

the sequence is not specified, it will be assumed to be the positive sequence.

A similar definition exists for a set of three-phase currents.

**Definition 1.2: Balanced Set of Three-Phase Currents.** A set of three-phase currents,  $i_a(t)$ ,  $i_b(t)$ ,  $i_c(t)$ , is called balanced if and only if:

The currents vary sinusoidally with time.

The amplitudes of the electric currents are equal.

There is a  $120^\circ$  phase difference between any two.

As an example, the following set is balanced:

$$i_a(t) = \sqrt{2} I \cos(\omega t + \phi) \quad (1.5a)$$

$$i_b(t) = \sqrt{2} I \cos(\omega t - 120^\circ + \phi) \quad (1.5b)$$

$$i_c(t) = \sqrt{2} I \cos(\omega t - 240^\circ + \phi) \quad (1.5c)$$

The set above, as in the case of voltages, is called a positive phase sequence.

A third definition is introduced for a three-phase system.

**Definition 1.3: Symmetric Three-Phase System.** A three-phase passive system is called symmetric if and only if the following two statements are true:

It is a linear system.

If a balanced set of three-phase currents flows into the system when it is excited with a balanced set of three-phase voltages.

## Power Transmission Systems

The definition of a symmetric three-phase system is illustrated in Fig. 1.3. Practical three-phase systems comprise three-phase components that are symmetric or nearly symmetric. Three-phase transformers are symmetric three-phase devices, three-phase synchronous generators are nearly symmetric devices, overhead transmission lines are nearly symmetric, and so on. Traditional power system analysis techniques (i.e., load flow, fault analysis, and transient stability techniques) have been developed on the assumption of symmetric three-phase systems.

### 1.3 TRANSMISSION LINE DESIGN

Power transmission lines are designed to transmit ac or dc electric power. Ac transmission lines may be three-phase or single-phase. The components of overhead transmission lines are illustrated in Fig. 1.4. A three-phase overhead line consists of the three-phase conductors a, b, and c, which are suspended with insulators from towers. Most designs include an overhead ground wire (OHGW or shield wire) to provide protection against lightning. The OHGW is typically connected to the neutral of the system and may be grounded at each tower. The tower grounding system may consist of ground rods (illustrated in Fig. 1.4), rings, counterpoises, and so on. A typical overhead transmission line terminates to two substations. The OHGW is typically connected to the grounding system of the substations, which are illustrated in Fig. 1.4a as ground mats. A single-phase overhead distribution line is illustrated in Fig. 1.4b. It consists of one phase conductor and a multiply grounded neutral conductor. Overhead power lines are suspended on towers or poles. The design of transmission towers depends on the operating voltage

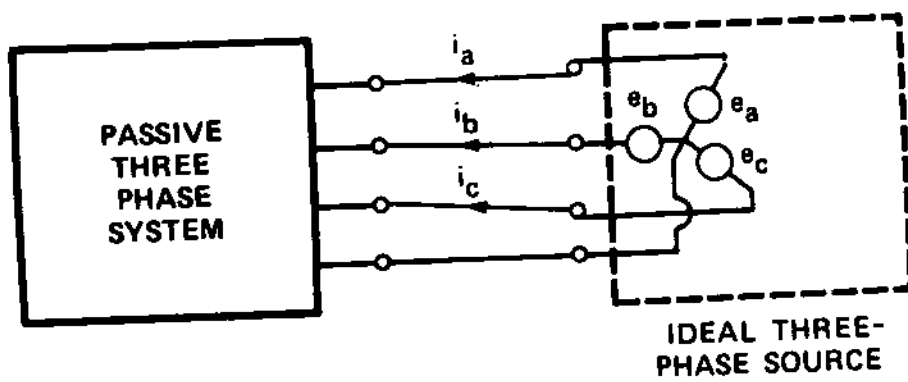


FIG. 1.3 Definition of a symmetric three-phase system.

$$\begin{pmatrix} \text{Balanced Voltages} \\ e_a(t), e_b(t), e_c(t) \end{pmatrix} = \begin{pmatrix} \text{Balanced Currents} \\ i_a(t), i_b(t), i_c(t) \end{pmatrix}$$

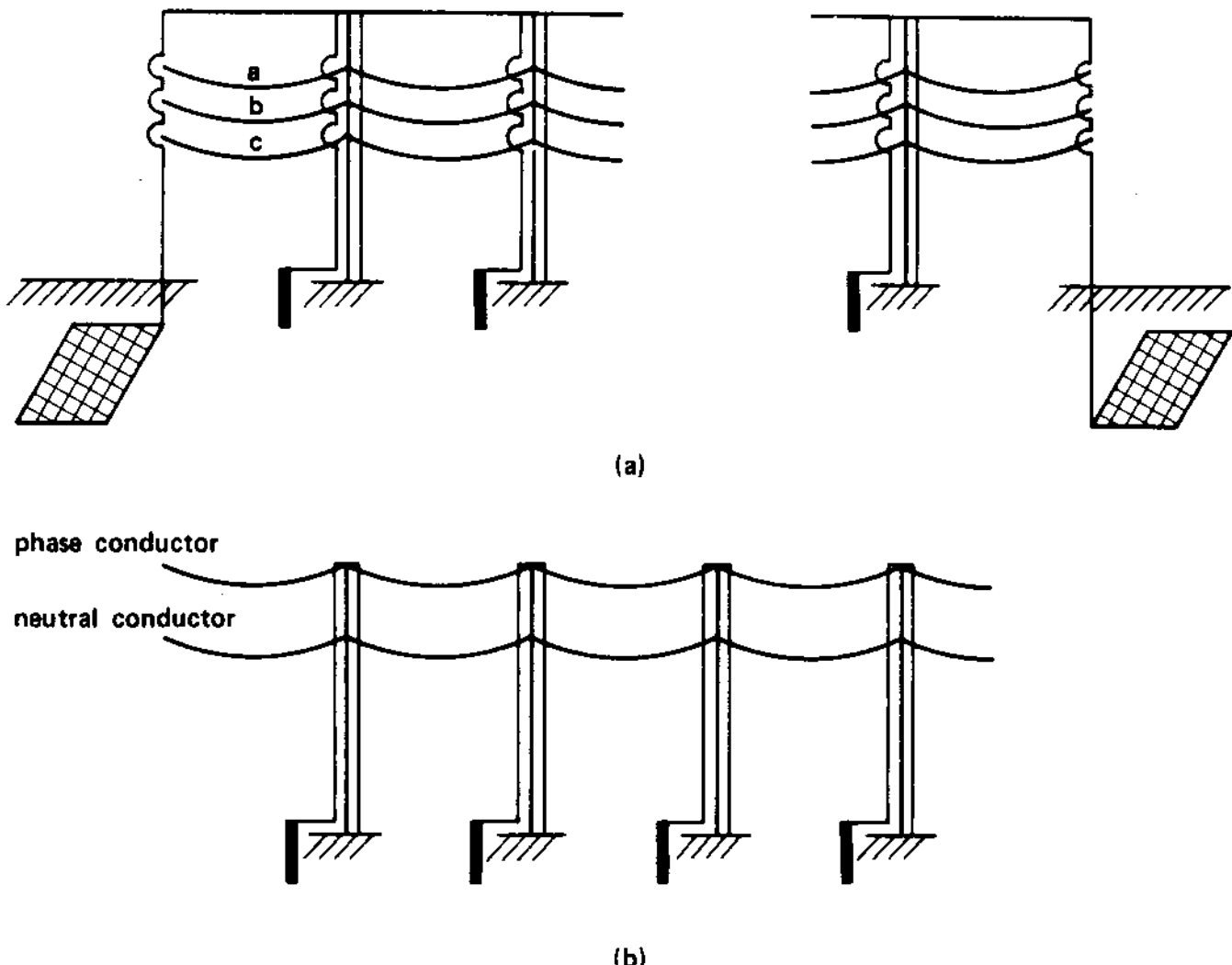


FIG. 1.4 Components of overhead transmission lines. (a) Three-phase transmission line, (b) single-phase distribution line.

of the line and other mechanical strength considerations. Three transmission tower designs are illustrated in Fig. 1.5, 1.6, and 1.7 for 230-, 115-, and 12-kV transmission lines, respectively. Note that the 12-kV line, which is typically used in distribution circuits, does not have an OHGW. Instead, it has a fourth conductor, the neutral, which is suspended below the phase conductors. The size of the neutral conductor is comparative to that of the phase conductors. The reason for this practice is the fact that distribution circuits are normally operated under unbalanced conditions, in which case the neutral conductor may carry a substantial electrical current.

Recent advances in technology have made dc transmission an economically attractive alternative over long distances. A typical dc transmission line is illustrated in Fig. 1.8. It consists of two conductors, the positive and negative poles, and an overhead ground conductor.

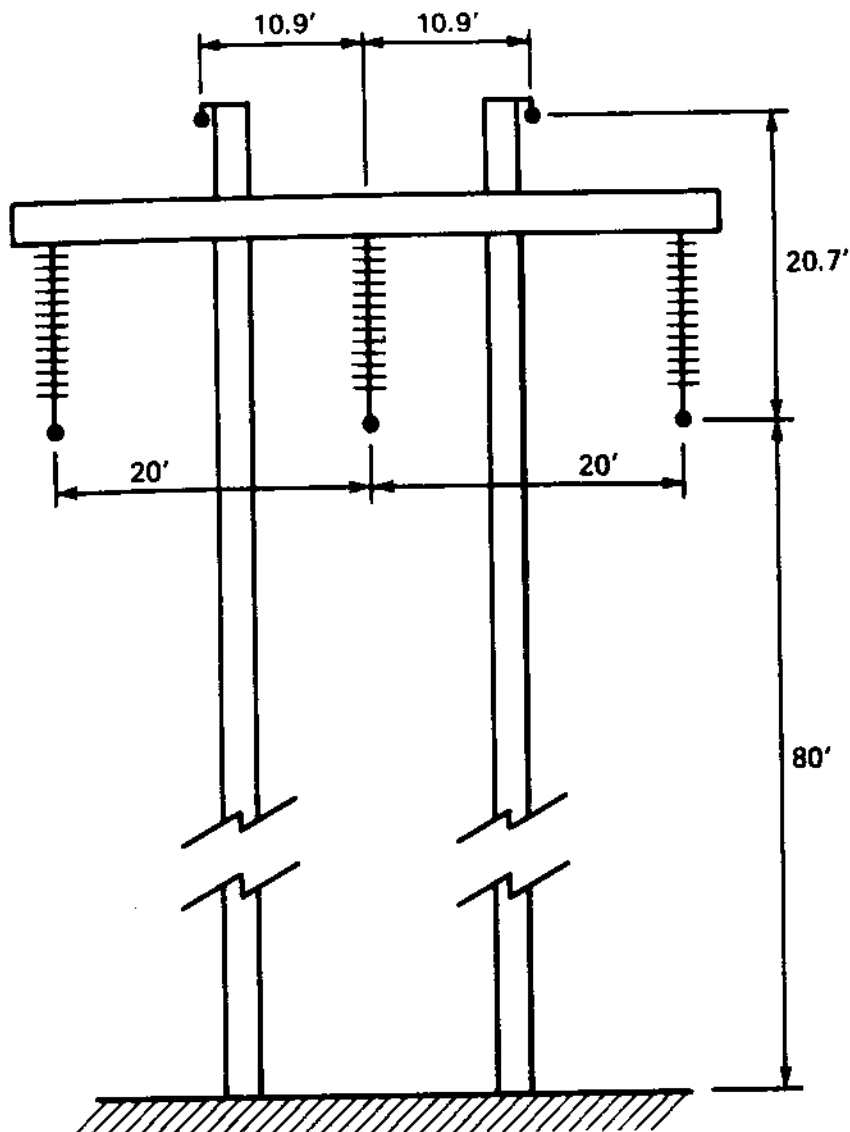


FIG. 1.5 Design of a 230-kV H-frame transmission tower. (Courtesy of Georgia Power Company.)

The illustrated designs of transmission lines will be utilized as examples throughout the book. Appropriate models of transmission lines will be developed. Specific examples are:

1. The sequence models of three-phase power lines will be developed. These models are applicable for power flow studies, short-circuit analysis, and stability studies.
2. Power line models with explicit representation of transmission tower grounding systems and substation grounding systems will be developed. These models are applicable for ground potential rise computations and the design of grounding systems.
3. Distributed parameter models of power lines will also be developed. These models are applicable for electrical transient analysis and the design of overvoltage protection.

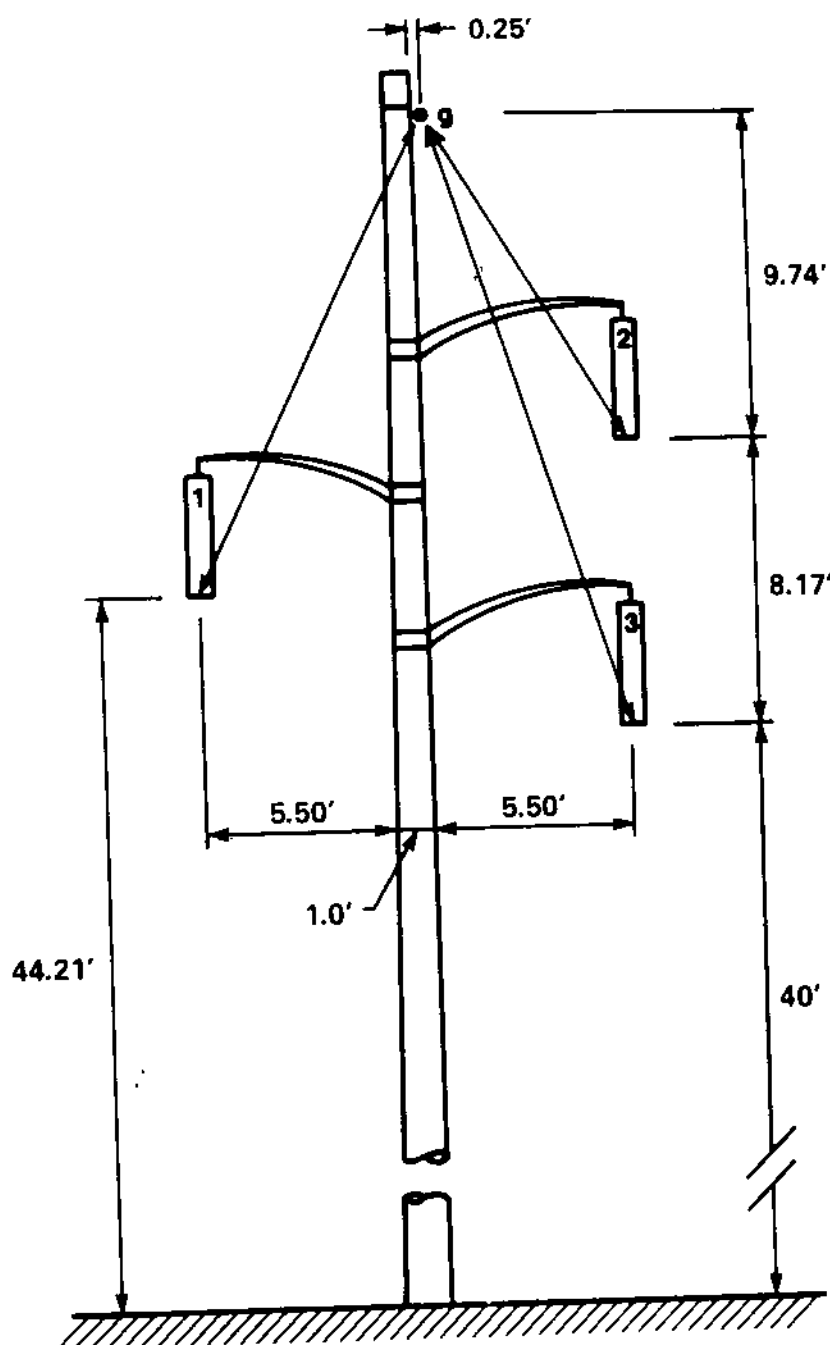


FIG. 1.6 Design of a 115-kV single-pole transmission tower. (Courtesy of Georgia Power Company.)

#### 1.4 DISTRIBUTION SYSTEM DESIGN

A distribution system comprises power lines and voltage-step-down equipment for electric service at industrial, commercial, and residential sites. A distribution system may comprise three-phase transmission lines, with typical operating voltages of 12 to 25 kV line to line, and three-phase, two-phase, or single-phase tapped lines. The construction of these lines may be by overhead or underground cable lines. These possibilities are illustrated in Fig. 1.9.

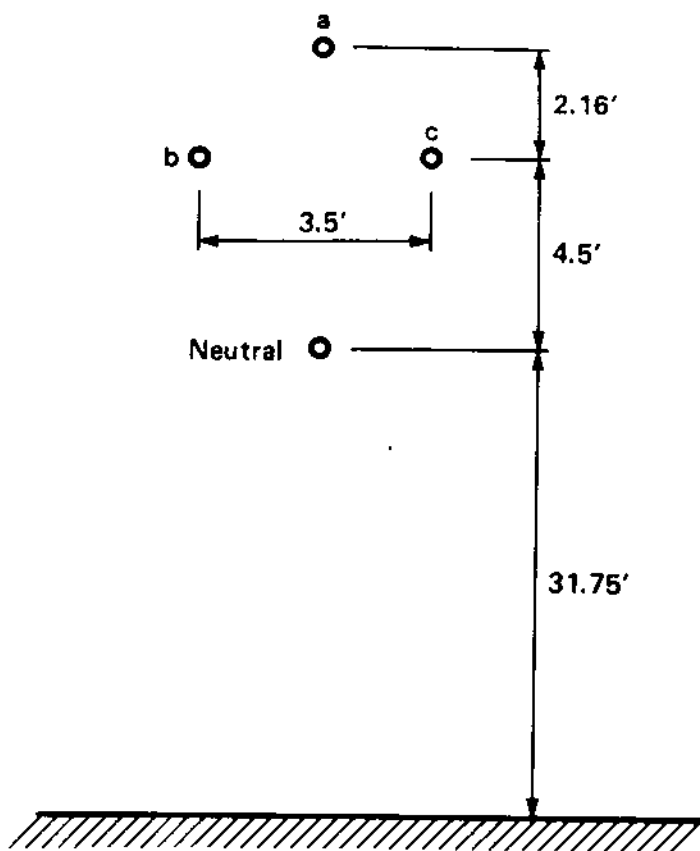


FIG. 1.7 Design of a 12-kV single-pole distribution tower. (Courtesy of Georgia Power Company.)

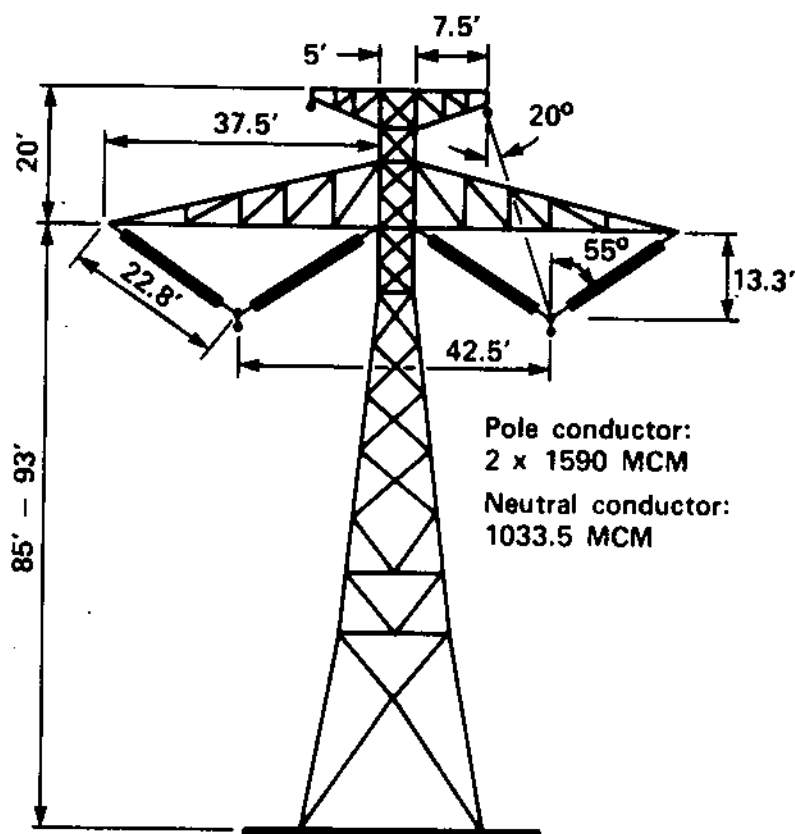


FIG. 1.8 Design of a  $\pm$  400-kV HVDC tower. (Courtesy of the Electric Power Research Institute.)

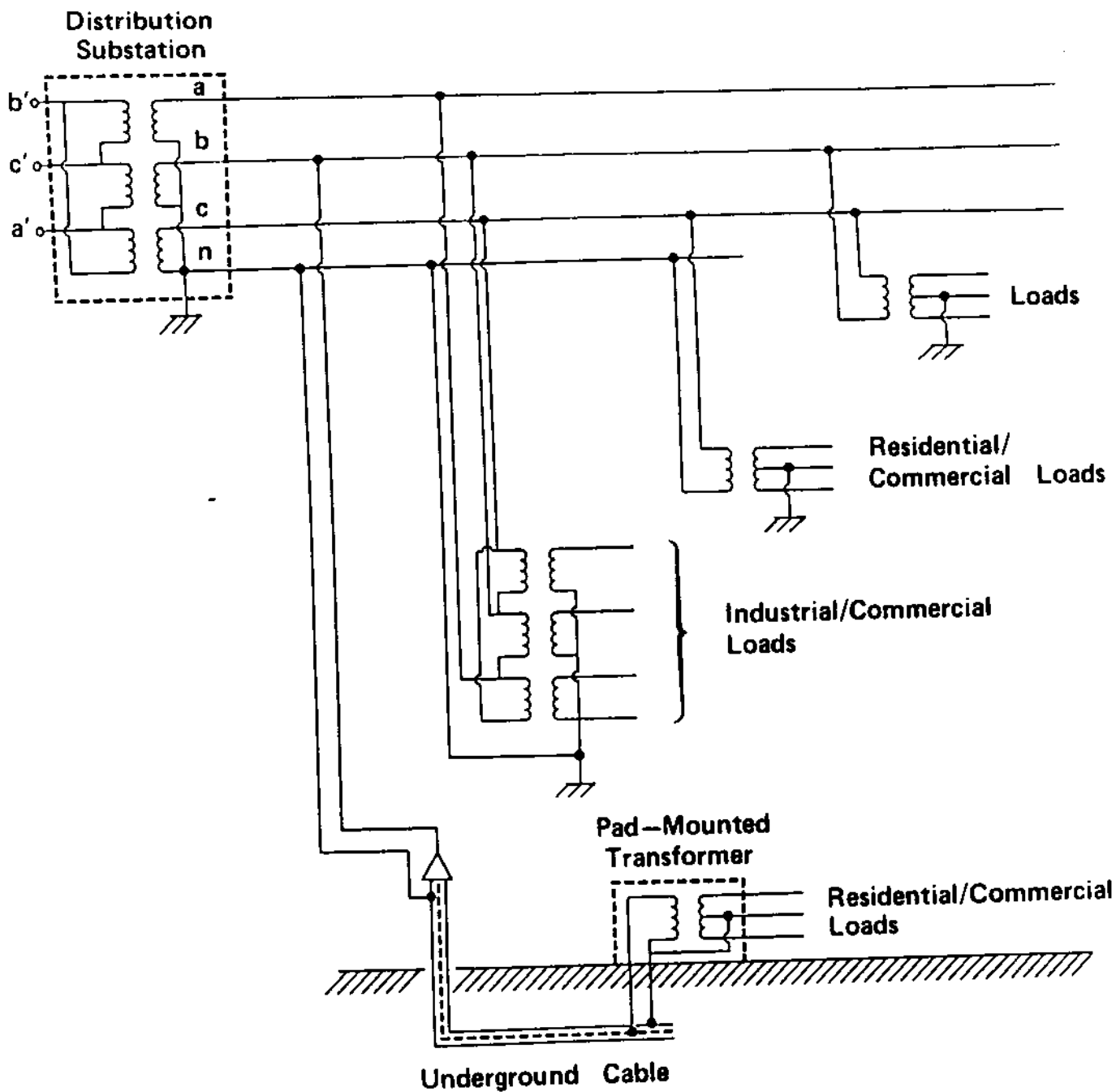


FIG. 1.9 A distribution system.

Fig. 1.9 suggests that distribution systems may operate (and in fact they do operate) under unbalanced conditions. This means that distribution systems present some unique analysis problems. In addition, recent advances in end use equipment technology has resulted in electric loads that may be interacting with the system dynamically. For example, solid-state motor controllers, rectifiers, and so on, inject harmonics into the distribution system. Analysis and understanding of these phenomena require that the distribution system be modeled and understood not only for the power frequency (60 Hz in the

United States, 50 Hz in Europe) but also for other frequencies, such as the harmonics of 60 Hz. The models discussed in this book are especially suitable for power frequency and harmonic analysis of the general distribution system of Fig. 1.9.

### 1.5 POWER SYSTEM GROUNDING

For several technical and safety reasons, electric power installations must be grounded. Grounding of power systems is achieved by embedding metallic structures (conductors) into earth and electrically connecting these conductors to the neutral of the power system. In this way a low impedance is provided between the power system neutral and the vast conducting soil, which guarantees that the voltage of the neutral, with respect to earth, will be low under all conditions.

Grounding is necessary for several reasons: (a) to assure correct operation of electrical devices, (b) to provide safety during normal or fault conditions, (c) to stabilize the voltage during transient conditions, and (d) to dissipate lightning strokes. The importance of grounding has long been recognized in power engineering. Today there are several standards that deal with various aspects of grounding on the performance of a power system. For example, ANSI/IEEE Standard 80 [18] addresses the impact of grounding system design on the safety of personnel in a power substation. ANSI/IEEE Standard 487 [58] addresses the topic of communication circuit protection serving power substations, which is primarily dependent on grounding.

In this book we examine methods of analysis of grounding systems and how these methods are utilized to assess the effects of grounding on power system performance or to design grounding systems.

### 1.6 POWER SYSTEM TRANSIENTS

Electrical transients in power systems play an important role in the design of electrical installations. There are numerous sources of electrical transients in power systems, such as lightning, switching, faults, and resonance conditions. Today, the phenomena leading to electrical transients are fairly well understood. It is important that power systems are designed so as to withstand the possible electrical transients that may occur. Overvoltage protection schemes are designed to ensure that the possible electrical overvoltages will not exceed the withstand capabilities of power apparatus with a certain protection margin. Recent trends in power apparatus design have resulted in increased significance of electrical transients. Two factors have contributed to this trend: (a) power apparatus is operating at higher voltage levels and with stricter voltage withstand capabilities,

and (b) the proliferation of apparatus can cause electrical transients, such as voltage correction capacitors, power electronics, series compensation capacitors, ac/dc converters, and so on. In this environment it is absolutely necessary that the mechanisms of possible overvoltages in specific systems be well understood and effective protection schemes designed.

We shall examine modeling techniques and analysis methods for the study of electrical transients in power systems. These methods are the basic tools for predicting possible problems in power systems and procedures for the protection of power apparatus.

### 1.7 SUMMARY AND DISCUSSION

In this introductory chapter, a general discussion of concepts related to grounding and transients of power systems has been presented. Typical designs of transmission circuits have been introduced and the major design factors have been discussed. It has been pointed out that models for the analysis of grounding systems and transients are related. In subsequent chapters we introduce the modeling procedures and the application of the models to the analysis and design of grounding systems, as well as to transient analysis and surge protection.

# 2

## Transmission Line Modeling Line Inductance

### 2.1 INTRODUCTION

In this chapter we are concerned with the inductance of a transmission line or the induced voltage along transmission lines due to the inductance. Analysis procedures are presented for the induced voltage along a line and the inductance of the line. Emphasis is placed on overhead transmission lines.

Conceptually, the phenomena to be studied can be explained through the simple one-conductor system illustrated in Fig. 2.1. Assume that electric current  $i(t)$ , which is time dependent, flows through this conductor. The current generates a magnetic field that is time dependent. Consider an infinitesimal length  $dx$  of conductor. Let  $d\lambda(t)$  be the magnetic flux linking the electric current  $i(t)$  flowing in the infinitesimal length  $dx$  of the conductor. By definition, the inductance of the length  $dx$  of the conductor is  $dL$ , where

$$dL = \frac{d\lambda(t)}{i(t)} \quad (2.1)$$

Since the magnetic flux linkage is time varying, a voltage  $dv(t)$  will be induced along length  $dx$  of the conductor:

$$dv(t) = \frac{d\lambda(t)}{dt} = dL \frac{di(t)}{dt}$$

Now assume that the inductance of the conductor is  $L$  henries per meter; then

$$dL = L dx$$

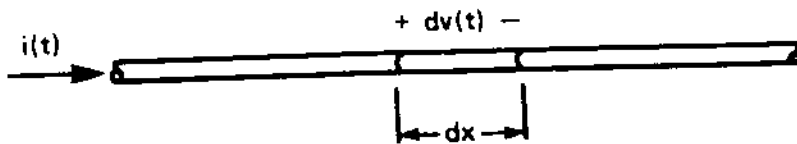


FIG. 2.1 A conductor carrying electric current  $i(t)$ . Path of return is not shown.

Upon substitution in the equations above and subsequent solution for  $L$ , we have

$$L = \frac{dv(t)/dx}{di(t)/dt} \quad \text{henries/meter} \quad (2.2)$$

Equation (2.1) or (2.2) defines the inductance of a conductor. Specifically, Eq. (2.1) states that the inductance equals the magnetic flux linkage divided by the electric current. Alternatively, Eq. (2.2) states that the inductance equals the induced voltage divided by the time derivative of the electric current. In our conceptual discussion of the inductance, we neglected a very important consideration. Specifically, we neglected the path of return of the electric current  $i(t)$ . The path of return drastically affects the induced voltage  $dv(t)$ , and thus the inductance of the conductor. This point will be clarified further in our discussion of specific transmission line configurations.

A transmission line is a complicated structure, comprising more than one conductor. Our objective in this chapter is to characterize each conductor with its inductance and also any pair of conductors with a mutual inductance.

## 2.2 MAGNETIC FIELD OF AN INFINITELY LONG CIRCULAR CONDUCTOR

In this section we introduce the basic concepts by considering the magnetic field of an infinitely long conductor of circular cross section. For simplicity, assume that the conductor material is nonmagnetic. In other words, the permeability of the conductor material is  $\mu_0$ . A cross section of the conductor is shown in Fig. 2.2a. The radius of the conductor is  $a$ . Further assume that the conductor carries an electric current  $i(t)$ , which is uniformly distributed in the cross section of the conductor (i.e., constant current density). Under these assumptions, it is relatively easy to compute the magnetic field of the configuration and subsequently the inductance of the line.

Because of the existing cylindrical symmetry, the magnetic field intensity  $\underline{H}$  at a point A, illustrated in Fig. 2.2a, will be perpendi-

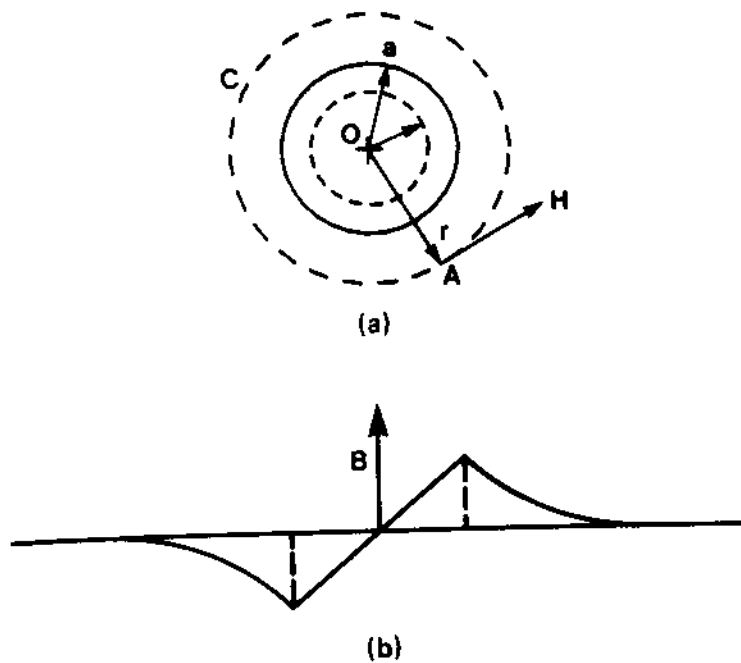


FIG. 2.2 Infinitely long circular conductor. (a) cross section, (b) magnetic flux density along a radial direction.

cular to the segment OA and the magnitude will be constant on the circular contour with center O and radius  $\overline{OA}$ . In other words, the magnitude of the magnetic field intensity,  $H$ , is a function of the radius  $\overline{OA} = r$  only [i.e.,  $H(r)$ ].  $H(r)$  is computed with a direct application of Ampère's law on the described configuration. There are two cases.

Case a. The point A is located outside the conductor:

$$\overline{OA} > a$$

Application of Ampère's law yields

$$i(t) = \int_C \underline{H}(r) \cdot d\underline{l} = 2\pi(\overline{OA})H(r) = 2\pi r H(r)$$

Upon solving for  $H(r)$ , we obtain

$$H(r) = \frac{i(t)}{2\pi r} \quad (2.3)$$

The magnetic flux density is given by

$$B(r) = \mu_0 H(r) = \frac{\mu_0 i(t)}{2\pi r} \quad (2.4)$$

Case b. The point A is located inside the conductor:

$$\overline{OA} < a$$

Application of Ampère's law yields

$$\text{electric current inside } C = \int_C \underline{H}(r) \cdot d\underline{l} = 2\pi(\overline{OA}) H(r) = 2\pi r H(r)$$

Under the assumption that the electric current density is constant inside the conductor, we have

$$\text{electric current inside } C = \frac{\pi r^2}{\pi a^2} i(t) = \left(\frac{r}{a}\right)^2 i(t) \quad r < a$$

Substitution and subsequent solution for  $H(r)$  yields

$$H(r) = \frac{ri(t)}{2\pi a^2} \quad r < a \quad (2.5)$$

and

$$B(r) = \mu_0 H(r) = \frac{\mu_0 ri(t)}{2\pi a^2} \quad r < a \quad (2.6)$$

The results are summarized in Fig. 2.2b, where the magnetic flux density  $B(r)$  is plotted as a function of  $r$  along a radial direction.

From the magnetic flux density  $B$ , the magnetic flux  $\Phi$  crossing any surface  $S$  is computed from the integral

$$\Phi = \int_S \underline{B} \cdot d\underline{s}$$

If the surface  $S$  crosses the conductor and since the electric current is distributed inside the conductor, the magnetic flux will link variable portions of the electric current. In this case the use of the concept of magnetic flux linkage is expedient. The magnetic flux linkage is defined by

$$\lambda = \int_S w \underline{B} \cdot d\underline{s}$$

where  $w$  is the portion of electric current linked with the infinitesimal magnetic flux  $\underline{B} \cdot d\underline{s}$ .

Given the magnetic flux linkage through a surface S, the induced voltage  $v(t)$  along the perimeter of the surface is computed by

$$v(t) = \frac{d\lambda(t)}{dt}$$

As an example, consider a rectangular surface S, of dimensions  $\ell$  and D, located on a plane passing through the axis of the conductor. The surface S is defined in Fig. 2.3. Consider the two illustrated infinitesimal strips of area  $\ell dr$  located on the surface S and parallel to the axis of the conductor. One infinitesimal strip is located inside the conductor at a distance  $r < a$  from the axis. The magnetic flux through this infinitesimal strip  $\ell dr$  which is located inside the conductor at a distance  $r$  links  $\pi r^2/\pi a^2$  percentage of the electric current. Thus the magnetic flux linkage  $d\lambda_{int}$  is

$$d\lambda_{int}(t) = \frac{\pi r^2}{\pi a^2} B(r) \ell dr = \frac{\mu_0 r^3 i(t)}{2\pi a^4} \ell dr$$

The magnetic flux linkage of the second infinitesimal strip  $\ell dr$ , which is located outside the conductor, links all the electric current through the conductor. The magnetic flux linkage of this infinitesimal strip  $d\lambda_{ext}$  is

$$d\lambda_{ext}(t) = \frac{\mu_0 i(t)}{2\pi r} \ell dr$$

The total magnetic flux linkage is

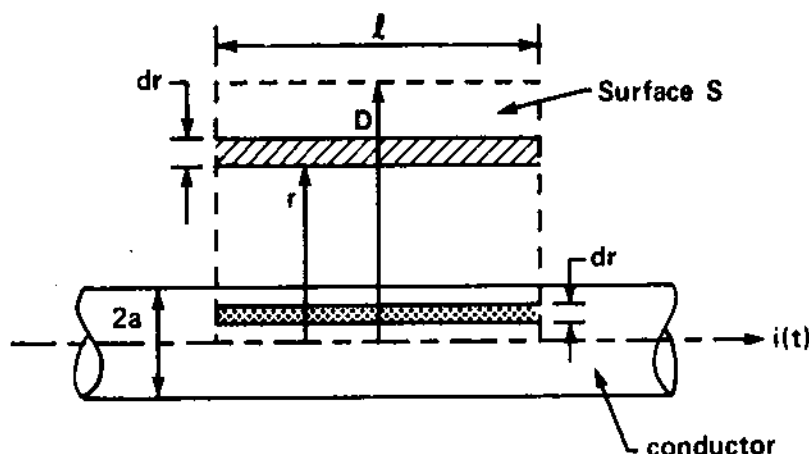


FIG. 2.3 Geometry of surface S.

$$\lambda(t) = \int_{r=0}^a \frac{\mu_0 r^3 i(t)}{2\pi a^4} \ell \, dr + \int_{r=a}^D \frac{\mu_0 i(t)}{2\pi r} \ell \, dr$$

Evaluation of the integrals gives us

$$\lambda(t) = \frac{\mu_0 \ell i(t)}{2\pi} \left( \frac{1}{4} + \ln \frac{D}{a} \right) \quad (2.7)$$

Equation (2.7) is usually written in the following compact form:

$$\lambda = \frac{\mu_0 i(t) \ell}{2} \ln \frac{D}{d} \quad (2.8)$$

where

$$d = ae^{-1/4}$$

$$\mu_0 = 4\pi \times 10^{-7} \text{ H/m} \quad (2.9)$$

The quantity  $d$  is known as the geometric mean radius of the conductor. The name was coined from the method of geometric mean distances, to be discussed later. The physical meaning of the geometric mean radius is that a thin hollow conductor of radius equal to the geometric mean radius and carrying the same electric current  $i(t)$  produces the same magnetic flux linkage as the conductor under consideration. This interpretation will be illustrated by the following example.

Example 2.1: An infinitely long hollow conductor of average radius  $d$  and infinitesimal thickness carries an electric current  $i(t)$ . Show that the magnetic flux linking a rectangular surface of dimensions  $\ell$  and  $D$ , with one  $\ell$ -long side located on the axis of the conductor, is

$$\lambda(t) = \frac{\mu_0 i(t) \ell}{2\pi} \ln \frac{D}{d}$$

Solution: The magnetic field density around this configuration is illustrated in Fig. E2.1b. Specifically, the magnetic field density is

$$B(r) = \begin{cases} 0 & r < d \\ \frac{\mu_0 i(t)}{2\pi r} & r > d \end{cases}$$

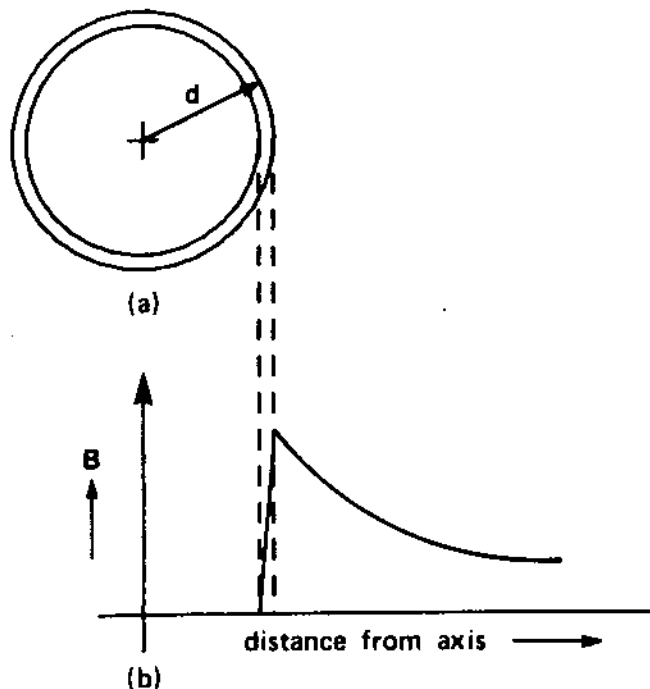


FIG. E2.1 Magnetic field around a hollow conductor carrying electric current.

The magnetic flux linkage is

$$\lambda(t) = \int_{r=d}^D \frac{\mu_0 i(t)}{2\pi r} \ell dr = \frac{\mu_0 i(t) \ell}{2\pi} \ln \frac{D}{d}$$

The induced voltage across the conductor due to the magnetic flux is readily computed from

$$v(t) = \frac{d \lambda(t)}{dt} = \frac{\mu_0 \ell}{2\pi} \ln \frac{D}{d} \frac{di(t)}{dt}$$

By definition, the inductance of the conductor is

$$L' = \frac{\lambda(t)}{i(t)} = \frac{\mu_0 \ell}{2\pi} \ln \frac{D}{d} \quad \text{henries}$$

On a per unit basis, the inductance is

$$L = \frac{\mu_0}{2\pi} \ln \frac{D}{d} \quad \text{henries/meter} \quad (2.10)$$

One should observe that the inductance of the conductor is dependent on the width  $D$  of the selected surface  $S$ . Since the width  $D$  can be selected arbitrarily, the result above does not have any

physical meaning. This peculiarity occurs because the path of return of the electric current  $i(t)$  has been neglected. It is apparent that in order to compute the inductance of the conductor in a unique and meaningful way, it is necessary to consider the entire circuit, that is, the path of return of the electric current. In any practical situation, all conductors or objects carrying electric current will be located in a finite area. In this case, as we shall see in subsequent sections, the inductance of the conductors can be uniquely defined. Despite the lack of realism of the configuration being considered, the results obtained are fundamental for the computation of the inductances of realistic transmission line configurations, as we shall see in subsequent sections.

### 2.3 MAGNETIC FIELD OF TWO CIRCULAR INFINITELY LONG CONDUCTORS

In this section we examine the magnetic field around a configuration consisting of two circular infinitely long and parallel conductors. It is assumed that each conductor carries electric current  $i(t)$  in opposite directions. Let the radii of the conductors be  $a$  and  $b$ , respectively. It is also assumed that the conductor material is nonmagnetic (i.e.,  $\mu = \mu_0$ ). The configuration is illustrated in Fig. 2.4. The figure also illustrates a rectangular surface  $S$ . The magnetic flux linkage through the surface  $S$  is to be computed. Assuming linear media, superposition applies. The magnetic flux linkage is computed as the sum of two terms: the flux linkage  $\lambda_{aa}$  due to current  $i(t)$  in conductor  $a$ , and the flux linkage  $\lambda_{ab}$  due to current  $i(t)$  in conductor  $b$ . Applying the results of Section 2.2 gives us

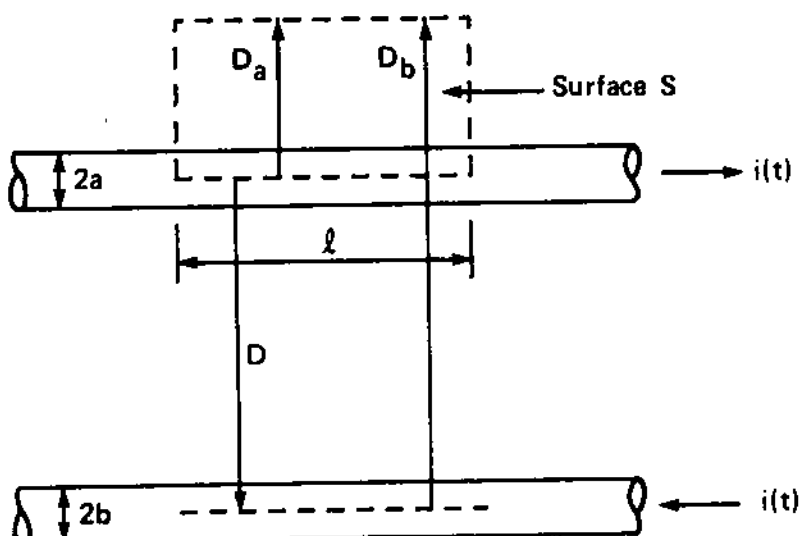


FIG. 2.4 A two-conductor transmission line.

$$\lambda_{aa}(t) = \frac{\mu_0 i(t) \ell}{2\pi} \ln \frac{D_a}{d_a}$$

$$\lambda_{ab}(t) = -\frac{\mu_0 i(t) \ell}{2\pi} \ln \frac{D_b}{D}$$

where

$$d_a = a e^{-0.25}$$

All other geometric parameters are defined in Fig. 2.5. Thus the magnetic flux linkage through surface S is

$$\lambda_a(t) = \lambda_{aa}(t) + \lambda_{ab}(t) = \frac{\mu_0 i(t) \ell}{2\pi} \left( \ln \frac{D_a}{d_a} - \ln \frac{D_b}{D} \right)$$

$$\lambda_a = \frac{\mu_0 i(t) \ell}{2\pi} \ln \frac{D_a D}{D_b d_a}$$

If the surface S is extended to infinity, then  $D_a \rightarrow \infty$ ,  $D_b = D + D_a \rightarrow \infty$ , and  $D_a/D_b \rightarrow 1.0$ . In this case the magnetic flux linkage of conductor a becomes

$$\lambda_a(t) = \lim \frac{\mu_0 i(t) \ell}{2\pi} \ln \left( \frac{D_a}{D_b} \frac{D}{d_a} \right) = \frac{\mu_0 i(t) \ell}{2\pi} \ln \frac{D}{d_a} \quad (2.11)$$

The magnetic flux linkage  $\lambda_b$  linking conductor b is computed in a similar way, yielding

$$\lambda_b(t) = \frac{\mu_0 i(t) \ell}{2\pi} \ln \frac{D}{d_b} \quad (2.12)$$

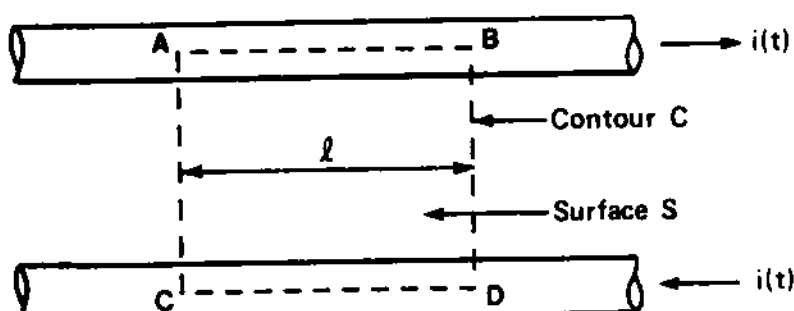


FIG. 2.5 An alternative way of computing the magnetic flux linkage of a two-conductor line.

where

$$d_b = b e^{-0.25}$$

The magnetic flux linkage linking a length  $\ell$  of the line, that is, a length  $\ell$  of both conductors a and b, is

$$\begin{aligned} \lambda(t) &= \lambda_a(t) + \lambda_b(t) = \frac{\mu_0 i(t) \ell}{2\pi} \left( \ln \frac{D}{d_a} + \ln \frac{D}{d_b} \right) \\ \lambda(t) &= \frac{\mu_0 i(t) \ell}{2\pi} \ln \frac{D^2}{d_a d_b} \end{aligned} \quad (2.13)$$

At this point, a number of important observations are pertinent.

First, observe that the same result of flux linkage will be obtained if the magnetic flux linkage encircled by a contour C illustrated in Fig. 2.5 is computed. However, it was convenient to use the results of the preceding paragraph. As an exercise, one should compute the flux linkage encircled by contour C (by computing an appropriate integral) and compare the result to Eq. (2.13). Second, by Faraday's law, the induced voltage  $v(t)$  by the magnetic field around contour C is given by  $-d\lambda/dt$ . This voltage is the induced voltage along the line:

$$v(t) = \frac{d\lambda}{dt} = \frac{\mu_0 \ell}{2\pi} \left( \ln \frac{D^2}{d_a d_b} \right) \frac{di(t)}{dt}$$

The inducted voltage  $v(t)$  is the sum of the induced voltages on conductor a (voltage from A to B; see Fig. 2.5) and on conductor b (voltage from D to C). Next, the inductance is computed from the defining equation

$$\begin{aligned} L' &= \frac{\lambda(t)}{i(t)} = \frac{\mu_0 \ell}{2\pi} \ln \frac{D^2}{d_a d_b} \quad \text{henries} \\ L &= \frac{\mu_0}{2\pi} \ln \frac{D^2}{d_a d_b} \quad \text{henries/meter} \end{aligned} \quad (2.14)$$

In case both conductors are identical,  $d_a = d_b = d$ ,

$$L = \frac{\mu_0}{\pi} \ln \frac{D}{d} \quad \text{henries/meter} \quad (2.15)$$

The inductive reactance of the line at frequency  $f$  is

$$x_1 = \omega L = \frac{\omega\mu_0}{\pi} \ln \frac{D}{d} \quad \text{ohms/meter} \quad (2.16)$$

where  $\omega = 2\pi f$  and  $f$  is the frequency of electric current in hertz. It is expedient to write the inductive reactance as the sum of two terms:

$$\begin{aligned} x_1 &= 2 \left( \frac{\omega\mu_0}{2\pi} \ln \frac{1}{d} + \frac{\omega\mu_0}{2\pi} \ln D \right) = 2(x_{kk} + x_{ki}) \\ x_{kk} &= \frac{\omega\mu_0}{2\pi} \ln \frac{1}{d} \end{aligned} \quad (2.17)$$

and

$$x_{ki} = \frac{\omega\mu_0}{2\pi} \ln D \quad (2.18)$$

The quantities  $x_{kk}$  and  $x_{ki}$  depend only on the geometric mean radius and the separation distance  $D$ , respectively. These quantities are known as the conductor component of inductive reactance, and the separation component of inductive reactance, respectively. As we shall see in Chapter 3, the geometric mean radius depends on the frequency of the electric current. For the normal operating frequency of power systems, the conductor component of inductive reactance and the geometric mean radius for all commercially available conductors have been tabulated.

Note that the mathematically rigorous reader will be offended by the expressions for  $x_{kk}$  and  $x_{ki}$ , because  $\ln D$  or  $\ln(1/d)$  do not make sense if they are considered individually. [What is  $\ln(5 \text{ m}) = ?$ ] It should be observed that if the quantities  $D$  and  $d$  are expressed in the same unit, the final result will be correct. For this reason the following convention has been accepted: The tables provide the values of  $x_{kk}$  and  $x_{ki}$  in (ohms/miles) under the understanding that the distances  $D$  and  $d$  are expressed in feet and that each quantity  $x_{kk}$ ,  $x_{ki}$  is meaningless if considered individually.

## 2.4 INTERPRETATION OF INDUCTIVE REACTANCE COMPONENTS

A useful way of interpreting the results of Section 2.3 is as follows. Recall that the magnetic flux linkage per unit length of conductor a due to current  $i(t)$  flowing through itself is

$$\lambda_{aa}(t) = \frac{\mu_0 i(t)}{2\pi} \ln \frac{D_a}{d_a} = \frac{\mu_0 i(t)}{2\pi} \ln \frac{1}{d_a} + \frac{\mu_0 i(t)}{2\pi} \ln D_a$$

The magnetic flux linkage of conductor a due to the electric current flowing in conductor b is

$$\lambda_{ab}(t) = \frac{\mu_0 i(t)}{2n} \ln D - \frac{\mu_0 i(t)}{2n} \ln D_b$$

Now recall that the second term,  $[\mu_0 i(t)/2\pi] \ln D_a$ , of  $\lambda_{aa}$  will cancel with the second term of  $\lambda_{ab}$  as  $D_a \rightarrow \infty$ . Consequently, these terms can be neglected. Then we can write

$$\lambda_{aa}(t) = \frac{\mu_0 i(t)}{2\pi} \ln \frac{1}{d}$$

and

$$\lambda_{ab}(t) = \frac{\mu_0 i(t)}{2n} \ln D$$

The induced voltage per unit length of the conductor due to the magnetic flux linkage  $\lambda_{aa}$  is

$$V_{aa}(t) = \frac{d\lambda_{aa}(t)}{dt} = \frac{\mu_0}{2\pi} \frac{di(t)}{dt} \ln \frac{1}{d}$$

For a sinusoidal electric current  $i(t)$  [i.e.,  $i(t) = \text{Re}\{Ie^{j\omega t}\}$ ] the induced voltage  $V_{aa}(t)$  will also be sinusoidal. Upon substitution of the electric current in the equation above and subsequent manipulations, the phasor of the induced voltage per unit length,  $\tilde{V}_{aa}$ , is computed to be

$$\tilde{V}_{aa} = \frac{j\omega\mu_0}{2\pi} \tilde{I} \ln \frac{1}{d} = x_{aa} \tilde{I} \quad (2.19)$$

where

$$x_{aa} = j\omega \frac{\mu_0}{2\pi} \ln \frac{1}{d}$$

It is expedient to call the voltage  $\tilde{V}_{aa}$  the induced voltage per unit length of a conductor due to its own current.

With a similar analysis, the induced voltage per unit length of conductor a due to the electric current flowing in conductor b is computed. Specifically,

$$V_{ab}(t) = \frac{d\lambda_{ab}}{dt} = \frac{\mu_0}{2\pi} \frac{di(t)}{dt} \ln D$$

The phasor of the induced voltage on conductor a due to the electric current in conductor b is

$$\tilde{V}_{ab} = j\omega \frac{\mu_0}{2\pi} \tilde{I} \ln D = x_{ab} \tilde{I} \quad (2.20)$$

where

$$x_{ab} = j\omega \frac{\mu_0}{2\pi} \ln D$$

The total induced voltage per unit length of conductor a is

$$\tilde{V}_a = \tilde{V}_{aa} + \tilde{V}_{ab} = x_{aa} \tilde{I} + x_{ab} \tilde{I}$$

A similar analysis will yield the induced voltage per unit length of conductor b,  $\tilde{V}_b$ :

$$\tilde{V}_b = -x_{bb} \tilde{I} - x_{ab} \tilde{I}$$

where

$$x_{bb} = x_{aa} = j \frac{\omega \mu_0}{2\pi} \ln \frac{1}{d}$$

The total induced voltage per unit length of the line is

$$\tilde{V} = \tilde{V}_a - \tilde{V}_b = 2(x_{aa} + x_{ab}) \tilde{I}$$

In order to adopt a convenient notation, assume that conductor a carries current  $\tilde{I}_a$  and conductor b carries current  $\tilde{I}_b$ , both currents flowing at the same direction, as in Fig. 2.6. Then

$$\tilde{I}_a = \tilde{I}$$

$$\tilde{I}_b = -\tilde{I}$$

The induced voltage per unit length of conductor a,  $\tilde{V}_a$ , is

$$\tilde{V}_a = x_{aa} \tilde{I}_a - x_{ab} \tilde{I}_b \quad (2.21)$$

The induced voltage per unit length of conductor b,  $\tilde{V}_b$ , is

$$\tilde{V}_b = x_{bb} \tilde{I}_b - x_{ab} \tilde{I}_a \quad (2.22)$$

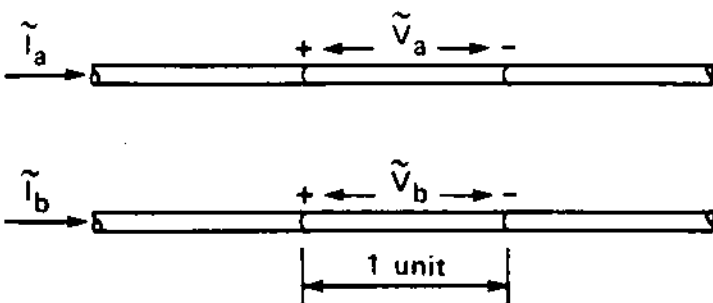


FIG. 2.6 Induced voltages in a two-conductor transmission line.

Note that the results above [Eqs. (2.21) and (2.22)] are valid under the condition that  $\tilde{I}_a + \tilde{I}_b = 0$ . The result above can be generalized to a configuration of  $n$  parallel infinitely long conductors. Specifically, the induced voltage per unit length of conductor  $k$  is

$$\tilde{V}_k = x_{kk} \tilde{I}_k - \sum_{\substack{i=1 \\ i \neq k}}^n x_{ki} \tilde{I}_i \quad (2.23)$$

where

- $\tilde{V}_k$  = induced voltage per unit length of conductor  $k$
- $x_{kk}$  = conductor component of inductive reactance
- $x_{ki}$  = separation component of inductive reactance between conductors  $k$  and  $i$
- $\tilde{I}_i$  = electric current flowing through conductor  $i$

Again, Eq. (2.23) is valid under the condition that the sum of all electric currents equals zero (i.e.,  $\sum_{i=1}^n \tilde{I}_i = 0$ ). This condition is crucial in the application of results above, because if not satisfied, Eq. (2.23) can provide erroneous results. From the practical point of view, to satisfy this condition it is necessary to account for all the paths of electric current.

## 2.5 PRACTICAL CONSIDERATIONS: USE OF TABLES

The preceding analysis suggests that the induced voltage on the conductors of a transmission line is readily computed with the aid of the

inductive reactance components  $x_{kk}$  and  $x_{ki}$ . As has been mentioned, extensive tables have been developed for the absolute value of  $x_{kk}$  for all commercially available conductors, as well as the absolute value of  $x_{ki}$ . The tables have been generated under the assumption that  $d$  and  $D$  are entered in feet, and  $x_{kk}$  or  $x_{ki}$  are computed in ohms per mile. Specifically, the equations for  $x_{kk}$  and  $x_{ki}$  have been simplified by substituting the constants  $\mu_0 = 4\pi \times 10^{-7}$  H/m,  $\pi = 3.14159$ ,  $\ln x = 2.3026 \log x$  and subsequent conversion of the units, yielding

$$x_{kk} = j0.00466f \log \frac{1}{d} \quad \text{ohms/mile}$$

$$x_{ki} = j0.00466f \log D \quad \text{ohms/mile}$$

where  $f$  is in hertz,  $d$  and  $D$  are in feet, and  $\log$  is the base 10 logarithm. The tables also provide the value of the geometric mean radius  $d$ , in feet. Tables for the most commonly used power conductors are given in Appendix A.

If it is desirable to work in the metric system, the following formula should be used:

$$x_{kk} = j\omega \frac{\mu_0}{2\pi} \ln \frac{1}{d} \quad \text{ohms/meter}$$

$$x_{ki} = j\omega \frac{\mu_0}{2\pi} \ln D \quad \text{ohms/meter}$$

where  $\omega$  is in radians per second,  $\mu_0 = 4\pi \times 10^{-7}$  H/m,  $d$  and  $D$  are both in feet or both in meters, and  $\ln$  is the natural logarithm (base e).

## 2.6 INDUCTIVE REACTANCE OF TYPICAL LINE CONFIGURATIONS

Inductive phenomena on transmission lines can be studied with the general equation (2.23). This equation is the basic tool by which the inductance of a transmission line can be computed. In this section we present the application of Eq. (2.23) to specific transmission lines configurations.

### 2.6.1 Single-Phase Transmission Line

The simplest single-phase line configuration is illustrated in Fig. 2.7. It consists of two parallel conductors of length  $\ell$ . The distance between the conductors is  $D$ . A source is connected at one end of the line and a load at the other end. It is of interest to compute the

inductive reactance per unit length of the line as well as the inductance per unit length of the line. If the length of the line is short, it can be assumed that at any point along the line, the electric current in conductors a, b is equal and of opposite direction. Thus

$$\tilde{I}_b = -\tilde{I}_a$$

The induced voltage per unit length of conductor a is

$$\tilde{V}_a = x_{aa}\tilde{I}_a - x_{ab}\tilde{I}_b = (x_{aa} + x_{ab})\tilde{I}_a \quad (2.24a)$$

Similarly, the induced voltage per unit length of conductor b is

$$\tilde{V}_b = x_{bb}\tilde{I}_b - x_{ba}\tilde{I}_a = -(x_{bb} + x_{ba})\tilde{I}_a \quad (2.24b)$$

The induced voltage per unit length of the line is

$$\tilde{V}_{line} = \tilde{V}_a - \tilde{V}_b = (x_{aa} + x_{ab} + x_{ba} + x_{bb})\tilde{I}_a$$

In the usual case, the two conductors are identical. Thus

$$x_{aa} = x_{bb} = j0.00466f \log \frac{1}{d} \quad \text{ohms/mile}$$

$$x_{ab} = x_{ba} = j0.00466f \log D \quad \text{ohms/mile}$$

and

$$\tilde{V}_{line} = 2(x_{aa} + x_{ab})\tilde{I}_a$$

The inductive reactance per unit length of the line is  $\tilde{V}_{line}/\tilde{I}_a$ :

$$x_{line} = 2(x_{aa} + x_{ab}) \quad \text{ohms/mile} \quad (2.25a)$$

The inductance per unit length of the line is  $x_{line}/j\omega$ :

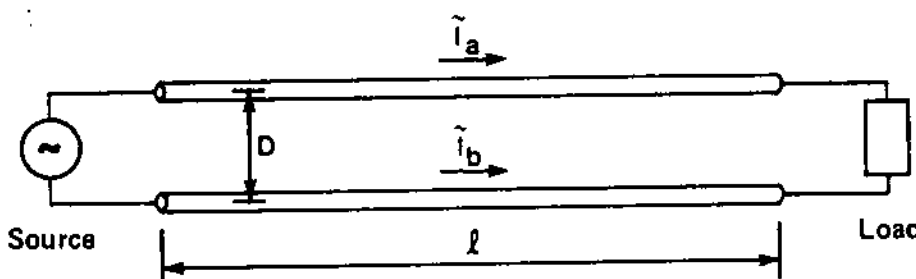


FIG. 2.7 The simplest single-phase line configuration.

$$L_{\text{line}} = \frac{2(x_{aa} + x_{ab})}{j\omega} \quad \text{henries/mile} \quad (2.25b)$$

Example 2.2: A single-phase transmission line consists of two 52,630-(circular mil) 1-strand copper conductors spaced 5 ft apart. The line supplies a single-phase load of 60 A at 60 Hz. Find the induced voltage per mile of line and the inductance per mile of line.

Solution: The diameter,  $2a$ , of the conductor is given by

$$(2a)^2 = 52,630 \text{ cm} \rightarrow 2a = 229 \text{ mils} \rightarrow 2a = 0.229 \text{ in.}$$

The geometric mean radius assuming uniform current distribution is

$$d = ae^{-0.25} = 0.08933 \text{ in.} = 0.007444 \text{ ft}$$

Evaluation of the inductive reactance components yields

$$x_{aa} = j0.5950 \Omega/\text{mi}$$

$$x_{ab} = j0.1954 \Omega/\text{mi}$$

The induced voltage per mile of line is

$$\tilde{V}_{\text{line}} = j94.85 \text{ V/mi}$$

The inductance per mile of line is

$$L_{\text{line}} = 0.004193 \text{ H/mi}$$

### 2.6.2 Three-Phase Transmission Line Without Neutral

The simplest three-phase line consists of three conductors, phase a, b, and c. It is assumed that no other path of electric current exists in the vicinity of the line. Such a line is illustrated in Fig. 2.8. It is assumed that the line is connected to a three-phase source at one end and to a three-phase load at the other end. The source and the load (Fig. 2.8) are shown to be wye connected. For purposes of our discussion, the connection of the source or the load is unimportant. The three phases carry electric currents  $\tilde{I}_a$ ,  $\tilde{I}_b$ , and  $\tilde{I}_c$ , respectively. Since for this simple three-phase line no other path of electric current exists in the vicinity of the line, the sum of the phase currents at any point along the line must equal zero:

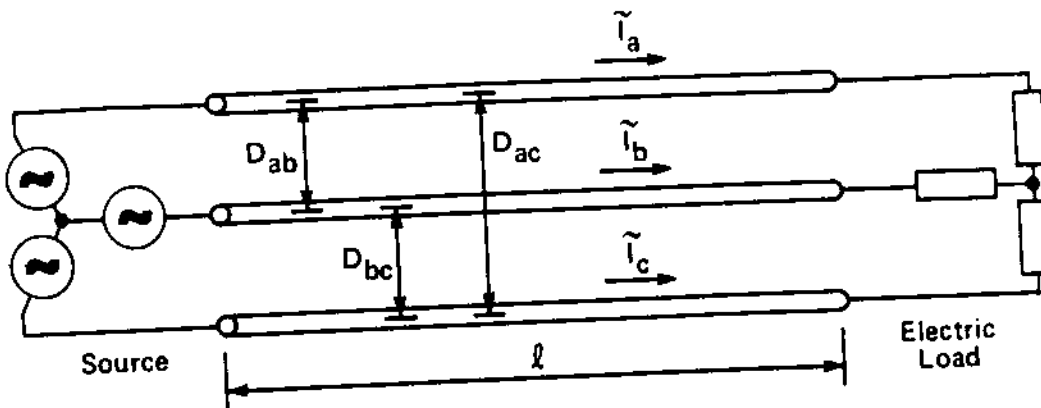


FIG. 2.8 The simplest three-phase line configuration.

$$\tilde{I}_a + \tilde{I}_b + \tilde{I}_c = 0$$

The flow of the electric currents  $\tilde{I}_a$ ,  $\tilde{I}_b$ , and  $\tilde{I}_c$ , will induce voltage on all three conductors. Consider, for example, the conductor of phase a:

1. Voltage equal to  $x_{aa}\tilde{I}_a$  will be induced on conductor a because of the magnetic field of its own current.
2. Voltage equal to  $-x_{ab}\tilde{I}_b$  will be induced on conductor a because of the magnetic field of current  $\tilde{I}_b$ .
3. Voltage equal to  $-x_{ac}\tilde{I}_c$  will be induced on conductor a because of the magnetic field of current  $\tilde{I}_c$ .

The total induced voltage  $\tilde{V}_a$  on conductor a is computed by superposition:

$$\tilde{V}_a = x_{aa}\tilde{I}_a - x_{ab}\tilde{I}_b - x_{ac}\tilde{I}_c \quad (2.26a)$$

Similarly, the total induced voltages on phases b and c are

$$(2.26b)$$

$$\tilde{V}_b = -x_{ab}\tilde{I}_a + x_{bb}\tilde{I}_b - x_{bc}\tilde{I}_c$$

$$(2.26c)$$

$$\tilde{V}_c = -x_{ac}\tilde{I}_a - x_{bc}\tilde{I}_b + x_{cc}\tilde{I}_c$$

Equations (2.26) provide the induced voltage per unit length on the three phases of the transmission line. The inductance of the transmission line can be extracted from these equations. In the next paragraph we consider the application of Eqs. (2.26) to the special case of a symmetric three-phase line.

Special Case:

A symmetric three-phase line is defined as one that comprises three identical conductors placed on the vertices of an equilateral triangle (i.e., the distance between any two of them is the same). Let this distance be D feet. Also let the geometric mean radius of the conductors be d. In this case, the inductive reactance components are

$$x_{ab} = x_{bc} = x_{ca} = x_m = j0.00466f \log D$$

and

$$x_{aa} = x_{bb} = x_{cc} = x_s = j0.00466f \log \frac{1}{d}$$

Now consider the equation for the induced voltage on phase a.

$$\begin{aligned}\tilde{V}_a &= x_{aa}\tilde{I}_a - x_{ab}\tilde{I}_b - x_{ac}\tilde{I}_c \\ &= x_s\tilde{I}_a - x_m(\tilde{I}_b + \tilde{I}_c)\end{aligned}$$

Since the sum of the three phase currents equals zero,

$$\tilde{I}_b + \tilde{I}_c = -\tilde{I}_a$$

Substitution gives us

$$\tilde{V}_a = x_s\tilde{I}_a + x_m\tilde{I}_a = (x_s + x_m)\tilde{I}_a$$

Similarly, the induced voltage on the other two phases is

$$\tilde{V}_b = (x_s + x_m)\tilde{I}_b$$

$$\tilde{V}_c = (x_s + x_m)\tilde{I}_c$$

The expressions above suggest that a symmetric three-phase line exhibits an equivalent reactance per phase and per unit length equal to

$$x_1 = x_s + x_m = j0.00466f \log \frac{D}{d} \quad \text{ohms/mile} \quad (2.27)$$

Also, the line exhibits an equivalent inductance per phase and per unit length equal to

$$L_1 = \frac{x_1}{j\omega} = 0.000742 \log \frac{D}{d} \quad \text{henries/mile}$$

Note that this conclusion has been reached under two assumptions: (a) the three-phase line is symmetric, and (b) the available paths for the flow of electric current are only the three phases a, b, and c.

In reality, it is impractical to construct a symmetric three-phase line. As a matter of fact, in practical transmission lines, the phase conductor spacing is not the same for different pairs of phases. In addition, a fourth or fifth path of electric current may exist: a neutral conductor and/or the conductive earth path. Nevertheless, the symmetric three-phase line is a useful simplification of a three-phase transmission line operating under or near balanced conditions.

### 2.6.3 Three-Phase Transmission Line with Neutral Conductor

A three-phase line with a neutral conductor is illustrated in Fig. 2.9. It consists of four parallel conductors. Three conductors are identical, the phase a, b, and c conductors. The neutral conductor is typically a different-size conductor. The line is connected to a three-phase source at one end and to a three-phase electric load at the other end. The source and the electric load may be wye or delta connected. The figure illustrates the case where both the source and the electric load are wye connected. We shall assume that the line neutral is connected to the source and load neutral. At any point along the line, the sum of all currents equals zero (i.e.,  $\tilde{I}_a + \tilde{I}_b + \tilde{I}_c + \tilde{I}_n = 0$ ). The induced voltage on each one of the four conductors per unit length of the line is obtained by application of Eq. (2.23):

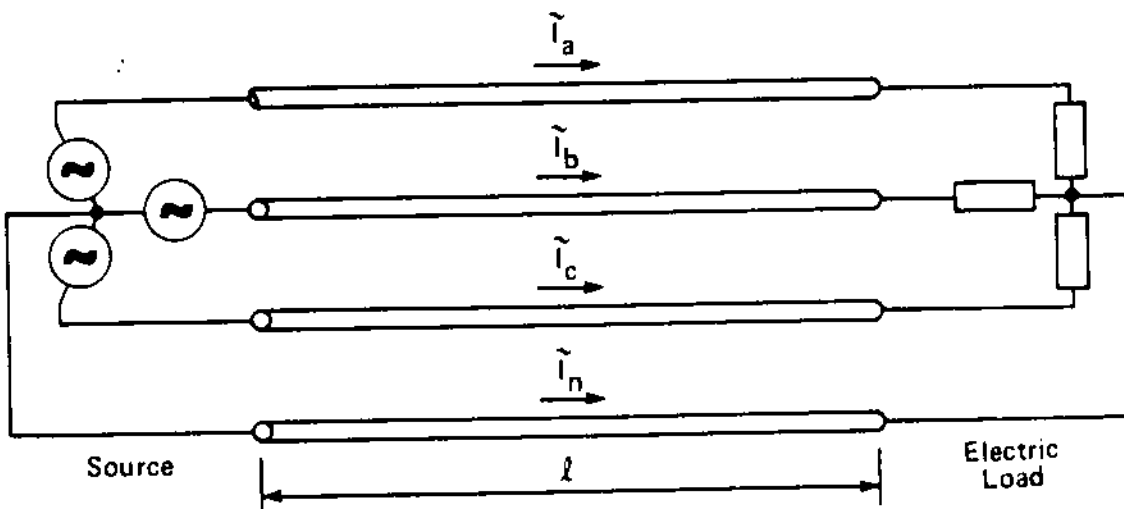


FIG. 2.9 A four-wire three-phase transmission line.

$$\tilde{V}_a = x_{aa}\tilde{I}_a - x_{ab}\tilde{I}_b - x_{ac}\tilde{I}_c - x_{an}\tilde{I}_n \quad (2.28a)$$

$$\tilde{V}_b = -x_{ab}\tilde{I}_a + x_{bb}\tilde{I}_b - x_{bc}\tilde{I}_c - x_{bn}\tilde{I}_n \quad (2.28b)$$

$$\tilde{V}_c = -x_{ac}\tilde{I}_a - x_{bc}\tilde{I}_b + x_{cc}\tilde{I}_c - x_{cn}\tilde{I}_n \quad (2.28c)$$

$$\tilde{V}_n = -x_{an}\tilde{I}_a - x_{bn}\tilde{I}_b - x_{cn}\tilde{I}_c + x_{nn}\tilde{I}_n \quad (2.28d)$$

where the inductive reactance components  $x_{aa}$ ,  $x_{ab}$ , ...,  $x_{an}$ , ... are computed in the usual way.

It should be noted that in the case of a balanced set of three-phase currents, the sum of the currents will be zero, and therefore,  $I_n = 0$ . In this case the equations reduce to those of the three-phase line without neutral. The neutral, therefore, does not affect the performance of the line (as far as inductive phenomena are concerned) during balanced operation.

#### 2.6.4 Induced Voltage on Communication Lines

Often, communication lines are suspended on the same towers as power lines. As an example, Fig. 2.10 illustrates a 115-kV transmission line and a communication line suspended on the same pole. A typical example is the wire pilot used for communication between two protective relays at the ends of a power line. Another typical example is a two-wire telephone line suspended on distribution poles. During normal operating conditions of the power line, voltage is induced on the communication line, which in most cases, is negligibly

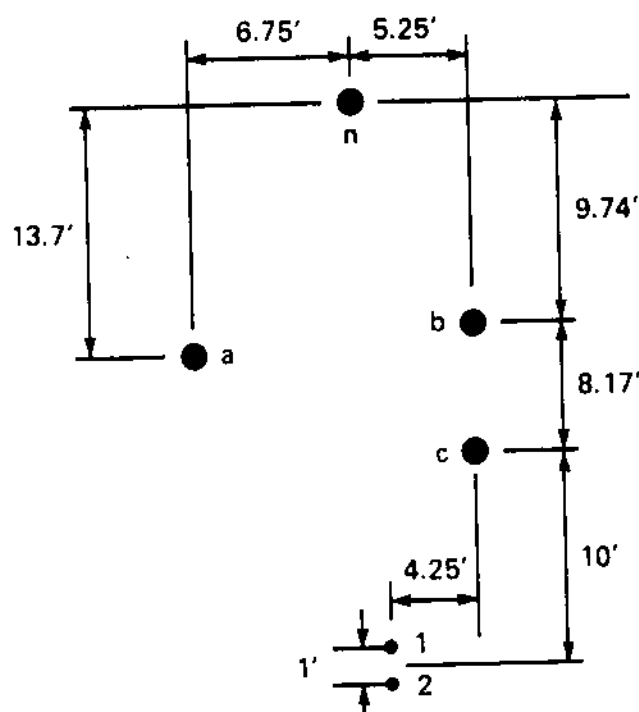


FIG. 2.10 A communication line suspended under a three-phase power line.

small. During fault conditions, however, the induced voltage on the communication line may assume substantial values. For the purpose of protecting the communication line, it is necessary to compute the maximum possible induced voltage on the communication line. A related analysis problem is the following. It is possible that substantial levels of harmonic currents flow in the phase conductors of the transmission line (due to end-use equipment that generates harmonics). These currents may induce low-level voltages on the communication line which manifest themselves as interference. Transposition of the communication line or use of twisted pairs may mitigate interference.

For the purpose of analytically evaluating protection needs or the level of interference, it is necessary to compute the induced voltage along a communication line. The basic tool for this analysis is Eq. (2.23). Consider, for example, the line of Fig. 2.10. Assume that the power line carries electric currents  $\tilde{I}_a$ ,  $\tilde{I}_b$ ,  $\tilde{I}_c$ , and  $\tilde{I}_n$  through the phase conductors a, b, c and the neutral conductor n, respectively. The induced voltage  $V_{cl}$  per unit length of the communication line is

$$\tilde{V}_{cl} = \tilde{V}_1 - \tilde{V}_2 \quad (2.29)$$

where  $\tilde{V}_1$  is the induced voltage on wire 1 per unit length, and  $\tilde{V}_2$  is the induced voltage on wire 2 per unit length.  $\tilde{V}_1$  and  $\tilde{V}_2$  are computed from

$$\begin{aligned}\tilde{V}_1 &= -x_{1a}\tilde{I}_a - x_{1b}\tilde{I}_b - x_{1c}\tilde{I}_c - x_{1n}\tilde{I}_n \\ \tilde{V}_2 &= -x_{2a}\tilde{I}_a - x_{2b}\tilde{I}_b - x_{2c}\tilde{I}_c - x_{2n}\tilde{I}_n\end{aligned}$$

In the computations above, the electric current of the communication line itself is neglected since it is much smaller than the electric currents of the power line.

## 2.7 TRANSPOSITION

A three-phase transmission line is seldom symmetric. Specifically, the inductive reactance components  $x_{ab}$ ,  $x_{ac}$ , and  $x_{cb}$  may all have different arithmetic values. In this case the induced voltages on the various conductors (phases) of the line will be of different numerical value even if balanced three-phase currents are flowing through the line. Thus the balanced operation of the line is disturbed, a rather bothersome condition. In order to achieve balanced three-phase induced voltages when balanced three-phase currents flow through the line, three-phase transmission lines are transposed. Transposition of the three-phase transmission lines is illustrated symbolically in Fig. 2.11. Note that in the second section, conductor a takes the

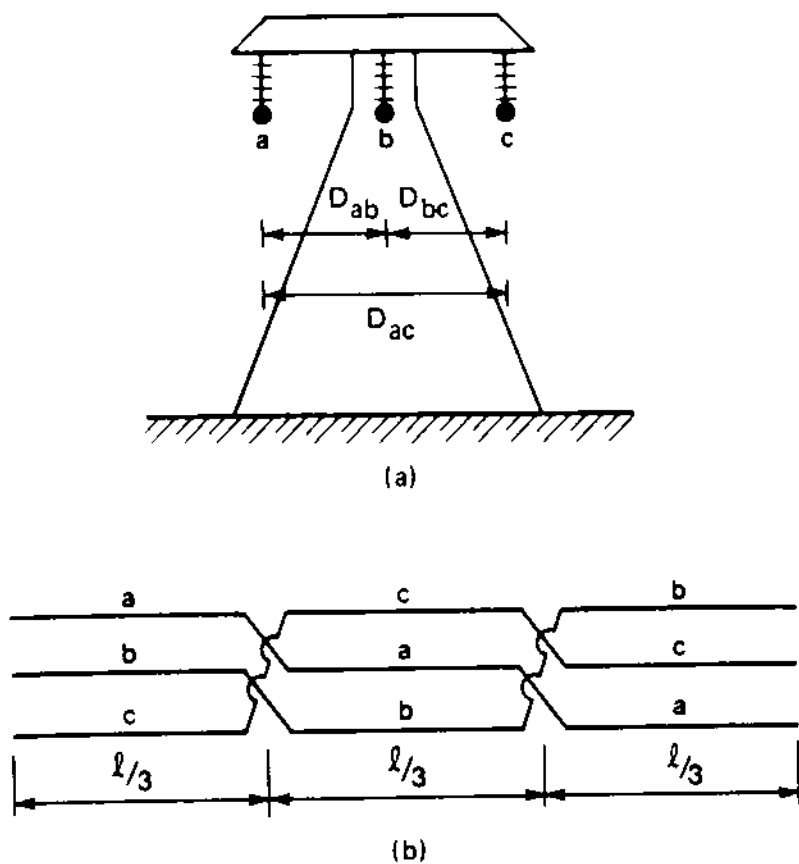


FIG. 2.11 A three-phase line transposition. (a) line configuration of first section, (b) schematic of transposition.

place of conductor b, conductor b takes the place of conductor c, and conductor c takes the place of conductor a. Similarly, the conductor location is rotated in the third section. If the three sections are all of equal length, as illustrated in Fig. 2.11b, the induced voltage on a specific phase is proportional to the electric current through the same phase assuming that  $\bar{I}_a + \bar{I}_b + \bar{I}_c = 0$ . For the purpose of proving this claim, consider a three-phase line with phase conductors of geometric mean radius  $d$  and the separation distances among the phase conductors in the first one-third length of the line equal to  $D_{ab}$ ,  $D_{ac}$ , and  $D_{bc}$ . The induced voltage on the phase a of the line will be  $\tilde{V}_a$ :

$$\tilde{V}_a = \tilde{V}_{a1} + \tilde{V}_{a2} + \tilde{V}_{a3} \quad (2.30)$$

where  $\tilde{V}_{a1}$  is the induced voltage on phase a of the first section of the line,  $\tilde{V}_{a2}$  is the induced voltage on phase a of the second section, and  $\tilde{V}_{a3}$  is the induced voltage on phase a of the third section. The induced voltages  $\tilde{V}_{a1}$ ,  $\tilde{V}_{a2}$ , and  $\tilde{V}_{a3}$  are

$$\tilde{V}_{a1} = \frac{(x_{aa}\tilde{I}_a - x_{ab1}\tilde{I}_b - x_{ac1}\tilde{I}_c)\ell}{3}$$

$$\tilde{V}_{a2} = \frac{(x_{aa}\tilde{I}_a - x_{ab2}\tilde{I}_b - x_{ac2}\tilde{I}_c)\ell}{3}$$

$$\tilde{V}_{a3} = \frac{(x_{aa}\tilde{I}_a - x_{ab3}\tilde{I}_b - x_{ac3}\tilde{I}_c)\ell}{3}$$

In the equations above,  $x_{kmi}$ ,  $k = a, b, c$  and  $m = a, b, c$  are the inductive reactance components of section  $i$  of the transposed line. Upon consideration of the transposed line (see Fig. 2.11a), it is concluded that

$$x_{bc3} = x_{ac2} = x_{ab1} = j \frac{\omega\mu}{2\pi} \ln D_{ab}$$

$$x_{ab3} = x_{bc2} = x_{ac1} = j \frac{\omega\mu}{2\pi} \ln D_{ac}$$

$$x_{ac3} = x_{ab2} = x_{bc1} = j \frac{\omega\mu}{2\pi} \ln D_{bc}$$

Substitution in Eq. (2.30) of the expressions above yields

$$\tilde{V}_a = \frac{[3x_{aa}\tilde{I}_a - (x_{ab1} + x_{ac1} + x_{bc1})(\tilde{I}_b + \tilde{I}_c)]\ell}{3}$$

Since the sum of all currents equals zero,

$$\tilde{I}_b + \tilde{I}_c = -\tilde{I}_a$$

Substitution yields

$$\tilde{V}_a = \left[ x_{aa} + \frac{1}{3} (x_{ab1} + x_{ac1} + x_{bc1}) \right] \tilde{I}_a \ell$$

Note that the induced voltage on phase  $a$  of a transposed line is proportional to the electric current through phase  $a$ . It is expedient to define the quantity  $x_1$  with

$$x_1 = \left[ x_{aa} + \frac{1}{3} (x_{ab} + x_{ac} + x_{bc}) \right] = j0.00466f \log \frac{D_m}{d} \quad (2.31)$$

where  $D_m = (D_{ab}D_{ac}D_{bc})^{1/3}$  and  $d$  is the GMR of phase  $a$ . In terms of the quantity  $x_1$ , the induced voltage on phase  $a$  is given by the simple expression

$$\tilde{V}_a = x_1 \tilde{I}_a \ell \quad (2.32a)$$

A similar expression is obtained for phases b and c:

$$\tilde{V}_b = x_1 \tilde{I}_b l \quad (2.32b)$$

$$\tilde{V}_c = x_1 \tilde{I}_c l \quad (2.32c)$$

A comparison of Eqs. (2.27) and (2.31) reveals that a transposed unsymmetrical three-phase line behaves as a symmetric three-phase transmission line. The equivalent separation distance between any two phases equals the geometric mean of the three separations  $D_{ab}$ ,  $D_{ac}$ ,  $D_{bc}$ :

$$D_m = (D_{ab} D_{ac} D_{bc})^{1/3}$$

Transposition of transmission lines is desirable to ensure balanced operation during normal operating conditions. However, the additional cost of transposition limits the practicality of transposition, especially for extra-high-voltage lines and above.

## 2.8 METHOD OF GEOMETRIC MEAN DISTANCES

The method of geometric mean distances is a simplification and algorithmization of the theory developed so far. It permits fast and accurate computation of the inductive reactance of a line consisting of complicated conductor structures. The basic concept will be illustrated with a two-conductor transmission line as shown in Fig. 2.12. Each conductor comprises a group of wires. Each group carries total electric currents  $\tilde{I}$  and  $-\tilde{I}$ , respectively. Group a consists of n identical subconductors and group b consists of m identical subconductors.

The described general configuration and conditions is encountered in overhead transmission lines with bundled conductors. Typical bundle conductors comprise two to five subconductors arranged in such a way that the separation distance between any two is several inches. The advantages of bundled conductors are discussed in the next section.



FIG. 2.12 A single-phase transmission line with bundle conductors.

The induced voltage on each subconductor  $a_1, a_2, \dots$ , and so on, is computed with the general formula (2.23):

$$\begin{aligned}\tilde{V}_{a_1} &= \left( x_{a_1 a_1} \tilde{I}_{a_1} - \sum_{i=2}^n x_{a_1 a_i} \tilde{I}_{a_i} - \sum_{j=1}^m x_{a_1 b_j} \tilde{I}_{b_j} \right) \\ \tilde{V}_{a_2} &= \left( x_{a_2 a_2} \tilde{I}_{a_2} - \sum_{\substack{i=1 \\ i \neq 2}}^n x_{a_2 a_i} \tilde{I}_{a_i} - \sum_{j=1}^m x_{a_2 b_j} \tilde{I}_{b_j} \right) \\ &\vdots \\ &\vdots \\ \tilde{V}_{a_n} &= \left( x_{a_n a_n} \tilde{I}_{a_n} - \sum_{i=1}^{n-1} x_{a_n a_i} \tilde{I}_{a_i} - \sum_{j=1}^m x_{a_n b_j} \tilde{I}_{b_j} \right)\end{aligned}$$

Now observe that the subconductors of group  $a$  are all connected in parallel and thus the voltage across each subconductor should be the same. Consideration of the equations above regarding the induced voltage across subconductors reveals that, in general, the induced voltages on the subconductors are not equal. In reality, what happens is that the electric current will distribute in such a way among the subconductors as to result in equal induced voltage along each subconductor. The analysis of this phenomenon is rather complex. Fortunately, however, in most practical applications, the electric current distributes approximately equally among the subconductors. For this reason it is assumed that the electric current through the subconductors of the same group is the same:

$$\tilde{I}_{ai} = \frac{\tilde{I}}{n}$$

and

$$\tilde{I}_{bj} = -\frac{\tilde{I}}{m}$$

Then the induced voltage along the conductor is computed as the average of the induced voltages on the subconductors, that is,

$$\tilde{V}_a = \frac{1}{n} (\tilde{V}_{a1} + \tilde{V}_{a2} + \dots + \tilde{V}_{an}) \quad (2.33)$$

Recall the defining equations for the inductive components:

$$x_{a_i a_i} = j0.00466f \log \frac{1}{d_{a_i}}$$

$$x_{a_i a_j} = j0.00466f \log D_{a_i a_j} \quad i \neq j$$

$$x_{a_i b_j} = j0.00466f \log D_{a_i b_j}$$

Upon substitution of the expressions above in Eq. (2.33), and subsequent manipulations,

$$\tilde{V}_a = j0.00466f \log \frac{D_{ab}}{D_a} \tilde{I} \quad (2.34)$$

where

$$D_{ab} = \left( \prod_{\substack{i=1, n \\ j=1, m}} D_{a_i b_j} \right)^{1/nm} \quad (2.35)$$

$$D_a = \left( \prod_{\substack{i=1, n \\ j=1, n}} D_{a_i a_j} \right)^{1/n^2} \quad (2.36)$$

and

$$D_{a_i a_i} = d_{a_i}$$

Comparison of Eq. (2.34) with the Eq. (2.24a) reveals that the present transmission line behaves as a single-phase line with separation distance between conductors equal to  $D_{ab}$  and geometric mean radius of conductor a equal to  $D_a$ . The quantity  $D_{ab}$ , which is a geometric average of the distance between any subconductor in group a and any subconductor in group b, is called the geometric mean distance (GMD) between groups a and b. Similarly, the quantity  $D_a$  is called the geometric mean radius (GMR) of group a.

The induced voltage along conductor b is computed with a similar procedure. The result is

$$\tilde{V}_b = j0.00466f \log \frac{D_{ab}}{D_b} \tilde{I} \quad (2.37)$$

where

$$D_b = \left( \prod_{\substack{i=1, m \\ j=1, m}} D_{b_i b_j} \right)^{1/m^2} \quad (2.38)$$

and

$$D_{b_i b_i} = d_{b_i}$$

Obviously,  $D_b$  shall be called the geometric mean radius (GMR) of group  $b$ .

The preceding analysis suggests that the examined transmission line with  $n + m$  subconductors is equivalent (for the purpose of computing the induced voltage along conductors) to a two-conductor single-phase line with geometric mean radii  $D_a$ ,  $D_b$  and separation distance  $D_{ab}$ . Alternatively, any group of subconductors forming one conductor (one phase of a transmission line) can be replaced with an equivalent conductor with a geometric mean radius given by Eq. (2.36). This procedure is known as the method of geometric mean distances. Applications are discussed next.

## 2.9 APPLICATIONS OF THE METHOD OF GEOMETRIC MEAN DISTANCES

In this section we present two typical applications of the method of geometric mean distances. Specifically, the analysis of a double-circuit three-phase line and the effects of conductor bundling are examined.

### 2.9.1 Double-Circuit Three-Phase Transmission Line

A double-circuit three-phase line is illustrated in Fig. 2.13. It comprises six phase conductors and two shield wires. Typically, the six conductors are paired into three groups to form a three-phase line. Specifically, with reference to Fig. 2.13, conductors  $a'$  and  $a''$  are connected at the ends of the line. Similarly, conductors  $b'$  and  $b''$ , and conductors  $c'$  and  $c''$  are connected together at the ends of the line. In this way, phase  $a$  of this line comprises two subconductors  $a'$  and  $a''$ , phase  $b$  comprises two subconductors  $b'$  and  $b''$ , and so on. In a double-circuit line the subconductors are placed symmetrically in such a way that the phase current is approximately equally distributed among the subconductors of the phases. Under these conditions, the two subconductors of a phase can be replaced

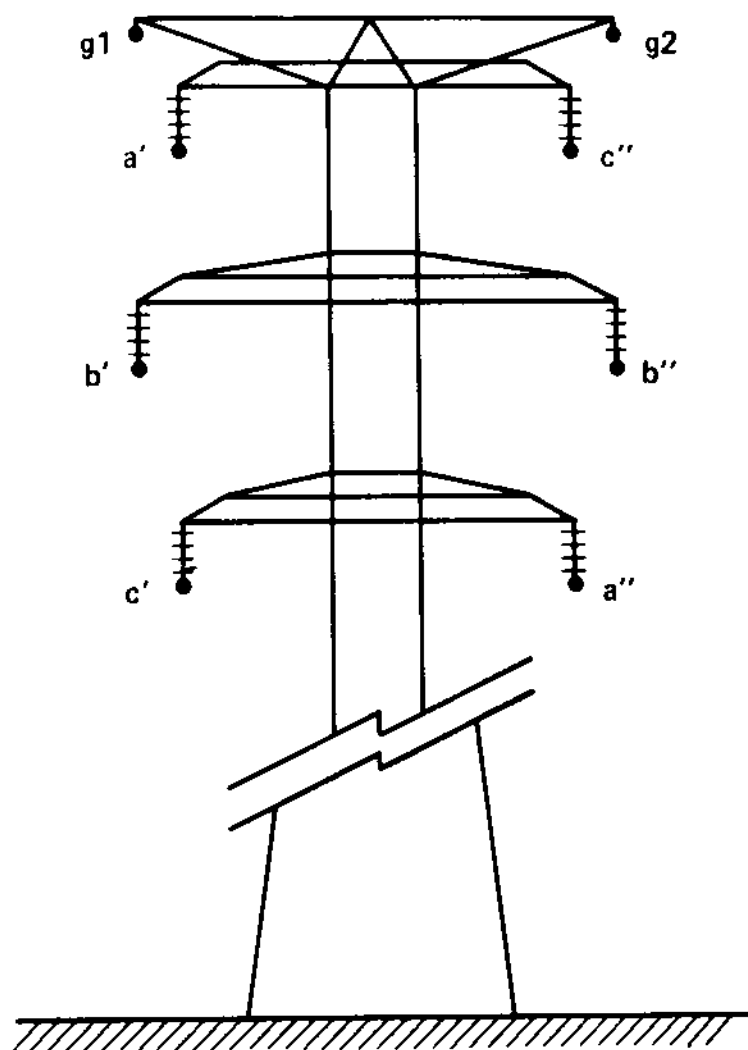


FIG. 2.13 A double-circuit three-phase transmission line.

with one equivalent conductor of a certain geometric mean radius and geometric mean distance from the other phases. Specifically,

$$d_a = (dD_{a'a''})^{1/2}$$

$$d_b = (dD_{b'b''})^{1/2}$$

$$d_c = (dD_{c'c''})^{1/2}$$

$$D_{ab} = (D_{a'b'} D_{a'b''} D_{a''b'} D_{a''b''})^{1/4}$$

$$D_{ac} = (D_{a'c'} D_{a'c''} D_{a''c'} D_{a''c''})^{1/4}$$

$$D_{bc} = (D_{b'c'} D_{b'c''} D_{b''c'} D_{b''c''})^{1/4}$$

where  $d$  is the geometric mean radius of the subconductors and,  $D_{ki}$  is the geometric mean distance between phases  $k$  and  $i$ .

The following example illustrates the application of the method of geometric mean distances on a double-circuit line.

Example 2.3: A double-circuit three-phase transmission line comprises six copper 300-kcm (kilocircular mils) 19-strand subconductors. The subconductors are arranged as in Fig. 2.13. Separation distances are as follows:

$$D_{a'a''} = D_{c'c''} = 34.058 \text{ ft}$$

$$D_{b'b''} = 28.0 \text{ ft}$$

$$D_{a'b''} = D_{b'a''} = D_{b'c''} = C_{c'b''} = 28.178 \text{ ft}$$

$$D_{a'b'} = D_{b'c'} = D_{a''b''} = D_{b''c''} = 13.34 \text{ ft}$$

$$D_{a'c'} = D_{a''c''} = 26.0 \text{ ft}$$

$$D_{a'c''} = D_{a''c'} = 22.0 \text{ ft}$$

Compute the induced voltages per mile in each phase. Assume that the line carries a balanced set of three-phase currents of magnitude 300 A and frequency 60 Hz.

Solution: First, the geometric mean distances are computed as follows:

$$d = 0.01987 \text{ ft}$$

$$d_a = d_c = (d D_{a'a''})^{1/2} = [(0.01987)(34.058)]^{1/2} = 0.8226 \text{ ft}$$

$$d_b = (d D_{b'b''})^{1/2} = [(0.01987)(28)]^{1/2} = 0.74589 \text{ ft}$$

$$D_{ab} = D_{bc} = (D_{a'b'} D_{a'b''})^{1/2} = 19.389 \text{ ft}$$

$$D_{ac} = (D_{a'c'} D_{a''c''})^{1/2} = 23.9165 \text{ ft}$$

Then

$$x_{aa} = x_{cc} = j0.00466f \log \frac{1}{D_{sa}} = j0.0237 \Omega/\text{mi}$$

$$x_{bb} = j0.00466f \log \frac{1}{D_{sb}} = j0.0356 \Omega/\text{mi}$$

and

$$x_{ab} = x_{ba} = x_{bc} = x_{cb} = j0.00466f \log D_{ab} = j0.36 \Omega/\text{mi}$$

$$x_{ca} = x_{ac} = j0.00466f \log D_{ac} = j0.3855 \Omega/\text{mi}$$

The three-phase balanced currents are

$$\tilde{I}_a = 300 \text{ A}$$

$$\tilde{I}_b = 300e^{-j120^\circ} \text{ A}$$

$$\tilde{I}_c = 300e^{-j240^\circ} \text{ A}$$

The induced voltages are

$$\tilde{V}_a = x_{aa}\tilde{I}_{aa} - x_{ab}\tilde{I}_b - x_{ac}\tilde{I}_c = 119.12e^{j86.81^\circ} \text{ V/mi}$$

$$\tilde{V}_b = -x_{ab}\tilde{I}_a + x_{bb}\tilde{I}_b - x_{bc}\tilde{I}_c = 118.68e^{-j30^\circ} \text{ V/mi}$$

$$\tilde{V}_c = -x_{ac}\tilde{I}_a - x_{bc}\tilde{I}_b + x_{cc}\tilde{I}_c = 119.12e^{-j146.81^\circ} \text{ V/mi}$$

Note that even if the currents are balanced, the induced voltages are unbalanced. ■

### 2.9.2 Effect of Bundle Conductors on Line Inductive Reactance

Bundle conductors are used on extra-high-voltage transmission lines for two reasons: (a) to reduce the inductive reactance of the line, and (b) to reduce corona phenomena (corona losses, radio and TV interference). In this section we examine the effects of conductor bundling on the inductive reactance of the line. A bundle conductor consists of a number of identical subconductors arranged in a symmetric configuration. Without substantial loss of accuracy, it can be assumed that the electric current of a phase conductor is equally distributed among the subconductors. In this case a bundle conductor can be replaced with an equivalent conductor of certain geometric mean radius and geometric mean distance from the other conductor by a direct application of the method of geometric mean distances. The procedure is straightforward and has been demonstrated in Section 2.9.1. Here we shall be concerned with the effects of bundling on the line inductance. These effects are illustrated by the following example.

Example 2.4: Consider a three-phase line with three bundle conductors which are horizontally arranged as in Fig. E2.2. Assume that each phase conductor consists of two identical subconductors of 1 in. diameter and spaced  $D_1$  feet apart horizontally. The horizontal separation between the centers of the bundles is 40 ft, as illustrated in Fig. E2.2. Assume that the transmission line is symmetrically transposed.

- (a) Calculate and plot the inductive reactance,  $x_1$ , as a function of  $D_1$ .
- (b) Calculate and plot the diameter of a single conductor as a function of  $D_1$  which is equivalent to the bundle in the sense that it yield the same inductive reactance  $x_1$  for the line.

Solution: (a) The geometric mean distance between the two phases and the geometric mean radius are

$$D_m \approx [(40)(40)(80)]^{1/3} = 50.4 \text{ ft}$$

$$d_s = (dD_1)^{1/2}$$

Assume uniform current distribution in each subconductor:

$$d = \frac{1}{24} e^{-1/4} \text{ ft} = 0.03245 \text{ ft}$$

Then

$$d_s = [(0.03245)D_1]^{1/2} = 0.1801389(D_1)^{1/2} \quad D_1 \text{ in feet}$$

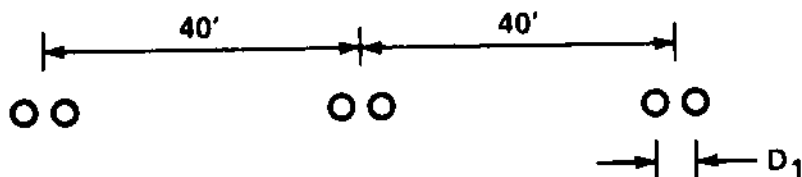


FIG. E2.2 A three-phase line with bundle conductors.

and

$$x_1 = j(0.00466) f \log \frac{D_m}{d_s}$$

or

$$x_1 = j(0.68413 - 0.1398 \log D_1) \quad \text{ohms/mile} \quad D_1 \text{ in feet}$$

Figure E2.3a shows a plot of  $x_1$  versus  $D_1$ . Clearly, the inductive reactance of the line is a decreasing function of the separation distance  $D_1$ .

(b) Consider a three-phase transposed transmission line consisting of solid round conductors spaced 40 ft apart horizontally. For the line above to be equivalent to the one with bundle conductors, in terms of inductive reactance, it is sufficient that each conductor has the same geometric mean radius as the bundle. Assuming that the current distribution inside this conductor is uniform, we have

$$d_s = e^{-1/4} \frac{D}{2} = 0.1801389(D_1)^{1/2}$$

where both  $D$  and  $D_1$  are expressed in feet. Solution for  $D$  yields

$$D = 0.4626(D_1)^{1/2} \quad D, D_1 \text{ in feet}$$

If  $D$ ,  $D_1$  are expressed in inches, the equation above transforms to

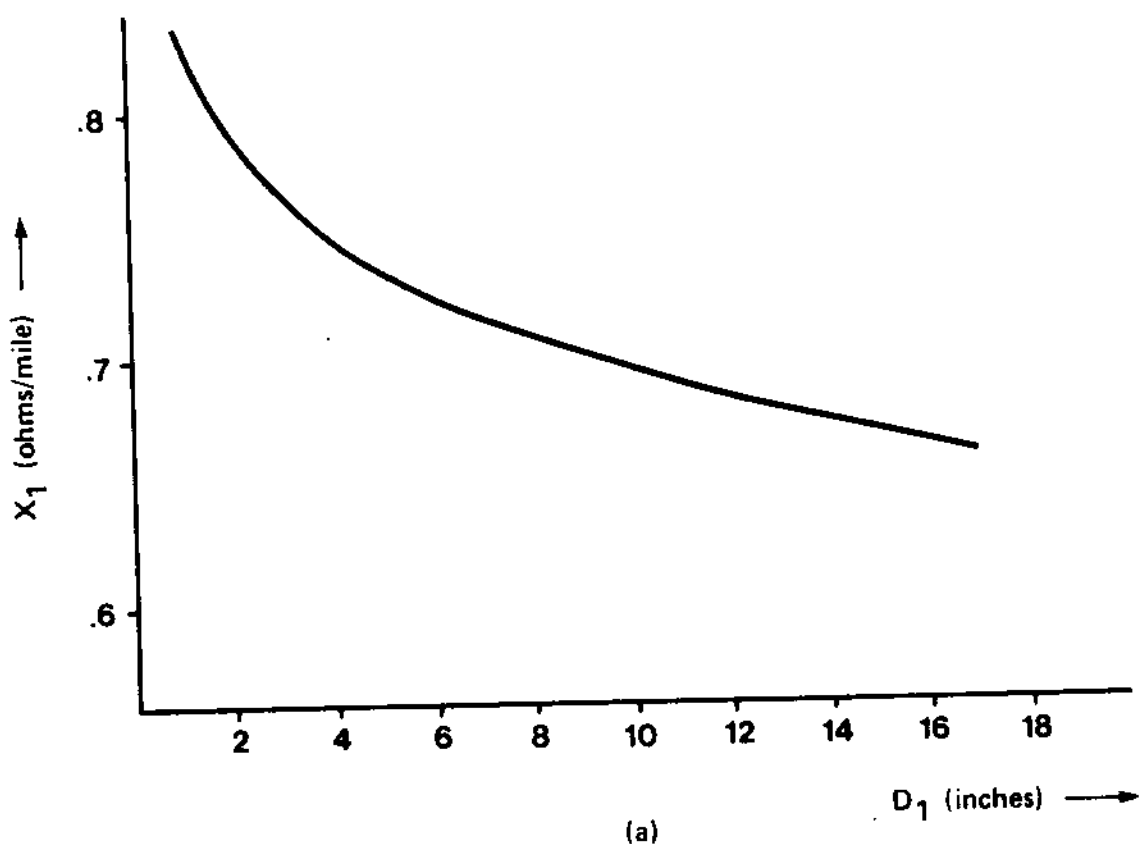
$$D' = 1.60249(D'_1)^{1/2} \quad D', D'_1 \text{ in inches}$$

Figure E2.3b shows a plot of  $D$  versus  $D_1$ .

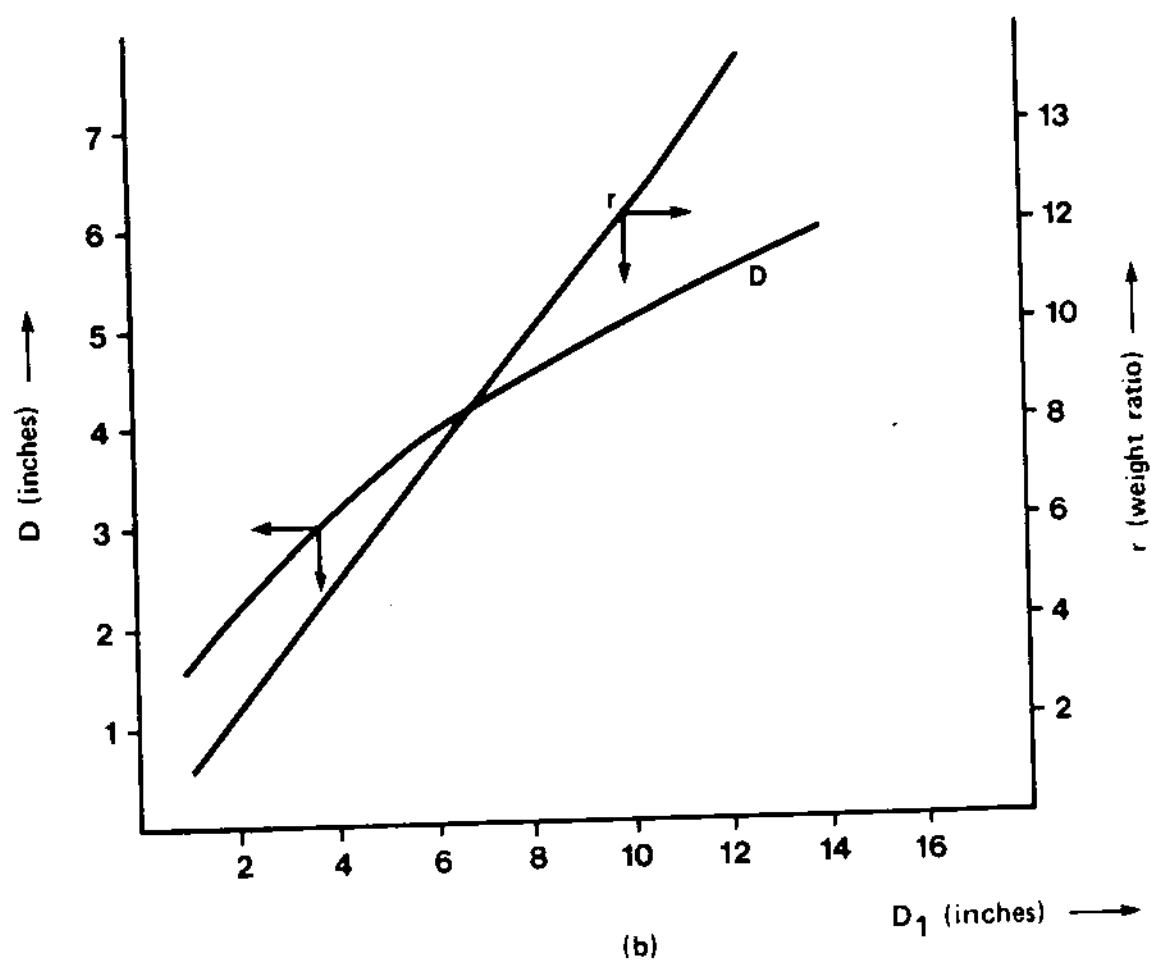
The ratio  $r$  of the weight of the equivalent solid conductor to the weight of the bundle conductor is computed as the ratio of the cross areas of the two conductors:

$$r = \frac{\pi D'^2 / 4}{2\pi(0.5)^2} = 1.284D'_1 \quad D'_1 \text{ in inches}$$

The ratio  $r$  as a function of the separation  $D'_1$  is also illustrated in Fig. E2.3b. Obviously, much more material is needed for a single solid conductor to yield the same inductive reactance as the bundle conductor. ■



(a)



(b)

FIG. E2.3 Inductive reactance and equivalent solid conductor of a bundle conductor transmission line.

## 2.10 INDUCTIVE REACTANCE OF THE EARTH PATH

Overhead or underground power transmission lines are characterized by the fact that earth is one of the paths for the flow of electric current. During normal operating conditions, some electric current is induced and flowing through the conductive earth soil. In general, the magnitude of this current is comparatively low. During abnormal operating conditions (faults), a substantial amount of electric current may flow through earth. This current (earth current) induces a voltage along the transmission line, thus affecting the performance of the power line under these conditions. As a matter of fact, most three-phase overhead transmission circuits are designed in such a way that during ground faults the majority of the fault current flows through the earth.

The distribution of the current in the earth follows a complex, nonuniform pattern. As a result, the computation of the inductive reactance of the earth path and the mutual inductance between the earth path and overhead conductors is very complex. These computations will be described in detail in Chapter 3. In this section a simplified formula will be given which results from the work of Carson [2] and Rudenberg [6]. This simplified formula is valid only for usual soil resistivities (50 to 500  $\Omega \cdot m$ ), for low frequencies such as the power frequency (50 or 60 Hz), and for usual overhead line configurations. Consider the simplest configuration of a single overhead conductor parallel to the surface of the earth and carrying electric current  $\tilde{I}$ . Assume that the conductor is grounded at the remote end. In this case, the current  $\tilde{I}$  returns through the earth. The configuration is illustrated in Fig. 2.14a and b. Carson [2] has given

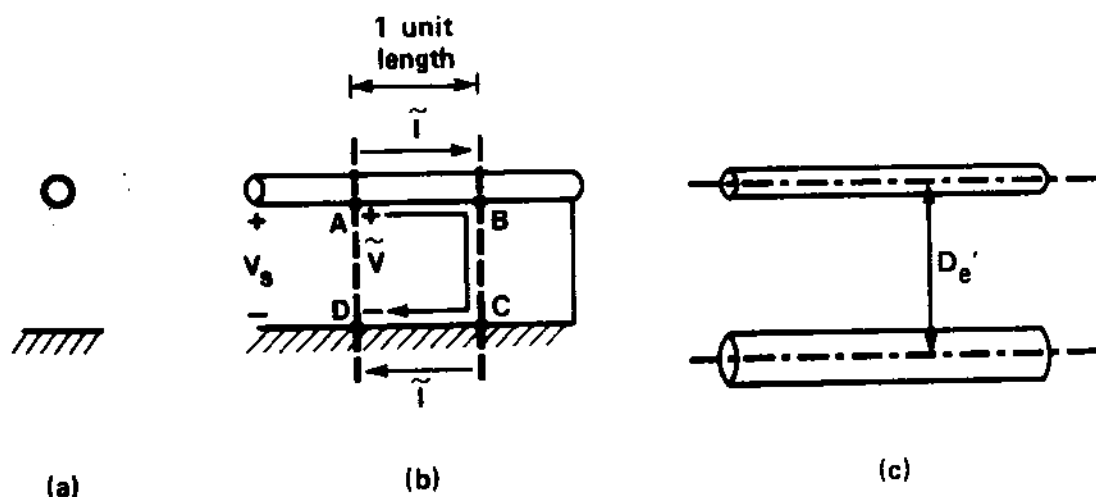


FIG. 2.14 A single conductor above earth. (a) Cross section, (b) longitudinal view, (c) equivalent conductor of the earth path.

a solution to this problem in terms of a complex infinite series. A simplified version of this result states that the induced voltage  $\tilde{V}$  along one unit length of the line as indicated in Fig. 2.14b is given approximately with

$$\tilde{V} = j \frac{\mu\omega}{2\pi} \left( \ln \frac{D_e}{d} \right) \tilde{I} \quad \text{volts/meter}$$

where

- $d$  = geometric mean radius of the overhead conductor
- $\tilde{I}$  = current through the overhead conductor (also through the earth in opposite direction)
- $\omega$  = angular frequency of the electric current
- $D_e$  = equivalent depth of return of earth currents which is approximately equal to  $2160(\rho/f)^{1/2}$  feet
- $\rho$  = soil resistivity, ohm-meters
- $f$  = frequency of the electric current, hertz (i.e.,  $f = \omega/2\pi$ )

Note that physically the induced voltage  $\tilde{V}$  occurs both along the conductor and along the earth. Specifically, the voltage  $\tilde{V}$  equals the induced voltage from point A to point B plus the induced voltage from point C to point D.

This simplified formula permits the representation of the earth path with an equivalent conductor for the representation of the earth path. For this purpose, consider Fig. 2.14c. The earth path has been substituted with a conductor of geometric mean radius  $d_e$ . The separation distance from the overhead conductor is  $D'_e$ . The induced voltage per unit length of this two-conductor configuration is

$$\tilde{V}' = j \frac{\omega\mu}{2\pi} \left( \ln \frac{D'_e}{dd_e} \right) \tilde{I} \quad \text{volts/meter}$$

To establish equivalence between the systems of Fig. 2.14b and c, the induced voltages must be equal. Thus

$$D_e = \frac{D'_e}{d_e}$$

Thus, for equivalence, the parameters  $d_e$  and  $D'_e$  of the equivalent conductor must be selected so as to satisfy the equation above. Note that at least one of the variables  $d_e$  or  $D'_e$  can be arbitrarily selected. It is convenient to select  $d_e = 1$  ft. Then the separation distance is

$$D'_e = \sqrt{D_e} \text{ feet} \quad \text{where } D_e \text{ is expressed in feet}$$

In summary, for the purpose of computing the inductive reactance, the earth path can be substituted with an equivalent conductor of geometric mean radius equal to 1 ft and at a distance of  $D'_e = \sqrt{D_e}$  from the overhead conductor. This result is a simplification valid for the usual soil resistivities (50 to 500  $\Omega \cdot \text{m}$ ), low frequencies (50 or 60 Hz), and usual overhead line configurations. Application of the simplified result above will be illustrated with an example.

Example 2.5: Consider the three-phase electric power line of Fig. E2.4. The phase conductors are ACSR, 556,500 cm, 26 strands. The line does not have an overhead ground wire. The soil resistivity is 75  $\Omega \cdot \text{m}$ . Compute the induced voltage per unit length of phase a assuming that the phase currents are  $\tilde{I}_a = 100 \text{ A}$ ,  $\tilde{I}_b = 20e^{-j100^\circ} \text{ A}$ , and  $\tilde{I}_c = 35e^{-j220^\circ} \text{ A}$ .

Solution: The induced voltage per unit length on phase a, including the effects of the earth current, is

$$\begin{aligned} \tilde{V}_a &= x_{aa}\tilde{I}_a - x_{ab}\tilde{I}_b - x_{ac}\tilde{I}_c - x_{ae}\tilde{I}_e \\ &\quad - (x_{ee}\tilde{I}_e - x_{ea}\tilde{I}_a - x_{eb}\tilde{I}_b - x_{ec}\tilde{I}_c) \end{aligned}$$

where

$$x_{aa} = j \frac{\omega \mu}{2\pi} \ln \frac{1}{d_a}$$

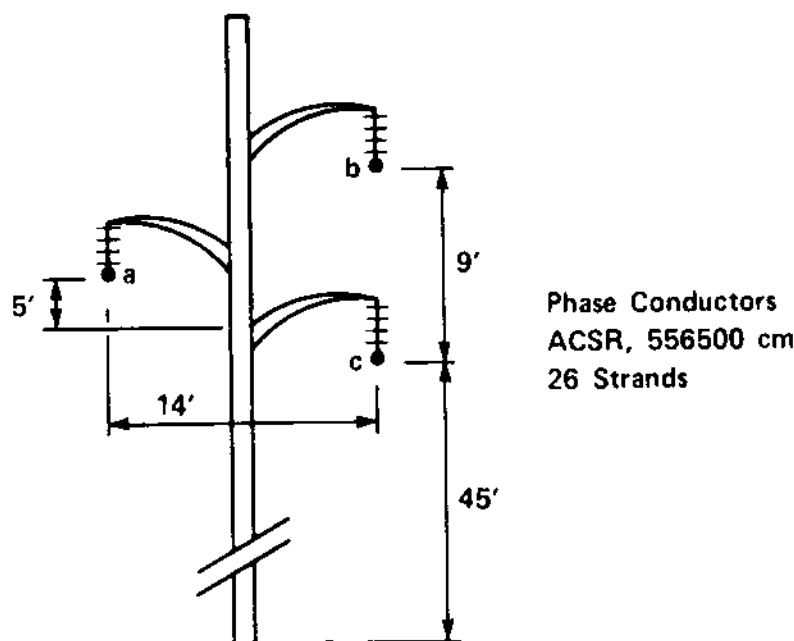


FIG. E2.4

$$x_{ab} = j \frac{\omega \mu}{2\pi} \ln D_{ab}$$

$$x_{ac} = j \frac{\omega \mu}{2\pi} \ln D_{ac}$$

$$x_{ae} = j \frac{\omega \mu}{2\pi} \ln D'_e$$

$$x_{ee} = j \frac{\omega \mu}{2\pi} \ln \frac{1}{d_e}$$

$$x_{ea} = x_{eb} = x_{ea} = j \frac{\omega \mu}{2\pi} \ln D'_e$$

Since there are four paths for the flow of the electric currents (i.e., the three phase conductors and the earth path) it follows that

$$\tilde{I}_a + \tilde{I}_b + \tilde{I}_c + \tilde{I}_e = 0$$

Upon solution of the equation above for the earth current  $\tilde{I}_e$  and substituting in the expression for the induced voltage, we have

$$\tilde{V}_a = x_{aa1} \tilde{I}_a - x_{ab1} \tilde{I}_b - x_{ac1} \tilde{I}_c$$

where

$$x_{aa1} = j \frac{\omega \mu}{2\pi} \ln \frac{D_e}{d} = j0.84852 \times 10^{-3} \Omega/m$$

$$x_{ab1} = j \frac{\omega \mu}{2\pi} \ln \frac{D_{ab}}{D_e} = j0.38538 \times 10^{-3} \Omega/m$$

$$x_{ac1} = j \frac{\omega \mu}{2\pi} \ln \frac{D_{ac}}{D_e} = -j0.38379 \times 10^{-3} \Omega/m$$

$$D_e = 2160(75/60)^{0.5} = 2415 \text{ ft}$$

$$d = 0.0315 \text{ ft}$$

$$D_{ab} = 14.56 \text{ ft}$$

$$D_{ac} = 14.87 \text{ ft}$$

Upon substitution of numerical values, we have

$$\tilde{V}_a = j(84.852 + 7.7076e^{-j100^\circ} + 13.4326e^{-j220^\circ}) \times 10^{-3} \text{ V/m}$$

or

$$\tilde{V}_a = 0.07355e^{j84.58^\circ} \text{ V/m}$$

$$= 118.34e^{j84.58^\circ} \text{ V/mi} *$$

## 2.11 SUMMARY AND DISCUSSION

In this chapter we presented basic techniques for calculation of the inductive reactance of transmission lines. The method of geometric mean distances allows a simple formula to be applied to any transmission line configuration. Any path of electric current, which has cylindrical symmetry, can be characterized with a geometric mean radius and geometric mean distances from any other path. Equation (2.23) is the basic tool for the computation of induced voltages along the conductor of a line.

The geometric mean radius of a conductor depends on the current distribution on the cross section of the path. In this chapter we have assumed that the electric current is uniformly distributed over the cross section of a conductor. In this case a simple formula provides the geometric mean radius. In Chapter 3 we argue that the current distribution inside a conductor is not uniform. It depends on the frequency of the applied currents and the dimensions and electric and magnetic properties of the conductor. In Chapter 3 we discuss methods by which the geometric mean radius can be accurately computed.

The distribution of electric current is especially complex in the cross section of the earth path. An approximate formula has been presented for calculations of induced voltages from earth currents. The formula is applicable at low frequencies and for typical transmission line configurations. More general models for representing the earth path are discussed in Chapter 3.

## 2.12 PROBLEMS

Problem 2.1: Consider two infinitely long, parallel, nonmagnetic, conducting, solid cylinders of 1/2-in. diameter at a distance of 1 ft between centers. Assume that each conductor carries an electric current (dc) of 100 A in opposite directions.

- (a) Plot the variation of the magnetic flux density  $B$  (in webers per square meter) along a line connecting the centers of the conductors and perpendicular to their axes.
- (b) Calculate the inductance of the line in henries per meter.

Problem 2.2: A single-phase line consists of two 2/0, 7-strand copper conductors spaced 3 ft apart. The line is 0.5 mi long.

- Find the 60-Hz inductive reactance of this line.
- If this line carries a 60-Hz current of 300 A rms, what is the induced voltage per mile in volts?
- What is the inductance of this line?

Problem 2.3: Compute the inductive reactance  $x_1$  in ohms per mile of a three-phase transposed transmission line. The phase conductors are bundled conductors consisting of two 300-kcm ACSR 26-strand subconductors. The spacing between subconductors is 10 in. The bundled conductors are vertically arranged, with 12 ft spacing between any two adjacent phases.

Problem 2.4: Consider Fig. P2.1. Which of the three-phase double-circuit transposed transmission lines (a) and (b) consisting of identical phase conductors has the least inductive reactance? Repeat for lines (c) and (d). (Notes: Letters a, b, and c denote the three phases, respectively. Primed letters denote the phases of the first circuit and double-primed letters denote the phases of the second circuit. Assume that subconductors of the same phase carry equal electric current.)

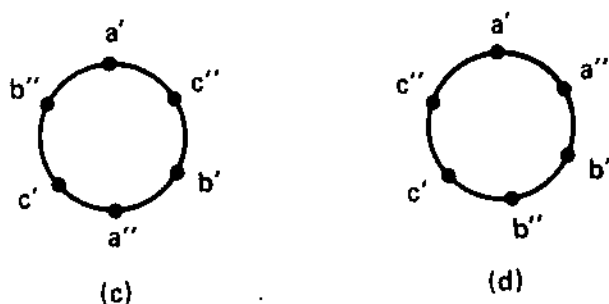
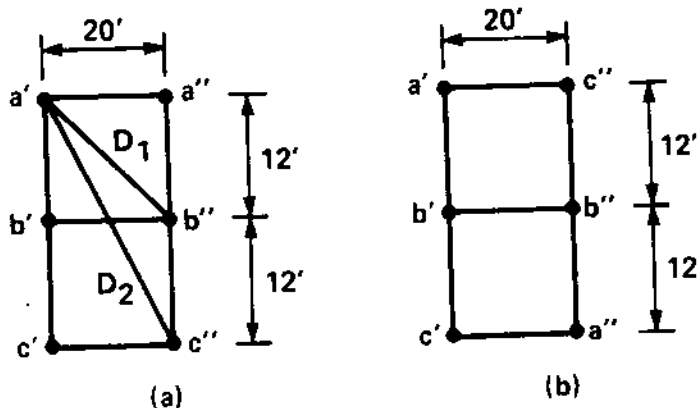


FIG. P2.1

Problem 2.5: Compute the geometric mean radius (GMR) of a hollow conductor of outside diameter  $2a$  and inside diameter  $2b$  as in Fig. P2.2. Assume constant current density inside the conductor.

Problem 2.6: A three-phase power line consisting of 350-kcm 19-strand copper conductors a, b, and c, and a communication line ( $\alpha, \beta$ ) consisting of No. 8 (16,510 cm) copper wires are shown in Fig. P2.3. The two lines parallel each other over a distance of 10 mi in the indicated relative positions. Neither line is transposed, and the power line carries balanced three-phase currents of 500 A, 60 Hz.

- What 60-Hz voltage can be measured on the open end of the communication line if the two conductors ( $\alpha, \beta$ ) are connected at the opposite end?
- What 60-Hz electric current is flowing in the communication line if each of its ends is closed through a  $50\text{-}\Omega$  resistor? What is the 60-Hz voltage across these resistors?
- How does the symmetrical transposition of the power line affect the answers to parts (a) and (b)?
- How does the symmetrical transposition of the communication line affect the answers to parts (a) and (b)?

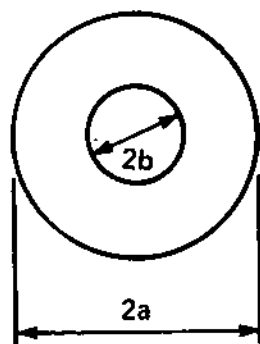


FIG. P2.2

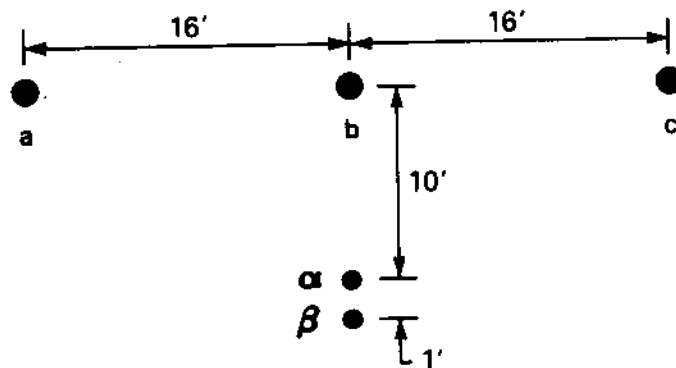


FIG. P2.3 Relative position of the three-phase line and the communication line.

Problem 2.7: Compute the inductive reactance of a coaxial cable with dimensions as in Fig. P2.4. Assume uniform current distribution in both conductors.

Problem 2.8: Figure P2.5 illustrates two 115-kV transmission lines, suspended on the same tower. The phases of the first line are denoted with a, b, c and the phases for the second line with the letters a'', b'', c''. The first line carries a balanced three-phase load of 300 A; that is,  $\tilde{I}_A = 300 \text{ A}$ ,  $\tilde{I}_B = 300e^{-j120^\circ} \text{ A}$ , and  $\tilde{I}_C = 300e^{-j240^\circ} \text{ A}$ . The second line is not energized. Both lines are 15 mi long. All phase conductors are ACSR, 300 kcm, 26 strands. Compute the induced voltage per unit length on phase a''.

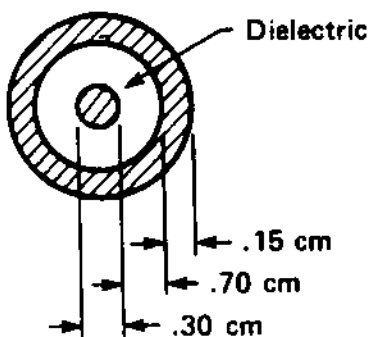


FIG. P2.4

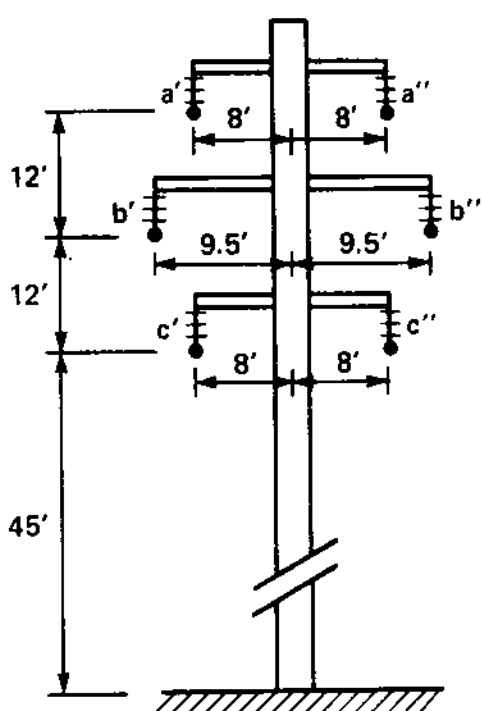


FIG. P2.5

# 3

## Transmission Line Modeling Line Resistance

### 3.1 INTRODUCTION

In this chapter we discuss the phenomena affecting the distribution of electric current inside conductors. These phenomena manifest themselves by altering the resistance and the inductive reactance of conductors. The cause of these phenomena is the interaction between electric currents and the alternating magnetic flux generated by the electric currents. Depending on the geometry of the problem examined, these phenomena are known as skin effect, proximity effect, and eddy currents. A brief description of these phenomena follows.

1. Skin effect: the time-varying magnetic field produced by the flow of ac current inside a conductor results in an uneven distribution of electric current in the cross section of the same conductor. The electric current tends to concentrate near the surface of the conductor ("skin"), away from the center. A pictorial view of the skin effect is given in Fig. 3.1a, where the dot density corresponds to the electric current density.
2. Proximity effect: the time-varying magnetic field produced by the flow of ac current in a conductor results in an uneven electric current distribution in the cross section of a nearby conductor. A pictorial view of the proximity effect is given in Fig. 3.1b, where again the dot density corresponds to the electric current density.
3. Eddy currents: an alternating magnetic field in a conducting medium of arbitrary shape causes the flow of electric currents. These currents are called eddy currents.

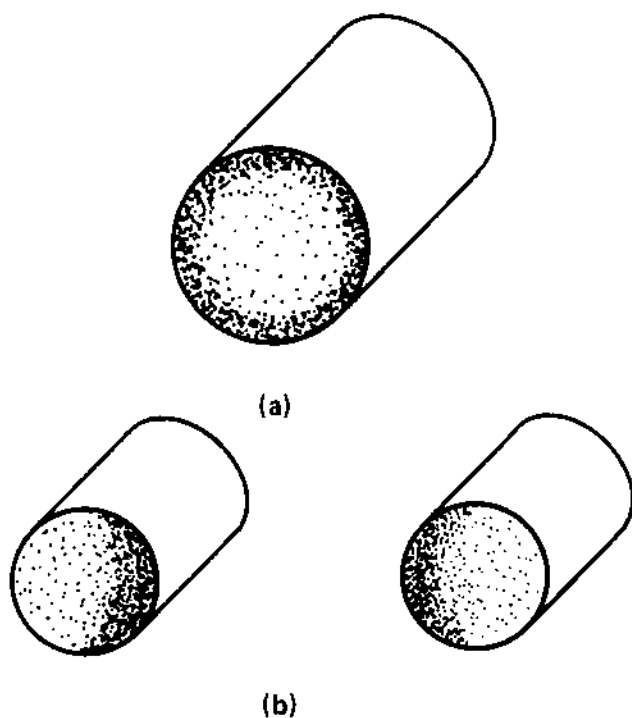


FIG. 3.1 Pictorial illustration of electric current distribution in conductors. (a) Skin effect, (b) proximity effect.

Of the phenomena mentioned, the skin effect is present in every conductor. The intensity of the phenomenon depends on the frequency of the electric current, the properties of the material, and the diameter of the conductor. The proximity effect is not substantial for overhead power transmission lines, due primarily to the relatively large separation distances among conductors. The proximity effect may be substantial in three-phase cables, where the conductors are very close to each other. Eddy currents are important in electro-mechanical devices, transformers, electric motors, and other devices that generate localized alternating magnetic fields in conducting media (magnetic core).

The analysis of these phenomena is complex. Closed-form solutions can be obtained only for relatively few simple cases. Such a case is the analysis of the skin effect in circular conductors. In this chapter we examine the skin effect in circular conductors. The quantitative effects of this phenomenon on the resistance and the inductive reactance of conductors will be discussed. Finally, the distribution of alternating current in earth will be analyzed to determine the effective resistance and reactance of the earth path.

### 3.2 CONDUCTOR RESISTANCE TO THE FLOW OF DC CURRENT

When direct current flows through a homogeneous round cylindrical conductor, the electric current is uniformly distributed inside the conductor. Assuming that the cross section of the conductor is  $A$  (squared meters) and the resistivity of the conductor material is  $\rho$  (ohm · meters), the resistance of the conductor is

$$r_{dc} = \rho \frac{1}{\pi a^2} \quad \text{ohms/meter} \quad (3.1)$$

Power conductors are made exclusively from copper or aluminum. The resistivity of power conductor materials is regulated by international and national standards. Typical values are as follows:

Copper at 20°C:	$\rho = 1.75 \times 10^{-8} \Omega \cdot m$
International annealed copper at 20°C:	$\rho = 1.7241 \times 10^{-8} \Omega \cdot m$
Other materials:	
Hard aluminum (ASA-C11) at 20°C:	$\rho = 2.828 \times 10^{-8} \Omega \cdot m$
Steel at 20°C:	$\rho = (10 \text{ to } 20) \times 10^{-8} \Omega \cdot m$ (depending on carbon content and annealing)

Often, the conductivity of power conductor materials is measured on a relative basis. For this purpose the conductivity of the international annealed copper at 20°C,  $\sigma_{IAC}$ , is taken as the basis. The conductivity of this material is

$$\sigma_{IAC} = \frac{1}{\rho} = 0.58 \times 10^8 \text{ S/m} \quad (3.2)$$

The conductivity  $\sigma$  of any other material is expressed in percent as follows:

$$\sigma(\%) = \frac{\sigma}{\sigma_{IAC}} \times 100 \quad (3.3)$$

For example, the conductivity of hard aluminum (ASA-C11) at 20°C is

$$\sigma(\%) = \frac{(10^8 / 2.828)(100)}{0.58 \times 10^8} = 61\%$$

The resistivity depends strongly on the temperature. For the temperature range at which power conductors operate, the dependence of resistivity on temperature can be expressed by a simple linear function,

$$\rho(t) = \rho(20^\circ\text{C})[1 + \alpha(t - 20)] \quad (3.4)$$

where  $\alpha$  is a constant characterizing the material and is measured in  $(^\circ\text{C})^{-1}$ . Values of  $\alpha$  for the most frequently used materials in power conductors are as follows:

Copper:  $\alpha = 0.0034$  to  $0.004/\text{ }^\circ\text{C}$   
 Aluminum:  $\alpha = 0.0032$  to  $0.0056/\text{ }^\circ\text{C}$

Many power conductors are stranded. In this case the effective dc resistance is slightly higher than the one computed with Eq. (3.1) because of the spiraling of the strands. Specifically, because of spiraling, some of the strands are longer than the actual length of the conductor. Thus for stranded conductors the difference in strand length must be accounted in the computation of the dc resistance.

### 3.3 SKIN EFFECT IN CIRCULAR CONDUCTORS

As has been mentioned, the distribution of alternating current in a conductor is not uniform. The phenomenon is known as the skin effect and affects the resistance and inductance of a conductor. In this section we discuss the skin effect on a circular conductor. Models will be derived for the computation of the resistance and inductance of a conductor under nonuniform current distribution.

#### 3.3.1 Basic Equations

Consider an infinitely long circular conductor. Assume that a sinusoidal electric current of frequency  $f$  is flowing through the conductor. Our objective is to devise a mathematical model for the prediction of the electric current distribution inside the conductor. For this purpose it is assumed that the conductor medium possesses the following properties:

- It is linear (material properties independent of field strength).
- It is isotropic (identical properties in every direction).
- It is homogeneous (material properties independent of position).
- It is nondispersive (material properties independent of time).

The typical power conductor materials (copper, aluminum) possess these properties.

Consider a part of the conductor of length  $\ell$  as in Fig. 3.2. Also consider an attached system of cylindrical coordinates (with the  $z$  axis on the axis of the conductor). The vectors of electric and magnetic field intensity will be parallel to the  $z$  axis and perpendicular to the plane through the conductor axis, respectively. Because of the cylindrical symmetry, the magnetic and electric field intensities,  $H$  and  $E$ , and the current density  $J$  will be independent of the angle  $\phi$  of the mentioned system of cylindrical coordinates. In addition, assuming that the length  $\ell$  of the conductor is much shorter than the wavelength of the applied voltage (i.e.,  $\ell \ll c/f$ ), the quantities  $H$ ,  $E$ , and  $J$  are also independent of  $z$ . Thus, for the case considered,  $H$ ,  $E$ , and  $J$  depend on the radial distance  $r$  from the axis of the conductor and time  $t$  only. In addition, the direction of the electric field intensity, and therefore the current density, is parallel to the  $z$  axis, while the direction of the magnetic field intensity is perpendicular to the radial distance from the conductor axis. Mathematically, these quantities are expressed as

$$\underline{E} = E(r, t) \underline{z} \quad (3.5a)$$

$$\underline{H} = H(r, t) \underline{\phi} \quad (3.5b)$$

$$\underline{J} = J(r, t) \underline{z} \quad (3.5c)$$

where  $\underline{z}$  and  $\underline{\phi}$  are the unit vectors of the cylindrical system of coordinates.

The quantities  $\underline{H}$ ,  $\underline{E}$ , and  $\underline{J}$  must satisfy Maxwell's equations. In cylindrical coordinates and for the defined problem, Maxwell's equations yield [3]

$$\frac{dE(r, t)}{dr} = \frac{dB(r, t)}{dt} \quad (3.6)$$

$$\frac{dH(r, t)}{dr} + \frac{1}{r} H(r, t) = J(r, t) + \frac{dD(r, t)}{dt} \quad (3.7)$$

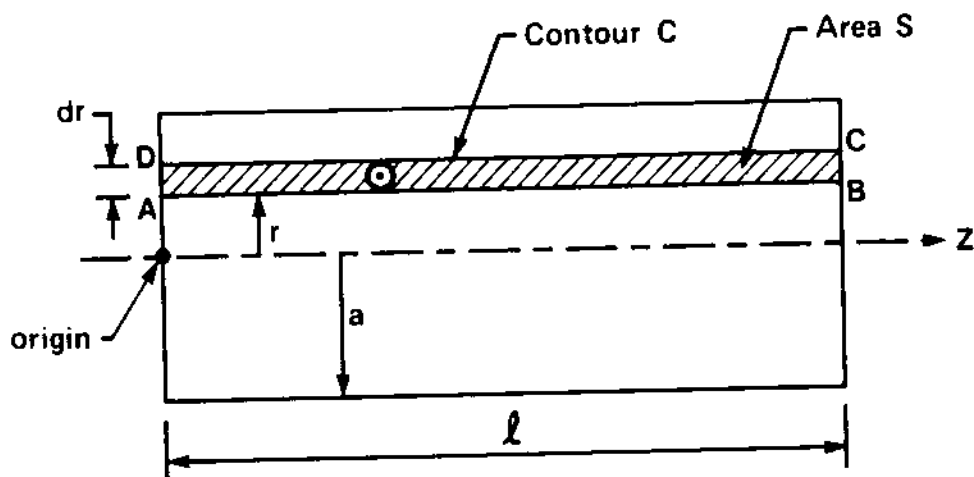


FIG. 3.2 Side view of a cylindrical conductor.

$$\mathbf{B}(\mathbf{r}, t) = \mu \mathbf{H}(\mathbf{r}, t) \quad (3.8a)$$

$$\mathbf{D}(\mathbf{r}, t) = \epsilon \mathbf{E}(\mathbf{r}, t) \quad (3.8b)$$

$$\mathbf{J}(\mathbf{r}, t) = \sigma \mathbf{E}(\mathbf{r}, t) \quad (3.8c)$$

where

$\mu$  = permeability of conductor material

$\epsilon$  = permittivity of conductor material

$\sigma$  = conductivity of conductor material

Equations (3.6), (3.7), and (3.8) result from direct application of Maxwell's equations (differential form) in cylindrical coordinates and assuming that the field quantities depend on  $r$  and  $t$  only, as delineated in Eqs. (3.5).

In order to obtain a better understanding of the physical phenomena involved, Eqs. (3.6) and (3.7) will be derived. Consider Fig. 3.2. An infinitesimal strip, parallel to the axis of the conductor, is illustrated. The strip defines an area  $S$  and a contour  $C$ . The dimensions of the area  $A$  are  $\ell$  by  $dr$ . Application of Faraday's law on the area  $S$  defined by the contour  $C$  yields

$$-\int_C \underline{\mathbf{E}} \cdot d\underline{\ell} = \frac{d}{dt} \int_S \underline{\mathbf{B}} \cdot d\underline{s} \quad (3.9)$$

Equation (3.9) states that the voltage induced along the contour  $C$  equals the time derivative of the magnetic flux crossing the area  $S$ .

The electric and magnetic field intensities in the surface  $S$  are given by Eqs. (3.5). The scalar functions,  $E(r, t)$  and  $H(r, t)$ , are continuous. In this case, the left-hand side of Eq. (3.9) is computed as the sum of the contributions from the sections AB, BC, CD, and DA of contour C:

$$-\int_C \underline{\mathbf{E}}(r, t) \cdot d\underline{\ell} = -\int_{AB} \underline{\mathbf{E}} \cdot d\underline{\ell} - \int_{BC} \underline{\mathbf{E}} \cdot d\underline{\ell} - \int_{CD} \underline{\mathbf{E}} \cdot d\underline{\ell} - \int_{DA} \underline{\mathbf{E}} \cdot d\underline{\ell}$$

Note that

$$\int_{BC} \underline{\mathbf{E}} \cdot d\underline{\ell} = \int_{DA} \underline{\mathbf{E}} \cdot d\underline{\ell} = 0$$

because the electric field intensity  $\underline{\mathbf{E}}$  is perpendicular to the contour  $C$  along the paths BC or DA. Also,

$$\int_{AB} \underline{\mathbf{E}} \cdot d\underline{\ell} = E(r, t) \ell$$

$$\int_{CD} \underline{E} \cdot d\underline{\ell} = -E(r + dr, t) \ell$$

Thus

$$-\int_C \underline{E}(r, t) \cdot d\underline{\ell} = [E(r + dr, t) - E(r, t)] \ell$$

The right-hand side of Eq. (3.9) is computed in a similar way. The vector  $\underline{B}$  is perpendicular to the surface  $S$  and continuous. Thus

$$\int_S \underline{B}(r, t) \cdot d\underline{s} = B(r, t) \ell \ dr$$

Upon substitution of the results above into Eq. (3.9) and division by  $(dr \ell)$ , the following equation is obtained:

$$\frac{E(r + dr, t) - E(r, t)}{dr} = \frac{d}{dt} B(r, t)$$

By definition, the left-hand side of the equation above is the derivative of  $E(r, t)$  with respect to  $r$ . Thus

$$\frac{dE(r, t)}{dr} = \frac{dB(r, t)}{dt}$$

This is exactly Eq. (3.6). The derivation of Eq. (3.7) follows a similar procedure. For this purpose, consider a cross section of the conductor as in Fig. 3.3. Also consider the infinitesimal area  $S$  which is defined by the contour  $C$ . Ampère's law applied to the area  $S$  and contour  $C$  states that

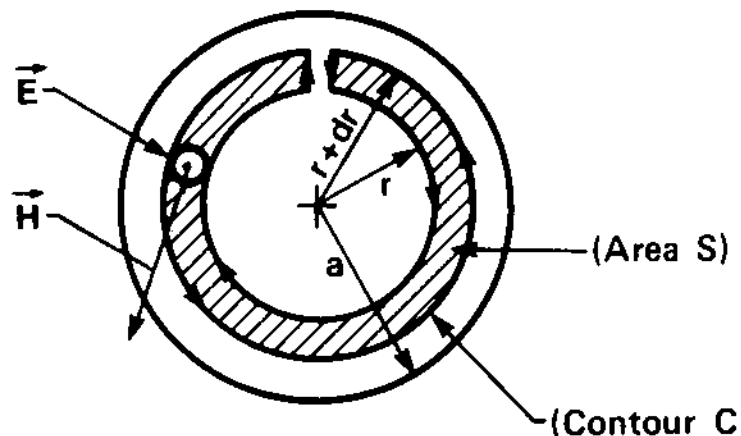


FIG. 3.3 Cross section of a cylindrical conductor.

$$\int_C \underline{H} \cdot d\underline{\ell} = \frac{d}{dt} \int_S \underline{D} \cdot d\underline{s} + \int_S \underline{J} \cdot d\underline{s} \quad (3.10)$$

The components of Eq. (3.10) are computed as follows:

$$\int_C \underline{H} \cdot d\underline{\ell} = 2\pi(r + dr)H(r + dr, t) - 2\pi r H(r, t)$$

$$\frac{d}{dt} \int_S \underline{D} \cdot d\underline{s} = \frac{d}{dt} D(r, t)[\pi(r + dr)^2 - \pi r^2]$$

$$\int_S \underline{J} \cdot d\underline{s} = J(r, t)[\pi(r + dr)^2 - \pi r^2]$$

Upon substitution of the results above into Eq. (3.10) and subsequent division by  $2\pi r dr$ , the following equation is obtained:

$$\frac{H(r + dr, t) - H(r, t)}{dr} + \frac{H(r + dr, t)}{r} = \frac{2r + dr}{2r} J(r, t) \\ + \frac{d}{dr} D(r, t) \frac{2r + dr}{2r}$$

Upon consideration that  $dr$  is an infinitesimal distance, the equation above becomes identical to Eq. (3.7):

$$\frac{dH(r, t)}{dr} + \frac{H(r, t)}{r} = J(r, t) + \frac{dD(r, t)}{dt}$$

In summary, two differential equations [Eqs. (3.6) and (3.7)] relating the magnetic and electric field intensities and the current density have been developed. Together with the constitutive relations [Eqs. (3.8)], they completely define a mathematical model for the study of the skin effect in cylindrical conductors.

It is expedient to transform Eqs. (3.6) and (3.7) in the frequency domain. For this purpose the quantities  $H$ ,  $E$ , and  $J$  are assumed to vary sinusoidally with time, that is,

$$H(r, t) = \sqrt{2} \operatorname{Re}\{\tilde{H}(r) \cdot e^{j\omega t}\} \quad (3.11a)$$

$$E(r, t) = \sqrt{2} \operatorname{Re}\{\tilde{E}(r) \cdot e^{j\omega t}\} \quad (3.11b)$$

$$J(r, t) = \sqrt{2} \operatorname{Re}\{\tilde{J}(r) \cdot e^{j\omega t}\} \quad (3.11c)$$

where  $\omega$  is the circular frequency, and  $\tilde{H}(r)$ ,  $\tilde{E}(r)$ , and  $\tilde{J}(r)$  are complex functions (phasors). Substitution of Eqs. (3.11) into Eqs. (3.6), (3.7), and (3.8) and subsequent elimination of the term  $e^{j\omega t}$  yields

$$\frac{d\tilde{E}(r)}{dr} = j\omega\mu\tilde{H}(r) \quad (3.12)$$

$$\frac{d\tilde{H}(r)}{dr} + \frac{\tilde{H}(r)}{r} = \tilde{J}(r) + j\omega\epsilon\tilde{E}(r) \quad (3.13)$$

$$\tilde{B}(r) = \mu\tilde{H}(r) \quad (3.14a)$$

$$\tilde{D}(r) = \epsilon\tilde{E}(r) \quad (3.14b)$$

$$\tilde{J}(r) = \sigma\tilde{E}(r) \quad (3.14c)$$

Elimination of the magnetic field intensity phasor  $\tilde{H}(r)$  from the equations above yields

$$\frac{1}{j\omega\mu} \frac{d^2\tilde{E}(r)}{dr^2} + \frac{1}{j\omega\mu r} \frac{d\tilde{E}(r)}{dr} = \tilde{J}(r) + j\omega\epsilon\tilde{E}(r)$$

Finally, upon elimination of the electric field intensity phasor  $\tilde{E}(r)$ , with the aid of Eq. (3.14c),

$$\frac{d^2\tilde{J}(r)}{dr^2} + \frac{1}{r} \frac{d\tilde{J}(r)}{dr} - (j\omega\mu\sigma - \omega^2\mu\epsilon)\tilde{J}(r) = 0 \quad (3.15)$$

Equation (3.15) determines the current density in a cross section of a cylindrical conductor when the electric current is sinusoidal of circular frequency  $\omega$ . For power conductors, this differential equation can be further simplified as follows. Observe that the term  $\omega^2\mu\epsilon$  is orders of magnitude smaller than  $\omega\mu\sigma$  even in very high frequencies. For example, for copper conductors at frequency 1 MHz, the term  $\omega^2\mu\epsilon$  is approximately 100,000 times less than the term  $\omega\mu\sigma$ . Thus the term  $\omega^2\mu\epsilon$  may be neglected. Then Eq. (3.15) becomes

$$\frac{d^2\tilde{J}(r)}{dr^2} + \frac{1}{r} \frac{d\tilde{J}(r)}{dr} - jk^2\tilde{J}(r) = 0 \quad 0 < r < a \quad (3.16)$$

where

$$k^2 \triangleq \omega\mu\sigma \quad (3.17)$$

In summary, the electric current density inside a circular conductor is determined by the solution of Eq. (3.16).

### 3.3.2 General Solutions

The general solution of the differential equation (3.16) describing the skin effect in circular conductors is well known. It is given in terms of two functions,  $I_0$  and  $K_0$  [11]:

$$\tilde{J}(r) = \tilde{A}_1 I_0(krj^{0.5}) + \tilde{A}_2 K_0(krj^{0.5}) \quad (3.18)$$

The functions  $I_0$  and  $K_0$  are known as the modified Bessel functions of first and second kind, respectively. The functions  $I_0$  and  $K_0$  represent two independent solutions of the differential equation (3.16). They are defined as follows:

$$I_0(z) = 1 + \frac{(z/2)^2}{(1!)^2} + \frac{(z/2)^4}{(2!)^2} + \frac{(z/2)^6}{(3!)^2} + \dots \quad (3.19a)$$

$$K_0(z) = -(\ln \frac{z}{2} + \gamma) I_0(z) + \left(\frac{z}{2}\right)^2 + \left(1 + \frac{1}{2}\right) \frac{(z/2)^4}{(2!)^2}$$

$$+ \left(1 + \frac{1}{2} + \frac{1}{3}\right) \frac{(z/2)^6}{(3!)^2} + \dots \quad (3.19b)$$

where  $\gamma = 1.7811 \dots$  and  $z$  is any complex number. The derivation of the two independent solutions above for Eq. (3.16) is beyond the scope of this book. The interested reader can consult references 9 and 11 for further study.

The functions  $I_0(krj^{0.5})$  and  $K_0(krj^{0.5})$  assume complex values and in general can be expressed in cartesian or polar coordinates:

Cartesian coordinates

$$I_0(xj^{0.5}) = \text{ber}(x) + j\text{bei}(x)$$

$$K_0(xj^{0.5}) = \text{ker}(x) + j\text{kei}(x)$$

Polar coordinates

$$I_0(xj^{0.5}) = M_0(x)e^{j\theta_0(x)}$$

$$K_0(xj^{0.5}) = N_0(x)e^{j\phi_0(x)}$$

where  $x$  is a real number. The cartesian coordinates of the modified Bessel functions are known as the Kelvin functions.

The functions  $I_0$  and  $K_0$  are entire functions on the complex plane and linearly independent. At  $r = 0$ , the function  $I_0$  is bounded, but the function  $K_0$  assumes unbounded values. Figure 3.4 provides a qualitative description of the functions  $I_0$  and  $K_0$ . Figure 3.5 illustrates the cartesian components  $\text{ber}(x)$ ,  $\text{bei}(x)$ ,  $\text{ker}(x)$ , and  $\text{kei}(x)$  versus the argument  $x$ , while Fig. 3.6 illustrates the polar components

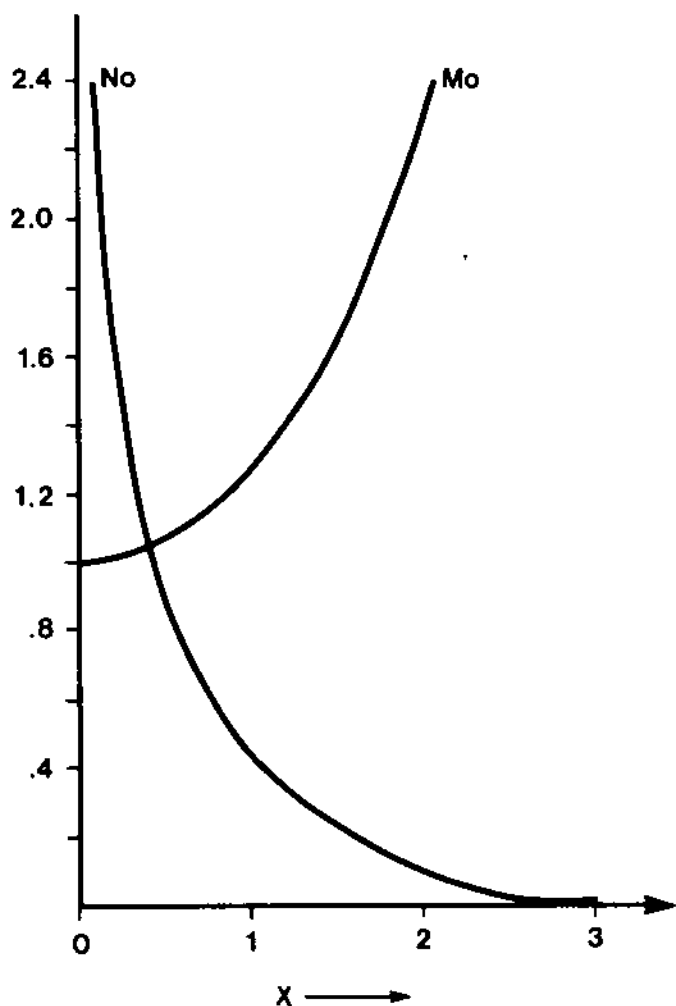


FIG. 3.4 Qualitative variation of the absolute value of the functions  $I_0(xj^{0.5})$  and  $K_0(xj^{0.5})$ .

$M_0(x)$ ,  $\theta_0(x)$ ,  $N_0(x)$ , and  $\phi_0(x)$  (modulus and phase) versus the argument  $x$ . The modulus and phase of the functions  $I_0(xj^{0.5})$  is also tabulated in Table 3.1 for values of the argument  $x$  from 0.0 to 10.0. Figures 3.5 and 3.6 and Table 3.1 can be used for practical computations.

In conclusion, the general solution to the differential equation (3.16) is a linear combination of the modified Bessel functions  $I_0$  and  $K_0$ , as expressed in Eq. (3.18). The solution provides the electric current density inside a cylindrical conductor. The constants  $\tilde{A}_1$  and  $\tilde{A}_2$  depend on specific conditions such as total current through the conductor, and so on. Such specific conditions will be examined next.

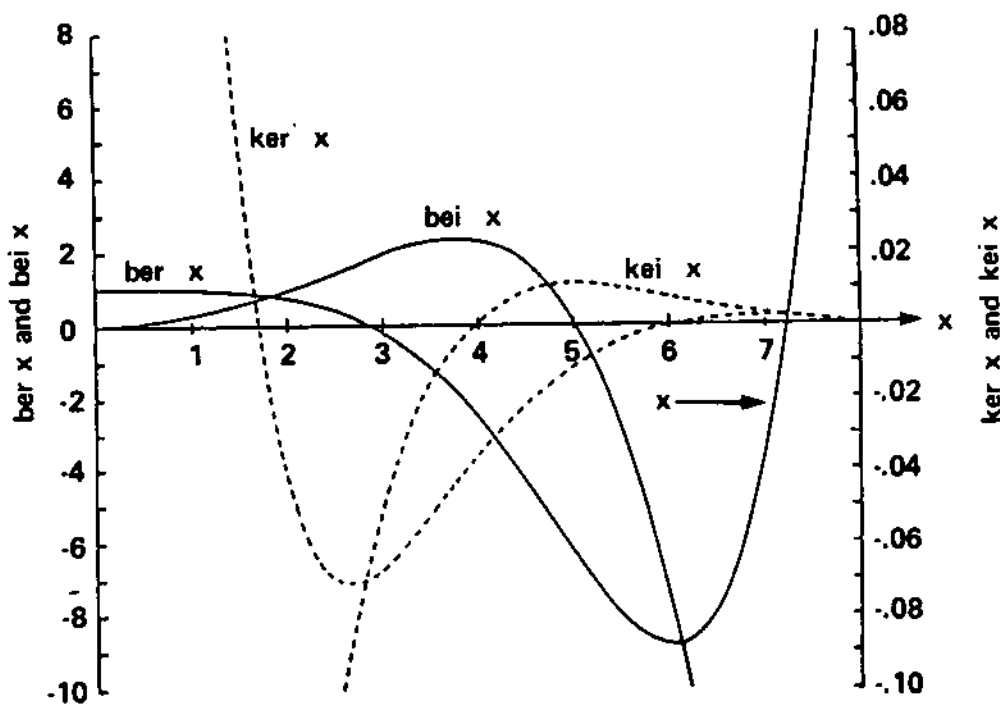


FIG. 3.5 Variation of the cartesian coordinates of the modified Bessel functions in the range  $(0 \leq x \leq 8)$ .

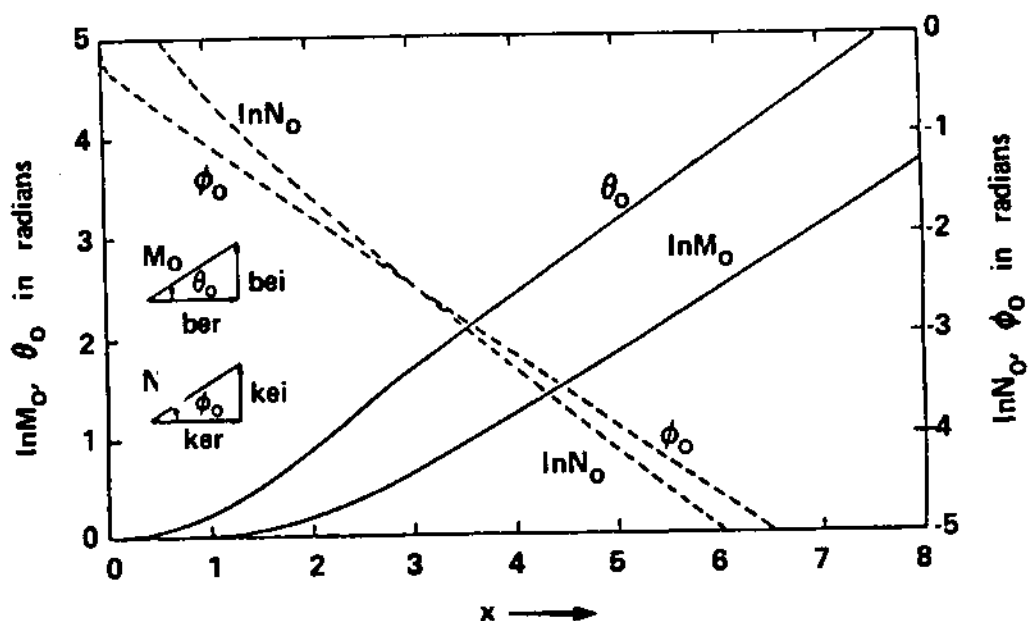


FIG. 3.6 Variation of the polar coordinates of the modified Bessel functions in the range  $(0 \leq x \leq 8)$ .

TABLE 3.1 Modulus and Phase of the Modified Bessel Functions

Z	$M_0(z)$	$\theta_0(z)$	$M_1(z)$	$\theta_1(z)$	Z	$M_0(z)$	$\theta_0(z)$	$M_1(z)$	$\theta_1(z)$
000	1.0000	.000	.0000	135.00	1.30	1.0438	23.75	6548	147.07
025	1.0000	.009	.0125	135.00	1.35	1.0508	25.54	6808	148.02
050	1.0000	.036	.0250	135.02	1.40	1.0586	27.37	7070	148.99
075	1.0000	.081	.0375	135.04	1.45	1.0672	29.26	7333	150.00
100	1.0000	.143	.0500	135.07	1.50	1.0767	31.19	7598	151.04
125	1.0000	.224	.0625	135.11	1.55	1.0871	33.16	7866	152.12
150	1.0000	.322	.0750	135.16	1.60	1.0984	35.17	8136	153.23
175	1.0000	.439	.0875	135.22	1.65	1.1108	37.22	8408	154.38
200	1.0000	.573	.1000	135.29	1.70	1.1242	39.30	8684	155.55
225	1.0000	.725	.1125	135.36	1.75	1.1387	41.41	8962	156.76
250	1.0001	.895	.1250	135.45	1.80	1.1544	43.54	9244	158.00
275	1.0001	1.083	.1375	135.54	1.85	1.1712	45.70	9530	159.27
300	1.0001	1.289	.1500	135.64	1.90	1.1892	47.88	9819	160.57
325	1.0002	1.513	.1625	135.76	1.95	1.2085	50.08	1.0113	161.90
350	1.0002	1.754	.1750	135.88	2.00	1.2290	52.29	1.0412	163.27
375	1.0003	2.014	.1875	136.01	2.05	1.2509	54.51	1.0715	164.66
400	1.0004	2.291	.2000	136.15	2.10	1.2741	56.74	1.1024	166.08
425	1.0005	2.587	.2125	136.29	2.15	1.2986	58.98	1.1339	167.53
450	1.0006	2.900	.2250	136.45	2.20	1.3246	61.22	1.1659	169.00
475	1.0008	3.231	.2375	136.62	2.25	1.3520	63.46	1.1987	170.50
500	1.0010	3.579	.2500	136.79	2.30	1.3808	65.71	1.2321	172.03
525	1.0012	3.946	.2626	136.97	2.35	1.4111	67.95	1.2663	173.58
550	1.0014	4.330	.2751	137.17	2.40	1.4429	70.19	1.3012	175.16
575	1.0017	4.732	.2876	137.37	2.50	1.5111	74.65	1.3736	178.39
600	1.0020	5.152	.3001	137.58	2.60	1.5855	79.09	1.4498	181.70
625	1.0024	5.589	.3126	137.80	2.70	1.6665	83.50	1.5300	185.10
650	1.0028	6.044	.3252	138.03	2.80	1.7541	87.87	1.6148	188.57
675	1.0032	6.517	.3377	138.26	2.90	1.8486	92.21	1.7046	192.11
700	1.0037	7.007	.3502	138.51	3.00	1.9502	96.52	1.7999	195.71
725	1.0043	7.515	.3628	138.76	3.10	2.0592	100.79	1.9011	199.37
750	1.0049	8.040	.3753	139.03	3.20	2.1760	105.03	2.0088	203.08
775	1.0056	8.582	.3879	139.30	3.30	2.3009	109.25	2.1236	206.83
800	1.0064	9.141	.4004	139.58	3.40	2.4342	113.43	2.2458	210.62
825	1.0072	9.718	.4130	139.87	3.50	2.5764	117.60	2.3763	214.44
850	1.0081	10.312	.4256	140.17	3.60	2.7280	121.75	2.5154	218.30
875	1.0091	10.923	.4382	140.48	3.70	2.8894	125.87	2.6640	222.17
900	1.0102	11.550	.4508	140.80	3.80	3.0613	129.99	2.8226	226.07
925	1.0114	12.194	.4634	141.12	3.90	3.2443	134.10	2.9920	229.98
950	1.0127	12.855	.4760	141.46	4.00	3.4391	138.19	3.1729	233.90
975	1.0140	13.533	.4886	141.80	4.50	4.6179	158.59	4.2782	253.67
1.000	1.0155	14.226	.5013	142.16	5.00	6.2312	178.93	5.8091	273.55
1.025	1.0171	14.936	.5140	142.52	5.50	8.4473	199.28	7.9253	293.48
1.050	1.0188	15.662	.5267	142.89	6.00	11.5008	219.63	10.8502	313.45
1.075	1.0207	16.403	.5394	143.27	6.50	15.7170	239.96	14.8961	333.46
1.100	1.0227	17.160	.5521	143.65	7.00	21.5478	260.29	20.5002	353.51
1.125	1.0248	17.933	.5648	144.05	7.50	29.6223	280.61	28.2736	373.59
1.150	1.0270	18.720	.5776	144.46	8.00	40.8175	300.92	39.0696	393.69
1.175	1.0294	19.523	.5904	144.87	8.50	56.3585	321.22	54.0807	413.82
1.200	1.0320	20.340	.6032	145.29	9.00	77.9564	341.52	74.9742	433.96
1.225	1.0347	21.172	.6161	145.73	9.50	108.0038	361.81	104.0822	454.11
1.250	1.0376	22.017	.6290	146.17	10.00	149.8476	382.10	144.6708	474.28

### 3.3.3 Solution for Solid Conductors

The electric current density anywhere in a solid conductor must be finite. In the general solution [Eq. (3.19)] observe that  $K_0(krj^{0.5})$  goes to infinity as  $r \rightarrow 0$ . Since the current density should be finite for  $r = 0$ , it is concluded that the constant  $\tilde{A}_2$  must be identical to zero:

$$\tilde{A}_2 = 0$$

Thus the general solution of the current density for a solid conductor is

$$\tilde{J}(r) = \tilde{A}_1 I_0(krj^{0.5}) \quad (3.20)$$

and the instantaneous current density is

$$J(r, t) = \sqrt{2} \operatorname{Re}\{\tilde{A}_1 I_0(krj^{0.5}) e^{j\omega t}\}$$

To simplify calculations, the modified Bessel function  $I_0$  is written in polar form:

$$\tilde{J}(r) = \tilde{A}_1 M_0(kr) e^{j\theta_0(kr)}$$

The constant  $\tilde{A}_1$  is determined from boundary conditions. For example, assuming that the current density just below the surface of the conductor is  $J_0$ , the constant  $\tilde{A}_1$  is computed from

$$J_0 = \tilde{J}(a) = \tilde{A}_1 M_0(ka) e^{j\theta_0(ka)} \rightarrow$$

$$\tilde{A}_1 = \frac{J_0}{M_0(ka)} e^{-j\theta_0(ka)}$$

Substitution in Eq. (3.20) yields

$$\tilde{J}(r) = J_0 \frac{M_0(kr)}{M_0(ka)} e^{j[\theta_0(kr) - \theta_0(ka)]} \quad 0 \leq r \leq a \quad (3.21)$$

The expression above provides all the information regarding the distribution of the current density. It is given in terms of the current density  $J_0$ , just below the surface of the conductor. As an example, Fig. 3.7 illustrates the current density distribution in a 1.162 cm-radius solid conductor for various frequencies. Note that even at  $f = 60$  Hz, the skin effect is substantial. At higher frequencies,

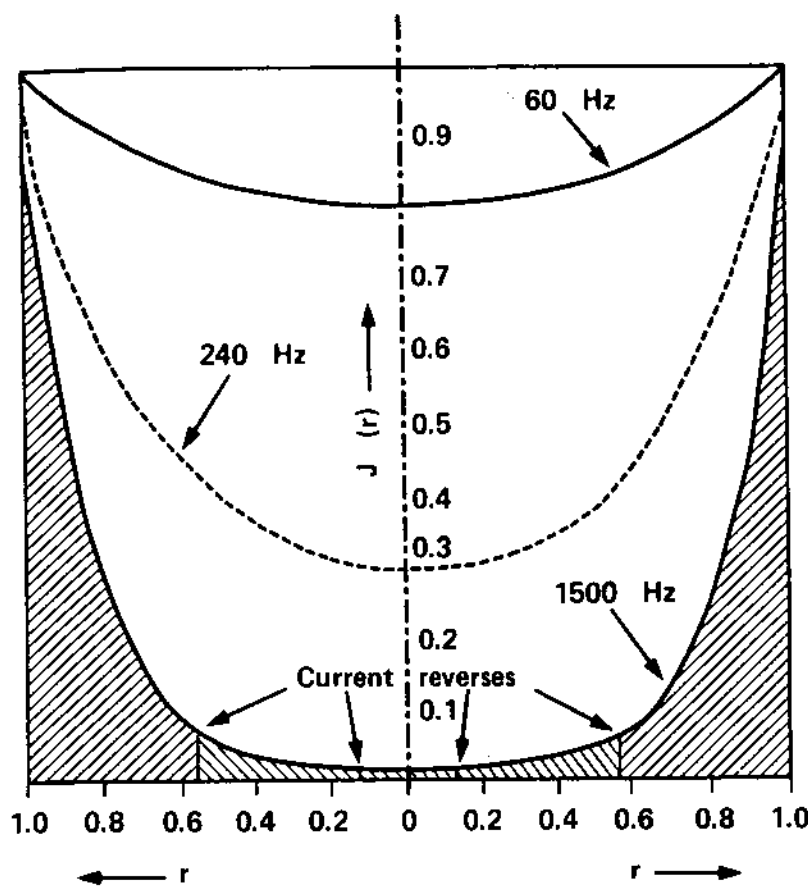


FIG. 3.7 Magnitude of electric current density versus distance from axis in a 1.162-cm radius copper conductor at various frequencies.

reversals of the current can be observed. For the example of Fig. 3.7, two reversals occur at the frequency 1500 Hz (twenty-fifth harmonic of 60 Hz). This happens because the phase angle [ $\theta_0(kr) - \theta_0(ka)$ ] can take all values from 0 to more than  $2\pi$  for high values of  $k$ , ( $\omega$ ) (see, e.g., Table 3.1). Note that the curves are normalized with respect to  $J_0$ , resulting in different total current through the conductor.

The instantaneous value of the current density in a solid conductor is obtained directly from Eq. (3.21):

$$J(r,t) = \sqrt{2} J_0 \frac{M_0(kr)}{M_0(ka)} \cos[\theta_0(kr) - \theta_0(ka) + \omega t] \quad (3.22)$$

$0 \leq r \leq a$

In the next section the two basic equations [(3.21) and (3.22)] will be utilized to answer the following questions: (a) what is the total current through the conductor, and (b) what is the resistance of the conductor?

### Total AC Current in a Solid Conductor

The total electric current through a solid conductor is obtained with an integration of the current density over the cross section of the conductor. For this purpose consider a circular infinitesimal strip at a distance  $r$  from the axis of the conductor. Since the electric current density is a function of the distance  $r$  only, the current density over the infinitesimal strip will be the same, equal to  $\tilde{J}(r)$ . The total current through the infinitesimal strip is

$$d\tilde{I} = \tilde{J}(r)2\pi r dr$$

The total current  $\tilde{I}_t$  through the conductor will be

$$\tilde{I}_t = \int_{r=0}^{r=a} \tilde{J}(r)2\pi r dr$$

Substituting  $\tilde{J}(r)$  from Eq. (3.21) yields

$$\tilde{I}_t = 2\pi J_0 \frac{1}{I_0(kaj^{0.5})} \int_0^a r I_0(krj^{0.5}) dr \quad (3.23)$$

For the computation of the integral above, the following identity of the modified Bessel functions is recalled:

$$\int_0^z w I_0(w) dw = z I_1(z)$$

where  $I_1(z)$  is a modified Bessel function of first kind and first order. The modulus and phase of the function  $I_1(z)$ , defined by  $I_1(zj^{0.5}) = M_1(z)e^{j\theta_1(z)}$ , are tabulated in Table 3.1 for practical computations. Direct application of this identity yields

$$\int_0^a r I_0(krj^{0.5}) dr = \frac{a}{k} I_1(kaj^{0.5}) e^{-j\pi/4}$$

Utilizing the property above, the integral is computed in terms of the function  $I_1$ , yielding

$$\tilde{I}_t = J_0 \frac{2\pi a I_1(kaj^{0.5})}{k I_0(kaj^{0.5})} e^{-j(3\pi/4)} \quad (3.24)$$

Elimination of  $J_0$  from Eqs. (3.23) and (3.21) will yield the electric current density in terms of the total electric current through the conductor:

$$\tilde{J}(r) = \tilde{I}_t \frac{k}{2\pi a} \frac{M_0(kr)}{M_1(ka)} e^{j[\theta_0(kr) - \theta_1(ka) + 3\pi/4]} \quad (3.25)$$

Equation (3.25) is more useful since the total electric current through the conductor is readily known.

#### Heat Dissipation in a Solid Conductor

The heat dissipated in a solid conductor is computed by appropriate integration of the heat dissipation in a certain length of the conductor. For this purpose consider a conductor segment of length  $\ell$ . Consider also a circular infinitesimal strip of thickness  $dr$  at a distance  $r$  from the axis of the conductor. This circle defines an elementary ring of length  $\ell$ , radius  $r$ , and infinitesimal thickness  $dr$ . The electric current flowing through the ring is

$$d\tilde{I}(r) = \tilde{J}(r) 2\pi r dr$$

The resistance of the elementary ring is

$$dR = \frac{1}{\sigma} \frac{\ell}{2\pi r dr}$$

Let the dissipated heat (ohmic losses) in the elementary ring per unit length be  $dP(r)$ . Then

$$\begin{aligned} dP(r)\ell &= dR |d\tilde{I}(r)|^2 \\ &= \frac{\ell}{\sigma} 2\pi r dr |\tilde{J}(r)|^2 \end{aligned}$$

Upon substitution of the current density  $\tilde{J}(r)$  from Eq. (3.21) and subsequent manipulations, we have

$$dP(r) = \frac{2\pi r}{\sigma} J_0^2 \frac{[ber(kr)]^2 + [bei(kr)]^2}{M_0^2(ka)} dr$$

The total heat dissipated in the conductor segment will be obtained from the following integral:

$$P = \frac{2\pi J_0^2}{\sigma M_0^2(ka)} \int_{r=0}^a r([ber(kr)]^2 + [bei(kr)]^2) dr$$

The integral above is computed with the aid of the following identity of the modified Bessel functions:

$$\int_{r=0}^a r([\text{ber}(kr)]^2 + [\text{bei}(kr)]^2) dr = \frac{a}{k} [\text{ber}(ka)\text{bei}'(ka) - \text{bei}(ka)\text{ber}'(ka)]$$

where the primed ('') functions denote the derivative of the function with respect to the argument. Upon application of the identity above, the ohmic losses per unit length of conductor are

$$P = \frac{2\pi J_0^2 a}{k\sigma} \frac{\text{ber}(ka)\text{bei}'(ka) - \text{bei}(ka)\text{ber}'(ka)}{[\text{ber}(ka)]^2 + [\text{bei}(ka)]^2} \quad (3.26)$$

This formula can be brought into a simpler form by recalling the following properties of the Kelvin functions:

$$\begin{aligned} \text{ber}'(x) &= M_1(x) \cos \left[ \theta_1(x) - \frac{\pi}{4} \right] \\ \text{bei}'(x) &= M_1(x) \sin \left[ \theta_1(x) - \frac{\pi}{4} \right] \end{aligned}$$

Upon substitution in the formula above and after manipulation, we obtain

$$P = J_0^2 \frac{2\pi a}{k\sigma} \frac{M_1(ka)}{M_0(ka)} \sin \left[ \theta_1(ka) - \theta_0(ka) - \frac{\pi}{4} \right] \quad (3.27)$$

An alternative formula can be obtained by substituting the "skin" density  $J_0$  with the total current  $I_t$  from Eq. (3.24). The result is

$$P = I_t^2 \frac{k}{2\pi a\sigma} \frac{M_0(ka)}{M_1(ka)} \sin \left[ \theta_1(ka) - \theta_0(ka) - \frac{\pi}{4} \right] \quad (3.28)$$

### 3.3.4 Effective Resistance of a Solid Conductor

For a given conductor of length  $\ell$ , the effective resistance to the flow of ac current is defined by

$$r_{ac} \stackrel{\Delta}{=} \frac{P}{I_{rms}^2} \quad (3.29)$$

where  $P$  is the heat dissipated in the conductor and  $I_{rms}$  is the rms value of the total electric current through the conductor. Recalling Eq. (3.28), the effective resistance of the conductor is given by

$$r_{ac} = \frac{k}{2\pi\sigma} \frac{M_0(ka)}{M_1(ka)} \sin \left[ \theta_1(ka) - \theta_0(ka) - \frac{\pi}{4} \right] \quad (3.30)$$

A more convenient form of the effective resistance if in terms of the conductor resistance to the flow of dc currents:

$$r_{dc} = \frac{1}{\sigma\pi a^2} \quad \text{ohms/meter}$$

Specifically, the ratio of  $r_{ac}$  to  $r_{dc}$  is computed to be

$$x_s = \frac{r_{ac}}{r_{dc}} = \frac{ka}{2} \frac{M_0(ka)}{M_1(ka)} \sin \left[ \theta_1(ka) - \theta_0(ka) - \frac{\pi}{4} \right] \quad (3.31)$$

Note that the increase depends only on the quantity  $ka$ , which depends on the conductor material properties and the frequency of the applied currents. Also note that as  $\omega \rightarrow 0$ , the ratio  $x_s$  goes to 1.0.

### 3.3.5 Effects of Skin Effect on Nonmagnetic Conductor Reactance

The reactance of transmission lines is affected by the skin and proximity effects. In this section we discuss the impact of skin effect on conductor reactance. Quantitatively, the effect is described with the concept of the geometric mean radius. Specifically, the geometric mean radius depends on the distribution of the electric current inside the conductor. In Chapter 2 the geometric mean radius for a circular, solid, nonmagnetic conductor, assuming uniform current distribution, has been computed to be  $d = ae^{-0.25}$ , where  $a$  is the radius of the conductor. In the presence of the skin effect, the electric current distribution is not uniform. Let's assume that the geometric mean radius in this case is  $d'$ , different than  $d$ . In general, the geometric mean radius  $d'$  must be a number between 0 and  $a$ , the radius of the conductor. It is expedient to express  $d'$  as

$$d' = ae^{-\xi/4} \quad (3.32)$$

where  $\xi$  is a number between 0 and 1. The value of the parameter  $\xi$  depends on frequency. When the frequency of the applied currents is zero (dc current), the geometric mean radius is equal  $d$  ( $d' = d$ ). Thus  $\xi = 1$ . When the frequency of the applied currents is very high, the skin effect forces all the current to the surface of the conductor. Thus  $d' = a$  and  $\xi = 0$ . For intermediate frequencies, the

parameter  $\xi$  is computed as follows. Let  $\lambda_i$  be the internal magnetic flux linkage of the conductor assuming uniform current distribution. It has been found (Chapter 2) that for a nonmagnetic circular conductor,

$$\lambda_i = \frac{\mu_0 I_t}{2\pi} \cdot \frac{1}{4}$$

The same component, with nonuniform current distribution, is computed to be

$$\lambda'_i = \frac{\mu_0 I_t}{2\pi} \cdot \frac{\xi}{4}$$

Thus

$$\xi = \frac{\lambda'_i}{\lambda_i} \quad (3.33)$$

The component  $\lambda'_i$  can be computed in a straightforward manner by integrating the magnetic flux linkage inside the conductor only, as was done in Chapter 2. However, the resulting integral equations in this case are very complex. A simpler approach is to consider the voltage per unit length of the conductor. On the "skin" of the conductor, the voltage per unit length is by definition equal to the electric field intensity  $E(a, t)$ . Recall Ohm's law:

$$E(a, t) = \frac{1}{\sigma} J(a, t)$$

In the frequency domain

$$\begin{aligned} \tilde{E}(a) &= \frac{1}{\sigma} \tilde{J}(r) = \tilde{I}_t \frac{k}{2\pi a \sigma} \frac{M_0(ka)}{M_1(ka)} e^{j[\theta_0(ka) - \theta_1(ka) + 3\pi/4]} \\ &= \tilde{I}_t \frac{k}{2\pi a \sigma} \frac{M_0(ka)}{M_1(ka)} \left\{ \cos \left[ \theta_0(ka) - \theta_1(ka) + \frac{3\pi}{4} \right] \right. \\ &\quad \left. + j \sin \left[ \theta_0(ka) - \theta_1(ka) + \frac{3\pi}{4} \right] \right\} \end{aligned}$$

In the equation above, observe that the voltage per unit length of the conductor has two components. One is due to the resistance of the conductor and it is in phase with the conductor current,  $\tilde{I}_t$ . The other is due to the alternating magnetic flux linkage inside the conductor and it is  $90^\circ$  out of phase with the conductor current,  $\tilde{I}_t$ . The latter voltage, denoted by  $\tilde{E}_i(a)$ , is

$$\tilde{E}_i(a) = \tilde{I}_t \frac{k}{2\pi a \sigma} \frac{M_0(ka)}{M_1(ka)} j \sin \left[ \theta_0(ka) - \theta_1(ka) + \frac{3\pi}{4} \right]$$

Since the voltage is due to the alternating magnetic flux  $\lambda_i^!$  inside the conductor, it should be also equal to

$$\tilde{E}_i(a) = j\omega \tilde{\Lambda}_i^!$$

where  $\tilde{\Lambda}_i^!$  is the phasor of the magnetic flux linkage  $\lambda_i^!$ . Upon solution for  $\tilde{\Lambda}_i^!$ ,

$$\tilde{\Lambda}_i^! = \tilde{I}_t \frac{k}{2\pi a \sigma \omega} \frac{M_0(ka)}{M_1(ka)} \sin \left[ \theta_0(ka) - \theta_1(ka) + \frac{3\pi}{4} \right]$$

or

$$\lambda_i^! = I_t \frac{k}{2\pi a \sigma \omega} \frac{M_0(ka)}{M_1(ka)} \sin \left[ \theta_0(ka) - \theta_1(ka) + \frac{3\pi}{4} \right]$$

Upon substitution into Eq. (3.33), the parameter  $\xi$  is

$$\xi = \frac{4}{ka} \frac{M_0(ka)}{M_1(ka)} \sin \left[ \theta_0(ka) - \theta_1(ka) + \frac{3}{4}\pi \right] \quad (3.34)$$

Note that the properties of Bessel functions guarantee that

$$\lim_{ka \rightarrow 0} \xi = 1 \quad \text{and} \quad \lim_{ka \rightarrow \infty} \xi = 0$$

In summary, the geometric mean radius of a solid nonmagnetic conductor is computed with Eq. (3.32), where the parameter  $\xi$  is given with Eq. (3.34). The equations account for the nonuniform current distribution inside the conductor due to the skin effect.

### 3.3.6 Method of Depth of Penetration

It should be apparent from previous sections that models for analysis of the skin effect are complex. A simpler but approximate way for accounting for the skin effect is the method of depth of penetration. This method states that the ac resistance of a conductor is approximately equal to the dc resistance of a hollow conductor of thickness equal to the depth of penetration,  $\delta$ , which is defined by

$$\delta = \frac{2}{k} = \frac{2}{(\mu\omega\sigma)^{0.5}} \quad (3.35)$$

For cylindrical solid conductors, the method is applied as follows: The ac resistance of a solid conductor of radius  $a$  is approximately equal to the dc resistance of a hollow conductor of outside radius  $a$  and inside radius  $a - \delta$  as in Fig. 3.8. Thus

$$r_{ac} = \rho \frac{\ell}{\pi(2a - \delta)\delta} \quad (3.36)$$

where  $\delta = 2/k$ . Because  $\delta$  depends on frequency, it is possible that  $\delta$  is greater than the radius  $a$  for very low frequencies. This means that the skin effect is negligible. In this case,  $r_{ac} \approx r_{dc} = \rho\ell/\pi a^2$ .

### 3.4 RESISTANCE AND GEOMETRIC MEAN RADIUS OF MAGNETIC CONDUCTORS

Power conductors are typically made of copper or aluminum. Many times, in order to increase the strength of copper or aluminum conductors, steel strands are added to the power conductors. A typical case is that of the ACSR (aluminum conductor steel reinforced) conductors. Other typical cases are the Alumoweld and Copperweld conductors, which are steel wires with a thin layer of aluminum or copper, respectively. These conductors as well as steel wires are typically used as overhead shield wires of transmission lines. In many applications, the presence of these wires does not substantially affect the performance of the line. For this reason, their presence is neglected. In certain applications, however, such as computation of ground potential rise, transmission losses, and so on, the presence of steel wires may affect line performance. In these cases it is necessary to compute the resistance and reactance of steel wires. Because of the high relative value of magnetic permeability of these wires, the skin effect substantially affects the resistance and reactance.

For the computation of the resistance and reactance (or alternatively, geometric mean radius) of steel conductors, the analysis presented in the previous sections should be repeated under the condition that the magnetic permeability of the conductor is  $\mu = \mu_r \mu_0$ , where  $\mu_r \neq 1$ . The results are

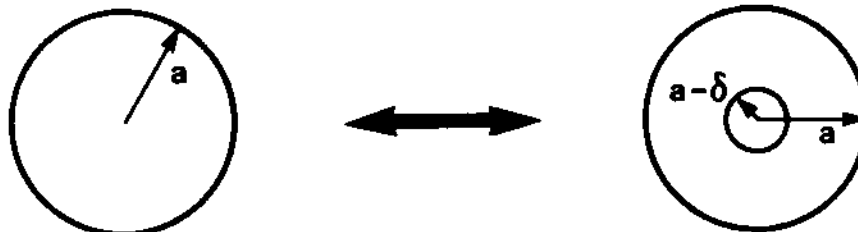


FIG. 3.8 Computation of conductor AC resistance with the method of depth of penetration.

$$\tilde{J}(r) = \tilde{I}_t \frac{k}{2\pi a} \frac{M_0(kr)}{M_1(kr)} e^{j[\theta_0(kr) - \theta_1(ka) + 3\pi/4]} \quad (3.37a)$$

$$r_{ac} = \frac{k}{2\pi a \sigma} \frac{M_0(ka)}{M_1(ka)} \sin \left[ \theta_1(ka) - \theta_0(ka) - \frac{\pi}{4} \right] \quad (3.37b)$$

$$d' = ae^{-\mu_r \xi / 4} \quad (3.37c)$$

where

$$k = \sqrt{\mu_r \mu_0 \omega \sigma}$$

$$\xi = \frac{4}{ka} \frac{M_0(ka)}{M_1(ka)} \sin \left[ \theta_0(ka) - \theta_1(ka) + \frac{3}{4}\pi \right]$$

Application of the equations above will be demonstrated with an example.

Example 3.1: Overhead ground wires are many times constructed from 0.1047-in.-diameter steel strands. Compute the 60-Hz resistance and geometric mean radius of a steel strand. The resistivity and permeability of the steel are  $\rho = 2.2 \times 10^{-7} \Omega \cdot m$  and  $\mu = 4\pi \times 10^{-5} H/m$ .

Solution: The relative permeability is

$$\mu_r = \mu/\mu_0 = 100.0$$

Thus

$$k = \sqrt{(100)(4\pi \times 10^{-7})(377)\left(\frac{1}{2.2}\right)10^7} = 464.05 \text{ m}^{-1}$$

$$a = 0.1047/2 \text{ in.} = 0.00133 \text{ m}$$

$$ka = 0.617$$

From Table 3.1 we obtain

$$M_0(ka) = 1.0022$$

$$\theta_0(ka) = 5.45^\circ$$

$$M_1(ka) = 0.3086$$

$$\theta_1(ka) = 137.73^\circ$$

Upon substitution into Eqs. (3.37b and 3.37c), we have

$$r_{ac} = 0.03963 \Omega/m = 63.76 \Omega/mi$$

$$\xi = 0.9992$$

$$d' = 1.888 \times 10^{-14} m = 6.195 \times 10^{-14} ft$$

Observe that the geometric mean radius of magnetic wires is extremely small. This should not cause any alarm. All it means is that the inductive reactance of magnetic wires, which is proportional to the logarithm of  $1/d'$ , is very high. Tables for steel wires list only the resistance and inductive reactance. The geometric mean radius, being a very small number, is not listed.

### 3.5 CURRENT DISTRIBUTION IN EARTH

Electric power systems are grounded; that is, the neutral is connected to earth-embedded metallic structures. As a result, electric currents are injected or induced in the soil. This phenomenon occurs both during normal operating conditions or fault conditions. Although the total earth current may be very small during normal operating conditions, during fault conditions the total earth current may be a substantial percentage of the fault current. The effects of earth currents are examined in Chapter 5. In this section we discuss the current distribution in earth and the basic equations by which the resistance and inductance of the earth path can be computed.

Analysis of voltages and currents in the earth is a rather complex problem. Alternating current in the earth is distributed in a rather complex manner. Figure 3.9 provides a qualitative illustration of this distribution for a system of one conductor above earth. The density of the dots signifies the density of the electric current. Note that just below the conductor, the current density is maximum. The current density decreases as the distance from the conductor increases. Carson [2] has provided a solution for the electromagnetic field and the current density inside the earth. The solution is given in terms of two functions P and Q, each function expressed with an infinite series. This solution will be discussed next and expressions for the few first terms of the P and Q functions will be given. For most applications, the Carson solution has been simplified or suitable alternative formulas have been developed. Two such approximate solutions are discussed next: (a) the equivalent depth of return method, and (b) the complex depth of return method.

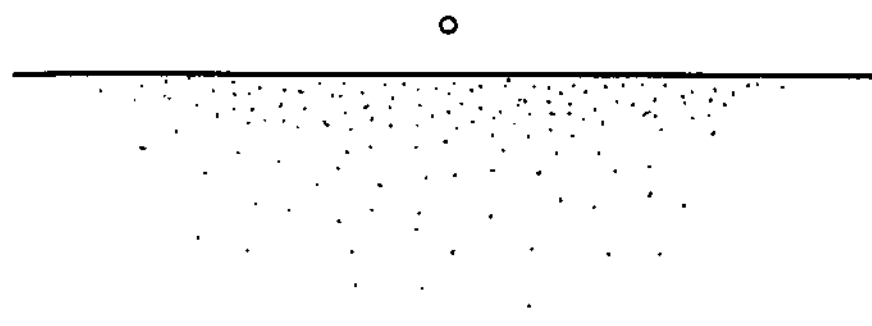


FIG. 3.9 Illustration of the current distribution in the earth.

### 3.5.1 The P and Q Form

It has been mentioned that Carson [2] provided a general solution for the problem illustrated in Fig. 3.9. His solution is in terms of an infinite series. Specifically, the solution is given in terms of two functions,  $P$  and  $Q$ , which are expressed as an infinite series of trigonometric functions. In his 1929 paper, Carson derived the solution in the now obsolete cgs system of units. Here we present the same solution in the mksa (metric) system of units and in a form that expresses the induced voltage along a conductor due to the combined effect of the conductor impedance and the earth path impedance. Specifically, consider the system of Fig. 3.10. It illustrates two parallel conductors above earth. Conductor  $a$  carries electric current  $\tilde{I}_a$  and conductor  $b$  carries current  $\tilde{I}_b$ , both in the

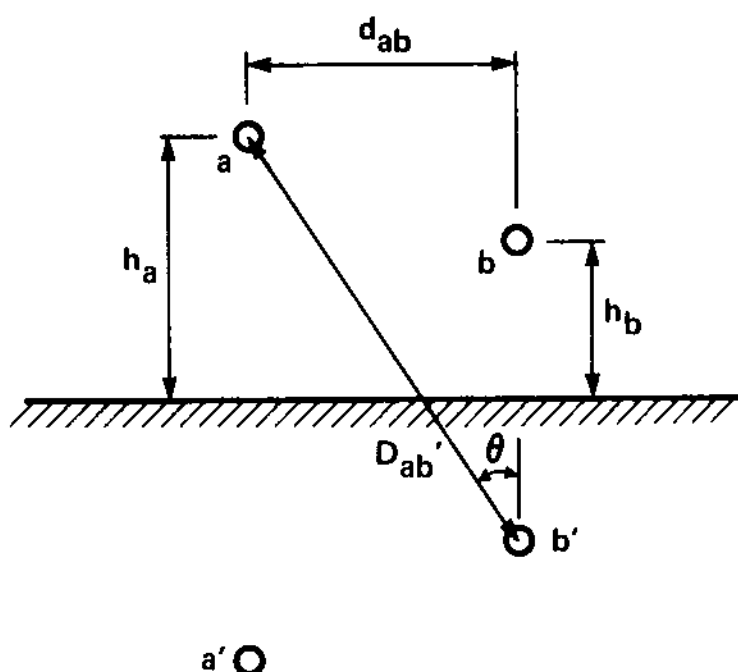


FIG. 3.10 Illustration of two parallel conductors above earth.

same direction. It is assumed that the current returns through the earth path (i.e., the earth current is  $\tilde{I}_e = -\tilde{I}_a - \tilde{I}_b$ ). Under these conditions the induced voltage on conductor a is

$$\begin{aligned}\tilde{V}_a &= \left[ r_a + j \frac{\omega\mu}{2\pi} \log \frac{D_{aa'}}{d_a} + \frac{2\omega\mu}{2\pi} (P_{aa} + jQ_{aa}) \right] \tilde{I}_a \\ &\quad - \left[ j \frac{\omega\mu}{2\pi} \ln \frac{D_{ab'}}{D_{ab}} + \frac{2\omega\mu}{2\pi} (P_{ab} + jQ_{ab}) \right] \tilde{I}_b\end{aligned}\quad (3.38)$$

where

$$\begin{aligned}P_{aa} &= \frac{\pi}{8} - \frac{x}{3\sqrt{2}} + \frac{x^2}{16} \left( 0.6728 + \ln \frac{2}{x} \right) + \frac{x^3}{45\sqrt{2}} - \frac{\pi x^4}{1536} \\ &\quad + \dots\end{aligned}\quad (3.39)$$

$$\begin{aligned}Q_{aa} &= -0.0386 + \frac{1}{2} \ln \frac{2}{x} + \frac{x}{3\sqrt{2}} - \frac{\pi x^2}{64} + \frac{x^3}{45\sqrt{2}} - \frac{x^4}{384} \\ &\quad - \frac{x^4}{384} \left( \ln \frac{2}{x} + 1.0895 \right) + \dots\end{aligned}\quad (3.40)$$

$$x = kD_{aa'} = 2kh_a$$

$D_{aa'}$  = distance between conductor a and its image (see Fig. 3.10)

$h_a$  = conductor a height above earth

$$\begin{aligned}P_{ab} &= \frac{\pi}{8} - \frac{1}{3\sqrt{2}} y \cos \theta + \frac{y^2}{16} \cos 2\theta \left( 0.6728 + \ln \frac{2}{y} \right) \\ &\quad + \frac{y^2}{16} \theta \sin 2\theta + \frac{y^3 \cos 3\theta}{45\sqrt{2}} - \frac{\pi y^4}{1536} \cos 4\theta + \dots\end{aligned}$$

$$\begin{aligned}Q_{ab} &= -0.0386 + \frac{1}{2} \ln \frac{2}{y} + \frac{1}{3\sqrt{2}} y \cos \theta - \frac{\pi y^2}{64} \cos 2\theta \\ &\quad + \frac{y^3}{45\sqrt{2}} \cos 3\theta - \frac{y^4}{384} \theta \sin 4\theta - \frac{y^4}{384} \cos 4\theta \left( \ln \frac{2}{y} + 1.0895 \right) \\ &\quad + \dots\end{aligned}$$

$$y = kD_{ab'}$$

$D_{ab'}$  = distance between conductor a and the image of conductor b (see Fig. 3.10)

$\theta = \arcsin(d_{ab}/D_{ab}')$ ; the angle  $\theta$  is indicated in Fig. 3.10

The number of terms to be retained in the infinite series P and Q depends on the frequency of the electric currents and the level of accuracy required.

### 3.5.2 Equivalent Depth of Return Method

The simplest model of the earth path is based on the concept of the equivalent depth of return. The model is valid only for relatively low frequencies. The steps for the derivation of the approximation are as follows. Consider the problem of one overhead conductor above the earth, as in Fig. 3.9. Usually, the height of the conductor  $h$  is much larger than its radius. Rudenberg [6] has suggested that the distribution of electric current inside the earth can be approximated with

$$\tilde{J}(r) = \frac{jk^2}{2\pi} \tilde{I}_t K_0(krj^{0.5}) \quad (3.41)$$

where

- $\tilde{J}(r)$  = current density in the earth at a distance  $r$  from the conductor
- $\tilde{I}_t$  = total current through the conductor
- $j$  = imaginary unit [ $= (-1)^{1/2}$ ]
- $k^2$  =  $\omega\mu\sigma$
- $K_0$  = modified Bessel function of the second kind, zero order

Rudenberg did not provide any reasoning for suggesting the foregoing formula. We can argue that he arrived at this suggestion by considering the general solution for the electric current density in cylindrical geometry [i.e., Eq. (3.18)]. While Eq. (3.18) is not applicable to the problem illustrated in Fig. 3.9 [recall that Eq. (3.18) was derived by assuming radial symmetry, i.e., solution independent of the angular coordinate  $\phi$ ], Rudenberg assumed that it is a reasonable approximation since the height  $h$  is typically large (more than 10 m). Upon acceptance of this assumption, observe that as  $r \rightarrow \infty$ , the electric current density must vanish. Since  $I_0(krj^{0.5}) \rightarrow \infty$  as  $r \rightarrow \infty$ , it is concluded that the constant  $A_1$  must be identically zero. Thus the solution is

$$\tilde{J}(r) = \tilde{A}_2 K_0(krj^{0.5}) \quad (3.42)$$

The total current through the infinite medium is

$$\tilde{I}_t = \int_{r=h}^{\infty} \tilde{A}_2 K_0(krj^{0.5}) 2\pi r dr$$

Recall the following integral of the modified Bessel function  $K_0$ :

$$\int_z^{\infty} w K_0(w) dw = z K_1(z)$$

Upon application of the identity above, we obtain

$$\tilde{I}_t = \frac{2\pi h j^{0.5}}{k} \tilde{A}_2 K_1(khj^{0.5}) \quad (3.43)$$

Elimination of the constant  $\tilde{A}_2$  from Eq. (3.42) with the aid of Eq. (3.43) yields

$$\tilde{J}(r) = j \frac{k^2 \tilde{I}_t}{2\pi} \frac{K_0(krj^{0.5})}{khj^{0.5} K_1(khj^{0.5})} \quad (3.44)$$

It should be observed that for typical soil and typical height  $h$  of conductors above earth, the quantity  $kh$  is very small. For example, assuming soil resistivity  $100 \Omega \cdot m$ , 60 Hz, and  $h = 10 m$ ,  $kh = 0.02176$ . Now recall a property of the modified Bessel function,  $K_0$ ; that is, for  $kh$  very small ( $< 0.5$ ),

$$khj^{0.5} K_1(khj^{0.5}) \approx 1.0$$

Thus

$$\tilde{J}(r) = j \frac{k^2 \tilde{I}_t}{2\pi} K_0(krj^{0.5})$$

which is exactly the equation suggested by Rudenberg. The induced voltage  $\tilde{V}$  per unit length on the surface of the earth along the conductor is computed from

$$\tilde{V} = \frac{1}{\sigma} \tilde{J}(r = h) = \frac{j k^2}{2\pi\sigma} \tilde{I}_t K_0(khj^{0.5}) \quad (3.45)$$

As we have discussed before, this voltage will have two components: one due to the resistance of the earth path which is in phase with the earth current, and another due to the changing magnetic flux density inside the earth. The latter voltage is  $90^\circ$  out of phase with the

earth current. This observation provides the procedure for the computation of the resistance and reactance of the earth path. Specifically, the resistance per unit length of the earth path is

$$R_e = \operatorname{Re} \left\{ \frac{\tilde{V}}{\tilde{I}_t} \right\} = \operatorname{Re} \left\{ \frac{jk^2}{2\pi\sigma} K_0(khj^{0.5}) \right\}$$

The inductive reactance per unit length of the earth path is

$$X_e = \operatorname{Im} \left\{ \frac{\tilde{V}}{\tilde{I}_t} \right\} = \operatorname{Im} \left\{ \frac{jk^2}{2\pi\sigma} K_0(khj^{0.5}) \right\}$$

A simplification of these formulas is achieved by recalling that for usual soil resistivities and transmission line designs, the argument  $kh$  of the modified Kelvin function is very small. In this case the asymptotic expansion of the modified Bessel function for small arguments can be utilized:

$$K_0(khj^{0.5}) \approx \ln \frac{1.123}{kh} - \frac{j\pi}{4}$$

Upon substitution of this expression in the equations for  $R_e$  and  $X_e$ , we have

$$R_e = \frac{\omega\mu}{8}$$

$$X_e = \frac{\omega\mu}{2\pi} \ln \left( \frac{399.6}{h} \sqrt{\frac{\rho}{f}} \right) \quad h \text{ in meters}$$

Note that  $X_e$  is the internal inductive reactance of the earth path. Considering the conductor and the earth path as a single-phase line, the voltage per unit length of this line is

$$\tilde{V} = j \frac{\mu_0 \omega \tilde{I}_t}{2\pi} \ln \frac{h}{d} + j \frac{\mu_0 \omega \tilde{I}_t}{2\pi} \ln \left( \frac{399.6}{h} \sqrt{\frac{\rho}{f}} \right) + r \tilde{I}_t + \frac{\omega\mu_0}{8} \tilde{I}_t$$

or

$$\tilde{V} = \left( r + \frac{\omega\mu_0}{8} \right) \tilde{I}_t + j \frac{\mu_0 \omega}{2\pi} \tilde{I}_t \ln \left( \frac{399.6}{d} \sqrt{\frac{\rho}{f}} \right)$$

Define  $D_e$ , the equivalent depth of return of earth currents:

$$D_e = 399.6 \sqrt{\frac{\rho}{f}} \quad \text{meters}$$

The formula above reads

$$\tilde{V} = \left( r + \frac{\omega\mu_0}{8} \right) \tilde{I}_t + j \frac{\mu_0\omega}{2\pi} \tilde{I}_t \ln \frac{D_e}{d} \quad (3.46)$$

where

- $d$  = geometric mean radius of the overhead conductor
- $r$  = conductor series resistance
- $\tilde{I}_t$  = total electric current through the overhead conductor (also through the earth in opposite direction)
- $f$  = frequency of current
- $D_e$  = equivalent depth of return of earth currents

Note that utilization of the earth as the return path has the effect of increasing the resistance by  $\omega\mu_0/8$ . The effect of the earth path on the reactance is expressed in terms of the equivalent depth of return,  $D_e$ .

The previous analysis suggests that the assumption made by Rudenberg that the earth current distributes in the earth according to Eq. (3.41), results in an equivalent depth of return equal to

$$D_e = 399.6 \sqrt{\frac{\rho}{f}} \text{ meters} = 1311 \sqrt{\frac{\rho}{f}} \text{ feet} \quad (3.47)$$

A better approximation for the equivalent depth of return is obtained by considering directly Carson's solution discussed in Section 3.5.1. By retaining only the first-order terms in Carson's solution, the following approximate formula for the depth of return is obtained:

$$D_e = 2160 \sqrt{\frac{\rho}{f}} \text{ feet} \quad (3.48)$$

The reader is encouraged to derive Eq. (3.48) by utilizing the results of Section 3.5.1.

The formula developed for the induced voltage on an overhead conductor using the earth as the return path can be converted into the English system of units, yielding

$$\tilde{V} = (r + 0.00159f)\tilde{I}_t + j0.00466f \left( \log \frac{D_e}{d} \right) \tilde{I}_t \text{ volts/mile} \quad (3.49)$$

Recall that the inductive component of formula (3.49) was introduced in Chapter 2. It was utilized to derive the parameters of an equivalent conductor for the earth path. It was shown that the earth path can be substituted for by an equivalent conductor of geometric mean radius of 1 ft located at a distance  $D'_e = \sqrt{D_e}$  from the

overhead conductor. By inspection of Eq. (3.49) it is apparent that the resistance of this equivalent conductor is  $0.00159f$  ohms per mile, where  $f$  is in hertz.

### 3.5.3 Complex Depth of Return Method

In recent years, Semlyen and Deri [12] suggested a closed-form approximation to Carson's solution. This form, appropriately modified for consistency with the nomenclature of this book, is presented next. Consider the system illustrated in Fig. 3.10. The induced voltage on conductor a is expressed in terms of the complex depth  $p$ , defined by

$$p = \frac{1}{k} j^{-0.5} \quad (3.50)$$

$$k = (\mu\omega\sigma)^{0.5}$$

The induced voltage per unit length of conductor a is

$$\tilde{V}_a = \left[ r_a + j \frac{\omega\mu}{2\pi} \ln \frac{2(h_a + p)}{a} + j \frac{\omega\mu}{2\pi} \frac{\xi}{4} \right] \tilde{I}_a - j \frac{\omega\mu}{2\pi} \ln \frac{\left[ (h_a + h_b + 2p)^2 + d_{ab}^2 \right]^{0.5}}{\left[ (h_a - h_b)^2 + d_{ab}^2 \right]^{0.5}} \tilde{I}_b$$

where

$h_a, h_b$  = heights of conductors a and b above ground (see Fig. 3.10)

$d_{ab}$  = horizontal separation between conductors a and b (see Fig. 3.10)

and

$$\xi = \frac{4}{ka} \frac{M_0(ka)}{M_1(ka)} \sin \left[ \theta_0(ka) - \theta_1(ka) + \frac{3\pi}{4} \right]$$

A study [13] of the closed-form solution above reported that the approximation yields a remarkably close agreement with the exact Carson's solution in a wide range of frequencies (0 to 10 MHz) for typical overhead line configurations. In the next paragraph, as well as in Chapter 6, we compare the approximate solutions to the exact solution and provide a quantitative analysis of the error of the approximation.

### 3.5.4 Comparison of the Earth Path Models

The preceding discussion presented three of the most widely used methods to evaluate the self- and mutual impedance of conductors above earth. The exact solution to this problem is complex. On the other hand, approximate solutions are available. The approximate method based on the equivalent depth of return,  $D_e$ , is quite simple. The approximate method based on the concept of the complex depth of return is more involved but still simple enough to be manageable. In order to get an idea of the quality of accuracy of the approximate methods, in this section we present an accuracy analysis of these methods. For this purpose a system of two conductors above earth is considered. The soil resistivity is assumed to be  $100 \Omega \cdot m$ . For this system the following quantities have been computed:

Self-resistance of one conductor

Self-inductance of one conductor

Mutual resistance between the two conductors

Mutual inductance between the two conductors

The quantities above have been computed as a function of frequency in the range 60 to 1200 Hz (first 20 harmonics of 60 Hz). The results are illustrated in Figs. 3.11 through 3.16. In all figures the exact value of the parameter is illustrated by a solid line. The computed error of the two approximate methods is also illustrated in the figures. The error analysis of the two mutual parameters (resistance and inductance) is performed for two distinct configurations (Figs. 3.13 through 3.16). The figures are self-explanatory. The method based on the equivalent depth of return is more accurate at low frequencies. The error increases at higher frequencies. The method based on the complex depth of return exhibits an error that is "flat" over the frequency range. Note that the inductance error is, in general, much smaller than the resistance error. For overhead transmission lines, the inductive reactance is the dominant component of the impedance for frequencies of 60 Hz or higher. This means that the impedance error committed with the approximate solution will be relatively small, as indicated in Figs. 3.12, 3.14, and 3.16. However, for applications where the resistance plays an important role, such as loss evaluation and analysis of resonance conditions, the error introduced with the approximate methods may be substantial.

Throughout this book, the simplest method (based on the equivalent depth of return  $D_e$ ) will be utilized to achieve maximum clarity of presentation. It should be understood that at any application this method can be replaced by the exact solution or the method based on the complex depth of return.

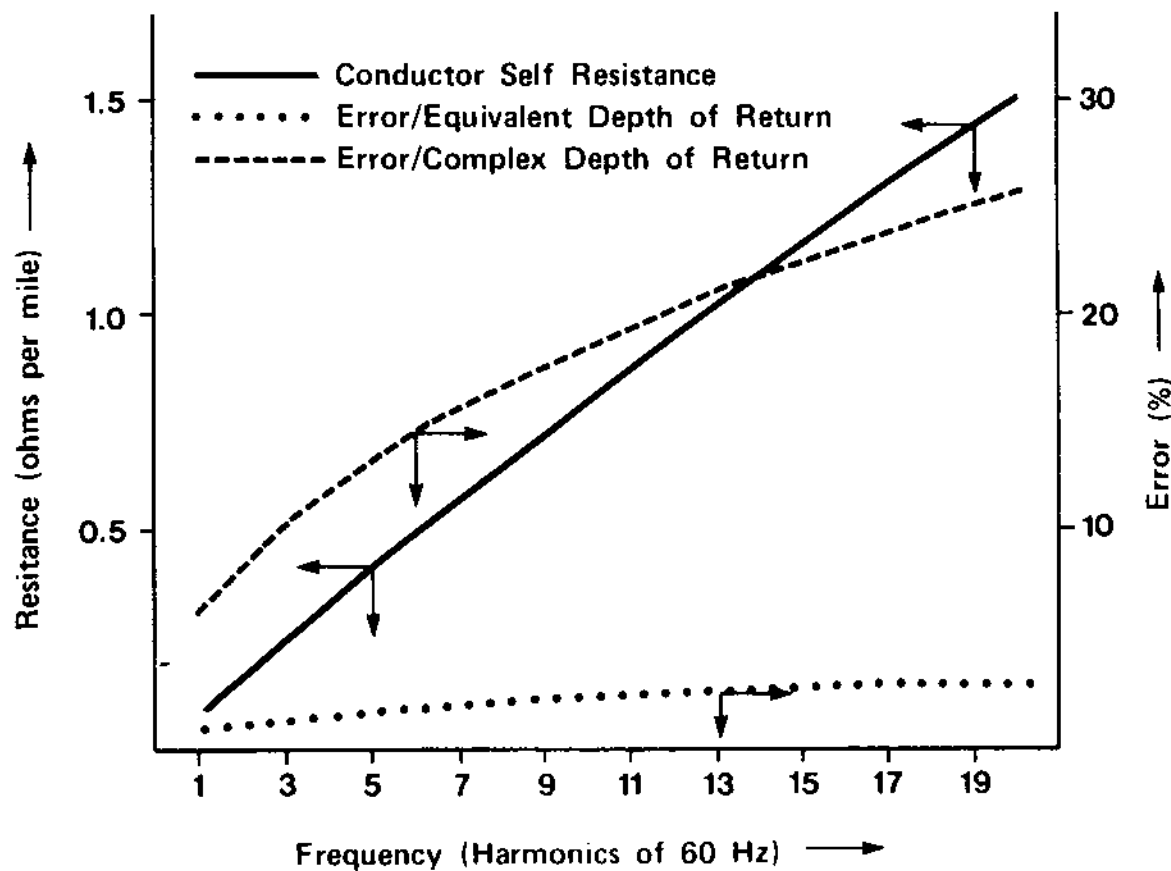


FIG. 3.11 Conductor self-resistance versus frequency. Comparison of two approximate solutions with exact solutions.

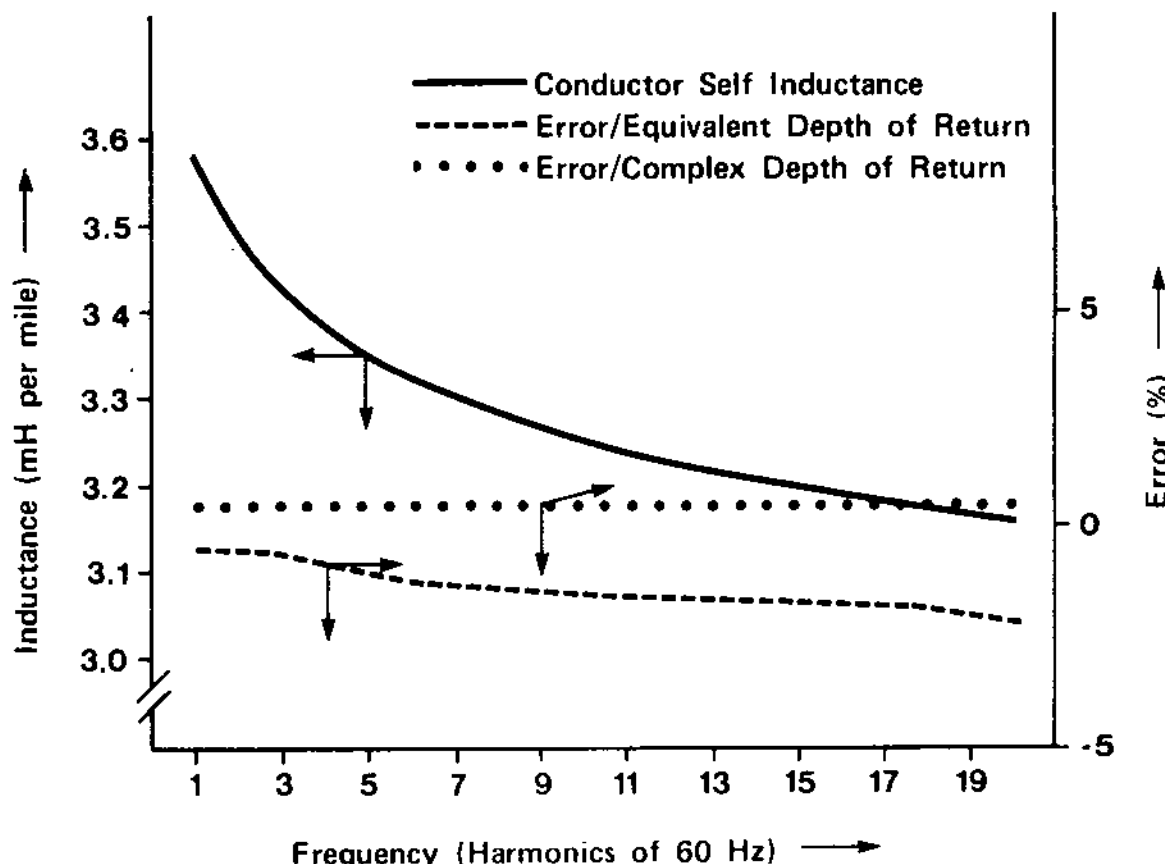


FIG. 3.12 Conductor self-inductance versus frequency. Comparison of two approximate solutions with the exact solutions.

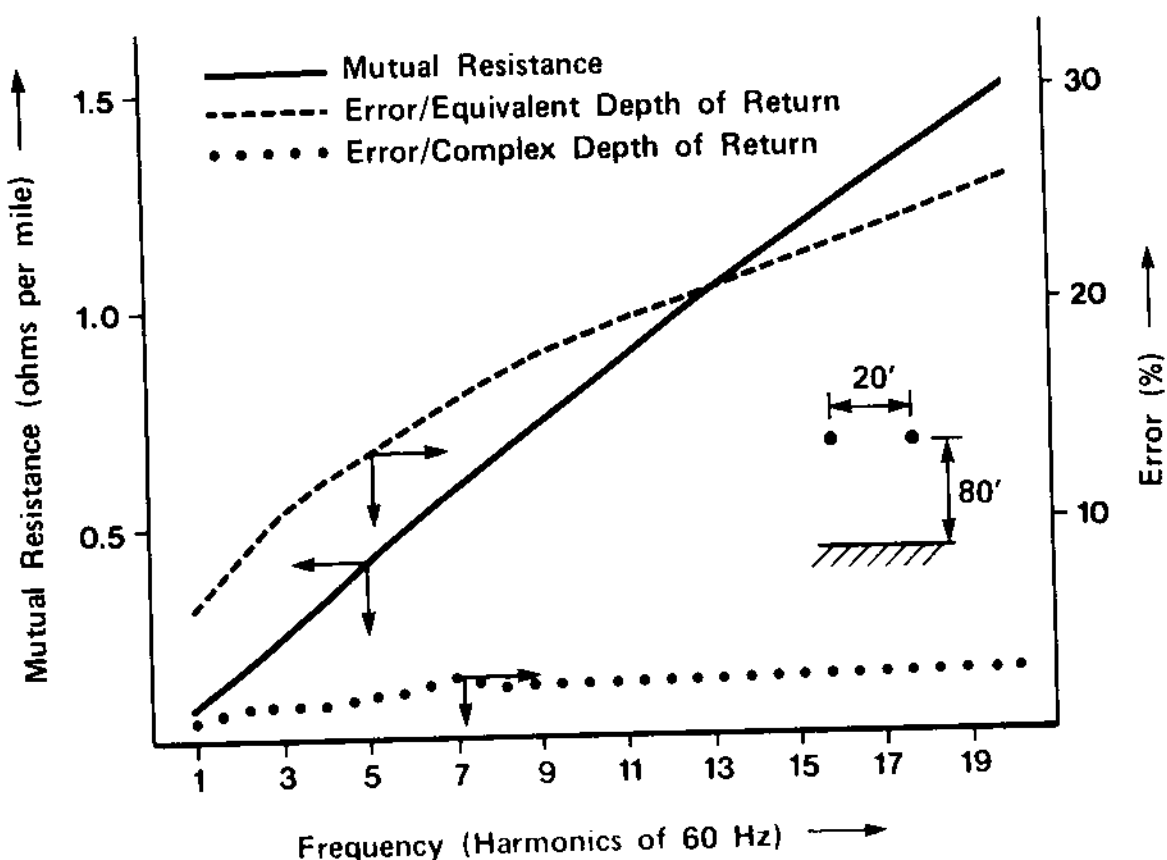


FIG. 3.13 Mutual resistance between two conductors above earth versus frequency. Comparison of two approximate solutions with exact solution.

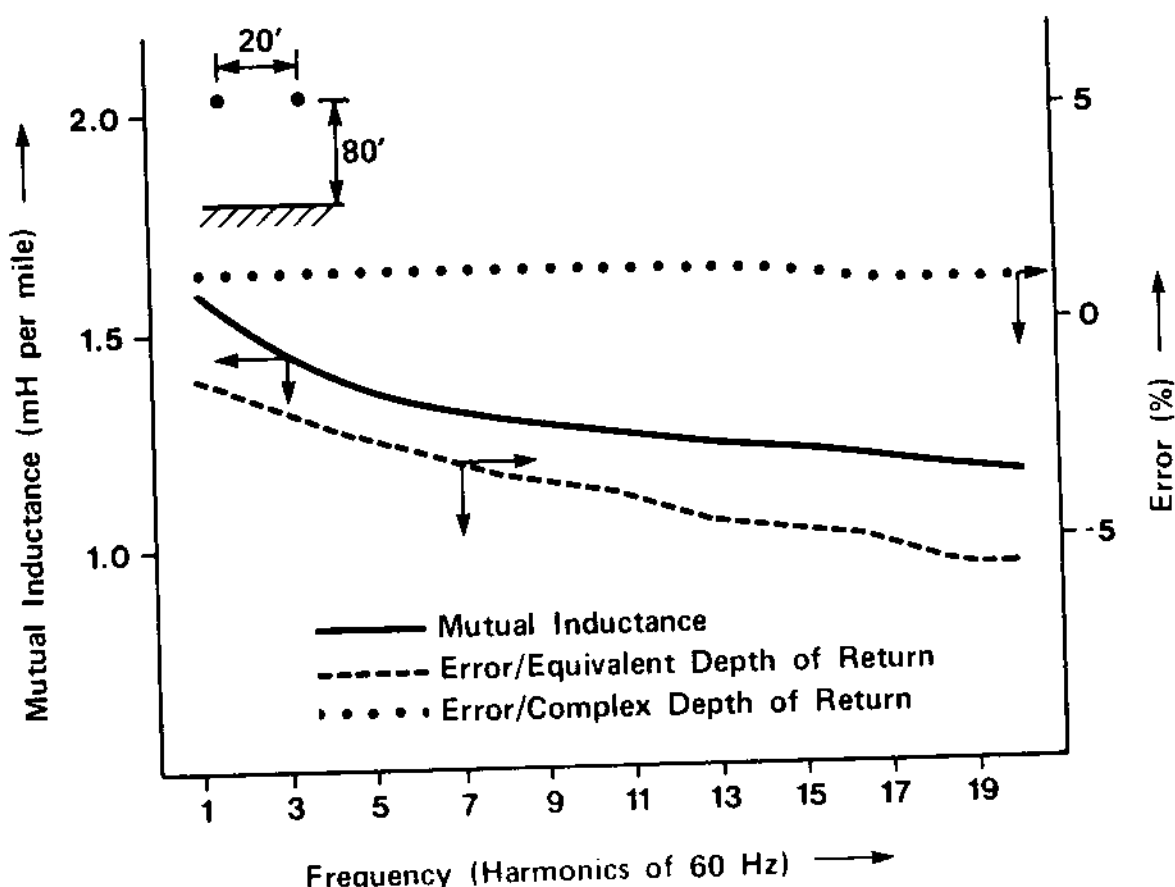


FIG. 3.14 Mutual inductance between two conductors above earth versus frequency. Comparison of two approximate solutions with exact solution.

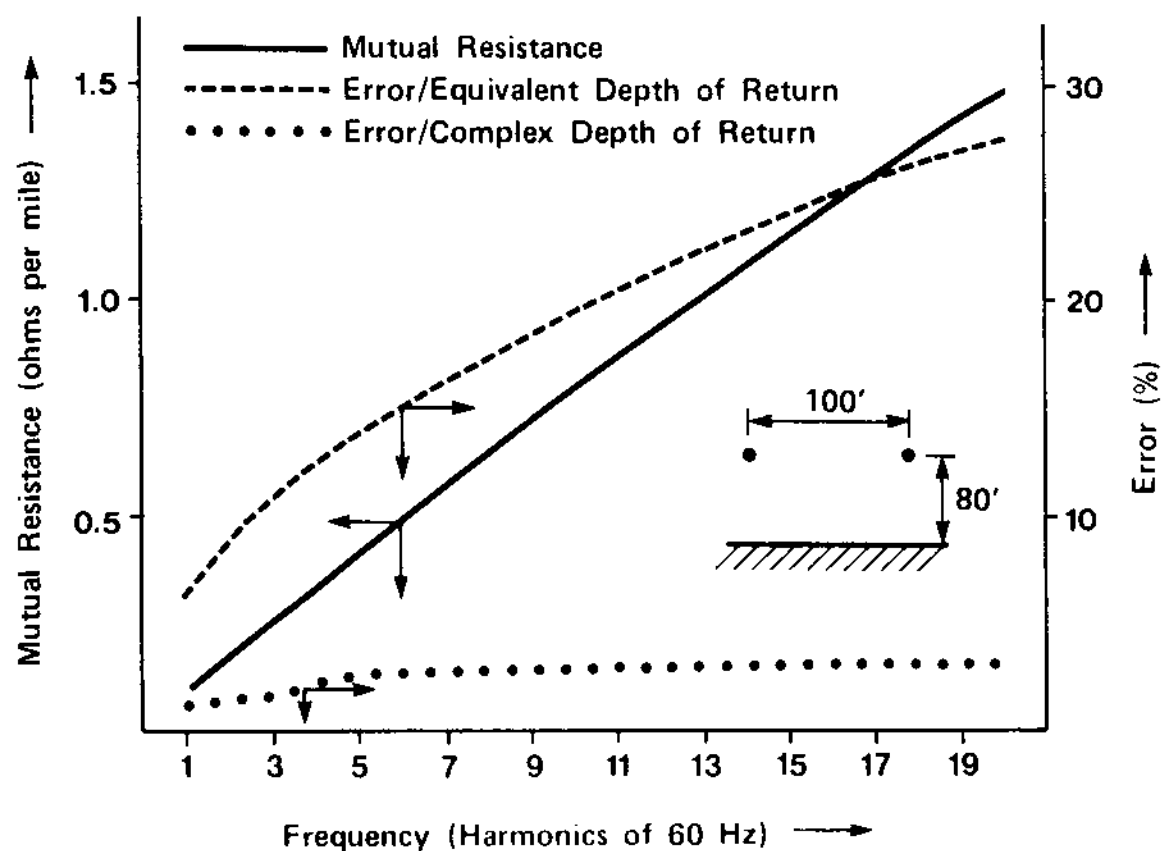


FIG. 3.15 Mutual resistance between two conductors above earth versus frequency. Comparison of two approximate solutions with exact solution.

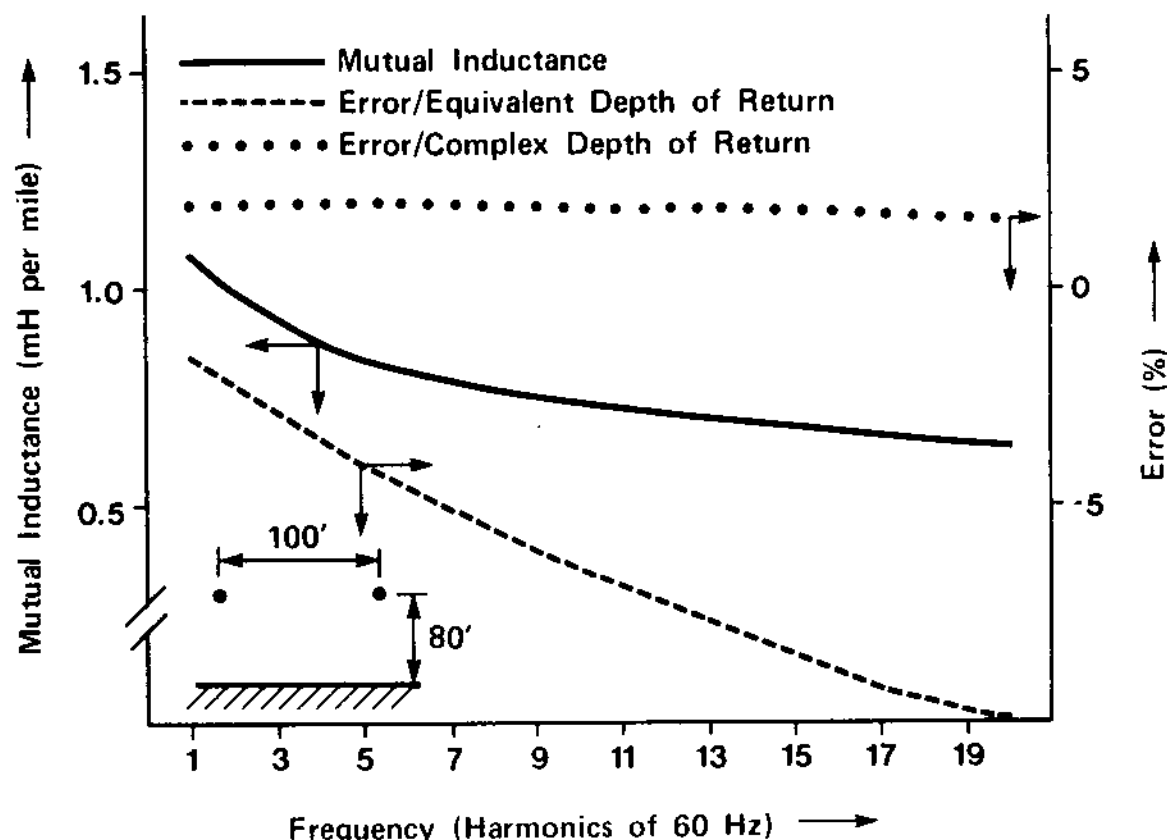


FIG. 3.16 Mutual inductance between two conductors above earth versus frequency. Comparison of two approximate solutions with exact solution.

### 3.6 SUMMARY AND DISCUSSION

In this chapter we have discussed phenomena affecting the electric current distribution in conductors and the earth. The distribution of alternating current is nonuniform, due to the interaction of the alternating magnetic field with the electric currents. Quantitative analysis of these phenomena allows computation of the effective resistance and inductance of electrical conductors at a given frequency. Closed-form solutions are only possible for solid circular conductors.

Of great practical importance is the computation of the impedance of the earth path. The exact solution is given in terms of an infinite series. Simplified but approximate solutions are available. Two such simplified solutions have been discussed and an accuracy analysis of these methods has been presented.

### 3.7 PROBLEMS

Problem 3.1: How much will the ac resistance of a 750-kcm solid copper conductor of 97% conductivity be at 25 and 60 Hz, at a temperature of 75°C? Use the depth of penetration method and check by the use of accurate methods.

Problem 3.2: Consider an annealed copper solid conductor of 1.0 in. diameter at a temperature of 20°C.

- (a) Plot the variation of the rms current density and the phase angle of the current density along the diameter for the following frequencies: 60 and 180 Hz.
- (b) Plot the variation along the diameter of the instantaneous current density for times  $t = 0, 0.002778$ , and  $0.005556$  s, and a frequency of 60 Hz.

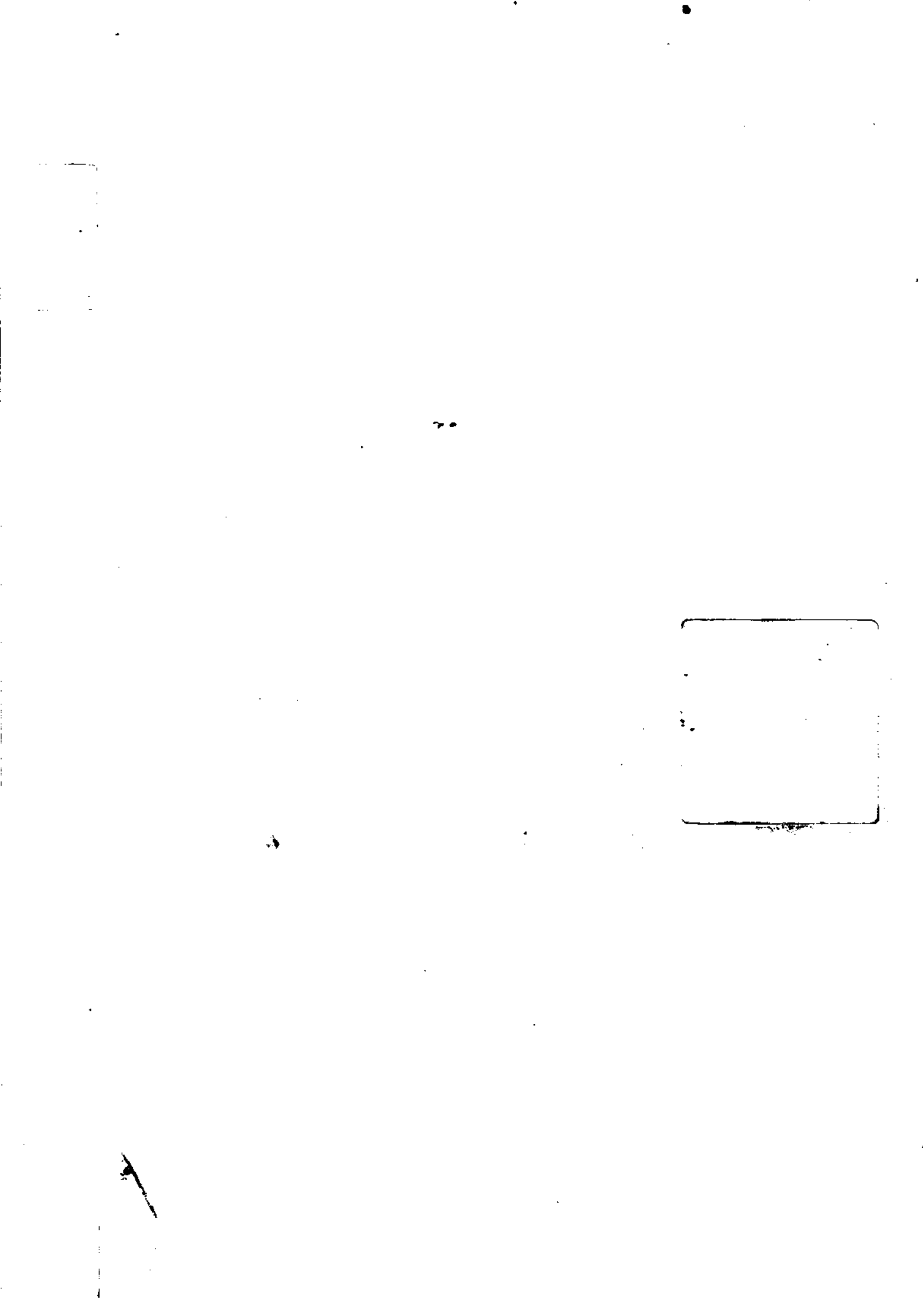
Problem 3.3: Consider a 300-kcm solid circular copper conductor of resistivity  $\rho = 1.78 \times 10^{-8} \Omega \cdot \text{m}$  at 20°C. The temperature coefficient of resistance is  $\alpha = 0.004/\text{°C}$ . Compute the 60-Hz ac resistance of the conductor in ohms per meter at 20 and 75°C.

Problem 3.4: Consider a solid copper conductor of 97% conductivity and diameter 2 in.

- (a) Compute the geometric mean radius at 20°C and 75°C for ac currents of 60 Hz.
- (b) Compute the 60-Hz inductive reactance in ohms per mile of a single-phase line at 20 and 75°C. The line consists of two conductors identical to the one in part (a) and spaced 5 ft apart.

Problem 3.5: A certain manufacturer of cable conductors decides to manufacture their 2000-kcm aluminum conductors from 72 aluminum strands as follows. First, the aluminum strands are covered with a thin insulating film. Then they are randomly twisted and compressed to form a 2000-kcm conductor. This conductor is practically solid. However, the presence of the insulating film around the strands and the production process (strands are randomly twisted with each other) results in a uniform distribution of electric current inside the conductor under low-frequency ac operation. Compute the reduction of the ac resistance of this conductor at 60 Hz due to the process above. The resistivity of the aluminum is  $2.83 \times 10^{-8} \Omega \cdot \text{m}$ .

Problem 3.6: Compute the geometric mean radius of a steel conductor of outside diameter  $5/16$  in., resistivity  $10 \times 10^8 \Omega \cdot \text{m}$ , and relative permeability  $\mu_r = 50$ .



# 4

## Transmission Line Modeling Line Capacitance

### 4.1 INTRODUCTION

In this chapter we discuss methods by which the capacitance of a transmission line can be computed. For this purpose we employ an approach analogous to the one for computing the inductive reactance of a transmission line. Recall that for the computation of the inductive reactance, the magnetic field around the transmission line was examined. For the computation of the line capacitance, the electric field around the line will be examined. The source of this electric field is electric charge, which is deposited on the surface of the line conductors. The analysis of the electric field results in a model relating the electric charge and the conductor voltage. The time derivative of the total electric charge on the surface of the conductors is by definition the capacitive current (or the charging current) of the line. Utilizing this definition, the model can be transformed into a relationship between the line voltage and the capacitive current. The line capacitance can be extracted from this model.

This general approach will be utilized to introduce the analysis of capacitive phenomena in lines in a step-by-step procedure. Specifically, first the simplest case of a single circular conductor will be examined to establish the basic equation. Then the analysis will be extended to two parallel conductors and the general n-conductor line configuration.

#### 4.2 ELECTRIC FIELD AROUND A CIRCULAR INFINITELY LONG CONDUCTOR

In this section we examine the simple case of one circular infinitely long conductor. We shall assume that the conductor is electrically charged and we shall seek the relationship between the electric charge and the conductor voltage. Specifically, assume that the conductor is charged with electric charge  $q$  (coulombs per meter). Because of symmetry, the electric charge is uniformly distributed on the conductor surface. The electric charge generates an electric field around the conductor. Because of symmetry, the electric field intensity  $\underline{E}$  will be radially directed and the magnitude will depend only on the distance of the point of observation from the axis of the conductor, as illustrated in Fig. 4.1,

$$\underline{E} = E(r)\underline{a}_r \quad (4.1)$$

where  $\underline{a}_r$  is a unit vector in the radial direction  $r$ .

Consider a cylinder of length  $l$  and circular bases of radius  $r$ . The axis of the cylinder is taken on the axis of the conductor as in Fig. 4.1. Let  $S$  be the surface of the cylinder and  $V$  its volume. Application of Gauss's law yields

$$\iiint_V \rho \, dv = \iint_S \underline{D} \cdot d\underline{s} \quad (4.2)$$

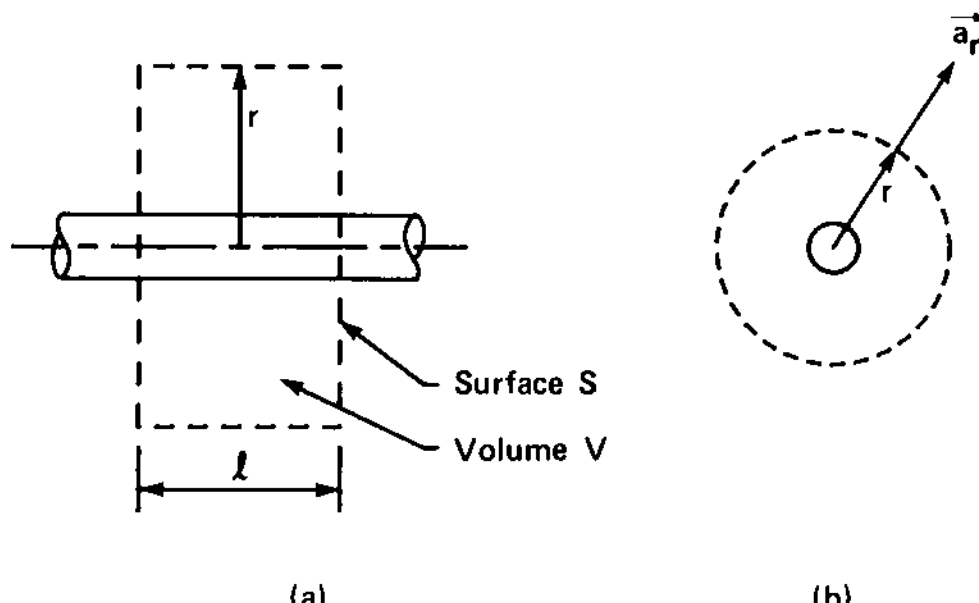


FIG. 4.1 An infinitely long circular conductor. (a) Side view, (b) cross section.

where

$\rho$  = electric charge density, C/m<sup>3</sup>

$\underline{D}$  = electric field density

$dv$  = infinitesimal volume

$d\underline{s}$  = infinitesimal surface area

The volume integral of the electric charge density inside the volume of the cylinder equals the total electric charge enclosed in the volume. It can be immediately computed by observing that electric charge exists only on the conductor surface at a density of  $q$  coulombs per meter. Thus

$$\iiint_V \rho dv = q\ell$$

The surface integral on the right-hand side of Eq. (4.2) is computed as follows:

$$\iint_S \underline{D} \cdot d\underline{s} = \iint_{S_1} \underline{D} \cdot d\underline{s} + \iint_{S_2} \underline{D} \cdot d\underline{s} + \iint_{S_3} \underline{D} \cdot d\underline{s}$$

where  $S_1$ ,  $S_2$  are the bases of the cylinder and  $S_3$  is the side surface of the cylinder. Note that because the electric field is radially directed, the contributions of the bases of the cylinder will vanish, that is,

$$\iint_{S_1} \underline{D} \cdot d\underline{s} = \iint_{S_2} \underline{D} \cdot d\underline{s} = 0$$

As has been discussed, the magnitude of the electric field intensity  $E$  and therefore  $D$  is a function of the radial distance  $r$  only. Thus on the surface  $S_3$ , the magnitude of the electric field density,  $D(r)$ , is constant. In addition, the vector  $\underline{D}$  is perpendicular to the surface  $S_3$  and thus parallel to  $d\underline{s}$ . Thus

$$\iint_{S_3} \underline{D} \cdot d\underline{s} = 2\pi r\ell D(r)$$

Substitution into Eq. (4.2) yields

$$q\ell = 2\pi r\ell D(r)$$

Upon solution for  $D(r)$ , we have

$$D(r) = \frac{q}{2\pi r} \quad (4.3)$$

If the permittivity of the medium is  $\epsilon$ , then

$$D(r) = \epsilon E(r)$$

and thus

$$E(r) = \frac{q}{2\pi\epsilon r} \quad (4.4)$$

The electric field inside the conductor is zero.

The computed electric field intensity provides the basis for computation of the potential difference between any two points A and B. This difference is called the voltage  $V_{AB}$  between points A and B, defined by

$$V_{AB} = \phi(A) - \phi(B) = \int_{C_{A \rightarrow B}} \underline{E}(r) \cdot d\underline{l}$$

If points A and B are located on the same radial direction, the computation of the line integral is straightforward.

$$\int_{C_{A \rightarrow B}} \underline{E}(r) \cdot d\underline{l} = \int_{r=r_A}^{r=r_B} E(r) dr = \frac{q}{2\pi\epsilon} \ln \frac{r_B}{r_A}$$

and therefore

$$V_{AB} = + \frac{q}{2\pi\epsilon} \ln \frac{r_B}{r_A} \quad (4.5)$$

Equation (4.5) relates the electric charge on the conductor to the potential difference between two points located at a radial distance  $r_B$  and  $r_A$ , respectively, from the axis of the conductor. Equation (4.5) is the basic equation utilized in the analysis of capacitance effects of transmission lines.

#### 4.3 ELECTRIC FIELD OF TWO PARALLEL INFINITELY LONG CIRCULAR CONDUCTORS

In this section we examine the electric field generated by two parallel infinitely long circular conductors charged with electric charge. For this purpose, consider two parallel infinitely long circular conductors.

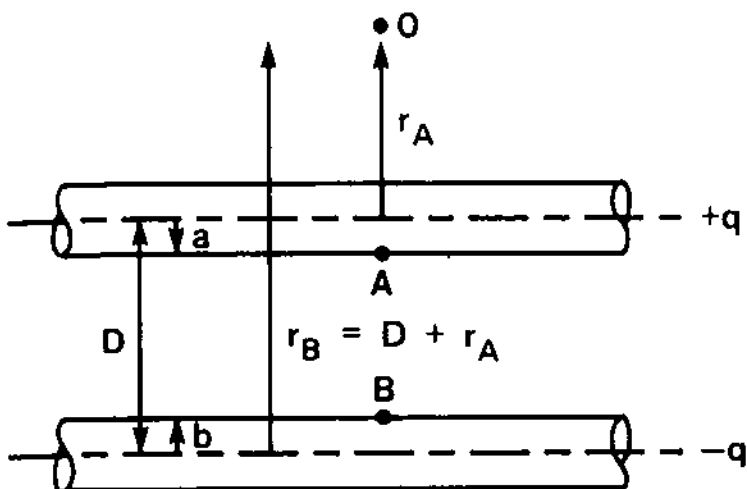


FIG. 4.2 Two parallel infinitely long circular conductors.

Assume that conductor 1 is charged with electric charge  $q$  (coulombs per meter), while conductor 2 is charged with  $-q$  (coulombs per meter). The system is illustrated in Fig. 4.2.

The distance between the axes of the two conductors is  $D$ , which is much greater than their radii  $a$  or  $b$ . In general, the presence of conductor 1 will affect the way the electric charge is distributed on the surface of conductor 2, and vice versa. Because  $D \gg a$  or  $b$ , it can be assumed that the distribution of the electric charge on each conductor is not affected by the presence of the other conductor. This assumption permits the utilization of the results of the preceding section and the analysis is simple. For overhead transmission lines, this analysis is also accurate. To justify the assumption, the exact solution will be given later and the quality of the approximation will be examined.

For the purpose of computing the potential difference between the two conductors, it suffices to compute the potential difference between any two points  $A$  and  $B$  located on the surface of the conductors. For simplicity, select two points  $A$  and  $B$  to be located on the surface of the conductors and on the plane through the axes of the conductors, as illustrated in Fig. 4.2. Next, the voltage between points  $A$  and  $B$  is computed by superposition and utilizing the results of the preceding section. Specifically, the contribution to the voltage from the electric charge  $+q$  of conductor 1 is

$$V_{AB}^+ = + \frac{q}{2\pi\epsilon} \ln \frac{r_B}{r_A} = + \frac{q}{2\pi\epsilon} \ln \frac{D - b}{a}$$

The contribution to the voltage from the electric charge  $-q$  of conductor 2 is

$$V_{AB}^- = -\frac{q}{2\pi\epsilon} \ln \frac{r'_B}{r'_A} = -\frac{q}{2\pi\epsilon} \ln \frac{b}{D-a}$$

The voltage between points A and B is

$$V_{AB} = V_{AB}^+ + V_{AB}^-$$

Upon substitution for  $V_{AB}^+$  and  $V_{AB}^-$ , we have

$$V_{AB} = \frac{q}{2\pi\epsilon} \ln \frac{(D-a)(D-b)}{ab}$$

By recalling that  $D \gg a, b$ , the expression for the voltage can be simplified:

$$V_{AB} = \frac{q}{2\pi\epsilon} \ln \frac{D^2}{ab} \quad (4.6)$$

The capacitance of the configuration of two conductors is

$$C = \frac{q}{V_{AB}} = \frac{2\pi\epsilon}{\ln(D^2/ab)} \quad \text{farads/meter} \quad (4.7)$$

Equation (4.7) provides the capacitance of two parallel conductors. In the derivation of this equation, it has been assumed that the conductors are far apart in such a way that the electric field of one does not affect the electric charge distribution on the other conductor. Thus the result above is approximate. The quality of this approximation is examined next.

#### 4.3.1 Quality of Approximation

The assumption that the electric charge distribution on one conductor is not affected by the presence of the other conductor is only approximately valid if  $D \gg a$ . To obtain a quantitative measure of the quality of the approximation, it is expedient to consider the exact solution and compare it with the approximate one. For this purpose we consider two parallel infinitely long identical conductors of radius  $a$  and located at a distance  $D$ . The system is illustrated in Fig. 4.3. The two conductors are charged with electric charge  $+q$  and  $-q$  per unit length, respectively. The exact solution for the electric field of this configuration is well known and illustrated in Fig. 4.3. Specifically, the electric field in the region between the two conductors is identical to the electric field generated by two line charges of density  $+q$  and  $-q$  per unit length, respectively, and located on the plane defined by the axes of the two conductors and at a distance  $y$  from their axes.

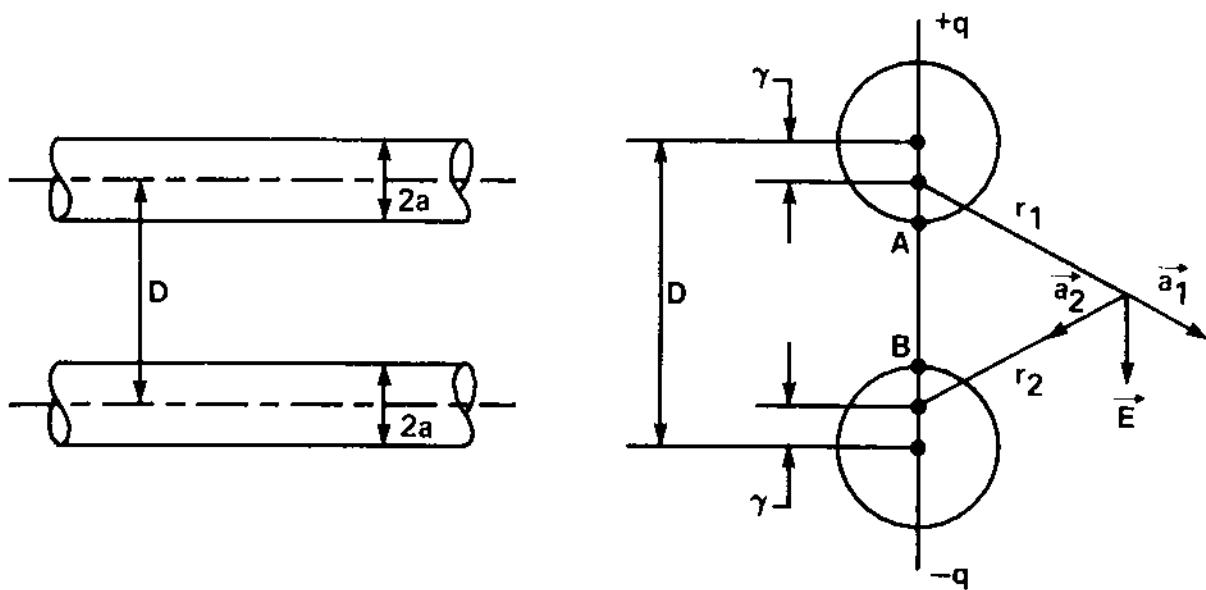


FIG. 4.3 The electric field of two parallel circular conductors.

The distance  $\gamma$  equals  $D/2 - \sqrt{(D/2)^2 - a^2}$ . The proof that this is the exact solution is based on the fact that the electric field of the two line charges generate two equipotential surfaces which coincide with the surfaces of the two conductors [3]. Thus the solution exactly matches the boundary conditions of the problem. The voltage between the two conductors equals the potential difference between any two points located on conductors 1 and 2, respectively. For simplicity, consider points A and B in Fig. 4.3. The voltage  $V_{AB}$  is

$$V_{AB} = \int_A^B \underline{E} \cdot d\underline{r} = \int_{r=a-\gamma}^{D-a-\gamma} \left[ \frac{q}{2\pi\epsilon r} + \frac{q}{2\pi\epsilon(D - 2\gamma - r)} \right] dr$$

Upon computation of the integral, we obtain

$$V_{AB} = \frac{q}{\pi\epsilon} \ln \frac{D - a - \gamma}{a - \gamma} \quad (4.8)$$

The exact capacitance of the configuration per unit length is

$$C_e = \frac{q}{V_{AB}} = \frac{\pi\epsilon}{\ln [(D - a - \gamma)/(a - \gamma)]} \quad (4.9)$$

Using the approximate formula (4.7), an error  $e$  is committed that is equal to

$$e = \ln \frac{D - a - \gamma}{a - \gamma} \left\{ \frac{1}{\ln(D/a)} - \frac{1}{\ln[(D - a - \gamma)/(a - \gamma)]} \right\} \quad (4.10)$$

**TABLE 4.1 Computational Error Due to the Assumption of Uniform Charge Distribution (Conductor Diameter: 2.54 cm)**

Separation D (cm)	r (cm)	Error e
3	0.70181	-0.310021
5	0.34661	-0.052421
10	0.16398	-0.008012
20	0.08097	-0.001473
30	0.05386	-0.000592
100	0.01613	-0.000037

As an example, consider two conductors of 1 in. (2.54 cm) in diameter. The error as a function of the separation distance D is given in Table 4.1. Note that when the separation distance becomes four times the diameter, the error is less than 1%. For larger separations, the error becomes negligibly small for practical applications. For typical overhead transmission lines, the separation distance between conductors is much larger than their radius. Thus the assumption of uniform charge distribution at the presence of neighboring conductors in overhead transmission lines is quite accurate. However, for three-phase cables, the conductors are much closer together (approximately one diameter). Thus in three-phase cables, this assumption may incur a substantial error. In subsequent analyses for the purpose of computing the capacitance of overhead lines, the simplified equations will be utilized.

#### 4.4 CAPACITANCE OF A GENERAL N-CONDUCTOR OVERHEAD TRANSMISSION LINE

Consider a configuration of n conductors which are parallel and infinitely long. The conductor cross section is circular. Figure 4.4 shows a cross section of the configuration. Assume that electric charge  $q_i(t)$  per unit length has been accumulated on the surface of conductor i which is uniformly distributed over the surface of the conductor. As a first step, we consider the potential of conductor i with respect to an arbitrarily selected point of reference X, which is illustrated in Fig. 4.4. For this purpose the principle of superposition and the results of Section 4.2 are employed to yield

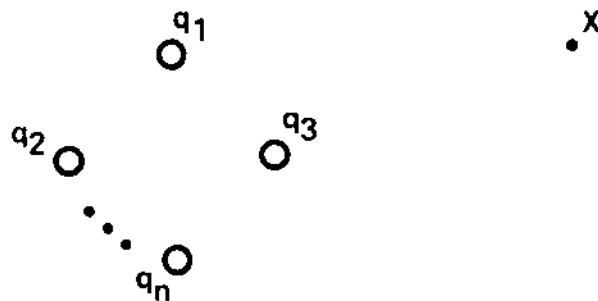


FIG. 4.4 A general configuration of  $n$  parallel circular conductors.

$$e_i(t) = \phi_i(t) - \phi_x(t) = \frac{1}{2\pi\epsilon} \sum_{j=1}^n q_j(t) \ln \frac{D_{jx}}{D_{ij}} \quad (4.11)$$

where

- $D_{ij}$  = distance between the axes of conductors  $i$  and  $j$
- $D_{jx}$  = distance between the axis of conductor  $j$  and point  $x$
- $\phi_i(t)$  = potential of conductor  $i$  at time  $t$
- $\phi_x(t)$  = potential of point  $X$  at time  $t$

Note that  $D_{ii} = a_i$ , the radius of the conductor  $i$ .

Equation (4.11) expresses the potential difference between conductor  $i$  and an arbitrarily selected point  $X$ . If point  $X$  is taken to infinity, the voltage  $e_i(t)$  will become the absolute voltage of the conductor. To derive the absolute voltage of conductor  $i$ , the general expression for  $e_i(t)$  is rewritten as

$$e_i(t) = \frac{1}{2\pi\epsilon} \sum_{j=1}^n q_j(t) \ln \frac{1}{D_{ij}} + \frac{1}{2\pi\epsilon} \sum_{j=1}^n q_j(t) \ln D_{jx}$$

Now observe that if the  $n$  conductors are the only objects with electric charge, the sum of the electric charges,  $q_1(t), \dots, q_n(t)$ , must equal zero, that is,

$$\sum_{j=1}^n q_j(t) = 0 \quad (4.12)$$

In this case it can be shown that

$$\lim_{x \rightarrow \infty} \sum_{j=1}^n q_j(t) \ln D_{jx} \rightarrow 0 \quad (4.13)$$

Then the absolute voltage of conductor i is

$$e_i(t) = \sum_{j=1}^n \frac{q_j(t)}{2\pi\epsilon} \ln \frac{1}{D_{ij}} \quad (4.14)$$

The proof of the limit of Eq. (4.13) follows.

Proof: Equation (4.12) is solved for  $q_n(t)$ :

$$q_n(t) = - \sum_{j=1}^{n-1} q_j(t)$$

Upon substitution in Eq. (4.13), we have

$$\begin{aligned} \sum_{j=1}^n q_j(t) \ln D_{jx} &= \sum_{j=1}^{n-1} q_j(t) \ln D_{jx} - \ln D_{nx} \sum_{j=1}^{n-1} q_j(t) \\ &= \sum_{j=1}^{n-1} q_j(t) \ln \frac{D_{jx}}{D_{nx}} \end{aligned}$$

As  $x \rightarrow \infty$ ,  $D_{jx}$ ,  $D_{nx} \rightarrow \infty$  and the ratios  $D_{jx}/D_{nx} \rightarrow 1.0$ . Thus

$$\lim_{x \rightarrow \infty} \sum_{j=1}^n q_j(t) \ln D_{jx} = \lim_{x \rightarrow \infty} \sum_{j=1}^{n-1} q_j(t) \ln \frac{D_{jx}}{D_{nx}} = 0$$

It is expedient to repeat the assumptions under which Eq. (4.14) has been obtained:

Assumption 1:  $\sum_{j=1}^n q_j = 0$

Assumption 2:  $D_{ij} \gg a_i$   
 $i \neq j$

The first assumption is valid for any transmission line configuration, assuming that all conductors have been accounted for. For overhead lines, since the conducting soil represents one of the conductors, this means that the earth must be also accounted for. The second assumption is always valid for overhead circuits. For cables, it introduces an error depending on cable configuration.

Equation (4.14) can be transformed into an equation relating the conductor capacitive current to the conductor voltage. For this purpose, Eq. (4.14) is differentiated with respect to time.

$$\frac{de_i(t)}{dt} = \sum_{j=1}^n \frac{1}{2\pi\epsilon} \frac{dq_j(t)}{dt} \ln \frac{1}{D_{ij}}$$

By definition, the time derivative of the conductor electric charge is the capacitive current (or charging current):

$$\frac{dq_j(t)}{dt} \stackrel{\Delta}{=} i'_j(t) \quad \text{capacitive current of conductor } j$$

Upon substitution, we have

$$\frac{de_i(t)}{dt} = \sum_{j=1}^n \frac{i'_j(t)}{2\pi\epsilon} \ln \frac{1}{D_{ij}} \quad i = 1, 2, \dots, n \quad (4.15)$$

Equation (4.15) is the basic equation for modeling the capacitive effects of a multiconductor power line. For sinusoidal steady-state analysis, Eq. (4.15) is converted into an algebraic equation. For this purpose, recall that under sinusoidal steady-state conditions, the voltages and currents will have the following general time variation:

$$e_i(t) = \operatorname{Re}\{\sqrt{2} \tilde{E}_i e^{j\omega t}\}$$

$$i'_j(t) = \operatorname{Re}\{\sqrt{2} \tilde{I}'_j e^{j\omega t}\}$$

where  $\tilde{E}_i$  and  $\tilde{I}'_j$  are complex numbers representing the phasors of the voltage and the capacitive current. Substitution in Eq. (4.15) and solution for  $\tilde{E}_i$  gives us

$$\tilde{E}_i = \sum_{j=1}^n \frac{\tilde{I}'_j}{j\omega 2\pi\epsilon} \ln \frac{1}{D_{ij}} \quad i = 1, 2, \dots, n \quad (4.16)$$

where  $D_{ij} = a_i$ , the radius of conductor i.

It is expedient to define the following quantities:

$$x'_{ij} = \frac{1}{j\omega 2\pi\epsilon} \ln D_{ij} \quad i \neq j \quad \text{ohm-meters} \quad (4.17a)$$

$$x'_{ii} = \frac{1}{j\omega 2\pi\epsilon} \ln \frac{1}{a_i} \quad \text{ohm-meters} \quad (4.17b)$$

which will be called the separation component of the capacitive reactance and the conductor component of the capacitive reactance, respectively. These quantities depend on the geometry and material of the transmission line and the frequency of the voltage. In terms of the components of the capacitive reactance, Eq. (4.16) takes the following simple form:

$$\tilde{E}_i = x'_{ii} \tilde{I}_i - \sum_{\substack{j=1 \\ j \neq i}}^n x'_{ij} \tilde{I}_j \quad (4.18)$$

As we shall see in the next section, the components of capacitive reactance for all commercially available conductors have been tabulated. As in the case of the components of inductive reactance, note that the mathematically rigorous reader will be offended by the expressions for  $x'_{ii}$  and  $x'_{ij}$  since they involve the terms  $\ln(1/a_i)$  and  $\ln(D_{ij})$ . It should be observed that if the quantities  $a_i$  and  $D_{ij}$  are expressed in the same unit, the final result will be correct. For this reason it has been accepted that  $a_i$  and  $D_{ij}$  will be expressed in feet under the understanding that each quantity  $x'_{ii}$ ,  $x'_{ij}$  is meaningless if considered individually.

In summary, the capacitive effects of a power line are represented with Eq. (4.15). Specifically, for each conductor in a power line one equation can be written relating the capacitive current of the conductors and the time derivative of the conductor voltage. For sinusoidal steady-state analysis, these equations are converted into a set of algebraic equations [Eq. (4.18)] relating the phasors of the conductor capacitive currents to the phasor of the conductor voltage.

#### 4.5 PRACTICAL CONSIDERATIONS: USE OF TABLES

The preceding analysis suggests that the capacitive currents of a transmission line can readily be computed with the aid of the capacitive reactance components  $x'_{ii}$  and  $x'_{ij}$ . As in the case of inductive reactances, extensive tables have been developed for the absolute

value of  $x'_{ij}$  for all commercially available conductors and the normal operating frequency of power systems. The tables have been generated under the assumption that the radius  $a_i$  and the distance  $D_{ij}$  are entered in feet and the capacitive reactance is computed in megohm-miles. Specifically, Eqs. (4.17) have been simplified by substituting the constants  $\epsilon = 8.854 \times 10^{-12} \text{ F/m}$ ,  $\pi = 3.14159$ ,  $\omega = 2\pi f$ ,  $\ln x = 2.3026 \log x$ , and subsequent conversion of the units, yielding

$$x'_{ij} = \frac{4.1}{jf} \log D_{ij} \quad i \neq j \quad \text{megohm-miles} \quad (4.19a)$$

$$x'_{ii} = \frac{4.1}{jf} \log \frac{1}{a_i} \quad \text{megohm-miles} \quad (4.19b)$$

where  $f$  is in hertz,  $a_i$ ,  $D_{ij}$  in feet, and  $\log$  represents the base 10 logarithm. Tables of capacitive reactance components for the most commonly used power conductors are given in Appendix A.

## 4.6 APPLICATIONS

Equation (4.18) is the basis for the analysis of all phenomena related to the capacitance of a transmission line. In this section we present examples of applications of the basic formula (4.18).

### 4.6.1 Single-Phase Line

A single-phase line is illustrated in Fig. 4.5. Our objective is to compute the capacitive current of the single-phase line. To simplify the procedure, it will be assumed that the voltage of the conductors  $a$  and  $b$  is  $\tilde{E}_a$ ,  $\tilde{E}_b$ , respectively, and that the voltage is constant

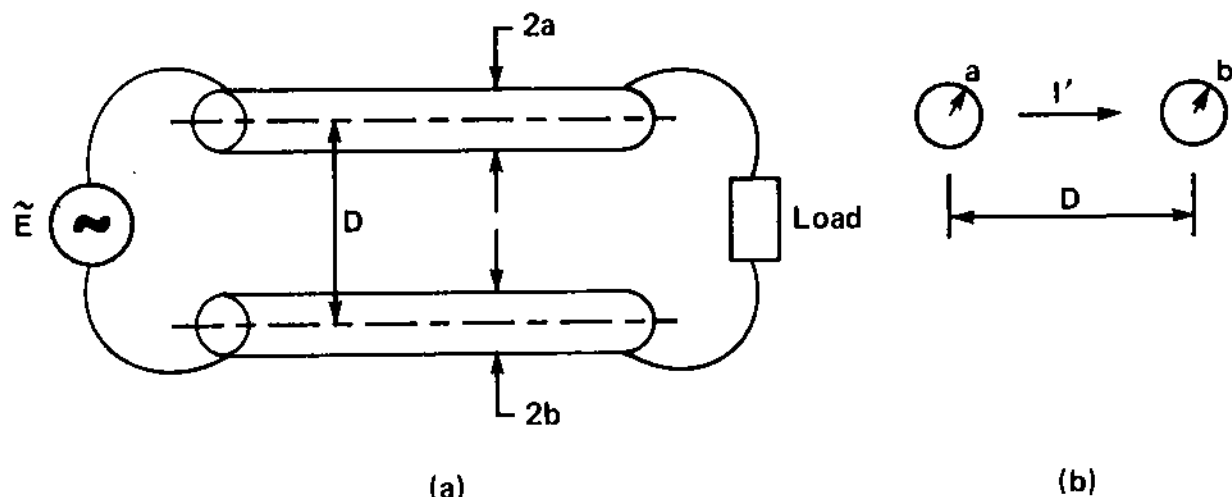


FIG. 4.5 A single-phase line. (a) Side view, (b) cross section.

throughout the length of the line. Assuming sinusoidal steady state and upon application of Eq. (4.18), we obtain

$$\begin{aligned}\tilde{E}_a &= x'_{aa} I'_a - x'_{ab} I'_b \\ \tilde{E}_b &= -x'_{ab} I'_a + x'_{bb} I'_b\end{aligned}$$

where

$$x'_{aa} = \frac{1}{j\omega 2\pi\epsilon} \ln \frac{1}{a}$$

$$x'_{bb} = \frac{1}{j\omega 2\pi\epsilon} \ln \frac{1}{b}$$

$$-x'_{ab} = \frac{1}{j\omega 2\pi\epsilon} \ln D$$

Assuming that there are not other conductors in the vicinity of this line yields

$$\tilde{I}'_a = -\tilde{I}'_b = \tilde{I}'$$

Then

$$\tilde{E}_a = (x'_{aa} + x'_{ab}) \tilde{I}'$$

$$\tilde{E}_b = -(x'_{ab} + x'_{bb}) \tilde{I}'$$

The potential difference between the two conductors is equal to the source voltage  $\tilde{E}$ . Thus

$$\tilde{E} = \tilde{E}_a - \tilde{E}_b = (x'_{aa} + x'_{bb} + 2x'_{ab}) \tilde{I}'$$

Thus the capacitive reactance of the line is

$$x'_1 = x'_{aa} + x'_{bb} + 2x'_{ab} = \frac{1}{j\omega 2\pi\epsilon} \ln \frac{D^2}{a \cdot b}$$

The capacitive current of the line is

$$\tilde{I}' = \frac{\tilde{E}}{x'_1} \quad (4.20)$$

Example 4.1: Consider a single-phase line consisting of 556,500-cm ACSR conductors with 30 strands located 18 ft apart. The

operating voltage of the line is 115 kV, 60 Hz. Compute the capacitive reactance and the capacitive current of the line.

Solution: The parameters of the conductor are obtained from Table A.2. The outside diameter is 0.953 in. The listed parameter  $x'_{kk}$  is

$$x'_{kk} = -j0.0956 \text{ M}\Omega\cdot\text{mi} \text{ at } 60 \text{ Hz}$$

The parameter  $x'_{kk}$  can be also computed as follows:

$$x'_{kk} = -j \frac{1}{\omega 2\pi\epsilon} \ln \frac{1}{a} = -j153.5 \text{ M}\Omega\cdot\text{m} = -j0.0954 \text{ M}\Omega\cdot\text{mi}$$

Since the separation distance D is 18 ft, the component  $x'_{ik}$  is computed.

$$x'_{ik} = -j \frac{1}{\omega 2\pi\epsilon} \ln (D) = -j137.8 \text{ M}\Omega\cdot\text{m} = -j0.0856 \text{ M}\Omega\cdot\text{mi}$$

The capacitive reactance of the line is

$$x'_l = -j2(0.0956 + 0.0859) \text{ M}\Omega\cdot\text{mi} = -j0.3630 \text{ M}\Omega\cdot\text{mi}$$

The capacitive current of the line is

$$\tilde{I}' = \frac{115 \text{ kV}}{-j0.363 \text{ M}\Omega\cdot\text{mi}} = j0.3168 \text{ A/mi}$$

#### 4.6.2. Three-Phase Line

Figure 4.6 illustrates a three-phase line without ground wires. Assume that there are no other conductors in the vicinity of the line.

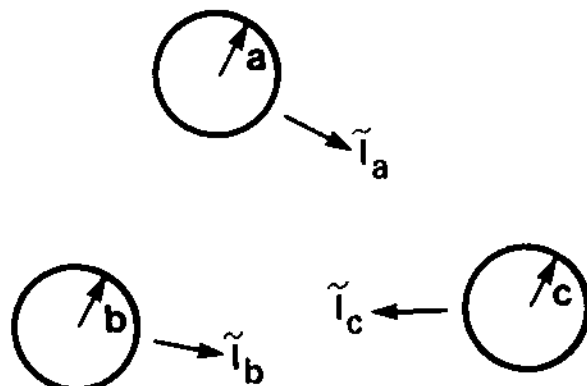


FIG. 4.6 Three-phase line without ground wire.

The operating voltage of the three conductors is  $\tilde{E}_a$ ,  $\tilde{E}_b$ , and  $\tilde{E}_c$ , respectively. For the purpose of computing the capacitive reactance and currents of the line, the general equation (4.18) is applied on each of the three conductors, yielding

$$\begin{aligned}\tilde{E}_a &= x'_{aa} \tilde{I}'_a - x'_{ab} \tilde{I}'_b - x'_{ac} \tilde{I}'_c \\ \tilde{E}_b &= -x'_{ab} \tilde{I}'_a + x'_{bb} \tilde{I}'_b - x'_{bc} \tilde{I}'_c \\ \tilde{E}_c &= -x'_{ac} \tilde{I}'_a - x'_{bc} \tilde{I}'_b + x'_{cc} \tilde{I}'_c\end{aligned}$$

where

$$\begin{aligned}x'_{aa} &= \frac{1}{j\omega 2\pi\epsilon} \ln \frac{1}{a} \\ x'_{bb} &= \frac{1}{j\omega 2\pi\epsilon} \ln \frac{1}{b} \\ x'_{cc} &= \frac{1}{j\omega 2\pi\epsilon} \ln \frac{1}{c} \\ x'_{ab} &= \frac{1}{j\omega 2\pi\epsilon} \ln D_{ab} \\ x'_{ac} &= \frac{1}{j\omega 2\pi\epsilon} \ln D_{ac} \\ x'_{bc} &= \frac{1}{j\omega 2\pi\epsilon} \ln D_{bc}\end{aligned}$$

Since the three conductors are alone in free space,  $\tilde{I}'_a + \tilde{I}'_b + \tilde{I}'_c = 0$ . Simultaneous solution of the set of equations yields the capacitive currents,  $\tilde{I}'_a$ ,  $\tilde{I}'_b$ ,  $\tilde{I}'_c$ :

$$\tilde{I}'_a = \frac{x'_c \tilde{E}_{ba} - x'_b \tilde{E}_{ac}}{A} \quad (4.21a)$$

$$\tilde{I}'_b = \frac{x'_a \tilde{E}_{cb} - x'_c \tilde{E}_{ba}}{A} \quad (4.21b)$$

$$\tilde{I}'_c = \frac{x'_b \tilde{E}_{ac} - x'_a \tilde{E}_{cb}}{A} \quad (4.21c)$$

where

$$\tilde{E}_{ij} = \tilde{E}_j - \tilde{E}_i$$

$$A = x'_a x'_b + x'_b x'_c + x'_a x'_c$$

$$x'_a = x'_{aa} + x'_{ab} + x'_{ac} - x'_{bc}$$

$$x'_b = x'_{bb} + x'_{ba} + x'_{bc} - x'_{ac}$$

$$x'_c + x'_{cc} + x'_{ac} + x'_{bc} - x'_{ab}$$

Typically, the three conductors of a three-phase line are identical (i.e.,  $a = b = c$ ). Now consider, as a special case, that the three-phase conductors are located on the vertices of an equilateral triangle (i.e.,  $D_{ab} = D_{bc} = D_{ac} = D$ ). As we have seen in Chapter 2, this is a symmetric three-phase line. For this line Eqs. (4.21) are simplified to

$$\tilde{I}'_a = \frac{\tilde{E}_{ba} - \tilde{E}_{ac}}{3(x'_s + x'_m)} = \frac{\tilde{E}_a}{x'_s + x'_m} \quad (4.22a)$$

$$\tilde{I}'_b = \frac{\tilde{E}_{cb} - \tilde{E}_{ba}}{3(x'_s + x'_m)} = \frac{\tilde{E}_b}{x'_s + x'_m} \quad (4.22b)$$

$$\tilde{I}'_c = \frac{\tilde{E}_{ac} - \tilde{E}_{cb}}{3(x'_s + x'_m)} = \frac{\tilde{E}_c}{x'_s + x'_m} \quad (4.22c)$$

where

$$x'_s = x'_{aa} = x'_{bb} = x'_{cc}$$

$$x'_m = x'_{ab} = x'_{ac} = x'_{bc}$$

Equations (4.22) indicate that in a symmetric three-phase line, the capacitive current of each conductor is proportional to its voltage. In other words, each phase exhibits the same capacitive reactance, which is equal to

$$x'_1 = x'_s + x'_m = \frac{1}{j\omega 2\pi\epsilon} \ln \frac{D}{a} \quad (4.23)$$

Equations (4.22) also suggest that the symmetric three-phase line can be represented with the equivalent circuit of Fig. 4.7.

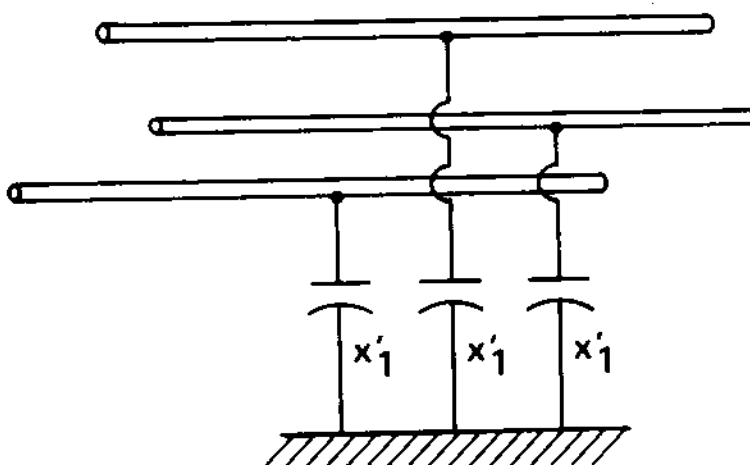


**FIG. 4.7** Equivalent capacitive circuit of a symmetric three-phase line.

#### 4.7 EFFECTS OF EARTH AND NEUTRAL/GROUND WIRES

Most overhead transmission lines have ground wires to protect them against lightning. Overhead distribution lines have neutral conductors for unbalanced current return. All overhead power lines are suspended above earth. Neutral/ground wires and the earth are conducting media in the vicinity of the line which may be charged with electric charge due to the electric field of the line. Alternatively, these conducting media alter the electric field of the line and affect the capacitance of the line. In this section we examine methods by which the effects of earth and neutral or overhead ground wires on line capacitance can be quantified.

The effect of neutral/ground wires can be computed in a straightforward way by treating these wires in the same way as the phase conductors. It should be observed that the voltage of the neutral/ground wires will be much different from the voltage of the phase conductors. Actually, the voltage of neutral or ground wires is approximately zero at normal operating conditions. For usual applications it is assumed that the voltage of neutral or ground wires is exactly zero.

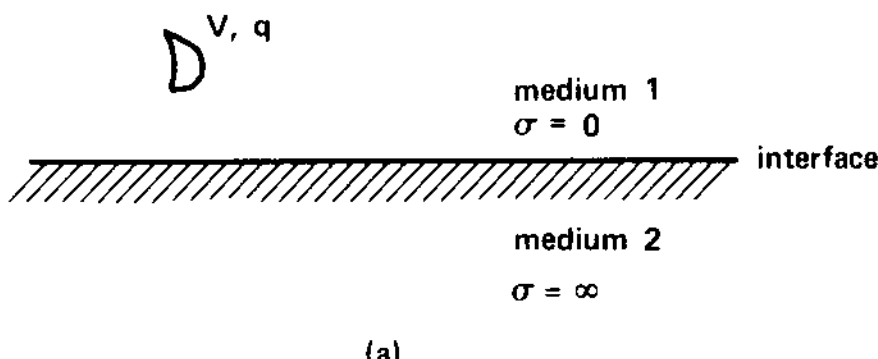
Computation of the effect of earth on the capacitive reactance of a line, in general, is a difficult problem. To simplify the analysis, it is assumed that the earth is a semi-infinite perfectly conducting medium. In this case the theory of images is applied directly, yielding a rather simple analysis procedure. Specifically, the problem of a transmission line located above earth is replaced with another equivalent problem which does not include the earth, but includes the images of the conductors with respect to the surface of the earth. In

subsequent paragraphs, the theory of images is reviewed and its application to the problem mentioned is demonstrated.

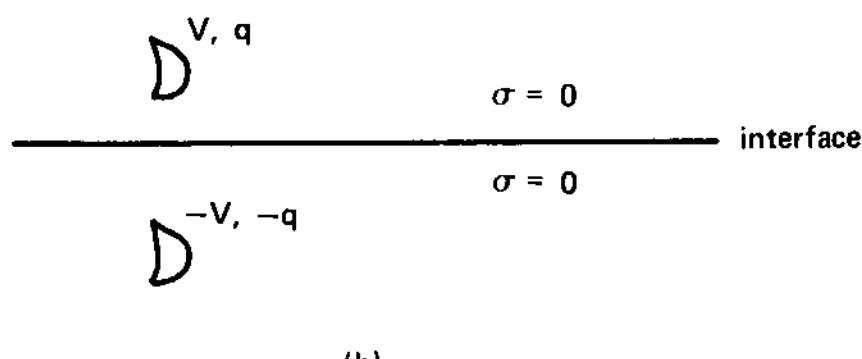
#### 4.7.1 Theory of Images

Consider a space consisting of two media: a nonconducting and a highly conducting medium. Assume the interface to be a plane, as illustrated in Fig. 4.8a. Further assume that in the nonconducting medium, there are objects that are charged with electric charge. Such an object of arbitrary shape is illustrated in Fig. 4.8a. The charged object will establish an electric field in medium 1. The electric field in medium 2 will be zero since medium 2 is a perfect conductor.

The theory of images [3] guarantees that the electric field in the space of medium 1 established by the charged objects is identical to the electric field generated by two objects located in the free space, as illustrated in Fig. 4.8b. The second object is the geometric image of the actual object with respect to the plane interface of the two media. If the electric charge on the object is  $q$ , the electric charge of the image is  $-q$ . This condition guarantees that the electric field intensity on the interface will be perpendicular to the plane interface.



(a)



(b)

FIG. 4.8 Application of the theory of images. (a) Physical configuration, (b) equivalent configuration.

Thus the boundary conditions of the problem are matched. A consequence of this condition is that if the voltage of the object is  $V$ , the voltage of its image will be  $-V$ .

#### 4.7.2 Application of the Theory of Images to Overhead Transmission Lines

Consider the general transmission line suspended above earth, as illustrated in Fig. 4.9a. Application of the theory of images results in the equivalent configuration of Fig. 4.9b. Subsequently, the capacitive currents of the conductors are computed as follows: The voltages of the conductors,  $\tilde{V}_1, \tilde{V}_2, \dots$ , are expressed in terms of the capacitive currents  $\tilde{I}_1, \tilde{I}_2, \dots$ . In this analysis the capacitive currents of the images are also included.

$$\tilde{V}_i = - \sum_{\substack{j=1 \\ j \neq i}}^n x'_{ij} \tilde{I}'_j + x'_{ii} \tilde{I}'_i + \sum_{j=1}^n x'_{ij'} \tilde{I}'_j \quad i = 1, 2, \dots, n \quad (4.24)$$

where

$$x'_{ij} = \frac{1}{j\omega 2\pi\epsilon} \ln D_{ij}$$

$$x'_{ij'} = \frac{1}{j\omega 2\pi\epsilon} \ln D_{ij'}$$

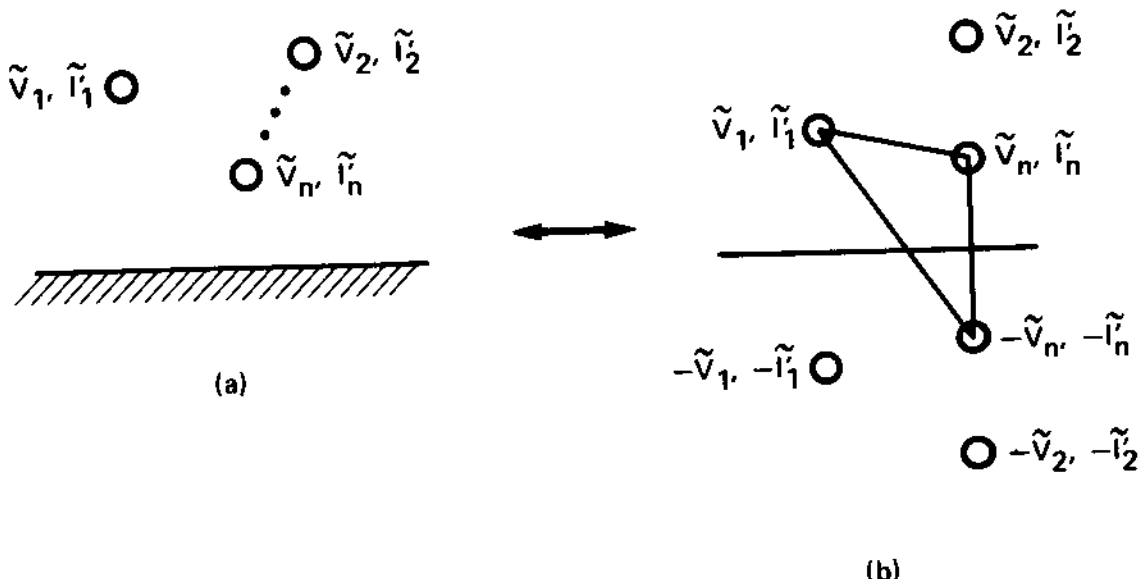


FIG. 4.9 General transmission line above ground. (a) Line geometr  
(b) line conductors and conductor images.

and

- $D_{ij}$  = distance between conductors  $i, j$
- $D_{ij'}$  = distance between conductor  $i$  and the image of conductor  $j$  (which is the same as the distance between conductor  $j$  and the image of conductor  $i$ )

Equation (4.24) is rewritten in a compact form.

$$\tilde{V}_i = - \sum_{\substack{j=1 \\ j \neq i}}^n (x'_{ij} - x'_{ij'}) \tilde{I}'_j + (x'_{ii} + x'_{ii'}) \tilde{I}'_i \quad i = 1, 2, \dots, n$$

Note that

$$\begin{aligned} x'_{ij} - x'_{ij'} &= \frac{1}{j\omega 2\pi\epsilon} (\ln D_{ij} - \ln D_{ij'}) = \frac{1}{j\omega 2\pi\epsilon} \ln \frac{D_{ij}}{D_{ij'}} \\ x'_{ii} + x'_{ii'} &= \frac{1}{j\omega 2\pi\epsilon} (\ln \frac{1}{a} + \ln D_{ii'}) = \frac{1}{j\omega 2\pi\epsilon} \ln \frac{D_{ii'}}{a_i} \end{aligned}$$

Then

$$\tilde{V}_i = \frac{\tilde{I}'_i}{j\omega 2\pi\epsilon} \ln \frac{D_{ii'}}{a_i} - \sum_{\substack{j=1 \\ j \neq i}}^n \frac{\tilde{I}'_j}{j\omega 2\pi\epsilon} \ln \frac{D_{ij}}{D_{ij'}} \quad i = 1, 2, \dots, n \quad (4.25)$$

Assuming that the voltages  $\tilde{V}_i$ ,  $i = 1, \dots, n$ , are known, Eq. (4.25) is solved to provide the capacitive currents  $\tilde{I}'_i$ ,  $i = 1, 2, \dots, n$ . The earth will also carry a capacitive current,  $\tilde{I}'_e$ , which is given by the equation

$$\tilde{I}'_e = \sum_{i=1}^n \tilde{I}'_i$$

The procedure is illustrated with an example involving a single-phase line.

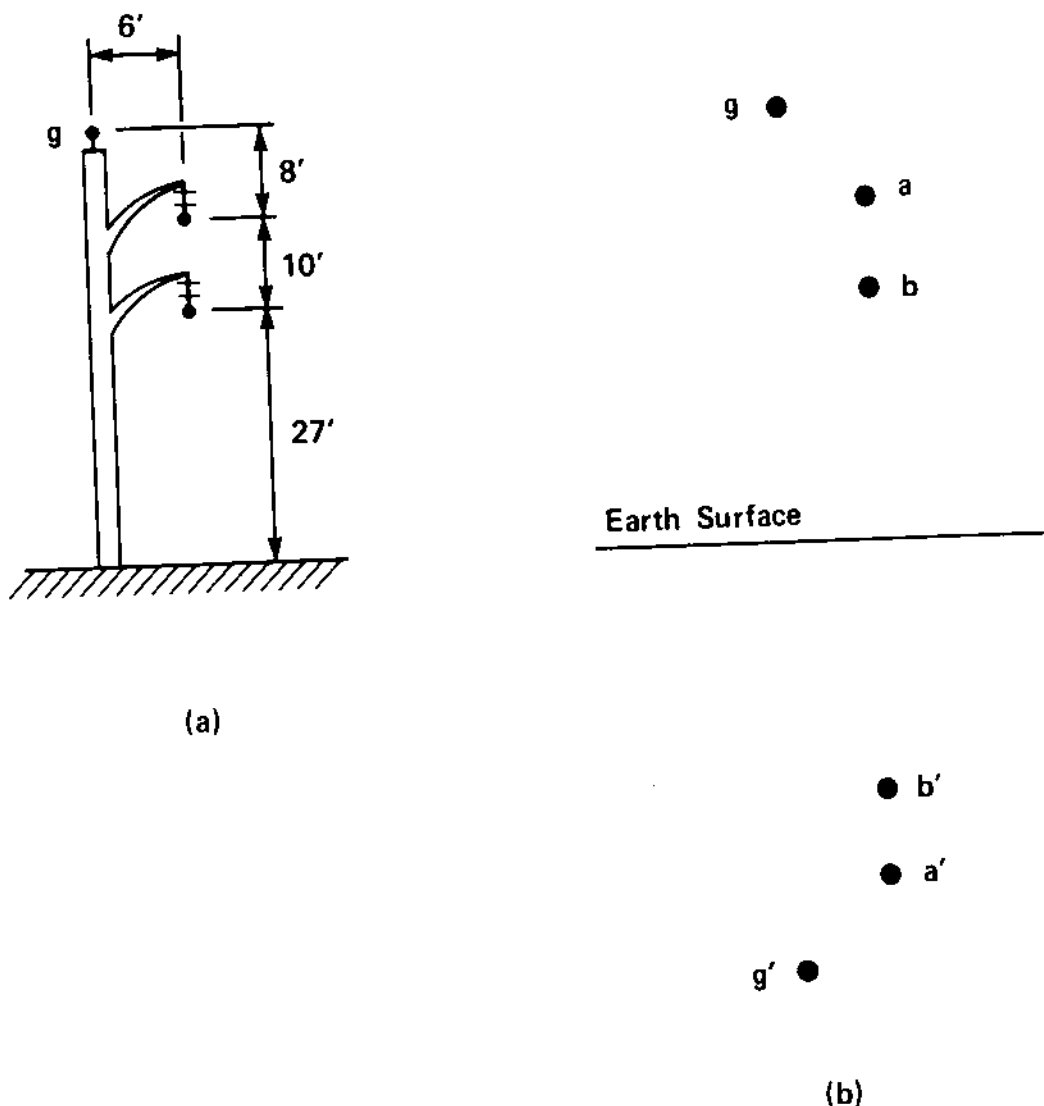


FIG. E4.1 A single-phase line. (a) Line geometry, (b) conductors and images.

Example 4.2: Compute the capacitive currents of the single-phase line of Fig. E4.1a. The line consists of 300-kcm ACSR phase conductors with 26 strands. The shield wire is 4/0, ACSR, 6 strands. The line operates symmetrically at 115 kV and 60 Hz. The overhead ground wire is grounded. Thus assume that its voltage is zero.

Solution: Let the capacitive currents of the conductors be  $\tilde{I}_a$ ,  $\tilde{I}_b$ ,  $\tilde{I}_g$ . Upon application of the theory of images, the relationship among the capacitive currents and the conductor voltages are

$$\begin{aligned}\tilde{E}_a &= \frac{1}{j\omega 2\pi\epsilon} \left( \tilde{I}'_a \ln \frac{D_{aa'}}{r_a} - \tilde{I}'_b \ln \frac{D_{ab}}{D_{ab'}} - \tilde{I}'_g \ln \frac{D_{ag}}{D_{ag'}} \right) \\ \tilde{E}_b &= \frac{1}{j\omega 2\pi\epsilon} \left( -\tilde{I}'_a \ln \frac{D_{ab}}{D_{a'b}} + \tilde{I}'_b \ln \frac{D_{bb'}}{r_b} - \tilde{I}'_g \ln \frac{D_{bg}}{D_{bg'}} \right) \\ \tilde{E}_g &= \frac{1}{j\omega 2\pi\epsilon} \left( -\tilde{I}'_a \ln \frac{D_{ga}}{D_{ga'}} - \tilde{I}'_b \ln \frac{D_{gb}}{D_{gb'}} + \tilde{I}'_g \ln \frac{D_{gg'}}{r_g} \right)\end{aligned}$$

Since the line operates symmetrically and the shield wire is grounded,

$$\tilde{E}_g = 0$$

$$\tilde{E}_a = \frac{115 \text{ kV}}{2} = 57.5 \text{ kV}$$

$$\tilde{E}_b = -\frac{115 \text{ kV}}{2} = -57.5 \text{ kV}$$

The distances in feet are taken from Fig. E4.1b.

$$D_{aa'} = 74 \text{ ft}$$

$$D_{bb'} = 54 \text{ ft}$$

$$D_{gg'} = 90 \text{ ft}$$

$$D_{ag'} = D_{a'g} = 82.219 \text{ ft}$$

$$D_{bg'} = D_{b'g} = 72.25 \text{ ft}$$

$$D_{ab'} = D_{a'b} = 64 \text{ ft}$$

$$D_{ab} = 10 \text{ ft}$$

$$D_{ag} = 10 \text{ ft}$$

$$D_{bg} = 18.9736 \text{ ft}$$

From Table A.2:

$$r_a = r_b = \frac{0.68}{24} = 0.02833 \text{ ft}$$

$$r_g = \frac{0.563}{24} = 0.023458 \text{ ft}$$

Upon substitution of numerical values,

$$j1.2059 \times 10^{-3} = 7.8678\tilde{I}'_a + 1.8563\tilde{I}'_b + 2.1068\tilde{I}'_g$$

$$-j1.2059 \times 10^{-3} = 1.8563\tilde{I}'_a + 7.5528\tilde{I}'_b + 1.337\tilde{I}'_g$$

$$0 = 2.1068\tilde{I}'_a + 1.337\tilde{I}'_b + 8.252\tilde{I}'_g$$

The solution to the system of equations above is

$$\tilde{I}'_a = j0.20734 \times 10^{-3} \text{ A/m} = j0.3336 \text{ A/mi}$$

$$\tilde{I}'_b = -j0.20719 \times 10^{-3} \text{ A/m} = -j0.3333 \text{ A/mi}$$

$$\tilde{I}'_g = -j0.01937 \times 10^{-3} \text{ A/m} = -j0.0312 \text{ A/mi}$$

The capacitive current  $\tilde{I}'_e$  of the earth is

$$\tilde{I}'_e = -\tilde{I}'_a - \tilde{I}'_b - \tilde{I}'_g = j0.0309 \text{ A/mi} \bullet$$

#### 4.8 SUMMARY AND DISCUSSION

In this chapter we have examined the phenomena relating to the electric field around a transmission line. The electric field is generated by electric charge which accumulates on the surface of the line conductors as well as the surface of the earth. In transmission lines operating under ac voltage, the electric charge varies with time as the voltage varies with time. The time derivative of the electric charge is the capacitive (or charging) current of the line conductors. A relationship has been developed which relates the instantaneous value of a conductor voltage to the electric charges on the conductors of the line [Eq. (4.14)]. For sinusoidal steady-state analysis, this relationship is transformed into Eq. (4.18), which relates the phasor of a conductor voltage to the capacitive currents of the line conductors. These two equations provide the basic tool to determine line capacitive currents and line capacitance. The effects of earth are accounted with the use of the method of images. In this case Eq. (4.25) provides the relationship between the phasor of a conductor voltage to the capacitive currents of the line conductors. Equation (4.25) is the basic analysis tool for the capacitive effects of overhead transmission lines.

#### 4.9 PROBLEMS

Problem 4.1: A dc transmission line consists of two solid copper conductors a, b of diameter 1.5 in. The conductors are 50 ft above ground and at a distance of 30 ft between centers. A third (ground return) conductor, g, is located 60 ft above ground and symmetrical-  
ly arranged with respect to conductors a and b. The diameter of conductor g is 1.0 in. The voltages of conductors a and b are  $E_a = 250 \text{ kV}$  and  $E_b = -250 \text{ kV}$ , respectively.

- (a) Calculate the electric charge of conductors a, b, and g, neglecting the effect of ground.
- (b) Calculate the electric charge of conductors a, b, and g without neglecting the effect of ground.

Probelm 4.2: A voltage of 46 kV (rms, 60 Hz) is applied between two parallel, long, conducting cylinders of  $\frac{1}{2}$  in. diameter each and spaced D feet between centers. If the electric field intensity on the surface of the conductors is not to exceed 12 kV/cm, compute the minimum allowable spacing D between the centers of the conductors.

Problem 4.3: A three-phase transmission line consisting of  $\frac{1}{2}$ -in.-diameter solid copper conductors arranged horizontally 10 ft apart is energized with balanced three-phase voltages, 115 kV rms line to line.

- (a) Where does the maximum electric field intensity occur?
- (b) Compute the maximum electric field intensity in volts per meter.

Problem 4.4: Compute the capacitive currents of a three-phase 115-kV (line-to-line) line under nominal operating conditions. The transmission tower configuration is illustrated in Fig. 1.6. The phase conductors are ACSR, 336,400 cm, 30 strands. The shield wire is steel with a diameter of  $5/16$  in. (Your answer should be in amperes per mile.) Do not neglect the effects of earth.

Problem 4.5: A single-phase 15-kV transmission line operates symmetrally ( $\pm 7.5 \text{ kV}$ ). The line consists of copper conductors 33,100 cm, single strand. The geometry of the line is illustrated in Fig. P4.1.

- (a) Compute the capacitive currents of the line. Do not neglect the effects of earth.
- (b) Where is the maximum electric field?

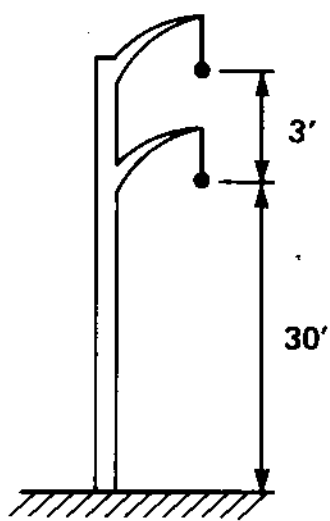


FIG. P4.1

- (c) Compute the maximum electric charge accumulated on the surface of the top conductor in coulombs per mile.
- (d) Compute the maximum electric field in volts per meter.

# 5

## Power System Grounding I Modeling Techniques

### 5.1 INTRODUCTION

Electric power systems are grounded (connected to earth by means of earth-embedded electrodes) for a number of reasons: (a) to assure correct operation of electrical devices, (b) to provide safety during normal or fault conditions, (c) to stabilize the voltage during transient conditions and therefore to minimize the probability of a flash-over during transients, (d) to dissipate lightning strokes, and so on. In general, a structure is called grounded if it is electrically connected to earth-embedded metallic structures. The earth-embedded metallic structures will be called the grounding system and provide a conducting path of electricity to earth. A typical substation grounding system consists of a ground mat, ground rods, and other earth-embedded metallic structures. A typical transmission tower grounding system consists of rings, counterpoises, ground rods, and so on. A typical transmission pole grounding system consists of ground rods, butt straps, counterpoises, and additional equipment. A typical grounding system for a house consists of one or more ground rods.

The purpose of the grounding system is to provide a low-impedance electrical contact between the neutral of an electrical system and earth. Ideally, the potential of the neutral of a three-phase system should be the same as that of the earth. In this case, human beings and animals are safe whenever they touch metallic structures connected to the system neutrals. Unfortunately, the impedance of the grounding system to earth is always a finite number. Thus the potential of grounded structures may become different than the potential at various points on earth during abnormal operation. Abnormal operation includes highly unbalanced operating conditions or fault conditions.

Depending on the level of the potential difference between earth points and grounded structures, a hazardous condition may be generated for human beings. This condition may result from two distinct possibilities:

1. A person touching a grounded structure which has a potential that is different from that of the point of earth at which the person is standing. In this case, the person is subjected to a voltage that will generate an electric current through his or her body. The voltage to which the human body is subjected is called the touch voltage.
2. A person walking on the surface of the earth will experience a voltage between his or her feet. This voltage will generate electric body currents. In this case, the voltage to which the person is subjected is called the step voltage.

The flow of electric current through the human body is a source of danger. Standards define limits on body currents that can be caused by touching grounding structures under adverse conditions. Consequently, grounding systems should be designed such that the possible electric body current in an operator or bystander should not exceed this limit under any foreseeable adverse conditions. In this respect, the objective of analysis procedures for grounding systems is to answer the following two questions:

1. What are the reasonable assumptions in the definition of foreseeable adverse conditions (worst condition)?
2. What is the highest possible body current during the worst conditions?

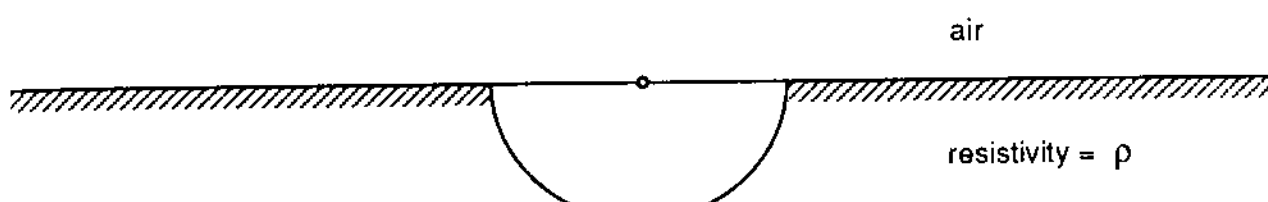
In this book we examine analysis techniques of grounding systems and how these techniques are utilized in the design of grounding systems. For simplicity, the analysis problem to determine the safety of electric power installations will be partitioned into two problems. The first analysis problem addresses the determination of the maximum voltage elevation of grounded structures [ground potential rise (GPR)] under all foreseeable adverse conditions. For this purpose, the fault condition resulting in the highest ground potential rise must be identified and analyzed. This analysis problem is examined in Chapter 7. The second analysis problem addresses the computation of the maximum body current in a person located in the ground/field given the ground potential rise. This analysis problem is examined in this chapter. In Chapter 8 we examine how these two analysis problems are utilized in the design of grounding systems.

## 5.2 ANALYSIS OF SIMPLE GROUNDING SYSTEMS

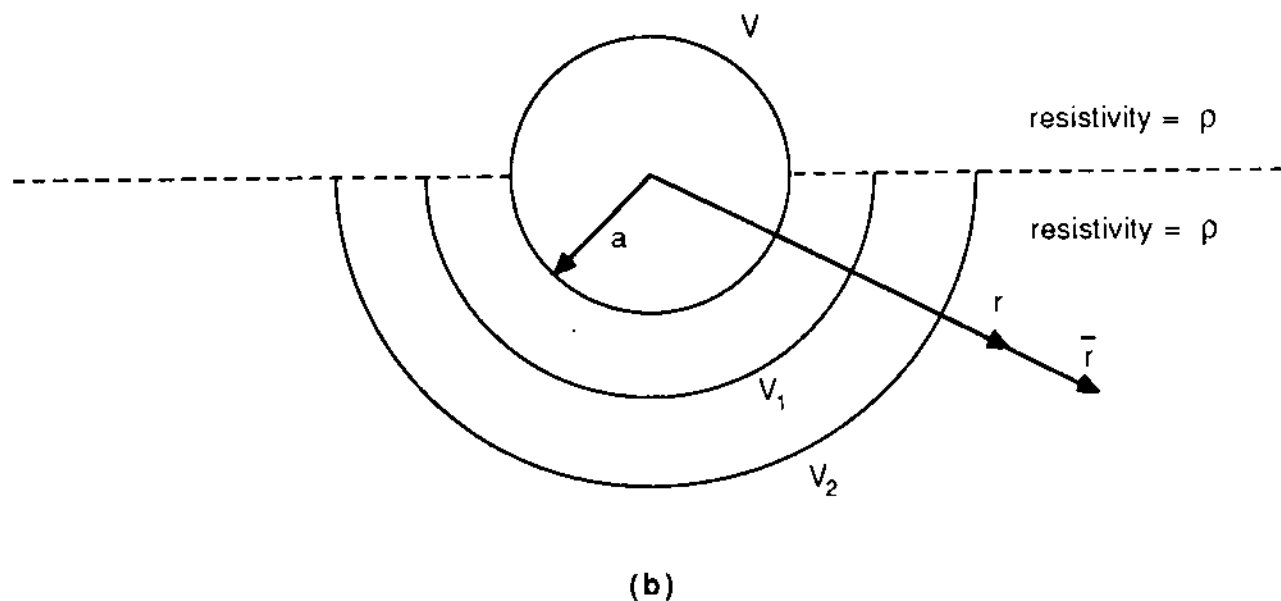
In this section we examine simple grounding systems. The analysis of these systems is simple and provides the basic concepts underlying the design of grounding systems. In later sections the analysis is extended to practical systems.

### 5.2.1 Hemispherical Electrode at the Surface of the Earth

The simplest grounding system from the analysis point of view is a hemispherical electrode embedded in earth of resistivity  $\rho$  as shown in Fig. 5.1a. The center of the hemispherical electrode is located on



(a)



(b)

FIG. 5.1 Hemispherical electrode embedded in earth. (a) Actual system, (b) equivalent system for analysis purposes.

the surface of the earth. Assume that the potential of the hemisphere is  $V$ . In this case electric current will flow from the surface of the electrode into the earth. Because of symmetry, the flow of the electric current in the semi-infinite earth will be the same as in the system of Fig. 5.1b, which illustrates a sphere embedded in an infinite medium of resistivity  $\rho$ . In other words, the flow of the current will be such that the equipotential surfaces generated will be concentric spherical surfaces. If total current  $I$  flows from the surface of the hemisphere into earth (Fig. 5.1a), total current  $2I$  will flow from the sphere into earth (Fig. 5.1b). The current density  $J(r)$  at a point located  $r$  distance from the center of the electrode will be

$$J(r) = \frac{2I}{4\pi r^2} \underline{r} \quad \text{amperes/m}^2 \quad r \geq a \quad (5.1)$$

where  $a$  is the radius of the hemisphere and  $\underline{r}$  is a unit vector in the radial direction. By Ohm's law, the electric field intensity at a point located  $r$  distance from the center of the hemisphere will be

$$\underline{E}(r) = \rho J(r) \underline{r} \quad r \geq a \quad (5.2)$$

The potential of the hemisphere with respect to a point  $x$  located at a distance  $r = r_1$  from the center of the hemisphere will be given by the equation

$$V(r_1) = \int_{r=a}^{r_1} J(r) \rho \, dr$$

Upon substitution and evaluation of the integral, we have

$$V(r_1) = \frac{\rho I}{2\pi} \left( \frac{1}{a} - \frac{1}{r_1} \right) \quad (5.3)$$

The potential of the sphere with respect to remote earth,  $V_\infty$ , is obtained by letting  $r_1 \rightarrow \infty$ .

$$V_\infty = \frac{\rho I}{2\pi a} \quad (5.4)$$

The potential on the surface of the earth along a line passing through the center of the hemisphere is illustrated in Fig. 5.2. The resistance of the hemisphere to remote earth is

$$R = \frac{V}{I} = \frac{\rho}{2\pi a} \quad (5.5)$$

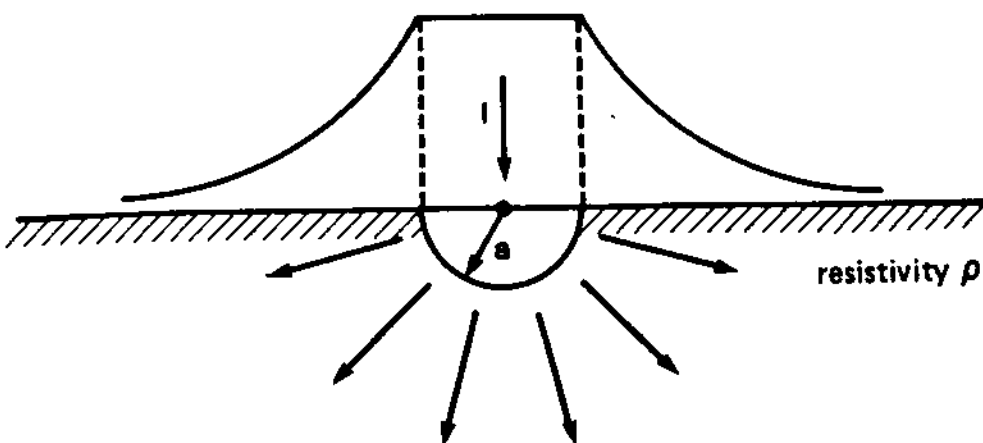


FIG. 5.2 Potential distribution on the surface of the earth generated by a hemisphere.

### 5.2.2 Two Hemispheres Embedded on the Surface of the Earth

The next simplest configuration comprises two hemispheres embedded on the surface of the earth as in Fig. 5.3a. An electric current source is connected between the two hemispheres, which will cause total electric current  $I$  to flow through the earth. For analysis purposes it can be assumed that the presence of one hemisphere does not affect the current distribution on the surface of the other hemisphere. This assumption is valid assuming that the distance between the two hemispheres is much larger than their radii. In this case, the results of Section 5.2.1 can be employed directly. The solution for this case is obtained by superposition. Specifically, the electric current density  $J(x,y)$  at a point  $(x,y)$ , illustrated in Fig. 5.3a, is

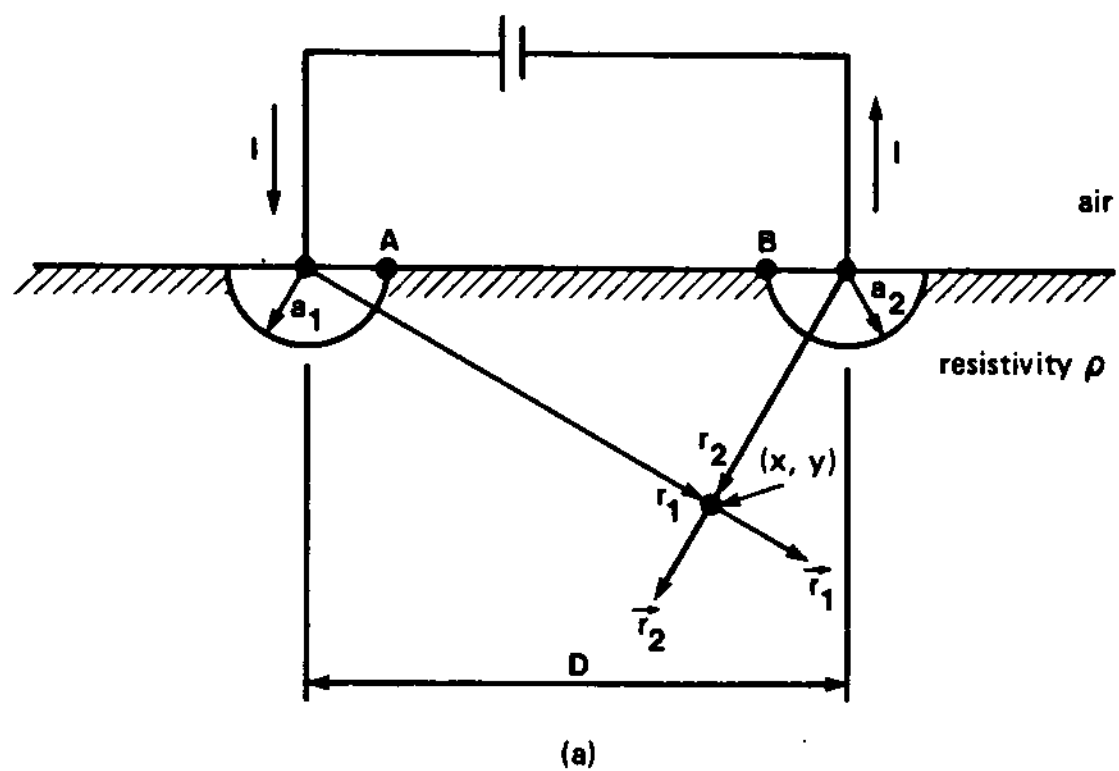
$$J(x,y) = \frac{2I}{4\pi r_1^2} \underline{r}_1 + \frac{-2I}{4\pi r_2^2} \underline{r}_2 \quad \text{amperes/m}^2 \quad (5.6)$$

where  $r_1, r_2$  are distances illustrated in Fig. 5.3a and  $\underline{r}_1, \underline{r}_2$  are unit vectors illustrated in Fig. 5.3a. The first term is the contribution to the electric current density from the first hemisphere and the second term is the contribution from the second hemisphere. Similarly, the electric field intensity  $E(x,y)$  is computed to be

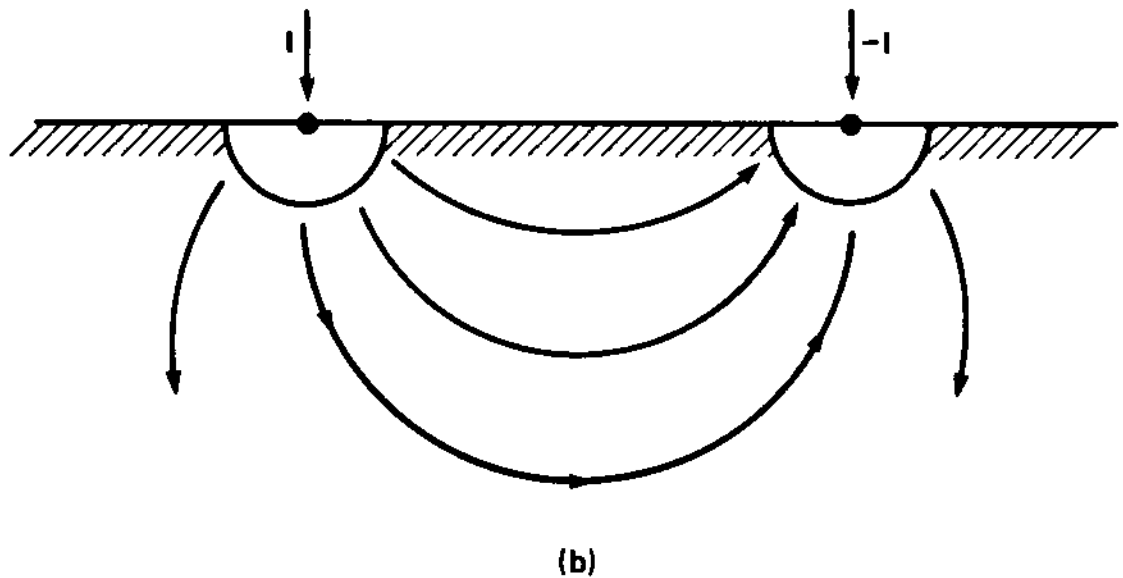
$$\underline{E}(x,y) = \rho \frac{2I}{4\pi r_1^2} \underline{r}_1 - \rho \frac{2I}{4\pi r_2^2} \underline{r}_2 \quad \text{volts/meter} \quad (5.7)$$

The voltage between the electrodes is computed from

$$V = \int \underline{E}(x,y) \cdot d\underline{r}$$



(a)



(b)

FIG. 5.3 Two hemispherical electrodes, (a) configuration, (b) lines of current flow.

Selecting an integration path along the line AB and carrying out the integration yields

$$V = \rho \frac{I}{2\pi} \left( \frac{1}{a_1} - \frac{1}{D - a_2} + \frac{1}{a_2} - \frac{1}{D - a_1} \right) \quad (5.1)$$

If both hemispheres are identical (i.e.,  $a_1 = a_2$ ), then

$$V = \frac{\rho I}{\pi} \left( \frac{1}{a} - \frac{1}{D-a} \right) \quad (5.9)$$

The resistance between the two hemispheres is

$$R = \frac{V}{I} = \frac{\rho}{\pi} \left( \frac{1}{a} - \frac{1}{D-a} \right) \quad (5.10)$$

The lines of flow of electric current are illustrated in Fig. 5.3b.

### 5.2.3 Sphere Buried in Earth

Another simple configuration is a sphere buried in earth at depth  $D$ , as illustrated in Fig. 5.4a. The solution is obtained using the theory of images, as illustrated in Fig. 5.4b. Specifically, the theory of images guarantees that the flow of electric current in the semi-infinite conductive medium will be the same as for the system of Fig. 5.4b, which comprises the original sphere and its image with respect to the interface in an infinite medium of resistivity  $\rho$ . If the original sphere injects a total current  $I$  into the soil, its image should also inject a total current  $I$ . In general, the electric current distribution on the surface of the sphere will be nonuniform. The exact solution is very complex. A simpler, but approximate solution is obtained by observing that if the distance  $D$  is much greater than the radius of the sphere, the current  $I$  will be approximately uniformly distributed on the surface of the sphere. In this case the current density, electric field intensity, and voltage in the semi-infinite region below the interface are given by

$$\underline{J}(x, y) = \frac{I}{4\pi r_1^2} \underline{r}_1 + \frac{I}{4\pi r_2^2} \underline{r}_2 \quad \text{amperes/m}^2 \quad (5.11)$$

$$\underline{E}(x, y) = \rho \frac{I}{4\pi r_1^2} \underline{r}_1 + \rho \frac{I}{4\pi r_2^2} \underline{r}_2 \quad \text{volts/meter} \quad (5.12)$$

$$V = \int \underline{E}(x, y) \cdot d\underline{r}$$

where  $r_1$ ,  $r_2$  are the distances of the point of interest from the centers of the sphere and its image, respectively (see Fig. 5.4b), and  $\underline{r}_1$ ,  $\underline{r}_2$  are unit vectors illustrated in Fig. 5.4b. The voltage of the sphere is obtained from the last formula if the integration is computed along any line starting on the surface of the sphere and terminating at infinity. Such a line is shown starting at point A. Upon evaluation of the integral along this line, we obtain

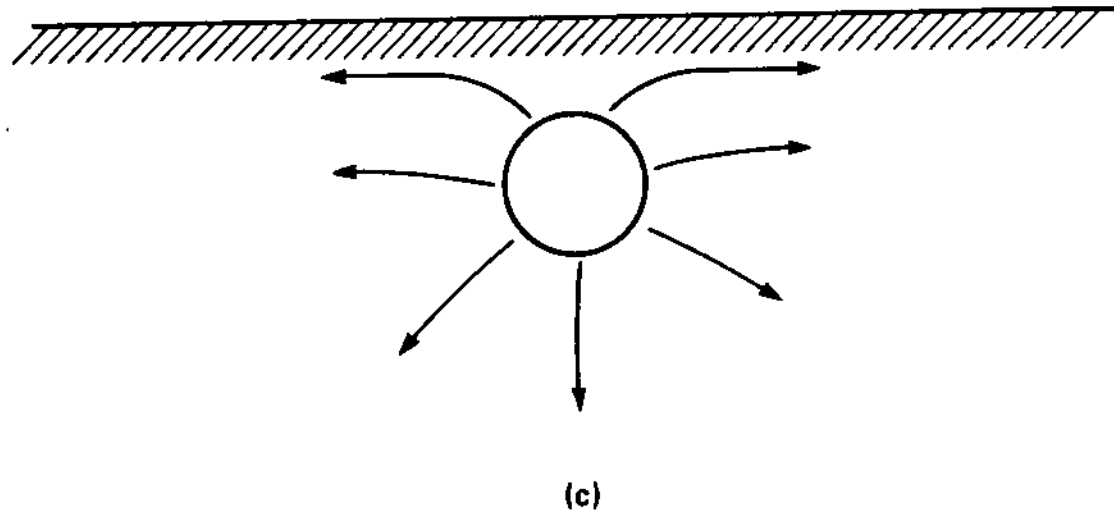
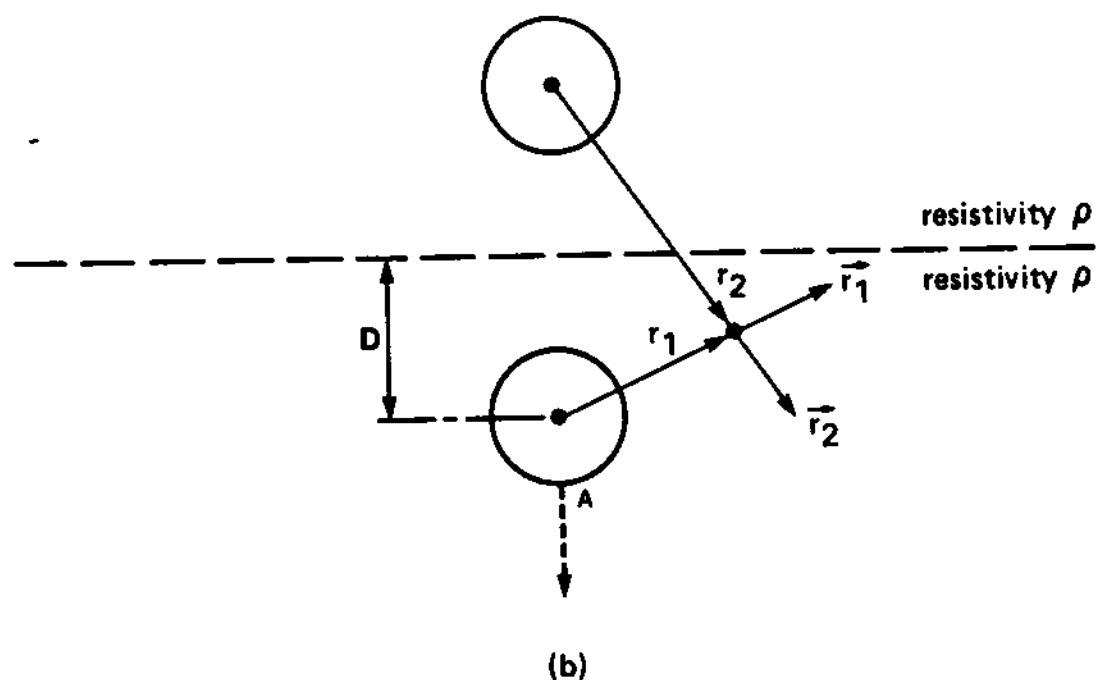
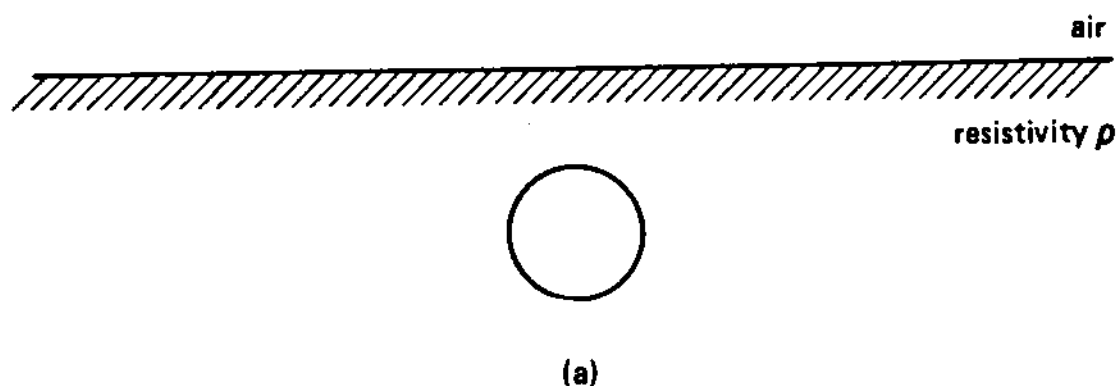


FIG. 5.4 Spherical electrode embedded in earth. (a) Actual configuration, (b) analysis equivalent configuration, (c) lines of current flow

$$V = \rho \frac{I}{4\pi} \left( \frac{1}{a} + \frac{1}{2D + a} \right) \quad (5.13)$$

The voltage at a point  $x$  located  $r_1$  distance from the sphere and  $r_2$  from its image is

$$V(x) = \rho \frac{I}{4\pi} \left( \frac{1}{r_1} + \frac{1}{r_2} \right) \quad (5.14)$$

#### 5.2.4 Other Simple Grounding Systems

While the ground electrodes considered in previous sections are simple to analyze, they are impractical for use in power system groundings. Practical grounding structures consist of ground rods, strips, rings, disks, ground mats, and so on. Some of the simplest practical grounding electrodes are illustrated in Fig. 5.5. Accurate analysis of the grounding systems of Fig. 5.5 requires numerical techniques

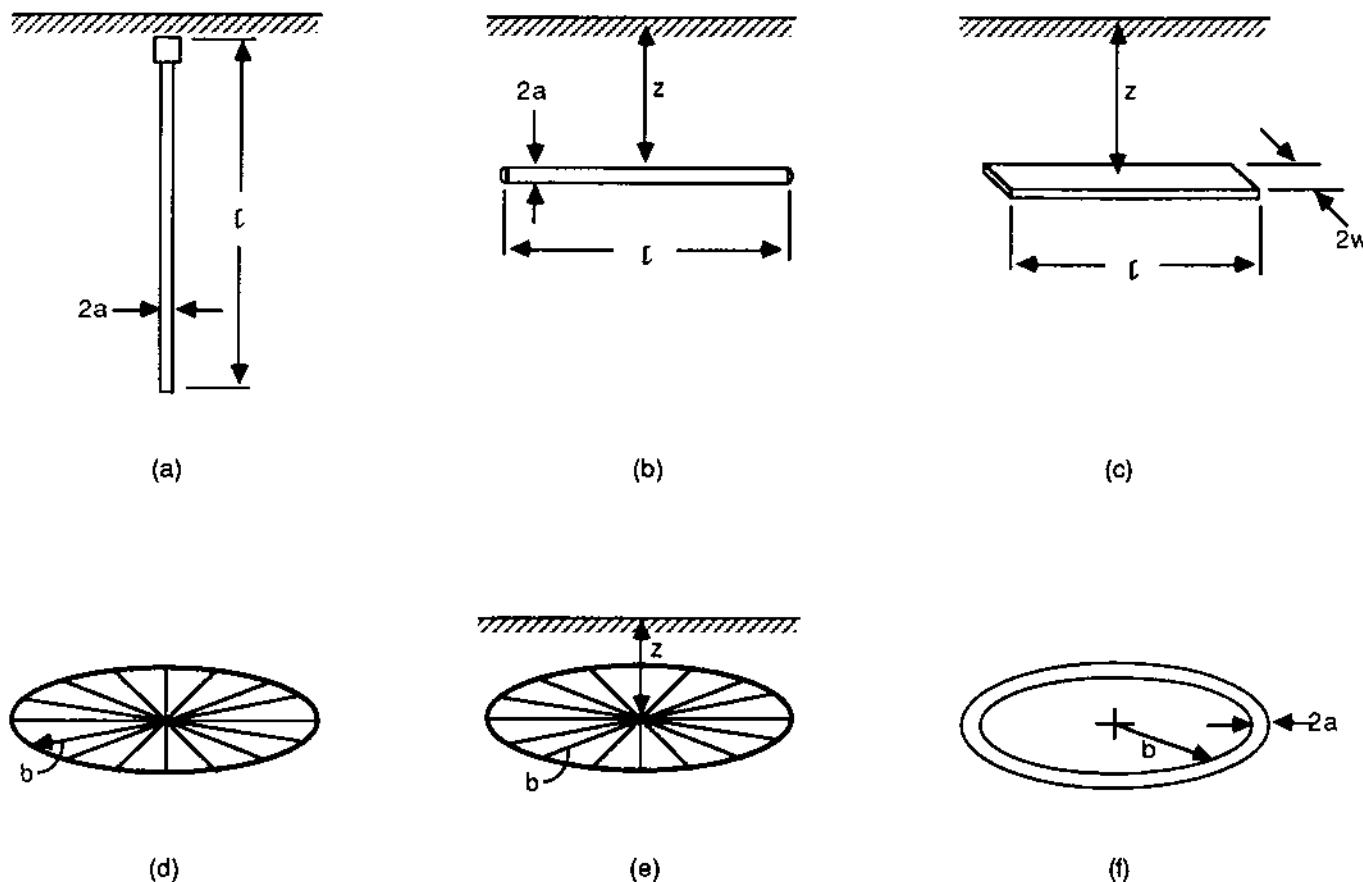


FIG. 5.5 Simple grounding systems. (a) Ground rod, (b) buried wire, (c) buried strip, (d) thin plate in infinite medium, (e) thin plate near the soil surface, (f) ring in infinite medium.

which will be presented later. Often it is necessary to estimate the resistance of a grounding system with simplified formulas. Such formulas for the simple grounding systems of Fig. 5.5 are as follows:

Ground rod (Fig. 5.5a)

$$R = \frac{\rho}{2\pi\ell} \ln \frac{2\ell}{a} \quad (5.15)$$

Buried wire (Fig. 5.5b)

$$R = \frac{\rho}{2\pi\ell} \left( \ln \frac{\ell}{a} + \ln \frac{\ell}{2z} \right) \quad z \geq 6a \quad (5.16)$$

Buried strip (Fig. 5.5c)

$$R = \frac{\rho}{2\pi\ell} \left( \ln \frac{2\ell}{w} + \ln \frac{\ell}{2z} \right) \quad z \geq 3w \quad (5.17)$$

Disk in infinite medium (Fig. 5.5d)

$$R = \frac{\rho}{8b} \quad (5.18)$$

Disk near the soil surface (Fig. 5.5e)

$$R = \frac{\rho}{4b} \quad (5.19)$$

Ring in infinite medium (Fig. 5.5f)

$$R = \frac{\rho}{4\pi^2 b} \ln \frac{8b}{a} \quad (5.20)$$

The foregoing results have been obtained with a simplified analysis procedure. Later, in Section 5.4, a rigorous analysis will be presented. Then the exact results will be simplified to obtain some of the approximate formulas presented. In this way some insight into the underlying simplifying assumptions will be acquired.

To complete the analysis of simple grounding systems, in the next section we present the computation of electric currents through the human body, using simplified equations. A simple procedure for safety assessment of grounding systems will also be outlined.

### 5.3 BODY CURRENTS DUE TO TOUCH AND STEP VOLTAGES

In this section we discuss a simplified procedure to determine the electric current that will flow in a human body due to touch or step voltages. For this purpose consider Figs. 5.6a and 5.7a, which

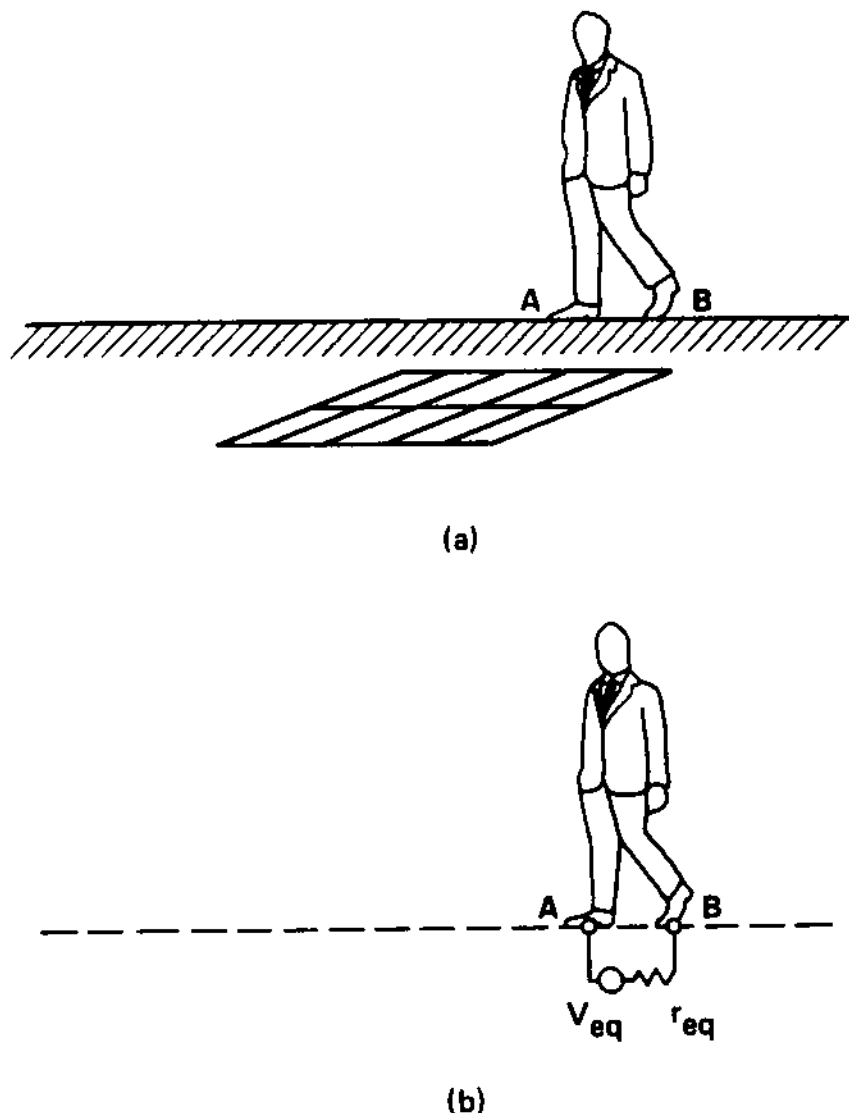
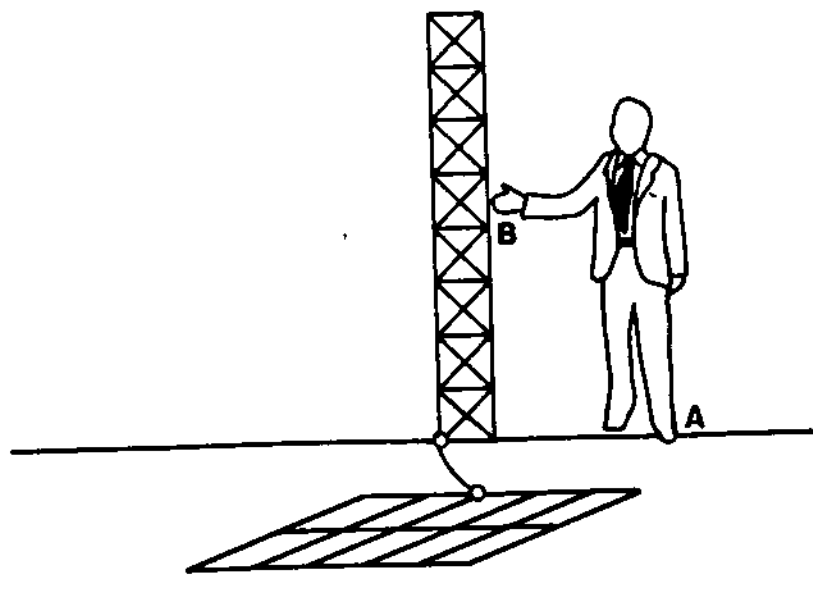
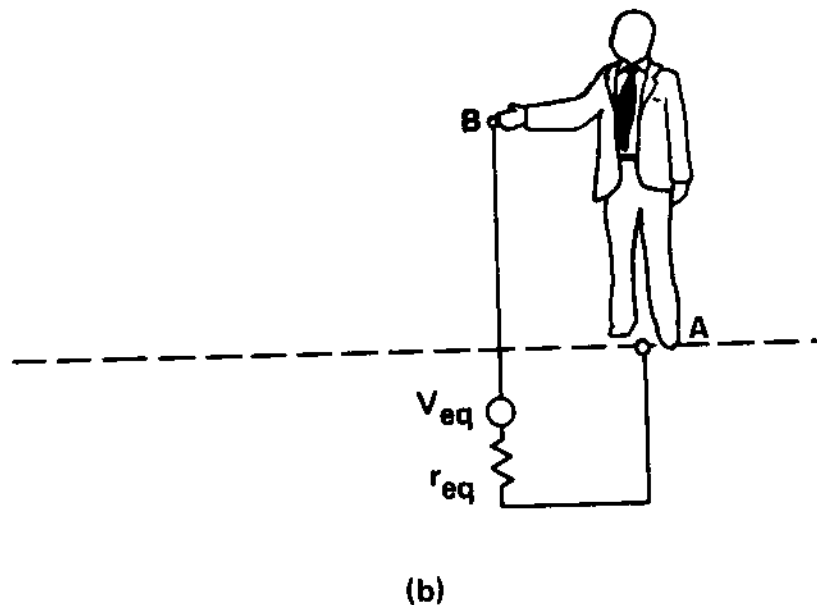


FIG. 5.6 Definition of equivalent circuit for the computation of body currents due to a step voltage.

illustrate human beings in the vicinity of a substation ground mat subjected to step and touch voltages, respectively. The computational procedure for body currents consists of computing a Thévenin equivalent circuit connected to the points of contact of the human body with the ground field (i.e., points A and B in Figs. 5.6b and 5.7b). The Thévenin equivalent circuit comprises two parameters: (a) the equivalent voltage source, and (b) the equivalent resistance. The voltage source equals the open-circuit voltage, meaning in this case the voltage at the points of contact when the human being is not touching. This voltage will be the step or touch voltage, respectively. The equivalent internal resistance between the points of contact can be accurately computed with numerical techniques [15].



(a)



(b)

FIG. 5.7 Definition of equivalent circuit for the computation of body currents due to a touch voltage.

For fast but approximate computations, the human foot can be modeled as a plate touching the surface of the earth. The resistance of the plate to remote earth is approximately (see Section 5.2.4)

$$R = \frac{\rho}{4b}$$

where  $\rho$  is the resistivity of the earth and  $b$  is the radius of the plate. The human foot definitely is not a circular plate. However, it has been observed with scale models and numerical studies that the area of the foot in touch with the earth is the determining variable. For this reason,  $b$  can be approximated with

$$b = \sqrt{\frac{A}{\pi}}$$

where  $A$  is the area of the foot in touch with the earth. For an adult with large feet, the area  $A$  of the person's feet is approximately  $200 \text{ cm}^2$ . Thus the value of  $b$  is computed to be

$$b \approx 0.08 \text{ m}$$

In this case the resistance of one foot touching the earth is

$$R = \frac{\rho}{(4)(0.08)} \approx 3\rho \text{ ohms} \quad (5.21)$$

where  $\rho$  is expressed in ohm·meters. Thus, approximately, the equivalent resistance  $r_{eq}$  in Fig. 5.6b is

$$r_{eq} = 3\rho + 3\rho = 6\rho \quad (5.22)$$

while the equivalent resistance in Fig. 5.7b, where the resistances of the two feet to soil are connected in parallel, is

$$r_{eq} = \frac{(3\rho)(3\rho)}{3\rho + 3\rho} = 1.5\rho \quad (5.23)$$

The equivalent resistance,  $r_{eq}$ , in Fig. 5.7b, should also take into account the resistance of the grounding system. However, for practical grounding systems, this resistance is typically small compared to the resistance  $1.5\rho$ , and thus omitted.

Once the Thévenin equivalent circuit has been computed, the electric current through the human body,  $i_b$ , is computed from

$$i_b = \frac{V_{eq}}{r_{eq} + r_b} \quad (5.24)$$

where  $r_b$  is the resistance of the human body between the points of contact. The resistance  $r_b$  of the human body depends on many factors, such as size, skin condition, pressure at the contact, and level of voltage  $V_{eq}$ , among others. Reasonable values are  $2000 \Omega$  for the resistance from one foot to another foot and  $1000 \Omega$  for the resistance from foot to arm. Occasionally, the pessimistic values  $1000$  and  $500 \Omega$

respectively, are used. ANSI/IEEE Standard 80 [18] suggests the value  $1000 \Omega$ . An example will illustrate the body current computations.

Example 5.1: A hemispherical electrode of radius  $a = 6$  ft is embedded in earth. A person is standing 9 ft away from the center of the hemisphere and holding a metallic structure electrically connected to the hemisphere, as in Fig. E5.1. Assume that an electric current of 100 A is injected into the earth through the hemisphere. Compute (a) the ground potential rise of the hemisphere and (b) the electric current through the human body. Assume a soil resistivity of  $100 \Omega \cdot \text{m}$ .

Solution:

a. The resistance of the hemisphere is

$$R = \frac{\rho}{2\pi a} = \frac{100}{(2\pi)(6)(0.3048)} \Omega = 8.7 \Omega$$

The ground potential rise is

$$\text{GPR} = IR = (100)(8.7) = 870 \text{ V}$$

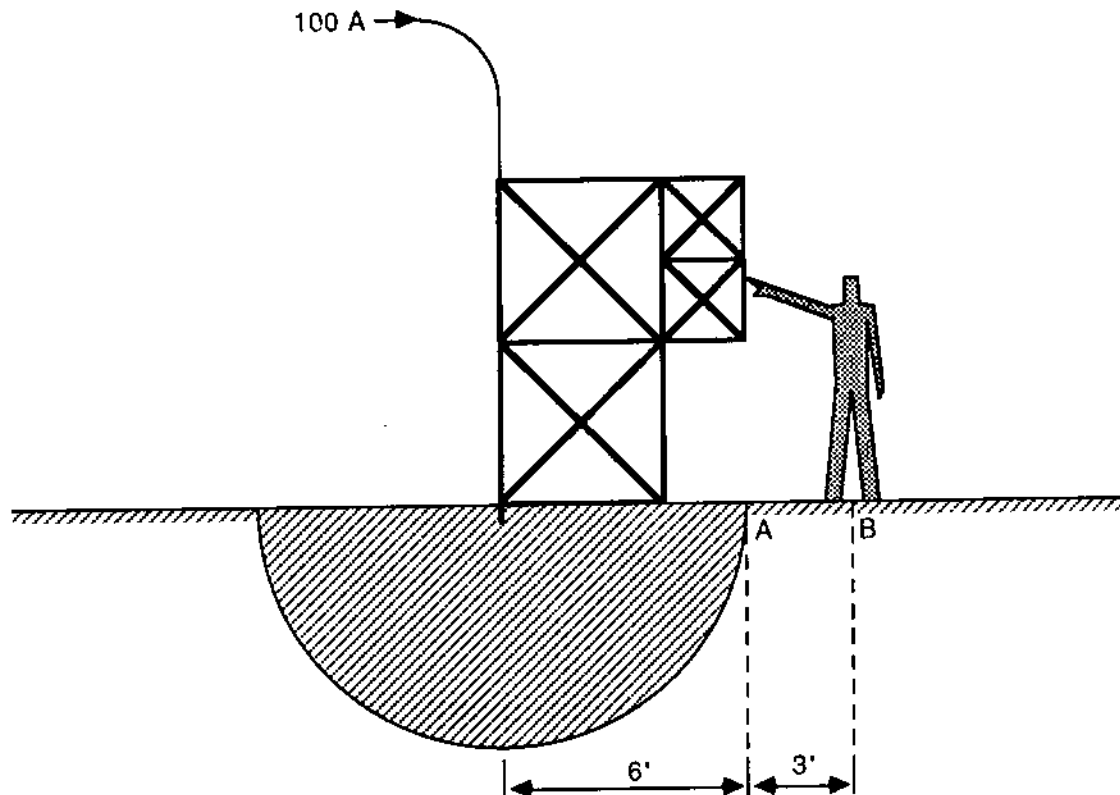


FIG. E5.1 Human being subjected to touch voltage near a hemispherical ground electrode.

b. The electric body current is

$$i_b = \frac{v_{eq}}{r_{eq} + r_b}$$

where  $v_{eq}$  is the touch voltage and

$$r_{eq} = 1.5\rho$$

$$r_b = 1000 \Omega$$

The touch voltage is computed with the equations developed in Section 5.2.1:

$$\text{voltage of grounded structure } V_A = 870 \text{ V}$$

$$\text{voltage of earth 3 ft away from electrode } V_B = \frac{\rho I}{2\pi r_1}$$

$$V_{eq} = 870.0 - \frac{\rho I}{2\pi r_1}$$

where  $r_1 = (9)(0.3048)$  m. Substitution gives us

$$V_{eq} = 289.8 \text{ V}$$

$$r_{eq} = 150.0 \Omega$$

The body current is

$$i_b = 0.252 \text{ A}$$

#### 5.4 GROUNDING SYSTEM SAFETY ASSESSMENT

The electric body current analysis presented in the preceding section together with our knowledge about tolerable body currents provides the basis for safety assessment of grounding systems. Research by Dalziel [19,20], Biegelmeier [21], and others suggests the following:

1. Electric currents below 5 mA are not hazardous.
2. Electric currents above 5 mA cause effects on human bodies which depend on the individual, duration, and magnitude of current. Electric currents above a certain value for a given combination of these parameters cause what is known in medical jargon as ventricular fibrillation. This condition refers to the case in which the heart beat stops irrecoverably. The threshold of ventricular

fibrillation for a typical adult male subjected to 60-Hz ac current of 1-s duration is on the order of 200 to 300 mA [21].

Based on available experimental data and accepted safety factors, the ANSI/IEEE Standard 80 [18] suggests the following rule. Electric body currents below  $116 \text{ mA}/\sqrt{t}$ , where  $t$  is the duration of the current in seconds, can be tolerated by the average person. Thus, according to this standard, the maximum allowable body current is

$$i_{b,\text{allowable}} = \frac{0.116}{\sqrt{t}} \quad \text{amperes}$$

where  $t$  is the duration of the electric current in seconds. On the other hand, the electric body current is

$$i_b = \frac{V_{eq}}{r_{eq} + r_b}$$

In the equation above,  $V_{eq}$  is the Thévenin equivalent voltage, which equals the step or touch voltage. Thus combining the two preceding equations, the maximum allowable step or touch voltage is computed:

$$V_{eq,\text{allowable}} = (r_{eq} + r_b) \frac{0.116}{\sqrt{t}} \quad (5.25)$$

To obtain the maximum allowable step voltage,  $r_{eq}$  should be replaced with  $6\rho$ . To obtain the maximum allowable touch voltage,  $r_{eq}$  should be replaced by  $1.5\rho$ . For body resistance  $r_b$ , the value of  $1000 \Omega$ , suggested by the IEEE Standard 80, can be used, yielding

$$V_{touch,\text{allowable}} = (1.5\rho + 1000) \frac{0.116}{\sqrt{t}} \quad \text{volts} \quad (5.26)$$

$$V_{step,\text{allowable}} = (6\rho + 1000) \frac{0.116}{\sqrt{t}} \quad \text{volts} \quad (5.27)$$

Thus, for a grounding system to be safe, the maximum touch and step voltage should not exceed the foregoing values. It is obvious from the equations above that safety can be assessed in terms of the touch and step voltages instead of the body currents. Safety assessment refers to the procedure by which the actual maximum touch and step voltages are computed and compared to the maximum allowable (safe) touch and step voltages. The actual maximum touch and step voltages can be computed using the simplified analyses outlined in previous sections or the rigorous analysis to be presented subsequently.

## 5.5 NUMERICAL ANALYSIS TECHNIQUES

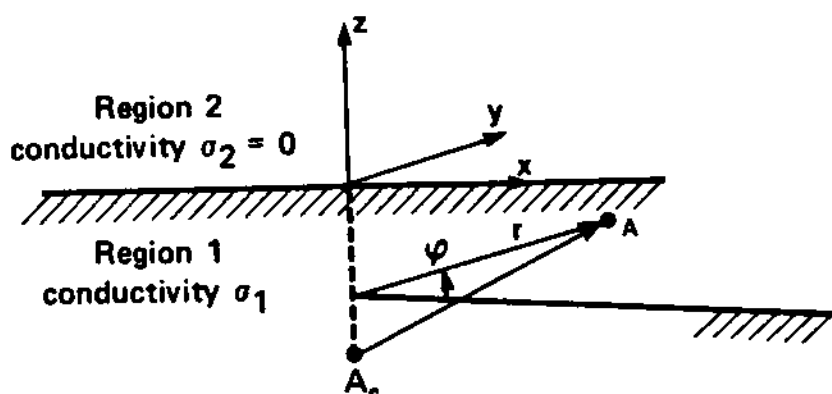
In this section we examine numerical analysis techniques of grounding systems. When an electric fault occurs somewhere in a power system, the grounding systems connected to the neutral of the power system are activated, that is, their potential becomes different than zero. We shall refer to this potential as the ground potential rise (GPR). As a result of the GPR, electric current emanates from the surface of the elements of the grounding system and flows into earth. This current will be called the earth current. The earth current sets up an electric potential field inside and on the surface of the earth. The frequency of the earth current is equal to the power frequency (60 Hz for the U.S. system or 50 Hz for Europe). It may also comprise a decaying dc component. The conditions described suggest that we need to be concerned only with the analysis of the flow of low-frequency electric current in the earth. This analysis is simplified on the observation that for usual grounding systems and soil resistivities, the flow of low-frequency electric currents is approximately that of dc currents (dc analysis). This fact is justified as follows: Consider the usual soil resistivities 50 to 1000  $\Omega \cdot m$ . The depth of penetration,  $\delta$ , given with the equation  $\delta = 2/\sqrt{\mu\omega\rho}$  (see Chapter 3), for the typical soil resistivities and the power frequency (50 or 60 Hz) is in the range 459 to 2054 m. The size of typical grounding systems is on the order of a few meters to 200 m. Since the size of the grounding system is much smaller than the depth of penetration, dc analysis suffices for most practical applications.

Dc analysis, as applied to grounding systems, will be introduced next. The procedures will be developed step by step starting from the simplest analysis problem and building up.

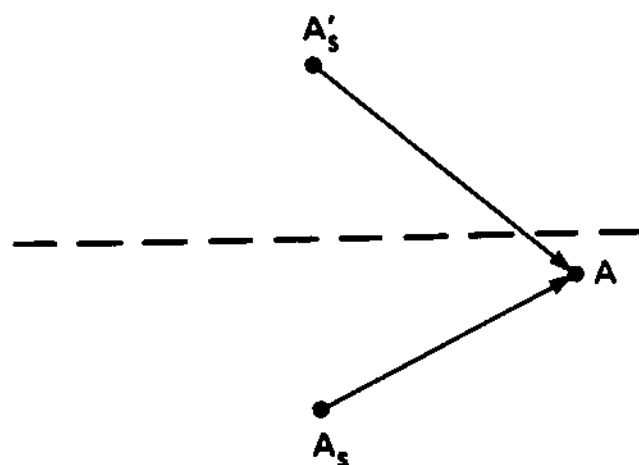
### 5.5.1 Basic Equations and Solutions

The fundamental analysis problem is illustrated in Fig. 5.8. Consider an infinitesimal section of an earth-embedded metallic structure. Assume that total electric current  $I_S$  emanates from the surface of the infinitesimal section and is flowing into earth. We shall refer to this current source as a point current source. The location of the source is at point  $A_S$ , as illustrated in Fig. 5.8. For this system we address the following question: What is the voltage at a point A in the earth? The voltage,  $V(r, \phi, z)$ , at a point  $(r, \phi, z)$  inside the earth must satisfy the Laplace equation

$$\nabla^2 V(r, \phi, z) = \frac{1}{r} \frac{\partial}{\partial r} \left( r \frac{\partial V(r, \phi, z)}{\partial r} \right) + \frac{1}{r^2} \frac{\partial^2 V(r, \phi, z)}{\partial \phi^2} + \frac{\partial^2 V(r, \phi, z)}{\partial z^2} = 0.0 \quad (5.28)$$



(a)



(b)

FIG. 5.8 A point current source inside the semiinfinite conducting earth.

where  $r$ ,  $\phi$ ,  $z$  are the coordinates of the point  $A$  relative to a system of cylindrical coordinates as indicated in Fig. 5.8a. Because of the symmetry of the problem, the solution is independent of the coordinate  $\phi$ . Thus  $V(r, \phi, z) = V(r, z)$ . In this case the Laplace equation reads

$$\nabla^2 V(r, z) = \frac{1}{r} \frac{\partial}{\partial r} r \frac{\partial V(r, z)}{\partial r} + \frac{1}{r^2} \frac{\partial^2 V(r, z)}{\partial z^2} = 0 \quad (5.29)$$

The general solution to this equation is well known [3]. It is given in terms of the Bessel function of zero order,  $J_0$ :

$$V(r, z) = \frac{I_S}{4\pi\sigma_1} \int_{k=0}^{\infty} \theta(k) J_0(kr) e^{+kz} dk \quad (5.30)$$

where  $k$  is a dummy variable and  $\theta(k)$  is an arbitrary function of  $k$ .

For a specific problem, the function  $\theta(k)$  is determined from boundary conditions. Note that the solution has two possible functional forms, corresponding to the + and - signs, which correspond to propagation in the  $+z$  and  $-z$  direction, respectively.

The general solution for the voltage in region 2 is

$$V_2(r, z) = \frac{I_S}{4\pi\sigma_1} \int_0^{\infty} \theta_2(k) J_0(kr) e^{-kz} dk \quad z > 0 \quad (5.31)$$

In the general equation above, the term corresponding to propagation is the  $+z$  direction ( $e^{+kz}$ ) must be omitted because  $V_2(r, z) \rightarrow 0$  as  $z \rightarrow +\infty$ .

The general solution for the voltage in region 1 is

$$V_1(r, z) = \frac{I_S}{4\pi\sigma_1} \int_0^{\infty} J_0(kr) e^{-k|z-z_s|} dk + \frac{I_S}{4\pi\sigma_1} \int_0^{\infty} \theta_1(k) J_0(kr) e^{+kz} dk \quad z \leq 0 \quad (5.32)$$

In the general solution above, the term corresponding to propagation in the  $-z$  direction ( $e^{-kz}$ ) has been omitted because  $V_1(r, z) \rightarrow 0$  as  $z \rightarrow -\infty$ .

In the set of two equations above, two unknown functions appear,  $\theta_1(k)$  and  $\theta_2(k)$ . The boundary conditions at the interface of the two regions will provide two equations which, if solved, will determine  $\theta_1(k)$  and  $\theta_2(k)$ . At the interface, the voltage must be a continuous function and the electric current must also be a continuous function. These requirements result in the following boundary conditions:

$$V_1(r, 0) = V_2(r, 0) \quad \text{for every } r \quad (5.33)$$

$$\sigma_1 \frac{\partial V_1(r, 0)}{\partial z} = \sigma_2 \frac{\partial V_2(r, 0)}{\partial z} \quad \text{for every } r \quad (5.34)$$

Note that

$$V_2(r, 0) = \frac{I_S}{4\pi\sigma_1} \int_0^{\infty} \theta_2(k) J_0(kr) dk$$

$$V_1(r,0) = \frac{I_S}{4\pi\sigma_1} \int_0^\infty J_0(kr) e^{+kz_s} dk + \frac{I_S}{4\pi\sigma_1} \int_0^\infty \theta_1(k) J_0(kr) dk$$

$$\sigma_1 \frac{\partial V_1(r,0)}{\partial z} = - \frac{I_S k}{4\pi} \int_0^\infty J_0(kr) e^{+kz_s} dk + \frac{I_S k}{4\pi} \int_0^\infty \theta_1(k) J_0(kr) dk$$

$$\sigma_2 \frac{\partial V_2(r,0)}{\partial z} = 0$$

Upon substitution into the boundary conditions, we obtain

$$\theta_2(k) = e^{-kz_s} + \theta_1(k)$$

$$-e^{-kz_s} + \theta_1(k) = 0$$

Solving for the functions  $\theta_1(k)$  and  $\theta_2(k)$  gives us

$$\theta_1(k) = e^{-kz_s} \quad (5.35)$$

$$\theta_2(k) = 2e^{-kz_s} \quad (5.36)$$

Finally, upon substitution of the computed functions  $\theta_1(k)$  and  $\theta_2(k)$ , the general solutions for the voltage in regions 1 and 2 are obtained:

$$V_2(r,z) = \frac{I_S}{4\pi\sigma_1} \int_0^\infty 2J_0(kr) e^{-k|z-z_s|} dk \quad (5.37)$$

$$V_1(r,z) = \frac{I_S}{4\pi\sigma_1} \int_0^\infty J_0(kr) e^{-k(z+z_s)} dk + \frac{I_S}{4\pi\sigma_1} \int_0^\infty J_0(kr) e^{k(z+z_s)} dk \quad (5.38)$$

In subsequent discussions we shall be concerned with the voltage in region 1 only.

The integrals appearing in the equation for the voltage  $V_1(r, z)$  are evaluated by utilizing the following identity of Bessel functions:

$$\int_0^\infty J_0(kr)e^{ka} dk \equiv \frac{1}{(r^2 + a^2)^{0.5}}$$

The final result is

$$V_1(r, z) = \frac{I_S}{4\pi\sigma_1} \left\{ \frac{1}{[r^2 + (z - z_s)^2]^{0.5}} + \frac{1}{[r^2 + (z + z_s)^2]^{0.5}} \right\} \quad (5.39)$$

In cartesian coordinates, Eq. (5.39) reads

$$V_1(r, z) = \frac{I_S}{4\pi\sigma_1} \left\{ [(x - x_s)^2 + (y - y_s)^2 + (z - z_s)^2]^{-0.5} + [(x - x_s)^2 + (y - y_s)^2 + (z + z_s)^2]^{-0.5} \right\} \quad (5.40)$$

The derived result is interpreted as follows: The voltage in region 1 is identical to the voltage generated by two point sources of magnitude  $I_S$  located at points  $(x_s, y_s, z_s)$  and  $(x_s, y_s, -z_s)$  in an infinite region of conductivity  $\sigma_1$ . In other words, the interface between regions 1 and 2 has the effect of generating the image of the point source with respect to the plane interface. This interpretation is illustrated in Fig. 5.8b.

The result derived is the basic building block of all numerical analysis procedures of grounding systems. In subsequent paragraphs we discuss these procedures.

### 5.5.2 Numerical Analysis of Grounding Systems: Matrix Method

The basic equation (5.40) can be utilized in a number of ways for the purpose of analysis of a practical grounding system. The basic idea in all methods is to divide a grounding system into small segments. Then utilization of the basic equations results in a relationship between the voltage of these segments and the electric current emanating from the surface of the segments. Consider, for example, the simple system of Fig. 5.9a. The ground electrodes are divided into  $n$  very small segments. Let total electric current  $I_i$  emanate from the surface of segment  $i$  and flow into earth as is illustrated in Fig.

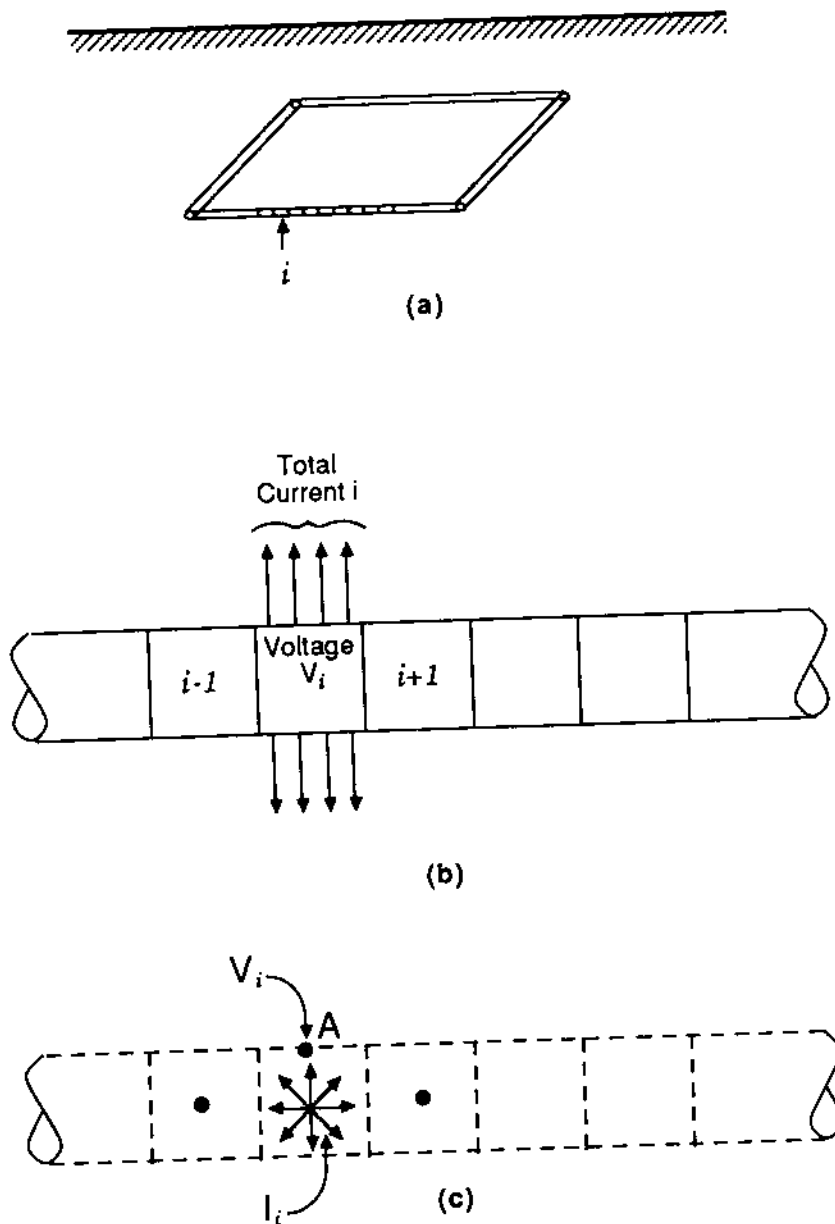


FIG. 5.9 Illustration of the matrix method. (a) Simple grounding system, (b) small segments  $i-1, i, i+1$ , (c) mathematical model of segment  $i$ .

5.9b. The figure also illustrates the neighbors of segment  $i$ . If segment  $i$  is very small, it can be represented with a point source of electric current  $I_i$  located at the center of the segment; the voltage at the surface of the segment is  $V_i$ . This is illustrated in Fig. 5.9c. The same model can be assumed for segments  $i - 1$ ,  $i + 1$ , and all other segments. Then the basic equations are utilized to develop relationships among the electric currents  $I_i$ ,  $i = 1, 2, \dots, n$ , and the voltages  $V_i$ ,  $i = 1, 2, \dots, n$ . Specifically, the voltage  $V_i$  (i.e., voltage of segment  $i$ ) at point A will be

$$V_i = \sum_{j=1}^n f(x_{Ai}, y_{Ai}, z_{Ai}, x_j, y_j, z_j, \sigma) I_j \quad (5.41)$$

where

$$f(x_{Ai}, y_{Ai}, z_{Ai}, x_j, y_j, z_j, \sigma) = \frac{1}{4\pi\sigma} \left\{ [(x_{Ai} - x_j)^2 + (y_{Ai} - y_j)^2 + (z_{Ai} - z_j)^2]^{-0.5} + [(x_{Ai} - x_j)^2 + (y_{Ai} - y_j)^2 + (z_{Ai} + z_j)^2]^{-0.5} \right\}$$

and

- $(x_{Ai}, y_{Ai}, z_{Ai})$  = coordinates of point A located on the surface of segment i
- $(x_j, y_j, z_j)$  = coordinates of the center of segment j
- $I_j$  = total electric current emanating from the surface of segment j

In general, n such equations can be written, one for each segment:

$$\begin{aligned} V_1 &= \sum_{j=1}^n f(x_{A1}, y_{A1}, z_{A1}, x_j, y_j, z_j, \sigma) I_j \\ V_2 &= \sum_{j=1}^n f(x_{A2}, y_{A2}, z_{A2}, x_j, y_j, z_j, \sigma) I_j \\ &\dots \\ V_n &= \sum_{j=1}^n f(x_{An}, y_{An}, z_{An}, x_j, y_j, z_j, \sigma) I_j \end{aligned} \quad (5.42)$$

If the voltages  $V_i$ ,  $i = 1, 2, \dots, n$ , are known, then the equations above can be solved to yield the electric currents  $I_j$ ,  $j = 1, 2, \dots, n$ . Once the electric currents are specified, the voltage  $V(x, y, z)$  at any point  $(x, y, z)$  in the earth can be computed from the equation

$$V(x, y, z) = \sum_{j=1}^n f(x, y, z, x_j, y_j, z_j, \sigma) I_j \quad (5.43)$$

In general, grounding systems are constructed with copper conductors. In this case, because of the high conductivity of copper, the entire grounding system is at essentially the same potential, the ground potential rise (GPR). Thus the voltage of all segments is the same and equal to  $V$  (i.e.,  $V_1 = V_2 = V_3 = \dots = V_n = V$ ). Equations (5.42) can be written in compact matrix notation:

$$\mathbf{V}\mathbf{1} = [\text{VDF}]\mathbf{I} \quad (5.44)$$

where

$$\mathbf{1}^T = [1 \ 1 \ 1 \ \dots \ 1]$$

$$[\mathbf{I}]^T = [I_1 \ I_2 \ \dots \ I_n]$$

$$[\text{VDF}]_{i,j} = f(x_{Ai}, y_{Ai}, z_{Ai}, x_j, y_j, z_j, \sigma)$$

and  $V$  is the ground potential rise of the grounding system.

The electric currents  $[\mathbf{I}]$  are computed from

$$[\mathbf{I}] = [\text{VDF}]^{-1} \mathbf{1}V \quad (5.45)$$

Note that the electric currents are proportional to the ground potential rise. Thus a resistance can be computed for the grounding system as the ratio of the ground potential rise over the total electric current. Specifically, the total electric current is

$$I_T = \sum_{j=1}^n I_j = \mathbf{1}^T [\mathbf{I}] \quad (5.46)$$

and

$$R = \frac{V}{I_T} \quad (5.47)$$

This method bears the name "matrix method" because it involves the matrix  $[\text{VDF}]$ . The entries of this matrix will be called voltage distribution factors (VDFs) because they provide the voltage at a given point due to the flow of a specific current source. The voltage distribution factors have dimensions of resistance (ohms). For this reason they are often referred to in the literature as transfer resistances, mutual resistances, and self-resistances. However, their physical meaning is not related to the concept of resistance. Thus it is more appropriate to give them a different name. We shall refer to this quantity as the voltage distribution factor.

### 5.5.3 Combined Integration/Matrix Method

The matrix method is conceptually simple. However, it is impractical because it involves the inversion of a large matrix. In this section we discuss another method that is suitable for practical applications.

The matrix method provides the electric current distribution along the conductors of a grounding system. Such analyses indicate that the distribution of electric current is more or less uniform along the conductor except at the end of the conductor or where there are conductor crossings. The actual current distribution along the conductors of a grounding system can be approximated with a staircase function. This approximation is equivalent to assuming that the current density is constant along small segments of the conductor. Since the current density along the conductors is not known *a priori*, a method will be developed for the computation of the current density. For this purpose the conductors of a grounding system are partitioned into a number of finite segments. The electric current density along a given finite segment is assumed constant but unknown. Next, expressions are developed relating the voltage at a point to the total current emanating from the finite segment. Then the matrix method is applied to yield the unknown values of the electric current. The size of the involved matrix is equal to the number of selected segments. Thus the size of the matrix can be kept relatively small by appropriate segmentation of the grounding system conductors. It should be emphasized that the number of segments determines how accurately the actual current distribution will be represented by a staircase function. More segments will result in a better approximation but in a larger matrix (and, therefore, more computations). Appropriate application of this method provides a good compromise between accuracy and efficiency. The method bears the name "combined integration/matrix method" because it involves integration along the length of a finite segment and subsequent application of the matrix method, as will be shown subsequently.

From the previous discussion it is obvious that application of the combined integration/matrix method requires the development of relationships between the total electric current emanating the surface of a finite length of conductor and the voltage at a given point in earth. These relationships will be developed next.

Consider two conductor segments of length  $2L_1$  and  $2L_2$ , respectively, as in Fig. 5.10. The two conductor segments are part of a grounding system. The coordinates of the center of the conductor segments are  $(x_1, y_1, z_1)$  and  $(x_2, y_2, z_2)$ , respectively. Assume that a total electric current,  $I_1$ , emanates from the outside surface of conductor segment 1 and flows into earth. Also assume that the flow of current is uniform over the outside surface of the conductor segment (constant surface density). The following three elementary problems are defined:

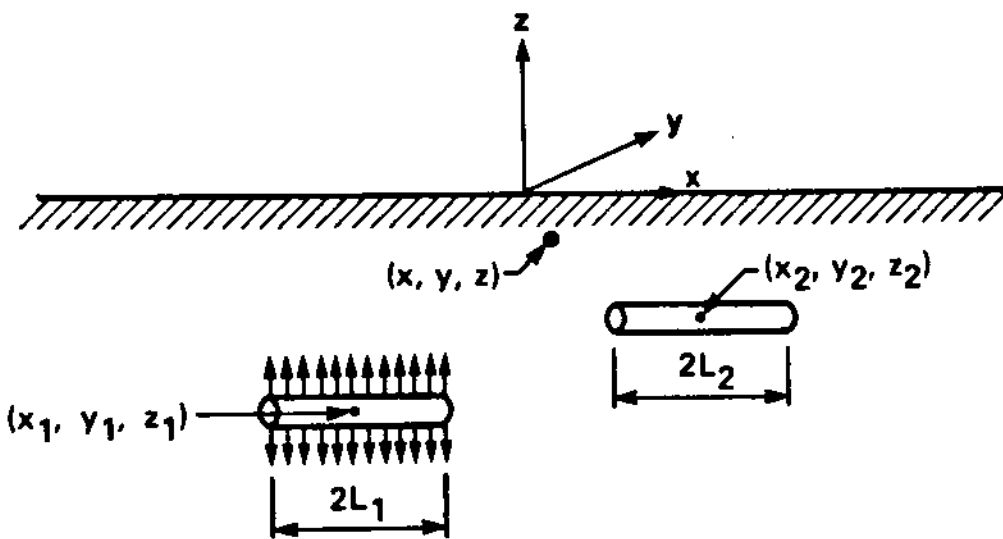


FIG. 5.10 Two earth embedded conductor segments of lengths  $2L_1$  and  $2L_2$  respectively.

Problem 1: Compute the voltage at a point  $(x, y, z)$  in the earth due to the flow of the electric current  $I_1$  (current of conductor segment 1).

Problem 2: Compute the voltage "transferred" to conductor segment 2 because of the flow of the electric current  $I_1$  (current of conductor segment 1).

Problem 3: Compute the voltage of the conductor segment 1 due to the flow of its own current,  $I_1$ .

It is shown later that the voltage at any point  $(x, y, z)$  or the "transferred" voltage to another conductor or the voltage of the conductor itself is proportional to the total electric current emanating from the conductor, that is,

$$V = R_t I \quad (5.4)$$

where

$I$  = total electric current emanating the surface of the conductor under consideration

$R_t$  = a function depending on the geometry of the system and the conductivity of the soil (this function, which has dimensions of resistance, is a generalization of the voltage distribution factors introduced earlier); it will be also referred to as VDF

Because of the large number of configurations that earth-embedded conductors may assume, the number of possible geometric arrangements for the three problems is large. To limit the possibilities,

assume that earth-embedded conductors are oriented only along the three coordinate axes  $x$ ,  $y$ , or  $z$ . In this case only three distinct geometric arrangements need to be considered for problem 1, leading to three distinct expressions for the VDF between a conductor segment and a point. These expressions are summarized in Table 5.1. Similarly, only six distinct geometric arrangements need to be considered for problem 2, leading to six distinct expressions for the VDF between two conductor segments. These equations are summarized in Table 5.2. Finally, for problem 3, only three distinct geometric arrangements need to be considered, leading to three distinct expressions, which are summarized in Table 5.3. The derivation of these expressions is illustrated with four sample calculations: (a) VDF between an  $x$ -directed conductor segment and a point  $(x, y, z)$ , (b) VDF between two  $x$ -directed conductor segments, (c) VDF between an  $x$ -directed conductor segment and a  $y$ -directed conductor segment, and (d) self-VDF of an  $x$ -directed conductor segment.

#### VDF Between an $x$ -Directed Conductor Segment and a Point $(x, y, z)$

Consider the conductor segment 1 illustrated in Fig. 5.10 and an arbitrary point  $(x, y, z)$  in the earth. Our objective will be to compute the voltage at point  $(x, y, z)$ , due to the flow of current  $I_1$ , neglecting all other sources of electric current (i.e., neglecting the presence of other conductor segments). The electric current  $I_1$  is assumed to be uniformly distributed on the surface of the conductor. Typically, the radius of the conductor is small (less than  $1/2$  in.). In this case it is reasonable to assume that the source of this current is an ideal line source located on the axis of the conductor segment. The line current density is  $I_1/2L_1$  (amperes per meter). The electric current of an infinitesimal length of the line source,  $dx_s$ , is  $I_1 dx_s/2L_1$ . The contribution of this current to the voltage at point  $(x, y, z)$  is

$$dV(x, y, z) = \frac{I_1}{8L_1 \pi \sigma} \left\{ \left[ (x - x_s)^2 + A_{\pm}^2 \right]^{-0.5} + \left[ (x - x_s)^2 + A_{\mp}^2 \right]^{-0.5} \right\} \quad (5.49)$$

where

$$A_{\pm}^2 = (y - y_1)^2 + (z \pm z_1)^2$$

Figure 5.11 illustrates the geometry of the infinitesimal current source and the point of interest  $(x, y, z)$ . For simplicity, the conductor segment length will be denoted as  $2L$  and the total current as  $I$ .

TABLE 5.1 Equations for Voltage Distribution Factors Between a Conductor Segment and a Point  
(Transfer Resistance)

Direction of conductor segment a,b	Voltage distribution factors <sup>c</sup>
x-directed	$\frac{1}{8L\pi\sigma} [F_1(x - x_1 + L, A_x^-) - F_1(x - x_1 - L, A_x^-) + F_1(x - x_1 + L, A_x^+) - F_1(x - x_1 - L, A_x^+)]$
y-directed	$\frac{1}{8L\pi\sigma} [F_1(y - y_1 + L, A_y^-) - F_1(y - y_1 - L, A_y^-) + F_1(y - y_1 + L, A_y^+) - F_1(y - y_1 - L, A_y^+)]$
z-directed	$\frac{1}{8L\pi\sigma} [F_1(z - z_1 + L, A_z^-) - F_1(z - z_1 - L, A_z^-) + F_1(z + z_1 + L, A_z^+) - F_1(z + z_1 - L, A_z^+)]$

aConductor segment length is 2L.

bConductor segment is centered at  $(x_1, y_1, z_1)$ .

c $F_1(t,u) = \ln[t + (t^2 + u^2)^{0.5}]$ ;  $A_x^\pm = [(y - y_1)^2 + (z \pm z_1)^2]^{0.5}$ ;  $A_y^\pm = [(x - x_1)^2 + (z \pm z_1)^2]^{0.5}$ ;  $A_z^\pm = [(x - x_1)^2 + (y - y_1)^2]^{0.5}$ .

TABLE 5.2 Equations for Voltage Distribution Factors Between Two Conductor Segments  
(Mutual Resistance)

Conductor direction <sup>a,b</sup>		Voltage distribution factors <sup>c,d</sup>	
Segment 1	Segment 2		
x-directed	x-directed	$\frac{1}{16L_1 L_2 \pi \sigma}$	$[F_2(x_2 - x_1 + L_1 + L_2, B_x^-) - F_2(x_2 - x_1 + L_1 - L_2, B_x^-)$ $+ F_2(x_2 - x_1 - L_1 + L_2, B_x^-) + F_2(x_2 - x_1 - L_1 - L_2, B_x^-)$ $+ F_2(x_2 - x_1 + L_1 + L_2, B_x^+) - F_2(x_2 - x_1 + L_1 - L_2, B_x^+)$ $- F_2(x_2 - x_1 - L_1 + L_2, B_x^+) + F_2(x_2 - x_1 - L_1 - L_2, B_x^+)]$
y-directed	y-directed	$\frac{1}{16L_1 L_2 \pi \sigma}$	$[F_2(y_2 - y_1 + L_1 + L_2, B_y^-) - F_2(y_2 - y_1 + L_1 - L_2, B_y^-)$ $- F_2(y_2 - y_1 - L_1 + L_2, B_y^-) + F_2(y_2 - y_1 - L_1 - L_2, B_y^-)$ $+ F_2(y_2 - y_1 + L_1 + L_2, B_y^+) - F_2(y_2 - y_1 + L_1 - L_2, B_y^+)$ $- F_2(y_2 - y_1 - L_1 + L_2, B_y^+) + F_2(y_2 - y_1 - L_1 - L_2, B_y^+)]$

TABLE 5.2 (Continued)

Conductor direction a, b		Voltage distribution factors c,d	
Segment 1	Segment 2		
z-directed	z-directed	$\frac{1}{16L_1 L_2 \pi \sigma}$ [ $F_2(z_2 - z_1 + L_1 + L_2, B_z^-) - F_2(z_2 - z_1 + L_1 - L_2, B_z^+)$ $- F_2(z_2 - z_1 - L_1 + L_2, B_z^-) + F_2(z_2 - z_1 - L_1 - L_2, B_z^+)$ $+ F_2(z_2 + z_1 + L_1 + L_2, B_z^-) - F_2(z_2 + z_1 + L_1 - L_2, B_z^+)$ $- F_2(z_2 + z_1 - L_1 + L_2, B_z^-) + F_2(z_2 + z_1 - L_1 - L_2, B_z^+)$ ]	
x-directed	y-directed	$\frac{1}{16L_1 L_2 \pi \sigma}$ [ $F_3(x_2 - x_1 + L_1, y_2 - y_1 + L_2, z_2 - z_1) - F_3(x_2 - x_1 + L_1, y_2 - y_1 - L_2, z_2 - z_1)$ $- y_1 - L_2, z_2 - z_1) - F_3(x_2 - x_1 - L_1, y_2 - y_1 + L_2, z_2 - z_1)$ $+ F_3(x_2 - x_1 - L_1, y_2 - y_1 - L_2, z_2 - z_1) + F_3(x_2 - x_1 + L_1, y_2 - y_1 + L_2, z_2 + z_1)$ $- F_3(x_2 - x_1 - L_1, y_2 - y_1 + L_2, z_2 + z_1) + F_3(x_2 - x_1 - L_1, y_2 - y_1 - L_2, z_2 + z_1)$ $- y_1 - L_2, z_2 + z_1) ]$	

$\text{x-directed}$ $\frac{1}{16L_1 L_2^{\pi\sigma}} [F_3(x_2 - x_1 + L_1, z_2 - z_1 + L_2, y_2 - y_1) - F_3(x_2 - x_1 + L_1, z_2 - z_1 - L_2, y_2 - y_1)$ $- z_1 - L_2, y_2 - y_1) - F_3(x_2 - x_1 - L_1, z_2 - z_1 + L_2, y_2 - y_1)$ $+ F_3(x_2 - x_1 - L_1, z_2 - z_1 - L_2, y_2 - y_1) + F_3(x_2 - x_1 + L_1, z_2$ $+ z_1 + L_2, y_2 - y_1) - F_3(x_2 - x_1 + L_1, z_2 + z_1 - L_2, y_2 - y_1)$ $- F_3(x_2 - x_1 - L_1, z_2 + z_1 + L_2, y_2 - y_1) + F_3(x_2 - x_1 - L_1, z_2$ $+ z_1 - L_2, y_2 - y_1)]$	$\text{y-directed}$ $\frac{1}{16L_1 L_2^{\pi\sigma}} [F_3(y_2 - y_1 + L_1, z_2 - z_1 + L_2, x_2 - x_1) - F_3(y_2 - y_1 + L_1, z_2$ $- z_1 - L_2, x_2 - x_1) - F_3(y_2 - y_1 - L_1, z_2 - z_1 + L_2, x_2 - x_1)$ $+ F_3(y_2 - y_1 - L_1, z_2 - z_1 - L_2, x_2 - x_1) + F_3(y_2 - y_1 + L_1, z_2$ $+ z_1 + L_2, x_2 - x_1) - F_3(y_2 - y_1 + L_1, z_2 + z_1 - L_2, x_2 - x_1)$ $- F_3(y_2 - y_1 - L_1, z_2 + z_1 + L_2, x_2 - x_1) + F_3(y_2 - y_1 - L_1, z_2$ $+ z_1 - L_2, x_2 - x_1)]$
---	---

a Segment 1 length is  $2L_1$ . Segment 2 length is  $2L_2$ .

b Segment 1 is centered at  $(x_1, y_1, z_1)$ . Segment 2 is centered at  $(x_2, y_2, z_2)$ .

$$c B_x^{\pm} = [(y_2 - y_1)^2 + (z_2 \pm z_1)^2]^{0.5}, B_y^{\pm} = [(x_2 - x_1)^2 + (z_2 \pm z_1)^2]^{0.5}, B_z^- = [(x_2 - x_1)^2 + (y_2 - y_1)^2]^{0.5}.$$

d The functions  $F_2$  and  $F_3$  are defined in the text.

TABLE 5.3 Equations for Self-Voltage Distribution Factors ("Self-Resistance")

Direction of conductor segment <sup>a,b</sup>	Self-voltage distribution factors <sup>c</sup>
x-directed	$\frac{1}{16L\pi\sigma} [F_2(2L,a) + F_2(-2L,a) - 2a + F_2(2L, z_1 \sqrt{2}) + F_2(-2L, z_1 \sqrt{2}) - 2 z_1 \sqrt{2}]$
y-directed	$\frac{1}{16L\pi\sigma} [F_2(2L,a) + F_2(-2L,a) - 2a + F_2(2L, z_1 \sqrt{2}) + F_2(-2L, z_1 \sqrt{2}) - 2 z_1 \sqrt{2}]$
z-directed	$\frac{1}{16L\pi\sigma} [F_2(2L,a) + F_2(-2L,a) - 2a + F_2(2 z_1  + 2L,a) + F_2(2 z_1  - 2L,a) - 2F_2(2 z_1 ,a)]$

aConductor segment length is  $2L$ .

bConductor segment is centered at  $(x_1, y_1, z_1)$ .  
 $cF_2(t,u) = t \ln[t + (t^2 + u^2)^{0.5}] - (t^2 + u^2)^{0.5}$ .

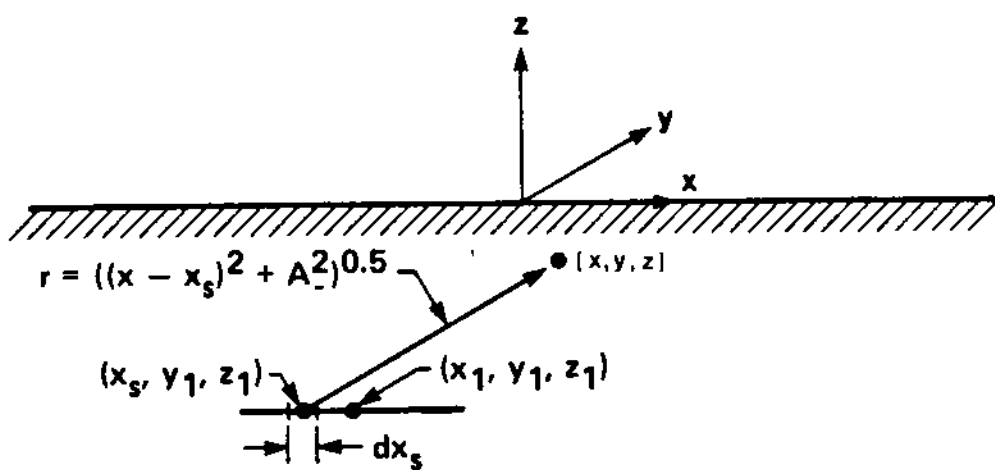


FIG. 5.11 Illustration of a conductor segment represented with a line current source of constant current density.

The voltage at point  $(x, y, z)$  results from the contributions of all infinitesimal current sources, that is,

$$\begin{aligned} V(x, y, z) &= \int dV(x, y, z) \\ &= \frac{I}{8L\pi\sigma} \int_{x_s=x_1-L}^{x_1+L} \left\{ [ (x - x_s)^2 + A_-^2 ]^{-1/2} \right. \\ &\quad \left. + [ (x - x_s)^2 + A_+^2 ]^{-1/2} \right\} dx_s \end{aligned}$$

The integral above is evaluated with the aid of the following indefinite integral:

$$\int (t^2 \pm u^2)^{-0.5} dt = \ln[t + (t^2 \pm u^2)^{0.5}]$$

The result is

$$\begin{aligned} V(x, y, z) &= \frac{I}{8L\pi\sigma} [ F_1(x - x_1 + L, A_-) - F_1(x - x_1 - L, A_-) \\ &\quad + F_1(x - x_1 + L, A_+) - F_1(x - x_1 - L, A_+) ] \quad (5.50) \end{aligned}$$

where

$$F_1(t, u) = \ln[t + (t^2 + u^2)^{0.5}] \quad (5.51)$$

Comparison of the derived formula to the one defining the VDF yields

$$\text{VDF} = \frac{1}{8L\pi\sigma} \ln[F_1(x - x_1 + L, A_-) - F_1(x - x_1 - L, A_-) + F_1(x - x_1 + L, A_+) - F_1(x - x_1 - L, A_+)] \quad (5.5)$$

In summary, Eq. (5.52) provides the voltage distribution factor (otherwise known as transfer resistance) between a conductor segment of length  $2L$ , oriented parallel to the  $x$  axis, and a point  $(x, y, z)$ .

### VDF Between Two $x$ -Directed Conductor Segments

Consider the configuration of two conductor segments as illustrated in Fig. 5.10. The coordinates of the centers of the two conductor segments are  $(x_1, y_1, z_1)$  and  $(x_2, y_2, z_2)$ , respectively. The lengths of the segment are  $2L_1$  and  $2L_2$ , respectively. The total electric current of conductor segment 1 is  $I_1$ . The flow of the current  $I_1$  will "transfer" a potential to the conductor segment 2. Let this potential be  $V_2$ . Our objective is to compute this voltage. A reasonably accurate way to compute this voltage is to compute the average voltage along the centerline of the conductor segment 2, assuming that the second conductor does not exist. The coordinates of a point on the centerline of the conductor segment 2 are  $(x, y_2, z_2)$ , where  $x$  varies in the interval  $[x_2 - L_2 \leq x \leq x_2 + L_2]$ . The voltage at point  $(x, y_2, z_2)$  is given from Eq. (5.52):

$$V_2(x, y_2, z_2) = \frac{I_1}{8L_1\pi\sigma} [F_1(x - x_1 + L_1, B_-) - F_1(x - x_1 - L_1, B_-) + F_1(x - x_1 + L_1, B_+) - F_1(x - x_1 - L_1, B_+)]$$

where

$$B_{\pm} = [(y_2 - y_1)^2 + (z_2 \pm z_1)^2]^{0.5}$$

The average voltage along the centerline of the conductor segment is

$$V_2 = \frac{1}{2L_2} \int_{x=x_2-L_2}^{x_2+L_2} V_2(x, y_2, z_2) dx \quad (5.5)$$

The integral above is evaluated with the aid of the following indefinite integral:

$$\int F_1(t, u) dt = t \ln[t + (t^2 + u^2)^{0.5}] - (t^2 + u^2)^{0.5}$$

The result is

$$\begin{aligned} V_2 = & \frac{I_1}{16L_1 L_2 \pi \sigma} [F_2(x_2 - x_1 + L_1 + L_2, B_-) + F_2(x_2 - x_1 + L_1 \\ & + L_2, B_+) - F_2(x_2 - x_1 + L_1 - L_2, B_-) - F_2(x_2 - x_1 \\ & + L_1 - L_2, B_+) - F_2(x_2 - x_1 - L_1 + L_2, B_-) - F_2(x_2 \\ & - x_1 - L_1 + L_2, B_+) + F_2(x_2 - x_1 - L_1 - L_2, B_-) \\ & + F_2(x_2 - x_1 - L_1 - L_2, B_+)] \end{aligned} \quad (5.54)$$

where

$$F_2(t, u) = t \ln[t + (t^2 + u^2)^{0.5}] - (t^2 + u^2)^{0.5} \quad (5.55)$$

Comparison of the equations above with the one defining the VDF yields

$$\begin{aligned} \text{VDF} = & \frac{1}{16L_1 L_2 \pi \sigma} [F_2(x_2 - x_1 + L_1 + L_2, B_-) + F_2(x_2 - x_1 \\ & + L_1 + L_2, B_+) - F_2(x_2 - x_1 + L_1 - L_2, B_-) - F_2(x_2 \\ & - x_1 + L_1 - L_2, B_+) - F_2(x_2 - x_1 - L_1 + L_2, B_-) \\ & - F_2(x_2 - x_1 - L_1 + L_2, B_+) + F_2(x_2 - x_1 - L_1 - L_2, B_-) \\ & + F_2(x_2 - x_1 - L_1 - L_2, B_+)] \end{aligned} \quad (5.56)$$

In summary, Eq. (5.56) provides the voltage distribution factor (otherwise known as mutual resistance) between two x-directed conductor segments of length  $2L_1$  and  $2L_2$ , respectively.

#### VDF Between an x-Directed and a y-Directed Conductor Segment

The configuration of two conductor segments, one x-directed and the other y-directed, is illustrated in Fig. 5.12. Let the x-directed conductor segment be of length  $2L_1$  and centered at the point  $(x_1, y_1, z_1)$ . The y-directed conductor segment is of length  $2L_2$  and centered at the point  $(x_2, y_2, z_2)$ . The total electric current of the x-directed conductor segment is  $I_1$ . Our objective is to compute the voltage transferred to the y-directed segment due to the current of the x-directed segment. Again, a reasonably accurate way to compute

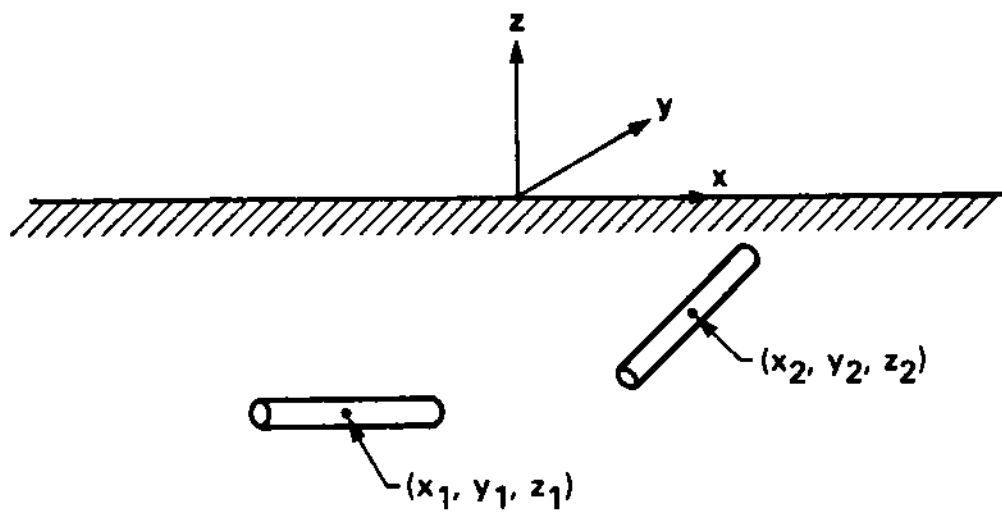


FIG. 5.12 Two-earth embedded conductor segments ( $x$ - and  $y$ -directed).

the voltage is to compute the average voltage along the center line of the  $y$ -directed conductor segment assuming that the  $y$ -directed conductor does not exist. The coordinates of a point on the center line of the  $y$ -directed conductor are  $(x_2, y, z_2)$ , where  $y$  varies in the interval  $[y_2 - L_2 \leq y \leq y_2 + L_2]$ . The voltage at point  $(x_2, y, z_2)$  due to the current of the  $x$ -directed conductor is given with an appropriate application of Eq. (5.52):

$$V_2(x_2, y, z_2) = \frac{I_1}{8L_1\pi\sigma} [F_1(x_2 - x_1 + L_1, C_-) - F_2(x_2 - x_1 - L_1, C_-) + F_1(x_2 - x_1 + L_1, C_+) - F_1(x_2 - x_1 - L_1, C_+)]$$

where

$$C_{\pm} = [(y - y_1)^2 + (z_2 \pm z_1)^2]^{0.5}$$

The voltage of the  $y$ -directed conductor is computed as the average of  $V_2(x_2, y, z_2)$  along the centerline:

$$V_2 = \frac{1}{2L_2} \int_{y=y_2-L_2}^{y_2+L_2} V_2(x_2, y, z_2) dy \quad (5.52)$$

The integral above is evaluated with the aid of the following indefinite integral:

$$\begin{aligned} F_3(t, u, v) &= \int \ln[t + (t^2 + u^2 + v^2)^{0.5}] du \\ &= -u + u \ln[t + (t^2 + u^2 + v^2)^{0.5}] + t \ln[u + (t^2 + u^2 + v^2)^{0.5}] \\ &\quad + 2v \tan^{-1} \frac{t + u + (t^2 + u^2 + v^2)^{0.5}}{v} \end{aligned}$$

Applying the integral above for each one of the four terms involved in Eq. (5.57) yields

$$\begin{aligned} V_2 = \frac{I_1}{16L_1 L_2 \pi \sigma} & [F_3(x_2 - x_1 + L_1, y_2 - y_1 + L_2, z_2 - z_1) \\ & - F_3(x_2 - x_1 + L_1, y_2 - y_1 - L_2, z_2 - z_1) \\ & + F_3(x_2 - x_1 + L_1, y_2 - y_1 + L_2, z_2 + z_1) \\ & - F_3(x_2 - x_1 + L_1, y_2 - y_1 - L_2, z_2 + z_1) \\ & - F_3(x_2 - x_1 - L_1, y_2 - y_1 + L_2, z_2 - z_1) \\ & + F_3(x_2 - x_1 - L_1, y_2 - y_1 - L_2, z_2 - z_1) \\ & - F_3(x_2 - x_1 - L_1, y_2 - y_1 + L_2, z_2 + z_1) \\ & + F_3(x_2 - x_1 - L_1, y_2 - y_1 - L_2, z_2 + z_1)] \end{aligned} \quad (5.58)$$

The voltage distribution factor (VDF) (or transfer resistance) equals the voltage  $V_2$  divided by the current  $I_1$ .

#### Self-VDF of an x-Directed Conductor

The self-VDF is defined as the ratio of the voltage rise of an earth-embedded conductor segment to the total electric current flowing into earth from the outside surface of the conductor. The computation of the self-VDF requires consideration of the finite diameter of the conductor segment. Specifically, as in our previous discussions, the conductor segment is modeled as a line current source located on the axis of the conductor. A constant current density along the line current source is assumed. Then the voltage of the conductor segment is computed as the average voltage on the cylindrical surface of the conductor segment. Because the conductor segment length is typically much larger than the radius, the two end surfaces of the segment are ignored.

Let the length of the conductor segment be  $2L$ , its radius  $a$ , and the total current  $I$ . The current density of the line source is

$$k = \frac{I}{2L}$$

Consider an infinitesimal cylindrical surface of the conductor segment at location  $x$  as illustrated in Fig. 5.13. An infinitesimal length  $dx_s$  of the line current source is also shown. This length represents an infinitesimal current source of current  $I dx_s / 2L$ . Now consider a point  $(x, y, z)$  located on the infinitesimal cylindrical surface. The voltage at this point due to the infinitesimal current source is

$$dV(x, y, z) = \frac{I dx_s}{8L\pi\sigma} \left\{ [ (x_s - x)^2 + a^2 ]^{-0.5} + [ (x_s - x)^2 + A_+^2 ]^{-0.5} \right\} \quad (5.1)$$

where

$$A_+ = [(y - y_1)^2 + (z + z_1)^2]^{0.5}$$

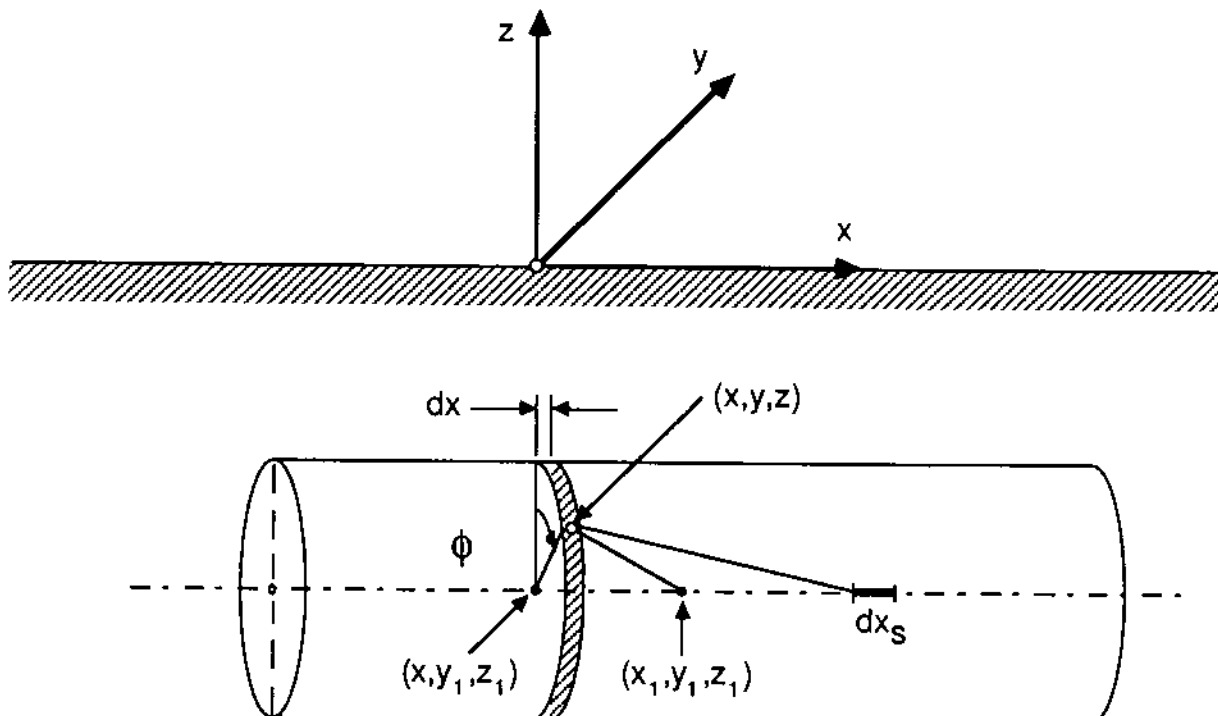


FIG. 5.13 Illustration of an  $x$ -directed conductor segment. (Conductor radius is enlarged to illustrate the analysis procedure.)

Assuming that the conductor is buried in earth at a depth much greater than the radius  $a$ , the  $A_+$  quantity is approximated by

$$A_+ \approx (2z_1^2)^{1/2}$$

The voltage at point  $(x, y, z)$  will be equal to the sum of the contributions from all infinitesimal sources:

$$V(x, y, z) = \int_{x_s=x_1-L}^{x_1+L} dV(x, y, z)$$

Upon substitution of  $A_+$  and evaluation of the integral, we have

$$\begin{aligned} V(x, y, z) &= \frac{I}{8L\pi\sigma} [F_1(x - x_1 + L, a) - F_1(x - x_1 - L, a) \\ &\quad + F_1(x - x_1 + L, |z_1|\sqrt{2}) - F_1(x - x_1 \\ &\quad - L, |z_1|\sqrt{2})] \end{aligned} \quad (5.60)$$

where the function  $F_1$  is defined with Eq. (5.51).

The average voltage around the infinitesimal cylindrical strip of Fig. 5.13 will be equal to  $V(x, y, z)$  since from Eq. (5.60) it is apparent that the voltage  $V(x, y, z)$  depends only on the coordinate  $x$ . Thus

$$V(x) = V(x, y, z)$$

Now the voltage elevation of the conductor is computed as the average voltage along all infinitesimal cylindrical surfaces:

$$V_1 = \frac{1}{2L} \int_{x=x_1-L}^{x_1+L} V(x) dx \quad (5.61)$$

Upon evaluation of the integral,

$$\begin{aligned} V_1 &= \frac{I}{16\pi\sigma L^2} [F_2(2L, a) - F_2(0, a) - F_2(0, a) + F_2(-2L, a) \\ &\quad + F_2(2L, |z_1|\sqrt{2}) - F_2(0, |z_1|\sqrt{2}) - F_2(0, |z_1|\sqrt{2}) \\ &\quad + F_2(-2L, |z_1|\sqrt{2})] \end{aligned} \quad (5.62)$$

where the function  $F_2$  is defined with Eq. (5.55). Note that  $F_2(0,a) = -a$ ,  $F_2(0,|z_1|\sqrt{2}) = -|z_1|\sqrt{2}$ .

The self-VDF of the conductor segment is computed as the ratio of the voltage  $V_1$  to the current  $I$ :

$$\begin{aligned} \text{VDF} &= \frac{1}{16\pi\sigma L^2} [F_2(2L,a) + F_2(-2L,a) - 2a + F_2(2L,|z_1|\sqrt{2}) \\ &\quad + F_2(-2L,|z_1|\sqrt{2}) - 2|z_1|\sqrt{2}] \end{aligned} \quad (5.63)$$

In summary, Eq. (5.63) provides the self-VDF (otherwise known as the self resistance) of an x-oriented conductor segment.

#### 5.5.4 Discussion on Numerical Techniques

In this section we have discussed numerical techniques for grounding system analysis. The basic analytical result is Eq. (5.40), which provides the voltage at a point in earth due to a point current source. This equation is the basis for all numerical analysis techniques of grounding systems. We discussed the matrix method as well as the combined integration/matrix method. Other ramifications of these methods can be found in the literature. The combined integration/matrix method is based on the concept of voltage distribution factors, defined as the transferred voltage to a point or conductor segment due to the electric current of an earth-embedded conductor segment. Typical VDFs have been derived. A summary of VDFs for conductor segments oriented parallel to any one of the three coordinate axes (x, y, or z) is given in Tables 5.1, 5.2, and 5.3. These tables can be used for the analysis of most practical grounding systems. The voltage distribution functions in Tables 5.1, 5.2, and 5.3 are valid under the assumption that the earth is a semi-infinite conducting medium of constant conductivity  $\sigma$ . This is far from being true. The conductivity of soil exhibits spatial and seasonal variations. Analysis that will take these variations into account is practically impossible. On the other hand, the effects of variations of soil resistivity are substantial. In any case, the soil conductivity below a certain distance from the surface of the earth remains approximately constant (practically invariant with time). The conductivity of the top layer may vary with weather conditions (e.g., higher conductivity after a rainy day). It is expedient to model the earth as a stratified semi-infinite medium. This earth model makes the analysis complex and impractical. As a compromise between modeling simplicity and the need to model stratified earth, a two-layer soil model is typically assumed. The analysis presented in the previous sections can easily be extended to accommodate the two-layer soil model. However, this analysis is not presented here because it is beyond the scope of the book. The reader

is referred to references 14, 15, and 22. The soil model is discussed further in Chapter 8.

## 5.6 ANALYSIS OF SPATIALLY SMALL GROUNDING SYSTEMS

Spatially small grounding systems can be analyzed with the basic equations developed in Sections 5.5 and 5.6. Such simple grounding systems are illustrated in Fig. 5.14. Specifically, a single earth-embedded conductor, a star configuration of conductors, and a substation ground mat with rectangular meshes is illustrated.

The analysis can be done in two ways. One way is to assume that a certain electric current is injected through the grounding system into earth. Then the voltage distribution in earth can be computed. The other way is to assume that a certain voltage is applied at a certain point of the grounding system. Then the electric current flowing into earth and the voltage distribution in earth can be computed. Since the soil is a linear medium, the two approaches are equivalent.

In the analysis of grounding systems, it is customary to neglect the voltage drop along the conductors of a grounding system. Since most of the grounding systems are constructed with copper conductors

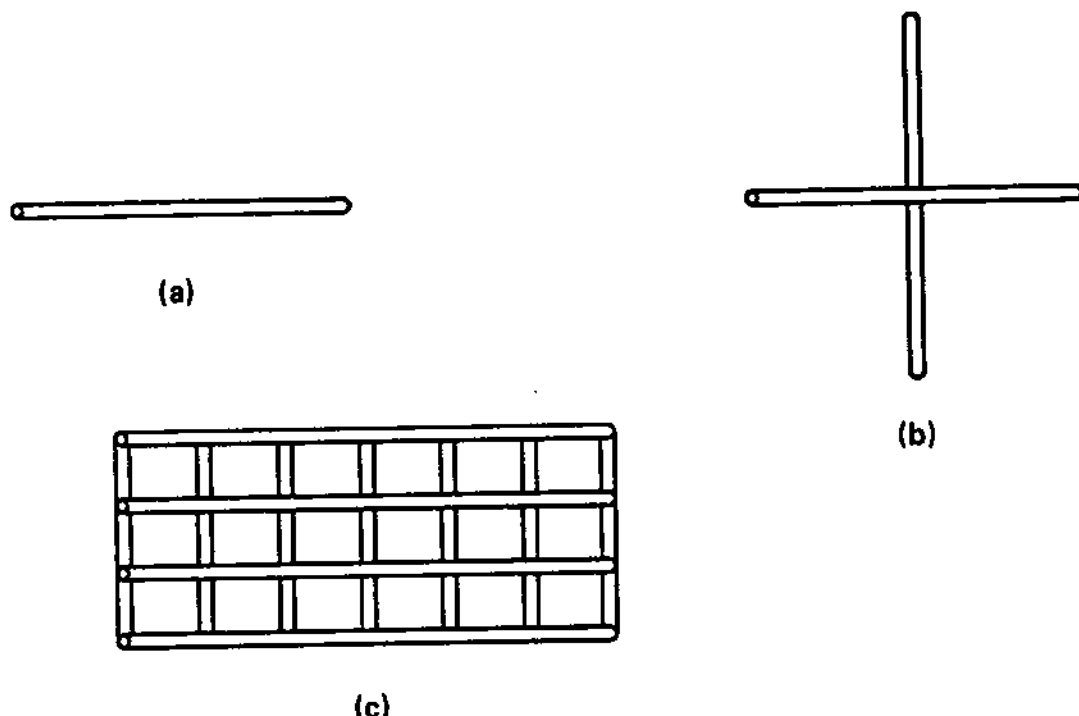


FIG. 5.14 Simple grounding systems. (a) Earth embedded wire, (b) star configuration of earth embedded wire, (c) substation ground mat with rectangular meshes.

and their dimensions are relatively small (i.e., grounding system of a power substation), this assumption is realistic. This means that all the metallic parts of a grounding system are raised to the same potential, the ground potential rise.

The procedure will be demonstrated with the analysis of an earth-embedded wire. For this purpose the earth-embedded wire is partitioned into  $n$  finite conductor segments. It is assumed that the electric current emanating from the surface of any one of the  $n$  segments is uniformly distributed along the finite segment. The total electric current emanating from conductor segment  $i$  is  $I_i$ . Then the equations of Tables 5.2 and 5.3 are utilized to relate the voltage of conductor segment  $i$ ,  $V_i$ , to the electric currents. Specifically, the voltage  $V_i$  of segment  $i$  will be constructed from the contributions from the currents of all segments:

$$V_i = \sum_{j=1}^n R_{tij} I_j \quad (5.64)$$

where  $R_{tij}$  is the VDF between segments  $i$  and  $j$  (self is  $i = j$ ). It has been mentioned that in practical cases the voltage of all segments will be approximately equal. Thus

$$V_i = V \quad \text{for every } i$$

Then writing one equation for each conductor segment yields

$$V = \sum_{j=1}^n R_{t1j} I_j$$

$$V = \sum_{j=1}^n R_{t2j} I_j$$

.

.

.

$$V = \sum_{j=1}^n R_{tnj} I_j$$

The system of equations above relates the voltage of the wire to the flow of current into earth,  $I_j$ ,  $j = 1, 2, \dots, n$ . If the voltage  $V$  is known, the foregoing system of equations can be solved to yield the electric currents  $I_j$ ,  $j = 1, 2, \dots, n$ .

Once the electric currents have been computed, other quantities of interest may be computed. These are:

Resistance. The resistance of the grounding structure is

$$R = \frac{V}{I_1 + I_2 + \dots + I_n} \quad (5.65)$$

Voltage in earth. The voltage at any point in the earth A can be computed utilizing the formulas of Table 5.1 as follows:

$$V(A) = \sum_{j=1}^n R_{tAj} I_j \quad (5.66)$$

where  $R_{tAj}$  is the VDF between segment j and point A (Table 5.1) and  $V(A)$  is the voltage at point A.

The procedure will be illustrated with an example.

Example 5.2: Consider a grounding system consisting of two 10-m-long, 2/0 copper conductors buried 0.75 m below the surface of the earth. The soil resistivity is  $200 \Omega \cdot \text{m}$ . Two insulated wires of negligible resistance are connected to the two copper conductors. The terminals of the two wires are indicated as A and B in Fig. E5.2. Assume that terminals A and B are connected. An electric current of 75 A is injected at terminals A and B.

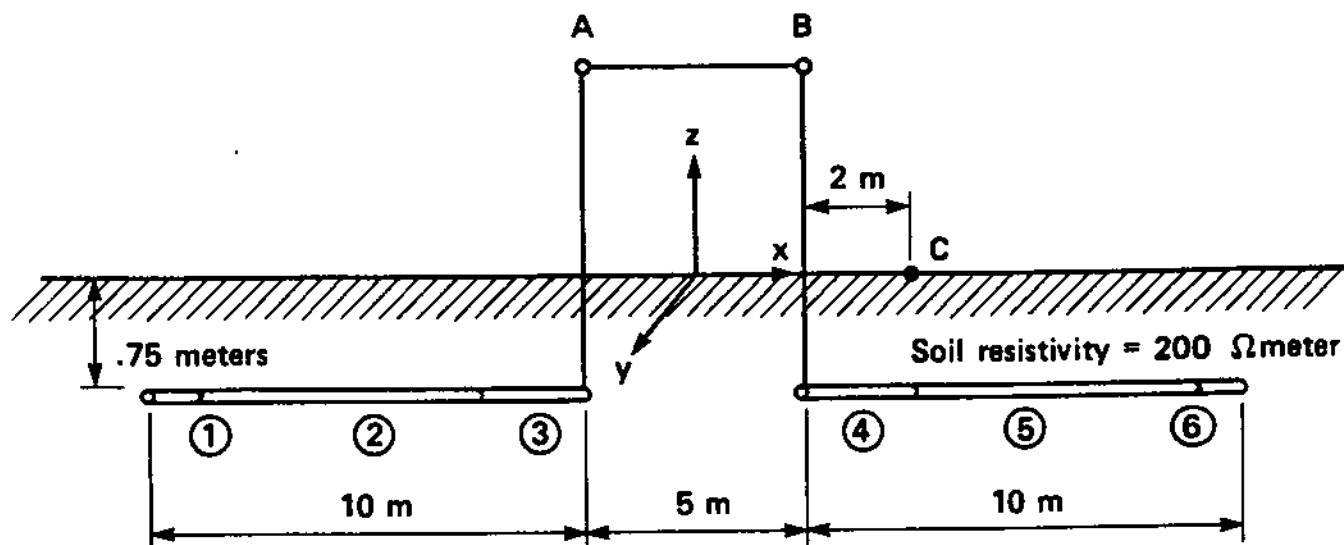


FIG. E5.2 A grounding system consisting of two 10 m, 2/0 copper conductors.

- (a) Compute the resistance of the grounding system.
- (b) Compute the ground potential rise of the system.
- (c) Assume that a person is standing on point C and touching terminals A and B. Compute the touch voltage applied to the person.

Solution: (a) The two conductors are partitioned into six segments as illustrated in Fig. E5.2a. Then a system of cartesian coordinates is selected as illustrated in Fig. E5.2a. Now the parameters of the six conductor segments are defined with respect to the coordinate system and tabulated in Table E5.1. Upon computation of the voltage distribution factors (VDF) between any two conductor segments (using the equations of Tables 5.2 and 5.3), the following matrix equation is obtained:

$$\begin{bmatrix} V_1 \\ V_2 \\ V_3 \\ V_4 \\ V_5 \\ V_6 \end{bmatrix} = \begin{bmatrix} 177.522 & 8.824 & 3.530 & 2.121 & 1.648 & 1.325 \\ 8.824 & 39.920 & 9.455 & 3.144 & 2.200 & 1.648 \\ 3.530 & 9.455 & 104.530 & 5.320 & 3.144 & 2.121 \\ 2.121 & 3.144 & 5.320 & 104.530 & 9.455 & 3.530 \\ 1.648 & 2.200 & 3.144 & 9.455 & 39.920 & 8.824 \\ 1.325 & 1.648 & 2.121 & 3.530 & 8.824 & 177.522 \end{bmatrix} \begin{bmatrix} I_1 \\ I_2 \\ I_3 \\ I_4 \\ I_5 \\ I_6 \end{bmatrix}$$

Upon solution of the matrix equations above for the electric currents, we obtain

$$\begin{bmatrix} I_1 \\ I_2 \\ I_3 \\ I_4 \\ I_5 \\ I_6 \end{bmatrix} = 10^{-2} \begin{bmatrix} 0.5698 & -0.1228 & -0.0073 & -0.0061 & -0.0142 & -0.0022 \\ -0.1228 & 2.5959 & -0.2245 & -0.0542 & -0.1043 & -0.0142 \\ -0.0073 & -0.2245 & 0.9809 & -0.0379 & -0.0542 & -0.0061 \\ -0.0061 & -0.0542 & -0.0379 & 0.9809 & -0.2245 & -0.0073 \\ -0.0142 & -0.1043 & -0.0542 & -0.2245 & 2.5959 & -0.1228 \\ -0.0022 & -0.0142 & -0.0061 & -0.0073 & -0.1228 & 0.5698 \end{bmatrix} \begin{bmatrix} V_1 \\ V_2 \\ V_3 \\ V_4 \\ V_5 \\ V_6 \end{bmatrix}$$

In the equations above,  $I_1$  is the total current injected into the soil from conductor segment 1,  $V_1$  is the voltage of conductor segment 1, and so on. Since all conductor segments are electrically connected, then

$$V_1 = V_2 = V_3 = V_4 = V_5 = V_6 = V$$

TABLE E5.1 Parameters of the Conductor Segments of the Grounding System of Fig. E5.2

Segment	Coordinates of conductor segment center (m)			Conductor segment length (m)	Diameter (m)	Orientation <sup>a</sup>
	$\underline{x}$	$\underline{y}$	$\underline{z}$			
1	-12.0	0.0	-0.75	1.0	0.0105	1
2	-8.0	0.0	-0.75	7.0	0.0105	1
3	-3.5	0.0	-0.75	2.0	0.0105	1
4	3.5	0.0	-0.75	2.0	0.0105	1
5	8.0	0.0	-0.75	7.0	0.0105	1
6	12.0	0.0	-0.75	1.0	0.0105	1

<sup>a</sup>1, x-directed; 2, y-directed; 3, z-directed.

For the computation of the resistance, it suffices to assume a value for  $V$ , solve for the currents, and then compute the resistance as the ratio of the voltage  $V$  over the current. Assuming that  $V = 100$  V and solving for the electric currents yields

$$I_1 = 0.4171 \text{ A}$$

$$I_2 = 2.0759 \text{ A}$$

$$I_3 = 0.6508 \text{ A}$$

$$I_4 = 0.6508 \text{ A}$$

$$I_5 = 2.0759 \text{ A}$$

$$I_6 = 0.4171 \text{ A}$$

The total current is

$$I_T = I_1 + I_2 + \dots + I_6 = 6.2876 \text{ A}$$

The resistance is

$$R = \frac{V}{I_T} = 15.9 \Omega$$

- (b) The ground potential rise (GPR) of the system is

$$\text{GPR} = (75 \text{ A})(15.9 \Omega) = 1192.5 \text{ V}$$

- (c) The touch voltage at point C will be equal to the ground potential rise (1192.5 V) minus the voltage at point C. The voltage at point C is given with the equation

$$V_C = \sum_{j=1}^6 R_{tcj} I_j$$

The electric currents  $I_j$ ,  $j = 1, 2, \dots, 6$ , are computed from the equations in part (a) by letting  $V_1 = V_2 = \dots = V_6 = \text{GPR} = 1192.5$  V. The result is

$$I_1 = 4.9718 \text{ A}$$

$$I_2 = 24.7551 \text{ A}$$

$$I_3 = 7.7608 \text{ A}$$

$$I_4 = 7.7608 \text{ A}$$

$$I_5 = 24.7551 \text{ A}$$

$$I_6 = 4.9718 \text{ A}$$

The voltage distribution factors  $R_{tcj}$  are computed with the equations of Table 5.1. The computed  $R_{tcj}$  values are

$$R_{tc1} = 1.927748 \Omega$$

$$R_{tc2} = 2.610968 \Omega$$

$$R_{tc3} = 3.981866 \Omega$$

$$R_{tc4} = 27.174290 \Omega$$

$$R_{tc5} = 13.321710 \Omega$$

$$R_{tc6} = 4.229192 \Omega$$

The voltage at point C is computed to be

$$V_c = 666.8 \text{ V}$$

The touch voltage is

$$V_{touch} = 525.7 \text{ V}$$

Example 5.2 suggests that analysis of grounding systems with hand calculators is at best tedious. Computer analysis is the preferred mode. Today there are several computer codes for the analysis of grounding systems. One of these codes is the program SGSYS developed under the sponsorship of the Electric Power Research Institute. A couple of typical computer-generated results are discussed next.

The objective of the first example is to demonstrate the current distribution along the conductors of a grounding system. Figure 5.15 illustrates the current distribution along a 60-m 2/0 copper conductor embedded in earth 0.5 m below the earth's surface. The earth resistivity is assumed to be  $100 \Omega \cdot \text{m}$ . Note that the current density is almost constant along the conductor except at the ends, where it is much larger. Figure 5.16 illustrates typical voltage profiles on the surface of the earth above the buried conductor. Observe that the voltage on the surface of the earth just above the center of the conductor assumes a maximum value [nearly 70% of the conductor voltage (GPR)]. Then it decays rapidly for points away from the conductor.

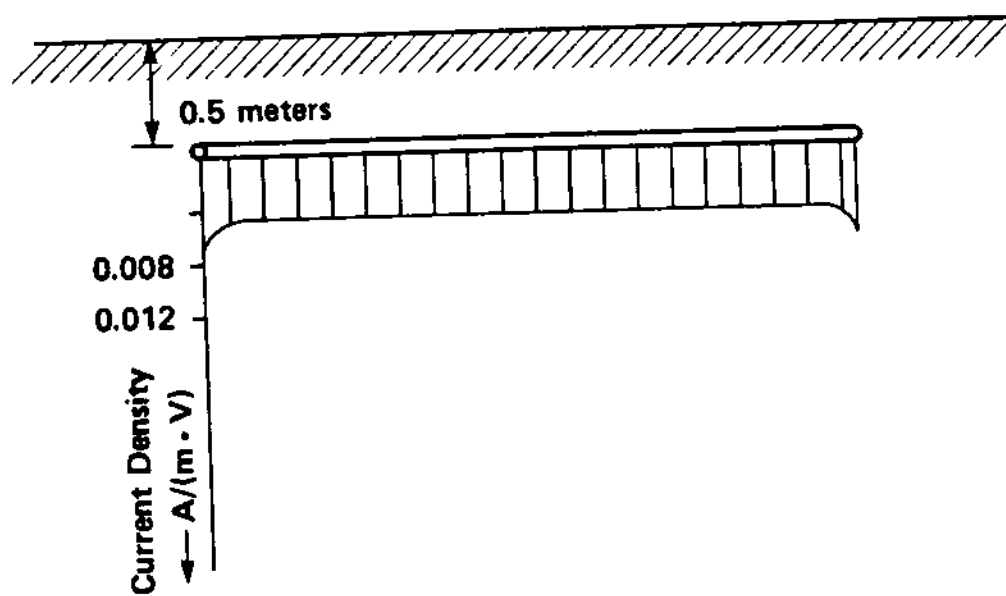


FIG. 5.15 Current distribution along a 60 m 2/0 copper conductor.  
(Burial depth = 0.5 m, soil resistivity = 100  $\Omega\text{-meter}$ , total current = .29  $\text{A/V}$ , resistance to remote earth = 3.47  $\Omega$ .)

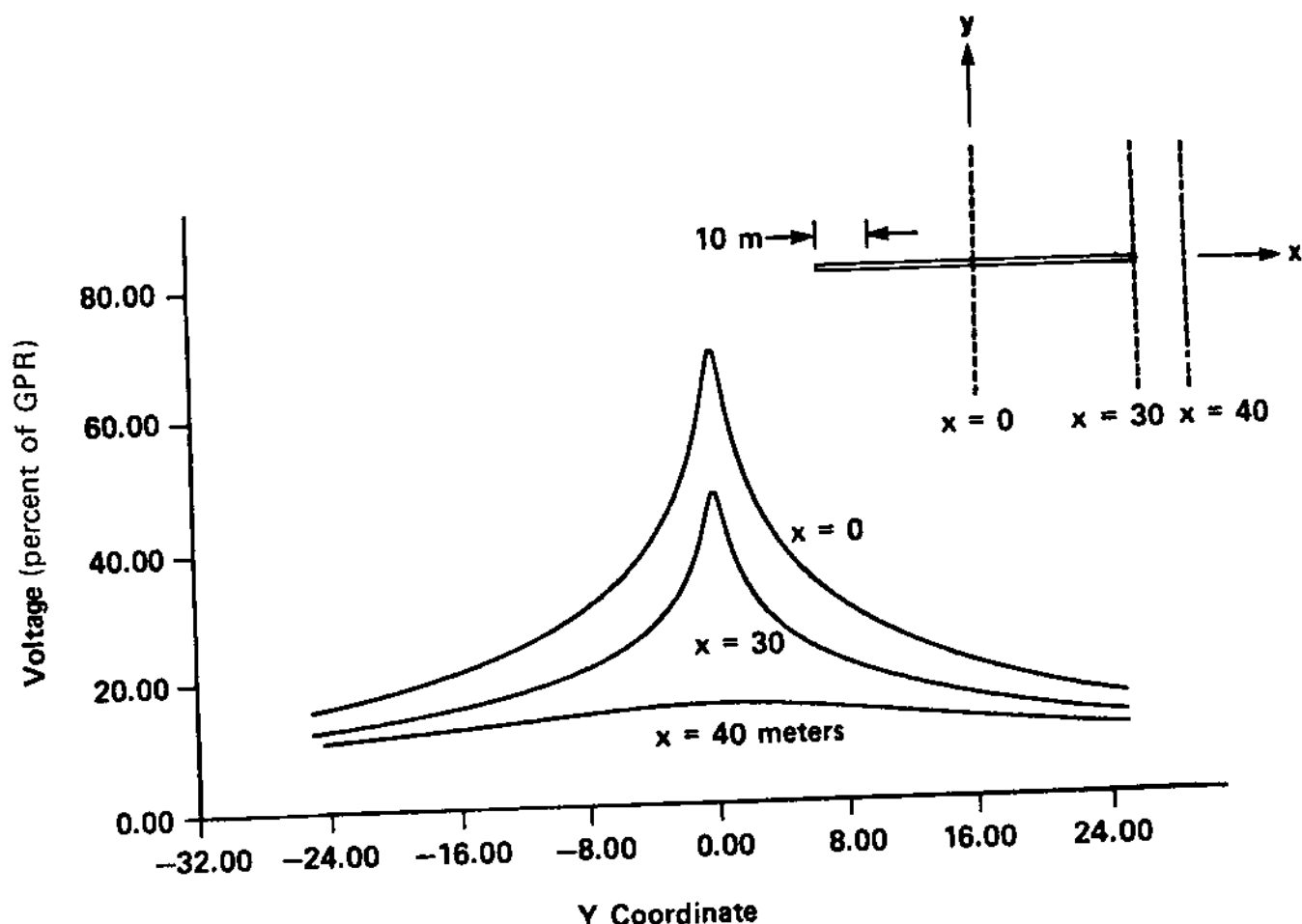


FIG. 5.16 Voltage profile on the surface of earth above a 60 m 2/0 copper conductor. (Burial depth = 0.5 meters, soil resistivity = 100  $\Omega\text{-meter}$ , resistance to remote earth = 3.47  $\Omega$ .)

Another computer-generated result is illustrated in Fig. 5.17. The figure illustrates the voltage profile on the surface of the earth along a diagonal line above an 8 mesh by 8 mesh ground mat. The parameters of the ground mat are listed on Fig. 5.17. The voltage profile on the surface of the earth can provide touch and step voltages. As an example, note that a person standing on the earth just above the center of the corner mesh of the mat (point C in Fig. 5.17) and touching a grounded structure will be subjected to the voltage  $V_{touch}$ , which is illustrated in Fig. 5.17. Similarly, a person standing with one of his or her feet on point B1 and the other on point B2 (which are 3 ft apart) will be subjected to a step voltage of  $V_{step}$ , illustrated in Fig. 5.17.

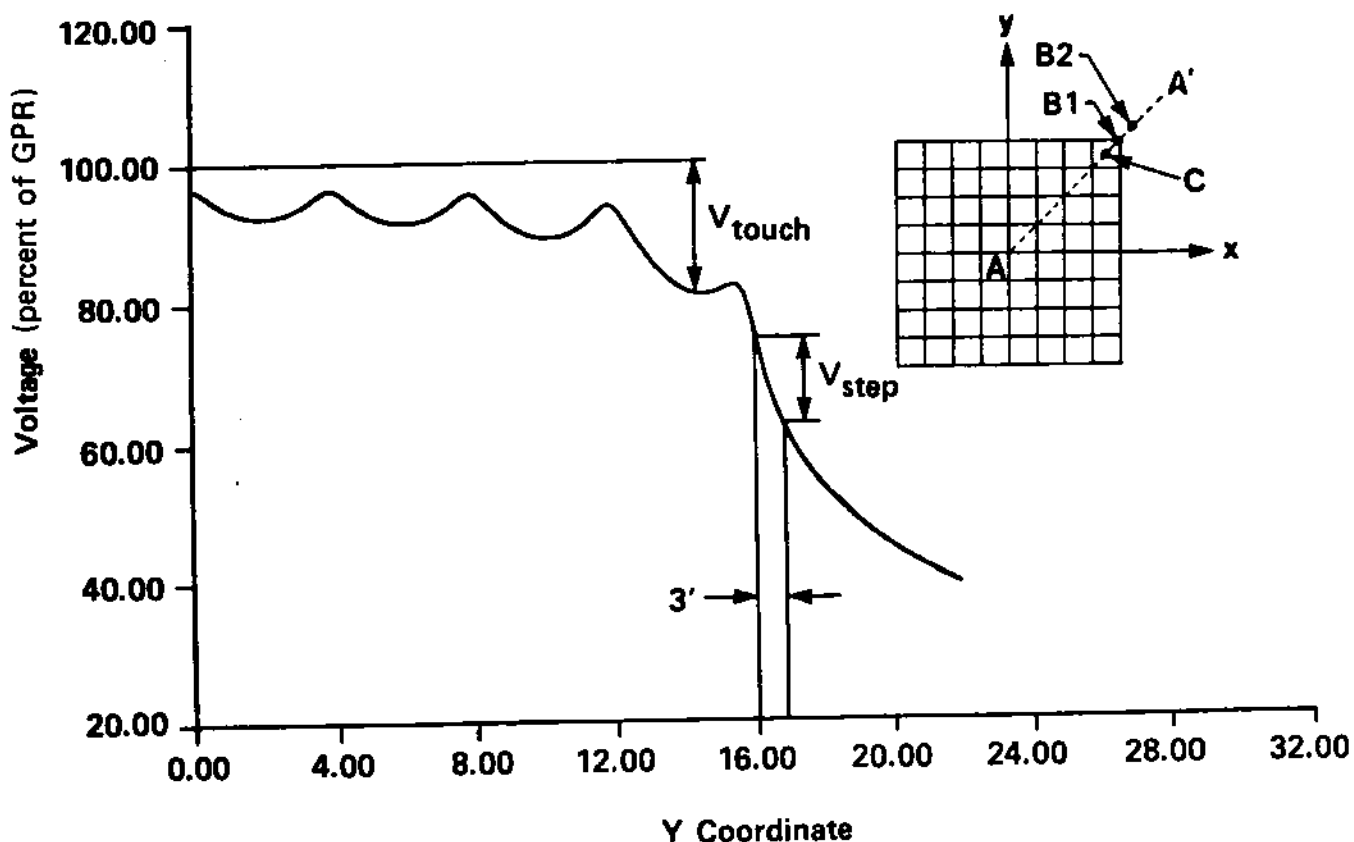


FIG. 5.17 Voltage profile along line AA'. Ground mat is 8 mesh by 8 mesh, 4 m by 4 m mesh size, 2/0 copper conductor. (Burial depth = 0.5 m, ground mat resistance to remote earth = 14.2  $\Omega$ .)

## 5.7 SIMPLIFIED EQUATIONS

The developed formulas are practically unusable for computer-based analysis. For fast approximate calculations, simpler formulas can be derived by taking into consideration the specific structure of grounding systems. Such simple formulas have been presented in Section 5.2. In this section typical simplified formulas are considered and the approximations involved in deriving these formulas are discussed.

### 5.7.1 Equations for the Resistance of Grounding Systems

In this section we examine the simplified equations for resistance of two typical cases, a ground rod and a substation ground mat. Consider a ground rod as in Fig. 5.5a. Typically, a ground rod is approximately 8 ft long and of diameter on the order of less than 1 in. Thus  $\ell \gg a$ . Assume that the ground rod is buried in such a way that the top point of the rod is near the surface of the earth. In this case the z coordinate of the center of the ground rod is  $|z_1| = \ell/2$ . Assuming uniform current distribution along the ground rod, the resistance of the ground rod is given in Table 5.3, assuming that  $\ell = 2L$  and  $|z_1| = \ell/2 = L$ . Substitution gives us

$$\begin{aligned} R &= \frac{1}{16L^2\pi\sigma} [F_2(2L,a) + F_2(-2L,a) - 2a + F_2(4L,a) - a \\ &\quad - 2F_2(2L,a)] \\ &= \frac{1}{16L^2\pi\sigma} [F_2(4L,a) - F_2(2L,a) + F_2(-2L,a) - 3a] \end{aligned}$$

Upon substitution of the functions  $F_2$ , we have

$$\begin{aligned} R &= \frac{1}{16L^2\pi\sigma} (4L \ln\{4L + [(4L)^2 + a^2]^{1/2}\} - [(4L)^2 + a^2]^{1/2}) \\ &\quad - 2L \ln\{2L + [(2L)^2 + a^2]^{1/2}\} - 2L \ln\{-2L + [(2L)^2 \\ &\quad + a^2]^{1/2}\} - 3a \} \end{aligned}$$

Note the following approximations:

$$4L + [(4L)^2 + a^2]^{1/2} \approx 8L + \frac{a^2}{8L} \approx 8L$$

$$2L + [(2L)^2 + a^2]^{1/2} \approx 4L + \frac{a^2}{4L} \approx 4L$$

$$-2L + [(2L)^2 + a^2]^{1/2} \approx \frac{a^2}{4L}$$

$$[(4L)^2 + a^2]^{1/2} \approx 4L + \frac{a^2}{8L} \approx 4L$$

Substitution of these approximations yields

$$R = \frac{1}{16L^2 \pi \sigma} \left( 4L \ln 8L - 4L - 2L \ln 4L - 2L \ln \frac{a^2}{4L} - 3a \right)$$

The result above can be rewritten in the following form:

$$\begin{aligned} R &= \frac{1}{16L^2 \pi \sigma} \left[ 2L \ln \frac{8L}{4L} - 4L - 3a + 2L \ln \frac{(8L)(4L)}{a^2} \right] \\ &= \frac{1}{16L^2 \pi \sigma} \left[ (4L \ln 2 - 4L - 3a) + 4L \ln \frac{(2)(2L)}{a} \right] \end{aligned}$$

Now observe that the quantity  $4L \ln 2 - 4L - 3a$  is very small compared to the quantity  $4L \ln[(2)(2L)/a]$ . If this quantity is neglected,

$$R = \frac{1}{4L \pi \sigma} \ln \frac{(2)(2L)}{a}$$

or

$$R = \frac{\rho}{2\pi l} \ln \frac{2l}{a}$$

where  $l = 2L$  is the length of the ground rod. The formula above is exactly the approximate equation (5.15) given for the resistance of a ground rod in Section 5.2.4. It is expedient to summarize the assumptions utilized in the derivation of the approximate equation:

- (a) the current distribution along the ground rod is uniform, and
- (b) the length of the ground rod,  $l$ , is much larger than its radius,  $a$ .

As a second typical system, consider a substation ground mat. Typically, a ground mat consists of conductors placed 5 to 20 ft apart and the ground mat may comprise many parallel conductors. It is buried in earth typically 1 to 5 ft deep. By construction, then, a ground mat resembles a plate with its distance to the surface of the soil much smaller than its dimensions. Studies of the resistance of ground mats reveal that the most important parameter that determines the resistance is the area covered by the mat. The specific shape of the ground mat (square, rectangular, etc.) is of secondary

importance. Thus, as a first approximation, we can claim that the resistance of the ground mat is approximately equal to the resistance of a disk near the soil surface which has an area equal to the area of the ground mat. Assuming that the area of the ground mat is  $A$  and the radius of the disk is  $b$ ,  $b = \sqrt{A/\pi}$ . Now, recall that the resistance of a disk near the soil surface is  $R = \rho/4b$  [Eq. (5.19)]. Upon substitution, the approximate resistance of a ground mat of area  $A$  is

$$R = \frac{\rho\sqrt{\pi}}{4\sqrt{A}} \quad (5.67)$$

Note that since the equation above is approximate, alternative formulas are possible.

### 5.7.2 Equations for Touch and Step Voltages

The computation of the touch and step voltages by use of numerical techniques has been discussed. In this section we discuss simplified equations for touch and step voltages. In general, it is very difficult to develop simplified equations for these two quantities because of the complexity of the problem. Based on experimental data, Koch [26] has suggested the following empirical formulas applicable to square ground grids:

$$E_m = \frac{\rho K_m K_i I_e}{L}$$

$$E_s = \frac{\rho K_s K_i I_e}{L}$$

where

$\rho$  = soil resistivity

$I_e$  = total current injected into the soil from the ground grid (earth current)

$L$  = total length of the ground grid conductor

$K_i$  = "nonuniformity factor," which accounts for the fact that the current distribution is not uniform along the grid conductors

and  $K_m$  and  $K_s$  are geometric factors defined with the following approximate formulas:

$$K_m = \frac{1}{2\pi} \ln \frac{D^2}{16hd} + \frac{1}{\pi} \ln \left( \prod_{i=3}^n \frac{2i-3}{2i-2} \right)$$

$$K_s = \frac{1}{\pi} \left[ \frac{1}{h} + \frac{1}{D+h} + \sum_{i=3}^n \frac{1}{(i-1)D} \right]$$

where

- n = number of parallel grid conductors
- D = spacing between two adjacent conductors
- d = diameter of the conductors
- h = burial depth

In addition, Koch [26] suggested the following empirical formula for the "nonuniformity factor"  $K_i$ :

$$K_i = 0.65 + 0.172n$$

The approximate formulas above have been compared extensively against computer models and found to be acceptably accurate only for square or nearly square ground grids. In addition, a number of improvements were made to these formulas and reported in reference 18. The simplified equations discussed in this section are useful for obtaining a first-order approximation of the performance of a grounding system with a hand-held calculator.

## 5.8 EQUIVALENT-CIRCUIT REPRESENTATION OF GROUNDING SYSTEMS

The analysis of grounding systems is often better understood through the use of equivalent circuits. Specifically, it is possible to represent a general grounding system with an equivalent circuit. The conceptual basis for such an equivalent circuit is illustrated in Fig. 5.18. The figure illustrates three conductor segments buried in earth. Assume that each conductor segment is connected to a thin wire that is brought outside the soil. Further assume that the thin wires are insulated from the soil in such a way that electric current may not flow from the surface of the thin wire into earth. Under these conditions, the presence of the thin wires does not affect the electric current flow or the voltage distribution in the soil. On the other hand, the entire system appears as a system with three terminals. It is well known from theory that given any linear system with terminals, no matter how complex, it can be represented with a circuit that has the same input/output relationships as the actual system. Thus the grounding system of Fig. 5.18a can be represented with the equivalent circuit of Fig. 5.18b. The equivalent circuit is purely resistive because we assume that the grounding system is energized with low-frequency currents and voltages (see Section 5.5).

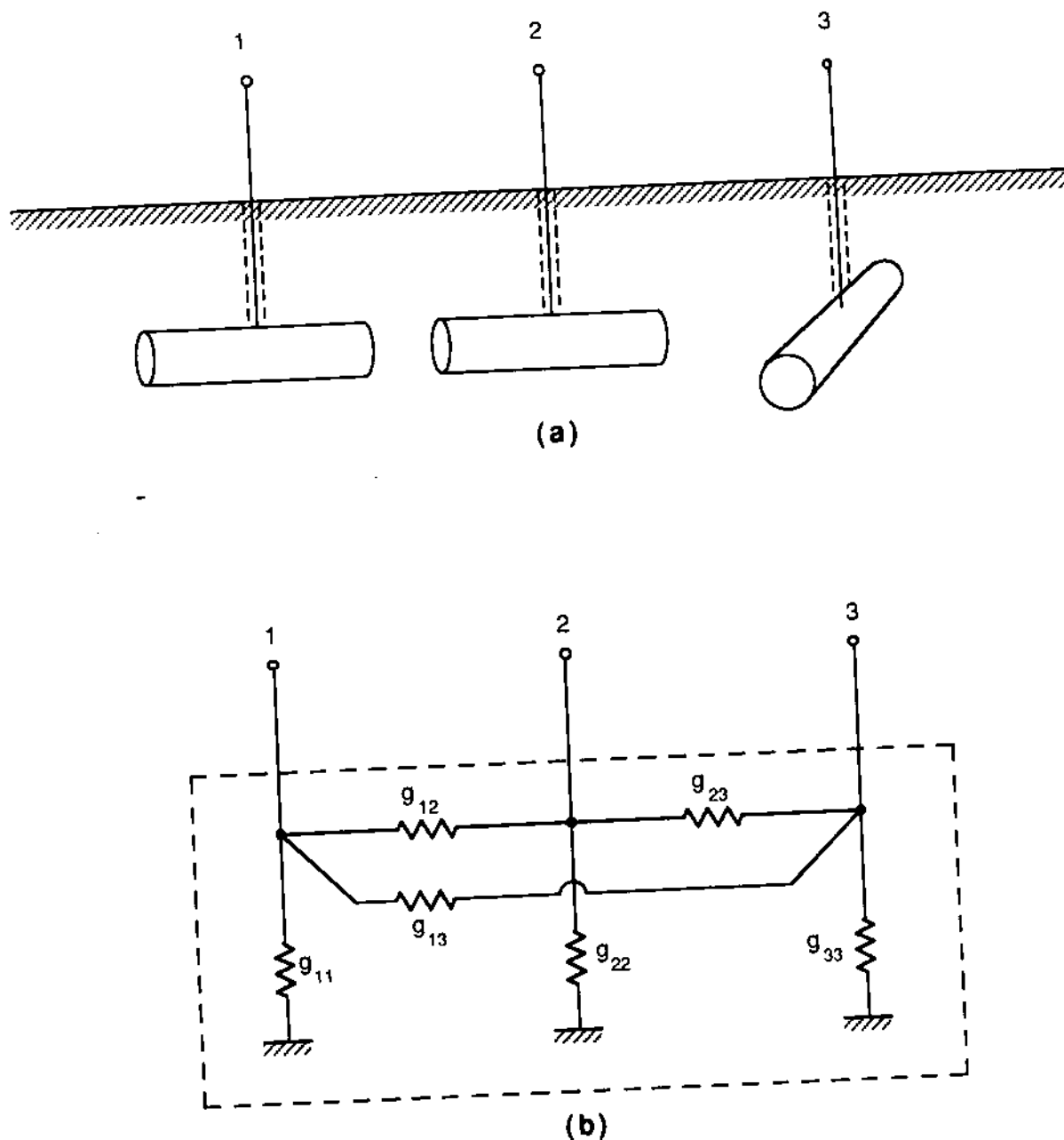


FIG. 5.18 Representation of the soil surrounding a grounding system by an equivalent circuit. (a) Earth embedded conductors, (b) equivalent circuit of the surrounding soil.

The parameters of the equivalent circuit are computed from the requirement that the input/output relationship of the systems of Fig. 5.18a and b should be identical. The input/output relationship of the system of Fig. 5.18b is expressed in terms of the admittance matrix as follows:

$$\begin{bmatrix} I_1 \\ I_2 \\ I_3 \end{bmatrix} = \begin{bmatrix} g_{11} + g_{12} + g_{13} & -g_{12} & -g_{13} \\ -g_{12} & g_{12} + g_{22} + g_{23} & -g_{23} \\ -g_{13} & -g_{23} & g_{13} + g_{23} + g_{33} \end{bmatrix} \begin{bmatrix} V_1 \\ V_2 \\ V_3 \end{bmatrix} \quad (5.68)$$

The input/output relationship for the system of Figure 5.18a is developed by applying the results of previous sections. Specifically, the voltage of conductor segments 1, 2, and 3 is given by the equations

$$V_1 = R_{t11}I_1 + R_{t12}I_2 + R_{t13}I_3$$

$$V_2 = R_{t12}I_1 + R_{t22}I_2 + R_{t23}I_3$$

$$V_3 = R_{t13}I_1 + R_{t23}I_2 + R_{t33}I_3$$

where

$I_i$  = electric current flowing from the surface of conductor segment  $i$  into earth, which is the same as the electric current flowing into the terminal  $i$

$V_i$  = voltage of segment  $i$ , which is the same as the voltage of terminal  $i$

$R_{tij}$  = voltage distribution factor between conductor segments  $i$  and  $j$

In compact matrix form, these equations read

$$[V] = [R][I] \quad (5.69)$$

where

$$[V] = \begin{bmatrix} V_1 \\ V_2 \\ V_3 \end{bmatrix} \quad \text{and} \quad [I] = \begin{bmatrix} I_1 \\ I_2 \\ I_3 \end{bmatrix}$$

The equation above is solved for the currents  $[I]$ , to yield

$$[I] = [Y][V] \quad (5.70)$$

where  $[Y] = [R]^{-1}$ . Equation (5.70) represents the input/output relationship of the system of Fig. 5.18a. For equivalence, Eqs. (5.68) and (5.70) must be identical. Thus

$$\begin{aligned} g_{11} + g_{12} + g_{13} &= y_{11} \\ -g_{12} &= y_{12} \\ -g_{13} &= y_{13} \quad \text{etc.} \end{aligned}$$

where  $y_{ij}$  is the  $(i,j)$  entry of the matrix  $[Y]$ , Eq. (5.70). Upon solution for the unknown conductances of the equivalent circuit, we have

$$\begin{aligned} g_{12} &= -y_{12} \\ g_{13} &= -y_{13} \\ g_{11} &= y_{11} + y_{12} + y_{13} \\ g_{23} &= -y_{23} \\ g_{22} &= y_{12} + y_{22} + y_{32} \\ g_{33} &= y_{13} + y_{23} + y_{33} \end{aligned}$$

The result for the simple system of Fig. 5.18 can be generalized. The conductor segments can be part of the same conductor or of different conductors which are not electrically connected. Assume that the grounding system is divided into  $n$  segments. Writing one equation for the voltage of each segment  $i$ , the following equation in compact matrix form is obtained:

$$[V] = [R][I]$$

where

$$[V] = \begin{bmatrix} V_1 \\ V_2 \\ \vdots \\ V_n \end{bmatrix} \quad [I] = \begin{bmatrix} I_1 \\ I_2 \\ \vdots \\ I_n \end{bmatrix}$$

and

- $V_i$  = voltage of the outside surface of conductor segment  $i$
- $I_i$  = total current emanating from the surface of conductor segment  $i$
- $[R]$  = symmetric  $n \times n$  matrix

Solution of the equation above for the currents [I] yields

$$[I] = [Y][V]$$

where  $[Y] = [R]^{-1}$ .

The parameters of the equivalent circuit are obtained from matrix Y as follows:

1. The negative value of the entry  $Y_{ij}$ ,  $i \neq j$  of the matrix (Y) equals the conductance of an element connected between conductor segments i and j.
2.  $\sum_{j=1}^n Y_{ij}$  equals the conductance of an equivalent-circuit element connected between conductor segment i and remote earth.

Note that the equivalent circuit represents the soil surrounding the grounding system. Since a grounding system will typically be connected to a power system, the equivalent circuit can be used to represent the grounding system in the power system network. The equivalent-circuit approach is particularly useful in the analysis of systems with multiple grounds. This problem will be addressed next.

#### 5.8.1 Analysis of Systems with Multiple Grounds

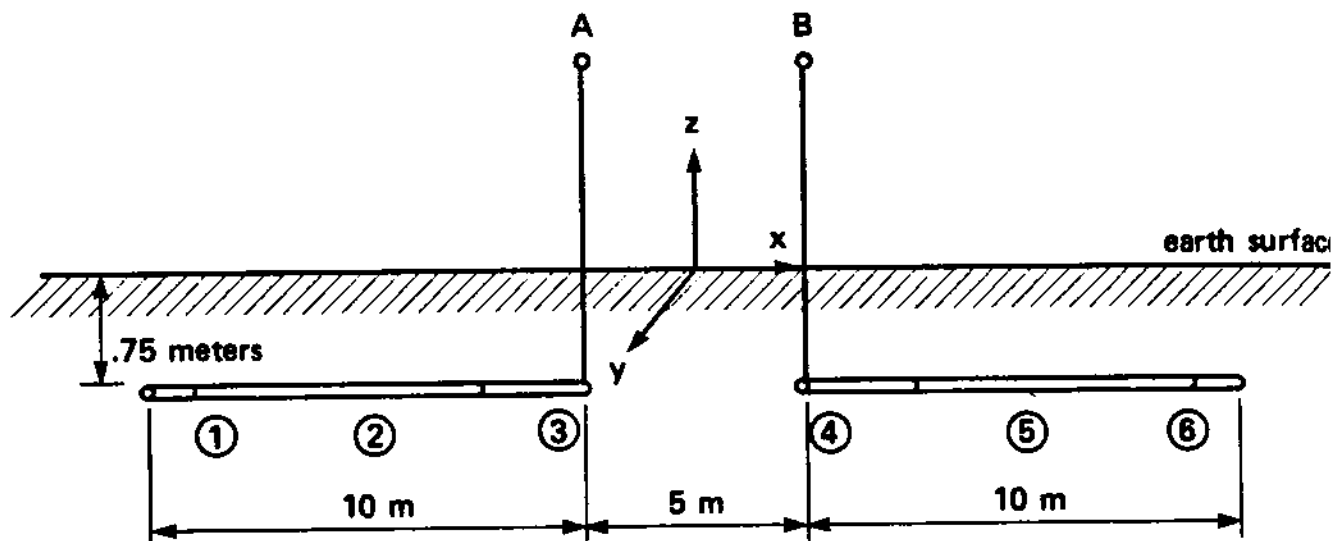
A system with multiple grounds is defined as one that comprises two or more groups of earth-embedded conductors which are not bonded together. Each group of conductors is electrically connected to other groups through the conductive soil. Examples of systems with multiple grounds are:

1. A substation ground mat and the buried portions of fence poles which are not bonded to the substation ground mat
2. A substation ground mat and a nearby buried metallic pipe which is not bonded to the ground mat

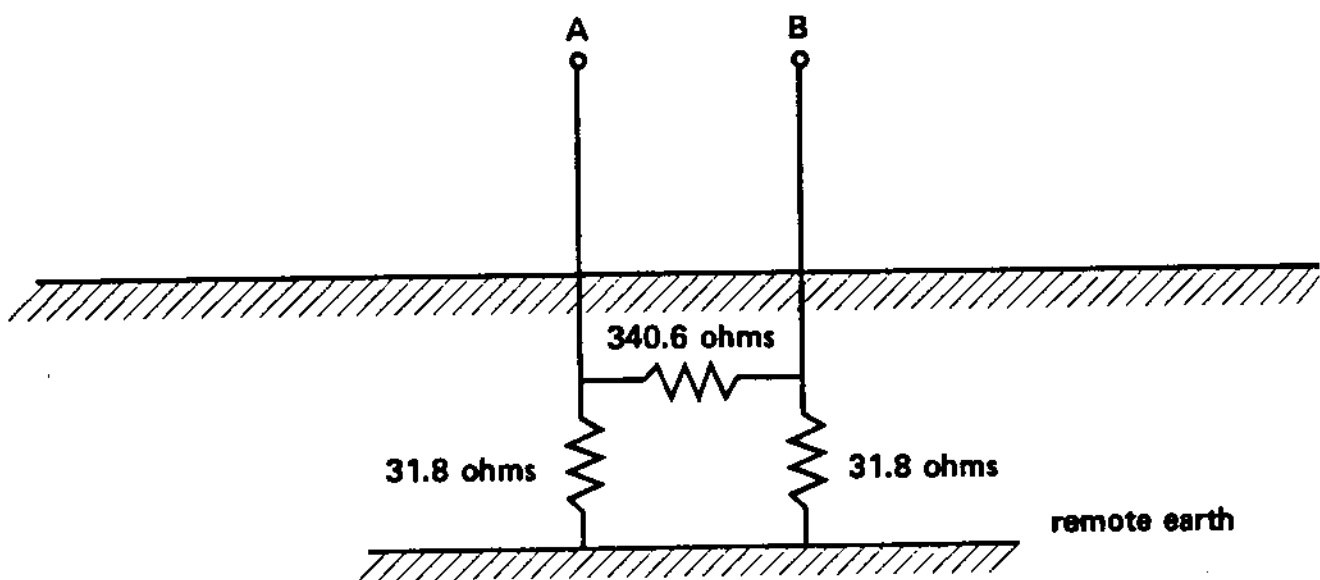
During electric faults in the power system or unbalanced operation, the ground potential rise will, in general, be different for different grounds of the system. In this case it is necessary to compute the potential rise of the different grounds. This objective is best attained through the use of equivalent circuits. Specifically, first an equivalent-circuit representation of the system of multiple grounds is computed. Then this circuit is connected to the circuit representing the power system. Subsequent solution of the resulting circuit provides the ground potential rise at each ground. The procedure will be illustrated with an example.

Example 5.3: Consider the grounding system of Example 5.2. Assume that terminals A and B are not connected as illustrated in Fig. E5.3a.

- Compute an equivalent-circuit representation of the grounding system as "seen" at terminals A and B. The soil resistivity is  $200 \Omega \cdot m$ .
- If electric current of 75 A is injected at node A, compute the ground potential rise of ground A and the transfer potential to ground B.



(a)



(b)

FIG. E5.3 A system with two grounds. (a) Physical arrangement, (b) equivalent circuit.

Solution: (a) The two conductors are segmented into six unequal conductor segments as in Example 5.2. The parameters of the conductor segments are illustrated in Table E5.1. The equations relating the conductor segment voltages to the conductor segment currents are given in Example 5.2. The equivalent circuit, as seen at terminals A and B of this two-ground system, is obtained as follows:

step 1. Assume that terminal A is maintained at V volts and terminal B is maintained at zero volts. In this case

$$V_1 = V_2 = V_3 = V$$

$$V_4 = V_5 = V_6 = 0$$

Assuming an arbitrary value for V (i.e.,  $V = 100$  V) and subsequent solution for the currents yields

$$I_1 = 0.4396 \text{ A}$$

$$I_2 = 2.2486 \text{ A}$$

$$I_3 = 0.7490 \text{ A}$$

$$I_4 = -0.0982 \text{ A}$$

$$I_5 = -0.1728 \text{ A}$$

$$I_6 = -0.0226 \text{ A}$$

The electric currents flowing in terminals A and B are

$$I_A = I_1 + I_2 + I_3 = 3.4372 \text{ A}$$

$$I_B = I_4 + I_5 + I_6 = -0.2936 \text{ A}$$

Therefore,

$$g_{AB} = -\frac{I_B}{V} = 0.002936 \text{ S}$$

$$g_{AA} = \frac{I_A + I_B}{V} = 0.031436 \text{ S}$$

or

$$R_{AB} = g_{AB}^{-1} = 340.6 \Omega$$

$$R_{AA} = g_{AA}^{-1} = 31.8 \Omega$$

The element  $g_{BB}$  of the equivalent circuit can be computed with a similar procedure. Since the system is symmetric,  $g_{BB} = g_{AA}$  and thus  $R_{BB} = 31.8 \Omega$ . Figure E5.3b illustrates the equivalent circuit.

- (b) When an electric current of 75 A is injected at ground A, the ground potential rise of ground A is

$$GPR_A = (75 \text{ A})R_{eq}$$

where  $R_{eq} = 31.8 \Omega$  in parallel with  $(31.8 + 340.6) \Omega = 29.298 \Omega$ . Thus

$$GPR_A = 2197.3 \text{ V}$$

The transfer voltage to ground B is the voltage at node B under the specified conditions. Thus

$$\begin{aligned} GPR_B &= 2197.3 \text{ V} \times \frac{31.8}{340.6 + 31.8} \\ &= 187.65 \text{ V} \end{aligned}$$

Note that this voltage is being transferred to ground B through the conductive soil alone.

## 5.9 PARAMETRIC ANALYSIS OF SUBSTATION GROUND MATS

The design of substation ground mats is dictated by safety considerations. The objective is the minimization of possible body currents in persons working or walking in and around the substation. As we have discussed, this objective is translated to the minimization of the maximum touch and step voltages. From the previous sections it is apparent that the analysis of grounding systems requires extensive computations, which for all practical purposes can only be made with a digital computer. It is, however, expedient to know the influence of the various parameters on the performance of grounding systems. In this section we present parametric results of substation grounding systems consisting of ground mats. These results provide, at a glance, information about the general behavior of such systems.

The parametric results have been obtained as follows: A ground mat with square meshes is considered. The parameters of the ground mat are:

Number of meshes in one direction: 6

Mesh size: 4 m  $\times$  4 m

Conductor size: 2/0 copper

Soil: Uniform of 200  $\Omega \cdot \text{m}$

Burial depth: 0.76 m

The resistance of this ground mat is computed to be 3.86  $\Omega$ . The maximum touch voltage for this grounding system occurs near the middle of the corner mesh. This voltage will be called the maximum mesh voltage. The maximum mesh voltage is computed to be 19.2% of the ground potential rise. Also, the maximum step voltage for this system occurs at a point located just above the outer corner of the ground mat and a direction along the diagonal of the ground mat. The location of the maximum step and mesh voltage is illustrated in Fig. 5.19. The computed maximum step voltage is 9.8% of the ground potential rise. Next, the resistance and the maximum step and mesh voltages were computed for various parameter values. Specifically, all parameters except one were kept constant. Then the resistance and maximum step and mesh voltages were computed versus the variable parameter. The results are illustrated in Figs. 5.20 through 5.24.

Figure 5.20 illustrates the effects of the ground mat size. As the number of meshes in one direction changes while the mesh size is kept constant, the size of the ground mat changes. Note that the resistance varies almost inversely proportional to the square root of the ground mat area. The maximum step and mesh voltages decrease modestly with the number of meshes in one direction.

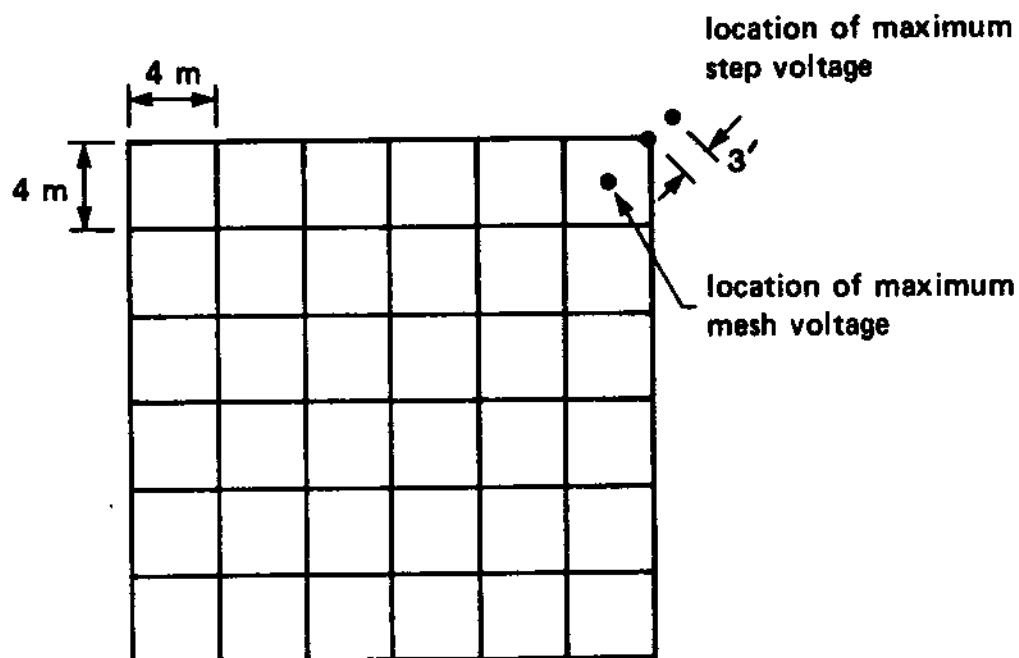


FIG. 5.19 The geometry of the ground mat for the parametric study.

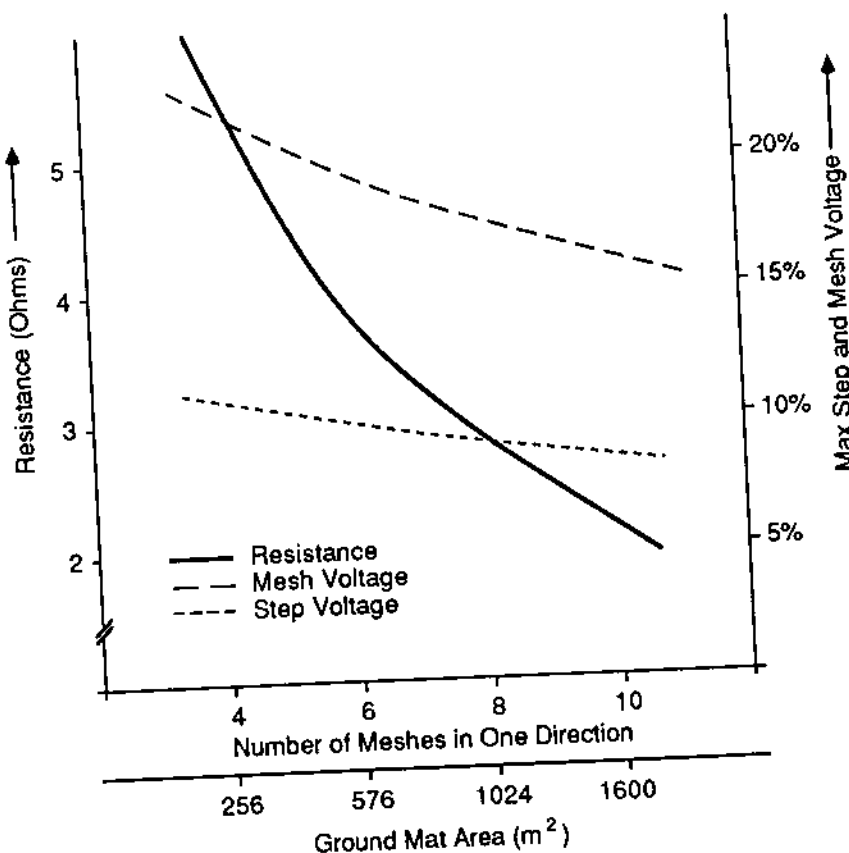


FIG. 5.20 Resistance, mesh and step voltages vs. number of meshes in one direction. (Conductor spacing = 4 meters, conductor size is 2/0 copper, burial depth = .76 meters, soil is uniform,  $200 \Omega\text{-meter}$ .)

Figure 5.21 illustrates the effects of the mesh size. The resistance varies almost inversely proportional to the mesh spacing or inversely proportional to the square root of the ground mat area. The maximum step voltage decreases moderately with the mesh size, while the maximum mesh voltage increases substantially with the mesh size.

Figure 5.22 illustrates the effects of the burial depth. The maximum step voltage drastically decreases as the burial depth increases. The resistance decreases moderately as the burial depth increases. The maximum mesh voltage attains a minimum for a burial depth of approximately 1 m and increases moderately for other burial depths.

Figure 5.23 illustrates the effects of conductor size. Specifically, four conductor sizes have been considered: 1/0, 2/0, 3/0, and 4/0 copper. Note that there is a substantial decrease of the resistance and maximum mesh voltage when the conductor size is increased from 1/0 to 2/0 copper. A further increase of the conductor size brings about only small decreases of the resistance and maximum mesh voltage and a small increase of the maximum step voltage. This suggests that grounding systems should be constructed with 2/0 copper unless other considerations (such as current-carrying capability) dictate larger sizes.

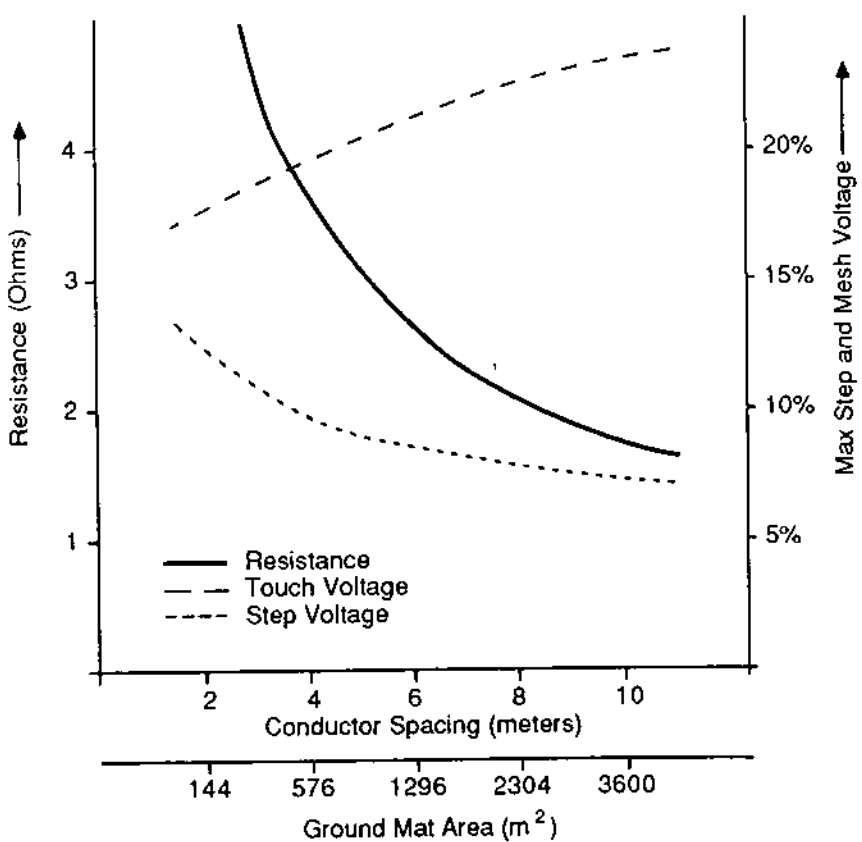


FIG. 5.21 Resistance, touch and step voltages vs. ground mat conductor spacing. (Number of meshes in one direction = 6, conductor size is 2/0 copper, burial depth = .76 m, soil is uniform, 200  $\Omega$ meter.)

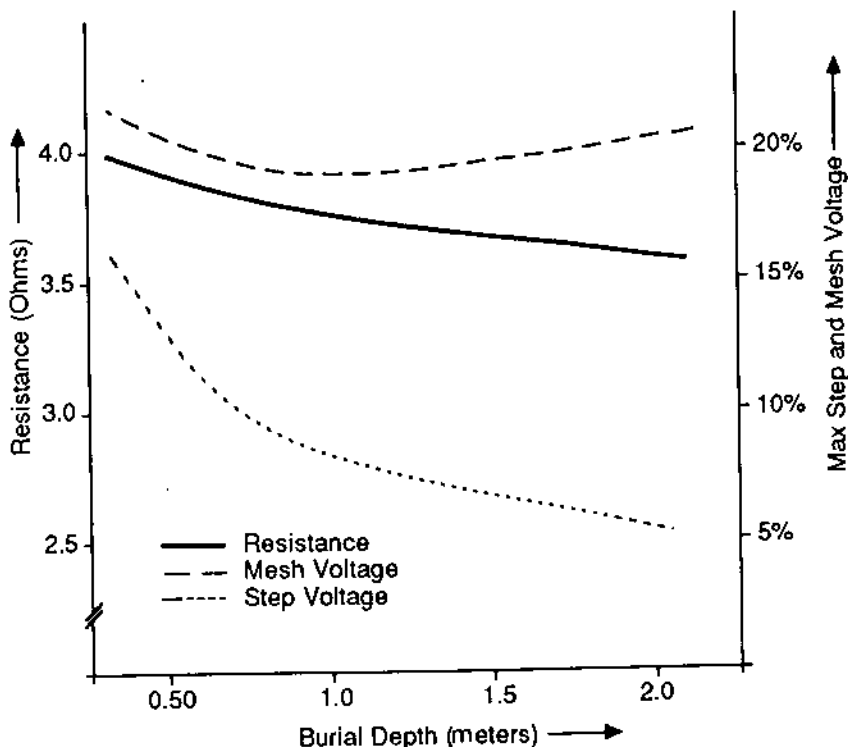


FIG. 5.22 Resistance, mesh and step voltages vs. ground mat burial depth. (Number of meshes in one direction = 6, conductor spacing = 4 m, conductor size is 2/0 copper, soil is uniform, 200  $\Omega$ meter.)

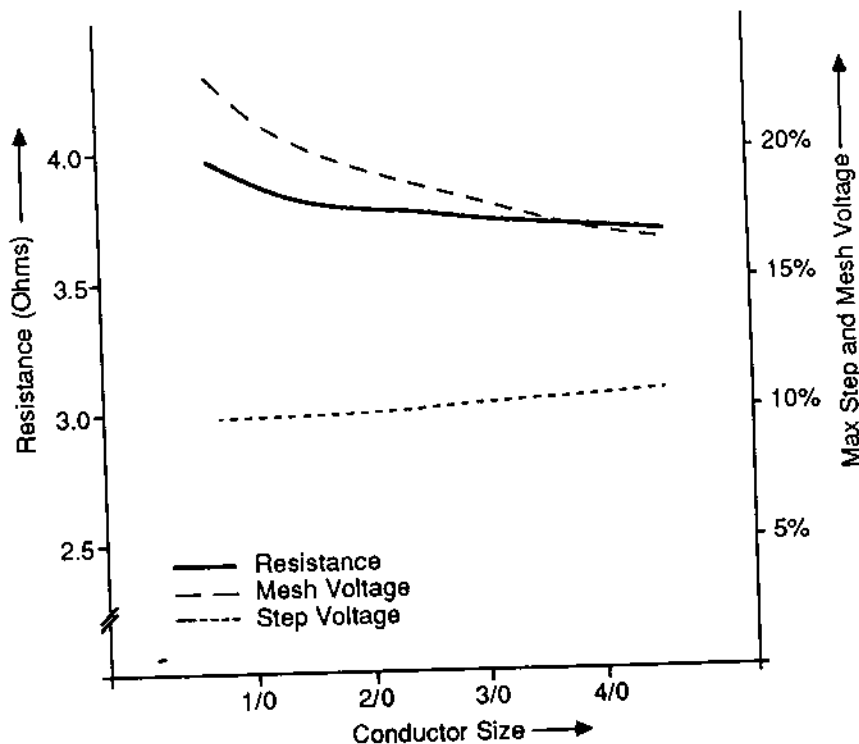


FIG. 5.23 Resistance, mesh and step voltages vs. ground mat conductor size. (Number of meshes in one direction = 6, conductor spacing = 4 m, burial depth = .76 m, soil is uniform, 200  $\Omega$ meter.)

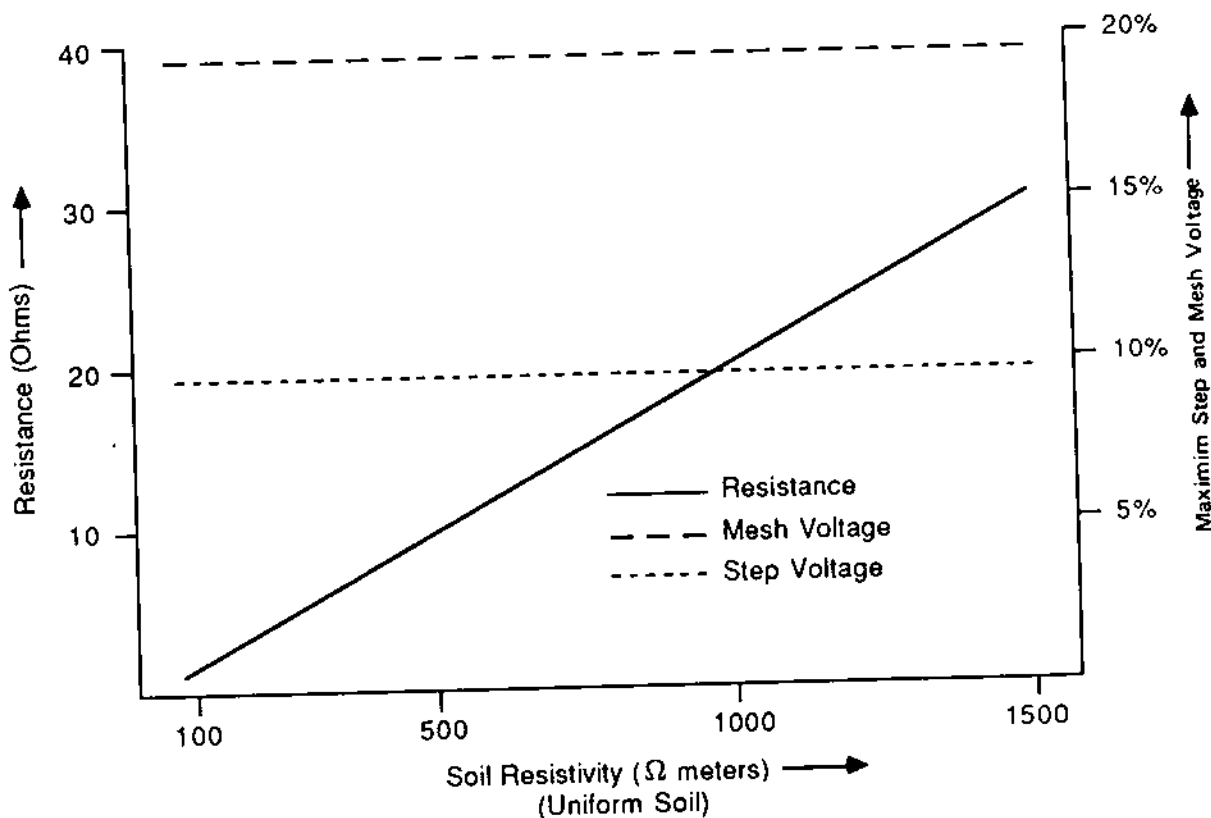


FIG. 5.24 Resistance, mesh and step voltages vs. soil resistivity. (Number of meshes in one direction = 6, conductor spacing = 4 m, conductor size is 2/0 copper, burial depth = .76 m.)

Figure 5.24 illustrates the effects of soil resistivity. The figure illustrates that the maximum step and mesh voltages as a percentage of the ground potential rise are insensitive to the soil resistivity. On the other hand, the resistance is proportional to the soil resistivity.

## 5.10 SUMMARY AND DISCUSSION

In this chapter we discussed analysis procedures of power system grounding systems. These techniques are applicable to the analysis of substation grounding systems as well as transmission tower grounding. The methodologies are based on dc analysis, which is accurate for spatially small systems energized with low-frequency currents and voltages. Under these conditions, the resistance of the grounding system is the dominant component of the impedance. The reactance is typically neglected. This approach is accurate for most practical grounding systems. For spatially large systems, however, especially grounding systems in low soil resistivity, it is possible that the reactance may be the dominant component of the impedance even at low frequencies (i.e., 60 Hz). The reactance of a grounding system can be computed with quasistatic analysis, which is not presented in this book. The interested reader can explore the subject in references 16, 17, and 25.

## 5.11 PROBLEMS

**Problem 5.1:** Consider the distribution pole grounding of Fig. P5.1. It consists of a single 8-ft ground rod driven into soil in such a way that the top of the rod is 2 ft below the soil surface. Compute the ground resistance assuming that the soil resistivity is  $200 \Omega \cdot m$  and the electric current is uniformly distributed along the ground rod.

- Use the exact equation of Table 5.3.
- Use the approximate equation.
- Compare the results in parts (a) and (b).

**Problem 5.2:** Consider a horizontal wire of length 20 m buried 0.5 m below earth surface in soil of resistivity  $100 \Omega \cdot m$ . Assuming uniform current distribution, compute the touch voltage at a point on the surface just above the center of the conductor when 200 A is injected into the horizontal conductor. The outside diameter of the wire is 0.741 in.

**Problem 5.3:** Compute the maximum allowable touch and step voltage in a power substation with soil resistivity of  $150 \Omega \cdot m$  and backup fault interruption time of 0.5 s. Assume that the tolerable body current cannot exceed  $116 \text{ mA} / \sqrt{t}$ , where  $t$  is the duration of electric shock.

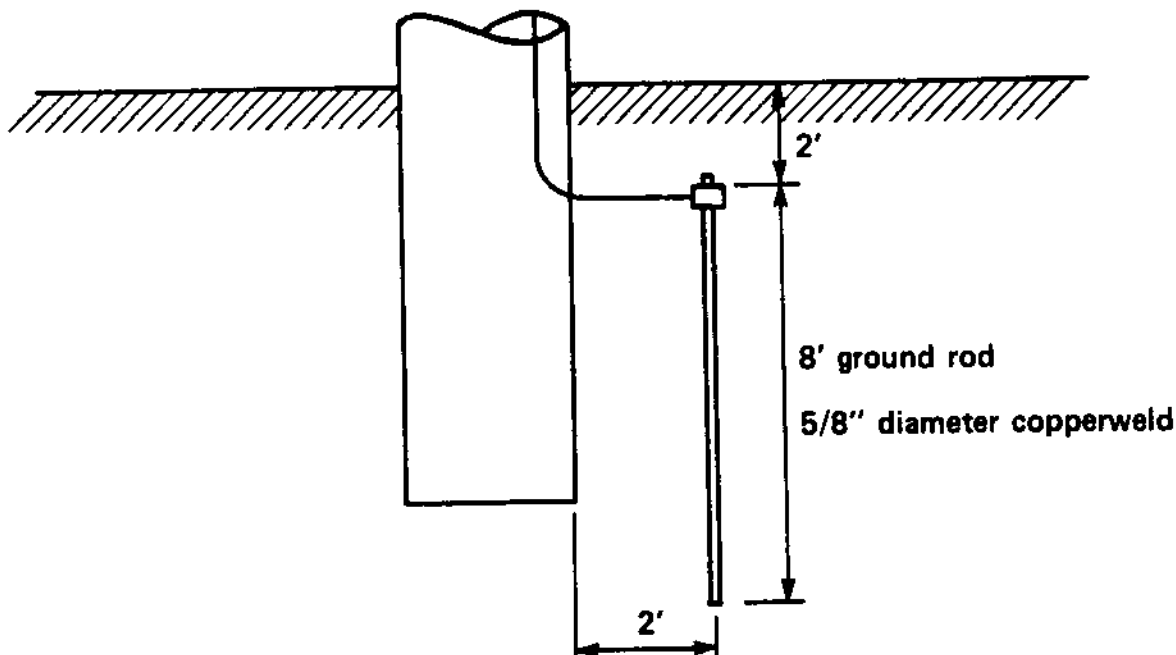


FIG. P5.1 Grounding configuration of a 12 kV distribution line pole.

**Problem 5.4:** A metallic cube is embedded in uniform soil of  $200 \Omega \cdot m$  as is illustrated in Fig. P5.2. The burial depth is 2 ft; each side of the cube is 1 ft. A total electric current of 100 A is flowing from the outside surface of the cube into earth. Compute the potential at point A on the surface of the earth located 3.5 ft off the center of the cube. Assume that the current distribution on the surface of the metallic cube is uniform.

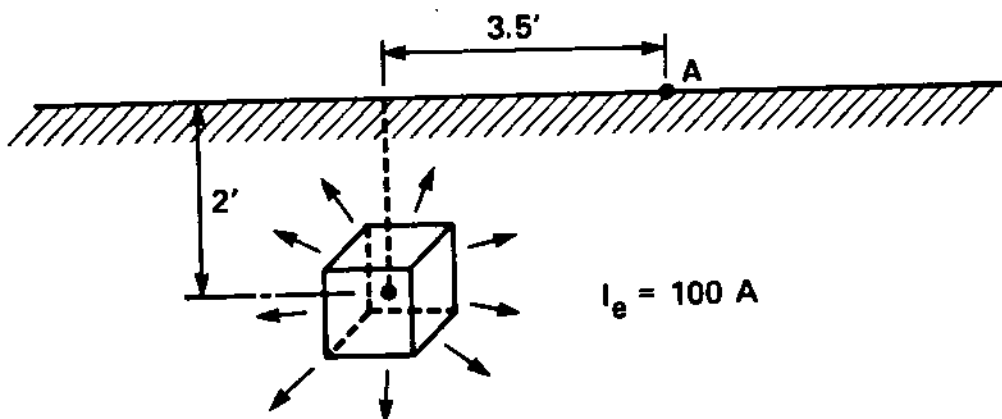
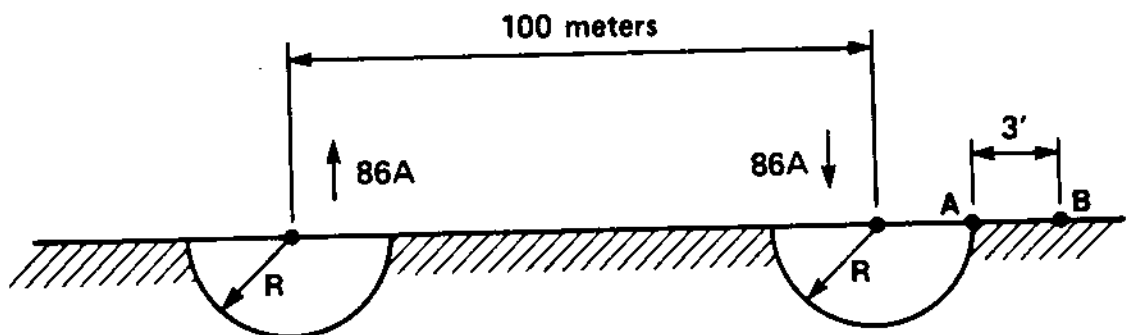


FIG. P5.2 A metallic cube embedded in earth.



$$V_{\text{touch}} = |V_{AB}|$$

FIG. P5.3 A grounding system consisting of two hemispheres.

Problem 5.5: A grounding system consists of two hemispheres embedded in earth. The distance between their centers is 100 m. During a certain fault condition, 86 A of electric current is injected into earth from one electrode and returns from the other electrode. It is desired to select the radius of the electrodes in such a way that the touch voltage defined in Fig. P5.3 will not exceed the value

$$V_{\max} = \frac{0.116 \text{ A}}{\sqrt{t}} (1.5\rho + 1000)$$

where  $t$  is the duration of the fault current in seconds and  $\rho$  is the soil resistivity. What is the minimum allowable radius of the electrodes if the soil resistivity is  $150 \Omega \cdot \text{m}$  and  $t = 0.25 \text{ s}$ ?

Problem 5.6: A grounding system of an ac/dc converter substation consists of a circular electrode buried in earth. Consider such a grounding system as in Fig. P5.4. The radius of the circular (ring) electrode is 500 m. It is buried at a depth of 3 m below the surface

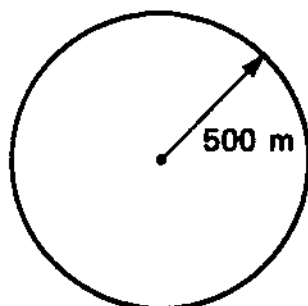


FIG. P5.4 Top view of a dc ground electrode.

of the earth. Assume that 1000 A of dc current is injected from the ground electrode into earth. Assume that the current is uniformly distributed around the electrode. Compute the voltage on the surface of the earth at the center of the electrode. The soil resistivity is 150  $\Omega \cdot m$ .

# 6

## Transmission Line Analysis

### 6.1 INTRODUCTION

In many power system analysis problems, the model of transmission lines is of fundamental importance. Some of the most important analysis problems are:

1. Power flow analysis
2. Short-circuit analysis
3. Harmonic analysis
4. Electrical transient analysis

The conditions involved in these analysis problems range from the steady-state low-frequency (50 or 60 Hz) nearly balanced operation to very fast transients (switching surges or lightning-induced transients). In addition, certain phenomena (such as asymmetric operation, fault conditions, or transients) involve the earth as an alternative path of electric current flow. In these cases, accurate modeling of the earth path is required. Depending on the objectives of the analysis, modeling procedures of transmission lines may be rather complex.

Transmission line modeling procedures are drastically simplified by developing specific transmission line models for specific applications. These models result from specific simplifying approximations which are reasonable for the application under consideration. For example, the sequence circuits of a transmission line are utilized for power flow or short-circuit analysis. On the other hand, for fast electromagnetic transients the distributed nature of the transmission line parameters must be modeled explicitly.

The objective of this chapter is to develop the basis of all the widely used models for transmission line analysis and spell out the specific assumptions and simplifications leading to these models. For this purpose we shall consider the basic equations of a transmission line. These equations are in the form of first-order partial differential equations. From these equations we shall develop transmission line models suitable for representing the line during steady-state operation. Emphasis will be placed on assumptions and simplifications involved. Later, in Chapter 9, the same differential equations will be used to develop models for transient analysis.

## 6.2 THE GENERAL TRANSMISSION LINE MODEL

In this section we consider the transmission line equations that form the basis for all subsequent models of power lines. For clarity of presentation, the single-phase line will be treated separately from the three-phase line.

### 6.2.1 Single-Phase Transmission Line Model

As we have seen in Chapters 2, 3, and 4, a single-phase electric power transmission line is characterized by the following constants:

- r: series resistance (in ohms/meter)
- L: inductance (in henries/meter)
- C: capacitance (in farads/meter)

For generality, we shall also assume that the line is characterized by a shunt conductance g (in siemens/meter). Consider a single-phase transmission line of length  $\ell$  and parameters r, L, C, and g. The transmission line is illustrated in Fig. 6.1a. A point on the line is identified by the distance y, which is measured from the left terminal of the line as is indicated in Fig. 6.1a. Consider an infinitesimal section of the single-phase line, of length dy, at a distance y from the receiving end. The equivalent-circuit representation of this section is illustrated in Fig. 6.1b. Application of Kirchhoff's current and voltage laws on the circuit of Fig. 6.1b yields:

Kirchhoff's voltage law:

$$-v(y, t) - \left( r \frac{dy}{dt} + L \frac{dy}{dt} \frac{d}{dt} \right) i(y + dy, t) + v(y + dy, t) = 0$$

Kirchhoff's current law:

$$i(y, t) + g \frac{dy}{dt} v(y, t) + C \frac{dy}{dt} \frac{dv(y, t)}{dt} - i(y + dy, t) = 0$$

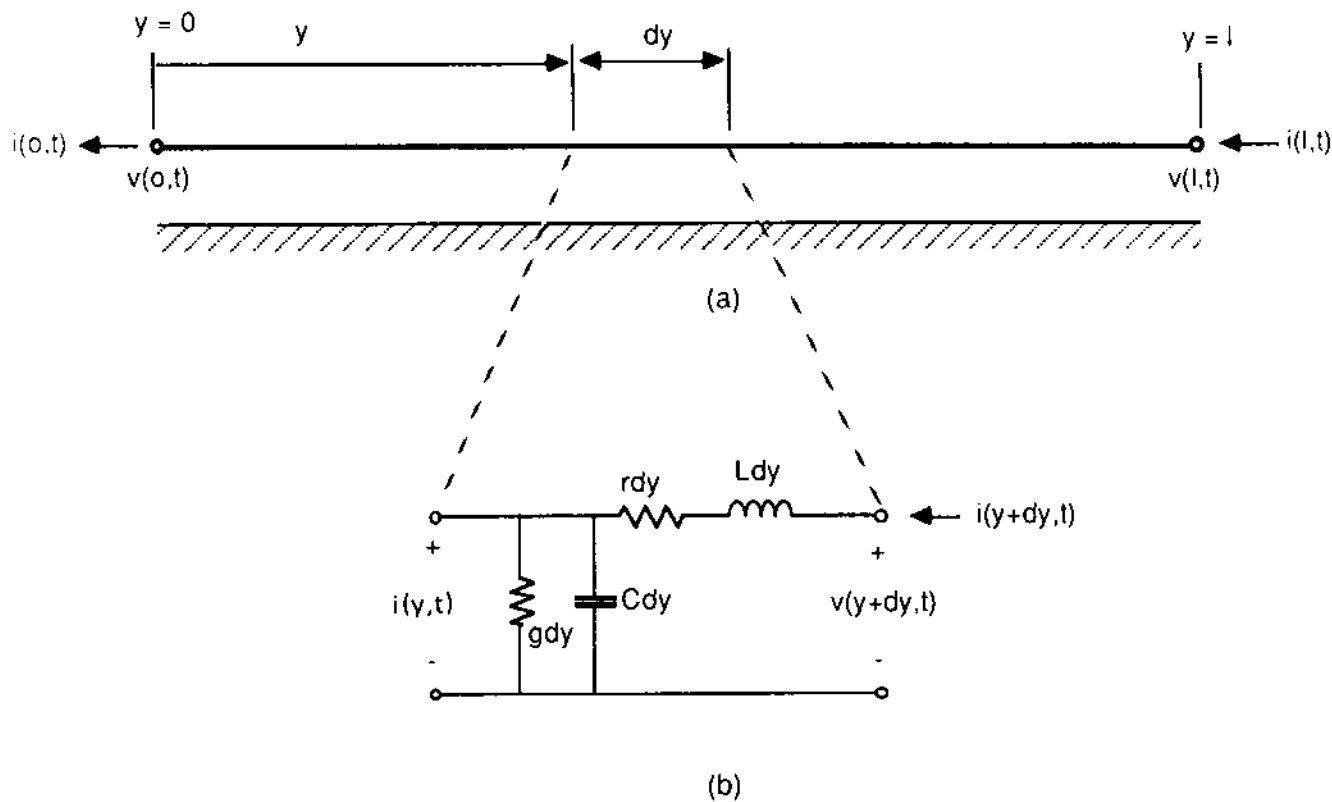


FIG. 6.1 General representation of a single phase line. (a) Schematic representation and notation, (b) equivalent circuit of an infinitesimal length.

The equations above are rewritten as follows:

$$\frac{v(y + dy, t) - v(y, t)}{dy} = ri(y + dy, t) + L \frac{d}{dt} i(y + dy, t)$$

$$\frac{i(y + dy, t) - i(y, t)}{dy} = gv(y, t) + C \frac{dv(y, t)}{dt}$$

Taking the limit as  $dy \rightarrow 0$  gives us

$$\frac{dv(y, t)}{dy} = ri(y, t) + L \frac{di(y, t)}{dt} \quad (6.1a)$$

$$\frac{di(y, t)}{dy} = gv(y, t) + C \frac{dv(y, t)}{dt} \quad (6.1b)$$

The partial differential equations (6.1) define the model of a single-phase transmission line in terms of the parameters  $r$ ,  $L$ ,  $g$ , and  $C$ .

Equations (6.1) are coupled first-order partial differential equations. It is possible to obtain an equivalent set of equations which

are not coupled. For this purpose Eq. (6.1b) is differentiated with respect to  $y$ :

$$\frac{d^2 i(y, t)}{dy^2} = g \frac{dv(y, t)}{dy} + C \frac{d}{dt} \frac{dv(y, t)}{dy}$$

Then the term  $dv(y, t)/dy$  is substituted from Eq. (6.1a) to yield

$$\frac{d^2 i(y, t)}{dy^2} = CL \frac{d^2 i(y, t)}{dt^2} + (gL + Cr) \frac{di(y, t)}{dt} + gri(y, t) \quad (6.2a)$$

Note that Eq. (6.2a) is decoupled (i.e., it is an equation in terms of the current function only). A similar procedure yields a differential equation in terms of the voltage function only:

$$\frac{d^2 v(y, t)}{dy^2} = CL \frac{d^2 v(y, t)}{dt^2} + (gL + Cr) \frac{dv(y, t)}{dt} + grv(y, t) \quad (6.2b)$$

The partial differential equations (6.1) or (6.2) described the performance of a single-phase line. They are applicable to transient analysis as well as steady-state analysis.

### 6.2.2 Three-Phase Transmission Line Model

In this section we extend the analysis of a single-phase transmission line to three-phase or multiphase transmission lines. Figure 6.2 illustrates a three-phase transmission line. The transmission line of Fig. 6.2 is the simplest three-phase overhead line. It comprises four paths of electric current flow: the three phase conductors and the earth. Shield or neutral conductors, which are present in most transmission lines, are omitted for the purpose of minimizing the complexity of the analysis. Now consider the three phase conductors. Each conductor is above earth. By utilizing the models developed in Chapters 3 and 4, each conductor  $i$  is characterized with a series self-resistance  $r_{ii}$ ; series mutual resistance to any other conductor  $j$ ,  $r_{ij}$ ; series self-inductance  $L_{iie}$ ; series mutual inductance to any other conductor  $j$ ,  $L_{ije}$ ; self-capacitance  $C_{ii}$ ; and mutual capacitance to any other conductor  $j$ ,  $C_{ij}$ . The series self- and mutual resistance and inductance can be computed using Carson's method or one of the two approximate methods discussed in Chapter 3. For simplicity, we shall use the approximate method referred to as the method of equivalent depth of return. According to this method, the series parameters will be given by the following equations (see Chapter 3):

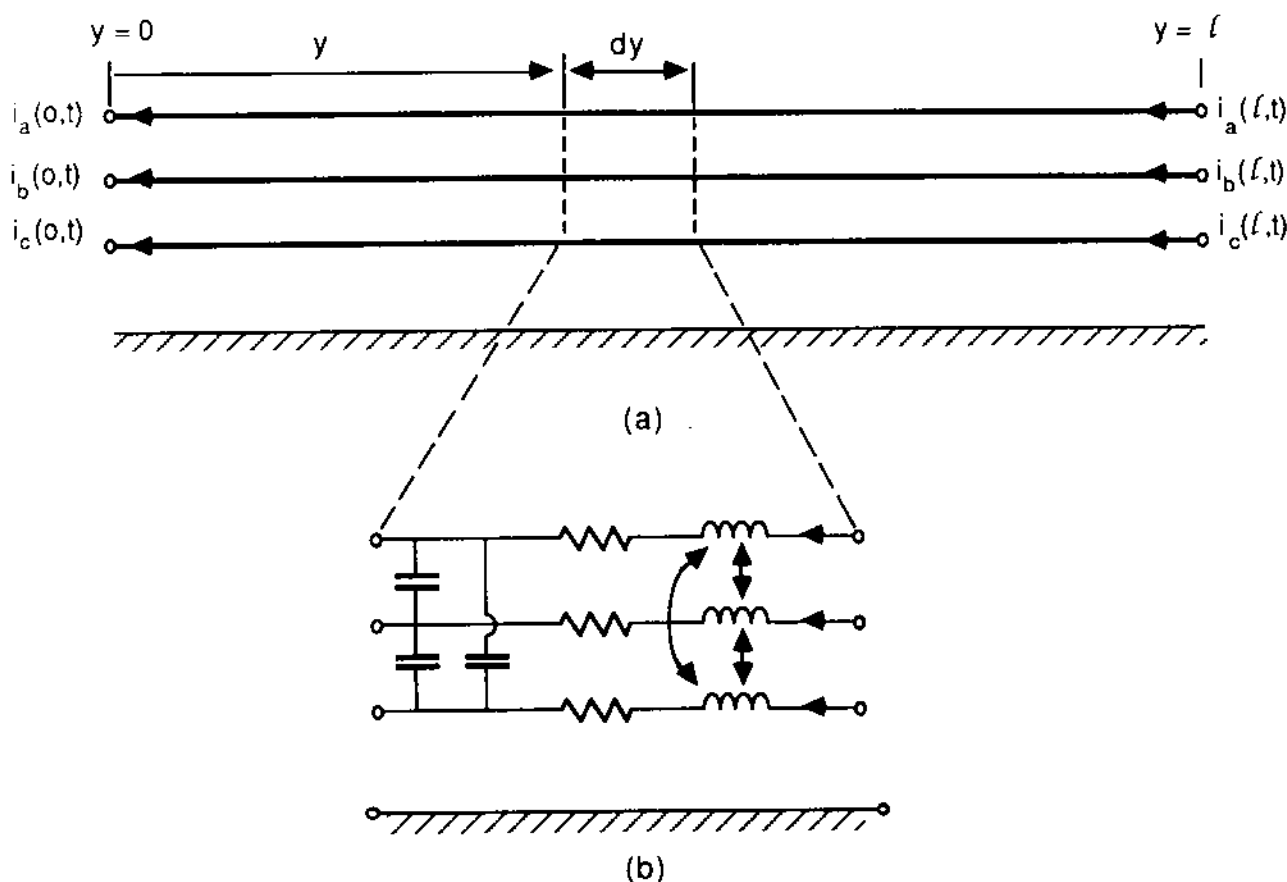


FIG. 6.2 General representation of a three phase line. (a) Schematic representation and notation, (b) equivalent circuit of an infinitesimal length.

$$\text{Self-resistance: } r_{ii} = r_i + r_e$$

$$\text{Mutual resistance: } r_{ij} = r_e$$

$$\text{Self-inductance: } L_{iie} = \frac{\mu}{2\pi} \ln \frac{D_e}{d}$$

$$\text{Mutual inductance: } L_{ije} = \frac{\mu}{2\pi} \ln \frac{D_e}{D_{ij}}$$

where

$$r_e = \omega \mu / 8$$

$r_i$  = conductor  $i$  resistance, ohms per meter

$d_i$  = conductor  $i$  geometric mean radius

$D_e$  =  $2160 \sqrt{\rho/f}$  feet

$\rho$  = soil resistivity

$f$  = frequency of currents

$D_{ij}$  = distance between conductors  $i$  and  $j$

The self- and mutual capacitances are computed using the methods developed in Chapter 4. First the matrix  $C'$  is computed:

$$C' = \begin{bmatrix} C'_{aa} & C'_{ab} & C'_{ac} \\ C'_{ba} & C'_{bb} & C'_{bc} \\ C'_{ca} & C'_{cb} & C'_{cc} \end{bmatrix}$$

where

$$C'_{ij} = (1/2\pi\epsilon) \ln(D_{ij}/D_{ij'})$$

and

$D_{ij}$  = distance between conductors  $i$  and  $j$  (when  $i = j$ ,  $D_{ii}$  equals the radius of conductor  $i$ )

$D_{ij'}$  = distance between conductor  $i$  and the image of conductor  $j$  with respect to the earth interface

Then the matrix  $C'$  is inverted to yield the matrix  $C$ :

$$C = C'^{-1} = \begin{bmatrix} C_{aa} & C_{ab} & C_{ac} \\ C_{ba} & C_{bb} & C_{bc} \\ C_{ca} & C_{cb} & C_{cc} \end{bmatrix}$$

The matrix above defines the self- and mutual capacitances. The self- and mutual parameters of the three phase conductors are represented schematically in Fig. 6.2b. For completeness, we also assume that there is self- and mutual conductance between the phase conductors, represented by the conductance matrix  $G$ .

Now application of Kirchhoff's voltage and current laws on the circuit of Fig. 6.2b yields

$$-v(y, t) - \left( R dy + L dy \frac{d}{dt} \right) i(y + dy, t) + v(y + dy, t) = 0$$

$$i(y, t) + Gv(y, t) dy + C dy \frac{dv(y, t)}{dt} - i(y + dy, t) = 0$$

where

$$i(y, t) = \begin{bmatrix} i_a(y, t) \\ i_b(y, t) \\ i_c(y, t) \end{bmatrix}$$

$$\mathbf{v}(y, t) = \begin{bmatrix} v_a(y, t) \\ v_b(y, t) \\ v_c(y, t) \end{bmatrix}$$

$$\mathbf{R} = \begin{bmatrix} r_e + r_a & r_e & r_e \\ r_e & r_e + r_b & r_e \\ r_e & r_e & r_e + r_c \end{bmatrix}$$

$$\mathbf{L} = \begin{bmatrix} L_{aae} & L_{abe} & L_{ace} \\ L_{bce} & L_{bbe} & L_{bce} \\ L_{cae} & L_{cbe} & L_{cce} \end{bmatrix}$$

$$\mathbf{G} = \begin{bmatrix} g_{aae} & g_{abe} & g_{ace} \\ g_{bae} & g_{bbe} & g_{bce} \\ g_{cae} & g_{cbe} & g_{cce} \end{bmatrix}$$

$$\mathbf{C} = \begin{bmatrix} C_{aa} & C_{ab} & C_{ac} \\ C_{ba} & C_{bb} & C_{bc} \\ C_{ca} & C_{cb} & C_{cc} \end{bmatrix}$$

Upon division of the matrix equations above by  $dy$  and taking the limit as  $dy \rightarrow 0$ , the following matrix differential equations are obtained:

$$\frac{dv(y, t)}{dy} = \mathbf{Ri}(y, t) + \mathbf{L} \frac{di(y, t)}{dt} \quad (6.3a)$$

$$\frac{di(y, t)}{dy} = \mathbf{Gv}(y, t) + \mathbf{Ci}(y, t) \quad (6.3b)$$

Again, as in the case of the single-phase line, the foregoing first-order matrix coupled partial differential equations can be transformed into uncoupled second-order matrix differential equations. The final result is

$$\frac{d^2i(y, t)}{dy^2} = \mathbf{CL} \frac{d^2i(y, t)}{dt^2} + (\mathbf{GL} + \mathbf{CR}) \frac{di(y, t)}{dt} + \mathbf{GRi}(y, t) \quad (6.4a)$$

$$\frac{d^2v(y,t)}{dy^2} = LC \frac{d^2v(y,t)}{ct^2} + (LG + RC) \frac{dv(y,t)}{dt} + RGv(y,t) \quad (6.4b)$$

It should be observed that the differential equations describing a multiphase transmission line are similar to the equations of a single-phase transmission line. The parameters of the single-phase line have been substituted by appropriate matrices. The computation of the matrices L, R, C, and G of the equations above are now demonstrated with an example.

Example 6.1: Consider a three-phase transmission line that is suspended on the transmission tower illustrated in Fig. 1.6. The position of the phase conductors is as follows: phase a, position 1; phase b, position 2; phase c, position 3. The phase conductors are ACSR, 336.4 kcm, 30 strand. The shield conductor is steel, 5/16 in. in diameter. The soil resistivity is 150  $\Omega \cdot m$ . Compute the resistance matrix, the inductance matrix, and the capacitance matrix of the line. The units should be ohms per meter, henries per meter, and microfarads per meter, respectively. Use the equivalent depth of return method. Neglect the shield conductor.

Solution:

Resistance: Conductors:  $r_c = 0.278 \Omega/m = 0.000173 \Omega/m$   
Earth:  $r_e = 0.0954 \Omega/m = 0.0000593 \Omega/m$

$$R = \begin{bmatrix} 0.2323 & 0.0593 & 0.0593 \\ 0.0593 & 0.2323 & 0.0593 \\ 0.0593 & 0.0593 & 0.2323 \end{bmatrix} \times 10^{-3} \Omega/m$$

Inductance:

$$L_{iie} = \frac{\mu_0}{2\pi} \ln \frac{D_e}{d_i}$$

$$d_i = 0.0255 \text{ ft}$$

$$L_{ije} = \frac{\mu_0}{2\pi} \ln \frac{D_e}{D_{ij}}$$

$$D_e = 2160 \sqrt{\frac{\rho}{f}} = 3415.25 \text{ ft}$$

$$D_{ab} = 12.636 \text{ ft}$$

$$D_{ac} = 12.717 \text{ ft}$$

$$D_{bc} = 8.17 \text{ ft}$$

Substitution gives us

$$L = \begin{bmatrix} 2.361 & 1.1199 & 1.2071 \\ 1.1199 & 2.361 & 1.1186 \\ 1.2071 & 1.1186 & 2.361 \end{bmatrix} \mu\text{H/m}$$

Capacitance: The matrix  $C'$  is computed:

$$C' = \frac{1}{2\pi\epsilon} \begin{bmatrix} 8.0457 & 1.9977 & 2.3788 \\ 1.9977 & 7.9591 & 1.9004 \\ 2.3788 & 1.9004 & 7.859 \end{bmatrix}$$

Upon inversion, the capacitance matrix is

$$C = \begin{bmatrix} 7.8844 & -1.4954 & -2.0248 \\ -1.4954 & 7.7016 & -1.4097 \\ -2.0248 & -1.4097 & 8.0324 \end{bmatrix} \times 10^{-6} \mu\text{F/m}$$

### 6.3 TRANSMISSION LINE MODELS FOR SINUSOIDAL STEADY STATE

Most of the time, power systems operate under sinusoidal steady-state conditions. In this case the imposed voltages and currents on the transmission line vary sinusoidally with frequency  $f$ . Since the transmission line is a linear system, the currents and voltages at any point in the transmission line will vary sinusoidally with time. Thus, in general,

$$i(y, t) = \operatorname{Re}\{\sqrt{2} \tilde{I}(y)e^{j\omega t}\} \quad (6.5a)$$

$$v(y, t) = \operatorname{Re}\{\sqrt{2} \tilde{V}(y)e^{j\omega t}\} \quad (6.5b)$$

where  $\tilde{I}(y)$ ,  $\tilde{V}(y)$  are complex numbers (phasors) and  $\omega = 2\pi f$ . The models of a single- or three-phase line under the conditions described are developed in the next sections.

## 6.3.1 Single-Phase Transmission Line

Upon substitution of Eqs. (6.5) into Eq. (6.2b), we obtain

$$\sqrt{2} \operatorname{Re} \left\{ e^{j\omega t} \frac{d^2 \tilde{V}(y)}{dy^2} \right\} = \sqrt{2} \operatorname{Re} \left\{ [-\omega^2 LC \tilde{V}(y) + j\omega(gL + Cr)\tilde{V}(y) + gr\tilde{V}(y)]e^{j\omega t} \right\}$$

The equation above must be satisfied for any time  $t$ . Thus the coefficients of the time functions on the two sides of the equation must be identical.

$$\frac{d^2 \tilde{V}(y)}{dy^2} = [-\omega^2 LC + j\omega(gL + Cr) + gr]\tilde{V}(y)$$

Upon factorization of the right-hand-side expression, we have

$$\frac{d^2 \tilde{V}(y)}{dy^2} = (r + j\omega L)(g + j\omega C)\tilde{V}(y) \quad (6.6a)$$

Application of the same procedure to Eq. (6.1a) yields

$$\frac{d\tilde{V}(y)}{dy} = (r + j\omega L)\tilde{I}(y) \quad (6.6b)$$

Now let's define

$$z \triangleq r + j\omega L = \text{series impedance per unit length of the line at frequency } \omega$$

$$y' \triangleq g + j\omega C = \text{shunt admittance per unit length of the line at frequency } \omega$$

With the new notation, Eqs. (6.6) become

$$\frac{d^2 \tilde{V}(y)}{dy^2} = zy'\tilde{V}(y) \quad (6.7a)$$

$$\frac{d\tilde{V}(y)}{dy} = z\tilde{I}(y) \quad (6.7b)$$

Equations (6.7) represent the single-phase line model at sinusoidal steady state. The general solution of Eq. (6.7a) is

$$\tilde{V}(y) = ae^{py} + be^{-py} \quad (6.8)$$

where  $a$ ,  $b$  are constants dependent on the boundary conditions of the line, and

$$p = \sqrt{zy'} = \left[ -\omega^2 LC + j\omega(gL + rC) + gr \right]^{0.5} \quad (6.9)$$

Note that  $p$  is dependent on the frequency  $f$  ( $\omega = 2\pi f$ ). The dimensions of the constant  $p$  are the inverse of length. The constant  $p$  characterizes the propagation of voltage through the transmission line. For this reason it is called the propagation constant. The real and imaginary parts of the propagation constant will be called the attenuation and phase constant, respectively. That is,  $p = k + j\eta$ , where  $k$  is the attenuation constant and  $\eta$  is the phase constant.

The general solution for the electric current phasor  $I(y)$  is obtained by substituting Eq. (6.8) into Eq. (6.7b). The result is

$$\tilde{I}(y) = \frac{1}{z} (ape^{py} - bpe^{-py})$$

Observe that

$$\frac{p}{z} = \frac{1}{\sqrt{zz'}}.$$

where  $z' = 1/y'$ . Define

$$Z_0 = \sqrt{zz'} \quad (6.10)$$

Note that the quantity  $Z_0$  has dimensions of impedance and it is characteristic of the transmission line under consideration. It will be called the characteristic impedance of the line. In terms of the characteristic impedance  $Z_0$ , the equation for the line current becomes

$$\tilde{I}(y) = \frac{a}{Z_0} e^{py} - \frac{b}{Z_0} e^{-py} \quad (6.11)$$

In summary, the general solution for the voltage and current phasors at a location  $y$  of a single-phase line is given by Eqs. (6.8) and (6.11). The solution is expressed in terms of the propagation constant  $p$ , the characteristic impedance  $Z_0$ , and two constants  $a$  and  $b$ . The quantities  $p$  and  $Z_0$  depend on the parameters of the line, while the constants  $a$ ,  $b$  are dependent on the boundary conditions. Consider, for example, the single-phase transmission line of Fig. 6.1. Let  $\tilde{V}_R$ ,  $\tilde{I}_R$  be the voltage and current phasors at the terminal  $y = 0$  of the line. Then

$$\tilde{V}(y = 0) = \tilde{V}_R = a + b$$

$$\tilde{I}(y = 0) = \tilde{I}_R = \frac{a}{Z_0} - \frac{b}{Z_0}$$

Upon solution of two equations above for the constants  $a$  and  $b$  we obtain

$$a = \frac{\tilde{V}_R + Z_0 \tilde{I}_R}{2}$$

$$b = \frac{\tilde{V}_R - Z_0 \tilde{I}_R}{2}$$

Substitution into Eqs. (6.8) and (6.9) gives us

$$\tilde{V}(y) = \tilde{V}_R \frac{e^{py} + e^{-py}}{2} + Z_0 \tilde{I}_R \frac{e^{py} - e^{-py}}{2}$$

$$\tilde{I}(y) = \frac{\tilde{V}_R}{Z_0} \frac{e^{py} - e^{-py}}{2} + \tilde{I}_R \frac{e^{py} + e^{-py}}{2}$$

By definition,  $(e^{py} + e^{-py})/2$  and  $(e^{py} - e^{-py})/2$  are the hyperbolic cosine and sine functions denoted with cosh and sinh, respectively. Thus

$$\tilde{V}(y) = \tilde{V}_R \cosh py + Z_0 \tilde{I}_R \sinh py \quad (6.12a)$$

$$\tilde{I}(y) = \frac{\tilde{V}_R}{Z_0} \sinh py + \tilde{I}_R \cosh py \quad (6.12b)$$

Equations (6.12) provide the voltage and current phasors at any location  $y$  along the line in terms of the voltage and current at the left terminal of the line ( $y = 0$ ). Of special interest are the voltage and current at the other end of the line ( $y = \ell$ ):

$$\tilde{V}_S = \tilde{V}(y = \ell) = \tilde{V}_R \cosh p\ell + Z_0 \tilde{I}_R \sinh p\ell$$

$$\tilde{I}_S = \tilde{I}(y = \ell) = \frac{\tilde{V}_R}{Z_0} \sinh p\ell + \tilde{I}_R \cosh p\ell$$

In compact matrix notation:

$$\begin{bmatrix} \tilde{V}_S \\ \tilde{I}_S \end{bmatrix} = \begin{bmatrix} \cosh p\ell & Z_0 \sinh p\ell \\ \frac{1}{Z_0} \sinh p\ell & \cosh p\ell \end{bmatrix} \begin{bmatrix} \tilde{V}_R \\ \tilde{I}_R \end{bmatrix} \quad (6.13)$$

This equation states that sending-end voltage and current are a linear combination of the receiving-end voltage and current, and vice versa. Three parameters describe this model completely: (a) the characteristic impedance of the line  $Z_0$ ; (b) the propagation constant of the line,  $p$ ; and (c) the length of the line,  $\ell$ . Note that the model depends only on the product  $p\ell$  and the characteristic impedance  $Z_0$ . Alternatively, the following parameters completely describe the single-phase transmission line: (a)  $A = \cosh p\ell$ , (b)  $B = Z_0 \sinh p\ell$ , and (c)  $C = (1/Z_0) \sinh p\ell$ . In terms of the parameters  $A$ ,  $B$ ,  $C$ , the line equations (6.13) become

$$\tilde{V}_S = A\tilde{V}_R + B\tilde{I}_R \quad (6.14a)$$

$$\tilde{I}_S = C\tilde{V}_R + A\tilde{I}_R \quad (6.14b)$$

These parameters are known as the  $A$ ,  $B$ ,  $C$  constants of the line. Note that

$$A^2 - BC = \cosh^2 p\ell - \sinh^2 p\ell = 1.0$$

Thus the parameters  $A$ ,  $B$ , and  $C$  are not independent. Knowledge of the two is enough to determine the third.

For numerical computations, the following relationships are useful:

$$\sinh(\alpha + j\beta) = \sinh \alpha \cos \beta + j \cosh \alpha \sin \beta$$

$$\cosh(\alpha + j\beta) = \cosh \alpha \cos \beta + j \sinh \alpha \sin \beta$$

where  $\alpha$ ,  $\beta$  are real numbers and

$$\cosh z = 1 + \frac{z^2}{2!} + \frac{z^4}{4!} + \frac{z^6}{6!} + \dots$$

$$\sinh z = z + \frac{z^3}{3!} + \frac{z^5}{5!} + \frac{z^7}{7!} + \dots$$

where  $z$  is any complex number.

In summary, a single-phase transmission line can be modeled as a two-port device, described by the constants  $A$ ,  $B$ , and  $C$ .

### 6.3.2 Three-Phase Transmission Line

The same analysis can be applied to three-phase transmission lines. Assuming sinusoidal steady state, Eqs. (6.4b) and (6.3a) of the three-phase transmission line become

$$\frac{d^2\tilde{V}(y)}{dy^2} = (R + j\omega L)(G + j\omega C)\tilde{V}(y) \quad (6.15a)$$

$$\frac{d\tilde{V}(y)}{dy} = (R + j\omega L)\tilde{I}(y) \quad (6.15b)$$

Define the following matrices:

$$Z \stackrel{\Delta}{=} R + j\omega L$$

$$Y' \stackrel{\Delta}{=} G + j\omega C$$

Then

$$\frac{d^2\tilde{V}(y)}{dy^2} = ZY'\tilde{V}(y) \quad (6.16a)$$

$$\frac{d\tilde{V}(y)}{dy} = Z\tilde{I}(y) \quad (6.16b)$$

The foregoing matrix differential equations in complex variables fully describe the performance of a general three-phase transmission line. Solution of these equations for specified boundary conditions will yield the electric currents and voltages of any phase at any location of the line. However, solution of the equations above is rather difficult. In the following section we discuss transformations that decompose the matrix equations (6.16) into scalar equations. In this way, the solution of the matrix equations (6.16) reduces to the solution of a set of scalar equations.

## 6.4 MODAL DECOMPOSITION

The model of a three-phase transmission line under sinusoidal steady-state conditions is defined by Eqs. (6.16). Solution of these equations is in general complex because the matrices  $Z$ ,  $Y'$  are full matrices resulting in a set of three coupled differential equations. To simplify the solution, observe that it is possible to find a transformation  $T$  of the voltage and current vectors  $\tilde{V}(y)$  and  $\tilde{I}(y)$  as follows:

$$T\tilde{V}(y) = \tilde{V}^m(y) \quad \text{or} \quad \tilde{V}(y) = T^{-1}\tilde{V}^m(y) \quad (6.17a)$$

$$T\tilde{I}(y) = \tilde{I}^m(y) \quad \text{or} \quad \tilde{I}(y) = T^{-1}\tilde{I}^m(y) \quad (6.17b)$$

where  $T$  is a  $3 \times 3$  matrix,  $\tilde{V}^m(y)$  are the transformed voltages at location  $y$  of the line, and  $\tilde{I}^m(y)$  are the transformed currents at location  $y$  of the line. Substitution of the transformation above into Eqs. (6.16) and subsequent premultiplication of the resulting equation by  $T$  results in

$$\frac{d^2\tilde{V}^m(y)}{dy^2} = TZY'T^{-1}\tilde{V}^m(y) \quad (6.18a)$$

$$\frac{d\tilde{V}^m(y)}{dy} = TZT^{-1}\tilde{I}^m(y) \quad (6.18b)$$

Now assume that  $T$  has been selected in such a way that the matrices  $TZY'T^{-1}$  and  $TZT^{-1}$  are diagonal matrices. In this case Eqs. (6.18) represent six uncoupled differential equations. The voltages  $\tilde{V}^m(y)$  are called the modal voltages of the line and the transformation  $T$  is called a modal transformation matrix. Similarly, the currents  $\tilde{I}^m(y)$  are called the modal currents. The procedure is called the modal decomposition. The advantages of modal decomposition are obvious. Solution of the decoupled equations (6.18) can be obtained with the techniques discussed in Section 6.3.1.

#### 6.4.1 Sequence Models

A special case of the modal decomposition results in what is known as the sequence models of a three-phase line. Specifically, many transmission lines are transposed or their construction is such that the mutual parameters (inductance, capacitance) are approximately the same for any pair of phases and the phase self-parameters are also approximately the same for the three phases. For this reason it is justifiable to approximate a three-phase power line with a symmetric line. Mathematically, this is equivalent to assuming that the matrices  $Z$  and  $Y'$  have the following symmetric structure:

$$Z = \begin{bmatrix} z_s & z_m & z_m \\ z_m & z_s & z_m \\ z_m & z_m & z_s \end{bmatrix}$$

$$Y' = \begin{bmatrix} y'_s & y'_m & y'_m \\ y'_m & y'_s & y'_m \\ y'_m & y'_m & y'_s \end{bmatrix}$$

Note that if the matrices  $Z$  and  $Y'$  do not have this form, which is usually the case, they are put in this form using the following equations:

$$z_s = \frac{1}{3} (z_{aa} + z_{bb} + z_{cc})$$

$$z_m = \frac{1}{3} (z_{ab} + z_{bc} + z_{ca})$$

$$y'_s = \frac{1}{3} (y'_{aa} + y'_{bb} + y'_{cc})$$

$$y'_m = \frac{1}{3} (y'_{ab} + y'_{bc} + y'_{ca})$$

The product  $ZY'$  of the two matrices is computed to be

$$ZY' = \begin{bmatrix} \alpha_1 & \alpha_2 & \alpha_2 \\ \alpha_2 & \alpha_1 & \alpha_2 \\ \alpha_2 & \alpha_2 & \alpha_1 \end{bmatrix}$$

where

$$\alpha_1 = z_s y'_s + 2z_m y'_m$$

$$\alpha_2 = z_m y'_m + z_s y'_m + z_m y'_s$$

Now under the discussed assumption of symmetry, the modal transformation matrix  $T$  is defined as follows:

$$T = \frac{1}{3} \begin{bmatrix} 1 & a & a^2 \\ 1 & a^2 & a \\ 1 & 1 & 1^2 \end{bmatrix} \quad a = e^{j120^\circ} \quad T^{-1} = \begin{bmatrix} 1 & 1 & 1 \\ a^2 & a & 1 \\ a & a^2 & 1 \end{bmatrix}$$

The modal voltages  $\tilde{V}^m(y)$  in this case will be denoted by

$$\tilde{V}_{120}(y) = \begin{bmatrix} \tilde{V}_1(y) \\ \tilde{V}_2(y) \\ \tilde{V}_0(y) \end{bmatrix}$$

and the modal currents will be denoted by

$$\tilde{I}_{120}(y) = \begin{bmatrix} \tilde{I}_1(y) \\ \tilde{I}_2(y) \\ \tilde{I}_0(y) \end{bmatrix}$$

Upon substitution of this modal transformation into Eqs. (6.18), we obtain

$$\frac{d^2\tilde{V}_{120}(y)}{dy^2} = M_{seq} \tilde{V}_{120}(y) \quad (6.19a)$$

$$\frac{d\tilde{V}_{120}(y)}{dy} = Z_{seq} \tilde{I}_{120}(y) \quad (6.19b)$$

where

$$M_{seq} = \begin{bmatrix} m_1 & 0 & 0 \\ 0 & m_1 & 0 \\ 0 & 0 & m_0 \end{bmatrix}$$

$$Z_{seq} = \begin{bmatrix} z_1 & 0 & 0 \\ 0 & z_1 & 0 \\ 0 & 0 & z_0 \end{bmatrix}$$

$$m_1 = \alpha_1 - \alpha_2 = p_1^2$$

$$m_0 = \alpha_1 + 2\alpha_2 = p_0^2$$

$$z_1 = z_s - z_m$$

$$z_0 = z_s + 2z_m$$

The matrix equations (6.19) represent six scalar equations. It is expedient to write the six scalar equations explicitly and grouped them into three groups of two as follows:

$$\frac{d^2\tilde{V}_1(y)}{dy^2} = p_1^2 \tilde{V}_1(y) \quad (6.20a)$$

$$\frac{d\tilde{V}_1(y)}{dy} = z_1 \tilde{I}_1(y) \quad (6.20b)$$

$$\frac{d^2\tilde{V}_2(y)}{dy^2} = p_1^2 \tilde{V}_2(y) \quad (6.21a)$$

$$\frac{d\tilde{V}_2(y)}{dy} = z_1 \tilde{I}_2(y) \quad (6.21b)$$

$$\frac{d^2\tilde{V}_0(y)}{dy^2} = p_0^2 \tilde{V}_0(y) \quad (6.22a)$$

$$\frac{d\tilde{V}_0(y)}{dy} = z_0 \tilde{I}_0(y) \quad (6.22b)$$

It is now apparent that Eqs. (6.20), (6.21), and (6.22) represent three single-phase lines. We shall refer to Eqs. (6.20) as the positive sequence model of the line, Eqs. (6.21) as the negative sequence model, and Eqs. (6.22) as the zero sequence model of the line. Note that the parameters  $(p_1, z_1)$  of the negative sequence model are identical to those of the positive sequence model. Collectively, we shall refer to Eqs. (6.19) or, equivalently, Eqs. (6.20), (6.21), and (6.22) as the sequence model of a three-phase line. The modal voltages and currents will be referred to as the symmetrical components of the currents and voltages. In addition, the parameters of the sequence models are defined as follows:

$p_1, p_0$  will be called the positive (or negative) and zero sequence propagation constants of the line.

$z_1, z_0$  will be called the per unit length positive (or negative) and zero sequence series impedance of the line.

For the purpose of completing the discussion of the sequence models, recall that

$$M_{seq} = TZY'T^{-1}$$

Consider the following:

$$TZY'T^{-1} = TZT^{-1}TY'T^{-1} = Z_{\text{seq}} TY'T^{-1}$$

Now define

$$Y'_{\text{seq}} = TY'T^{-1} \quad \text{and therefore} \quad M_{\text{seq}} = Z_{\text{seq}} Y'_{\text{seq}}$$

Upon evaluation of  $Y'_{\text{seq}}$ , we have

$$Y'_{\text{seq}} = \begin{bmatrix} y'_1 & 0 & 0 \\ 0 & y'_1 & 0 \\ 0 & 0 & y'_0 \end{bmatrix}$$

where

$$y'_1 = y'_s - y'_m$$

$$y'_0 = y'_s + 2y'_m$$

Note that  $y'_1$ ,  $y'_0$  are the per unit length positive (or negative) and zero sequence shunt admittance of the line.

In terms of the parameters  $y'_1$ ,  $y'_0$ , the propagation constants  $p_1$ ,  $p_2$ , and  $p_0$  are

$$p_1 = p_2 = \sqrt{z_1 y'_1} \quad (6.23a)$$

$$p_0 = \sqrt{z_0 y'_0} \quad (6.23b)$$

It should be apparent that for each of the sequence models a characteristic impedance can be defined as follows:

$$Z_0^1 = Z_0^2 = \sqrt{\frac{z_1}{y'_1}} \quad (6.24a)$$

$$Z_0^0 = \sqrt{\frac{z_0}{y'_0}} \quad (6.24b)$$

In summary, a specific modal decomposition of the three-phase line equations results in the sequence models of the line (i.e., the positive, negative, and zero sequence models). Each model is identical to a single-phase line model. The parameters of the positive sequence models are equal to the parameters of the negative sequence model.

A physical interpretation of the sequence models of a three-phase transmission line is expedient. For this purpose, assume that only one symmetrical component of the voltage or current is present. As an example, assume that only the positive sequence current is present [i.e.,  $\tilde{I}_1(y) \neq 0$ ,  $\tilde{I}_2(y) = 0$ , and  $\tilde{I}_0(y) = 0$ ]. The actual phase currents  $I_a(y)$ ,  $I_b(y)$ ,  $I_c(y)$  are obtained from the inverse transformation  $T^{-1}$ :

$$\tilde{I}_{abc}(y) = T^{-1} \begin{bmatrix} \tilde{I}_1(y) \\ 0 \\ 0 \end{bmatrix} = \begin{bmatrix} \tilde{I}_1(y) \\ \tilde{I}_1(y)e^{-j120^\circ} \\ \tilde{I}_1(y)e^{-j240^\circ} \end{bmatrix}$$

As is evident from the equation above, the three phase currents are balanced and of the positive sequence. The case is depicted in Fig. 6.3a, which illustrates the three phase currents. Note that the electric current in the ground is zero.

Similarly, if we assume that only the negative sequence component is present [i.e.,  $\tilde{I}_1(y) = 0$ ,  $\tilde{I}_2(y) \neq 0$ , and  $\tilde{I}_0(y) = 0$ ], the actual phase currents are

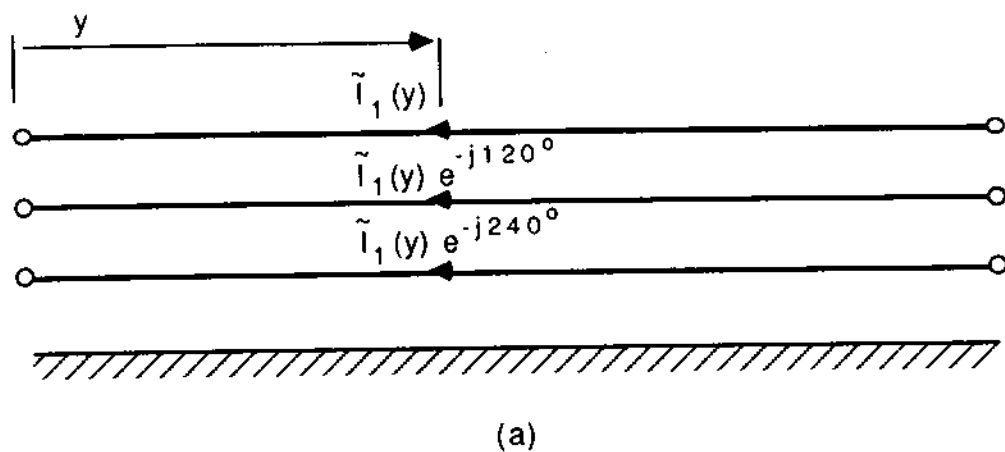
$$\tilde{I}_{abc}(y) = T^{-1} \begin{bmatrix} 0 \\ \tilde{I}_2(y) \\ 0 \end{bmatrix} = \begin{bmatrix} \tilde{I}_2(y) \\ \tilde{I}_2(y)e^{j120^\circ} \\ \tilde{I}_2(y)e^{j240^\circ} \end{bmatrix}$$

Again, as is evident from equation above, the three phase currents are balanced but of the negative sequence. The case is depicted in Fig. 6.3b, which illustrates the three phase currents. Note that the electric current in the earth is zero.

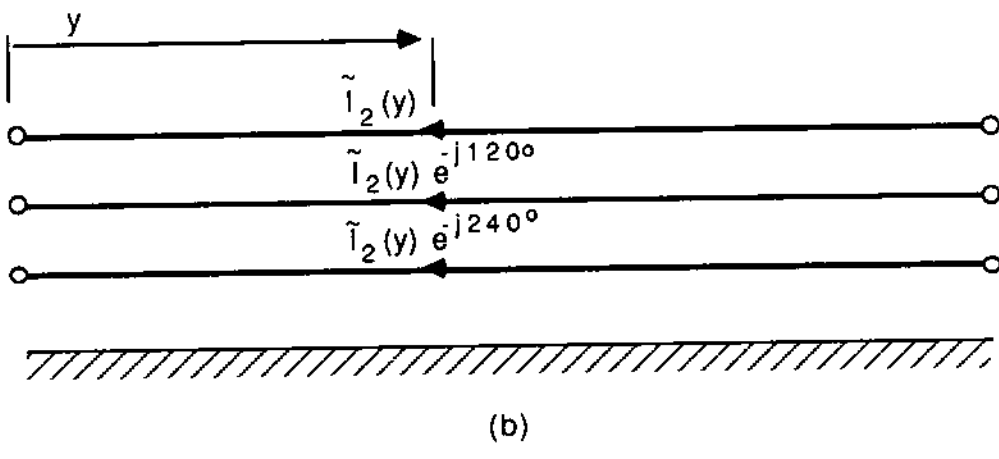
Finally, if we assume that only the zero sequence component is present, [i.e.,  $\tilde{I}_1(y) = 0$ ,  $\tilde{I}_2(y) = 0$ , and  $\tilde{I}_0(y) \neq 0$ ], the actual phase currents are

$$\tilde{I}_{abc}(y) = T^{-1} \begin{bmatrix} 0 \\ 0 \\ \tilde{I}_0(y) \end{bmatrix} = \begin{bmatrix} \tilde{I}_0(y) \\ \tilde{I}_0(y) \\ \tilde{I}_0(y) \end{bmatrix}$$

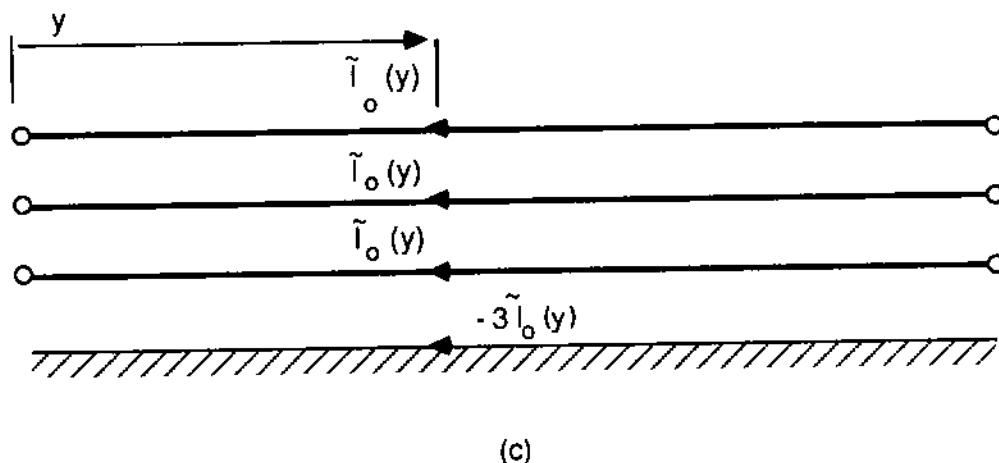
As is evident from the equation above, all three phase currents are identical. Sequence cannot be defined for these currents—thus the name "zero sequence." The earth current will be the negative of the sum of the phase currents [i.e.,  $-3\tilde{I}_0(y)$ ]. The case is depicted in Fig. 6.3c.



(a)



(b)



(c)

FIG. 6.3 Illustration of the symmetrical components on a transmission line. (a) Positive sequence components, (b) negative sequence components, (c) zero sequence components.

Example 6.2: Consider the transmission line of Example 6.1. Compute the sequence parameters of the line. Neglect the shield wire.

Solution: The symmetric Z matrix of the line, computed at 60 Hz, in  $\Omega/m$ , is

$$Z = \begin{bmatrix} 0.2323 + j0.8901 & 0.0593 + j0.4330 & 0.0593 + j0.4330 \\ 0.0593 + j0.4330 & 0.2323 + j0.8901 & 0.0593 + j0.4330 \\ 0.0593 + j0.4330 & 0.0593 + j0.4330 & 0.2323 + j0.8901 \end{bmatrix} \times 1$$

The symmetric Y' matrix of the line, computed at 60 Hz, is

$$Y' = \begin{bmatrix} j3.0331 & -j0.5556 & -j0.5556 \\ -j0.5556 & +j3.0331 & -j0.5556 \\ -j0.5556 & -j0.5556 & j3.0331 \end{bmatrix} \times 10^{-9} S/m$$

The product ZY' is

$$ZY' = \begin{bmatrix} -2.2186 + j0.6387 & -0.5782 + j0.0178 & -0.5782 + j0.0178 \\ -0.5782 + j0.0178 & -2.2186 + j0.6387 & -0.5782 + j0.0178 \\ -0.5782 + j0.0178 & -0.5782 + j0.0178 & -2.2186 + j0.6387 \end{bmatrix} \times 10^{-12} m^{-2}$$

Upon application of the transformation T, we have

$$z_1 = (0.173 + j0.4571) \times 10^{-3} \Omega/m$$

$$z_0 = (0.3509 + j1.7561) \times 10^{-3} \Omega/m$$

$$y'_1 = j3.5887 \times 10^{-9} S/m$$

$$y'_0 = j1.9219 \times 10^{-9} S/m$$

$$m_1 = (-1.6404 + j0.6209) \times 10^{-12} m^{-2}$$

$$m_0 = (-3.3750 + j0.6743) \times 10^{-12} m^{-2}$$

The characteristic impedance and propagation constants of the sequence components are:

$$Z_0^1 = \sqrt{\frac{z_1}{y'_1}} = 369e^{-j10.365^\circ} \Omega$$

$$p_1 = p_2 = \sqrt{z_1 y'_1} = 1.3244 \times 10^{-6} e^{j79.63^\circ} \text{ m}^{-1}$$

Zero sequence components:

$$z_0^0 = \sqrt{\frac{z_0}{y'_0}} = 965 e^{-j5.65^\circ} \Omega$$

$$p_0 = \sqrt{z_0 y'_0} = 1.8552 \times 10^{-6} e^{j84.35^\circ} \text{ m}^{-1}$$

In summary of this section, modal decomposition provides a tool for the solution of the equations of a multiphase line. A special case of modal decomposition, applicable to symmetric or nearly symmetric three-phase lines, yields the sequence models of a three-phase line. In this case the analysis of three-phase lines is reduced to the analysis of three single-phase transmission lines.

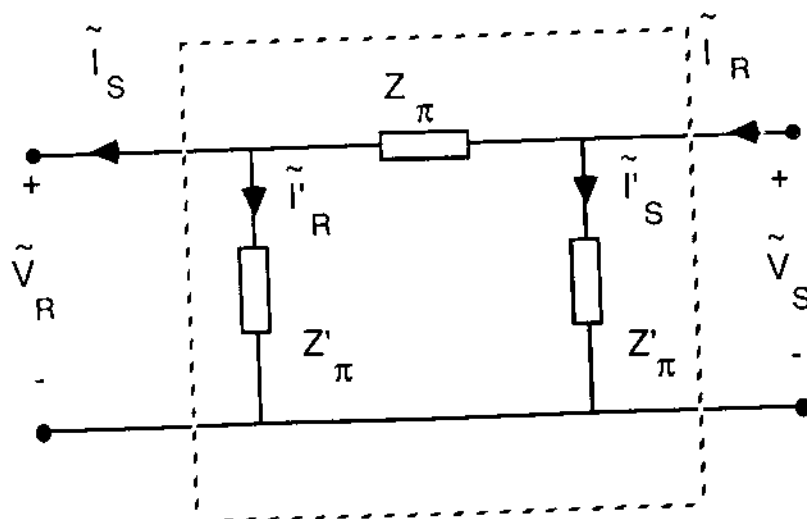
## 6.5 EQUIVALENT CIRCUITS

In Section 6.4 we have developed models of single-phase, as well as three-phase lines, under steady-state conditions. The models are in terms of the A, B, C parameters or alternatively, in terms of the characteristic impedance, propagation constant, and line length. An alternative representation of the transmission lines under steady-state conditions is by means of equivalent circuits. This approach is more attractive because of the familiarity of engineers with circuits. This section presents the computation of equivalent circuits from the transmission line parameters. Only the single-phase line case will be demonstrated. Since a three-phase line can be reduced to three single-phase lines by means of a modal decomposition, the extension to three-phase lines will be left to the reader as an exercise.

Consider Eqs. (6.13) of a single-phase line in terms of the terminal currents and voltages. From realization theory it is known that a two-port circuit can be found which is described with the same equations. Furthermore, this two-port circuit is not unique. From the multiplicity of equivalent circuits, two particular circuits have been popular among power engineers: (a) the  $\pi$  equivalent, and (b) the T equivalent. These circuits are introduced next.

### 6.5.1 $\pi$ -Equivalent Circuit

To a transmission line with constants A, B, C, corresponds a  $\pi$ -equivalent circuit with elements  $Z_\pi$ ,  $Z'_\pi$  as in Fig. 6.4. The elements  $Z_\pi$ ,  $Z'_\pi$  of the  $\pi$ -equivalent circuit are computed by equating the equations of the  $\pi$ -equivalent circuit to those of the transmission line. Specifically, the circuit of Fig. 6.4 is described by the following equations:

FIG. 6.4  $\pi$ -equivalent circuit.

$$\tilde{V}_S = \left( 1 + \frac{Z_\pi}{Z'_\pi} \right) \tilde{V}_R + Z_\pi \tilde{I}_R \quad (6.25a)$$

$$\tilde{I}_S = \frac{1}{Z'_\pi} \left( 2 + \frac{Z_\pi}{Z'_\pi} \right) \tilde{V}_R + \left( 1 + \frac{Z_\pi}{Z'_\pi} \right) \tilde{I}_R \quad (6.25b)$$

By comparison of the equations above to transmission line equations (6.14), we obtain

$$A = 1 + \frac{Z_\pi}{Z'_\pi}$$

$$B = Z_\pi$$

$$C = \frac{1}{Z'_\pi} \left( 2 + \frac{Z_\pi}{Z'_\pi} \right)$$

Solution of the foregoing equations for  $Z_\pi$ ,  $Z'_\pi$  yields

$$Z_\pi = B \quad (6.26a)$$

$$Z'_\pi = \frac{B}{A - 1} \quad (6.26b)$$

Equations (6.26) define the parameters of the  $\pi$ -equivalent circuit of a line.

### 6.5.2 T-Equivalent Circuit

To a transmission line with constants A, B, C corresponds a T-equivalent circuit with elements  $Z_T$ ,  $Z'_T$  as in Fig. 6.5. The elements  $Z_T$ ,  $Z'_T$  of the T-equivalent circuit are computed by equating the equations of the T-equivalent circuit to those of the transmission line. Specifically, the circuit of Fig. 6.5 is described by the equations

$$\tilde{V}_S = \left( 1 + \frac{Z_T}{Z'_T} \right) \tilde{V}_R + Z_T \left( 2 + \frac{Z_T}{Z'_T} \right) \tilde{I}_R \quad (6.27a)$$

$$\tilde{I}_S = \frac{1}{Z'_T} \tilde{V}_R + \left( 1 + \frac{Z_T}{Z'_T} \right) \tilde{I}_R \quad (6.27b)$$

Comparison of Eqs. (6.27) to the transmission line equations (6.14) gives us

$$A = 1 + \frac{Z_T}{Z'_T}$$

$$B = \left( 2 + \frac{Z_T}{Z'_T} \right) Z_T$$

$$C = \frac{1}{Z'_T}$$

Upon solution for the parameters  $Z_T$ ,  $Z'_T$ , we have

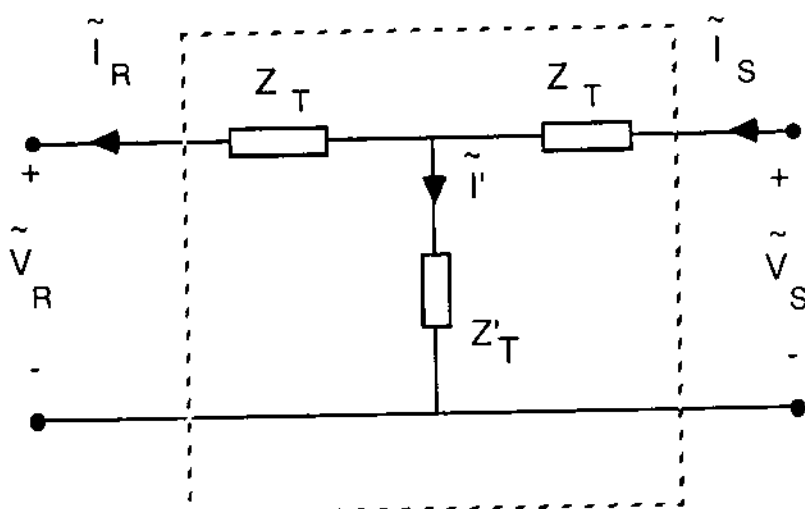


FIG. 6.5 T-equivalent circuit.

$$Z'_T = \frac{1}{C} \quad (6.28a)$$

$$Z_T = \frac{A - 1}{C} \quad (6.28b)$$

### 6.5.3 Nominal $\pi$ - and T-Equivalent Circuits

The nominal  $\pi$ - and T-equivalent circuits of a transmission line are approximations of the exact equivalents. In general, these approximations are valid for short lines; thus the name "short-line equivalent" is alternatively used. Consider the  $\pi$ - and T-equivalent circuits described by the parameters  $Z_\pi$ ,  $Z'_\pi$ ,  $Z_T$ , and  $Z'_T$ :

$$\begin{aligned} Z_\pi &= B = Z_0 \sinh p\ell \\ Z'_\pi &= \frac{B}{A - 1} = \frac{Z_0 \sinh p\ell}{\cosh p\ell - 1} \\ Z_T &= \frac{A - 1}{C} = Z_0 \frac{\cosh p\ell - 1}{\sinh p\ell} \\ Z'_T &= \frac{1}{C} = \frac{Z_0}{\sinh p\ell} \end{aligned}$$

The nominal  $\pi$ - and T-equivalent circuits are obtained by approximating the hyperbolic sine and cosine functions. Specifically, assuming that  $p\ell \ll 1$ , the functions are expanded into a series and then only the major terms are retained:

$$\begin{aligned} \sinh p\ell &\approx p\ell \\ \cosh p\ell &\approx 1 + \frac{(p\ell)^2}{2} \end{aligned}$$

Substitution of the approximations above in the equations for the parameters  $Z_\pi$ ,  $Z'_\pi$ ,  $Z_T$ , and  $Z'_T$  yields

$$Z_\pi \approx Z_0 p\ell = z\ell = (r + j\omega L)\ell \quad (6.29a)$$

$$Z'_\pi \approx \frac{Z_0 p\ell}{1 + (p\ell)^2/2 - 1} = 2 \frac{z'}{\ell} = \frac{2}{(g + j\omega C)\ell} \quad (6.29b)$$

$$Z_T = \frac{A - 1}{C} \approx \frac{1 + (p\ell)^2/2 - 1}{(1/Z_0)p\ell} = \frac{z\ell}{2} = (r + j\omega L) \frac{\ell}{2} \quad (6.29c)$$

$$\text{and } Z'_T = \frac{1}{C} = \frac{Z_0}{\sinh p\ell} \approx \frac{Z_0}{p\ell} = \frac{z'}{\ell} = \frac{1}{(g + j\omega C)\ell} \quad (6.29d)$$

The computation of equivalent circuits for a transmission line will be illustrated with an example.

Example 6.3: Consider the positive sequence model of the three-phase line of Example 6.2. The computed parameters are  $Z_0 = 369e^{-j10.36^\circ} \Omega$  and  $p = 1.3244 \times 10^{-6} e^{j79.63^\circ} m^{-1}$ . Assume that the line is 85 mi long and compute:

- (a) The  $\pi$ -equivalent circuit.
- (b) The T-equivalent circuit.
- (c) The nominal  $\pi$ -equivalent circuit.
- (d) The nominal T-equivalent circuit.

Solution: First, the A, B, C parameters of the line are computed as follows:

$$p\ell = 0.18113e^{j79.63^\circ}$$

$$\begin{aligned} \cosh p\ell &= 0.984659 + j0.005809 \\ &= 0.984676e^{j0.34^\circ} \end{aligned}$$

$$\begin{aligned} \sinh p\ell &= 0.032092 + j0.177323 \\ &= 0.180204e^{j79.74^\circ} \end{aligned}$$

$$A = 0.984676e^{j0.34^\circ}$$

$$B = 66.4953e^{j69.38^\circ} \Omega$$

$$C = 0.000488e^{j90.1^\circ} S$$

$$(a) Z_\pi = B = (23.417 + j62.235) \Omega$$

$$Z'_\pi = \frac{B}{A - 1} = (8.489 - j4053.59) \Omega$$

The  $\pi$ -equivalent circuit is illustrated in Fig. E6.1a.

$$(b) Z_T = \frac{A - 1}{C} = 33.615e^{j69.16^\circ} \Omega = (11.959 + j31.416) \Omega$$

$$Z'_T = \frac{1}{C} = 2049.18e^{-j90.1} \Omega = (-3.576 - j2049.18) \Omega$$

The T-equivalent circuit is illustrated in Fig. E6.1b.

$$(c) Z_\pi = z\ell = Z_0 p\ell = 66.837e^{j69.27} = 23.658 + j62.509$$

$$Z'_\pi = 2z'/\ell = 2Z_0/p\ell = 4074.42e^{-j90^\circ} = -j4074.4$$

The nominal  $\pi$ -equivalent circuit is illustrated in Fig. E6.1c.

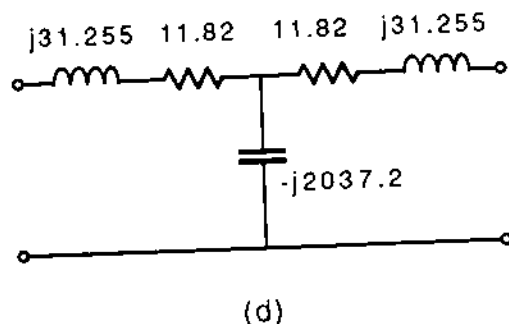
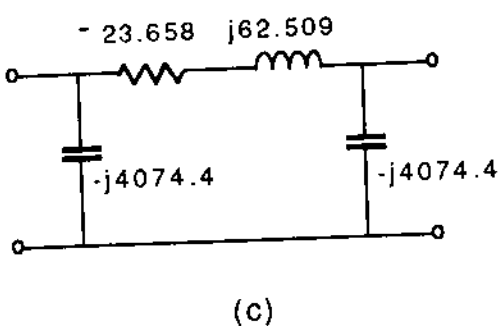
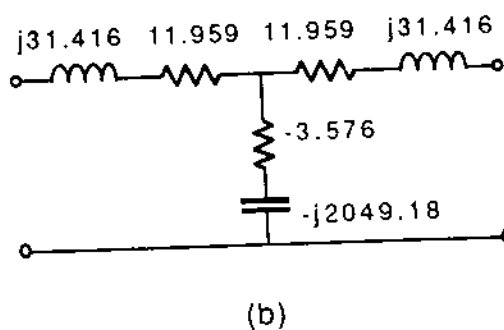
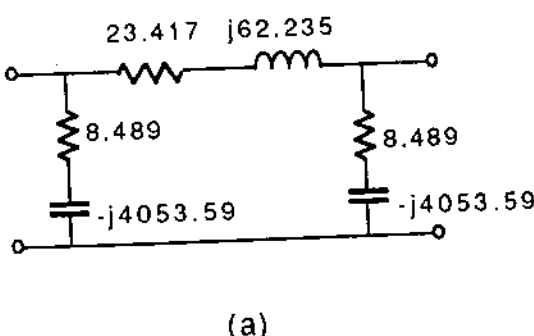


FIG. E6.1 The equivalent circuits of Example E6.3. (All indicated values are in ohms.)

$$(d) \quad Z_T = z\ell/2 = 11.82 + j31.255 \Omega$$

$$Z'_T = z'/\ell = -j2037.2 \Omega$$

The nominal T-equivalent circuit is illustrated in Fig. E6.1d.

## 6.6 COMPUTATION OF SEQUENCE PARAMETERS OF THREE-PHASE TRANSMISSION LINES

In previous sections we have seen that a special case of modal decomposition (symmetrical components transformation) of the three-phase line equations results in the sequence models. The transformation applies to both voltages and currents yielding the symmetrical components of these quantities as well as the line impedances yielding the sequence parameters of the line. In this section we are concerned with the computation of the sequence parameters of a three-phase line. One way to compute these parameters is through the

mathematical transformations of the resistance, inductance, and capacitance matrices of the line discussed in previous sections. An alternative way to compute these parameters is by utilizing the physical interpretation of the sequence models illustrated in Fig. 6.3. The figure illustrates that it is possible to excite the transmission line with a single mode (single symmetrical component). For example, the line is excited with positive sequence components only in Fig. 6.3a, with negative sequence components only in Fig. 6.3b, and with zero sequence components only in Fig. 6.3c. The impedance of the line to the flow of positive sequence component currents will be the positive sequence impedance, and so on. This observation suggests a simple two-step procedure to compute the sequence parameters of a line: (a) apply an excitation to the line corresponding to a single mode (symmetrical component), and (b) compute the line parameter. This procedure will be discussed for the purpose of computing the sequence series and shunt impedance of a three-phase line.

### 6.6.1 Series Impedance

The sequence series impedance of a three-phase line is computed with the following procedure:

- Step 1. Assume that sequence currents (positive, negative, or zero) flow through the transmission line,  $\tilde{I}_a$ ,  $\tilde{I}_b$ ,  $\tilde{I}_c$ .
- Step 2. Compute the voltages,  $\tilde{V}_a$ ,  $\tilde{V}_b$ ,  $\tilde{V}_c$ , per unit length of the line using the models developed in Chapters 2 and 3.
- Step 3. If the three-phase line were symmetric, the series impedance would be  $z = \tilde{V}_a/\tilde{I}_a = \tilde{V}_b/\tilde{I}_b = \tilde{V}_c/\tilde{I}_c$ . Since the line is not exactly symmetric, the series impedance per unit length of the line is computed as the average:

$$z = \frac{1}{3} \left( \frac{\tilde{V}_a}{\tilde{I}_a} + \frac{\tilde{V}_b}{\tilde{I}_b} + \frac{\tilde{V}_c}{\tilde{I}_c} \right) \quad (6.30)$$

The foregoing three-step procedure is straightforward for the computation of the positive and negative sequence series impedance. The voltage per unit length of the line for the three phases is

$$\begin{aligned}\tilde{V}_a &= r_c \tilde{I}_a + x_{aa} \tilde{I}_a - x_{ab} \tilde{I}_b - x_{ac} \tilde{I}_c \\ \tilde{V}_b &= -x_{ab} \tilde{I}_a + r_c \tilde{I}_b + x_{bb} \tilde{I}_b - x_{bc} \tilde{I}_c \\ \tilde{V}_c &= -x_{ac} \tilde{I}_a - x_{bc} \tilde{I}_b + r_c \tilde{I}_c + x_{cc} \tilde{I}_c\end{aligned}$$

Upon substitution of expressions above into Eq. (6.30) and observing that

$$\frac{\tilde{I}_b}{\tilde{I}_a} = \frac{\tilde{I}_c}{\tilde{I}_b} = \frac{\tilde{I}_a}{\tilde{I}_c} = e^{j240^\circ} = a^2$$

$$\frac{\tilde{I}_c}{\tilde{I}_a} = \frac{\tilde{I}_a}{\tilde{I}_b} = \frac{\tilde{I}_b}{\tilde{I}_c} = e^{j120^\circ} = a$$

$$x_{aa} = x_{bb} = x_{cc} = x_s$$

we have

$$z_1 = r_c + x_s - \frac{1}{3} (a + a^2)(x_{ab} + x_{bc} + x_{ca})$$

Note that  $a + a^2 = -1$ . Thus

$$z_1 = r_c + x_s + \frac{1}{3} (x_{ab} + x_{bc} + x_{ca})$$

Upon substitution of the inductive reactance components, we have

$$z_1 = r_c + j \frac{\mu\omega}{2\pi} \ln \frac{D}{d} \quad (6.31a)$$

where  $D = (D_{ab}D_{bc}D_{ca})^{1/3}$  and  $d$  is the geometric mean radius of the phase conductors. Converted into the English system of units, Eq. (6.31a) reads

$$z_1 = r_c + j0.00466f \log \frac{D}{d} \quad \Omega/\text{mi} \quad (6.31b)$$

where  $f$  is in hertz and  $r_c$  is in ohms per mile.

The computation of the zero sequence impedance is more complex, since the return of the zero sequence currents must be considered. In general, there are two return paths: (a) the shield/neutral wire, and (b) the earth path. Thus, in order to compute the zero sequence impedance, it is necessary to know what percentage of the zero sequence currents returns through the earth and what through the shield/neutral wire (current division). The problem appears to be complex since the current division depends on the grounding system of the line (tower footing grounding) and the grounding of the line at the two terminals of the line. Fortunately, transmission lines, in general, are grounded with low resistance grounds at the two ends (substation grounding resistance) and the tower footing resistances are relatively low. Under these conditions it can be assumed that the line is solidly grounded. This assumption introduces a small error in the computation of the line zero sequence parameters which is acceptable for most applications. In this case the transmission

line is said to be effectively grounded. The zero sequence current division of an effectively grounded line can be computed on the basis that the voltage drop along the shield/neutral conductor must be equal to the voltage drop along the earth path.

In terms of the return path of zero sequence currents, overhead power circuits can be classified into two categories: In the first category are transmission lines with high-strength-steel overhead ground wire. This design is usual for medium-voltage transmission circuits. Because the steel wires have a high resistance and substantial inductive reactance compared to those of the earth path, the zero sequence currents returns mostly through the earth path. For these circuits, as a first approximation, the shield wire is neglected in the computation of the zero sequence series impedance. In the second category are transmission lines with overhead ground wire(s) or neutral of relatively low impedance (i.e., ACSR, Alumoweld, two shield wires, etc.). This design is usual for distribution circuits and very high voltage transmission circuits. In this case the impedance of the shield or neutral wire is comparable to the impedance of the earth path. Thus in the computation of the zero sequence series impedance, the neutral wire must be considered. The point is illustrated further in Example 6.5. The computation of line series impedance is illustrated with two examples.

Example 6.4: Compute the positive sequence series impedance in ohms per mile of the transmission line of Example 6.1. The line is 115 kV, 24.6 mi long, and transposed. The phase conductors are ACSR, 336.4 kcm, 30 strands.

Solution:

$$z_1 = r_c + j0.00466f \log \frac{D}{d} \quad \Omega/\text{mi}$$

where

$r_c$  = conductor resistance, ohms per mile

$f$  = frequency of currents and voltages (60 Hz)

$D$  = geometric mean distance between phase conductors

$d$  = geometric mean radius of phase conductors

From Table A.2 the parameters of the phase conductors (ACSR, 336.4 kcm, 30 strands) are

$$r_c = 0.306 \quad \Omega/\text{mi}$$

$$d = 0.0255 \quad \text{ft}$$

For the computation of D, the following distances are taken from Fig. 1.6 (see also Example 6.1):

$$D_{ab} = 12.636 \text{ ft}$$

$$D_{ac} = 8.17 \text{ ft}$$

$$D_{bc} = 12.717 \text{ ft}$$

Thus

$$D = 10.949 \text{ ft}$$

and

$$z_1 = 0.306 + j0.7362 \Omega/\text{mi}$$

It should be noted that the negative sequence impedance is equal to the positive sequence impedance:

$$z_2 = 0.306 + j0.7362 \Omega/\text{mi}$$

Example 6.5: Consider the three-phase transmission line of Example 6.4. Compute the zero sequence series impedance of the line in ohms per mile. The line is transposed, the shield wire is 5/16-in.-diameter steel wire. The soil resistivity is  $100 \Omega \cdot \text{m}$ . Assume that the line is effectively grounded.

Solution: First the current division between the two return paths must be computed as illustrated in Fig. E6.2. The current division is computed on the assumption of an effectively grounded line. In this case

$$V_g = V_e$$

Assuming that electric current ( $\alpha 3I_0$ ) is flowing in the shield wire and  $\beta 3I_0$  is flowing in the earth, the voltages  $\tilde{V}_g$ ,  $\tilde{V}_e$  are computed as follows (transposed line):

$$\tilde{V}_g = \ell(r_g + x_{gg})(\alpha 3I_0) - \ell(x_{ag} + x_{bg} + x_{cg})I_0 - \ell x_{ge} e^{\beta 3I_0}$$

$$\tilde{V}_e = \ell x_{ee} e^{\beta 3I_0} - \ell(x_{ae} + x_{be} + x_{ce})I_0 - \ell x_{ge} \alpha 3I_0$$

$$\alpha 3I_0 + \beta 3I_0 = -3I_0$$

Solution for the variables  $\alpha$  and  $\beta$  yields

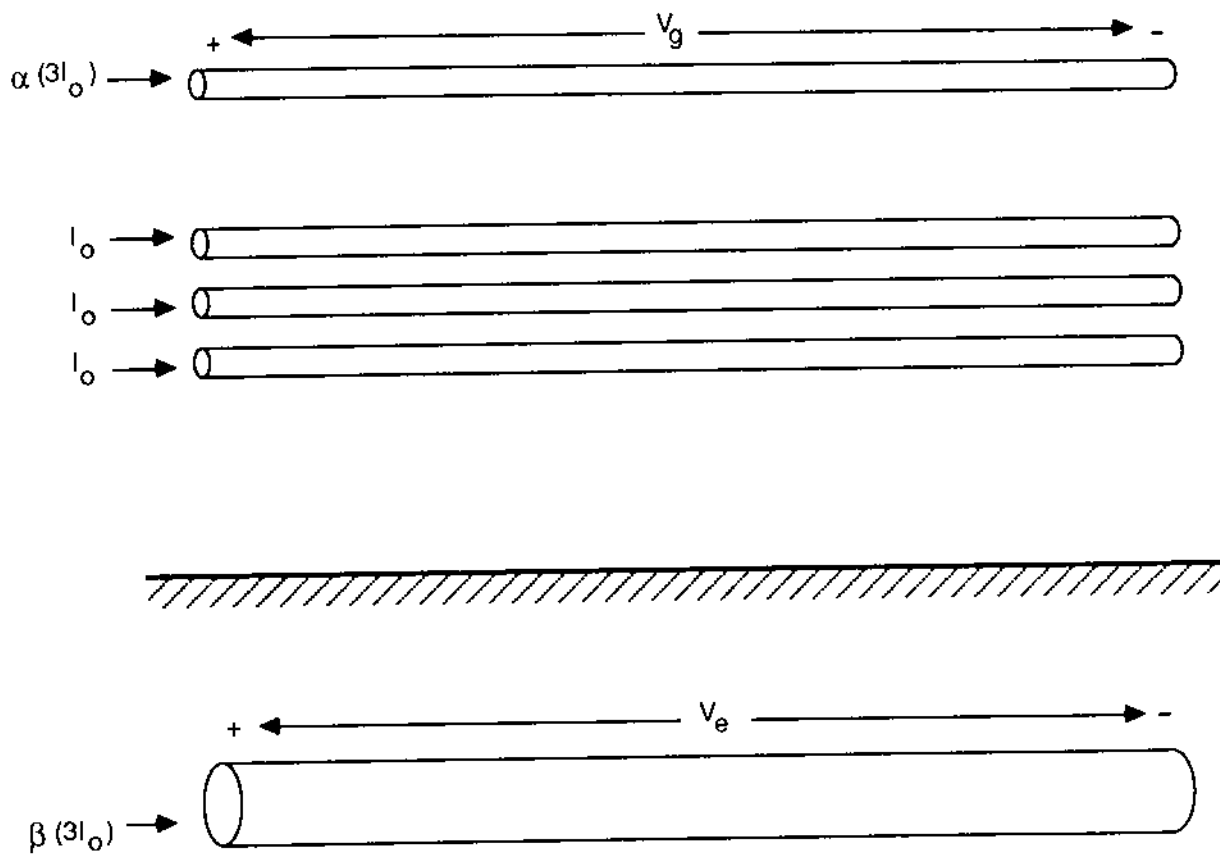


FIG. E6.2 Illustration for the computation of the zero sequence current split on a three phase transmission line.

$$\alpha = - \left[ 3 \left( r_g + r_e + j0.00466f \log \frac{D_e}{d_g} \right) \right]^{-1} \left( 3r_e + j0.00466 f \log \frac{D_e^3}{D_{ag} D_{bg} D_{cg}} \right)$$

$$\beta = -1 - \alpha$$

Next we substitute numerical values:

$$r_g = 5.83 \Omega/\text{mi}$$

$$r_e = 0.0954 \Omega/\text{mi}$$

$$f = 60 \text{ Hz}$$

$$D_e = 2160 \sqrt{\frac{\rho}{f}} = 2788 \text{ ft}$$

$$d_g = 0.0002 \text{ ft (from Table A.3)}$$

$$D_{ag} = 11.065 \text{ ft}$$

$$D_{bg} = 15.273 \text{ ft}$$

$$D_{cg} = 18.664 \text{ ft}$$

$$\alpha = 0.01527e^{j158.38^\circ}$$

$$\beta = -0.09858 - j0.005626 = 0.9858e^{j180.33^\circ}$$

Note that approximately 1.5% of the electric current returns through the shield wire. The remaining zero sequence current returns through the earth. Now the voltage of any phase conductor is computed as follows:

$$V_0 = \ell(r_c + x_{aa})I_0 - \frac{2\ell}{3}(x_{ab} + x_{ac} + x_{bc})I_0 - \frac{\ell}{3}(x_{ag} + x_{bg} + x_{cg})\alpha 3I_0 - \ell x_{ae}\beta 3I_0 - V_e$$

or

$$V_0 = \ell \left[ r_c + x_{aa} - \frac{2}{3}(x_{ab} + x_{ac} + x_{bc}) + x_{ae} + x_{be} + x_{ce} + 3x_{ae} \right] I_0 - \beta I_0 \ell (3r_e) - \alpha I_0 \ell (x_{ag} + x_{bg} + x_{cg} - 3x_{ae} - 3x_{ge})$$

The zero sequence series impedance per unit length is

$$Z_0 = \frac{V_0}{I_0 \ell} = \left( r_c + j0.00466f \log \frac{D_e^3}{\sqrt[3]{d^3 D_{ab}^2 D_{ac}^2 D_{bc}^2}} \right) - \beta 3r_e - \alpha j0.00466f \log \frac{D_{ag} D_{bg} D_{cg}}{D_e^3}$$

Next we substitute numerical values:

$$D_{ab} = 12.636 \text{ ft}$$

$$D_{ac} = 8.17 \text{ ft}$$

$$D_{bc} = 12.717 \text{ ft}$$

$$d = 0.0255 \text{ ft}$$

$$r_c = 0.306 \Omega/\text{mi}$$

$$z_0 = 0.306 + j2.754 - 0.9858e^{j180.33^\circ} (0.2862) \\ - 0.01527e^{j158.38^\circ} (-j1.9116) = 0.577 + j2.728 \Omega/\text{mi}$$

Example 6.5 clearly indicates that for effectively grounded lines with steel shield wires, a good approximation in the computation of the zero sequence impedance will be to assume that all electric current returns through the earth path. In this case, the zero sequence impedance is

$$z_0 = r_c + 3r_e + j(3)(0.00466)f \log \frac{D_e}{GMR_0}$$

where

$$GMR_0 = \left( d^3 D_{ab}^2 D_{ac}^2 D_{bc}^2 \right)^{1/9} \text{ feet} \\ D_e = 2160 \sqrt{\frac{\rho}{f}} \text{ feet}$$

Upon substitution of numerical values, we have

$$GMR_0 = 1.4515 \text{ ft}$$

$$D_e = 2788 \text{ ft}$$

$$r_c = 0.306 \Omega/\text{mi}$$

$$r_e = 0.0954 \Omega/\text{mi}$$

and

$$z_0 = 0.5922 + j2.7542$$

Observe that this value is slightly higher than the one computed earlier. Thus, when the presence of the shield wire is neglected, the zero sequence impedance is overestimated. The error may be substantial for lines with low-impedance neutrals. The impact of the shield/neutral conductors on the zero sequence series impedance of a line is discussed further in Section 6.10.

### 6.6.2 Shunt Admittance

The sequence shunt admittance of a three-phase line is computed using the following procedure.

- Step 1. Assume that sequence voltages (positive, negative, or zero) are applied to the transmission line,  $\tilde{V}_a$ ,  $\tilde{V}_b$ ,  $\tilde{V}_c$ .
- Step 2. Compute the line capacitive currents,  $\tilde{I}'_a$ ,  $\tilde{I}'_b$ ,  $\tilde{I}'_c$  per unit length of the line using the models discussed in Chapter 4.
- Step 3. If the three-phase line were symmetric, the shunt admittance will be  $y' = \tilde{I}'_a/\tilde{V}_a = \tilde{I}'_b/\tilde{V}_b = \tilde{I}'_c/\tilde{V}_c$ . Since the line is not exactly symmetric, the shunt admittance per unit length of the line is computed as the average:

$$y' = \frac{1}{3} \left( \frac{\tilde{I}'_a}{\tilde{V}_a} + \frac{\tilde{I}'_b}{\tilde{V}_b} + \frac{\tilde{I}'_c}{\tilde{V}_c} \right) \quad (6.32)$$

The procedure is illustrated with two examples.

Example 6.6: Consider the three-phase transmission line of Examples 6.4 and 6.5. Compute the positive-sequence shunt admittance of the line in siemens per mile.

Solution: First, we assume that the transmission line is energized with positive sequence three-phase voltages. Then we compute the capacitive currents for each one of the three phases. Figure E6.3 illustrates the line configuration and the images. The outside radii of the conductors are:

Phase conductors:  $0.741/24 = 0.03087$  ft

Shield wire:  $0.3125/24 = 0.01302$  ft

The geometric distances among phase conductors and images are as follows:

$$D_{a'a} = 78.60 \text{ ft}$$

$$D_{b'b} = 86.52 \text{ ft}$$

$$D_{c'c} = 70.18 \text{ ft}$$

$$D_{g'g} = 106.0 \text{ ft}$$

$$D_{ab} = (12^2 + 3.96^2)^{1/2} = 12.5365 \text{ ft}$$

$$D_{ac} = (12^2 + 4.21^2)^{1/2} = 12.7170 \text{ ft}$$

$$D_{ag} = (13.7^2 + 6.75^2)^{1/2} = 15.2726 \text{ ft}$$

$$D_{bc} = 8.17 \text{ ft}$$

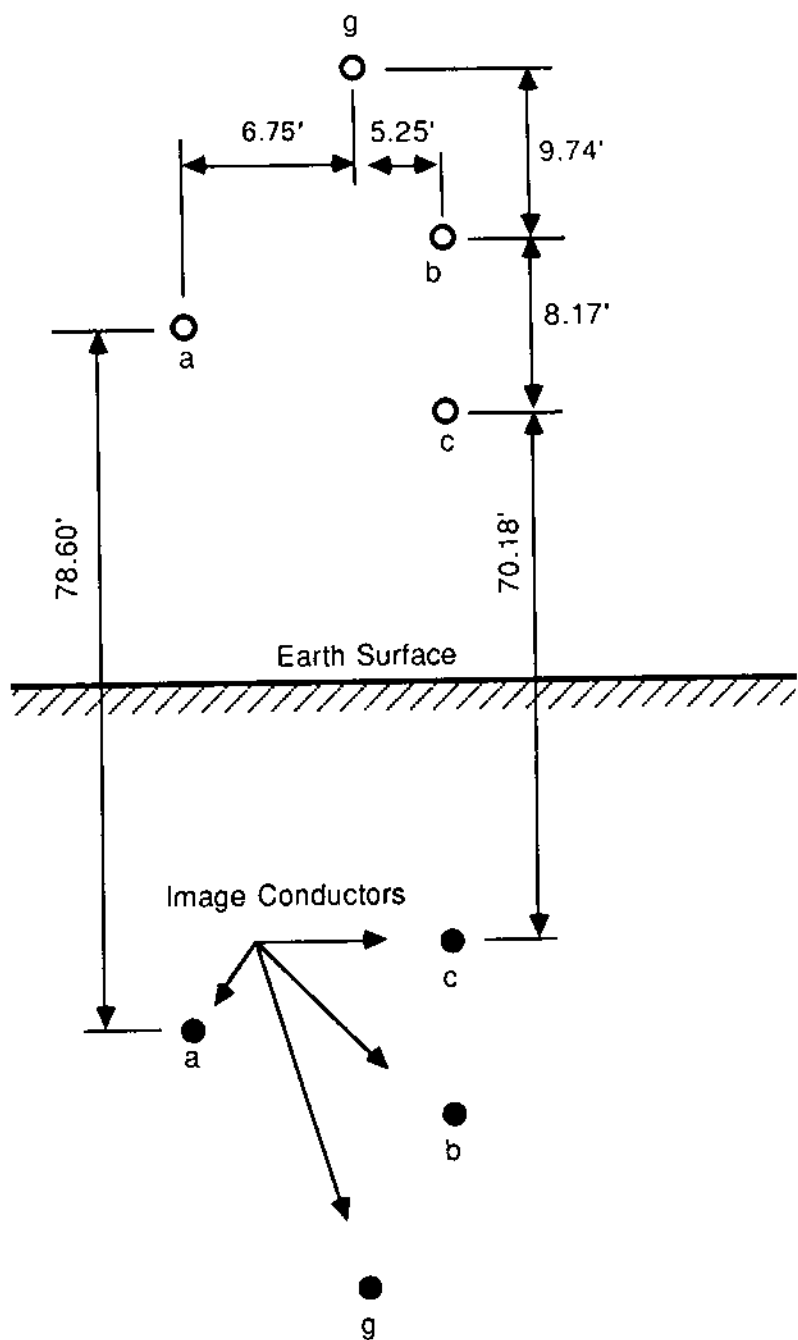


FIG. E6.3

$$D_{bg} = (9.74^2 + 5.25^2)^{1/2} = 11.0648 \text{ ft}$$

$$D_{cg} = (17.91^2 + 5.25^2)^{1/2} = 18.6636 \text{ ft}$$

$$D_{bc'} = D_{b'c} = 86.52 - 8.17 = 78.35 \text{ ft}$$

$$D_{ag'} = D_{a'g} = [6.75^2 + (92.30)^2]^{1/2} = 92.5464 \text{ ft}$$

$$D_{ab'} = D_{a'b} = [12^3 + (86.52 - 3.96)^2]^{1/2} = 83.4275 \text{ ft}$$

$$D_{ac'} = D_{a'c} = [12^2 + (70.18 + 4.21)^2]^{1/2} = 75.3516 \text{ ft}$$

$$D_{bg'} = D_{b'g} = [5.25^2 + (106 - 9.74)^2]^{1/2} = 96.4030 \text{ ft}$$

$$D_{cg'} = D_{c'g} = [(5.25^2 + (106 - 9.74 - 8.17)^2]^{1/2} = 88.2463 \text{ ft}$$

The equations relating the capacitive currents to the voltages are

$$\begin{bmatrix} 7.8422 & 1.8874 & 1.7792 & 1.8016 \\ 1.8874 & 7.9382 & 2.2607 & 2.1648 \\ 1.7792 & 2.2607 & 7.7289 & 1.5536 \\ 1.8016 & 2.1648 & 1.5536 & 9.0046 \end{bmatrix} \begin{bmatrix} I'_{a1} \\ I'_{b1} \\ I'_{c1} \\ I'_{g1} \end{bmatrix} = j20.972 \times 10^{-9} \begin{bmatrix} E_a \\ E_b \\ E_c \\ 0 \end{bmatrix}$$

In the equations above, the electric capacitive currents will be computed in amperes per meter when the voltages are expressed in volts. Thus substitution gives us

$$E_a = \frac{115,000}{\sqrt{3}}$$

$$E_b = E_a e^{-j120^\circ}$$

$$E_c = E_a e^{-j240^\circ}$$

and upon solution of the resulting equations, we obtain

$$I'_{a1} = 0.2293 \times 10^{-3} e^{j89.95^\circ} \text{ A/m}$$

$$I'_{b1} = 0.2441 \times 10^{-3} e^{-j26.96^\circ} \text{ A/m}$$

$$I'_{c1} = 0.2432 \times 10^{-3} e^{-j153.01^\circ} \text{ A/m}$$

$$I'_{g1} = 0.01498 \times 10^{-3} e^{-j179.24^\circ} \text{ A/m}$$

Upon substitution into Eq. (6.32), we have

$$y'_1 = \frac{10^{-9}}{3} (3.45356 e^{j89.95^\circ} + 3.6765 e^{j93.04^\circ} + 3.6629 e^{j86.99^\circ})$$

$$y'_1 = j3.5942 \times 10^{-9} \text{ S/m} = j5.783 \times 10^{-6} \text{ S/mi}$$

The shunt impedance is

$$z'_1 = \frac{1.0}{y'_1} = -j0.2782 \times 10^9 \Omega \cdot \text{m} = -j0.173 \times 10^6 \Omega \cdot \text{mi}$$

Note that the negative sequence shunt admittance and impedance will be equal to the positive sequence shunt admittance and impedance.

Example 6.7: Consider the three-phase transmission line of Examples 6.4, 6.5, and 6.6. Compute the zero sequence shunt admittance of the line in siemens per mile.

Solution: This problem will be solved in the same way as Example 6.6. Zero sequence voltages will be applied to the transmission line and the capacitive currents will be computed. The equation relating the voltage to the capacitive currents of the line are (see Example 6.6)

$$\begin{bmatrix} 7.8422 & 1.8874 & 1.7792 & 1.8016 \\ 1.8874 & 7.9382 & 2.2607 & 2.1648 \\ 1.7792 & 2.2607 & 7.7289 & 1.5536 \\ 1.8016 & 2.1648 & 1.5536 & 9.0046 \end{bmatrix} \begin{bmatrix} I'_{a1} \\ I'_{b1} \\ I'_{c1} \\ I'_{g1} \end{bmatrix} = j20.972 \times 10^{-9} \begin{bmatrix} V \\ V \\ V \\ 0 \end{bmatrix}$$

In the equations above, the capacitive currents will be computed in amperes per meter when the zero sequence voltage  $V$  is expressed in volts.

Assuming that  $V = 1.0$  and solving the resulting equations give us

$$I'_a = j2.0502 \times 10^{-9} \text{ A/m}$$

$$I'_b = j1.9375 \times 10^{-9} \text{ A/m}$$

$$I'_c = j1.9173 \times 10^{-9} \text{ A/m}$$

$$I'_g = -j1.2068 \times 10^{-9} \text{ A/m}$$

Upon substitution into Eq. (6.32), we obtain

$$y'_0 = j1.9665 \times 10^{-9} \text{ S/m} = j3.164 \times 10^{-6} \text{ S/mi}$$

The zero sequence shunt impedance is

$$z_0' = -j0.508 \times 10^9 \Omega \cdot m = -j0.3157 M\Omega \cdot mi$$

## 6.7 TRANSMISSION LINE MODELS BASED ON AN ADMITTANCE MATRIX

In previous sections we have discussed models of three-phase lines. We derived the sequence models of a three-phase line, which simplify the analysis but neglect asymmetries existing among the three phases. An alternative model of a three-phase line (or any other line) which does not require simplifying assumptions is by means of an admittance matrix. Specifically, since the transmission line is a linear system, a linear relationship between the line terminal currents and the line terminal voltages can be found. This relationship is expressed in terms of the line admittance matrix.

$$[I] = [Y][V] \quad (6.33)$$

where

$[I]$  = vector of line terminal currents flowing into the line

$[V]$  = vector of line terminal voltages

$[Y]$  = admittance matrix of the line

The admittance matrix representation of a line is simple and general. It applies to single or multiphase lines, it accounts for asymmetries in case of multiphase lines, it can account for line tower grounding, and so on. The computation of the admittance matrix of a line will be demonstrated with a single-phase line.

### 6.7.1 Admittance Matrix of a Single-Phase Line

The admittance matrix of a single-phase line can easily be derived as follows. Recall Eqs. (6.13) of a single-phase line in terms of the terminal voltages and currents:

$$\tilde{V}_S = (\cosh p\ell) \tilde{V}_R + Z_0(\sinh p\ell) \tilde{I}_R$$

$$\tilde{I}_S = \frac{1}{Z_0} (\sinh p\ell) \tilde{V}_R + (\cosh p\ell) \tilde{I}_R$$

Recall that the electric currents  $\tilde{I}_S$ ,  $\tilde{I}_R$  at the terminals of the line are defined as flowing from the right of the line to the left (see Fig. 6.1). Let's identify the line terminals with numerals (i.e., the sending end will be terminal 1, etc.) and define the terminal currents,  $I_1$  and  $I_2$ , as flowing into the line, that is,

$$\tilde{I}_1 = \tilde{I}_S$$

$$\tilde{I}_2 = -\tilde{I}_R$$

For uniformity, let's rename the terminal voltages  $\tilde{V}_S$  and  $\tilde{V}_R$ :

$$\tilde{V}_1 = \tilde{V}_S$$

$$\tilde{V}_2 = \tilde{V}_R$$

Upon substitution of the new variables into the equations of the line and subsequent solution for the currents  $\tilde{I}_1$  and  $\tilde{I}_2$ , we obtain

$$\begin{bmatrix} \tilde{I}_1 \\ \tilde{I}_2 \end{bmatrix} = \begin{bmatrix} \cosh p\ell / (Z_0 \sinh p\ell) & -1 / (Z_0 \sinh p\ell) \\ -1 / (Z_0 \sinh p\ell) & \cosh p\ell / (Z_0 \sinh p\ell) \end{bmatrix} \begin{bmatrix} \tilde{V}_1 \\ \tilde{V}_2 \end{bmatrix} \quad (6.34)$$

By comparison of Eq. (6.34) to Eq. (6.33), which defines the admittance matrix, the admittance matrix of the single-phase line is

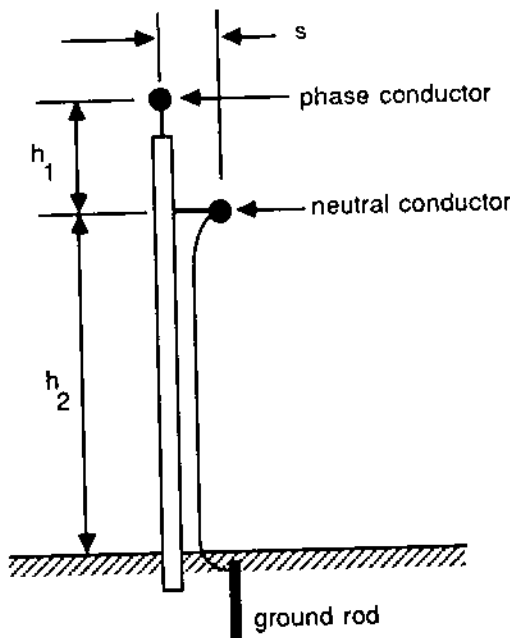
$$Y = \begin{bmatrix} \cosh p\ell / (Z_0 \sinh p\ell) & -1 / (Z_0 \sinh p\ell) \\ -1 / (Z_0 \sinh p\ell) & \cosh p\ell / (Z_0 \sinh p\ell) \end{bmatrix}$$

Note that the admittance matrix is a symmetric matrix. This is true for all transmission lines.

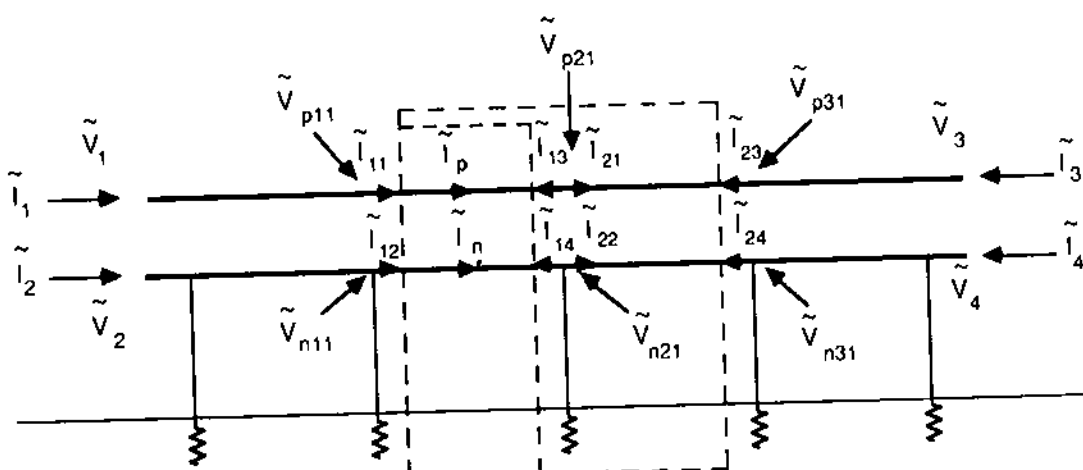
### 6.7.2 Transmission Line Models with Explicit Grounding Representation

An advantage of the transmission-line model based on the admittance matrix representation is the simplicity by which the grounding structures of the line can be incorporated. Modeling of the transmission tower grounds will be discussed by considering a single-phase line with multiple grounds. The line is illustrated in Fig. 6.6. It is a typical single-phase overhead distribution line. The line is multiply grounded, that is, the neutral conductor is connected to the pole grounding system at each pole. The length of the line is  $\ell$  miles. Also, the supporting poles are assumed to be at a regular distance of  $\ell_g$  and are grounded. It is desired to develop an admittance matrix representation of the transmission line relating the electric currents and voltages at the terminals of the line.

For this purpose, consider a single span of the line. Since the length of a span is typically short, the nominal  $\pi$ -equivalent circuit can be utilized to represent the span. Subsequently, the admittance matrix representation of one span is developed. Then the result is extended to the entire transmission line.



(a)



(b)

FIG. 6.6 A single phase line with multiple grounds. (a) Pole configuration, (b) longitudinal view.

The series impedance of the span is modeled with the equations

$$\tilde{V}_{p11} - \tilde{V}_{p21} = [(r_c + r_e + x_{ppe})\tilde{I}_p + (r_e + x_{pne})\tilde{I}_n] \ell_s$$

$$\tilde{V}_{n11} - \tilde{V}_{n21} = [(r_e + x_{pne})\tilde{I}_p + (r_e + r_n + x_{nne})\tilde{I}_n] \ell_s$$

where the currents and voltages are defined in Fig. 6.6. In compact matrix notation

$$\tilde{V}_{s1} - \tilde{V}_{s2} = (R_s + X_s)\tilde{I}$$

$$R_s = \begin{bmatrix} r_p + r_e & r_e \\ r_e & r_e + r_n \end{bmatrix} \ell_s$$

$$X_s = \begin{bmatrix} x_{ppe} & x_{pne} \\ x_{pne} & x_{nne} \end{bmatrix} \ell_s$$

$$V_{s1} = \begin{bmatrix} V_{p11} \\ V_{n11} \end{bmatrix} \quad V_{s2} = \begin{bmatrix} V_{p21} \\ V_{n21} \end{bmatrix} \quad I = \begin{bmatrix} I_p \\ I_n \end{bmatrix}$$

The capacitive reactance of the line is modeled with the equations

$$V_{s1} = X_{sh}(\tilde{I}_{s1} - \tilde{I})$$

$$V_{s2} = X_{sh}(\tilde{I} + \tilde{I}_{s2})$$

where

$$\tilde{I}_{s1} = \begin{bmatrix} \tilde{I}_{11} \\ \tilde{I}_{12} \end{bmatrix} \quad \tilde{I}_{s2} = \begin{bmatrix} \tilde{I}_{13} \\ \tilde{I}_{14} \end{bmatrix}$$

$$(X_{sh})_{ij} = \frac{4\pi}{jf} \left( \log \frac{D_{ij}}{D_{ij'}} \right) \frac{2}{\ell_s}$$

and

$f$  = frequency

$D_{ij}$  = geometric distance between conductors  $i, j$

$D_{ij'}$  = geometric distance between conductor  $i$  and image of  $j$

Solution of the foregoing equations for the electric currents yield

$$\tilde{I} = (R_s + X_s)^{-1}(\tilde{V}_{s1} - \tilde{V}_{s2})$$

$$\tilde{I} + \tilde{I}_{s2} = X_{sh}^{-1}\tilde{V}_{s2}$$

$$\tilde{I}_{s1} - \tilde{I} = X_{sh}^{-1}\tilde{V}_{s1}$$

Upon elimination of currents  $\tilde{I}$  and rearranging, we have

$$\begin{bmatrix} \tilde{I}_{s1} \\ \tilde{I}_{s2} \end{bmatrix} = \begin{bmatrix} (R_s + X_s)^{-1} + X_{sh}^{-1} & -(R_s + X_s)^{-1} \\ -(R_s + X_s)^{-1} & (R_s + X_s)^{-1} + X_{sh}^{-1} \end{bmatrix} \begin{bmatrix} \tilde{V}_{s1} \\ \tilde{V}_{s2} \end{bmatrix}$$

Thus the admittance matrix of one span is

$$Y_s = \begin{bmatrix} (R_s + X_s)^{-1} + X_{sh}^{-1} & -(R_s + X_s)^{-1} \\ -(R_s + X_s)^{-1} & (R_s + X_s)^{-1} + X_{sh}^{-1} \end{bmatrix}$$

The admittance of one span is then employed to compute the admittance of two spans, then three spans, and so on. In the procedure, the tower footing impedance is taken into consideration. The procedure will be illustrated as applied to the computation of the admittance matrix of two successive spans as illustrated in Fig. 6.6. The equations of one span are

$$\begin{bmatrix} \tilde{I}_{s1} \\ \tilde{I}_{s2} \end{bmatrix} = Y_s \begin{bmatrix} \tilde{V}_{s1} \\ \tilde{V}_{s2} \end{bmatrix}$$

The equations for the other span are

$$\begin{bmatrix} \tilde{I}_{s2r} \\ \tilde{I}_{s3} \end{bmatrix} = Y_s \begin{bmatrix} \tilde{V}_{s2} \\ \tilde{V}_{s3} \end{bmatrix}$$

where

$$\tilde{I}_{s2r} = \begin{bmatrix} \tilde{I}_{21} \\ \tilde{I}_{22} \end{bmatrix} \quad \tilde{I}_{s3} = \begin{bmatrix} \tilde{I}_{23} \\ \tilde{I}_{24} \end{bmatrix} \quad \tilde{V}_{s3} = \begin{bmatrix} \tilde{V}_{p31} \\ \tilde{V}_{n31} \end{bmatrix}$$

In addition, Kirchhoff's current law applied at the interconnection of the two spans:

$$\tilde{I}_{13} + \tilde{I}_{21} = 0$$

$$\tilde{I}_{14} + \tilde{I}_{22} + G_T \tilde{V}_{n21} = 0$$

where  $G_T$  is the admittance of the tower. In compact matrix notation

$$\tilde{I}_{s2} + \tilde{I}_{s2r} + Y_T \tilde{V}_{s2} = 0$$

where

$$Y_T = \begin{bmatrix} 0 & 0 \\ 0 & G_T \end{bmatrix}$$

In the equations above, the electric currents  $\tilde{I}_{s2}$  and  $\tilde{I}_{s2r}$  can be eliminated, yielding the admittance matrix representation of two spans, including the tower footing impedance. The elimination yields

$$\begin{aligned}\tilde{I}_{s1} &= \left[ (R_s + X_s)^{-1} + X_{sh}^{-1} - Y_1 \right] \tilde{V}_{s1} - Y_1 \tilde{V}_{s3} \\ \tilde{I}_{s3} &= -Y_1 \tilde{V}_{s1} + \left[ (R_s + X_s)^{-1} + X_{sh}^{-1} - Y_1 \right] \tilde{V}_{s3}\end{aligned}$$

where

$$Y_1 = (R_s + X_s)^{-1} \left[ Y_T + 2(R_s + X_s)^{-1} + 2X_{sh}^{-1} \right]^{-1} (R_s + X_s)^{-1}$$

Thus the admittance matrix representation of two spans, including tower footing impedance, is

$$Y_{2s} = \begin{bmatrix} (R_s + X_s)^{-1} + X_{sh}^{-1} - Y_1 & -Y_1 \\ -Y_1 & (R_s + X_s)^{-1} + X_{sh}^{-1} - Y_1 \end{bmatrix}$$

The procedure must be repeated for all spans of the line sequentially to yield the admittance matrix representation of the entire transmission line.

Example 6.8: A single-phase overhead transmission line has a multiply grounded neutral. The phase conductor is ACSR, 1/0, and the neutral conductor is ACSR, No. 2, 7 strands. The pole arrangement is illustrated in Fig. 6.6. The dimensions appearing in Fig. 6.6 are  $h_1 = 5$  ft,  $h_2 = 35$  ft,  $s = 0.5$  ft. The span length is  $\ell_s = 0.0833$  mi. The line is four span lengths long. The pole grounding system resistance is  $47 \Omega$  and the soil resistivity is  $100 \Omega \cdot \text{m}$ . Compute the admittance matrix of the single-phase line.

Solution: The matrices  $R_s$ ,  $X_s$ , and  $X_{sh}$  for one span of the line are computed. The data for the conductors are

$$r_p = 1.12 \Omega/\text{mi}$$

$$d_p = 0.00446 \text{ ft}$$

$$a_p = 0.199 \text{ in.} = 0.01658 \text{ ft}$$

$$r_n = 1.65 \Omega/\text{mi}$$

$$d_n = 0.00504 \text{ ft}$$

$$a_n = 0.1625 \text{ in.} = 0.01354 \text{ ft}$$

$$D_e = 2160 \sqrt{\rho/f} = 2788 \text{ ft}$$

$$r_e = 0.00159f = 0.0954 \Omega/\text{mi}$$

$$R_s = \begin{bmatrix} 0.0101243 & 0.00795 \\ 0.00795 & 0.14544 \end{bmatrix} \Omega$$

$$X_s = \begin{bmatrix} j0.135 & j0.06394 \\ j0.06394 & j0.1338 \end{bmatrix} \Omega$$

$$X_{sh} = \begin{bmatrix} -j6.0412 & -j1.9253 \\ -j1.9253 & -j6.0903 \end{bmatrix} \times 10^6 \Omega$$

Upon inversion of the matrices, we obtain:

$$(R_s + X_s)^{-1} = \begin{bmatrix} 4.25455 - j4.43095 & -1.99230 + j0.20462 \\ -1.99230 + j0.20462 & 4.26251 - j3.05667 \end{bmatrix}$$

$$X_{sh}^{-1} = \begin{bmatrix} j0.1841 & -j0.0582 \\ -j0.0582 & j0.1826 \end{bmatrix} \times 10^{-6} \text{ s}$$

$$Y_T + 2(R_s + X_s)^{-1} + 2X_{sh}^{-1} = \begin{bmatrix} 8.50910 - j8.86190 & -3.98460 + j0.40924 \\ -3.98465 + j0.40924 & 8.54629 - j6.11313 \end{bmatrix}$$

$$\left[ Y_T + 2(R_s + X_s)^{-1} + 2X_{sh}^{-1} \right]^{-1} = \begin{bmatrix} 0.05064 + j0.06749 & 0.00401 + j0.03192 \\ 0.00401 + j0.03192 & 0.07270 + j0.06524 \end{bmatrix}$$

$$Y_1 = \begin{bmatrix} 2.127060 - j2.215527 & -0.995910 + j0.102506 \\ -0.995910 + j0.102506 & 2.125816 - j1.528446 \end{bmatrix}$$

The admittance matrix of two spans is

$$Y_{2s} = \begin{bmatrix} Y_a & -Y_1 \\ -Y_1 & Y_a \end{bmatrix}$$

where

$$Y_a = \begin{bmatrix} 2.127490 - j2.215423 & -0.996390 + j0.102114 \\ -0.996390 + j0.102114 & 2.136693 - j1.528224 \end{bmatrix}$$

Similarly, the admittance matrix of four spans is computed by combining the admittances of two spans. The final result is

$$Y_{4s} = \begin{bmatrix} Y_{d4s} & -Y_{o4s} \\ -Y_{o4s} & Y_{d4s} \end{bmatrix}$$

where

$$Y_{o4s} = \begin{bmatrix} 1.063745 - j1.107712 & -0.498195 + j0.051057 \\ -0.498195 + j0.051057 & 1.063044 - j0.764097 \end{bmatrix}$$

$$Y_{d4s} = \begin{bmatrix} 1.063745 - j1.107711 & -0.498195 + j0.051057 \\ -0.498195 + j0.051057 & 1.073649 - j0.764127 \end{bmatrix}$$

In this section we discussed procedures by which the admittance matrix of any transmission line can be determined. This model is general—capable of representing line asymmetries and line tower footing impedance. The last capability is important for the purpose of computing the ground potential rise in grounded structures. This problem is discussed further in Chapter 7.

## 6.8 ADMITTANCE MATRIX MODEL OF MUTUALLY COUPLED TRANSMISSION LINES

In this section we present the fundamental equations utilized in modeling a single three-phase transmission line or  $n$  parallel mutually coupled transmission lines in terms of an admittance matrix. The modeling procedure will be demonstrated with a system of two parallel mutually coupled three-phase transmission lines. The system is illustrated in Fig. 6.7. The objective of the modeling procedure is to derive the admittance matrix of the system, that is, the relationship between the electric currents and voltages at the terminals of the lines [i.e., Eq. (6.33)]. For the case under consideration, the dimensions of the vectors  $I$  and  $V$  are  $2(3n + m)$ , where  $n$  is the number of mutually coupled lines and  $m$  is the number of neutral/shield wires. The matrix  $Y$  contains all the model information about these lines.

The admittance matrix of a system of mutually coupled lines is derived as follows. Consider the mutually coupled lines of Fig. 6.7a. Symbolically, the conductors of these lines appear in Fig. 6.7b. Let the line length be  $\ell$ . Assume that the span length is  $\ell_s$ . First, the model of one span is developed. For this purpose, consider span  $k$  illustrated in Fig. 6.7b. Let the currents flowing on the left side of the span be denoted by the subscript  $k$ , superscript  $l$ , and the currents flowing on the right side of the span be denoted by the subscript  $k$ , superscript  $r$ . As an example of this notation, the

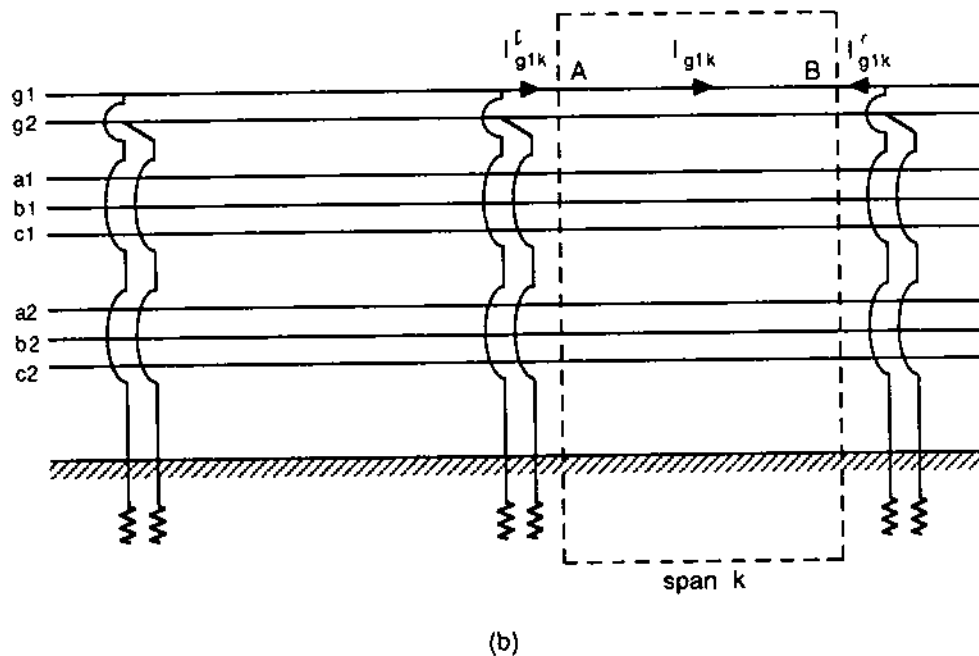
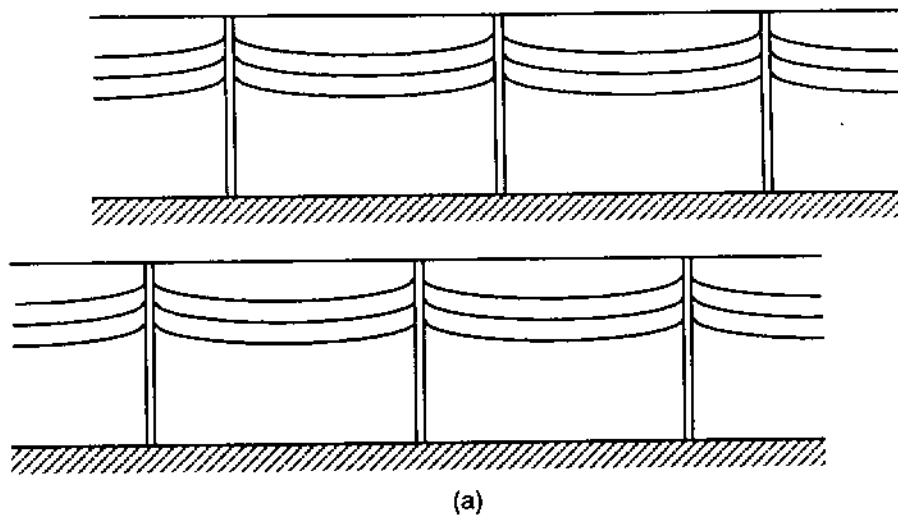


FIG. 6.7 Two mutually coupled transmission lines.

shield wire currents for shield wire  $g_1$  will be  $\tilde{I}_{g1k}^l$  and  $\tilde{I}_{g1k}^r$ , respectively, as indicated in Fig. 6.7b. Further assume that the line capacitance is lumped at the two ends of the span. Under this assumption the electric current in the conductors will be different from the current at the terminals of span. This current is denoted by the subscript  $k$ . As an example, the current of the shield wire  $g_1$  is denoted by  $I_{g1k}$  and illustrated in Fig. 6.7b. The voltage at the left-side terminals of the span are denoted by the subscript  $k$ . Thus the voltage at points A and B of the shield wire  $g_1$  are

denoted  $\tilde{V}_{g1k}$  and  $\tilde{V}_{g1k+1}$ , respectively. The induced voltage along a conductor of the span  $k$  is given as a linear combination of its own electric current and the currents flowing in the other conductors. As an example, the induced voltage along AB of the shield wire  $g1$  is given by

$$\begin{aligned}\tilde{V}_{AB} &= \tilde{V}_{g1k} - \tilde{V}_{g1k+1} \\ &= f_{g1g1} \tilde{I}_{g1k} + f_{g1g2} \tilde{I}_{g2k} + f_{g1a1} \tilde{I}_{a1k} + \cdots + f_{g1c2} \tilde{I}_{c2k}\end{aligned}\quad (6.35)$$

Note that in Eq. (6.35) the functions  $f_{g1g1}$ ,  $f_{g1g2}$ , and so on, are computed with Carson's theory (infinite series) or any of the alternative methods presented in Chapter 3. Writing one such equation for each conductor in the system, the following matrix equation is obtained:

$$\tilde{V}_k - \tilde{V}_{k+1} = X \tilde{I}_k \quad (6.36)$$

Now consider the capacitance of span  $k$ . We shall assume that the capacitance is lumped at the ends of the span. Half of the capacitance is lumped to the left end and half to the right end. The models developed in Chapter 4 can be utilized to compute the shunt impedance matrix of the half span,  $X_{sh}$ . Now observe that the capacitive current of the left half of the span is  $\tilde{I}_k^l - \tilde{I}_k^r$  and the capacitive current of the right half of the span is  $\tilde{I}_k^r + \tilde{I}_k^l$ . Thus

$$\tilde{V}_k = X_{sh} (\tilde{I}_k^l - \tilde{I}_k^r) \quad (6.37a)$$

$$\tilde{V}_{k+1} = X_{sh} (\tilde{I}_k^r + \tilde{I}_k^l) \quad (6.37b)$$

Equations (6.36) and (6.37) are solved for the electric currents  $\tilde{I}_k^l$  and  $\tilde{I}_k^r$  (after eliminating the currents  $\tilde{I}_k$ ), yielding

$$\begin{bmatrix} \tilde{I}_k^l \\ \tilde{I}_k^r \end{bmatrix} = \begin{bmatrix} Y_{S11} & Y_{S12} \\ Y_{S21} & Y_{S22} \end{bmatrix} \begin{bmatrix} \tilde{V}_k \\ \tilde{V}_{k+1} \end{bmatrix} \quad (6.38)$$

where

- $\tilde{I}_k^l$  = vector of electric currents on the left side of the span  $k$
- $\tilde{I}_k^r$  = vector of electric currents on the right side of the span  $k$
- $\tilde{V}_k$  = vector of conductor voltages on the left side of the span  $k$
- $\tilde{V}_{k+1}$  = vector of conductor voltages on the right side of the span  $k$

$$Y_{s11} = Y_{s22} = X^{-1} + X_{sh}^{-1}$$

$$Y_{s12} = Y_{s21} = -X^{-1}$$

The admittance matrix of the entire transmission line is computed by combining the admittance matrices of the individual spans and the tower footing admittance. The procedure is based on nodal analysis. Specifically, the nodal equations for two adjacent line spans are written and the voltages at the connection nodes of the two spans are eliminated. This procedure yields the admittance matrix of two spans. Then the procedure is repeated for the next span. The final result is the admittance matrix of the entire line. This procedure is demonstrated for a single-phase line in Section 6.7.1.

The procedure is computationally intense. However, the result is an exact representation of a transmission line. Specifically, line asymmetries and tower footing impedances are explicitly represented in the admittance matrix. In the next section we discuss how the sequence parameters of a set of mutually coupled lines can be computed from the admittance matrix.

### 6.9 COMPUTATION OF TRANSMISSION LINE SEQUENCE PARAMETERS FROM THE ADMITTANCE MATRIX

In this section we present procedures by which the transmission line parameters are computed directly from the admittance matrix. The procedure involves two steps. In the first step, the admittance matrix is simplified by eliminating the explicit representation of shield/neutral wires and neglecting line asymmetries. In the second step, the sequence parameters of the transmission line are computed by appropriate transformations. The two steps are discussed next.

Step 1. In this step the admittance matrix is simplified as follows. First, the voltage of the shield wires is assumed to be zero. This is equivalent to assuming that the shield wires are connected to the grounding system at the terminals of the lines and the impedance of the grounding system at the line terminals is negligibly small. In addition, the equations expressing the electric current through the shield wires are removed. The process results in a reduced-size admittance matrix equation for a system of  $n$  parallel mutually coupled transmission lines.

$$\tilde{I}_r = Y_r \tilde{V}_r \quad (6.39)$$

where

$$\tilde{I}_r = \begin{bmatrix} \tilde{I}_{aS1} \\ \tilde{I}_{bS1} \\ \tilde{I}_{cS1} \\ \tilde{I}_{aS2} \\ \tilde{I}_{bS2} \\ \vdots \\ \vdots \end{bmatrix} \quad \tilde{V}_r = \begin{bmatrix} \tilde{V}_{aS1} \\ \tilde{V}_{bS1} \\ \tilde{V}_{cS1} \\ \tilde{V}_{aS2} \\ \tilde{V}_{bS2} \\ \vdots \\ \vdots \end{bmatrix}$$

and  $\tilde{I}_{aS1}$ ,  $\tilde{V}_{aS1}$  is the phase a (sending end) current and voltage of line 1, and so on. Note that only phase currents and voltages exist in this equation. Also note that the voltage and current vectors are ordered in such a way that the three phases of any line are contingent. This form is convenient for the next step.

Step 2. In this step all the voltages and currents in Eq. (6.39) are substituted by their symmetrical components as follows:

$$\tilde{I}_{abcS1} = T^{-1} \tilde{I}_{120S1}$$

$$\tilde{I}_{abcR1} = T^{-1} \tilde{I}_{120R1}$$

$$\tilde{I}_{abcS2} = T^{-1} \tilde{I}_{120S2}$$

.

.

.

$$\tilde{V}_{abcS1} = T^{-1} \tilde{V}_{120S1}$$

$$\tilde{V}_{abcR1} = T^{-1} \tilde{V}_{120R1}$$

$$\tilde{V}_{abcS2} = T^{-1} \tilde{V}_{120S2}$$

.

.

.

where

$$\tilde{I}_{abcS1} = \begin{bmatrix} \tilde{I}_{aS1} \\ \tilde{I}_{bS1} \\ \tilde{I}_{cS1} \end{bmatrix} \quad \tilde{I}_{120S1} = \begin{bmatrix} \tilde{I}_{1S1} \\ \tilde{I}_{2S1} \\ \tilde{I}_{0S1} \end{bmatrix} \quad \text{etc.}$$

and  $T$  is the symmetrical component transformation defined in Section 6.4.1. Subscripts 1, 2, and 0 denote the positive, negative, and zero sequences, respectively.

Upon substitution into the admittance matrix equation (6.39) and subsequent manipulations,

$$\tilde{I}_{\text{seq}} = Y_{\text{seq}} \tilde{V}_{\text{seq}} \quad (6.40)$$

where

$$\tilde{I}_{\text{seq}} = \begin{bmatrix} \tilde{I}_{1S1} \\ \tilde{I}_{2S1} \\ \tilde{I}_{0S1} \\ \tilde{I}_{1S2} \\ \vdots \\ \vdots \\ \vdots \end{bmatrix}, \quad \tilde{V}_{\text{seq}} = \begin{bmatrix} \tilde{V}_{1S1} \\ \tilde{V}_{2S1} \\ \tilde{V}_{0S1} \\ \tilde{V}_{1S2} \\ \vdots \\ \vdots \\ \vdots \end{bmatrix}$$

and

$$Y_{\text{seq}} = \begin{bmatrix} T & 0 & \cdots \\ 0 & T & \cdots \\ \cdots & \cdots & \cdots \end{bmatrix} Y_r \begin{bmatrix} T^{-1} & 0 & \cdots \\ 0 & T^{-1} & \cdots \\ \cdots & \cdots & \cdots \end{bmatrix}$$

Next, the matrix  $Y_{\text{seq}}$  is partitioned into four square submatrices as follows:

$$Y_{\text{seq}} = \begin{bmatrix} Y_{11} & Y_{12} \\ Y_{21} & Y_{22} \end{bmatrix}$$

In general, the following relationships are valid:

$$Y_{22} = Y_{11}$$

and

$$Y_{12} = Y_{21}$$

Next, define

$$\begin{aligned} Y_{\text{seq,ser}} &= -Y_{12} \\ Z_{\text{seq,ser}} &= Y_{\text{seq,ser}}^{-1} \end{aligned} \quad (6.41a)$$

and

$$Y_{\text{seq,sh}} = Y_{11} + Y_{12} \quad (6.41b)$$

The matrix  $Z_{\text{seq,ser}}$  contains the series sequence parameters of the  $n$  parallel lines. The matrix  $Y_{\text{seq,sh}}$  provides the shunt sequence parameters of the line. These parameters are retrieved from matrices  $Z_{\text{seq,ser}}$  and  $Y_{\text{seq,sh}}$  as follows.

### Series Sequence Impedances

Positive sequence self-impedance of line  $i$ ,  $Z_1 = Z_{\text{seq,ser}}(i_1, i_2)$ , where

$$i_1 = 3(i - 1) + 1$$

$$i_2 = i_1$$

Negative sequence self-impedance of line  $i$ ,  $Z_2 = Z_{\text{seq,ser}}(i_1, i_2)$  where

$$i_1 = 3(i - 1) + 2$$

$$i_2 = i_1$$

Zero sequence self-impedance of line  $i$ ,  $Z_0 = Z_{\text{seq,ser}}(i_1, i_2)$  where

$$i_1 = 3(i - 1) + 3$$

$$i_2 = i_1$$

Zero sequence mutual impedance between lines  $i$  and  $j$ ,  $Z_{0m} = Z_{\text{seq,ser}}(i_1, i_2)$  where

$$i_1 = 3(i - 1) + 3$$

$$i_2 = 3(j - 1) + 3$$

### Shunt Sequence Admittances

Positive sequence self-shunt admittance of line  $i$ ,  $Y_1 = Y_{\text{seq,sh}}(i_1, i_2)$  where

$$i_1 = 3(i - 1) + 1$$

$$i_2 = i_1$$

Negative sequence self-shunt admittance of line  $i$ ,  $Y_2 = Y_{\text{seq,sh}}(i_1, i_2)$  where

$$i_1 = 3(i - 1) + 2$$

$$i_2 = i_1$$

Zero sequence self-shunt admittance of line  $i$ ,  $Y_0 = Y_{\text{seq},\text{sh}}(i_1, i_2)$   
where

$$i_1 = 3(i - 1) + 3$$

$$i_2 = i_1$$

Zero sequence mutual shunt admittance between lines  $i$  and  $j$ ,

$$Y_{0m} = Y_{\text{seq},\text{sh}}(i_1, i_2)$$

where

$$i_1 = 3(i - 1) + 3$$

$$i_2 = 3(j - 1) + 3$$

In summary, we have discussed procedures by which the line sequence parameters can be obtained from the admittance matrix of a set of mutually coupled lines.

### 6.10 COMPARISON OF TRANSMISSION LINE MODELS

As we discussed earlier, a three-phase transmission line can be represented with either the sequence models or the admittance matrix. The model equations are determined using the methods developed in Chapters 2, 3, and 4. The effects of the earth are accounted for by using Carson's theory (Chapter 3). Because this solution is complex, we discussed alternative but approximate methods in Chapter 3. It should be apparent that accurate modeling of an overhead transmission line requires that Carson theory be utilized to compute the resistance and inductance matrices of the line and that the line is represented with the admittance matrix. In practice, the sequence models are widely used. Typically, approximate methods are used for the computation of the sequence models. In order to determine the level of error of the approximate modeling procedures, we shall compare the various models of the line to the exact model. The comparison will extend to the first few harmonics of 60 Hz: specifically, from 60 to 2400 Hz. In this frequency range, three types of comparisons will be performed. First, the accuracy of the approximate equations for modeling self- and mutual resistance and inductance among line conductors will be examined. Second, the accuracy lost due to the sequence transformation will be examined. Third, the effects of shield or neutral conductors on the sequence parameters will be examined. Numerical results will be given for an example

230-kV three-phase transmission line. The design of the transmission tower is illustrated in Fig. 1.5. The line is 12.8 mi long, the phase conductors are ACSR, 795 kcm, 54 strands, and the overhead ground wires are Alumoweld 7, AWG No. 6. The tower ground resistance is  $25 \Omega$  and the length of one span is 0.1 mi.

Accuracy of Approximate Equations of Self- and Mutual Resistance and Inductance

Figure 6.8 illustrates the series impedance of the positive (or negative) sequence  $\pi$ -equivalent model as computed using the exact Carson's equations. The error of this quantity when computed with the equivalent depth of return method or the complex depth of return method is negligibly small (less than 0.3% in the frequency range specified). Figure 6.9 illustrates the series impedance of the zero sequence  $\pi$ -equivalent model using the exact equations. On

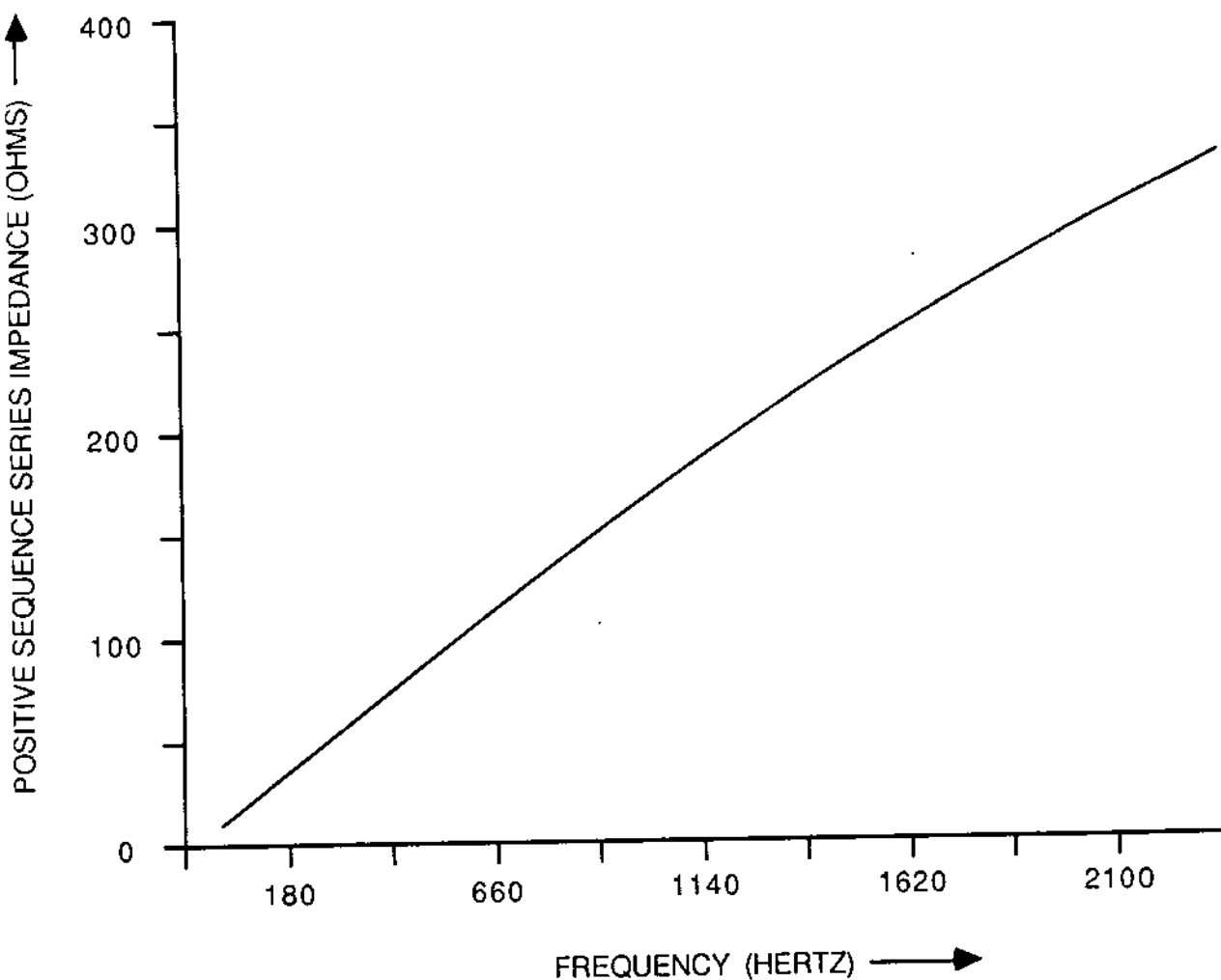


FIG. 6.8 Variation of the positive sequence series impedance with frequency.

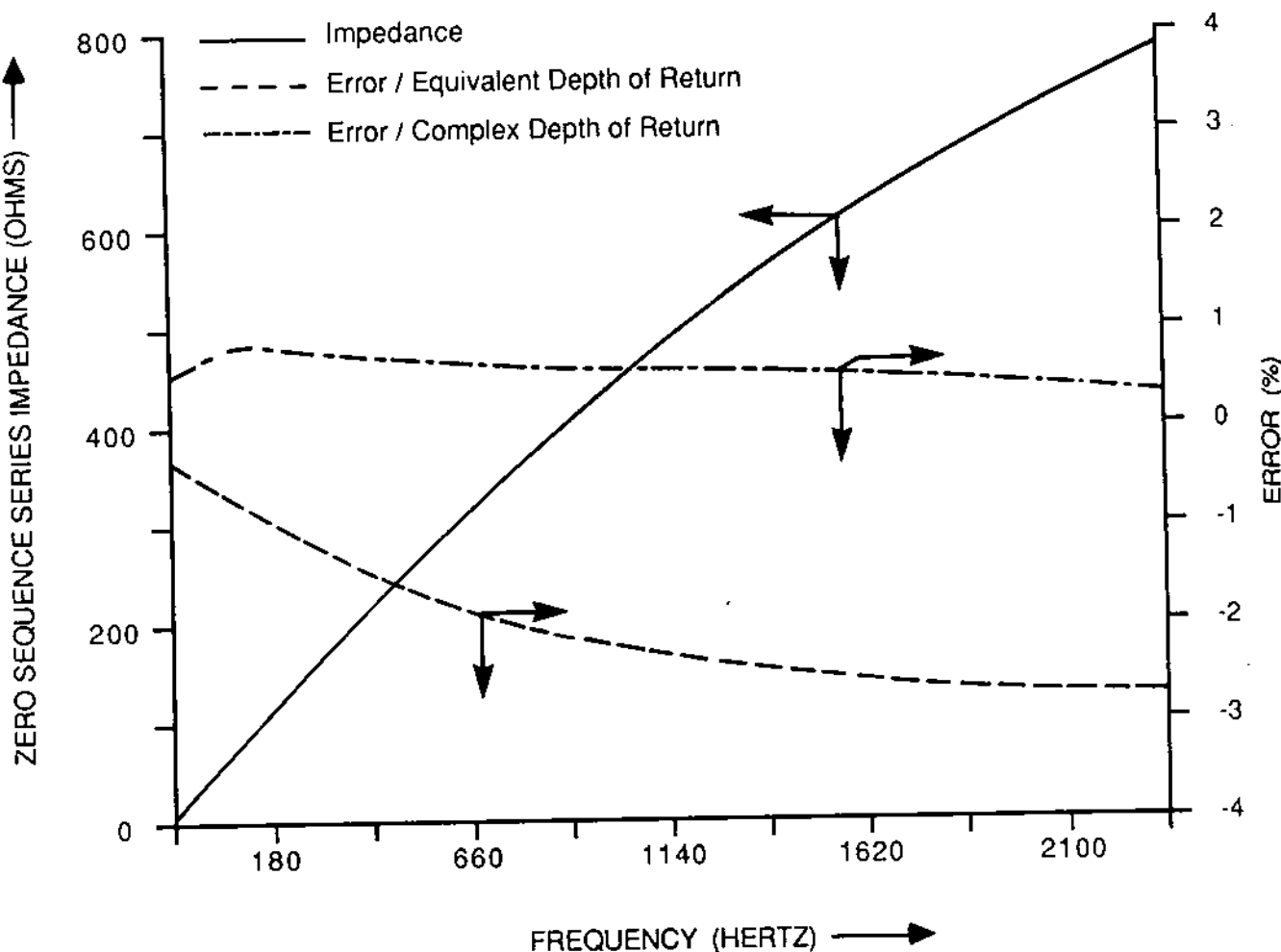


FIG. 6.9 Comparison of two approximate methods for the computation of the zero sequence series impedance.

In the same figure, the error of the impedance is illustrated for the two approximate methods. Note that the complex depth of return method yields an error of less than 1%, while the equivalent depth of return method yields an error less than 3.0% in the frequency range specified.

#### Accuracy of Sequence Transformation

The symmetrical component transformation requires that line asymmetries be neglected. To quantify the error committed, two line asymmetry factors,  $S_1$  and  $S_2$ , will be defined. For this purpose, consider the series impedance of the line. Let  $Z_{S\max}$  and  $Z_{S\min}$  be the maximum and minimum values of the mutual impedances between two phases. Similarly, consider the shunt admittance of the line. Let  $y'_{sh,\max}$  and  $y'_{sh,\min}$  be the maximum and minimum values of the mutual admittances between two phases. The asymmetry factors  $S_1$  and  $S_2$  are defined as follows:

$$S_1 = \frac{1}{2} \left| \frac{Z_{S\max} - Z_{S\min}}{Z_1} \right| \quad (6.42)$$

$$S_2 = \frac{1}{2} \left| \frac{y'_{sh,\max} - y'_{sh,\min}}{y'_1} \right| \quad (6.43)$$

where  $Z_1$  is the positive sequence series impedance and  $y'_1$  is the positive sequence shunt admittance. By definition, the asymmetry factors provide a measure of how much a balance set of voltages and currents is distorted by the line due to line asymmetries. Figure 6.10 provides a plot of the asymmetry factors  $S_1$  and  $S_2$  over the frequency range 60 to 2400 Hz for the example 230-kV line. Note that for this line the asymmetry factors are in the range 4 to 5%.

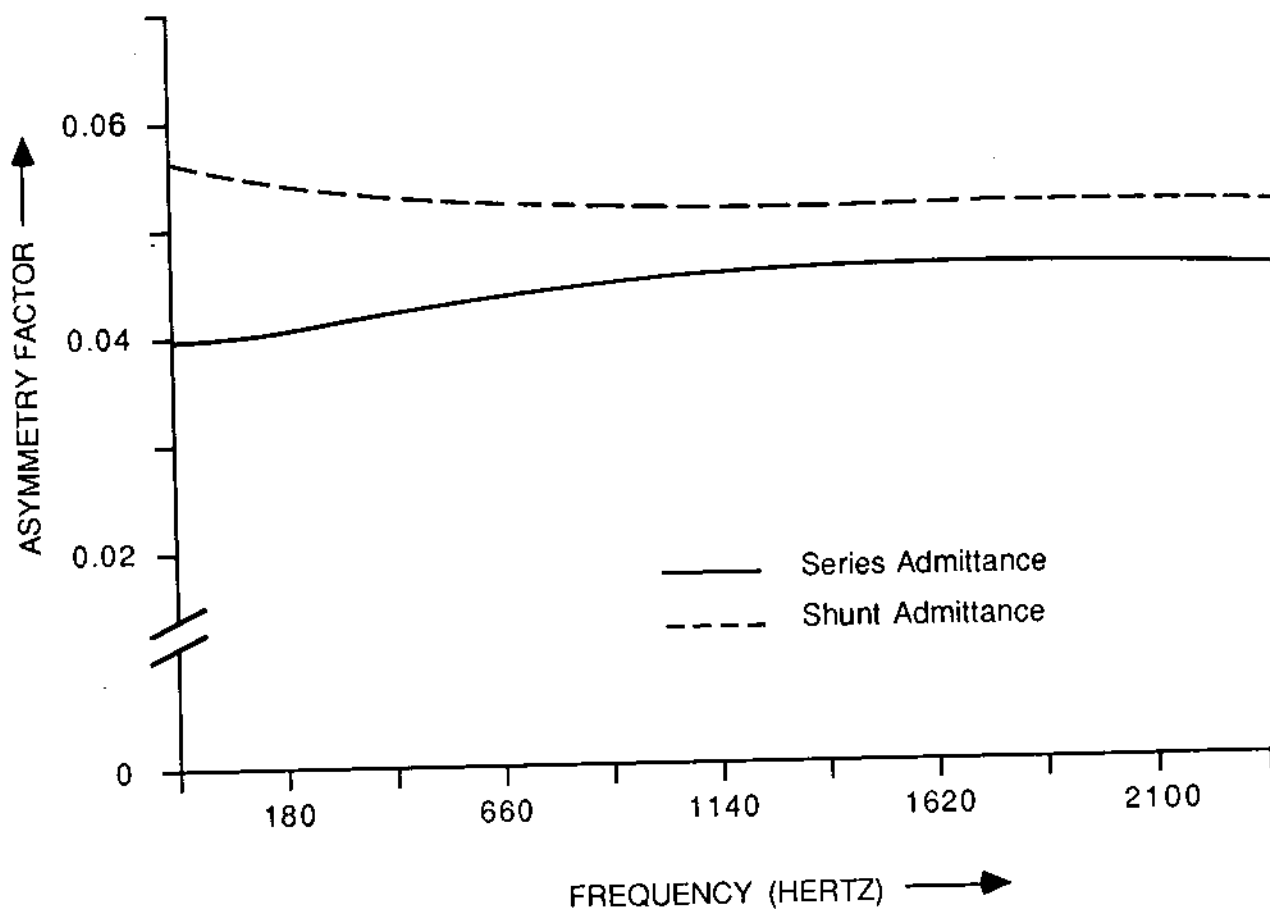


FIG. 6.10 Asymmetry factor versus frequency for the Example 230 kV three phase line.

### Effect of Shield/Neutral Wires

It has been mentioned that many times the shield or neutral wires of a line are neglected in the computation of the sequence parameters. This practice does not appreciably affect the positive sequence parameters, but may introduce a substantial error to the computation of the zero sequence parameters. To illustrate this point, the zero sequence series impedance of the example 230-kV three-phase line has been computed under three distinct conditions: (a) both overhead ground wires are present, (b) only one overhead ground wire is present, and (c) there is no overhead ground wire present. The results in the frequency range 60 to 2400 Hz are illustrated in Fig. 6.11. Note that the error is substantial for this line.

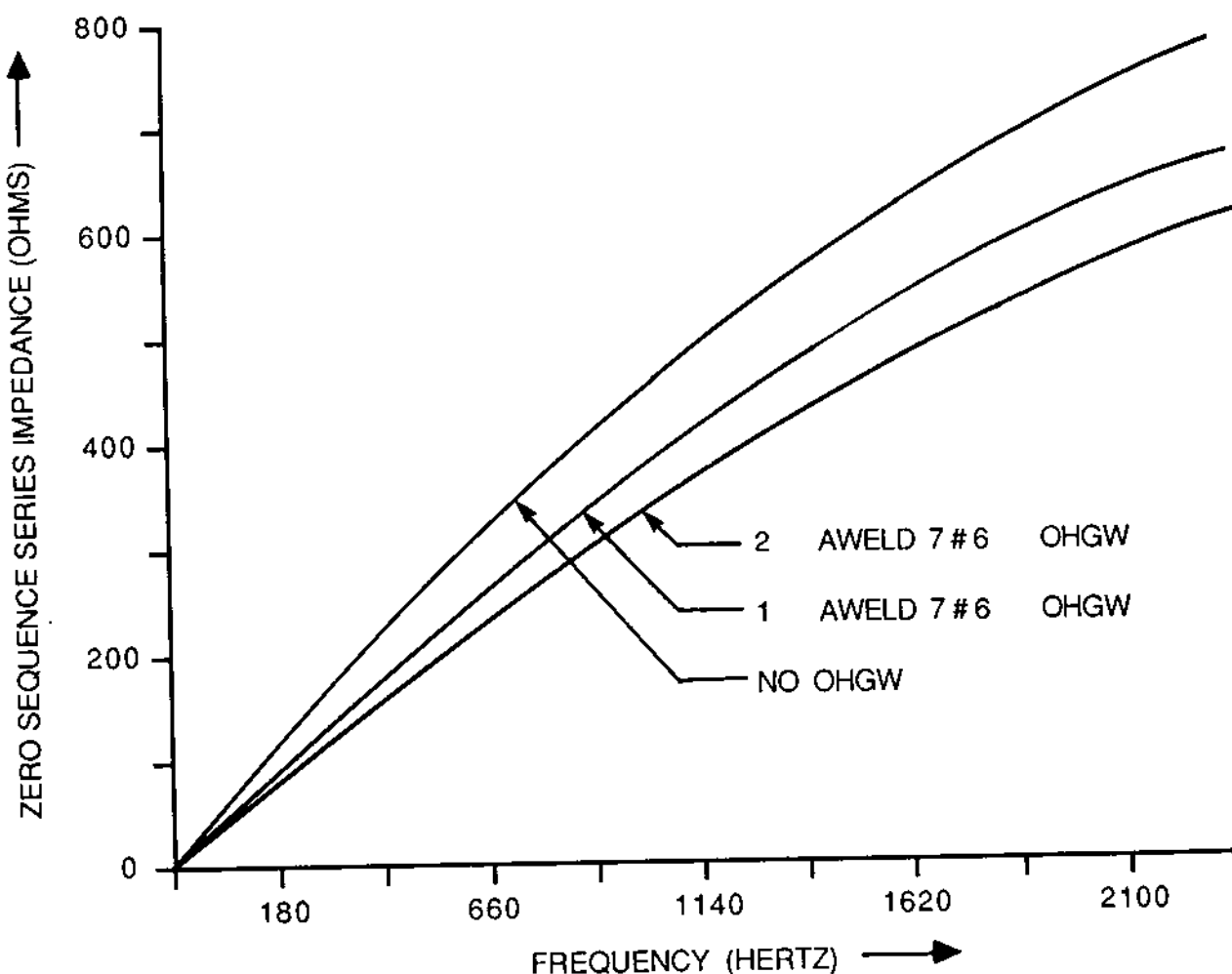


FIG. 6.11 Effects of overhead ground wires on the zero sequence series impedance of the example 230 kV line.

### 6.11 TRANSMISSION LINE POWER EQUATIONS

There are a number of applications, such as the power flow problem, stability analysis, and so on, in which the power transmitted through a transmission line is required in the formulation of the problem. In these applications it is assumed that the line operates under sinusoidal or nearly sinusoidal steady-state conditions. In this section we derive equations that describe the power flow through a transmission line. For this purpose the transmission line is typically represented with the sequence models. Depending on the application, the line may operate under balanced conditions (e.g., the power flow problem) or unbalanced conditions (e.g., stability analysis of unbalanced faults). In general, then, the power line may operate under unbalanced conditions. Let  $\tilde{V}_{s1}$ ,  $\tilde{V}_{s2}$ ,  $\tilde{V}_{s0}$  and  $\tilde{V}_{R1}$ ,  $\tilde{V}_{R2}$ ,  $\tilde{V}_{R0}$  be the sending and receiving bus positive, negative, and zero sequence voltages, respectively, and  $\tilde{I}_{s1}$ ,  $\tilde{I}_{s2}$ ,  $\tilde{I}_{s0}$ ,  $\tilde{I}_{R1}$ ,  $\tilde{I}_{R2}$ ,  $\tilde{I}_{R0}$  be the sending and receiving bus positive, negative, and zero sequence electric currents, respectively. The power injected at the sending end is  $S_s$ :

$$S_s = \tilde{V}_{abc}^T \tilde{I}_{abc}^* = [\tilde{V}_{s1} \quad \tilde{V}_{s2} \quad \tilde{V}_{s0}]^T T^{-1} \begin{bmatrix} \tilde{I}_{s1}^* \\ \tilde{I}_{s2}^* \\ \tilde{I}_{s0}^* \end{bmatrix} \\ = 3\tilde{V}_{s1}\tilde{I}_{s1}^* + 3\tilde{V}_{s2}\tilde{I}_{s2}^* + 3\tilde{V}_{s0}\tilde{I}_{s0}^* \quad (6.44a)$$

Similarly, the power delivered at the receiving end is  $S_R$ :

$$S_R = 3\tilde{V}_{R1}\tilde{I}_{R1}^* + 3\tilde{V}_{R2}\tilde{I}_{R2}^* + 3\tilde{V}_{R0}\tilde{I}_{R0}^* \quad (6.44b)$$

Equations (6.44) state that the power transmitted through a transmission line is computed from the symmetrical components of the voltages and currents. In addition, the contribution to the power flow from a specific symmetrical component is independent from the other two. As an example, for the power flow problem it is assumed that the line operation is balanced (i.e., only the positive sequence component is present). In this case the power flow equations become  $S_s = 3\tilde{V}_{s1}\tilde{I}_{s1}^*$  and  $S_R = 3\tilde{V}_{R1}\tilde{I}_{R1}^*$ .

It is expedient to express the power equations in terms of the line terminal voltages only. For this purpose the line terminal currents (each symmetrical component separately) are expressed in terms of the line terminal voltages (symmetrical components) and the line parameters. Subsequently, they are substituted into Eqs. (6.44) to yield the power equations in terms of the line terminal voltages only. It should be apparent that this procedure may be implemented

by selecting any of the three alternative sequence models of a three-phase line: (a) A, B, C constants, (b)  $\pi$ -equivalent circuits, or (c) T-equivalent circuits. In subsequent paragraphs we derive three alternative forms of the power equations based on the three alternative sequence models. For simplicity, we shall consider only one sequence model. Let the sending and receiving bus voltage of this model be  $\tilde{V}_S$  and  $\tilde{V}_R$  and the electric currents be  $\tilde{I}_S$  and  $\tilde{I}_R$ . The contribution of this sequence model to the power flow is

$$S_S = 3\tilde{V}_S \tilde{I}_S^* \quad (6.45a)$$

$$S_R = 3\tilde{V}_R \tilde{I}_R^* \quad (6.45b)$$

### 6.11.1 Power Equations in Terms of the A, B, C Constants

The power equations in terms of the A, B, C constants are derived as follows. Recall the line equations (6.14) in terms of the A, B, C constants. Upon solution of Eqs. (6.14) for the electric currents  $\tilde{I}_S$ ,  $\tilde{I}_R$  in terms of the voltages  $\tilde{V}_S$ ,  $\tilde{V}_R$ , we have

$$\tilde{I}_S = \frac{A}{B} \tilde{V}_S - \frac{1}{B} \tilde{V}_R$$

$$\tilde{I}_R = \frac{1}{B} \tilde{V}_S - \frac{A}{B} \tilde{V}_R$$

Note that the first equation is derived by taking into consideration the identity  $A^2 - CB = 1$ . Upon substitution of these equations into the power equations (6.45):

$$S_S = \frac{3A^*}{B^*} V_S^2 - \frac{3\tilde{V}_S \tilde{V}_R^*}{B^*} \quad (6.46a)$$

$$S_R = \frac{3A^*}{B^*} V_R^2 - \frac{3\tilde{V}_R \tilde{V}_S^*}{B^*} \quad (6.46b)$$

It is expedient to express the constants A, B and the voltages  $\tilde{V}_S$  and  $\tilde{V}_R$  in polar coordinates and the powers  $S_S$  and  $S_R$  in cartesian coordinates (real and reactive power) as follows:

$$A = ae^{j\alpha}$$

$$B = be^{j\beta}$$

$$\tilde{V}_S = V_S e^{j\delta_S}$$

$$\tilde{V}_R = V_R e^{j\delta_R}$$

$$S_S = P_S + jQ_S$$

$$S_R = P_R + jQ_R$$

Substitution of the expressions above gives us

$$S_S = P_S + jQ_S = \frac{3a}{b} V_S^2 e^{j(\beta-\alpha)} - \frac{3V_S V_R}{b} e^{j(\delta_S - \delta_R + \beta)}$$

$$S_R = P_R + jQ_R = \frac{3a}{b} V_R^2 e^{j(\beta-\alpha)} + \frac{3V_S V_R}{b} e^{j(\delta_R - \delta_S + \beta)}$$

Separation of the real and imaginary parts results in

$$P_S = \frac{3a}{b} V_S^2 \cos(\beta - \alpha) - \frac{3V_S V_R}{b} \cos(\delta_S - \delta_R + \beta) \quad (6.47a)$$

$$Q_S = \frac{3a}{b} V_S^2 \sin(\beta - \alpha) - \frac{3V_S V_R}{b} \sin(\delta_S - \delta_R + \beta) \quad (6.47b)$$

$$P_R = -\frac{3a}{b} V_R^2 \cos(\beta - \alpha) + \frac{3V_S V_R}{b} \cos(\delta_R - \delta_S + \beta) \quad (6.47c)$$

$$Q_R = -\frac{3a}{b} V_R^2 \sin(\beta - \alpha) + \frac{3V_S V_R}{b} \cos(\delta_R - \delta_S + \beta) \quad (6.47d)$$

Equations (6.47) are the power flow equations of the line in terms of the constants A, B, and C.

### 6.11.2 Power Equations in Terms of the $\pi$ Equivalent Circuit Parameters

The power equations in terms of the parameters of the  $\pi$  equivalent circuit,  $Z_\pi$  and  $Z'_\pi$ , are obtained as follows: First, the line terminal currents  $\tilde{I}_S$  and  $\tilde{I}_R$  are expressed in terms of the parameters  $Z_\pi$ ,  $Z'_\pi$  and the line terminal voltages.

$$\tilde{I}_S = \frac{\tilde{V}_S}{Z'_\pi} + \frac{1}{Z_\pi} (\tilde{V}_S - \tilde{V}_R)$$

$$\tilde{I}_R = \frac{1}{Z_\pi} (\tilde{V}_S - \tilde{V}_R) - \frac{\tilde{V}_R}{Z'_\pi}$$

Upon substitution in Eqs. (6.45) of the expressions above, the power equations of the transmission line are obtained in terms of the parameters  $Z_\pi$ ,  $Z'_\pi$ . A rather popular form of the power equations is based on representing the parameters  $Z_\pi$ ,  $Z'_\pi$  with their cartesian coordinates and the voltages  $\tilde{V}_S$  and  $\tilde{V}_R$  with their polar coordinates:

$$\frac{1}{Z'_\pi} = g - jb \quad g, b \geq 0$$

$$\frac{1}{Z_\pi} = g' + jb' \quad g', b' \geq 0$$

$$\tilde{V}_S = V_S e^{j\delta_S}$$

$$\tilde{V}_R = V_R e^{j\delta_R}$$

Upon substitution and separation of the real and imaginary parts of the two equations, the following power flow equations are obtained:

$$P_S = 3(g + g')V_S^2 - 3gV_S V_R \cos(\delta_S - \delta_R) + 3bV_S V_R \sin(\delta_S - \delta_R) \quad (6.48a)$$

$$Q_S = 3(b - b')V_S^2 - 3gV_S V_R \sin(\delta_S - \delta_R) - 3bV_S V_R \cos(\delta_S - \delta_R) \quad (6.48b)$$

$$P_R = -3(g + g')V_R^2 + 3gV_S V_R \cos(\delta_S - \delta_R) + 3bV_S V_R \sin(\delta_S - \delta_R) \quad (6.48c)$$

$$Q_R = -3(b - b')V_R^2 - 3gV_S V_R \sin(\delta_S - \delta_R) + 3bV_S V_R \cos(\delta_S - \delta_R) \quad (6.48d)$$

The transmission line power equations (6.48) are the most popular form for load flow applications.

### 6.11.3 Power Equations in Terms of the T-Equivalent-Circuit Parameters

The power flow equations in terms of the parameters of the T-equivalent circuit,  $Z_T$  and  $Z'_T$ , are derived in the same way as are the other power equations. Specifically, first the line equations in terms of the parameters of the T-equivalent circuit are solved for the currents  $\tilde{I}_S$  and  $\tilde{I}_R$ . Next the currents are substituted in the power flow equations. The final result is

$$S_S = 3 \frac{Z_T^* + Z'_T^*}{(2Z'_T^* + Z_T^*)Z_T^*} V_S^2 - 3 \frac{Z'_T^*}{2Z_T^*Z'_T^* - Z_T^{*2}} V_S V_R^*$$

$$S_R = 3 \frac{Z_T^* + Z'_T^*}{(2Z'_T^* + Z_T^*)Z_T^*} V_S^2 + 3 \frac{Z'_T^*}{(2Z'_T^* + Z_T^*)Z_T^*} V_S^* V_R$$

The equations above result in rather complicated expressions for real and reactive power. For this reason, these equations are not very popular models.

## 6.12 SUMMARY AND DISCUSSION

In this chapter we examined models of transmission lines. Specifically, the general model of single-phase as well as multiple-phase transmission lines was developed in terms of a set of differential equations. The single-phase transmission-line model, under sinusoidal steady-state conditions, can be represented as a two-port network with three constants A, B, C, or with an equivalent circuit. The  $\pi$ - and T-equivalent circuits of the line were developed. For short transmission lines, the approximate nominal  $\pi$ - and T-equivalent circuits may be used.

Three- or multiple-phase transmission lines are more complex since they are modeled by a set of coupled differential equations. Modal decomposition reduces a multiple-phase line into a number of single-phase lines. A special case of modal decomposition is the symmetrical components transformation, which applies to a symmetric three-phase transmission line. With the use of this transformation, a three-phase transmission line is represented with three sequence models: the positive, negative, and zero sequence models. Each sequence model can be represented with a two-port network with constants A, B, and C or with the  $\pi$ - or T-equivalent circuits.

The representation of a three-phase line with the sequence models is an approximation. Specifically, it neglects line asymmetries, and the explicit representation of the shield/neutral wires and grounding structures is lost. Representing a transmission line with the admittance matrix eliminates the need for these approximations. The admittance matrix representation of a line is suitable for computer-based computations. An accuracy analysis has been presented which provides quantitative results for a typical transmission line. The selection of the transmission line model depends on the application and the desired accuracy.

Finally, equations for the power flow through a line have been developed under sinusoidal conditions. The power equations are useful for several applications, such as power flow studies and stability analysis.

### 6.13 PROBLEMS

Problem 6.1: A 100-mi-long three-phase line has the following positive sequence parameters:

$$Z = 0.05 + j0.81 \Omega/\text{mi}$$

$$Z' = j29,500 \Omega \cdot \text{mi}$$

Calculate the following positive sequence parameters.

- (a) The characteristic impedance and propagation constant.
- (b) The A, B, C, parameters of the line.
- (c) The  $\pi$ -equivalent circuit impedances  $Z_\pi$  and  $Z'_\pi$ .
- (d) The T-equivalent circuit impedances  $Z_T$  and  $Z'_T$ .
- (e) The nominal  $\pi$ -equivalent circuit impedances.

Problem 6.2: A three-phase transmission line has the following positive sequence parameters:

Series impedance:  $Z = 0.12 + j.87 \Omega/\text{mi}$

Shunt impedance:  $Z' = -j0.1 \text{ M}\Omega \cdot \text{mi}$

Length:  $\ell = 130 \text{ mi}$

- (a) Compute the nominal  $\pi$ -equivalent model (positive sequence) of the line.
- (b) Compute the  $\pi$ -equivalent model (positive sequence) of the line.
- (c) Compare the two models in parts (a) and (b).

Problem 6.3: Consider a three-phase transmission line suspended on a tower similar to the one illustrated in Fig. 1.5. The line is 96.0 mi long and consists of 795-kcm 54-strand ACSR phase wires and 203.2-kcm ACSR overhead ground wires. Calculate the following zero sequence quantities.

- (a) Characteristic impedance and propagation constant.
- (b) A, B, C parameters.
- (c)  $\pi$ -equivalent circuit.
- (d) T-equivalent circuit.
- (e)  $\pi$ -equivalent nominal circuit.
- (f) T-equivalent nominal circuit.

Problem 6.4: Compute the zero sequence series impedance of a 12-kV overhead transmission line. The transmission pole design is illustrated in Fig. 1.7. The phase conductors are ACSR, 397.5 kcm, 26 strands. Assume the following two cases:

- (a) The line does not have a neutral conductor.
- (b) The line has a multiply grounded neutral conductor. Assume that the impedance of the grounds is negligibly small. The neutral conductor is ACSR, 4.0.

**Problem 6.5:** Consider the single-phase overhead distribution line of Fig. P6.1. The neutral conductor is effectively grounded; that is, the neutral conductor is connected at every pole to the grounding system of the pole which has a very small impedance. The phase conductor carries an electric load of 100 A. The current returns partly through the neutral conductor and partly through the earth. Compute the electric current through the neutral conductor,  $I_n$ , and the electric current through the earth,  $I_e$ . For this purpose, neglect the resistance and the capacitance of the line. Use the equivalent depth of return method. The soil resistivity is 150  $\Omega \cdot \text{m}$ .

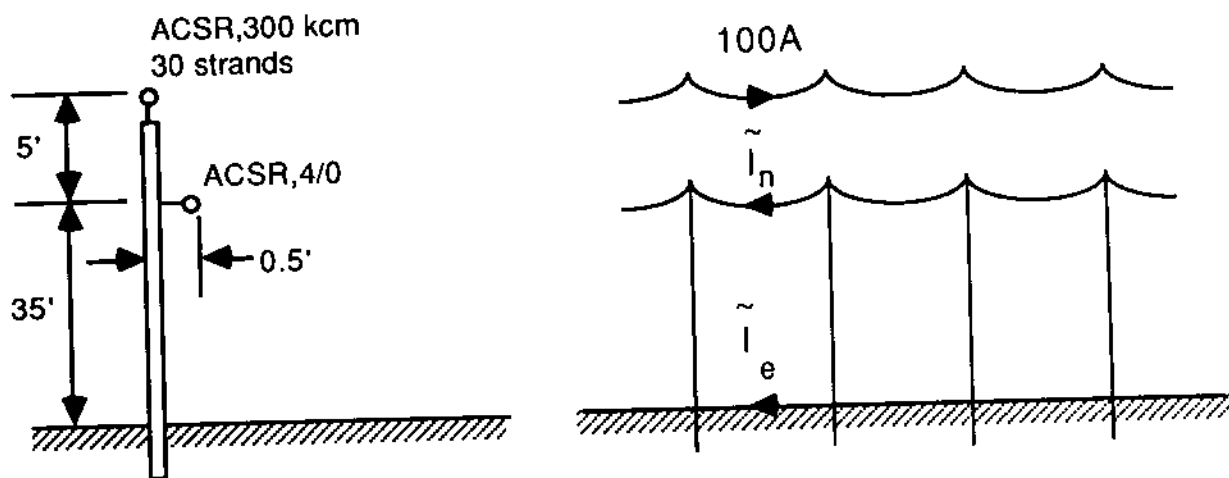
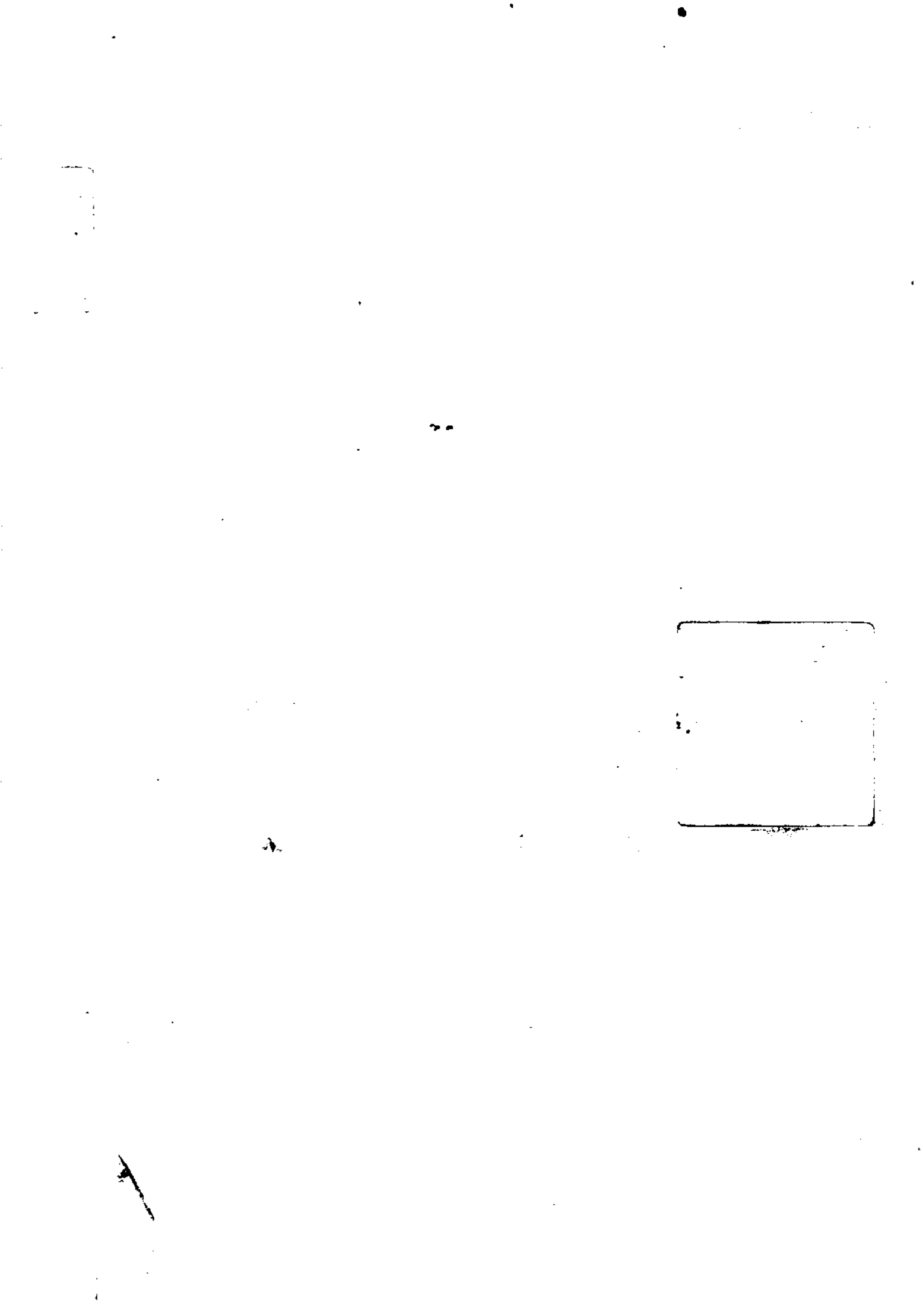


FIG. P6.1



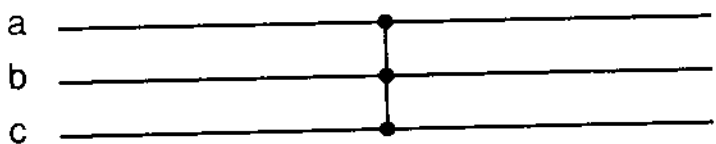
# 7

## Power System Fault Analysis

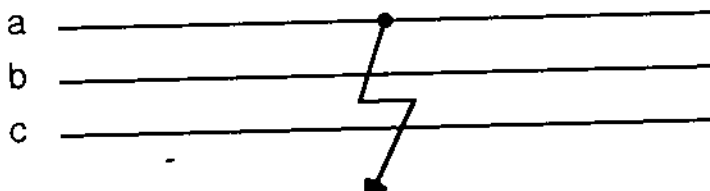
### 7.1 INTRODUCTION

The normal operating conditions of an electric power system are occasionally disrupted because of faults. A fault occurs because of insulation failure or when a conducting medium shorts one or more phases of the system. In general, the causes of faults are many: lightning, tree limbs falling on lines, wind damage, insulation deterioration, vandalism, and so on. In a three-phase system, a fault can involve two or more conductors. Depending on the number of conductors involved in a fault, they are classified into the following types: single line to ground, line to line, double line to ground, and/or three-phase faults. The fault types mentioned are illustrated in Fig. 7.1. Faults on electric power systems cause a number of undesirable effects: (a) flow of excessive electric current, which, in general, can damage equipment; (b) abnormal voltages (over-voltage or undervoltage) at other system points; (c) voltage elevation of system neutral (in case of asymmetrical faults), which present a hazard to human beings and animals; and (d) transferred or induced voltages on neighboring metallic structures and/or communication circuits which may be of significant strength.

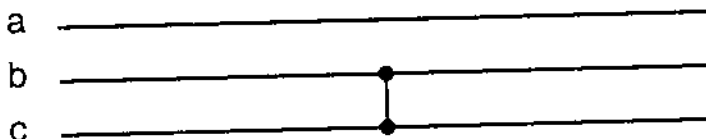
It is important to isolate the faulted power system element as soon as possible after fault initiation. For this purpose, power systems are equipped with a protective system comprising relays, breakers, fuses, and so on. The design of the protective system requires knowledge of the fault current levels. Thus it is necessary to determine the values of system voltages and currents during faulted conditions. This information is utilized in the selection of circuit breaker sizes, fuse size and characteristics, setting of relays, and



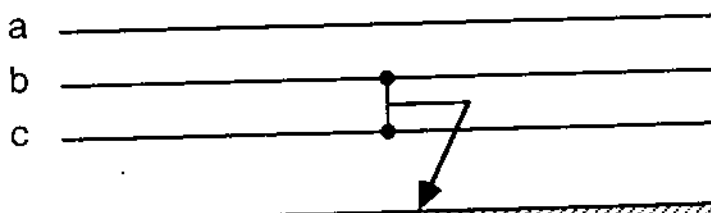
(a)



(b)



(c)



(d)

FIG. 7.1 Four types of power system faults. (a) Three phase fault, (b) single line to ground fault, (c) line to line fault, (d) double line to ground fault.

so on. Proper selection of protective devices enables the effective detection and isolation of faulted power system elements. Electric power faults are typically cleared within 2 to 60 cycles of power frequency (0.03 to 1 s). For certain types of faults, a substantial voltage rise may develop at the system neutral which affects the safety

of human beings and animals near the power system. To mitigate the hazardous effects of power system faults, power systems must be properly grounded. Analysis of power faults and neutral voltage elevation is necessary for the proper design of grounding systems, ensuring safety of personnel.

In this chapter we discuss the problem of power system fault analysis. Two distinct approaches will be presented. First, fault analysis of three-phase systems is approached in the conventional way through the use of symmetrical components. The basic assumptions and limitations of the method of symmetrical components are explicitly stated. The method of symmetrical components is extended to analyze current distribution among sky wires, neutrals, and earth. This extension of the method provides the basis for the computation of ground potential rise. Second, a general approach to the problem of fault analysis is presented. This method is applicable to symmetrical three-phase systems as well as asymmetrical three-phase systems and non-three-phase systems. The method provides the current distribution among overhead circuits and earth as well as the ground potential rise of the system neutrals.

## 7.2 REVIEW OF THE THEORY OF SYMMETRICAL COMPONENTS

The method of symmetrical components was introduced in Chapter 6 as a modal decomposition. It was applied to the transmission line equation. The transformation can be applied to any element of a three-phase system. Assuming that each element of the power system is symmetric, the transformation will result into three balanced sets or systems which are known as positive, negative, and zero sequence systems. In this way, the analysis of three-phase symmetric systems is decomposed into the analysis of three three-phase systems, each operating under balanced conditions. It is expedient to emphasize the underlying assumption for this decomposition.

**Sinusoidal steady state.**

All three-phase power system elements are symmetric.

All power system elements are linear.

Practical power systems meet the foregoing conditions only approximately. For example, a synchronous generator is behaving as a non-linear element during the transients of a fault. For most practical applications, however, it is approximated as a linear device. On the other hand, transposed transmission lines and most transformers are symmetric elements. Untransposed transmission lines and certain transformers are not symmetric three-phase elements. For these elements, the symmetrical component method represents an approximation. The

acceptability of the approximation depends on the application and the degree of asymmetry of the elements involved.

Traditionally, the approximation of electric power elements as symmetric elements has been accepted for most applications (i.e., fault analysis, load flow, and transient stability). In specific applications, additional simplifications may be involved. Specifically for fault analysis, the following additional simplifications are utilized:

Shunt elements in transformer models are neglected.

Shunt capacitance in transmission line models are neglected.

Electric load currents are neglected.

The first modeling simplification, in general, does not introduce a substantial error. The other two may introduce a substantial error, depending on the specific system conditions.

As we discussed in Chapter 6, the symmetrical component transformation is expressed with the following formula:

$$\begin{bmatrix} \tilde{V}_a \\ \tilde{V}_b \\ \tilde{V}_c \end{bmatrix} = T^{-1} \begin{bmatrix} \tilde{V}_1 \\ \tilde{V}_2 \\ \tilde{V}_0 \end{bmatrix} \quad (7.1)$$

where

$$\begin{aligned} \tilde{V}_{a,b,c} &= \text{three-phase voltage phasors} \\ \tilde{V}_{1,2,0} &= \text{symmetrical components} \end{aligned}$$

and

$$T = \frac{1}{3} \begin{bmatrix} 1 & a & a^2 \\ 1 & a^2 & a \\ 1 & 1 & 1 \end{bmatrix} \quad a = e^{j120^\circ} \quad (7.2)$$

A physical interpretation of the symmetrical component transformation of the power line equations was given in Chapter 6. In terms of phasor analysis, the transformation can be viewed as follows: An unbalanced three-phase system of phasors is transformed into three balanced systems of phasors known as the positive, negative, and zero phase sequence components. The positive sequence set consists of three phasors equal in magnitude,  $120^\circ$  out of phase, and rotating counterclockwise so that they reach their positive maximum values in the same sequence as that of the generators of the power system. Thus if the phase sequence or phase rotation of the power system is  $a, b, c$ , the positive sequence components will also have a phase rotation of  $a, b, c$ . The negative sequence set consists of three phasors equal in magnitude, displaced  $120^\circ$  apart, and rotating counter-

clockwise (i.e., in a sequence opposite to the positive). Thus if the positive sequence is a, b, c, the negative sequence is a, c, b. The zero sequence set contains three phasors equal in magnitude and in phase. Figure 7.2 illustrates the transformation for a set of three-phase voltages. Since the symmetrical components form three

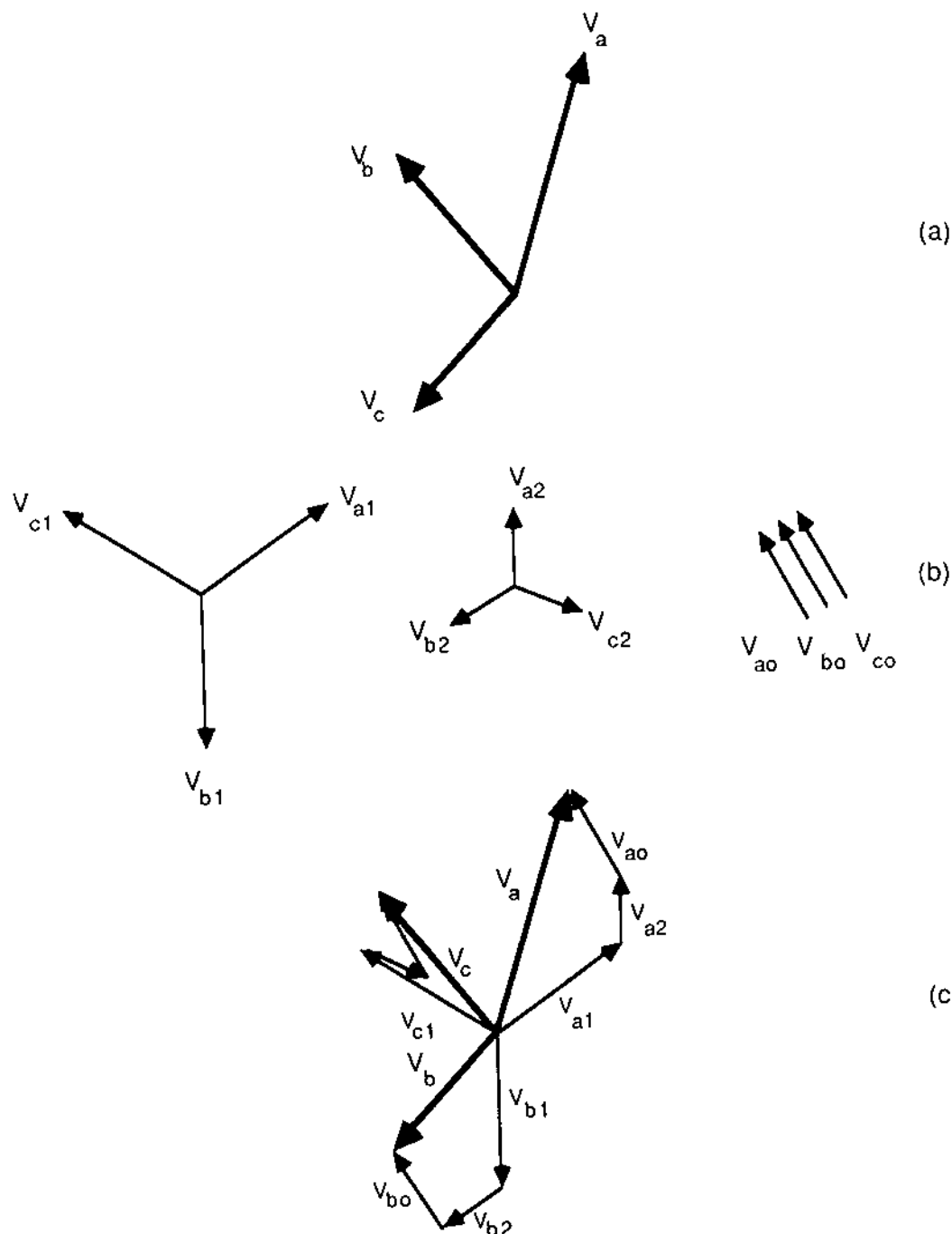


FIG. 7.2 Analysis of a set of three phase voltages into symmetrical components. (a) Phase voltages, (b) symmetrical components: positive, negative, and zero, (c) construction of phase voltages from the symmetrical components.

sets of balanced three-phase voltages, they can be uniquely defined with the phase a phasors only. Assume that the phase a phasors of the symmetrical components are denoted by  $\tilde{V}_{a1}$ ,  $\tilde{V}_{a2}$ , and  $\tilde{V}_{a0}$  for the positive, negative, and zero sequences, respectively. Then:

Positive sequence

$$\tilde{V}_{a1} = \tilde{V}_{a1} \quad (7.3a)$$

$$\tilde{V}_{b1} = a^2 \tilde{V}_{a1} \quad (7.3b)$$

$$\tilde{V}_{c1} = a \tilde{V}_{a1} \quad (7.3c)$$

Negative sequence

$$\tilde{V}_{a2} = \tilde{V}_{a2} \quad (7.4a)$$

$$\tilde{V}_{b2} = a \tilde{V}_{a2} \quad (7.4b)$$

$$\tilde{V}_{c2} = a^2 \tilde{V}_{a2} \quad (7.4c)$$

Zero sequence

$$\tilde{V}_{a0} = \tilde{V}_{a0} \quad (7.5a)$$

$$\tilde{V}_{b0} = \tilde{V}_{a0} \quad (7.5b)$$

$$\tilde{V}_{c0} = \tilde{V}_{a0} \quad (7.5c)$$

The actual phase quantities are reconstructed from the sequence components as follows (see Fig. 7.2):

$$\tilde{V}_a = \tilde{V}_{a1} + \tilde{V}_{a2} + \tilde{V}_{a0}$$

$$\tilde{V}_b = \tilde{V}_{b1} + \tilde{V}_{b2} + \tilde{V}_{b0}$$

$$\tilde{V}_c = \tilde{V}_{c1} + \tilde{V}_{c2} + \tilde{V}_{c0}$$

Upon substitution of the phasors  $\tilde{V}_{b1}$ ,  $\tilde{V}_{b2}$ ,  $\tilde{V}_{b0}$ ,  $\tilde{V}_{c1}$ ,  $\tilde{V}_{c2}$ , and  $\tilde{V}_{c0}$  in terms of the phase a phasors and casting the result in compact matrix notation, we have

$$\begin{bmatrix} \tilde{V}_a \\ \tilde{V}_b \\ \tilde{V}_c \end{bmatrix} = T^{-1} \begin{bmatrix} \tilde{V}_{a1} \\ \tilde{V}_{a2} \\ \tilde{V}_{a0} \end{bmatrix} \quad (7.6)$$

Upon premultiplication of Eq. (7.6) by T yields

$$\begin{bmatrix} \tilde{V}_{a1} \\ \tilde{V}_{a2} \\ \tilde{V}_{a0} \end{bmatrix} = T \begin{bmatrix} \tilde{V}_a \\ \tilde{V}_b \\ \tilde{V}_c \end{bmatrix} \quad (7.7)$$

Equation (7.7) provides the transformation of any set of three-phase phasors  $\tilde{V}_a$ ,  $\tilde{V}_b$ ,  $\tilde{V}_c$  into the symmetrical components  $\tilde{V}_{a1}$ ,  $\tilde{V}_{a2}$ , and  $\tilde{V}_{a0}$ . Note that only phase a of the symmetrical components is provided. The other phases, b and c, always exist and are determined from Eqs. (7.3), (7.4), and (7.5). For this reason the sequence components are always indicated with the phase a quantity only. For simplicity, the index of phase a is omitted and the symmetrical components are denoted by  $\tilde{V}_1$ ,  $\tilde{V}_2$ ,  $\tilde{V}_0$ ,  $\tilde{I}_1$ ,  $\tilde{I}_2$ , and  $\tilde{I}_0$ .

The importance of the sequence components stems from the fact that for a symmetric power system (or that part of a power system that is symmetric) there is no interaction between any two of the sequence components. In other words:

1. Positive sequence currents produce only positive sequence voltages, and vice versa.
2. Negative sequence currents produce only negative sequence voltages, and vice versa.
3. Zero sequence currents produce only zero sequence voltages, and vice versa.

When the voltages and currents of a symmetric three-phase system are transformed into symmetrical components, the system model is also transformed. In Chapter 6 we discussed how the line model is transformed into the sequence models. In this chapter we discuss how a general three-phase power system model is transformed. For this purpose, consider the system of Fig. 7.3a. Since the system is linear, the electric currents flowing into the system will be a linear combination of the terminal voltages. In compact matrix notation,

$$\tilde{I}_{abc} = Y_{abc} \tilde{V}_{abc} - \tilde{I}_{s,abc} \quad (7.8)$$

where

$$\tilde{I}_{abc} = \begin{bmatrix} \tilde{I}_a \\ \tilde{I}_b \\ \tilde{I}_c \end{bmatrix}$$

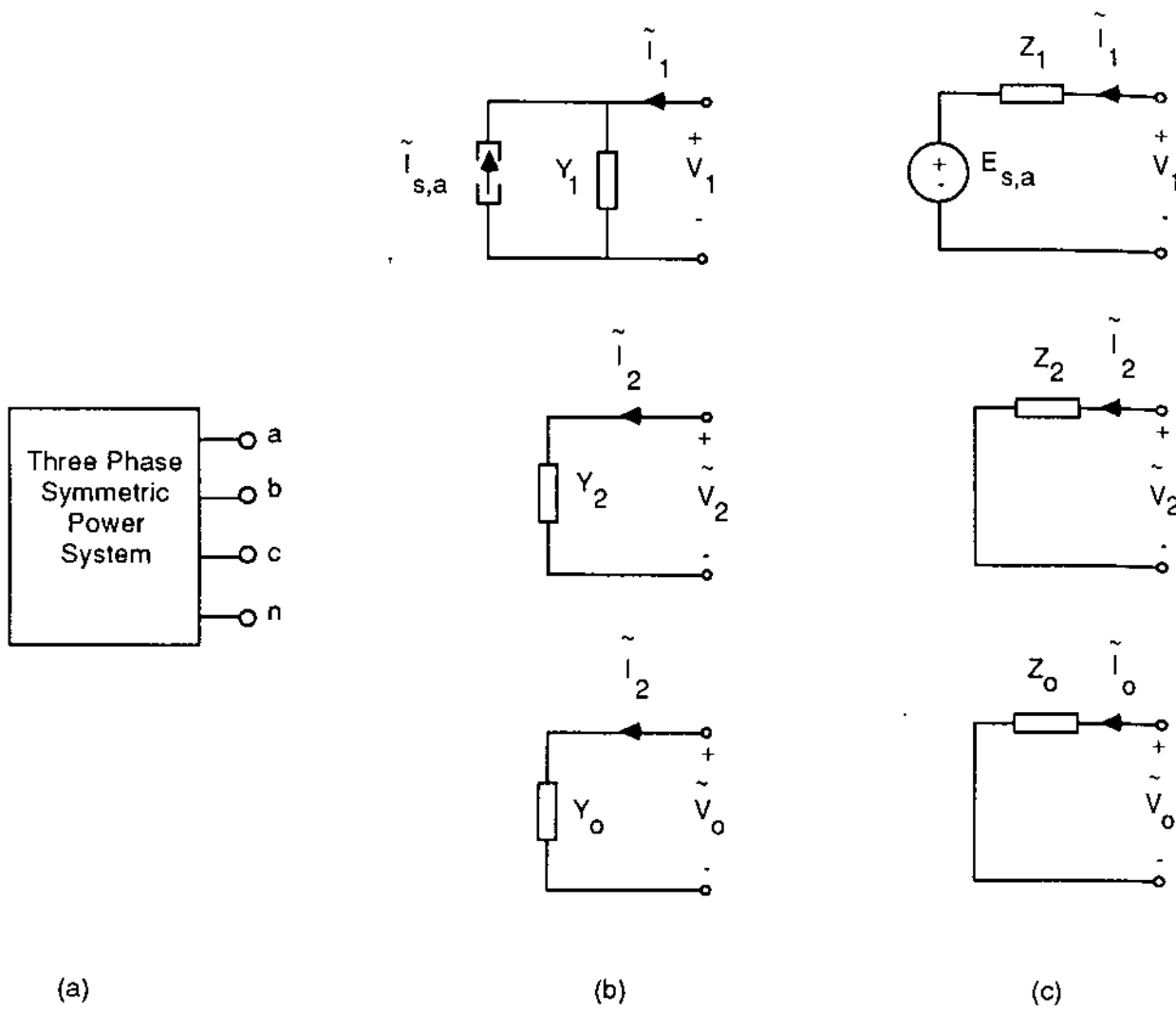


**FIG. 7.3** Decomposition of a symmetric three phase system into three sequence networks. (a) Three phase symmetric power system, (b) Norton equivalent sequence networks, (c) Thevenin equivalent sequence networks.

$$\tilde{V}_{abc} = \begin{bmatrix} \tilde{V}_a \\ \tilde{V}_b \\ \tilde{V}_c \end{bmatrix}$$

$\mathbf{Y}_{abc}$  is the admittance matrix of the system and  $\mathbf{i}_{s,abc}$  are the equivalent source currents in case the system comprises a three-phase generator. We shall assume that the equivalent source currents are of positive sequence and balanced, that is,

$$\tilde{I}_{s,abc} = \begin{bmatrix} \tilde{I}_{s,a} \\ a^2 \tilde{I}_{s,a} \\ a \tilde{I}_{s,a} \end{bmatrix}$$

Premultiplying the equation above by  $T$  and replacing  $\tilde{V}_{abc}$  with its equal  $T^{-1}\tilde{V}_{120}$ , one obtains

$$T\tilde{I}_{abc} = TY_{abc}T^{-1}\tilde{V}_{120} - T\tilde{I}_{s,abc}$$

or

$$\tilde{I}_{120} = Y_{120}\tilde{V}_{120} - \tilde{I}_{s,120} \quad (7.9)$$

where

$$\tilde{I}_{120} = T\tilde{I}_{abc} = \begin{bmatrix} \tilde{I}_1 \\ \tilde{I}_2 \\ \tilde{I}_0 \end{bmatrix}$$

$$\tilde{V}_{120} = T\tilde{V}_{abc} = \begin{bmatrix} \tilde{V}_1 \\ \tilde{V}_2 \\ \tilde{V}_0 \end{bmatrix}$$

$$\tilde{I}_{s,120} = \begin{bmatrix} \tilde{I}_{s,a} \\ 0 \\ 0 \end{bmatrix}$$

$$Y_{120} = TY_{abc}T^{-1}$$

Since we have assumed that the three-phase power system is symmetric, the matrix  $Y_{120}$  must be diagonal, that is,

$$Y_{120} = \begin{bmatrix} Y_1 & 0 & 0 \\ 0 & Y_2 & 0 \\ 0 & 0 & Y_0 \end{bmatrix} \quad (7.10)$$

Then Eq. (7.9) represents three decoupled equations. These equations are written explicitly as follows:

$$\tilde{I}_1 = Y_1\tilde{V}_1 - \tilde{I}_{s,a} \quad (7.11a)$$

$$\tilde{I}_2 = Y_2\tilde{V}_2 \quad (7.11b)$$

$$\tilde{I}_0 = Y_0\tilde{V}_0 \quad (7.11c)$$

Equations (7.11) represent three Norton equivalent circuits which are illustrated in Fig. 7.3b. We shall refer to these circuits as the Norton equivalent sequence networks. An alternative form results from solving Eqs. (7.11) for the voltages, yielding

$$\tilde{V}_1 = Z_1 \tilde{I}_1 + Z_1 \tilde{I}_{s,a} = Z_1 \tilde{I}_1 + \tilde{E}_{s,a} \quad (7.12a)$$

$$\tilde{V}_2 = Z_2 \tilde{I}_2 \quad (7.12b)$$

$$\tilde{V}_3 = Z_0 \tilde{I}_0 \quad (7.12c)$$

where  $Z_1 = 1/Y_1$ ,  $Z_2 = 1/Y_2$ ,  $Z_0 = 1/Y_0$ . Equations (7.12) represent three Thévenin equivalent circuits which are illustrated in Fig. 7.3c. We shall refer to these circuits as the Thévenin equivalent sequence networks or simply as the sequence networks.

The decomposition of a three-phase power system into three sequence networks can be done on a component-by-component basis. The sequence networks of each component must be connected in the same way as the components are connected to each other.

In the next three sections we discuss fault analysis procedures based on symmetrical components. Specifically, in Section 7.3 we discuss the representation of specific power system elements with sequence models. Then in Section 7.4 we discuss procedures for fault current computations.

### 7.3 SEQUENCE MODELS OF THREE-PHASE APPARATUS

Sequence models can be derived for any three-phase power system element, assuming that it is a symmetric three-phase system. As we discussed in Chapter 6, transmission lines are represented with three-sequence models. Usually, the  $\pi$ -equivalent circuit for each of the three sequence models is employed. Each  $\pi$ -equivalent circuit has two parameters: the series and the shunt impedance. Thus the three-sequence models of a three-phase line are determined with six parameters: (a) the series impedance of the sequence networks denoted by  $Z_1$ ,  $Z_2$ ,  $Z_0$  (positive, negative, and zero sequence, respectively) and (b) the shunt impedance of the sequence networks denoted by  $Z'_1$ ,  $Z'_2$ ,  $Z'_0$ .

In the next subsections we present a brief review of sequence parameters for the most common elements of electric power systems—generators and transformers.

#### 7.3.1 Synchronous Machines

Typical reactance values are available from the manufacturer. Three different values are specified for positive sequence: the subtransient reactance  $x_d''$ , the transient reactance  $x_d'$ , and the synchronous reactance  $x_d$ . These are the direct axis values and are used for calculation of the short-circuit current value at different times after the incidence of the short circuit. A similar set of reactances exist

for the quadrature axis,  $x''_q$ ,  $x'_q$ ,  $x_q$ . In selecting the appropriate generator reactance, one should bear in mind the following: For short-duration phenomena (less than 0.1 to 0.2 s), a synchronous generator behaves approximately as a constant-voltage source behind the subtransient reactance. For longer-duration phenomena (typically, 0.1 to 1.0 s), the synchronous generator behavior can be approximated by a constant-voltage source behind the transient reactance. In the steady state, the synchronous generator can be modeled as a constant-voltage source behind the synchronous reactance. For short-circuit analysis, the subtransient reactance values are used, as they give the highest initial current value. The transient reactance value is used for stability analysis. The synchronous reactance is used for sustained fault current calculations.

Whereas a synchronous machine has many positive sequence reactances, it has only one negative sequence reactance. A good approximation of the negative sequence reactance is given with the average of the direct axis and quadratic axis subtransient reactances. This is so because the flow of negative sequence currents through the machine appear as a double-frequency component rotating in the direction opposite to the rotation of the machine. Thus it scans the direct and quadrature axes twice per cycle. As a result, a good approximation of the negative sequence reactance is the average of the direct and quadrature axes subtransient reactance.

The zero sequence reactance of a synchronous machine is much less than the other reactances. For this reason, a synchronous machine is almost always grounded through an inductor to limit the zero sequence currents through the machine.

The resistance of the armature windings is so small that it is neglected in calculating the short-circuit currents. The resistance is of importance in determining the dc time constants of an asymmetrical short-circuit current. The sequence networks of a synchronous machine are illustrated in Fig. 7.4.

### 7.3.2 Transformers

Three-phase transformers are characterized by series and shunt impedances. In most applications (i.e., short-circuit analysis, load flow, etc.) the shunt impedance of a transformer is neglected.

In terms of construction, a three-phase transformer may consist of three single-phase transformers connected in a three-phase configuration or may be one single construction where all three phases share the same magnetic circuit (core or shell type). We shall refer to the first category as a three-phase transformer bank, while the second category will be referred to as a three-phase transformer.

The positive and negative sequence reactances of all transformers are identical and available from the manufacturer. The zero sequence reactance of three-phase transformer banks is either equal to the

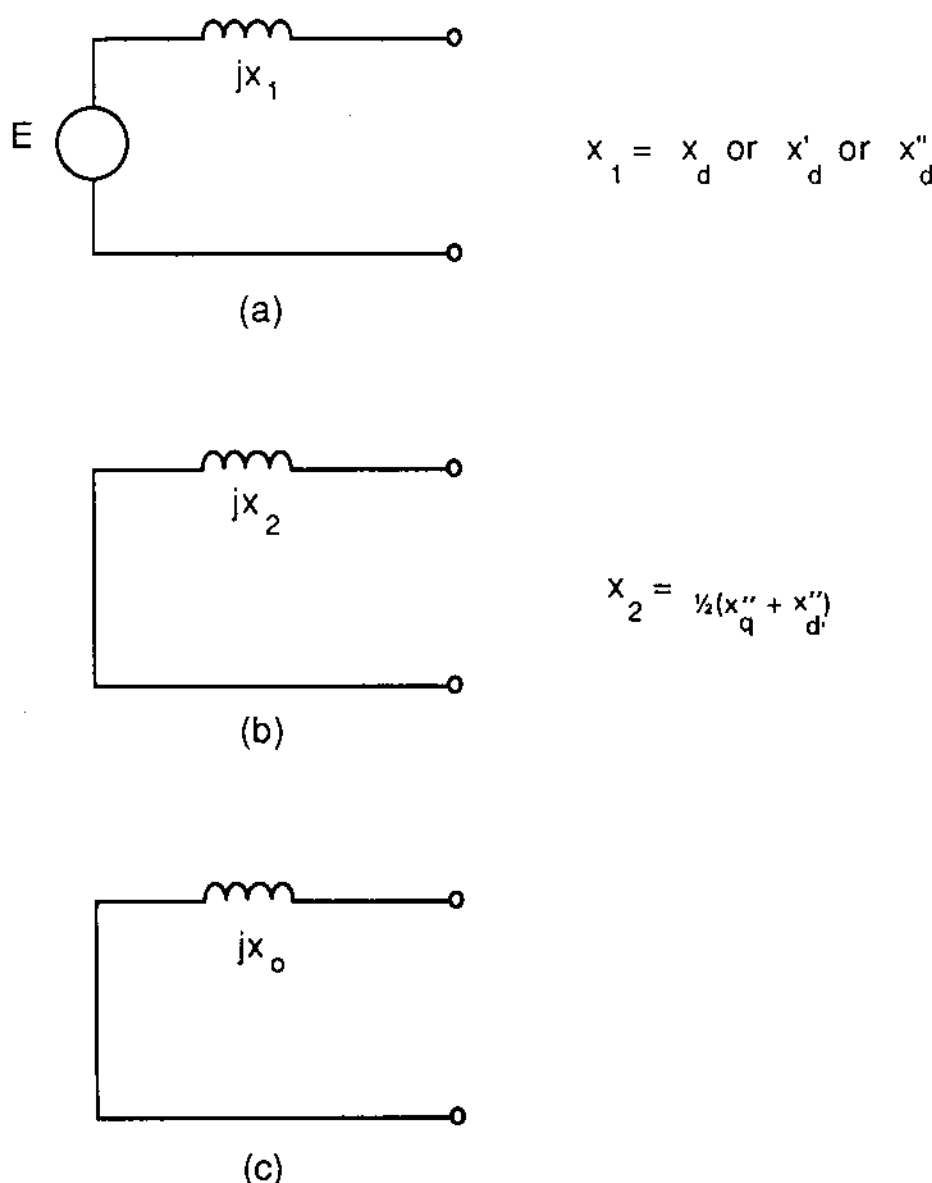


FIG. 7.4 The sequence networks of a synchronous machine. (a) Positive sequence network, (b) negative sequence network, (c) zero sequence network.

positive/negative sequence reactance (for wye-grounded/wye-grounded transformer connections) or infinite (for delta-connected transformers). In three-phase transformers, the magnetic circuit behaves as an equivalent delta winding which modulates the zero-sequence reactance of the transformer. Thus, depending on the design of the magnetic core, the zero sequence reactance may be different from the positive/negative sequence reactance. The resistance of transformer windings is very small and thus is neglected for most applications.

The zero sequence network of a three-phase transformer depends on the transformer connection. For reference, Fig. 7.5 illustrates

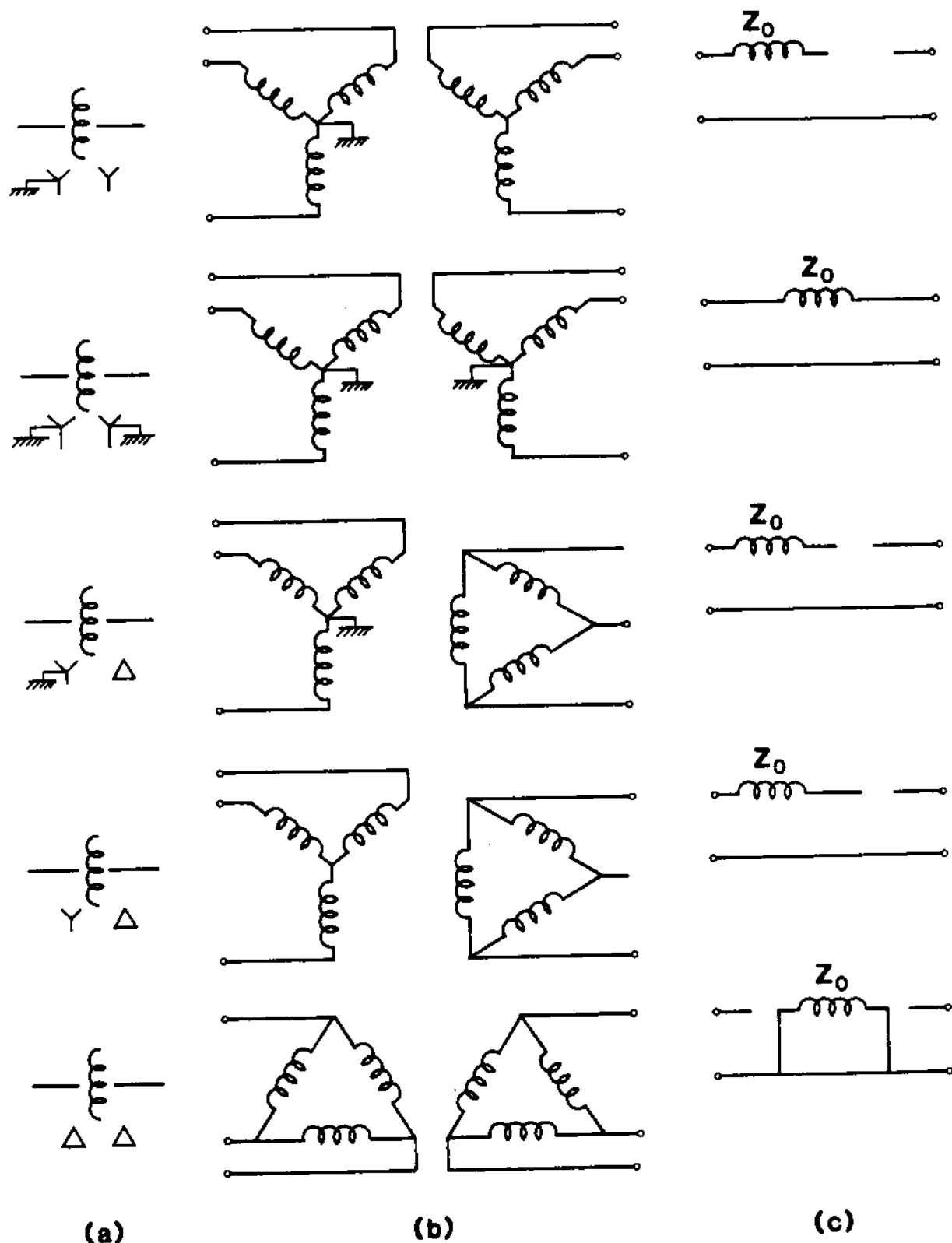


FIG. 7.5 Transformer zero sequence networks. (a) Symbol, (b) connection diagram, (c) zero sequence circuit. (From W. D. Stevenson, Jr., Elements of Power System Analysis, 4th Edition, McGraw-Hill Book Company, 1982.)

the zero sequence network for the most common transformer connections. The shunt impedance is neglected since it is normally very high.

#### 7.4 FAULT ANALYSIS BASED ON SEQUENCE MODELS

In this section we discuss short-circuit analysis techniques based on the sequence model representation of power system elements. We discuss symmetrical as well as asymmetrical short circuits, with emphasis on asymmetrical faults. Possible fault types are illustrated in Fig. 7.1. The principles of short-circuit analysis using the sequence models are illustrated in Fig. 7.6. Specifically, Fig. 7.6a illustrates a power system that is subjected to a fault. The power system is represented as a block with four terminals, the three phase conductors, and the neutral conductor. The fault, in general, is represented by a circuit connected to the four terminals of the power system. Let  $Y_{abc}^f$  be the admittance matrix of the fault circuit and  $Y_{abc}^s$  be the admittance matrix of the power system. With reference to Fig. 7.6a, the models of the power system and the fault are expressed by the equations

$$\tilde{I}_{abc}^s = Y_{abc}^s \tilde{V}_{abc} - \tilde{I}_{s,abc} \quad (7.13)$$

$$\tilde{I}_{abc}^f = Y_{abc}^f \tilde{V}_{abc} \quad (7.14)$$

where  $\tilde{I}_{abc}^s$ ,  $\tilde{I}_{abc}^f$ ,  $\tilde{V}_{abc}$  are vectors of the phase currents and voltages, and  $\tilde{I}_{s,abc}$  are Norton equivalent current sources, as has been the usual notation.

Equations (7.13) and (7.14) are transformed through the use of a symmetrical component transformation, yielding

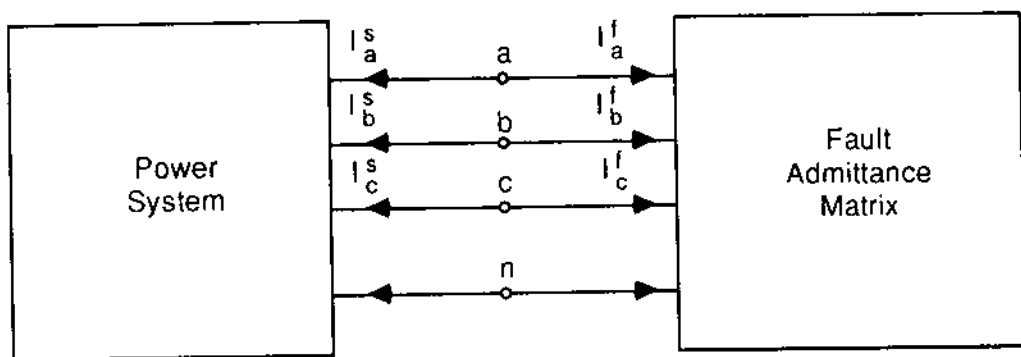
$$\tilde{I}_{120}^s = Y_{120}^s \tilde{V}_{120} - \tilde{I}_{s,120} \quad (7.15)$$

$$\tilde{I}_{120}^f = Y_{120}^f \tilde{V}_{120} \quad (7.16)$$

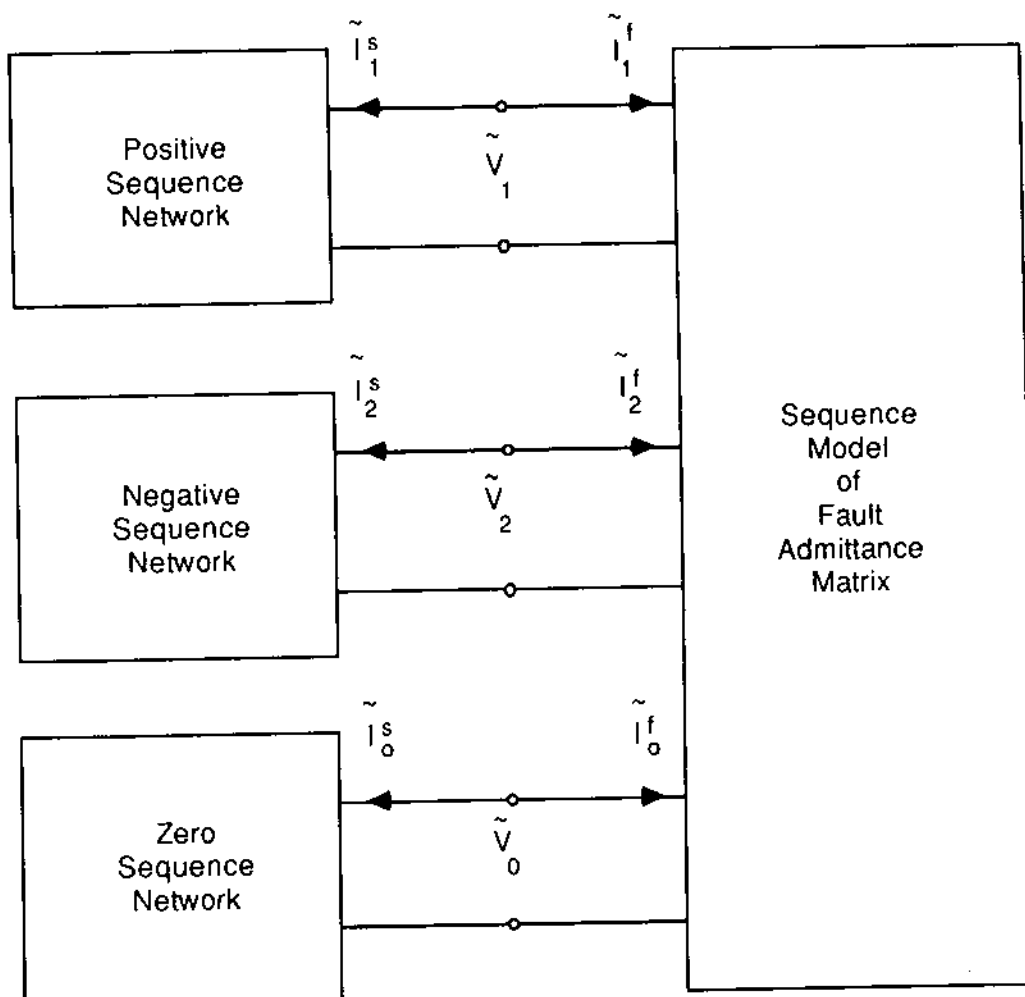
where

$$Y_{120}^s = T Y_{abc}^s T^{-1} \quad (7.17a)$$

$$Y_{120}^f = T Y_{abc}^f T^{-1} \quad (7.17b)$$



(a)



(b)

FIG. 7.6 Principle of short circuit analysis using symmetrical components.

We know that Eq. (7.15) represents the sequence networks of the power system, while Eq. (7.16) represents the sequence model of the fault admittance matrix. The transformed system is illustrated in Fig. 7.6b. Depending on the specific fault type, the sequence model of the fault admittance matrix represents a specific set of connections among the three sequence networks. In subsequent sections we consider specific fault types and derive the specific set of connections.

### Three-Phase Fault

A three-phase fault occurs when all three phases of a power system are connected to the system neutral through a very low impedance,  $Z_f$ . In this case

$$\tilde{I}_a^f = \frac{\tilde{V}_a}{Z_f} \quad (7.18a)$$

$$\tilde{I}_b^f = \frac{\tilde{V}_b}{Z_f} \quad (7.18b)$$

$$\tilde{I}_c^f = \frac{\tilde{V}_c}{Z_f} \quad (7.18c)$$

The equations above, written in compact matrix notation, provide the fault admittance matrix,  $Y_{abc}^f$ :

$$\begin{bmatrix} \tilde{I}_a^f \\ \tilde{I}_b^f \\ \tilde{I}_c^f \end{bmatrix} = \begin{bmatrix} 1/Z_f & 0 & 0 \\ 0 & 1/Z_f & 0 \\ 0 & 0 & 1/Z_f \end{bmatrix} \begin{bmatrix} \tilde{V}_a \\ \tilde{V}_b \\ \tilde{V}_c \end{bmatrix} \quad (7.19)$$

Upon transformation of above equation into the sequence model, we have

$$\begin{bmatrix} \tilde{I}_1^f \\ \tilde{I}_2^f \\ \tilde{I}_0^f \end{bmatrix} = \begin{bmatrix} 1/Z_f & 0 & 0 \\ 0 & 1/Z_f & 0 \\ 0 & 0 & 1/Z_f \end{bmatrix} \begin{bmatrix} \tilde{V}_1 \\ \tilde{V}_2 \\ \tilde{V}_0 \end{bmatrix} \quad (7.20)$$

Equation (7.20) suggests that a three-phase fault in the sequence models is represented with three impedances  $Z_f$  connected across each of the sequence networks. These connections are illustrated in Fig. 7.7.

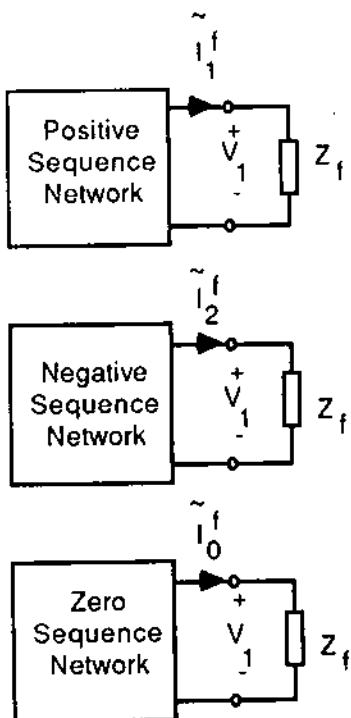


FIG. 7.7 Three-phase fault.

Line-to-Line Fault

A line-to-line fault occurs whenever a very low impedance,  $Z_f$ , is connected across two phases. Assuming that the faulted phases are b and c, the fault currents are

$$\tilde{I}_a^f = 0 \quad (7.21a)$$

$$\tilde{I}_b^f = \frac{\tilde{V}_b - \tilde{V}_c}{Z_f} \quad (7.21b)$$

$$\tilde{I}_c^f = \frac{\tilde{V}_c - \tilde{V}_b}{Z_f} \quad (7.21c)$$

Equations (7.21) written in compact matrix notation provide the fault admittance matrix,  $Y_{abc}^f$ :

$$\begin{bmatrix} \tilde{I}_a^f \\ \tilde{I}_b^f \\ \tilde{I}_c^f \end{bmatrix} = \begin{bmatrix} 0 & 0 & 0 \\ 0 & 1/Z_f & -1/Z_f \\ 0 & -1/Z_f & 1/Z_f \end{bmatrix} \begin{bmatrix} \tilde{V}_a \\ \tilde{V}_b \\ \tilde{V}_c \end{bmatrix} \quad (7.22)$$

Upon transformation of Eq. (7.22) into the sequence model, we have

$$\begin{bmatrix} \tilde{I}_1^f \\ \tilde{I}_2^f \\ \tilde{I}_0^f \end{bmatrix} = \begin{bmatrix} 1/Z_f & -1/Z_f & 0 \\ -1/Z_f & 1/Z_f & 0 \\ 0 & 0 & 0 \end{bmatrix} \begin{bmatrix} \tilde{V}_1 \\ \tilde{V}_2 \\ \tilde{V}_0 \end{bmatrix} \quad (7.23)$$

The admittance matrix above corresponds to an impedance  $Z_f$  connected between the positive and negative sequence network as illustrated in Fig. 7.8.

#### Line-to-Line-to-Ground Fault

This fault may occur in different ways: for example, when a very low impedance is connected between phases b and c and another low impedance between phase b and neutral; or when a very low impedance is connected between phase b and neutral and another between phase c and neutral. Consider the latter line-to-line-to-ground fault and assume that the fault impedance is  $Z_f$ . The fault currents will be

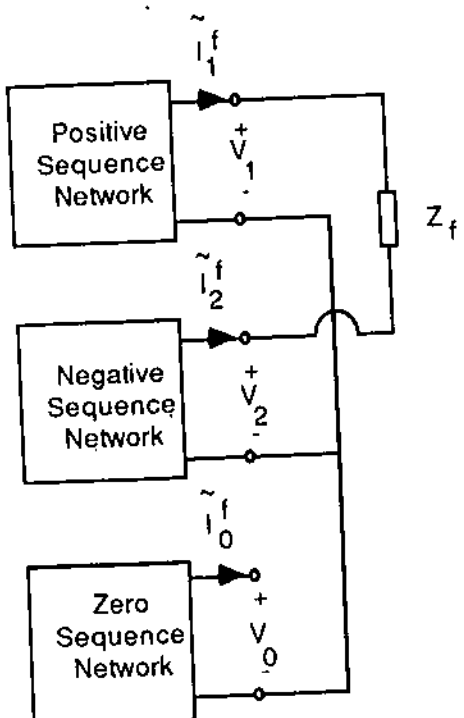


FIG. 7.8 Line-to-line fault.

$$\tilde{I}_a^f = 0 \quad (7.24a)$$

$$\tilde{I}_b^f = \frac{\tilde{V}_b}{Z_f} \quad (7.24b)$$

$$\tilde{I}_c^f = \frac{\tilde{V}_c}{Z_f} \quad (7.24c)$$

Equations (7.24) written in compact matrix notation provide the fault admittance matrix,  $Y_{abc}^f$ :

$$\begin{bmatrix} \tilde{I}_a^f \\ \tilde{I}_b^f \\ \tilde{I}_c^f \end{bmatrix} = \begin{bmatrix} 0 & 0 & 0 \\ 0 & 1/Z_f & 0 \\ 0 & 0 & 1/Z_f \end{bmatrix} \begin{bmatrix} \tilde{V}_a \\ \tilde{V}_b \\ \tilde{V}_c \end{bmatrix} \quad (7.25)$$

Upon transformation of Eq. (7.25) into the sequence model, we obtain

$$\begin{bmatrix} \tilde{I}_1^f \\ \tilde{I}_2^f \\ \tilde{I}_0^f \end{bmatrix} = \begin{bmatrix} 2/3Z_f & -1/3Z_f & -1/3Z_f \\ -1/3Z_f & 2/3Z_f & -1/3Z_f \\ -1/3Z_f & -1/3Z_f & 2/3Z_f \end{bmatrix} \begin{bmatrix} \tilde{V}_1 \\ \tilde{V}_2 \\ \tilde{V}_0 \end{bmatrix} \quad (7.26)$$

The admittance matrix equation (7.26) represents a circuit that connects a  $3Z_f$  impedance between any pair of sequence networks. These connections are illustrated in Fig. 7.9. If the fault impedance is zero, Fig. 7.9 suggests that the three sequence networks are connected in parallel.

#### Single Line-to-Ground Fault

This fault occurs whenever a very low impedance,  $Z_f$ , is connected between a phase and the neutral. Assuming that the faulted phase is phase a, the fault currents are

$$\tilde{I}_a^f = \frac{\tilde{V}_a}{Z_f} \quad (7.27a)$$

$$\tilde{I}_b^f = 0 \quad (7.27b)$$

$$\tilde{I}_c^f = 0 \quad (7.27c)$$

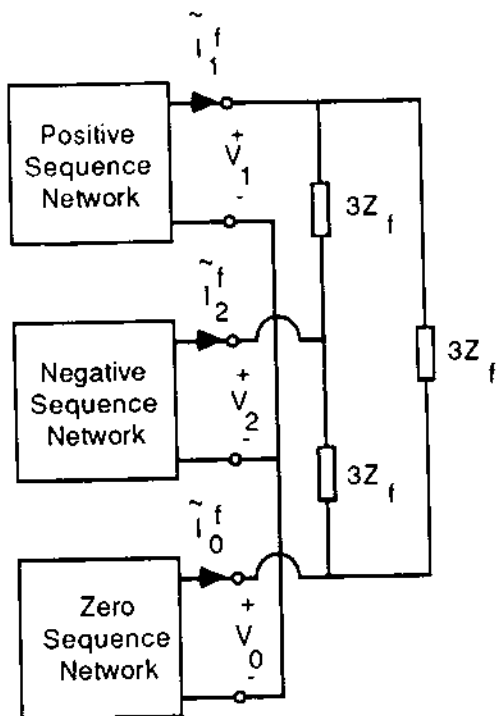


FIG. 7.9 Line-to-line-to-ground fault.

In compact matrix notation the equations above read

$$\begin{bmatrix} \tilde{I}_a^f \\ \tilde{I}_b^f \\ \tilde{I}_c^f \end{bmatrix} = \begin{bmatrix} 1/Z_f & 0 & 0 \\ 0 & 0 & 0 \\ 0 & 0 & 0 \end{bmatrix} \begin{bmatrix} \tilde{V}_a \\ \tilde{V}_b \\ \tilde{V}_c \end{bmatrix} \quad (7.28)$$

Upon transformation of the equation above into the sequence model, we have

$$\begin{bmatrix} \tilde{I}_1^f \\ \tilde{I}_2^f \\ \tilde{I}_0^f \end{bmatrix} = \begin{bmatrix} 1/3Z_f & 1/3Z_f & 1/3Z_f \\ 1/3Z_f & 1/3Z_f & 1/3Z_f \\ 1/3Z_f & 1/3Z_f & 1/3Z_f \end{bmatrix} \begin{bmatrix} \tilde{V}_1 \\ \tilde{V}_2 \\ \tilde{V}_0 \end{bmatrix} \quad (7.29)$$

The connectivity of the sequence networks from Eq. (7.29) is not obvious. Observe that Eq. (7.29) states that all the sequence currents are identical, that is,

$$\tilde{I}_1^f = \tilde{I}_2^f = \tilde{I}_0^f = \frac{\tilde{V}_1 + \tilde{V}_2 + \tilde{V}_0}{3Z_f}$$

These equations are satisfied only if the sequence networks are connected in series with the impedance  $3Z_f$ . The connections are illustrated in Fig. 7.10.

In summary, we have discussed procedures by which the sequence networks of a power system must be connected to provide a circuit for the computation of fault currents under specific fault conditions. Specifically, under steady-state but possibly unbalanced conditions, the system is represented with three sequence networks, as in Fig. 7.6b. At the point of a fault (symmetric or asymmetric), the sequence networks must be interconnected because it is this area where the sequence quantities interact. The type of interaction, and therefore the way the sequence networks should be interconnected, depend on the asymmetry. Figures 7.7 through 7.10 illustrate the connections required for the four types of faults mentioned earlier.

Computationally, the analysis of symmetrical or asymmetrical faults requires the following steps:

- Step 1. Compute the three equivalent circuits (Norton or Thévenin equivalent) at the fault location (positive, negative, and zero sequence).
- Step 2. Interconnect the three equivalent circuits depending on the fault type.
- Step 3. Compute the symmetrical components. Subsequently compute the phase quantities.

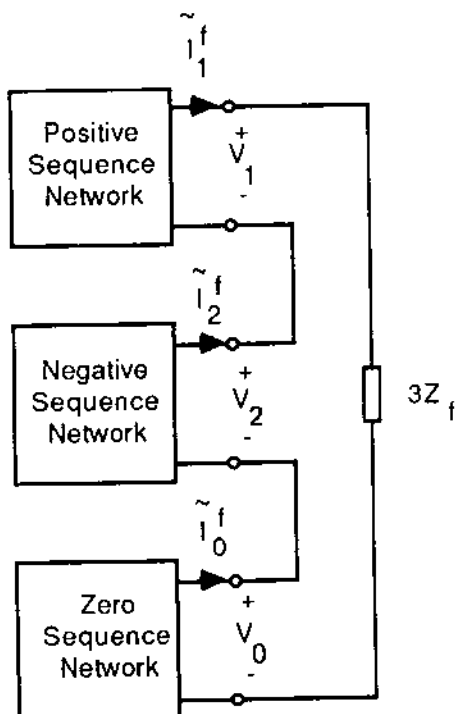


FIG. 7.10 Single phase-to-ground fault.

From the tasks above, the most complex and computationally demanding is task 1. It requires the formation of the three sequence networks and subsequent reduction of these to a Norton or Thévenin equivalent. The formation of the three sequence networks is accomplished through interconnection of the sequence models of individual devices. The procedure is straightforward and illustrated with an example.

Example 7.1: Consider the electric power system of Fig. E7.1. Assume a single phase-to-ground fault located on the line 20 mi from the transformer. Compute the fault current: (a) neglecting the load current, and (b) without neglecting the load current. Use symmetrical component theory in the computations. System data are as follows:

$$\begin{aligned}\text{Generator (80 MVA, 15 kV): } & x_d'' = 0.185 \text{ pu} \\ & x_2 = (x_d'' + x_q'')/2.0 = 0.28 \text{ pu} \\ & x_0 = 0.06 \text{ pu}\end{aligned}$$

$$\text{Transformer (80 MVA, 15/115 kV): } x_1 = x_2 = x_0 = j1.10 \text{ pu (on transformer rating)}$$

$$\begin{aligned}\text{Transmission line: } & z_1 = z_2 = 0.3 + j0.7334 \Omega/\text{mi} \\ & z_0 = 0.34 + j1.55 \Omega/\text{mi}\end{aligned}$$

$$\begin{aligned}\text{Electric load (three phase, delta connected): } & z_1 = z_2 = 200 - j20 \Omega \\ & z_0 = \infty\end{aligned}$$

Transformer shunt impedance and transmission line capacitive shunt impedance are to be neglected.

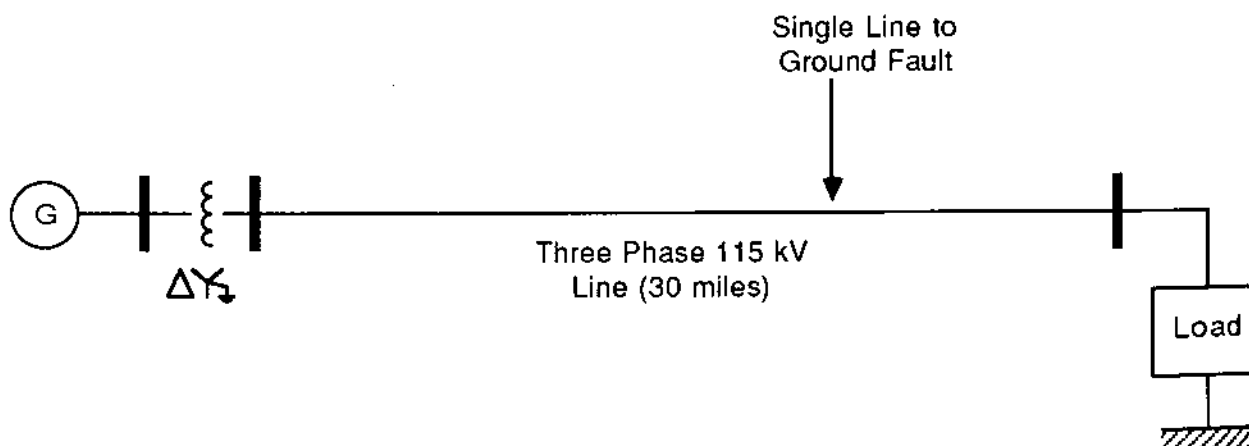


FIG. E7.1 A power system with a single line-to-ground fault.

Solution: All impedances will be converted in pu on an 80-MVA basis. At the 115-kV level, the base impedance is  $z_B = 115^2/80 = 165.3 \Omega$ . The sequence networks are constructed and illustrated in Fig. E7.2. The figure illustrates the electric load as well.

- (a) The electric load is neglected. The Thévenin equivalent sequence networks are illustrated in Fig. E7.3. The sequence currents are

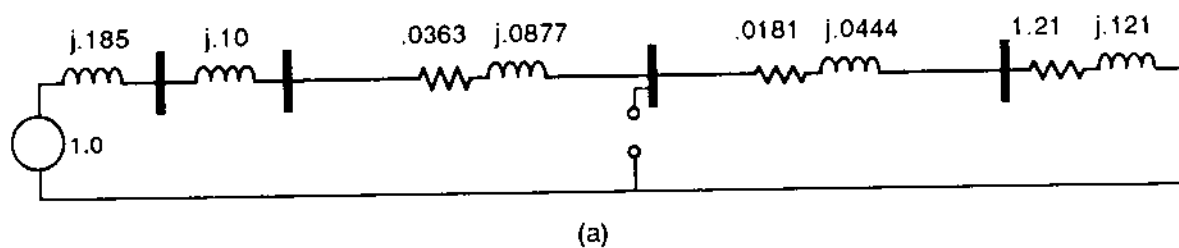
$$\tilde{I}_1 = \tilde{I}_2 = \tilde{I}_0 = \frac{1.0}{0.7671 + j1.1299} = 0.7322e^{-j55.8^\circ} \text{ pu}$$

The phase electric currents are

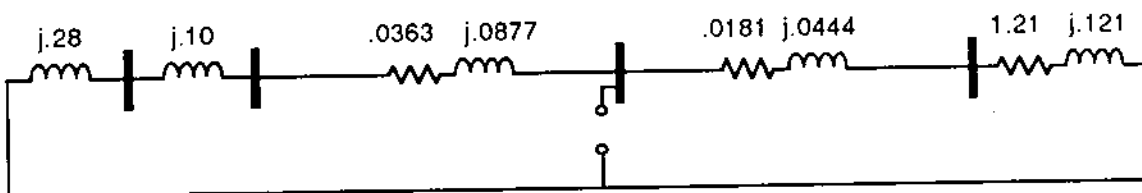
$$\tilde{I}_a = 3\tilde{I}_0 = 2.1966e^{-j55.8^\circ} \text{ pu} = 882.2e^{-j55.8^\circ} \text{ A}$$

$$\tilde{I}_b = 0$$

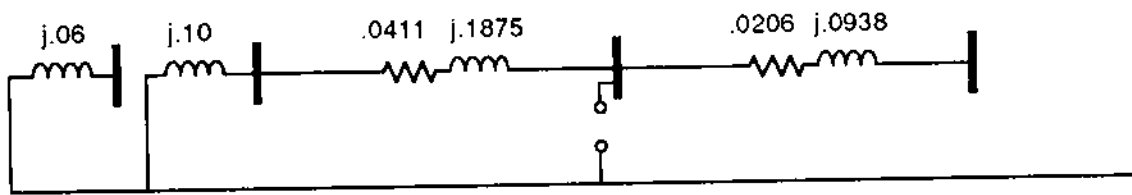
$$\tilde{I}_c = 0$$



(a)



(b)



(c)

FIG. E7.2 Sequence networks for the power system of Fig. E7.1.  
(a) Positive sequence, (b) negative sequence, (c) zero sequence.

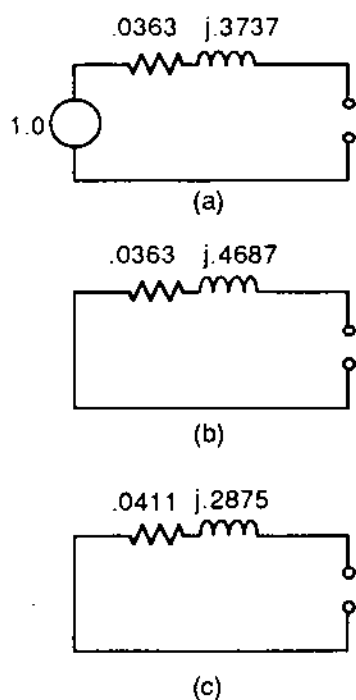


FIG. E7.3 Thévenin equivalent of the sequence networks of Fig. E7.2, neglecting electric load.

- (b) The electric load is not neglected. In this case the Thévenin equivalent sequence networks are computed and illustrated in Fig. E7.4. The sequence currents are

$$\tilde{I}_1 = \tilde{I}_2 = \tilde{I}_0 = \frac{0.902}{0.3256 + j0.9814} = 0.8723e^{-j71.64^\circ} \text{ pu}$$

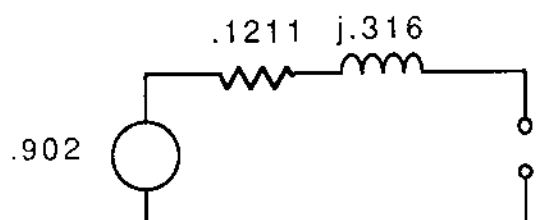
The phase electric currents are:

$$\tilde{I}_a = 3\tilde{I}_0 = 2.6169e^{-j71.64^\circ} \text{ pu} = 1051e^{-j71.64^\circ} \text{ A}$$

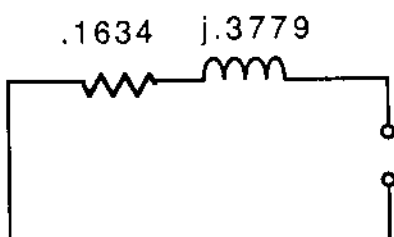
$$\tilde{I}_b = 0$$

$$\tilde{I}_c = 0$$

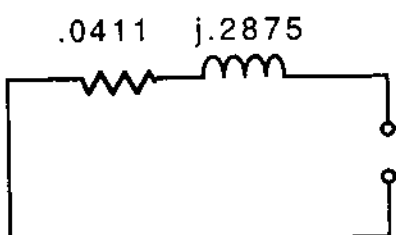
Comparing the two cases, it is obvious that the presence of the electric load increases the fault current. Of course, since the electric load is represented with a passive R, L equivalent, it does not contribute to the fault current. The increase in the fault current is due to the fact that the presence of the electric load allows the other two phases of the source (b and c) to contribute to the fault current through the load.



(a)



(b)



(c)

FIG. E7.4 Thévenin equivalent of the sequence networks of Fig. E7.2, including electric load.

## 7.5 GROUND POTENTIAL RISE DURING FAULTS

It was pointed out in Section 7.4 that two specific fault conditions yield substantial zero sequence electric currents. Since one of the paths for the flow of the zero sequence currents is the earth, electric current will flow into earth through the grounding system. This phenomenon results in the voltage elevation of grounded structures. Analysis of the ground potential rise requires that the grounding system be explicitly represented in the model of the system. In this and subsequent sections, we discuss relevant modeling and analysis procedures for the purpose of computing the ground potential rise.

An asymmetrical fault in a power system will cause a substantial amount of electric current to flow in the overhead sky wires, neutral conductors, earth, transmission towers, and so on. The distribution of electric current among the various alternative paths is determined by many parameters, such as conductor size, conductor separation, tower footing resistance, soil resistivity, and location and type of fault. Assuming that the fault current distribution has been determined, the ground potential rise can be computed directly from the earth current. Modeling and analysis procedures for the purpose of determining fault current distribution can be developed either using the symmetrical components method or direct analysis (i.e., in terms of phase quantities). The symmetrical components method is an approximation. The general assumptions and limitations of the methods have been discussed in Section 7.2. The direct analysis in terms of the phase quantities is exact, but it is computationally more intense. In subsequent sections both methods are presented and a comparison of the two methods is given.

## 7.6 FAULT CURRENT DISTRIBUTION BASED ON SEQUENCE MODELS

In this section we discuss analysis techniques for determining the fault current distribution among all alternative paths. Only the method based on the sequence models will be examined. One of the assumptions for the sequence models is that the power system elements are symmetric. A consequence of this assumption is that positive or negative sequence currents flow only in the phase conductors. Electric currents in the grounding system (earth) and shield or neutral conductors are of the zero sequence only. For analysis purposes it is necessary to construct the sequence networks of a given electric power system. The positive and negative sequence networks are computed in the usual way. The zero sequence network, however, must be constructed in such a way as to explicitly represent (a) the shield or neutral wires, (b) the earth path, (c) the tower footing resistances, and so on. Subsequently, the sequence networks are connected in a way corresponding to the type of fault (i.e., in series for a single line-to-ground fault, etc.). This procedure results in a large network problem. Upon solution of this network, the sequence components of the electric current and voltage everywhere in the system are obtained. From this information the actual electric current and voltage everywhere in the system can be computed with the inverse transformation of the symmetrical components.

As has been pointed out, the current distribution among phase conductors, sky wires, neutral conductors, and earth is determined only with the zero sequence network. This observation allows a simplification of the computational procedure. Specifically, we need

to analyze only the zero sequence network in order to determine the relative current distribution among all parallel paths. Actual fault current levels are determined through the usual fault analysis. The overall procedure involves the following steps:

- Step 1. Compute and lay out the zero sequence network for the system under consideration. Earth, shield wires, neutral wires, tower footing resistances, substation grounding impedances, and so on, should be explicitly represented.
- Step 2. For a specified fault location, compute the zero sequence current in the shield wires, neutral wires, towers, and so on, as a percentage of the zero sequence current injected at the location of the fault. Denote these currents by  $\tilde{I}_t$ ,  $\tilde{I}_s$ , and so on.
- Step 3. Compute the equivalent impedance of the zero sequence network at the location of the fault,  $Z_0$ . This is the zero sequence impedance of the system at the specified fault location.
- Step 4. Compute the positive and negative sequence impedance of the system at the location of the fault,  $Z_1$  and  $Z_2$ , respectively.
- Step 5. Compute the fault current  $\tilde{I}_f$  and the zero sequence current  $\tilde{I}_0$ . For this purpose the usual fault analysis equations should be employed.
- Step 6. Compute the actual current in the shield wires, towers, neutral wires, and so on, from the equations

$$\begin{aligned}\tilde{I}_{ti} &= \tilde{I}_{ti}(3I_0) \\ \tilde{I}_s &= \tilde{I}_s(3I_0) \quad \text{etc.}\end{aligned}$$

The computational procedure is straightforward. A couple of points, however, need further clarification: (a) the computation of the tower footing resistances and substation ground impedance, and (b) the construction of the zero sequence network in such a way as to retain the identity of shield wires, neutral wires, earth, and so on.

#### Computation of Grounding Structure Impedances

The computation of the grounding structure impedances, such as substation grounding, tower grounding, counterpoises, and so on, has been presented in Chapter 5.

#### Construction of the Zero Sequence Network

Construction of the zero sequence network is done as follows. Every path of zero sequence currents must be identified and characterized with self-impedance and possible mutual impedance with other paths.

For transmission lines, the earth path is modeled using the techniques presented in Chapters 2 and 3.

The construction of the zero sequence network with explicit representation of the shield wire, earth path, and so on, is illustrated in Fig. 7.11. Figure 7.11 illustrates the physical system with a set of unbalanced three-phase currents. The figure is helpful in determining the sequence network representation of the line. Consider one span of the line. In general, if currents  $\tilde{I}_a$ ,  $\tilde{I}_b$ ,  $\tilde{I}_c$ ,  $\tilde{I}_g$  flow in the phase conductors and shield wire of a specific span of the line, the induced voltages along the line conductors are

$$\Delta \tilde{V}_a = [(r_c + z_{se})\tilde{I}_a - z_{me}\tilde{I}_b - z_{me}\tilde{I}_c - z_{pge}\tilde{I}_g]\ell \quad (7.30a)$$

$$\Delta \tilde{V}_b = [-z_{me}\tilde{I}_a + (r_c + z_{se})\tilde{I}_b - z_{me}\tilde{I}_c - z_{pge}\tilde{I}_g]\ell \quad (7.30b)$$

$$\Delta \tilde{V}_c = [-z_{me}\tilde{I}_a - z_{me}\tilde{I}_b + (r_c + z_{se})\tilde{I}_c - z_{pge}\tilde{I}_g]\ell \quad (7.30c)$$

$$\Delta \tilde{V}_g = [-z_{pge}\tilde{I}_a - z_{pge}\tilde{I}_b - z_{pge}\tilde{I}_c + (r_g + z_{gge})\tilde{I}_g]\ell \quad (7.30d)$$

In formulas (7.30), and in compliance with the requirement of the symmetrical component transformation, it is assumed that there is symmetry in the line, thus  $z_{abe} = z_{ace} = z_{bce} = z_{me}$ . In addition,  $z_{age} = z_{bge} = z_{cge} = z_{pge}$ . These parameters are computed using the exact Carson's equations or any of the approximate methods discussed in Chapter 3. To simplify the equations we shall use the equivalent depth of return method (see Chapter 3). Using this method and putting the equations in compact matrix form, Eqs. (7.30) read

$$\Delta \tilde{V}_{abc} = [(r_c I + r_e II + X)\tilde{I}_{abc} + (r_e + x_{pge})\Pi\tilde{I}_g]\ell \quad (7.31a)$$

$$\Delta \tilde{V}_g = [(r_e + x_{pge})\tilde{I}_{abc}^T + (r_e + r_g + x_{gge})\tilde{I}_g]\ell \quad (7.31b)$$

where

$$\tilde{I}_{abc} = \begin{bmatrix} \tilde{I}_a \\ \tilde{I}_b \\ \tilde{I}_c \end{bmatrix} \quad \Delta \tilde{V}_{abc} = \begin{bmatrix} \Delta \tilde{V}_a \\ \Delta \tilde{V}_b \\ \Delta \tilde{V}_c \end{bmatrix}$$

$I = 3 \times 3$  identity matrix

$$II = \begin{bmatrix} 1 & 1 & 1 \\ 1 & 1 & 1 \\ 1 & 1 & 1 \end{bmatrix}$$

$X = 3 \times 3$  matrix of inductive reactances; if, using the method of equivalent depth of return (see Chapter 3), the  $i, j$  entry of the matrix is

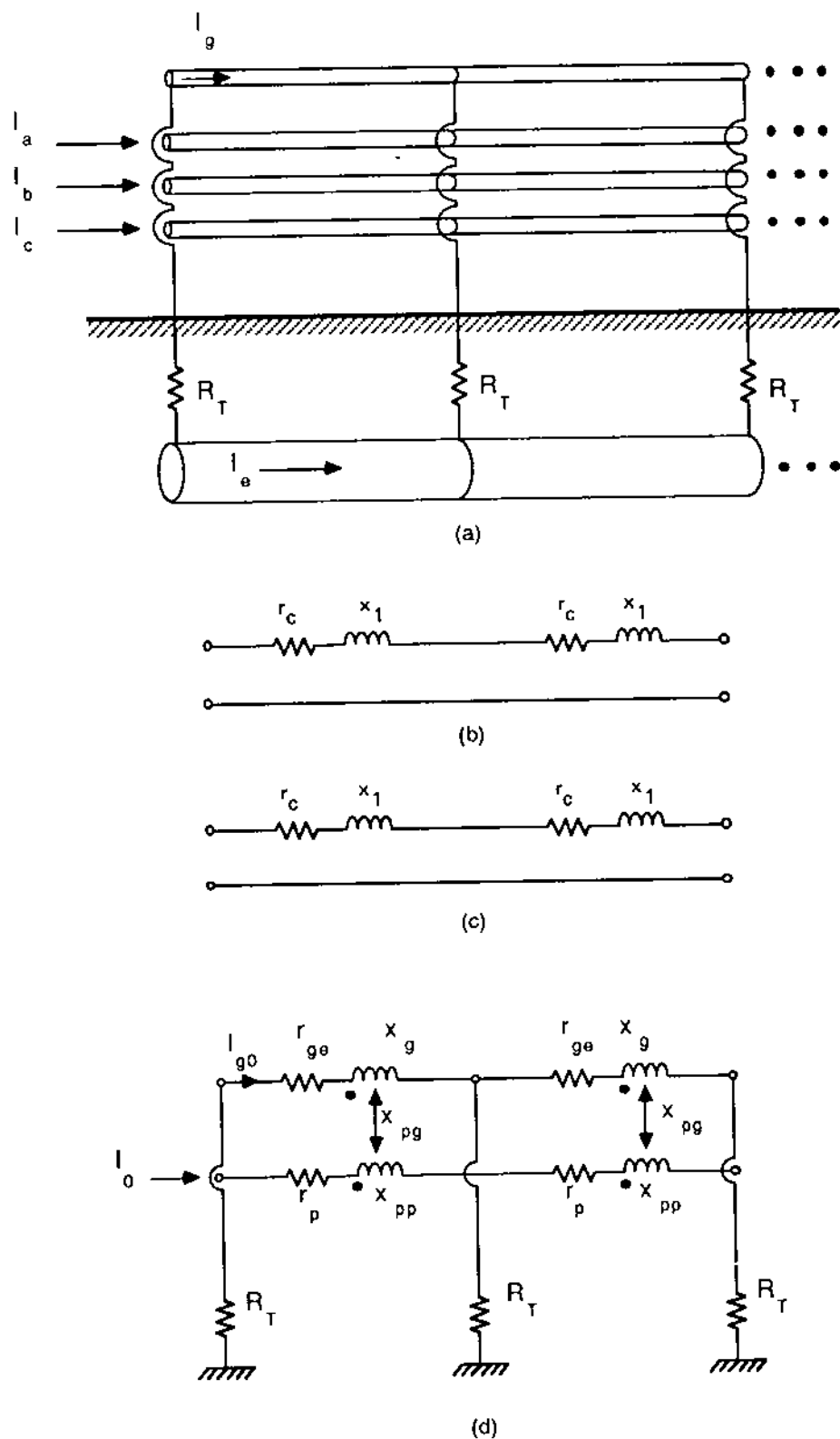


FIG. 7.11 Equivalent sequence networks of a transmission line. (a) Line construction with phase conductors, shield/neutral and earth path; (b) positive sequence network; (c) negative sequence network; (d) zero sequence network.

$$x_{i,j} = j0.00466f \log \frac{D_e}{D_{ij}}$$

$D_{ij}$  = geometric mean distance between conductors i and j

$$x_{pge} = j0.00466f \log \frac{D_e}{D_{pg}}$$

$$x_{gge} = j0.00466f \log \frac{D_e}{d_g}$$

$d_g$  = geometric mean radius of ground wire

$r_e$  = 0.00159f  $\Omega/\text{mi}$

$$\Pi = \begin{bmatrix} 1 \\ 1 \\ 1 \end{bmatrix}$$

Equations (7.31) are converted into the symmetrical components framework by substituting the three phase currents  $\tilde{I}_{abc}$ , and voltages  $\Delta\tilde{V}_{abc}$ , with their symmetrical components. The result is

$$\Delta\tilde{V}_{120} = [T(r_c I + r_e II + X)T^{-1}\tilde{I}_{120} + (r_e + x_{pge})T\Pi\tilde{I}_g] \ell \quad (7.32a)$$

$$\Delta\tilde{V}_g = [(r_e + x_{pge})(T^{-1}\tilde{I}_{120})^T + (r_e + r_g + x_{gge})\tilde{I}_g] \ell \quad (7.32b)$$

Expansion of Eqs. (7.32) yields

$$\Delta\tilde{V}_1 = (r_c + x_1)\tilde{I}_1 \ell \quad (7.33a)$$

$$\Delta\tilde{V}_2 = (r_c + x_1)\tilde{I}_2 \ell \quad (7.33b)$$

$$\Delta\tilde{V}_0 = (r_c + 3r_e + x_0)\tilde{I}_0 \ell + (r_e + x_{pge})\tilde{I}_g \ell \quad (7.33c)$$

$$\Delta\tilde{V}_g = 3(r_e + x_{pge})\tilde{I}_0 \ell + (r_e + r_g + x_{gge})\tilde{I}_g \ell \quad (7.33d)$$

The equations derived express the voltages versus the symmetrical component currents in the phases of the line and the actual current in the shield/neutral wire. In order to make the last two equations symmetric, the electric current  $\tilde{I}_g$  is substituted for by  $\tilde{I}_g = 3\tilde{I}_g 0$ . Now the equations read:

$$\Delta\tilde{V}_1 = (r_c + x_1)\tilde{I}_1 \ell \quad (7.34a)$$

$$\Delta\tilde{V}_2 = (r_c + x_1)\tilde{I}_2 \ell \quad (7.34b)$$

$$\Delta\tilde{V}_0 = (r_c + 3r_e + x_0)\tilde{I}_0 \ell + 3(r_e + x_{pge})\tilde{I}_g 0 \ell \quad (7.34c)$$

$$\Delta \tilde{V}_g = 3(r_e + x_{pge})\tilde{I}_0 \ell + 3(r_e + r_g + x_{gge})\tilde{I}_{g0} \ell \quad (7.34d)$$

Equations (7.34) represent the equivalent circuit shown in Fig. 7.11b, c, and d. Specifically, Fig. 7.11b illustrates the positive sequence network, Fig. 7.11c illustrates the negative sequence network and Fig. 7.11d illustrates the zero sequence network. Comparison of the equations to the equivalent circuit of Fig. 7.11d yields

$$r_p = (r_c + 3r_e) \ell$$

$$x_{pp} = x_0 \ell = j(3)(0.00466)(f) \log \frac{D_e}{D_0} \ell$$

$$r_{ge} = (3r_e + 3r_g) \ell$$

$$x_g = 3x_{gge} \ell = j(3)(0.00466)(f) \log \frac{D_e}{d_g} \ell$$

$$x_{pg} = (3r_e + 3x_{pge}) \ell = 3 \left[ r_e + j(0.00466)(f) \log \frac{D_e}{D_{pg}} \right] \ell$$

In summary, for analysis purposes of fault current distribution and of the ground potential rise of system neutrals, the sequence networks can be employed as an acceptable approximation. For this purpose, the zero sequence network of transmission lines must explicitly represent all the paths available to the flow of zero sequence currents. The zero sequence network of a transmission line that meets this requirement has been developed and illustrated in Fig. 7.11d. Once the sequence networks have been developed, the remaining of the procedure is similar to the usual fault analysis. The procedure will be illustrated with an example.

Example 7.2: Consider the electric power system of Fig. E7.5. The tower design of the 115-kV transmission line is illustrated in Fig. 1.6, while the tower design of the 12-kV line is illustrated

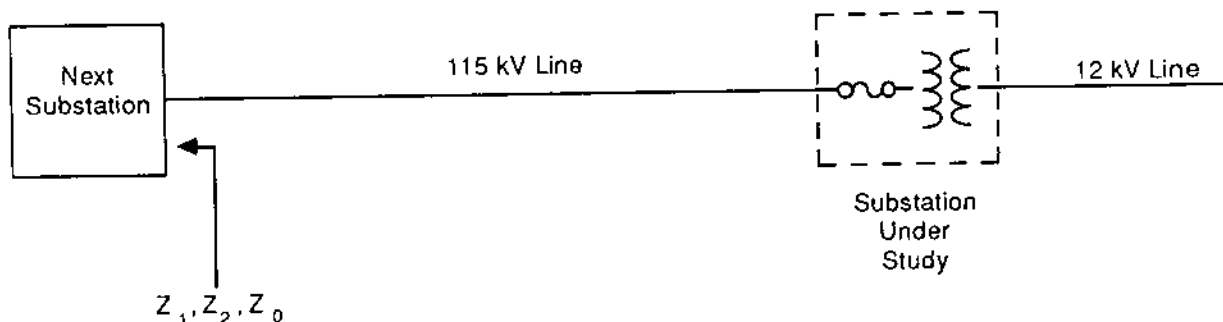


FIG. E7.5 Example system for ground potential rise computations.

in Fig. 1.7. The phase conductors of the 115-kV line are ACSR, 336.4 kcm, 30 strands. The overhead shield wire is a 5/16-in. steel wire. The phase conductors of the 12-kV distribution line are ACSR, 1/0, and the neutral conductor is ACSR, No. 2, 7 strands. The substation under study is a distribution substation with a 20-MVA 115/12-kV delta-wye-connected transformer of 10% reactance. The neutral is grounded with a ground mat. The resistance of the ground mat to remote earth is  $2 \Omega$ . The feeding substation, indicated as "next substation," has an equivalent positive, negative, and zero sequence impedance of  $Z_1 = Z_2 = j9.8 \Omega$ ,  $Z_0 = j6.6 \Omega$ , and it is grounded with a ground mat of  $2\Omega$  resistance. The 115-kV line is 23.5 mi long. The tower footing resistance of the line is  $30 \Omega$ , and the span length is 0.10 mi. The 12-kV line is 10 mi long, the tower grounding resistance is  $50 \Omega$ , and the span length is 0.0833 mi. The soil resistivity is  $265 \Omega \cdot \text{m}$ . Compute the fault current and the ground potential rise of the substation ground mat when a single line-to-ground fault occurs on the high side of the transformer.

Solution: The solution of this problem will be worked with the method of symmetrical components. The sequence networks of the system are illustrated in Fig. E7.6. The impedances illustrated in the figure are computed as follows.

115-kV line: The positive sequence series impedance of this line has been computed in Example 6.3. It is

$$d = 0.0255 \text{ ft}$$

$$D_m = 10.952 \text{ ft}$$

$$R_1 = 0.306 \Omega/\text{mi}$$

$$X_1 = 0.7362 \Omega/\text{mi}$$

Thus the total positive/negative sequence impedance is

$$Z_1 = Z_2 = (0.306 + j0.7362)(23.5) = 7.19 + j17.30 \Omega$$

The zero sequence network of this line is illustrated in Fig. E7.6. The illustrated impedances are computed as follows:

$$r_p = (r_c + 3r_e)\ell = [0.306 + (3)(0.00159)(60)](0.1) = 0.05922 \Omega$$

$$x_{pp} = j0.00466f \log \frac{D_e}{D_0} \ell$$

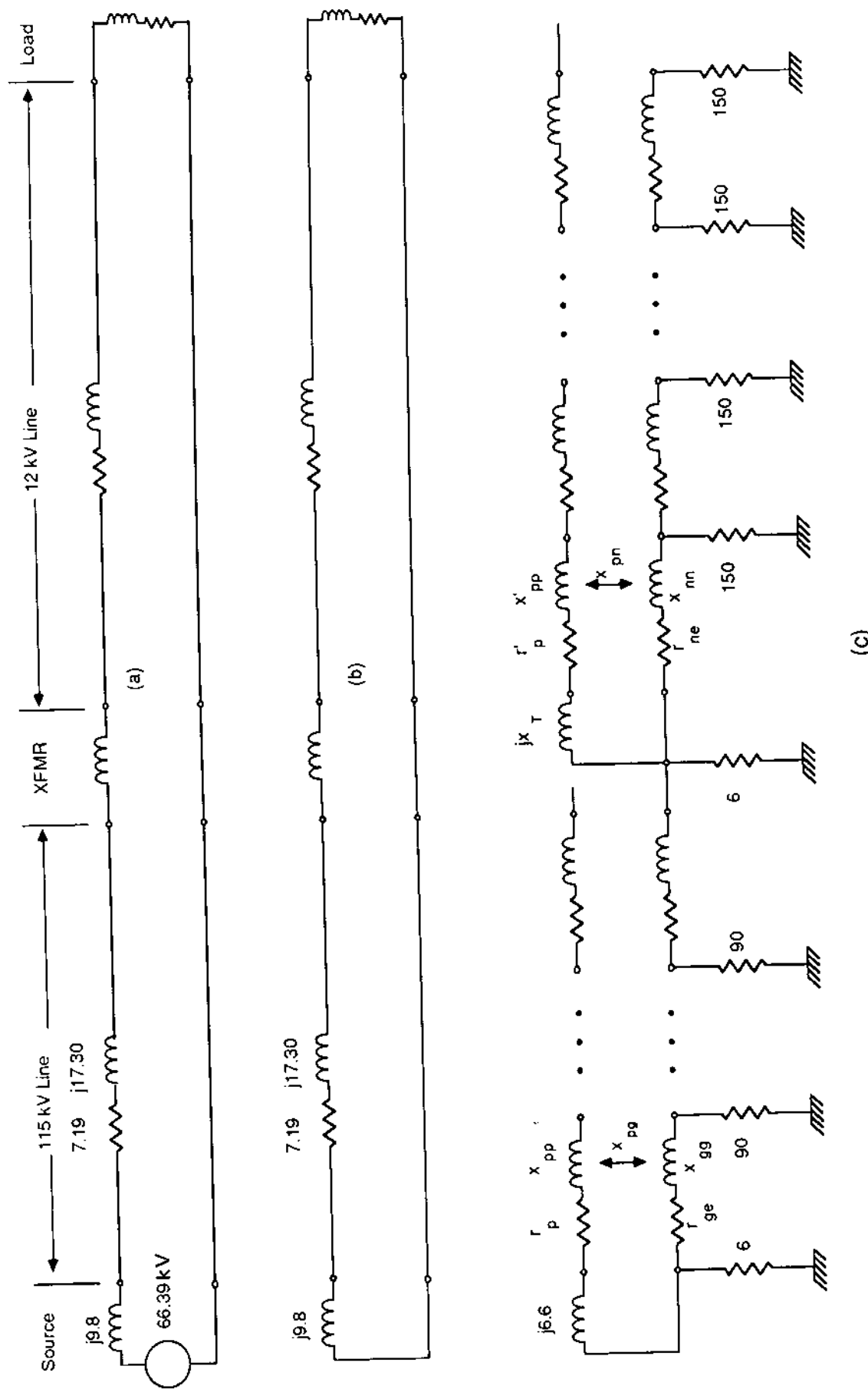


FIG. E7.6 The sequence networks of the power system of Fig. E7.5. (a) Positive sequence network, (b) negative sequence network, (c) zero sequence network.

$$D_e = 2160 \sqrt{\frac{\rho}{f}} = 4539 \text{ ft}$$

$$D_0 = [(0.0255)^3 (8.17)^2 (12.64)^2 (12.72)^2]^{1/9} = 1.4516 \text{ ft}$$

$$x_{pp} = j0.293 \Omega$$

$$r_{ge} = (3r_e + 3r_g)l = 2.34 \Omega$$

$$x_g = 3x_{gge}l = j.62 \Omega$$

$$x_{pg} = (3r_e + 3x_{pge})l$$

$$x_{pge} = j0.00466f \log \frac{D_e}{D_{pg}}$$

$$D_{pg} = [(11.065)(15.273)(18.644)]^{1/3} = 14.665 \text{ ft}$$

$$x_{pge} = j0.6967 \Omega/\text{mi}$$

$$x_{pg} = 0.0286 + j0.209 \Omega$$

12-kV line: The positive and negative sequence impedances per span length are

$$Z_1 = Z_2 = \left( r_c + j0.00466f \log \frac{D}{d} \right) l$$

$$r_c = 1.12 \Omega/\text{mi}$$

$$D = \frac{[(33)(33)(42)]^{1/3}}{12} = 2.98 \text{ ft}$$

$$d = 0.00446 \text{ ft}$$

$$l = 0.0833 \text{ mi}$$

$$Z_1 = Z_2 = 0.09329 + j0.06579 \Omega$$

The zero sequence impedances per span length are

$$r_{ne} = 3(r_e + r_n)l$$

$$r_e = 0.00159f \Omega/\text{mi}$$

$$r_n = 1.65 \Omega/\text{mi}$$

$$l = 0.0833 \text{ mi}$$

$$r_{ne} = 0.436 \Omega$$

$$x_{ne} = j(3)(0.00466)f \log \frac{D_e}{d_n} \ell$$

$$D_e = 2160 \sqrt{\frac{\rho}{f}} = 4539 \text{ ft}$$

$$d_n = 0.00504 \text{ ft}$$

$$x_n = j0.4212 \Omega$$

$$r'_p = (r_c + 3r_e)\ell$$

$$r_c = 1.12 \Omega/\text{mi}$$

$$r'_p = 0.117 \Omega$$

$$x'_{pp} = j0.00466f \log \frac{D_e}{d_p} \ell$$

$$d_p = [(0.00446)^3 (2.75)^2 (2.75)^2 (3.5)^2]^{1/9} = 0.341 \text{ ft}$$

$$x'_{pp} = j0.0977 \Omega$$

$$x_{pn} = (3r_e + 3x_{pne})\ell$$

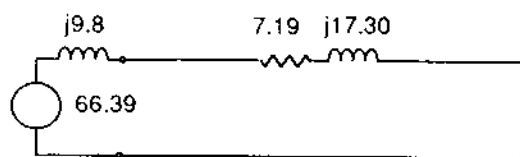
$$x_{pne} = j0.00466f \log \frac{D_e}{D_{pn}}$$

$$D_{pn} = [(6.66)(4.828)(4.828)]^{1/3} = 5.376 \text{ ft}$$

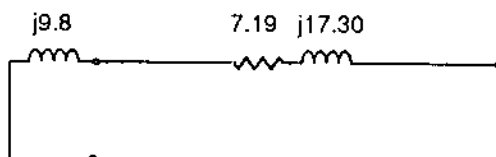
$$x_{pne} = 1.2473 \Omega/\text{mi}$$

$$x_{pn} = 0.0238 + j0.3117 \Omega$$

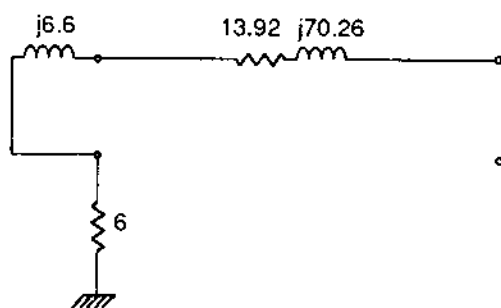
The sequence networks constructed suffice to perform the analysis. The networks are complex for manual computations. To obtain a solution that is tractable with a hand-held calculator, a number of simplifying assumptions will be introduced. First, the shield wire of the 115-kV line can be neglected since it will carry a very small percentage of the current. Also, since the electric load is delta connected, the zero sequence network of the 12-kV line will be open as indicated in Fig. E7.7. Thus the  $r_p$ ,  $x_{pp}$  branch of the 12-kV line can be eliminated since no electric current will flow through. The effect of the electric load is small. Thus the electric load can be neglected in the



(a)



(b)

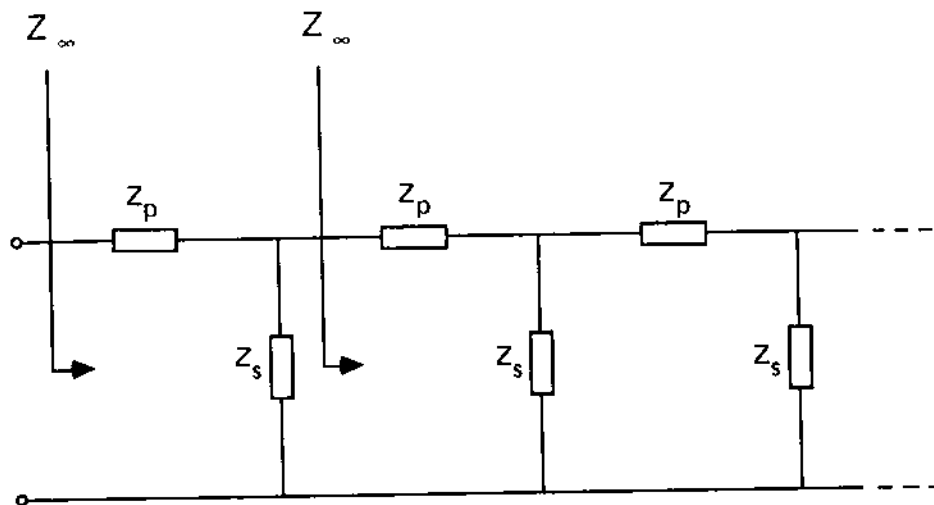


(c)

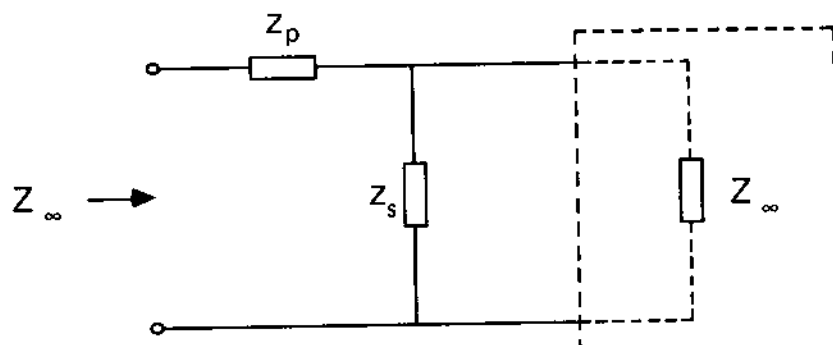
**FIG. E7.7** Simplified sequence networks for the system of Fig. E7.5.  
 (a) Positive sequence network, (b) negative sequence network, (c) zero sequence network.

positive and negative sequence networks. In this case the positive and negative sequence network of the transformer and the 12-kV line should be eliminated since no electric current will flow through.

The simplifications mentioned result in the sequence networks of Fig. E7.7. The zero sequence network of the 12-kV line is a ladder-type network. The number of legs of the ladder network is ( $n = 10 \text{ mi}/0.0833 \text{ mi per span}$ ) 120. An equivalent circuit of the ladder network can be computed using z-transform methods [27] or an approximate equivalent circuit assuming that the ladder network extends to infinity. The approximate equivalent circuit is computed as illustrated in Fig. E7.8. Under the assumption of an infinitely long ladder network, the equivalent impedance  $Z_\infty$  is the same at any node of the ladder network (see Fig. E7.8a). Thus, from Fig. E7.8b,



(a)



(b)

FIG. E7.8 Ladder network reductions. (a) Ladder network, (b) equivalent network.

$$Z_\infty = Z_s + \frac{Z_p Z_\infty}{Z_p + Z_\infty}$$

Upon manipulation of equation above, we have

$$Z_\infty^2 - (Z_p + Z_s)Z_\infty - Z_s Z_p = 0$$

Solution of the equation above for  $Z_\infty$  gives us

$$Z_\infty = \frac{Z_s}{2} + \left[ \left( \frac{Z_s}{2} \right)^2 + Z_s Z_p \right]^{1/2}$$

Note that the other solution of the quadratic equation is rejected on the basis that it yields a capacitive impedance.

Application of this equation to the problem yields

$$Z_{\infty} = 9.048 + j3.78 \Omega$$

Now the circuit of Fig. E7.7 is reduced to the one in Fig. E7.9. The figure also illustrates the connections of the sequence networks for a single line-to-ground fault on the high side of the transformer. The electric currents are

$$\tilde{I}_1 = \tilde{I}_2 = \tilde{I}_0 = \frac{66.39 \text{ kV}}{34.30 + j131.06 + Z_e} = (0.49 \text{ kA})e^{-j73.87^\circ}$$

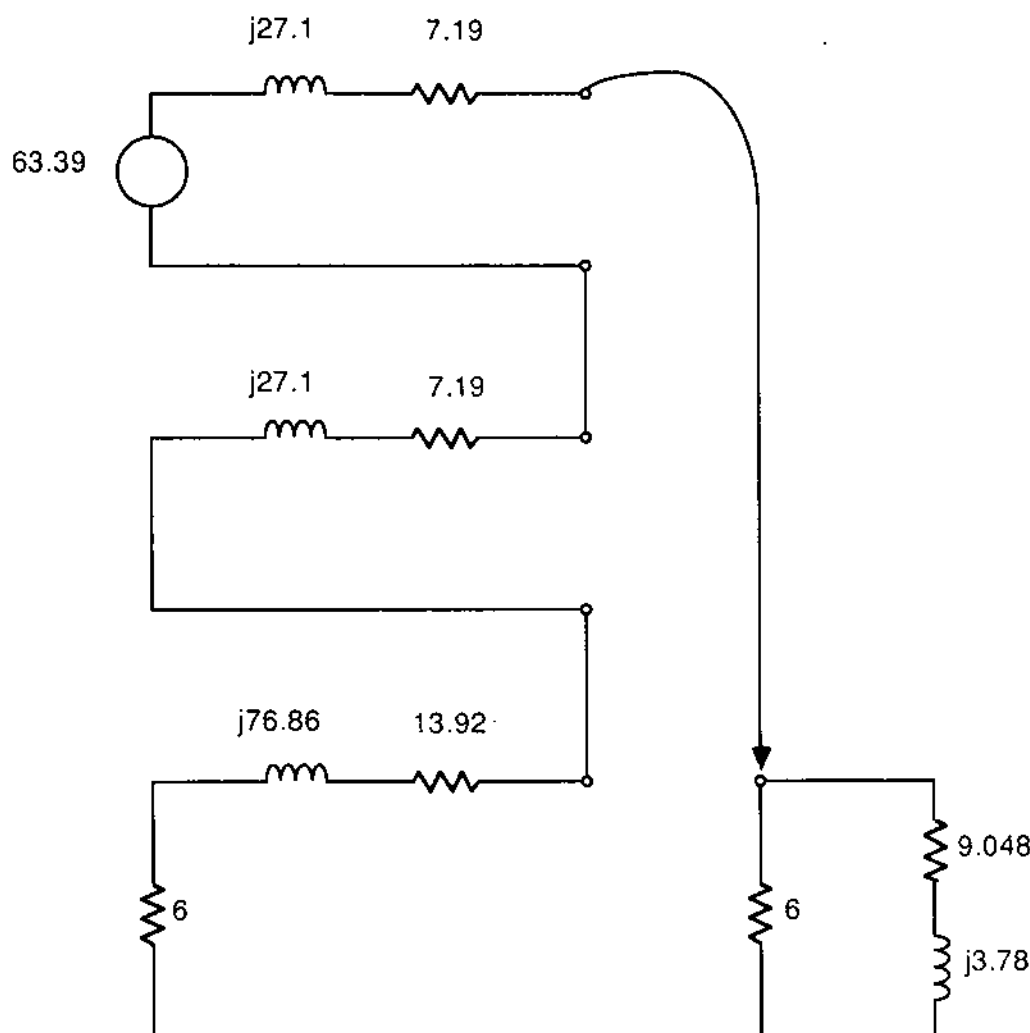


FIG. E7.9 Reduced sequence networks and connections for a single line to ground fault.

where

$$Z_e = 6.0 \parallel (9.048 + j3.78) = 3.75 + j0.565 \Omega$$

The fault current is

$$I_F = 1.47 \text{ kA}$$

The ground potential rise is

$$\text{GPR} = |Z_e I_0| = 1.858 \text{ kV}$$

The electric current division (earth current over fault current)

$$a = \left| \frac{Z_\infty}{6.0 + Z_\infty} \right| = 0.632$$

Example 7.2 has demonstrated the procedure for current distribution and ground potential rise computations using the sequence networks. A number of comments are pertinent to clarify the limitations of the method. First, if simplifying assumptions are not introduced, the resulting network problem is very large. Second and most important, the per unit system cannot be used. This is so because in this case electric current flows directly from the 115-kV system into the grounding structures of the 12-kV line without going through a transformer. This fact will necessitate the inclusion of ideal transformers for transformer representation. In general, the method becomes unattractive. For this reason and because the sequence models neglect line asymmetries, direct phase analysis becomes preferable for the analysis of fault current distribution. Direct phase analysis is presented in the next section.

## 7.7 DIRECT PHASE ANALYSIS

The symmetrical component method has been widely accepted and used in electric power engineering. However, its applicability is limited to power system analysis problems for which the assumption of symmetric three-phase systems is acceptable. For many analysis problems such as short-circuit analysis, power flow analysis, transient stability, and so on, this assumption has been widely accepted. For other applications, such as analysis of general multiphase networks or three-phase networks with single- and two-phase taps, the symmetrical component method becomes cumbersome. For the purpose of computing fault current distribution and ground potential rise, the symmetrical component method becomes very complex and thus unattractive. An

alternative approach is based on the admittance matrix representation of power system elements. We refer to this method as direct phase analysis. The method is simple and able to account for (a) asymmetries of power system elements (i.e., untransposed lines, etc.), (b) single- or two-phase systems, and (c) general multiphase systems. On the other hand, the method is computationally intensive.

### 7.7.1 Basis of the Method

The methodology is based on an admittance representation of symmetric or asymmetric single- or multiple-phase electric power system elements. For example, consider a single-phase transformer. This element can be viewed as a block with four terminals, as in Fig. 7.12. Neglecting magnetic core saturation, the device is linear. Thus a linear relationship exists among the terminal voltages and the terminal currents. That is,

$$\begin{bmatrix} \tilde{I}_1 \\ \tilde{I}_2 \\ \tilde{I}_3 \end{bmatrix} = Y \begin{bmatrix} \tilde{V}_1 \\ \tilde{V}_2 \\ \tilde{V}_3 \end{bmatrix} \quad (7.35)$$

Equation (7.35) is a general form of the Norton equivalent of the element under consideration. By definition, the matrix  $Y$  is the admittance matrix of the transformer. The admittance matrix is determined from consideration of the specific circuits of the element. In Chapter 6 we discussed the computation of the admittance matrix of a transmission line. In general, any linear power system element can assume a similar description. Once all elements are described in this fashion, nodal analysis is applied directly to analyze the electric power system at steady state.

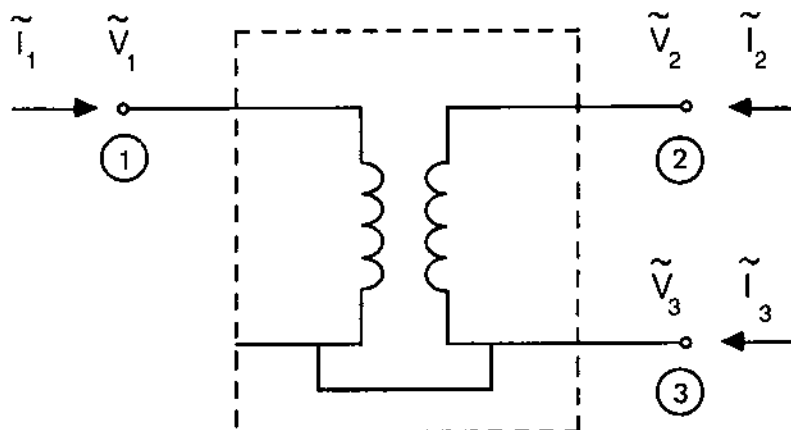


FIG. 7.12 A single phase transformer.

In subsequent sections the modeling procedure is described and the application of nodal analysis is outlined. An example will be employed to demonstrate the fault analysis in direct phase quantities.

### 7.7.2 Admittance Matrix of Power System Elements

In this section we present the basic modeling procedures by which the admittance matrix of power system elements are computed. The basic idea of these procedures is simple: The circuit equations describing the power system elements are written. Then all variables are eliminated except the terminal voltages and currents. The relationship between the currents and voltages provides the admittance matrix. Depending on the complexity of the power system element under consideration, the procedure may be simple or complex. The procedures are illustrated here with typical applications.

#### Single-Phase Transformer

A single-phase transformer is illustrated in Fig. 7.12. The equations describing the transformer are

$$\tilde{V}_1 - \tilde{V}_3 = (r_h + j\omega L_{hh})\tilde{I}_1 + j\omega L_{h\ell}\tilde{I}_2 \quad (7.36a)$$

$$\tilde{V}_2 - \tilde{V}_3 = (r_\ell + j\omega L_{\ell\ell})\tilde{I}_2 + j\omega L_{\ell h}\tilde{I}_1 \quad (7.36b)$$

$$0 = \tilde{I}_1 + \tilde{I}_2 + \tilde{I}_3 \quad (7.36c)$$

Equations (7.36) are written in compact matrix notation as follows:

$$A\tilde{V} = Z\tilde{I} \quad (7.37)$$

where

$$A = \begin{bmatrix} 1 & 0 & -1 \\ 0 & 1 & -1 \\ 0 & 0 & 0 \end{bmatrix} \quad (7.38)$$

$$Z = \begin{bmatrix} Z_h & Z_m & 0 \\ Z_m & Z_\ell & 0 \\ 1 & 1 & 1 \end{bmatrix} \quad (7.39)$$

$$Z_\ell = r_\ell + j\omega L_{\ell\ell}$$

$$Z_h = r_h + j\omega L_{hh}$$

$$Z_m = j\omega L_{h\ell} = j\omega L_{\ell h}$$

$$\tilde{I} = \begin{bmatrix} \tilde{I}_1 \\ \tilde{I}_2 \\ \tilde{I}_3 \end{bmatrix} \quad \tilde{V} = \begin{bmatrix} \tilde{V}_1 \\ \tilde{V}_2 \\ \tilde{V}_3 \end{bmatrix}$$

The matrix  $Z$  is not singular. Thus  $Z^{-1}$  exists. Premultiplication of Eq. (7.37) by  $Z^{-1}$  yields

$$\tilde{I} = Z^{-1} A \tilde{V} \quad (7.40)$$

Thus the admittance matrix of the single-phase transformer of Fig. 7.11 is

$$Y = Z^{-1} A \quad (7.41)$$

Example 7.3: A single-phase transformer is rated 15-kVA, 7200/240 V. The leakage impedance is 2.2% on its rating and the resistance is 0.8%. The magnetizing current is 0.7%. Compute the admittance matrix of the transformer.

Solution: Assuming that the transformer impedance is equally divided between the two windings (on a per unit basis), the parameters  $r_h$ ,  $L_{hh}$ , and so on, are computed as follows:

$$n = \frac{7200}{240} = 30$$

$$r_h = \frac{(0.4)((0.01)(7.2))^2}{0.015} = 13.824 \Omega$$

$$r_\ell = \frac{(0.4)(0.01)(0.24)^2}{0.015} = 0.01536 \Omega$$

$$\omega L_{h\ell} = \frac{(100.0/0.7)(7.2)(0.24)}{0.015} = 9600.0 \Omega$$

$$\omega L_{hh} = n \omega L_{h\ell} + \frac{(1.1)(0.01)(7.2)^2}{0.015} = 288038.016 \Omega$$

$$\omega L_{\ell\ell} = \frac{\omega L_{h\ell}}{n} + \frac{(1.1)(0.01)(0.24)^2}{0.015} = 320.04224 \Omega$$

$$Z_h = 13.824 + j288038.016 \Omega$$

$$Z_\ell = 0.01536 + j320.04224 \Omega$$

$$Z_m = j9600.0$$

Upon substitution into Eq. (7.41) and evaluation we have

$$Y = \begin{bmatrix} 0.004224 - j0.011616 & -0.12673 + j0.34851 & 0 \\ -0.12673 + j0.34851 & 3.8017 + j10.4565 & 0 + j0.001823 \\ 0 & 0 + j0.001823 & 0 - j0.001823 \end{bmatrix}$$

### Single-Phase Source

The admittance matrix representation of a single-phase source is computed as follows. The equations describing the model of Fig. 7.13 are

$$\tilde{V}_1 - \tilde{V}_2 = Z_s \tilde{I}_1 + \tilde{E}_s \quad (7.42a)$$

$$\tilde{I}_2 = -\tilde{I}_1 \quad (7.42b)$$

Upon solution of Eqs. (7.42) for  $\tilde{I}_1$ ,  $\tilde{I}_2$ :

$$\begin{bmatrix} \tilde{I}_1 \\ \tilde{I}_2 \end{bmatrix} = \begin{bmatrix} 1/Z_s & -1/Z_s \\ -1/Z_s & 1/Z_s \end{bmatrix} \begin{bmatrix} \tilde{V}_1 \\ \tilde{V}_2 \end{bmatrix} - \begin{bmatrix} \tilde{E}_s/Z_s \\ -\tilde{E}_s/Z_s \end{bmatrix} \quad (7.43)$$

Equation (7.43) is in the desired form.

**Example 7.4:** Consider a 7200-V single-phase source of internal impedance  $j2 \Omega$ . Compute the admittance matrix equation of the source.

**Solution:** The admittance matrix is

$$\begin{bmatrix} \tilde{I}_1 \\ \tilde{I}_2 \end{bmatrix} = \begin{bmatrix} -j0.5 & j0.5 \\ j0.5 & -j0.5 \end{bmatrix} \begin{bmatrix} \tilde{V}_1 \\ \tilde{V}_2 \end{bmatrix} - \begin{bmatrix} -j3600.0 \\ j3600.0 \end{bmatrix}$$

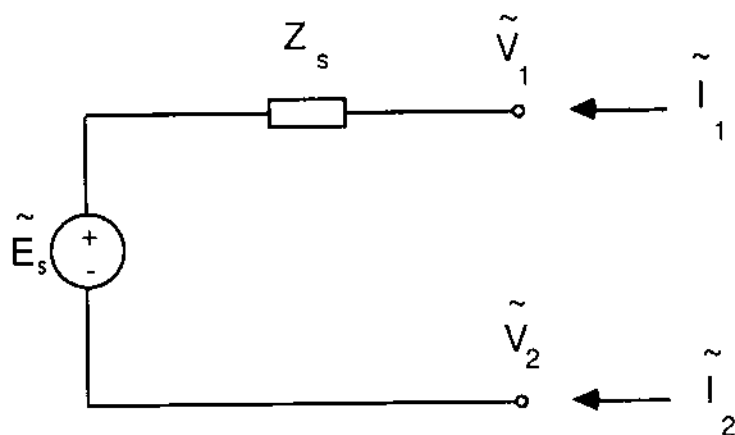


FIG. 7.13 A single phase source.

### Nodal Analysis

Consider an electric power system consisting of  $n$  interconnected elements. The admittance matrix representation for element  $k$  is

$$\tilde{I}^{(k)} = Y^{(k)} \tilde{V}^{(k)} - b^{(k)} \quad k = 1, \dots, n, \quad (7.44)$$

where  $Y^{(k)}$  is the admittance matrix of element  $k$  and  $b^{(k)}$  is the equivalent current source of element  $k$ .

For fault analysis, the fault is also considered as an element and the admittance matrix representation of the fault is computed. In this case one of Eqs. (7.44) represents the fault model. Equations (7.44) state that the electric current at any terminal of an electric power system element is a linear combination of the terminal voltages of the element plus a constant. On the other hand, the element may be connected to other elements. Consider an interconnection node  $j$  as illustrated in Fig. 7.14. Kirchhoff's current law applied at node  $j$  yields

$$\tilde{I}_{kj}^{(k)} + \tilde{I}_{mj}^m + \tilde{I}_{\ell j}^\ell = 0 \quad (7.45)$$

Now the electric currents appearing in Eq. (7.45) can be substituted from the Norton equivalent representation of the elements. The resulting equation will be in terms of node voltages only. The procedure must be repeated for every interconnection node in the system. In this way  $N$  independent equations will be obtained, where  $N$  is the number of interconnection nodes. Note that the number of unknown voltages will be also  $N$ . The  $N$  equations are written in matrix notation as follows:

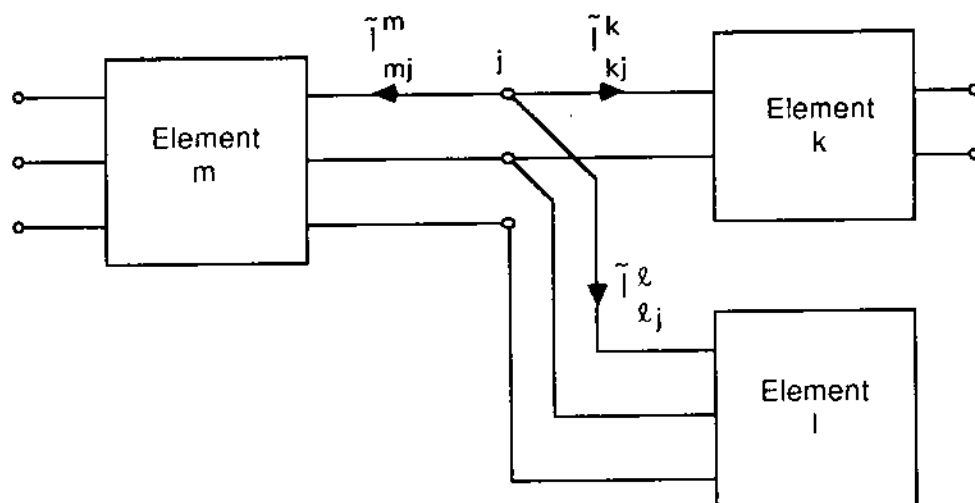


FIG. 7.14 A general interconnection node.

$$Y_N \tilde{V}_N = b_N \quad (7.46)$$

where

$Y_N$  = admittance matrix for the entire system constructed from the individual matrices  $Y(k)$ ,  $k = 1, 2, \dots, n$

$\tilde{V}_N$  = vector of voltages at the nodes of the system

$b_N$  = independent current sources, constructed from the individual current sources

Solution of Eq. (7.46) yields the voltage at every node in the system. Back substitution into Eqs. (7.44) yields the electric current at the terminals of each device. From this information, any other quantity of interest can be computed. For example, the ground potential rise of a substation grounding system is the voltage at the node representing the neutral, and so on. The procedure will be illustrated with an example.

Example 7.5: Consider the simple single-phase distribution system of Fig. E7.10. The single-phase distribution line is the line of Example 6.8. The equivalent single-phase source is a 7200-V source of internal impedance equal to  $j2.0 \Omega$ . The source ground impedance is  $25 \Omega$ . Assume a fault at the end of the distribution line. The fault impedance is  $0.1 \Omega$ . Compute (a) the fault current, (b) the ground potential rise at the fault location, and (c) the ground potential rise at the source.

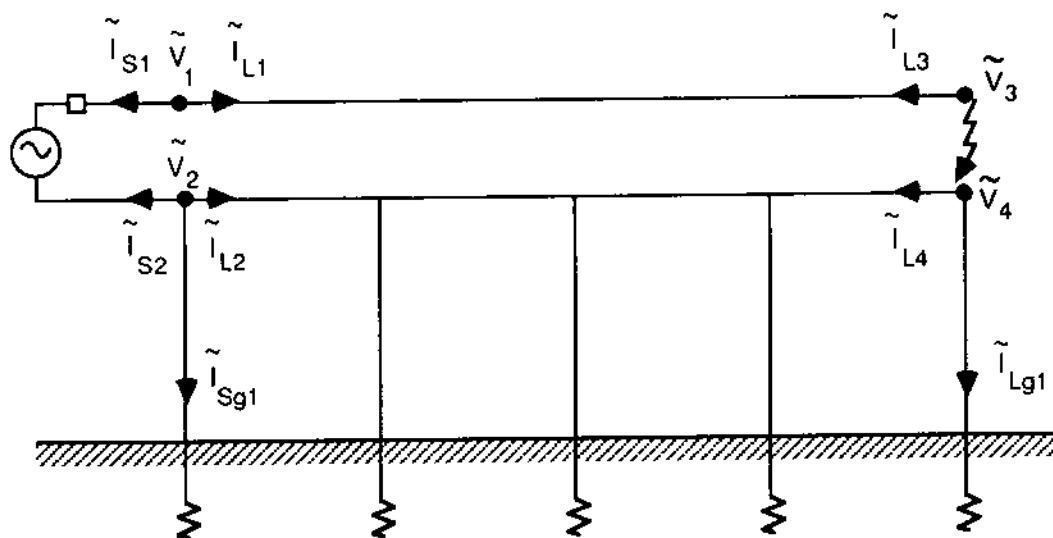


FIG. E7.10 Single phase distribution system.

Solution: The admittance matrix representation of the source and the distribution line has been computed in Examples 7.4 and 6.8, respectively. The source model is

$$\begin{bmatrix} \tilde{I}_{s1} \\ \tilde{I}_{s2} \end{bmatrix} = \begin{bmatrix} -j0.5 & +j0.5 \\ +j0.5 & -j0.5 \end{bmatrix} \begin{bmatrix} \tilde{V}_1 \\ \tilde{V}_2 \end{bmatrix} - \begin{bmatrix} -j3600.0 \\ j3600.0 \end{bmatrix}$$

The distribution line model is shown on page 299. The source ground model is

$$\tilde{I}_{sg1} = 0.04\tilde{V}_2$$

The remote end distribution line ground model is

$$\tilde{I}_{Lg1} = 0.02128\tilde{V}_4$$

The fault model is

$$\begin{bmatrix} \tilde{I}_{f1} \\ \tilde{I}_{f2} \end{bmatrix} = \begin{bmatrix} 10.0 & -10.0 \\ -10.0 & 10.0 \end{bmatrix} \begin{bmatrix} \tilde{V}_3 \\ \tilde{V}_4 \end{bmatrix}$$

Upon application of nodal analysis, the equation on page 299 is obtained. Upon solution of the equations, we obtain

$$\tilde{V}_1 = 1883 - j1523 = 2422e^{-j38.96^\circ} \text{ V}$$

$$\tilde{V}_2 = -460 + j412 = 617e^{j138.15^\circ} \text{ V}$$

$$\tilde{V}_3 = 826 - j896 = 1219e^{-47.33^\circ} \text{ V}$$

$$\tilde{V}_4 = 730 - j654 = 980e^{-j41.86^\circ} \text{ V}$$

The fault current is

$$\tilde{I}_f = 10.0(\tilde{V}_3 - \tilde{V}_4) = 960 - j2420 = 2603e^{j68.36^\circ} \text{ A}$$

The ground potential rise at the source is 617 V. The ground potential rise at the fault location is 980 V.

### 7.7.3 Discussion of Direct Phase Analysis

In this section we have presented procedures for fault analysis in power systems based on admittance matrix representation of power system elements. This representation of power system elements is

stribution line model:

$$\begin{bmatrix} L_1 \\ L_2 \\ L_3 \\ L_4 \end{bmatrix} = \begin{bmatrix} 1.063745 - j1.107711 & -0.498195 + j0.051057 & -1.063745 + j1.107712 & 0.498195 - j0.051057 \\ -0.498195 + j0.051057 & 1.073649 - j0.764127 & 0.498195 - j0.051057 & -1.063044 + j0.764097 \\ -1.063745 + j1.107712 & 0.498195 - j0.051057 & 1.063745 - j1.107711 & -0.498195 + j0.051057 \\ 0.498195 - j0.051057 & -1.063044 + j0.764097 & -0.498195 + j0.051057 & 1.073649 - j0.764127 \end{bmatrix} \begin{bmatrix} \tilde{V}_1 \\ \tilde{V}_2 \\ \tilde{V}_3 \\ \tilde{V}_4 \end{bmatrix}$$

quation obtained by nodal analysis:

$$\begin{bmatrix} 1.063745 - j1.607711 & -0.498195 + j0.551057 & -1.063745 + j1.107712 & 0.498195 - j0.051057 \\ -0.498195 + j0.551057 & 1.113649 - j1.264127 & 0.498195 - j0.051057 & -1.063044 + j0.764097 \\ -1.063745 + j1.107712 & 0.498195 - j0.051057 & 11.063745 - j1.107711 & -10.498195 + j0.051057 \\ 0.498195 - j0.051057 & -1.063044 + j0.764097 & -10.498195 + j0.051057 & 11.094929 - j0.764127 \end{bmatrix} \begin{bmatrix} \tilde{V}_1 \\ \tilde{V}_2 \\ \tilde{V}_3 \\ \tilde{V}_4 \end{bmatrix} = \begin{bmatrix} -j.36 \\ j.36 \\ 0 \\ 0 \end{bmatrix}$$

a generalization of Norton equivalents. The only assumption involved in this representation is that the power system elements are linear devices (i.e., the nonlinearities are ignored). The solution method is a straightforward application of nodal analysis. The procedure is computationally intensive and suitable for computer implementation. The advantage of the method stems from the capabilities of the admittance matrix representation. Specifically, the admittance matrix can model (a) transmission line asymmetries, (b) grounding systems, and so on. Thus this method is suitable to study the effects of asymmetries, ground potential rise, fault current distribution, and other factors.

## 7.8 TRANSFER VOLTAGES DURING FAULTS

Because the soil is not perfectly conducting, potential differences may be generated between two grounded points. As a matter of fact, electric currents do circulate in earth during even normal operating conditions. During fault conditions (especially asymmetric faults) the earth currents may be substantial, resulting in high-voltage elevation of grounding systems and transfer voltages to nearby metallic structures. These voltages may cause:

1. Safety problems
2. Misoperation or damage of communication circuits

Safety problems are generated whenever the voltages transferred to grounded structures are high enough to cause electric shocks to human beings or animals. Communication circuits are affected in two ways: (a) voltages are induced on these circuits from the electric currents of the power line which corrupt the useful signals with noise, increasing the possibility of misoperation, or (b) voltages may be transferred by conduction to communication circuits, which can cause interference problems or damage of communication equipment. The two interference mechanisms are illustrated in Fig. 7.15. The figure illustrates two communication circuits. Circuit 2 may be subjected to a voltage equal to the difference in the ground potential rise at the two grounds G1 and G2. Circuit 1 is parallel to the power line and is therefore subjected to induced voltage from the electric currents of the power line. Induced voltages are mitigated by transposing the communication circuit. In general, communication circuits must be protected against transferred or induced voltages. Protection schemes involve protection blocks, isolation transformers, neutralizing transformers, and so on. Judicious application of protection schemes requires that the maximum voltage on the communication circuit under any adverse conditions be computed.

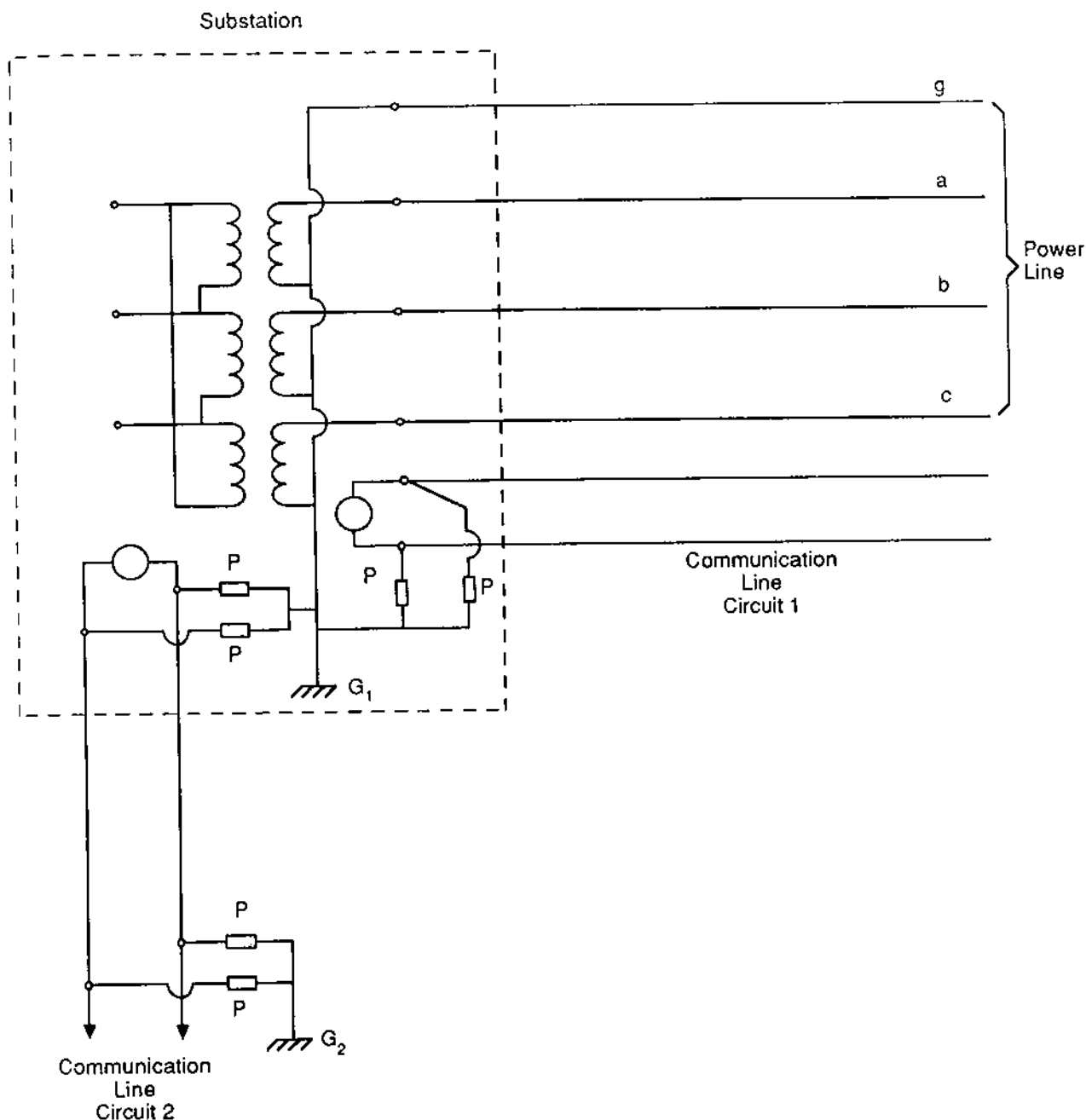


FIG. 7.15 Two mechanisms by which power lines can interfere with communication circuits. (a) Line 1 is subject to interference by induction, (b) line 2 is subject to interference by conduction.

The basic problem is illustrated by the simplified system of Fig. 7.16. A power transmission line is illustrated terminating in two substations. The substations each comprise a delta-wye-connected transformer. To the left of the figure is a source feeding the substation. Another power transmission line starts from the substation to the right of the figure. Both substations are grounded with a ground

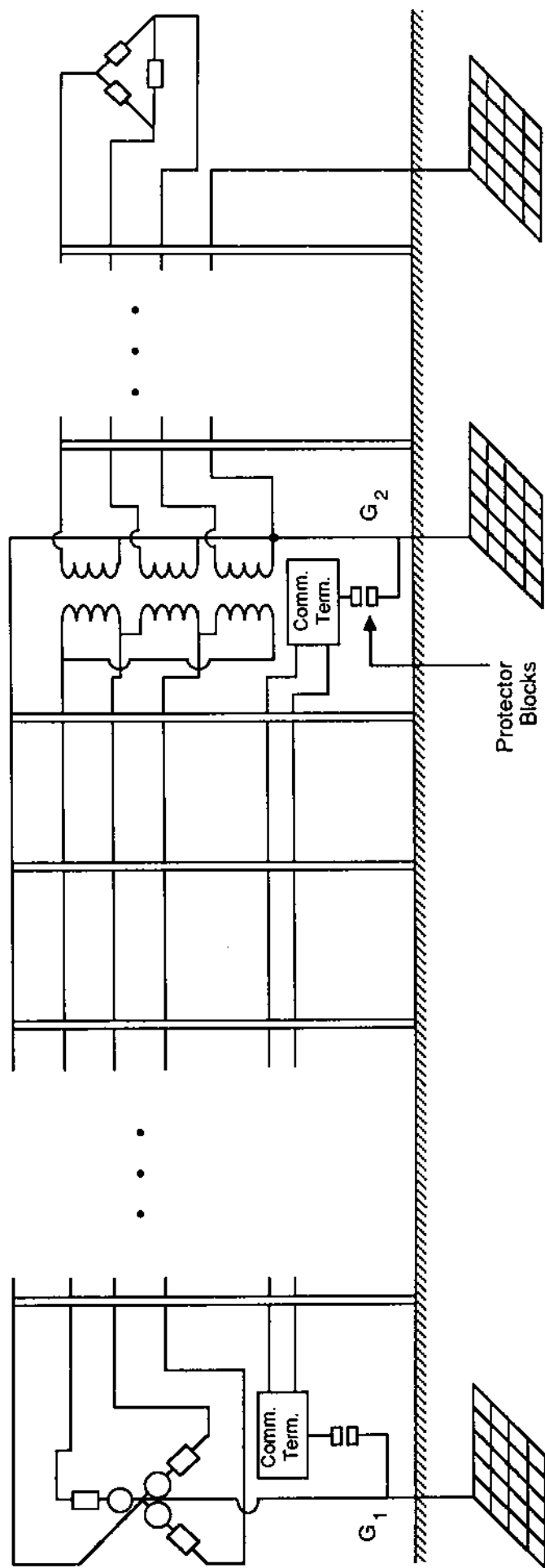


FIG. 7.16 Illustration of a communication circuit in the environment of a power system.

mat. A communication circuit  $t$  is suspended on the same towers as the power line. Typically, the communication circuit is connected to the substation grounding system through protector blocks. Our discussion will focus on the voltage induced or transferred to the communication circuit.

During normal operating conditions, almost balanced three-phase currents flow through the power line. The voltages induced on the communication line from each of the phase currents are approximately equal in magnitude. The phase difference between any two is  $120^\circ$ . Thus the total induced voltage is approximatley zero. On the other hand, the ground potential rise at the two grounds, G1 and G2, is small (smaller than the protection level of the protector blocks), and therefore the voltage transferred to the communication circuit is practically zero. However, during unbalanced conditions, the total induced voltage may be substantial. At the same time, the ground potential rise of the grounds, G1 and G2, may also be substantial. As a result, the communication circuit may be subjected to a substantial voltage and must be protected. Selection of the protection depends on the expected level of overvoltages during all foreseeable adverse conditions. Specifically, the protection scheme should be able to withstand the maximum voltage that may develop between points G1 and G2. Typical protection schemes of communication circuits are illustrated in Fig. 7.17. Scheme (a) involves protector blocks only. It provides protection for voltages up approximately to 300 V. Scheme (b) involves protector blocks and an isolation transformer. This scheme is capable of providing protection against much higher voltages, depending on the insulation level of the isolation transformer. Scheme (c) involves protection blocks and a neutralizing transformer. The neutralizing transformer is a three-winding transformer. The third winding will carry an electric current proportional to the voltage between points G1 and G2, which will insert a voltage on the communication circuit approximately equal but of opposite polarity (neutralizing voltage) of the voltage developed across the communication circuit (see Fig. 7.17c). Protection scheme (b) is simple, effective, and relatively inexpensive. The selection of the insulation level of the isolation transformer is based on the maximum voltage that can develop along the communication circuit under any foreseeable adverse conditions. For a specific condition, the voltage along the communication circuit can be computed using the direct phase analysis method. For this purpose, the wires of the communication circuit are modeled as conductors of the power line.

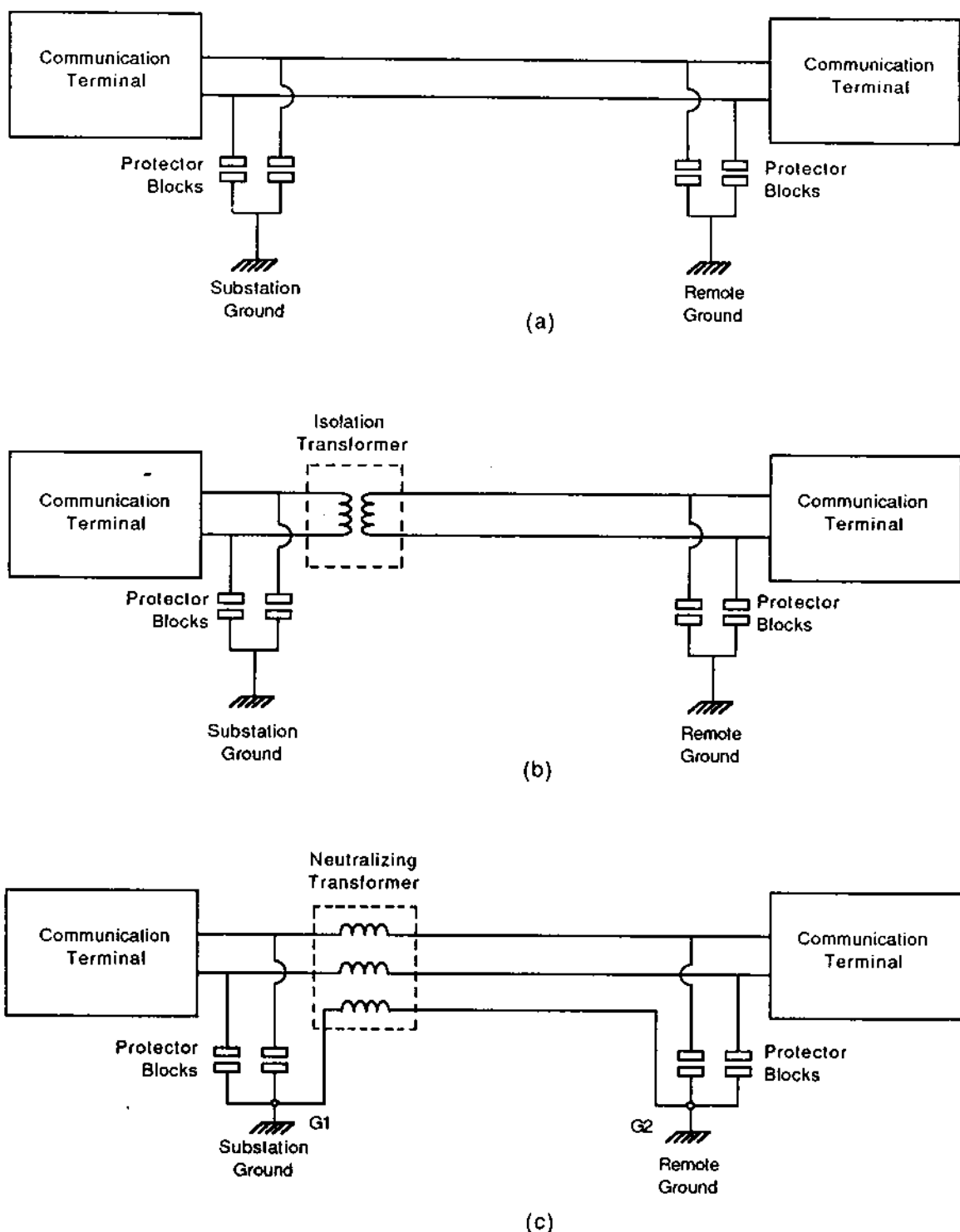


FIG. 7.17 Communication line protection schemes. (a) Protector blocks, (b) protector blocks and isolation transformer, (c) protector blocks and neutralizing transformer.

## 7.9 SUMMARY AND DISCUSSION

In this chapter we have discussed fault analysis methodologies. The conventional fault analysis method based on symmetrical components has been reviewed. An extension of the method has been presented which enables the computation of the fault current distribution and ground potential rise of grounding systems. The symmetrical component method neglects asymmetries existing in power system elements such as transmission lines. The direct phase analysis method has been presented, which takes asymmetries into consideration. Direct phase analysis is based on the admittance matrix representation of power system elements (or Norton equivalent) and nodal analysis. The method is computationally intensive and thus, by necessity, computer based.

## 7.10 PROBLEMS

**Problem 7.1:** A 40-mi three-phase 115-kV (line-to-line) transmission line is connected to an ideal three-phase balanced-voltage source as in Fig. P7.1a. The transmission line design is indicated in Fig. P7.1b. The phase conductors are ACSR, 397.5 kcm, 30 strands, while the shield wire is ACSR, 266.8 kcm, 26 strands. Compute the fault current (rms value) for a single phase (phase a)-to-ground fault at the remote end of the line. Neglect the capacitive current.

**Problem 7.2:** A three-phase transmission line connects two electrical power systems as in Fig. P7.2. Each of the power systems is represented as an equivalent source with the following sequence impedances:

$$Z_1 = j0.1 \text{ pu at } 100 \text{ MVA}$$

$$Z_2 = j0.1 \text{ pu at } 100 \text{ MVA}$$

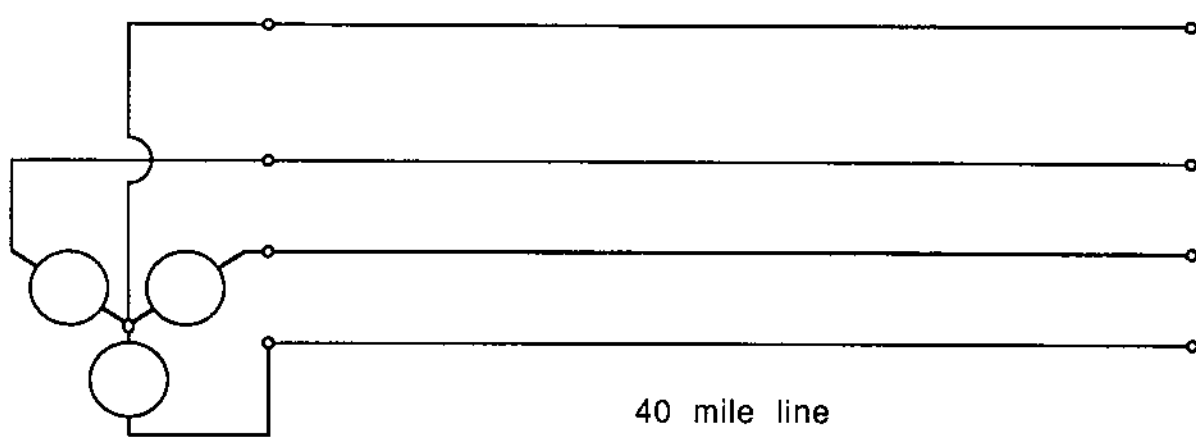
$$Z_0 = j0.06 \text{ pu at } 100 \text{ MVA}$$

The voltage sources behind the equivalent impedances are in phase. The parameters of the transmission line are

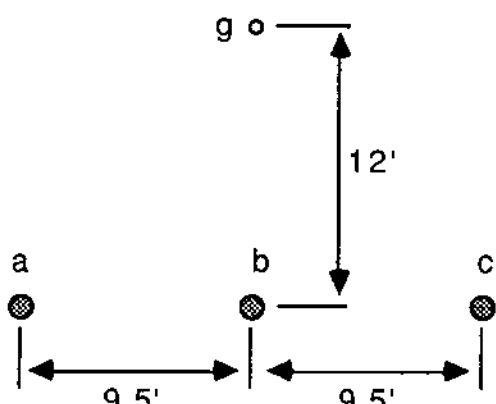
$$Z_1 = Z_2 = j0.8 \Omega/\text{mi}$$

$$Z_0 = j2.1 \Omega/\text{mi}$$

The operating voltage of the line is 115 kV line to line. The line length is 40 mi. Compute the fault current for a single line-to-ground fault at the middle of the line.



(a)



(b)

FIG. P7.1

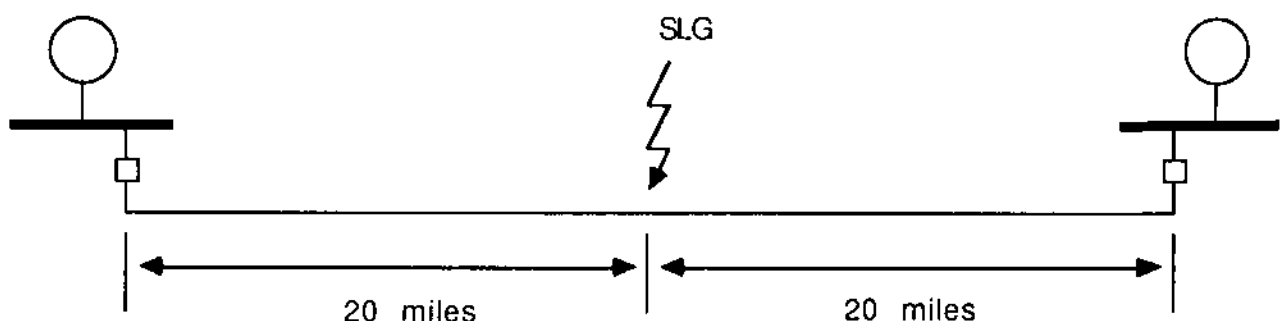


FIG. P7.2



FIG. P7.3

Problem 7.3: Consider the electric power distribution system of Fig. P7.3. Compute the ground potential rise for this system and for a single line-to-ground fault on the high side of the transformer (115 kV, delta side). The system parameters are:

Source: 115-kV line to line,  $Z_1 = Z_2 = j0.08$  pu on 100 MVA,  $Z_0 = j0.06$  pu on 100 MVA. The unit is grounded to its own grounding system through a coil. The total impedance (ground plus coil) is  $1.0 + j2.0 \Omega$ .

Transformer: 75 MVA, 115 kV/12 kV (delta-wye connected),  $Z_1 = Z_2 = Z_0 = j0.07$  pu on 75 MVA. The transformer is grounded. The ground resistance is  $1.5 \Omega$ .

Transmission line: The tower design is illustrated in Fig. 1.7. The phase conductors are ACSR, 1/0, and the neutral conductor is ACSR, No. 2, 7 strands.

Use the method of symmetrical components. Neglect the electric loads. Assume that the 12-kV line is infinitely long. The soil resistivity is  $100 \Omega \cdot m$ .

Problem 7.4: Consider an H-frame three-phase transmission line. The tower design of this line is illustrated in Fig. 1.5. The line is symmetrically transposed. The shield wires are 5/16-in. galvanized high-strength steel. The phase conductors are 500 kcm, ACSR, 30 strands. The tower footing resistance is  $25 \Omega$ . Tower separation is 500 ft. Soil resistivity is  $175 \Omega \cdot m$ . Compute the zero sequence network of the line which explicitly represents the shield wires and the tower footing ground impedance. Neglect the capacitive reactance.

Problem 7.5: Consider a three-phase transmission line with tower design as illustrated in Fig. 1.5. The line is effectively grounded. Compute the zero sequence series impedance of the line assuming that all the zero sequence current returns through the earth. Assume a  $175 \Omega \cdot m$  soil resistivity. The phase conductors are bundle conductors consisting of two subconductors spaced 12 in. apart. Each subcontractor is ACSR, 795 kcm, 54 strands.

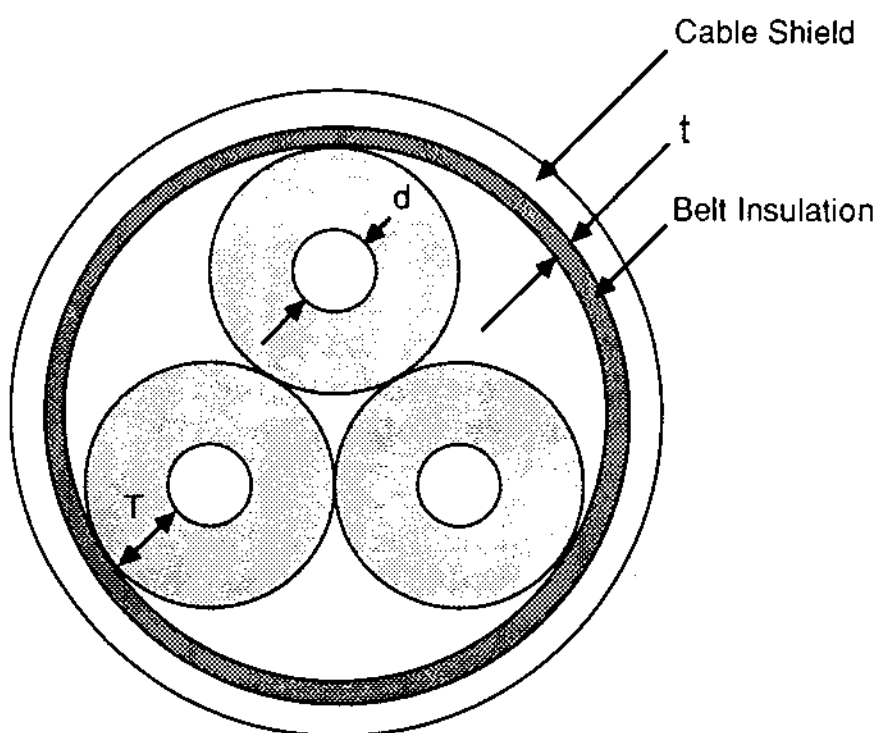


FIG. P7.4

Problem 7.6: Compute the zero sequence series impedance of the three-phase cable of Fig. P7.4. Neglect proximity effects. Assume that all zero sequence current returns through the cable shield. The geometric and electrical data of the cable are:

Conductor:  $d = 0.866$  in.

$\text{GMR} = 0.0305$  ft

$r = 0.091 \Omega/\text{mi}$

Insulation:  $T = 0.155$  in.

$t = 0.075$  in.

Cable shield:  $\text{GMR} = 1.237$  in.

$r = 0.558 \Omega/\text{mi}$

# 8

## Power System Grounding II Design Procedure

### 8.1 INTRODUCTION

The importance of well-designed grounding systems to the performance of power systems and safety of personnel has been recognized since the early days of power systems. Unfortunately, design procedures are hindered by a number of factors that are difficult to quantify. Based primarily on experience and simple analytical models, the first guide for the design of substation grounding systems was introduced in 1961: the ANSI/IEEE Standard 80. This document, together with two major revisions in 1976 and 1986, has been the primary tool available to substation engineers for analysis and design of substation grounding systems.

Standard 80 provides design criteria and guidance as to what should be considered in the process of designing a grounding system. In addition, it provides design equations applicable to simple grounding systems. The increased complexity and higher short-circuit capacities of present-day interconnected power systems requires improved analysis methods and design procedures for grounding systems. Improved analysis methods, which are computer based, have recently been developed. The basis and theoretical background for such methods have been discussed in Chapters 5 and 7. In this chapter we discuss utilization of these methods for a substation grounding system design.

## 8.2 BASIC PROBLEMS AND SOLUTIONS

The leading design criteria of substation grounding systems are (a) safety of personnel operating in and about the substation, and (b) minimization of ground potential rise, resulting in reduced protection requirements of communication equipment.

Hazards to personnel result primarily from touch, step, and transfer voltages during fault conditions on the interconnected power system. The protection requirements of communication circuits depend on the maximum possible ground potential rise and induced voltages. In general, the grounding system must be designed to:

1. Limit the ground potential rise of the substation ground mat to an acceptable value for any possible fault condition
2. Limit the resulting touch, step, and transfer voltages in and around the substation to values that are below the hazard level to human beings.

The two objectives are interrelated. Touch, step, and transfer voltages are proportional to the ground potential rise. The proportionality constants depend on the design of the grounding system. In general, the performance of a grounding system is determined from a large number of parameters, such as:

1. Soil resistivities in the vicinity of earth-embedded grounding conductors
2. Grounding grid area and geometry
3. Structure and parameters of the interconnected power system, including transformer connections, overhead ground wires, transmission tower grounding, counterpoise wires, and the use of URD cable

The basic problem in the design of grounding systems will be discussed with the aid of Fig. 8.1. The figure illustrates a distribution substation with one transformer, one transmission line, and one distribution line. Typically, the substation will have its own ground mat, ground rods, and so on. The towers/poles of the transmission line, as well as the distribution line, will have their own grounding system (counterpoise, ground rods, buttstrap, etc.). In normal operation, the voltage of the grounds will be near zero.

The power system of Fig. 8.1 is susceptible to short circuits inside the distribution substation or along the 115- or 12-kV lines. During an asymmetrical ground fault, electric current will flow from the grounding structures into earth. The level of the electric current flowing into earth (earth current) depends on the grounding structures, soil resistivities, design of the overhead power system, and location and type of the fault. The electric current flow in the

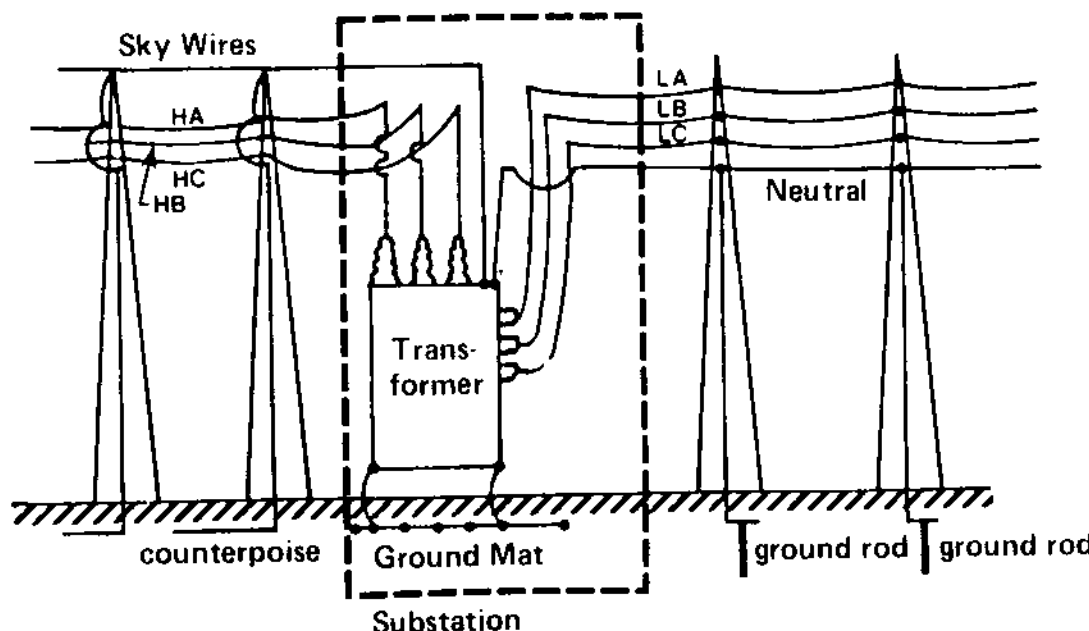


FIG. 8.1 Illustration of power system grounding structures.

earth causes the ground potential rise and potential distribution on the surface of the earth. The potential distribution in the earth determines touch, step, and transfer voltages. The grounding system is classified as safe if the touch, step, and transfer voltages meet postulated safety criteria. Thus grounding system analysis must address the following problems:

1. Determination of soil resistivities
2. Computation of maximum ground potential rise
3. Computation of touch, step, and transfer voltages
4. Safety assessment

Given a power system and the parameters of the grounding system, an analysis can be made to determine the maximum touch and step voltages that can occur in the system under adverse conditions. Analysis procedures for this purpose were discussed in previous chapters. With this in mind, the design procedure of a substation grounding system can proceed in an iterative fashion. The design engineer must assume a certain design and then perform an analysis of the design. The analysis determines whether the design criteria are met. In case they are not met, modifications must be made and the procedure repeated.

The general procedure outlined above involves the following specific tests:

Step 1. Perform soil resistivity measurement around the substation site.

Step 2. Analyze soil resistivity measurements to establish the soil parameters.

Step 3. Collect and prepare data for the interconnected power system.

Step 4. Assume a preliminary design for the substation ground grid.

Step 5. Compute the impedances of all grounding structures of the system, such as

- Substation ground resistance
- Tower footing resistance

Step 6. Perform a detail analysis of the substation grounding system to determine ground resistance, maximum touch voltage, and maximum step voltage as a percentage of ground potential rise.

Step 7. Identify the worst fault type and location and determine by computation the maximum earth current (or maximum ground potential rise).

Step 8. Perform a safety assessment. Specifically, compute the maximum touch voltage and maximum step voltage in volts.

Determine whether these values meet postulated safety criteria. If yes, the procedure stops here. Otherwise, the design must be modified and steps 6, 7, and 8 must be repeated.

The design procedure described is illustrated in Fig. 8.2. For a typical substation grounding system design, one or two iterations of the foregoing procedure will yield a design that meets design criteria. In subsequent sections we elaborate on the constituent components of the procedure described above.

### 8.3 DETERMINATION OF A SOIL MODEL

The first step in the design procedure is to determine the soil model in the vicinity of the substation. The soil model can be established through a number of field tests. Of those the most widely used are the Wenner method and the driven rod method. Both methods are very simple to implement. There are several commercial instruments for performing these measurements. The two methods are discussed in detail below.

#### 8.3.1 Wenner Method

The Wenner method is probably the most widely used in practice. It involves placing four small pins into the earth in a straight line, as illustrated in Fig. 8.3a. A source, connected between the outer pins, generates an electric current which is injected into the earth from one pin and collected at the other pin. The flow of this electric current in the earth generates a potential distribution in the soil. As a result, the potential at the location of the two inner pins is nonzero. The voltage between the two inner pins is measured

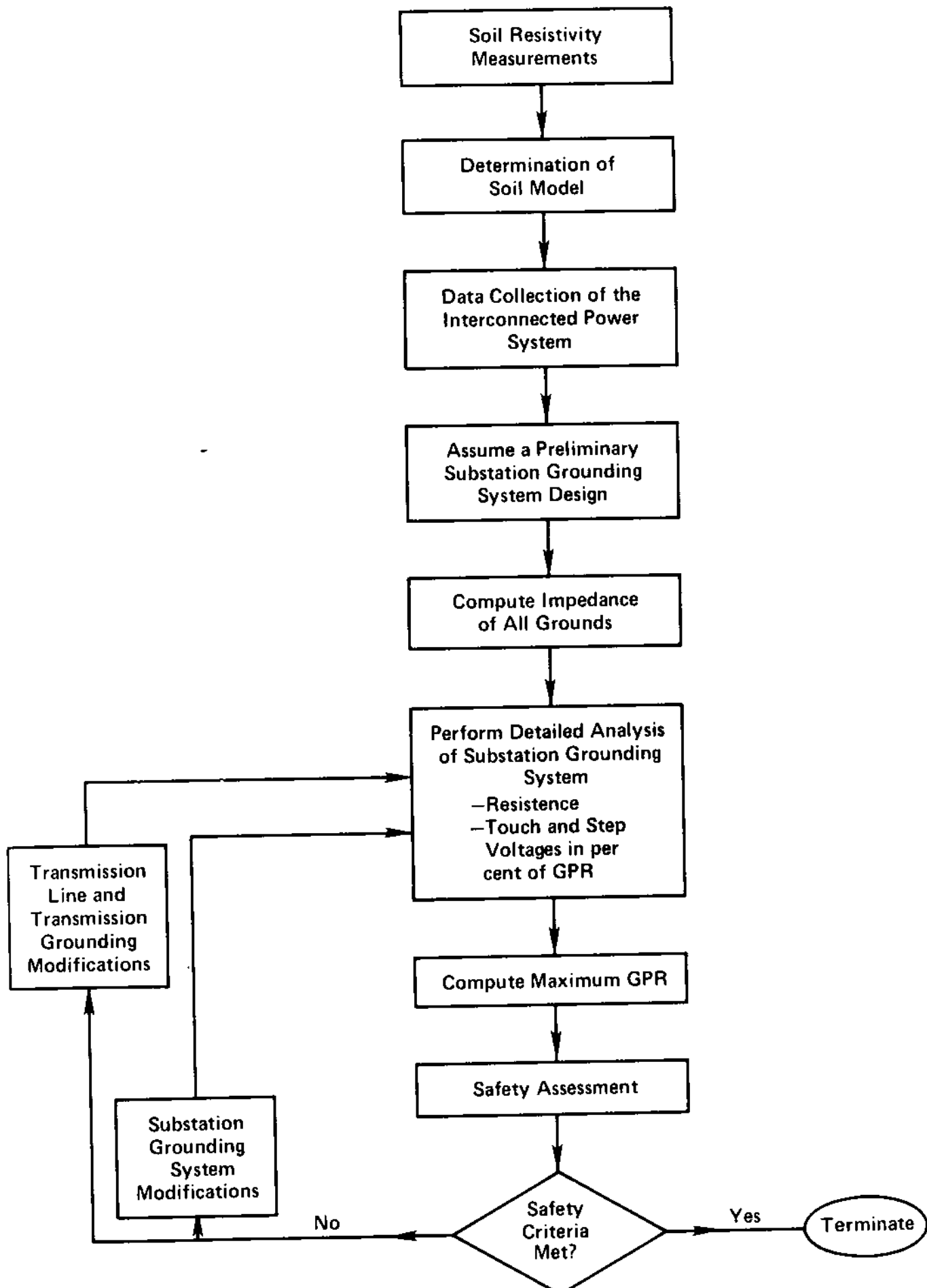


FIG. 8.2 Design procedure of substation grounding systems.

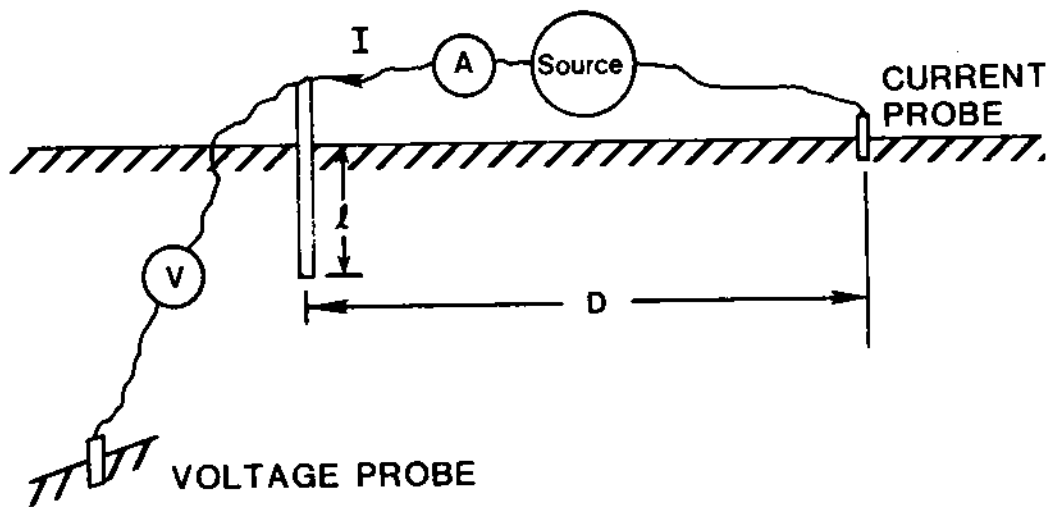
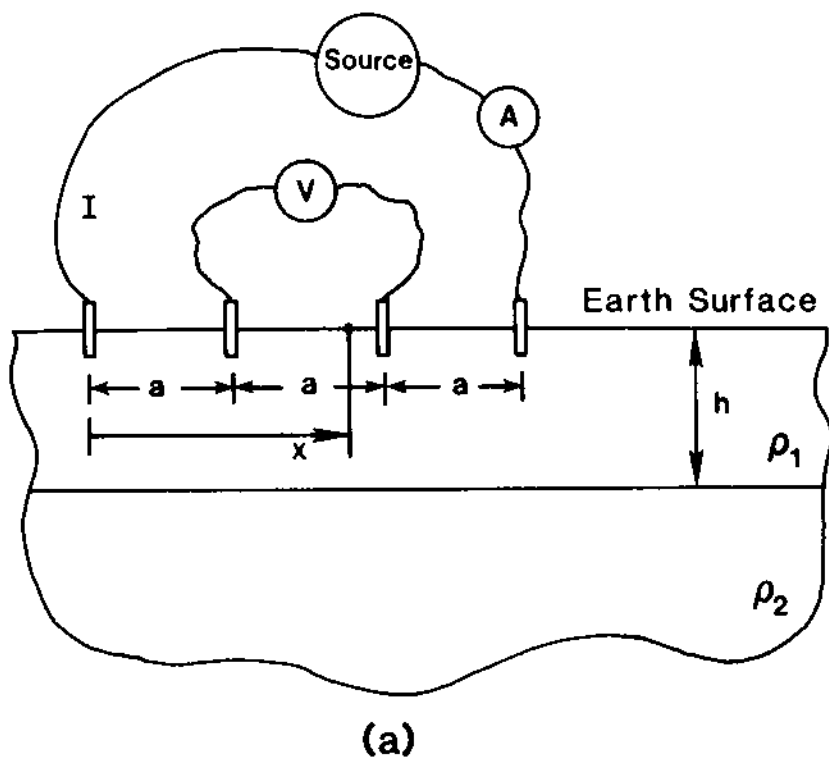


FIG. 8.3 Soil resistivity measurement system arrangements.  
(a) Wenner method, (b) driven rod method.

with a voltmeter. The injected current  $I$  and the measured voltage  $V$  are related to the resistivity of the soil. This relationship is obtained as follows. Assume that the length of the pin is very small compared to the separation distance between them. In this case the two outer pins can be considered as point current sources of current  $I$  and  $-I$ , respectively, located on the surface of the earth. The

voltage at a point along the line of the pins, located at a distance  $x$  from the pin injecting current  $I$  into the soil (see Fig. 8.3a) is given by the following equation (see Chapter 5):

$$V(x) = \frac{\rho I}{2\pi x} - \frac{\rho I}{2\pi(3a - x)} \quad (8.1)$$

The voltage of the two inner pins is  $V(a)$  and  $V(2a)$ , respectively. Thus the voltage  $V$  between the two inner pins is

$$V = V(a) - V(2a) = \frac{\rho I}{2\pi a} \quad (8.2)$$

Solving for the soil resistivity  $\rho$  gives us

$$\rho = 2\pi a \frac{V}{I} \quad (8.3)$$

In a uniform soil, the four-pin arrangement should provide the same soil resistivity irrespective of the separation distance  $a$ . When the soil is not uniform, which is the most common case, the method will provide the "apparent soil resistivity," which depends on the separation distance  $a$ . From this information it is possible to determine a nonuniform soil model, as we discuss in Section 8.3.3.

### 8.3.2 Driven Rod Method

The driven rod method, as the name suggests, consists of inserting a ground rod into soil. When a length  $\ell$  of the ground rod is driven into the soil, the resistance of the ground rod with respect to remote ground is measured. For this purpose, a source is employed which is connected between the driven rod and an auxiliary electrode (current probe) located a distance  $D$  away from the driven rod, as illustrated in Fig. 8.3b. This connection causes electric current  $I$  to be injected into the earth from the driven rod which is collected at the auxiliary electrode. Another auxiliary electrode is used to measure the voltage of the driven rod. This electrode (voltage probe) is placed away from the driven rod and away from the current probe to minimize interference. The driven rod resistance with respect to remote earth is approximately  $R = V/I$ . This resistance is related to the soil resistivity. An approximate expression of a ground rod resistance to remote earth was obtained in Chapter 5:

$$R = \frac{\rho}{2\pi\ell} \ln \frac{2\ell}{a} \quad (8.4)$$

Upon solution of Eq. (8.4) for the soil resistivity

$$\rho = \frac{2\pi\ell R}{\ln(2\ell/a)} \quad (8.5)$$

If the soil is uniform (constant resistivity throughout), the driven rod method should provide the same soil resistivity irrespective of the length  $\ell$  of the driven rod in contact with the soil. When the driven rod method is applied to a nonuniform soil, it will provide an "apparent soil resistivity" which will vary with the length of the ground rod in contact with the soil. From these data a nonuniform soil model can be derived as discussed in Section 8.3.3.

In the application of the driven rod method, the position of the current and voltage probe is important. Specifically, the current probe should be placed away from the driven rod so that the electric field around the ground rod is not affected by the presence of the current probe. Similarly, the voltage probe should be placed at a point of approximately zero voltage, that is, a point whose voltage is not affected by the presence of the ground rod and the current probe. For further information, consult reference 57.

### 8.3.3 Discussion on Soil Resistivity Measurements

In this section we presented two techniques by which field measurements of soil resistivities can be translated into a soil model. These computations in general are done by computer. There are a number of commercially available computer programs that interpret the field data into a soil model [39-41]. One such computer model developed by the author is discussed here.

This model is the program SOMIP (SOil Resistivity Measurement Interpretation Program). SOMIP effectively addresses the most important practical aspects of the problem, which are:

1. The present state of the art in grounding system analysis can accommodate a two-layer soil model.
2. Actual soil is almost never stratified into two layers with constant resistivity in the two layers. Resistivity varies with depth, there are local discontinuities, and so on. In a large substation area, soil resistivity may be different in one corner than another.
3. Commercially available measurement systems utilize finite probes in a specific configuration to measure a certain resistance. From resistance measurements, the soil resistivities must be extracted.

Specifically, item 3 is taken care of by exactly modeling the measurement system as a multiground system (see Chapter 5). Both Wenner method and driven rod method arrangements can be accommodated. Item 1 is taken care of by utilizing a statistical estimation

procedure which yields the best estimate of the parameters of a two-layer soil [40]. "Best" means that the computed parameters optimize the distance between the model and the measurements. By far the most difficult item to address is 2. The methodology in SOMIP employs error analysis of the estimation procedure to determine error bounds on the soil parameters as a function of confidence level. For more information, consult reference 40. The final output of model SOMIP is the best estimate of the parameters of a two-layer soil model and error bounds on the soil parameters versus confidence level.

Typical outputs from the program SOMIP are illustrated in Fig. 8.4. Soil resistivity measurements have been taken with the four-pin method at the Valdosta substation of Georgia Power Company. Note that Fig. 8.4a illustrates the best estimate of soil parameters. Figure 8.4b illustrates the error bounds on soil parameters versus the confidence level. Figures 8.4c and d illustrate how well the model fits into the measurements. These figures provide a pictorial view of the information obtained with the program SOMIP. Reference 40 provides additional information on the subject of soil resistivity measurement analysis.

#### 8.4 COMPUTATION OF GROUND RESISTANCES

It has been mentioned that the most important design parameter of a grounding system is the ground potential rise. Since the ground potential rise depends, among other parameters, on the ground resistances, an investigation of the ground potential rise requires knowledge of the ground resistances. Initially, the design of the grounding system is not known. It is then necessary to assume a preliminary design of the grounding system and proceed. At this point of the design process, it should be recognized that the preliminary design, as well as the final design, is more or less limited by the available real estate of the substation. Recall from Chapter 5 that the ground resistance is primarily dependent on the soil resistivity and the area of the grounding system. Specifically, an approximate expression of the resistance of a ground mat is

$$R = \frac{\rho\sqrt{\pi}}{4\sqrt{A}} \quad (8.6)$$

where  $\rho$  is the soil resistivity and  $A$  is the area covered by the grounding system.

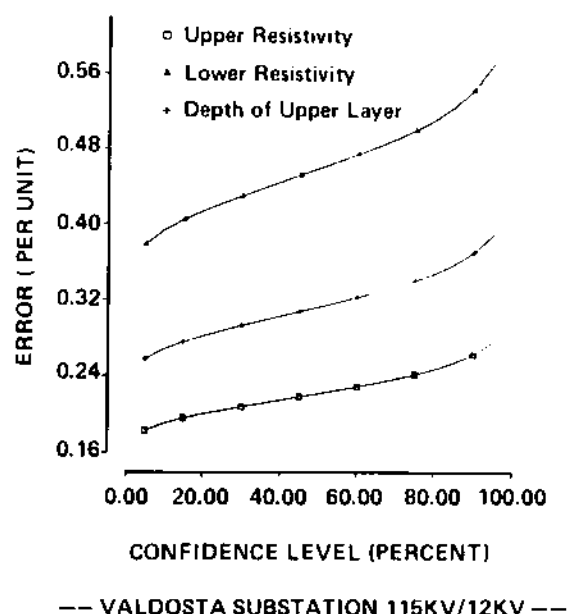
Other design changes, such as the addition of ground rods or more parallel conductors, will have a limited effect on the ground resistance. Thus on a preliminary basis, Eq. (8.6) suffices for an estimate of the ground resistance. In addition to the preliminary computation of the substation ground resistance, the ground re-

**FOUR PIN METHOD  
VALDOSTA SUBSTATION 115KV/12KV  
GEORGIA POWER COMPANY**

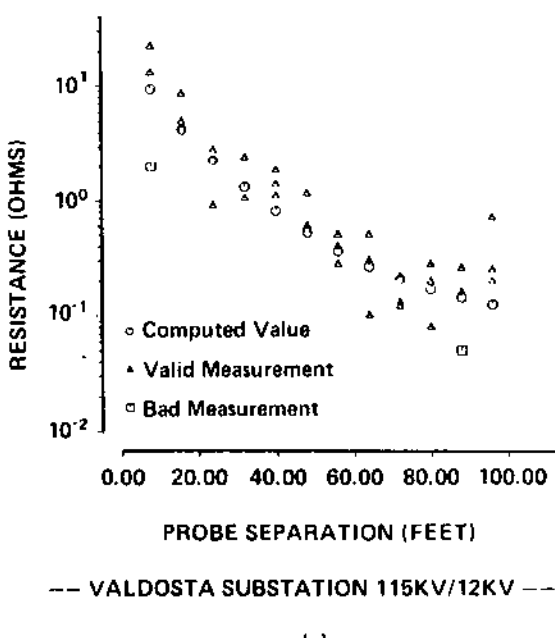
**Best Estimate of Soil Parameters:**

Upper Layer Soil Resistivity  
 $150.2 \text{ (ohm}^{\circ}\text{meter)}$   
 Depth of Upper Layer  
 $21.81 \text{ (feet)}$   
 Lower Layer Soil Resistivity  
 $19.4 \text{ (ohm}^{\circ}\text{meter)}$

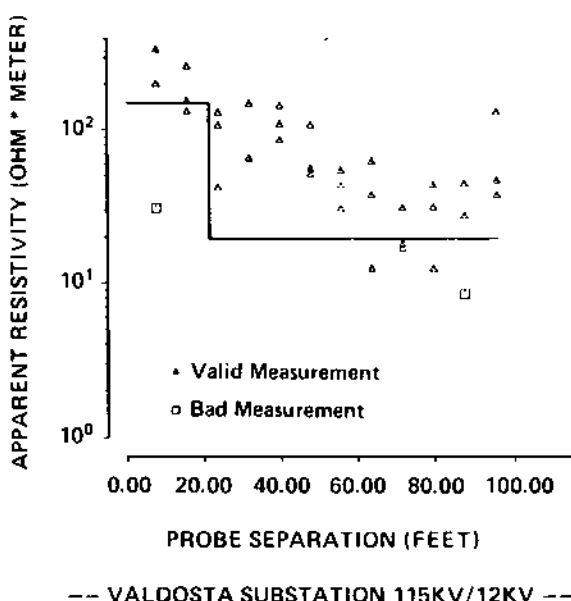
(a)



(b)



(c)



(d)

**FIG. 8.4** Typical output of the program SOMIP. Soil resistivity measurement at Valdosta substation. (a) Estimated soil resistivities, (b) quality of estimate, (c) and (d) model vs field data fit. (Courtesy of Georgia Power Company.)

sistance of distribution poles, transmission towers, and so on, should be computed. For this purpose the approximate formulas presented in Section 5.2 can be utilized. It should be emphasized that if computer-based analysis methods are available, the resistance of the preliminary substation grounding system and all other grounds (transmission towers, poles, etc.) can be accurately computed with these programs.

In summary, the ground resistance of all grounding structures in a system of interest must be computed. This information is required for a comprehensive investigation of the ground potential rise, discussed next.

## 8.5 MAXIMUM GROUND POTENTIAL RISE

Computational procedures for the ground potential rise have been presented in Chapter 7. In this chapter we consider the characteristics of the ground potential rise. For this purpose we examine the variation of the ground potential rise in simple power systems. Subsequently, we discuss the major parameters affecting the ground potential rise.

The ground potential rise is determined primarily by the parameters of the transmission circuits, transformers, generation, the location and type of fault, and the ground impedance. In general, three-phase faults or line-to-line faults do not result in substantial ground potential rise. Fault types that result in substantial ground potential rise are (a) single line-to-ground faults, and (b) double line-to-ground faults. For the purpose of designing grounding systems, it is important to determine the maximum possible ground potential rise. For a given system, there is a fault type at certain location which will result in a maximum ground potential rise for the grounding system under consideration. This fault condition (fault type and location) shall be called the worst fault condition. Conceptually, the determination of the worst fault condition is simple: One must consider all possible faults in a power system: for example, single and double line-to-ground faults inside the substation under consideration and similar faults along all transmission circuits connected to the substation. For each fault condition, the ground potential rise must be computed. The worst fault condition will be the one yielding the maximum ground potential rise. This conceptually simple procedure is computationally complex and possible only by computer. In subsequent paragraphs we shall discuss the basic characteristics of the ground potential rise.

### 8.5.1 Parametric Analysis of Ground Potential Rise

To obtain some insight into the behavior of the ground potential rise, we shall examine the variation of the ground potential rise of simple systems versus the most important system parameters affecting it.

For this purpose consider a simple system comprising a generation station, which is connected with a 25.6-mi 230-kV transmission line to a very large substation. The system is illustrated in Fig. 8.5. System data are listed in the figure. The tower design of the 230-kV transmission line is illustrated in Fig. 1.5. The phase conductors

$$\begin{aligned} S &= 300 \text{ MVA} \\ X_1 &= 0.18 \text{ pu} \\ X_2 &= 0.17 \text{ pu} \\ X_0 &= 0.09 \text{ pu} \end{aligned}$$

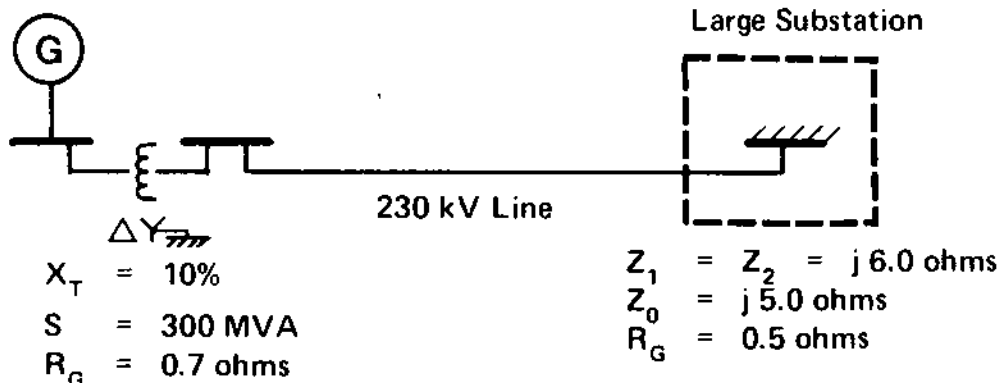


FIG. 8.5 Example system for ground potential rise study.

are ACSR, 1033.5 kcm, 54 strands. The overhead ground wires are Alumoweld 7, AWG No. 6. The tower grounding resistance is  $30 \Omega$  and the soil resistivity is  $100 \Omega \cdot \text{m}$ . For this system a single line-to-ground fault is placed on the transmission line at a distance  $x$  from the generation station. For this fault condition, the ground potential rise at the generation station is computed using the techniques presented in Chapter 7. The procedure is repeated for discrete  $x$  values, from  $x = 0$  (inside the generation station) to  $x = 25.6 \text{ mi}$  (inside the substation). Then the entire procedure is repeated for double line-to-ground faults. The computed ground potential rise versus the fault location is illustrated in Fig. 8.6a. The same analysis is performed assuming that one of the shield wires of the 230-kV line has been removed. The results are illustrated in Fig. 8.6b.

A number of comments are pertinent for the parametric results of Fig. 8.6. Consider the case of two overhead ground wires (Fig. 8.6a). Observe that the worst fault condition is a single line-to-ground fault approximately 4.5 mi from the generating station. The maximum GPR is 1995 V. Note that a fault on the high side of the step-up transformer yields a considerably lower ground potential rise. As the fault location moves away from the substation, the ground potential rise decreases initially and then starts increasing. It peaks for a fault at a distance of 4.5 mi from the generating station. Also note that for this system the single line-to-ground fault always yields a higher ground potential rise than does a double line-to-ground fault. (This is not in general true. Depending on system parameters, it is possible that a double line-to-ground fault will yield a higher ground potential rise.) It should be emphasized

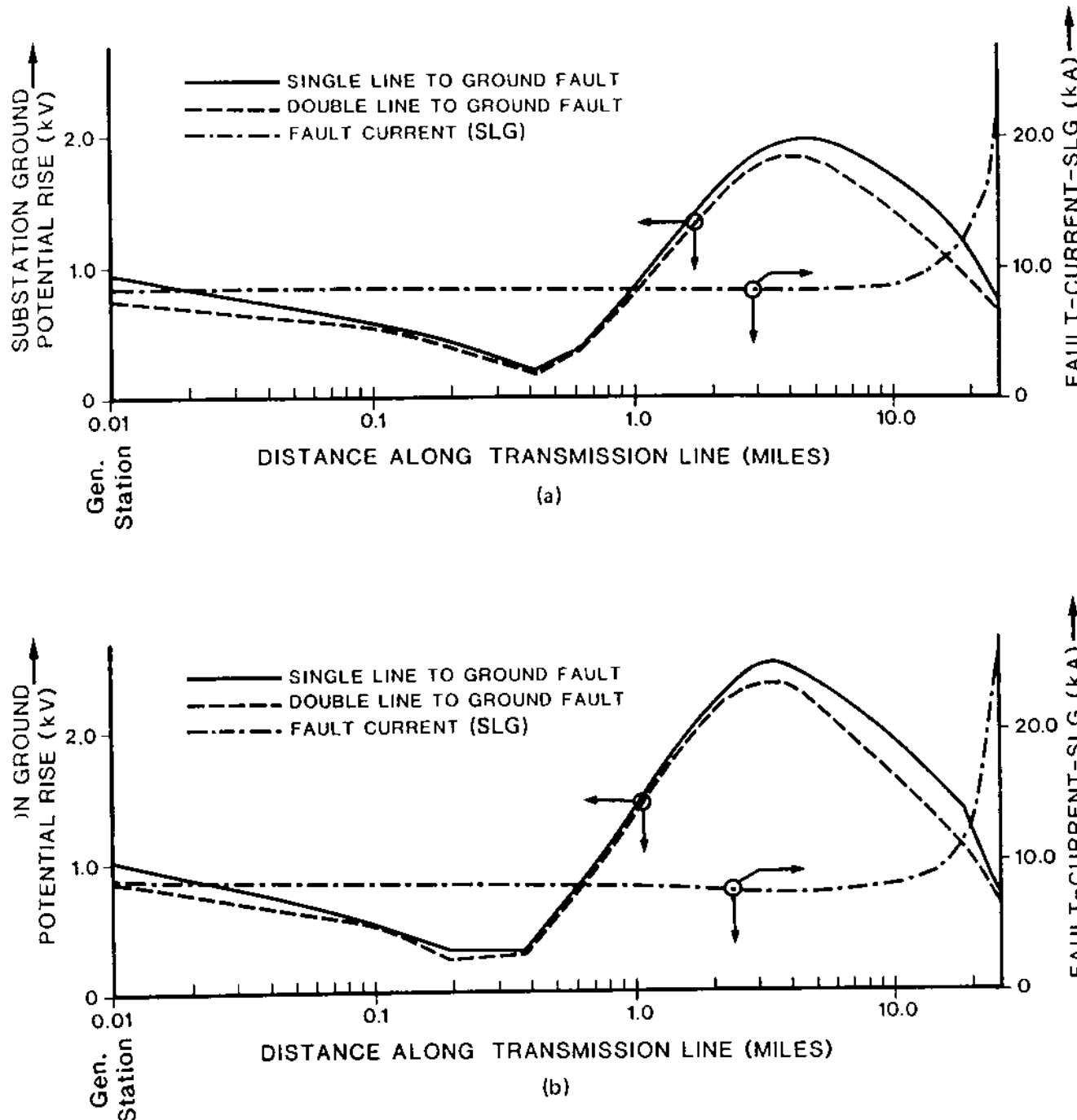


FIG. 8.6 Ground potential rise variation of a generation substation.  
 (a) Transmission line has two overhead ground wires, (b) Transmission line has one overhead ground wire.

that the worst fault type (in terms of ground potential rise) at a certain location is dependent on the system parameters. Now consider the case of one overhead ground wire (Fig. 8.6b). The same behavior of the ground potential rise is observed, except that the maximum ground potential rise occurs at a distance of 3.5 mi from the generating substation. The maximum ground potential rise is

2485 V. In general, removal of one of the shield wires results in a higher ground potential rise. This observation can be generalized. The addition of multiply grounded shield or neutral wires results in a lower ground potential rise, all other things being equal. The single line-to-ground fault current is also illustrated in Fig. 8.6.

Another usual case is illustrated in Fig. 8.7. The figure illustrates a distribution substation with one 6.4-mi-long 115-kV transmission line and one 1.6-mi-long 12-kV distribution line. The power system at the end of the 115-kV line is represented with an equivalent source. The sequence parameters of the source are illustrated in the figure. The tower design of the 115-kV transmission line is illustrated in Fig. 1.6. The phase conductors are ACSR, 336.4 kcm, 30 strands. The overhead shield wire is steel 5/16 in. in diameter. The tower design of the 12-kV distribution line is illustrated in Fig. 1.7. The phase conductors of the distribution line are ACSR, 1/0, and the neutral conductor is ACSR, No. 2, 7 strands. The parameters of the distribution substation transformer and the substation ground resistance are listed in the figure. The parametric analysis of the ground potential rise for this system is illustrated in Fig. 8.8. The figure illustrates the ground potential rise for single or double line-to-ground faults along the 115- and 12-kV lines. It also illustrates the fault current of the single line-to-ground fault. Note that for this system the worst fault condition is a single line-to-ground fault on the high side of the distribution transformer. This condition yields the maximum ground potential rise of 4109 V. Despite the fact that faults on the distribution line result in higher short-circuit current, they typically yield a smaller ground potential rise.

### 8.5.2 Discussion of Ground Potential Rise

In this section we discussed the basic factors affecting ground potential rise. The problem appears quite complex. Specific solutions to specific problems require computer analysis. A number of computer

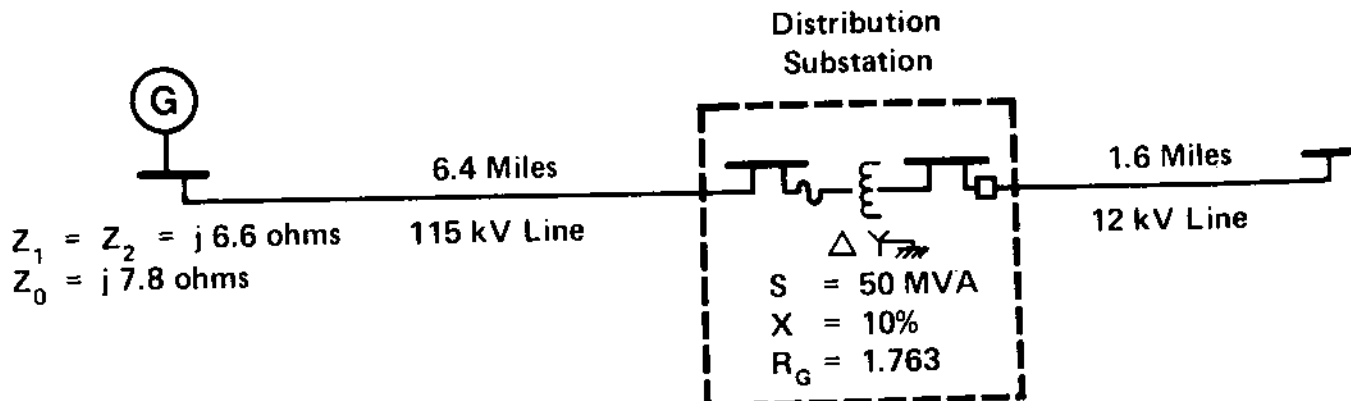


FIG. 8.7 A 115 kV/12 kV distribution substation.

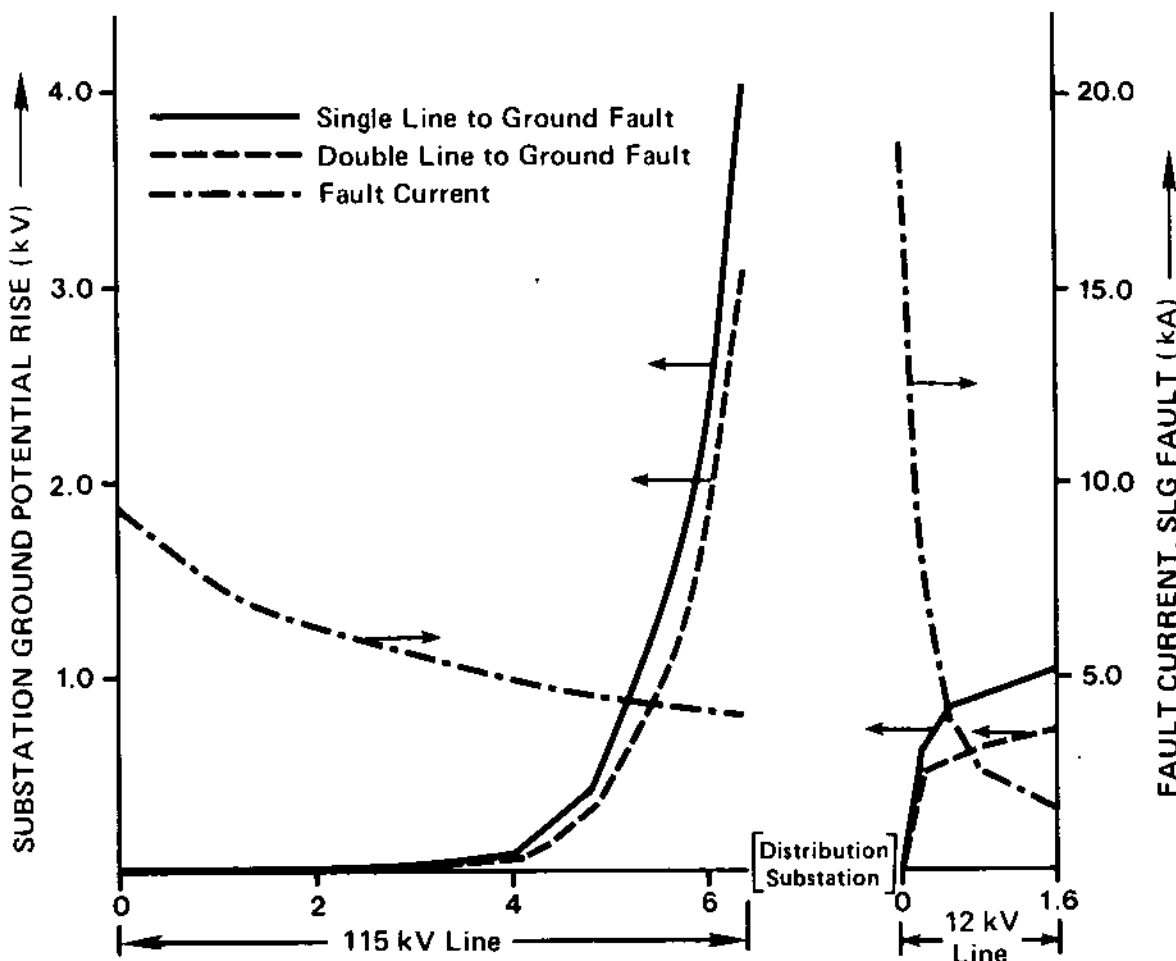


FIG. 8.8 Ground potential rise variation of a distribution substation.

models are available for this purpose. As an example, the program SMECC [37] computes the maximum ground potential rise for a given substation. Specifically, it determines the worst fault condition (fault type and location) that produces the maximum ground potential rise. The program employs a search algorithm which places faults on selected towers of transmission lines connected to the substation or inside the substation (high and low side). The faults are analyzed and the ground potential rise of the substation ground mat is monitored. The fault that results in the maximum ground potential rise is identified as the worst fault condition and the fault analysis results are reported. The computer model SMECC is based on the direct phase analysis method presented in Chapter 7. It can model systems comprising any number of (a) generators, (b) electric loads, (c) grounds, (d) delta-wye connected transformers, (e) wye-wye connected transformers, (f) transmission lines (single circuit or multiple circuits), and (g) autotransformers. For additional reading, consult reference 28.

Irrespective of what method or computer programs are used for this analysis, the investigation of the ground potential rise is the single most important task in the design process of a grounding system.

## 8.6 INVESTIGATION OF TOUCH AND STEP VOLTAGES

Once the ground potential rise is known for a grounding system, the touch and step voltages can be determined by computation. The calculation can be done with the simplified formulas (see Section 5.8) or with computer models. In either case it is important to determine the maximum touch and step voltages. In addition, an investigation should be performed to determine the existence of special points of danger. These topics are discussed next.

### 8.6.1 Determination of Maximum Touch and Step Voltages

In usual designs of substation grounding systems, the ground mat covers the entire area of the substation and extends a few feet past the substation fence. Usually, it is buried 1 to 3 ft below the surface of the earth. A human being may be standing anywhere inside the substation and touching a grounded structure while the worst fault condition occurs. The touch voltage at a point A on the surface of the earth inside the substation is

$$V_{\text{touch}} = \text{GPR} - V(A)$$

where GPR is the maximum ground potential rise and  $V(A)$  is the voltage of point A. The maximum touch voltage occurs at a point located approximately above the center of the outer mesh of the ground mat. Often, this touch voltage is referred to as mesh voltage. As an example, Fig. 8.9 illustrates the mesh voltages as a percentage of GPR for an 8 mesh x 8 mesh ground grid. Note that the maximum mesh voltage occurs in the corner mesh. The maximum step voltage will occur at the periphery of the ground mat near the corner. Approximate formulas for the maximum touch and step voltage in a typical rectangular ground mat are given in Chapter 5:

$$V_{\text{touch},\max} = \frac{\rho K_m K_i I_e}{L} \quad (8.7)$$

$$V_{\text{step},\max} = \frac{\rho K_s K_i I_e}{L} \quad (8.8)$$

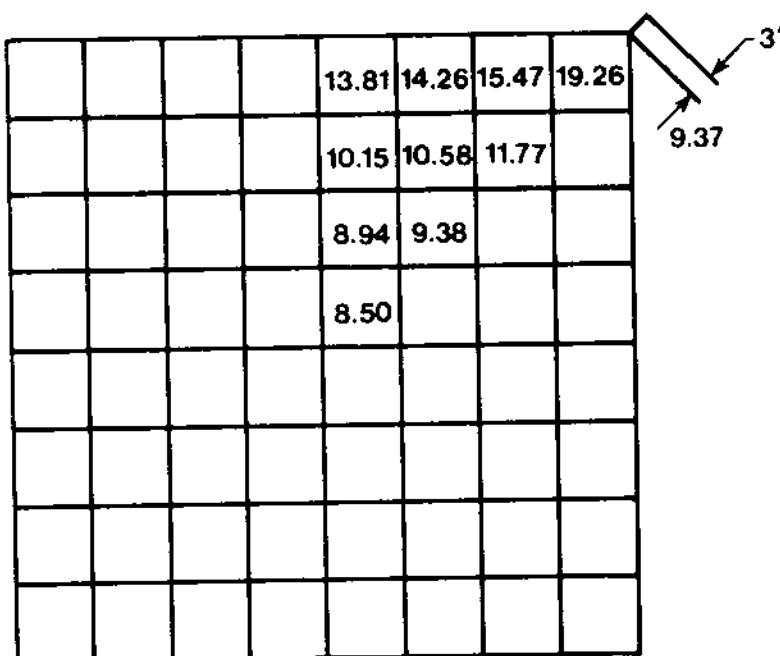


FIG. 8.9 Mesh voltages in an  $8 \times 8$  mesh ground mat. (Burial depth = 2 ft, mesh size =  $20 \times 20$  ft, uniform soil.)

where

$\rho$  = soil resistivity

$I_e$  = total current injected into earth

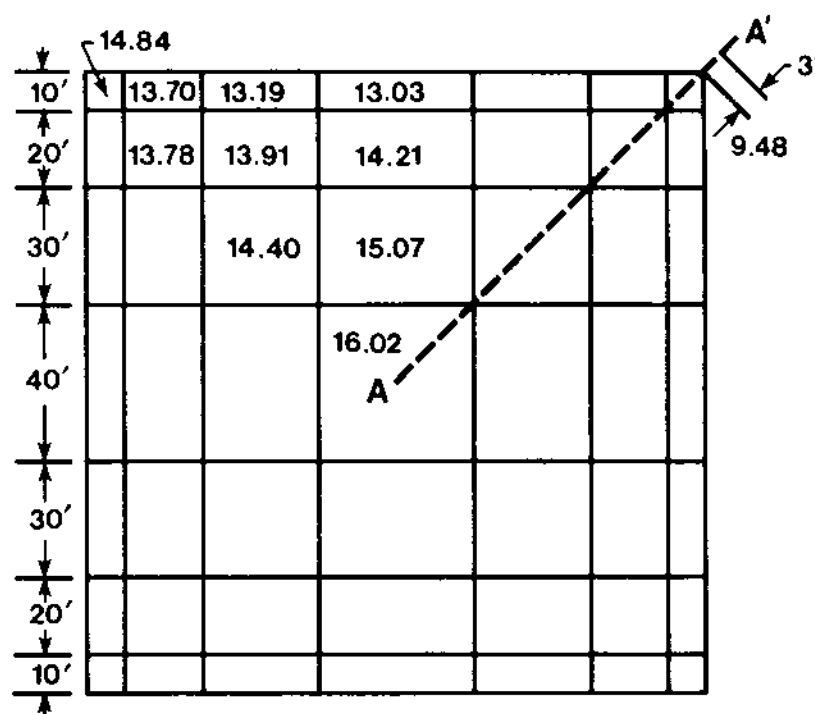
$L$  = total conductor length

$K_i$  = asymmetry factor (see Chapter 5)

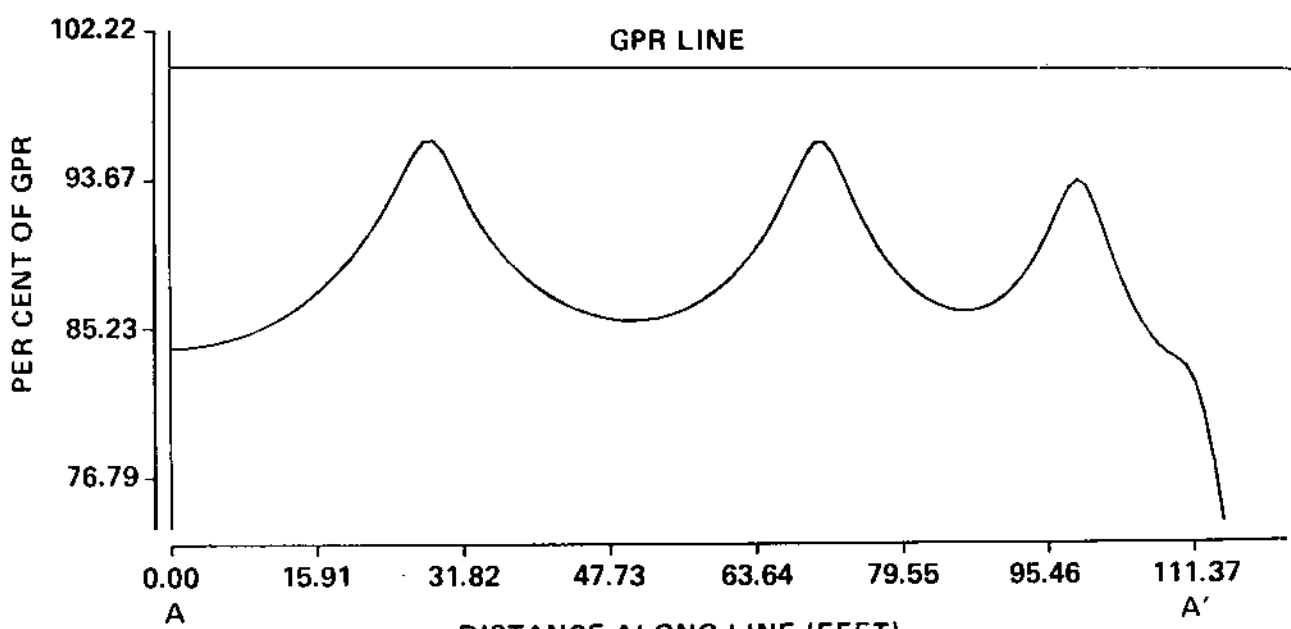
$K_m, K_s$  = geometric factors (see Chapter 5)

Recall that Eqs. (8.7) and (8.8) are applicable only to regular ground mats.

Many times, however, ground mats are irregular. In these cases it is not obvious where the maximum touch and step voltages will occur. In general, the maximum touch and step voltages will occur near the extremities of the ground mat. A good way to determine the maximum touch and step voltage in an irregular mat is to compute the voltage profile along the diagonal of meshes near the extremities of the ground mat. Practically, computation of the voltage profile requires the use of a computer model. The procedure is illustrated in Fig. 8.10, which deals with an irregular ground mat. Figure 8.10b illustrates the voltage profile along the diagonal of the ground mat. The difference between the ground potential rise (GPR line) and the voltage profile provides the touch voltage profile. By inspection, the maximum touch voltage occurs at the center of the ground mat. The mesh voltages are listed in Fig. 8.10a as a percentage of GPR. The maximum step voltage is also illustrated in the figure. A voltage profile provides a pictorial view of touch voltage distribution and indicates the location of the maximum touch voltage.



(a)



(b)

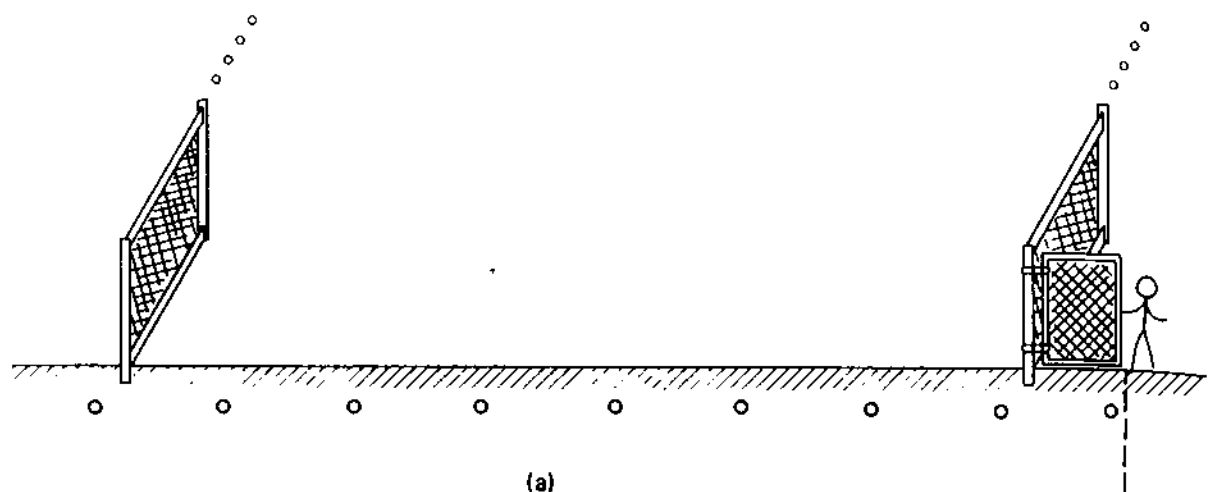
FIG. 8.10 Mesh voltages of an irregular ground mat. (a) Geometry of ground mat: burial depth = 2 ft, uniform soil, (b) voltage profile along line AA'.

### 8.6.2 Investigation of Special Points of Danger

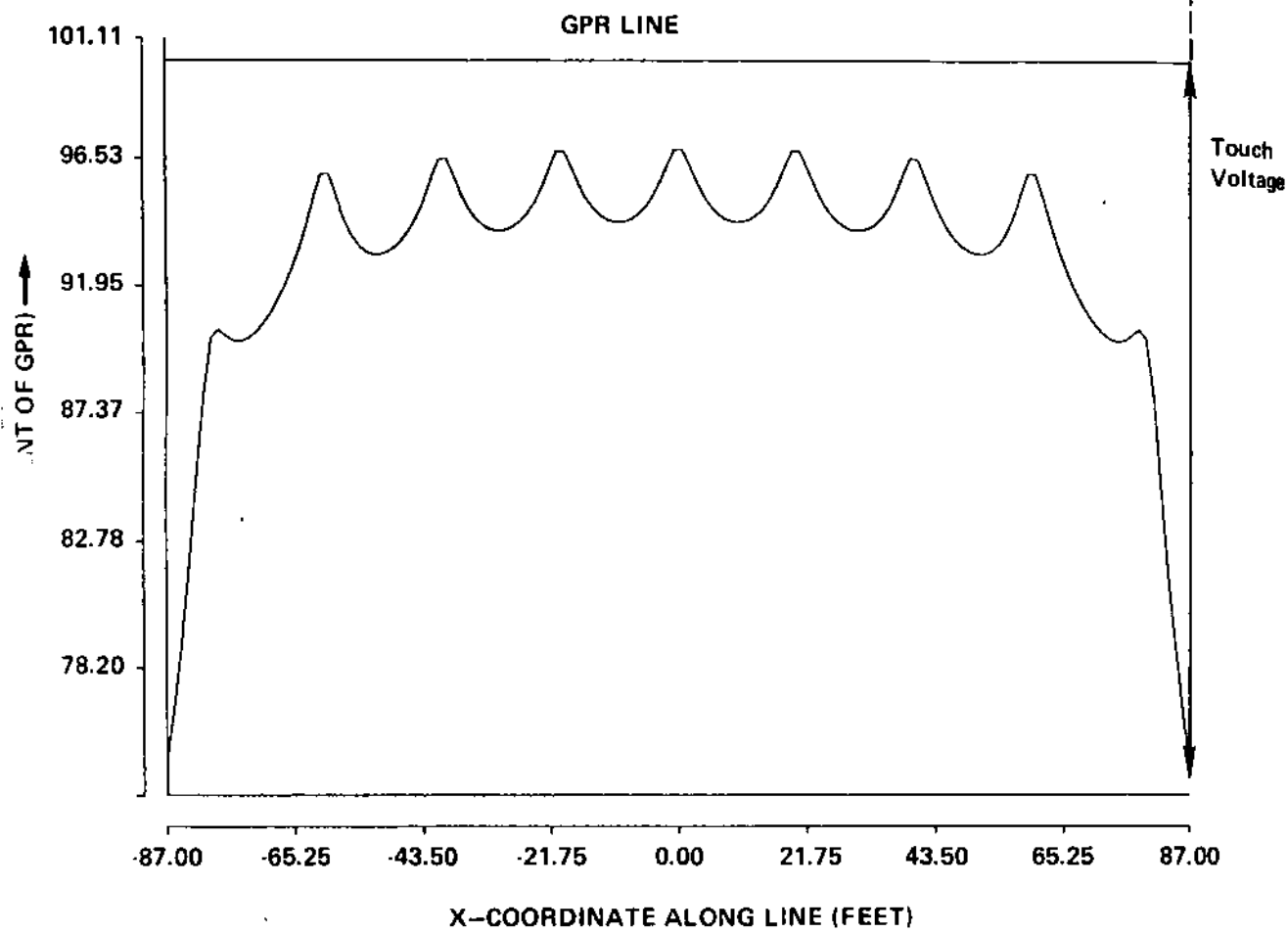
In a substation or an electric power installation, there may be points that could present higher danger under certain conditions. Such points are unique to specific installations. A somewhat common situation involving special points of danger occurs near the gate of a substation fence. The condition that results in higher danger is illustrated in Fig. 8.11. Assume that at the time someone is opening the gate, a fault resulting in maximum ground potential rise occurs. The human being holding the gate is subjected to a touch voltage  $V_T$  which is graphically determined in Fig. 8.11. Specifically, the figure illustrates that the ground grid extends 3 ft beyond the fence. The length of the gate is assumed to be 8 ft. Figure 8.11b illustrates the voltage profile on a line passing through the point where the person is standing. Assuming that the fence is bonded to the ground grid, the fence potential equals the ground potential rise. Thus the touch voltage is constructed as illustrated in Fig. 8.11b. Note that the touch voltage in this case may be considerably higher than the maximum mesh voltage. This special point of danger can be eliminated by extending the ground mat to cover the area spanned by the opening of the gate. In general, when a special point of danger is identified, it is possible to provide a simple solution.

### 8.6.3 Transfer Voltages to Nearby Metallic Structures

Earth-embedded metallic structures located in the vicinity of a grounding system but not electrically connected to a grounding system are subject to transfer voltages through the conductive soil. Such metallic structures include metallic pipes and fences. For certain geometric arrangements, it is possible that the transfer voltages may be substantial. In this case points of danger may be located away from the substation. Such a case is illustrated in Fig. 8.12. The figure illustrates the ground mat of a substation. Ten feet away from the ground mat there is a 320-ft metallic pipe that is bonded to the mat. Approximately 60 ft from the ground mat there is a fence which is not bonded to the pipe or the ground mat. The system is illustrated in Fig. 8.12a. Analysis reveals that a voltage will be transferred to the fence which will be 44.85% of the ground potential rise of the ground mat. Figure 8.12b illustrates the surface voltage profile along the line AA' illustrated in Fig. 8.12a and the voltage rise of the fence. Note that a person standing near point A' and touching the fence will be subjected to a touch voltage of  $V_T$ , illustrated in Fig. 8.12b. It is possible that this touch voltage will be substantial, presenting a safety hazard. In this case the system must be altered such that touch voltages resulting from the transferred voltage meet safety criteria.

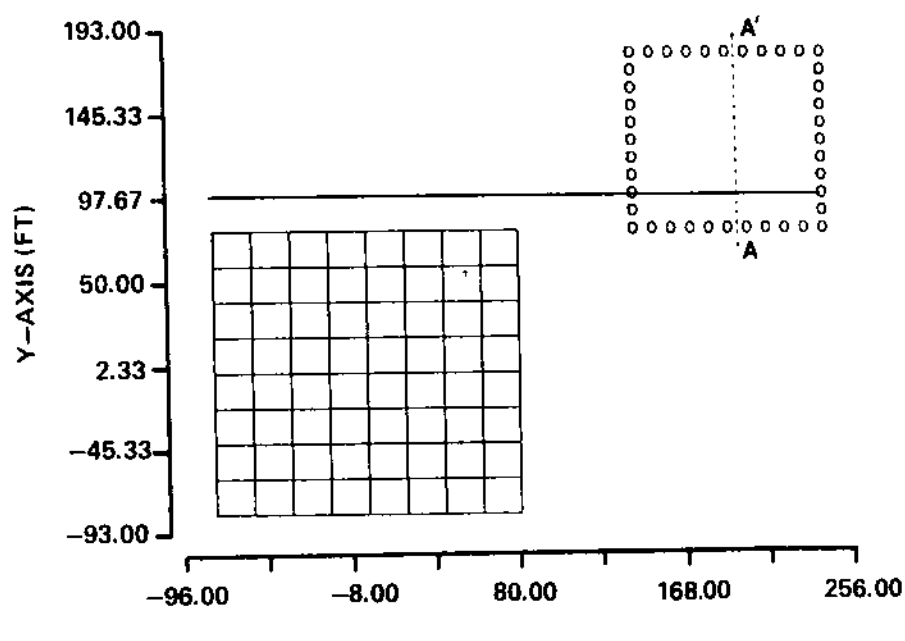


(a)

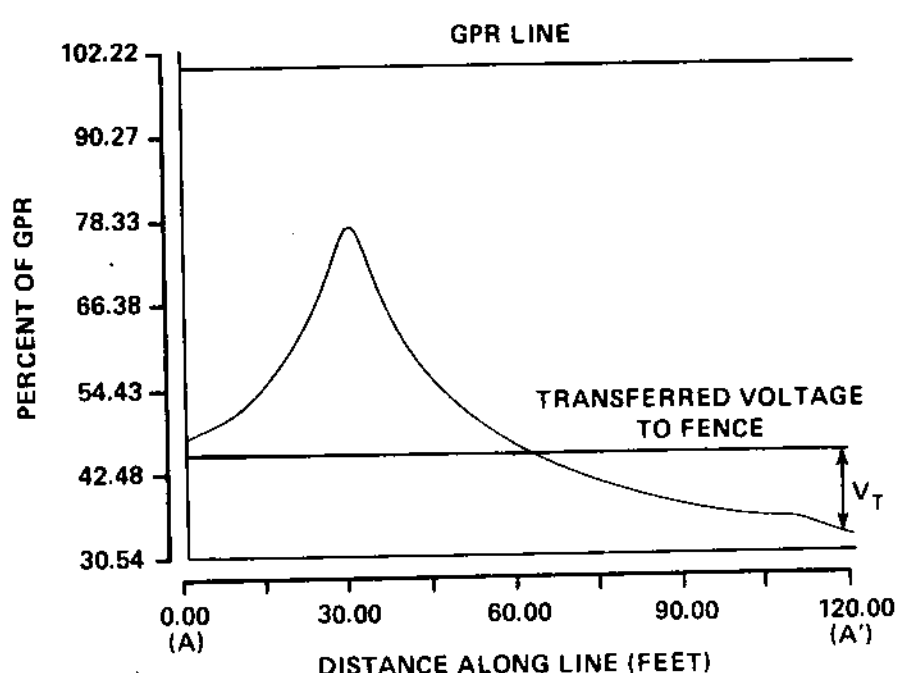


(b)

FIG. 8.11 Illustration of possible high touch voltage near the gate of a fence.



(a)



(b)

FIG. 8.12 Illustration of transfer voltages to nearby metallic structures and resulting touch voltages. (a) System configuration, (b) surface voltage profile along line AA'.

#### 8.6.4 Discussion of Touch and Step Voltages

In this section we have discussed procedures by which the maximum touch and step voltages in a substation can be determined. Special danger points have also been discussed. Exact analysis requires computer-based models. Several computed models exist for this purpose. One of these models is the program SGSYS. This program is capable of analyzing a grounding system consisting of one or more or any combination of the following elementary grounding structures: (a) ground mats, (b) ground rods, (c) fences, (d) metallic pipes, and so on. The elements of a grounding system may be bonded together or in groups, each group not connected directly to any other group (multiple grounds). The computer model produces the following information: (a) the resistance of the overall grounding system, (b) the touch voltage at a selected point, (c) the step voltage at a selected point and direction, (d) the voltage on a selected grid of points, (e) a plot of the voltage profile on a selected line segment, and (f) the transfer voltages on metallic structures not bonded to the grounding system, if such structures exist. The results illustrated in Figs. 8.9 through 8.12 have been obtained with program SGSYS.

### 8.7 SAFETY ASSESSMENT

Safety assessment is a procedure that determines whether the maximum touch and step voltages computed meet the postulated safety criteria. We shall assume the safety criteria suggested in ANSI/IEEE Standard 80 [18]. This criterion is defined in terms of the tolerable body currents, that is, the value of electric current that the average person can withstand without danger of electrocution (or the possibility of suffering ventricular fibrillation). Standard 80 suggests that the body current should not exceed the tolerable body current  $i_{bt}$ , defined by

$$i_{bt} = \frac{0.116 \text{ A}}{\sqrt{t}} \quad (8.9)$$

where  $t$  is the duration of the electric current in seconds.

In Section 5.4 we have seen how the tolerable body current is translated into a maximum allowable touch or step voltage. The equations are repeated here:

$$V_{\text{touch,allowable}} = \frac{0.116(1.5\rho + 1000)}{\sqrt{t}} \quad V \quad (8.10)$$

$$V_{\text{step,allowable}} = \frac{0.116(6\rho + 1000)}{\sqrt{t}} \quad V \quad (8.11)$$

where  $\rho$  is the soil resistivity expressed in ohm-meters and  $t$  is the duration of the electric shock expressed in seconds. The value of 1000 represents the resistance of the human body in ohms.

Then the safety of the grounding system is assessed with the equations

$$DV_{T,\max} \leq V_{\text{touch,allowable}} \quad (8.12)$$

$$DV_{S,\max} \leq V_{\text{step,allowable}} \quad (8.13)$$

where

$V_{T,\max}$ ,  $V_{S,\max}$  = steady-state rms values of the actual maximum touch and step voltages

$D$  = decrement factor, which accounts for the dc component of the touch and step voltages

The decrement factor  $D$  depends on the level of the dc component of the ground potential rise, the duration of the electric shock, and the attenuation rate of the dc component. For typical power systems and maximum dc component, the decrement factor  $D$  is tabulated in Table 8.1 as a function of the shock duration.

Equations (8.10) and (8.11) are valid for uniform soil of resistivity  $\rho$ . Often, the soil is not uniform or a layer of high resistivity is placed on the surface of the earth, for example, a layer of crushed stone (typically the layer is a few inches thick). In this case Eqs. (8.10) and (8.11) must account for the fact that the resistance of the human foot to earth is affected by the resistivity of the soil at the point of contact. This effect can be computed accurately using the methods presented in Chapter 5. An alternative procedure suggested in reference 18 is to incorporate a correction factor  $c_s$  in

TABLE 8.1 Decrement Factor D

Electric shock duration (Electric fault duration) (s)	Decrement factor, D
0.008	1.65
0.1	1.25
0.25	1.10
0.50 or more	1.00

Eqs. (8.10) and (8.11). The correction factor depends on the thickness of the upper layer  $h_s$  (crushed rock or whatever other material) and the relative soil resistivities between the upper layer and the remaining soil, defined by the constant K:

$$K = \frac{\rho - \rho_s}{\rho + \rho_s} \quad (8.14)$$

where  $\rho_s$  is the resistivity of the upper layer and  $\rho$  is the resistivity of soil below the upper layer. The correction factor  $c_s$  as a function of  $h_s$  and K is illustrated in Fig. 8.13. In terms of the correction factor  $c_s$ , Eqs. (8.10) and (8.11) become

$$V_{\text{touch,allowable}} = \frac{(0.116)(1.5c_s \rho_s + 1000)}{\sqrt{t}} \quad V \quad (8.15)$$

$$V_{\text{step,allowable}} = \frac{(0.116)(6c_s \rho_s + 1000)}{\sqrt{t}} \quad V \quad (8.16)$$

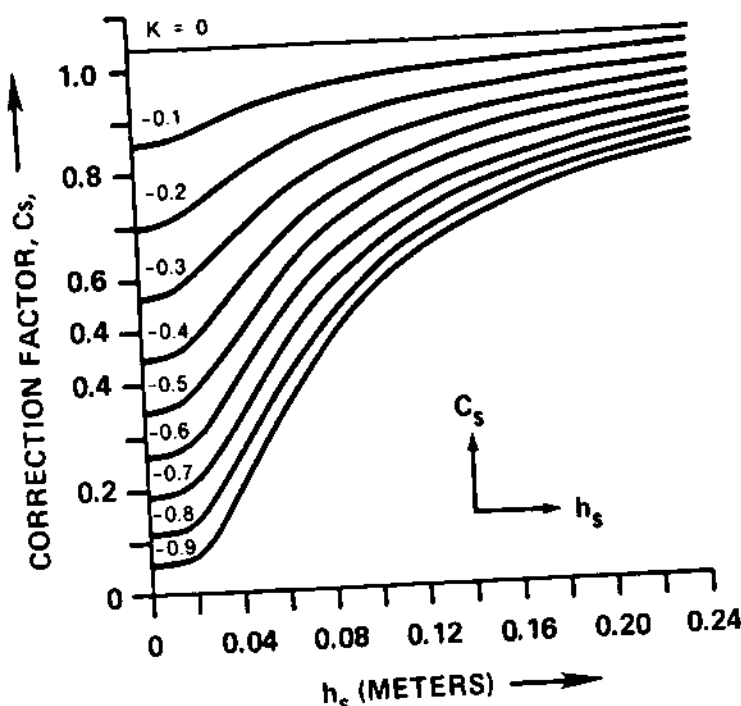


FIG. 8.13 Correction factor as a function of upper layer thickness  $h_s$  and factor K. (From: ANSI/IEEE Std 80, IEEE Guide for Safety in AC Substation Grounding.)

Equations (8.15) and (8.16) must be used whenever there is a layer of crushed rock of thickness  $h_s$  on the surface of the earth or when the soil is modeled as a two-layer soil.

## 8.8 MITIGATION OF TOUCH AND STEP VOLTAGES

More often than not, preliminary designs of grounding systems do not meet the stringent safety requirements of Standard 80. In this case it is imperative to modify the design such that safety requirements are met.

In general, two types of modifications can be made. One type of design modification results in increased allowable touch and step voltages. Specifically, the allowable touch and step voltages can be increased by placing a layer of high-resistivity material (such as crushed rock) on the surface of the earth and covering all areas of potentially high touch voltage. This layer acts as a high resistance between the energized ground grid and the point of contact of the human being with the soil and thus limits the level of the body current. Hence for a specified allowable body current, the touch or step voltage that will produce this body current is increased. Equations (8.15) and (8.16) should be used to determine the new allowable touch and step voltages.

The other type of design modifications aims at a reduction in the maximum possible touch and step voltages in a substation. Specifically, modifications can be made either to the grounding system itself or to the overall power system. A concise discussion of these modifications and their effects follows:

1. Changes in the design of the substation grounding system. These changes consist of reducing the mesh size of the ground mats, addition of ground rods, and so on. These changes result in a slight decrease in the ground resistance and a substantial reduction in the touch or step voltages as a percentage of the ground potential rise. The maximum ground potential rise decreases slightly with these changes since the ground resistance reduction is typically small.
2. Changes in the design of transmission circuits connected to the substation under study. These changes may involve increasing the size of the overhead shield wire (transmission lines) or the size of the neutral conductor (distribution lines) or improving the tower or pole grounding system. These changes, in general, reduce the maximum ground potential rise while the touch and step voltages as a percentage of the ground potential rise remain unaffected. Thus the absolute value of the touch and step voltages is decreased.

Recall that the design process of a grounding system is iterative, as discussed in Section 8.2. If a design does not meet safety requirements, the design must be modified as discussed above and within the physical constraints of the specific system. The new design is then analyzed and a safety assessment is performed. The procedure is repeated until the design meets safety requirements. In the next section this procedure is discussed in detail.

## 8.9 DESIGN EXAMPLES

In this section we illustrate the design procedure of grounding systems with two illustrative examples. The first example is a generation substation; the second example is a distribution substation. The two examples illustrate a few design options for the purpose of meeting safety requirements.

### 8.9.1 Design Example of a Generation Substation

Consider the generation station illustrated in Fig. 8.5. It comprises one 300-MVA 25-kV unit and a 300-MVA 25-kV/230-kV step-up transformer. The fault clearing time is 15 cycles (or 0.25 s). A 25.6-mi 230-kV line connects the generation station to the rest of the system. Other data are illustrated in Fig. 8.5. The 230-kV transmission line has two overhead ground wires, each Alumoweld 7, AWG No. 6. The size of the generation substation yard is 280 ft by 160 ft. A preliminary design of the ground mat is illustrated in Fig. 8.14. It consists of 20 ft x 20 ft meshes buried 2 ft below the surface of the earth, and is constructed with 4/0 copper conductor. The soil is uniform of resistivity 100  $\Omega \cdot m$ . The ground resistance of this ground mat is computed with a computer program to be 0.7  $\Omega$ . The study of the ground potential rise for this system has been discussed in Section 8.5.1 and is illustrated in Fig. 8.6. Note that the maximum ground potential rise is 1995 V and occurs for a single line-to-ground fault 4.5 mi from the generation substation (see Fig. 8.6a). With these data a safety assessment is performed for the system. Specifically, the allowable touch and step voltages are

$$V_{\text{touch,allowable}} = \frac{0.116(1.5\rho + 1000)}{\sqrt{t}} = 266.8 \text{ V}$$

$$V_{\text{step,allowable}} = \frac{0.116(6\rho + 1000)}{\sqrt{t}} = 371.2 \text{ V}$$

The actual maximum touch and step voltages, as a percentages of the ground potential rise, are 17.56 and 8.68, respectively (illustrated in Fig. 8.14). From Table 8.1 the decrement factor D is 1.10. The actual maximum touch and step voltages times the decrement factor are

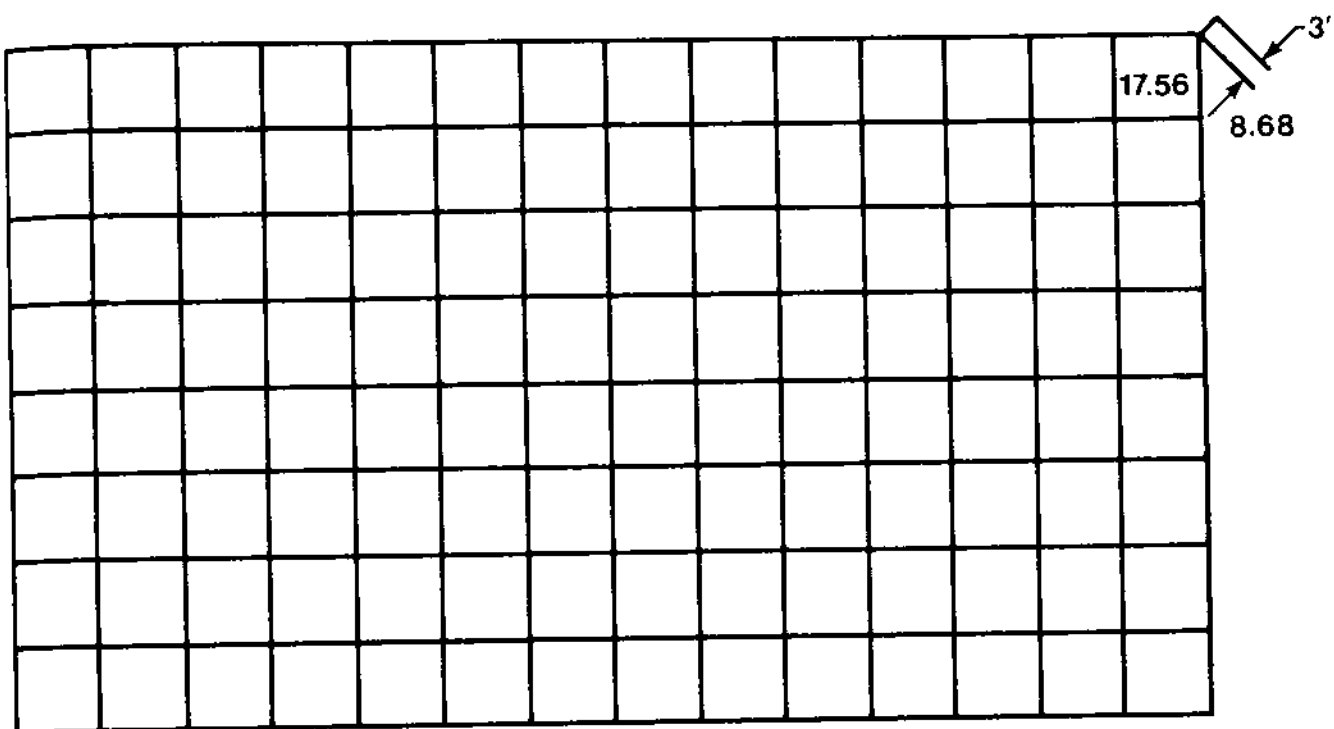


FIG. 8.14 Preliminary design of the generation substation ground mat.

$$DV_{touch,max} = (1.1)(0.1756)(GPR) = 385.33 \text{ V}$$

$$DV_{step,max} = (1.1)(0.868)(GPR) = 190.52 \text{ V}$$

Note that safety requirements [Eqs. (8.12) and (8.13)] are not met. To meet safety requirements, the system should be modified. Since the difference between the maximum touch voltage and the allowable touch voltage is relatively small, we shall try to reduce the maximum touch voltage by a design modification of the ground mat. For this purpose four conductors are added to the ground mat, as illustrated in Fig. 8.15. The new ground mat is analyzed using a computer program. The ground resistance is  $0.688 \Omega$  and the maximum mesh voltage is 13.47% of the ground potential rise. The mesh voltage of the outer six meshes, as well as the maximum step voltage, are illustrated in Fig. 8.15. The actual maximum touch and step voltages times the decrement factor for the new design are

$$DV_{touch,max} = (1.1)(0.1347)(GPR) = 292.0 \text{ V}$$

$$DV_{step,max} = (1.1)(0.0834)(GPR) = 183.0 \text{ V}$$

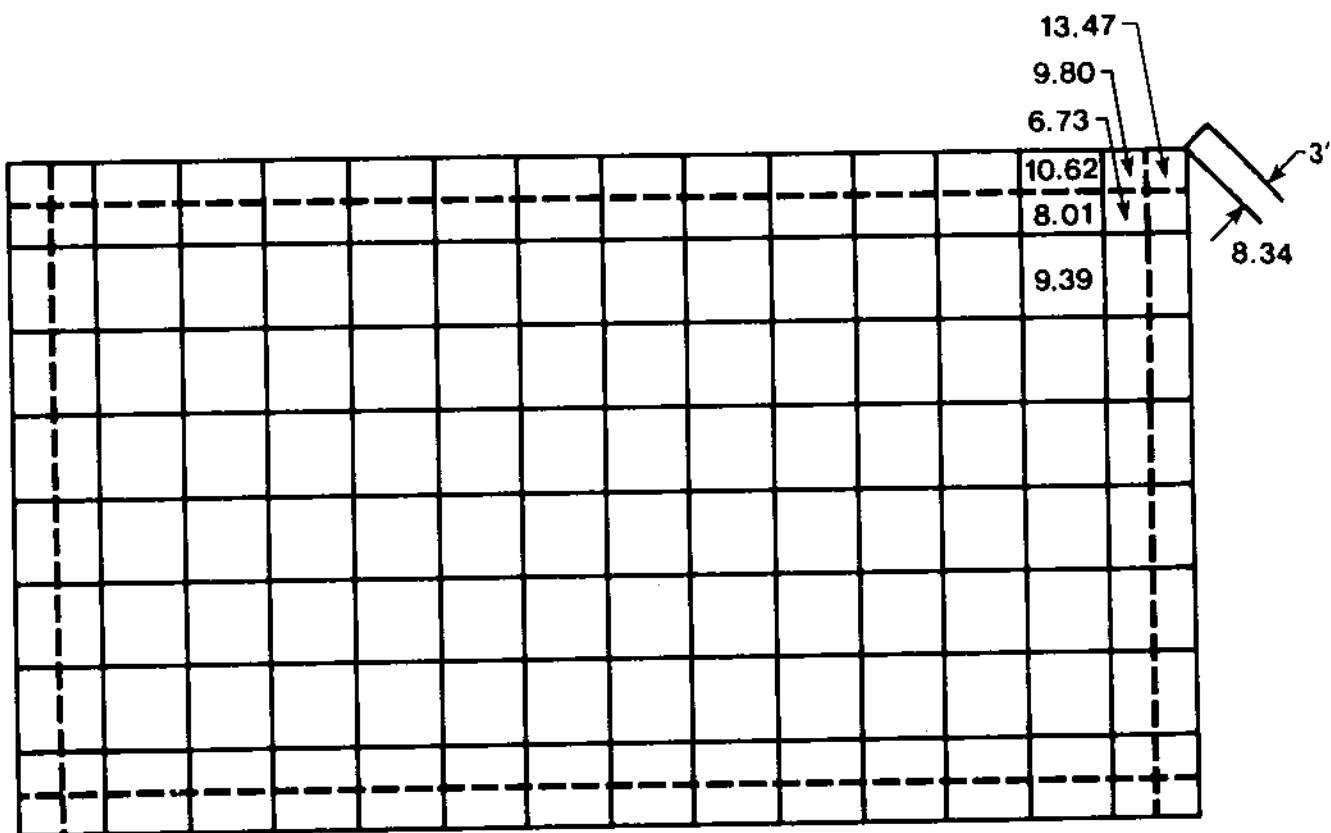


FIG. 8.15 Final design of the generation substation ground mat.

In the formula, the GPR of 1995 V was used. In reality, the GPR will be somewhat smaller because the ground resistance has been reduced from  $0.7 \Omega$  to  $0.688 \Omega$ . This reduction will be neglected for simplicity. Note that Eq. (8.13) is satisfied, whereas Eq. (8.12) is not satisfied but is close to being satisfied. An additional modification, for example, another conductor through the outer mesh, will satisfy safety requirements.

### 8.9.2 Design Example of a Distribution Substation

Consider the distribution substation illustrated in Fig. 8.7. The fault clearing time for this system is 20 cycles (0.33 s). The substation yard is square 160 ft by 160 ft. The preliminary design of the ground mat is identical to the one illustrated in Fig. 8.9. It is constructed from copper 4/0 conductor buried 2 ft below the soil surface. The soil resistivity is  $185 \Omega \cdot m$ . The computed resistance of the ground mat is  $1.763 \Omega$ . The maximum touch and step voltages for this system as a percentage of GPR are illustrated in Fig. 8.9. The ground potential rise for this system was investigated in Section 8.5.1 and is summarized in Fig. 8.8. The maximum ground potential rise is 4109 V and occurs for a single line-to-ground fault on the

high side of the distribution transformer. The decrement factor is computed from Table 8.1 with interpolation  $D = 1.066$ . The actual touch and step voltages times the decrement factor for this system are

$$DV_{\text{touch,max}} = (1.066)(0.1926)(4109) = 843.6 \text{ V}$$

$$DV_{\text{step,max}} = (1.066)(0.0937)(4109) = 410.4 \text{ V}$$

The allowable touch and step voltages are

$$V_{\text{touch,allowable}} = \frac{0.116(1.5\rho + 1000)}{\sqrt{t}} = 256.7 \text{ V}$$

$$V_{\text{step,allowable}} = \frac{0.116(6\rho + 1000)}{\sqrt{t}} = 423.9 \text{ V}$$

Note that for this system the allowable touch voltage is much smaller than the actual maximum touch voltage for the system. The allowable step voltage is greater than the maximum step voltage.

As a first design modification, assume that a 4-in. layer of crushed rock of resistivity  $2000 \Omega \cdot \text{m}$  (when wet) is added on the surface of the earth. In this case the allowable touch and step voltages will increase as follows:

$$V_{\text{touch,allowable}} = \frac{0.116(1.5c_s \rho_s + 1000)}{\sqrt{t}} = 550.5 \text{ V}$$

$$V_{\text{step,allowable}} = \frac{0.116(6c_s \rho_s + 1000)}{\sqrt{t}} = 1599.4 \text{ V}$$

where  $c_s$  is taken from Fig. 8.13 as follows:

$$\rho_s = 2000 \Omega \cdot \text{m}$$

$$h_s = 4 \text{ in.} = 0.1016 \text{ m}$$

$$K = \frac{\rho - \rho_s}{\rho + \rho_s} = -0.831$$

$$c_s = 0.58$$

By comparison of the allowable and maximum values, safety requirements are not met.

Now let's try a design modification for the purpose of reducing the maximum ground potential rise. Specifically, assume that the overhead shield wire of the 115-kV line is replaced with an ACSR 4/0 conductor for a length of 2 mi. An investigation of the maximum ground potential rise for the new system yields a value of 2676 V. The maximum touch and step voltages times the decrement factor are

$$DV_{\text{touch,max}} = (1.066)(0.1926)(2676) = 549.4 \text{ V}$$

$$DV_{\text{step,max}} = (1.066)(0.0937)(2676) = 267.2 \text{ V}$$

This design meets safety requirements [Eqs. (8.12) and (8.13)] and therefore is the final design.

The two design examples illustrate that in a design process there are many alternatives. In a specific design process one should select the least expensive design alternative. A discussion of the cost optimization of the final design is beyond the scope of this book.

## 8.10 SUMMARY AND DISCUSSION

In this chapter we have discussed design procedures of substation grounding systems. The objective of these procedures is to define a grounding system that meets safety requirements. ANSI/IEEE Standard 80 [18] delineates safety requirements for ac substation grounding systems. The design procedure is iterative, based on analysis and subsequent modification of the grounding system until the safety requirements are met. The single most important item of the process is accurate determination of the maximum ground potential rise. Other important items are investigation of special points of danger. A qualitative discussion and examples were presented, as were two comprehensive examples of the iterative design procedure. By necessity, computer-based models of grounding system are required in the design process.

# 9

# Power System Transients

## 9.1 INTRODUCTION

Electric power systems are subject to many types of disturbances that result in transients. For example, physical phenomena such as lightning may generate transient overvoltages. On the other hand, normal operating procedures, such as breaker closing and switching of equipment cause electrical transients. Abnormal conditions such as electrical faults also cause transients. The physical phenomena involved in power system transients may be classified into two categories:

1. Interaction between magnetic energy stored in inductors and electric energy stored in capacitors
2. Interaction between mechanical energy stored in rotating machines and electrical energy stored in circuits

The first category comprises purely electrical (or electromagnetic) transients. The second category consists of the electromechanical transients. Most power system transients are oscillatory in nature and therefore are characterized with the frequency of oscillations. Based on the frequency of oscillations, power system transients are classified as illustrated in Fig. 9.1. Our point of interest in this chapter will be the electrical transients.

Electrical transients result in abnormal voltages (overvoltages) and abnormal electric currents (overcurrents). Overcurrents may damage power equipment due to excessive heat dissipation. Overvoltages may result in flashovers (electrical discharges through the air) or insulation breakdown (electrical discharges through solid or

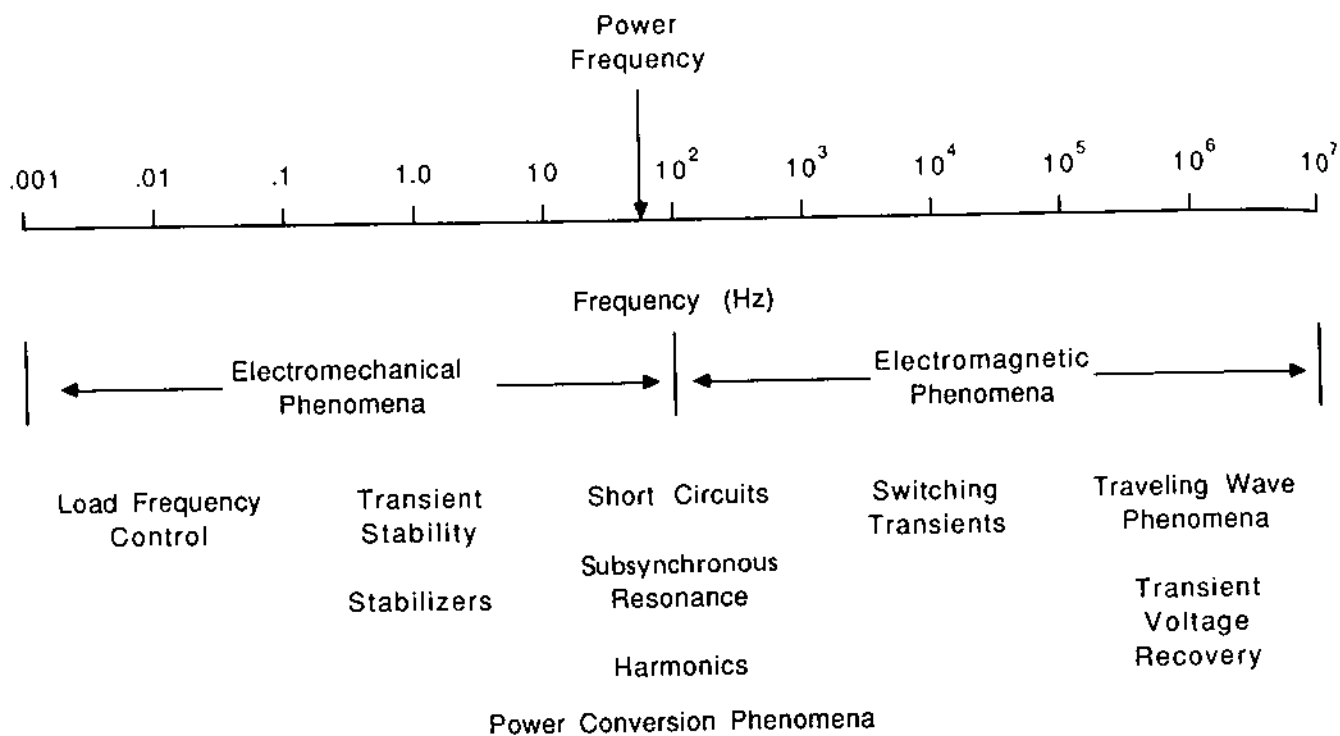


**FIG. 9.1** Classification of power system transients.

liquid insulating materials), device outages, and eventual deterioration of power system reliability. Normally, flashovers will cause a temporary power outage due to the temporary tripping of the equipment at which the flashover occurred, and the subsequent reclosing operation. Insulation breakdown, however, leads to permanent damage of transmission equipment and thus permanent outages. The equipment need to be repaired or replaced before being reconnected to the system. It should be apparent that electrical transients affect the reliable operation of power apparatus. In this chapter we investigate the mechanisms causing electrical transients (overvoltages or overcurrents) in transmission equipment, analysis techniques, and methods of mitigation of electrical transients or protection against transients.

Electrical transients can be studied by a number of methods. For power system electrical transients, the following methods can be applied:

1. Graphical methods
2. Analytical methods
3. Numerical methods
4. Using a transient network analyzer (TNA)

A transient network analyzer (TNA) is made of scaled-down power system model components that may be interconnected in such ways as to correspond to a system under study. Typically, the connections

are automatically performed with the aid of a digital computer. In addition, the digital computer may excite the system in a desirable way. The transient voltages and currents are recorded and may be plotted or analyzed as desired.

Methods 1, 2, and 3 are simulation methods. These methods enable solutions to the mathematical models describing the system under study. They differ only in the solution method, which, as the name indicates, are graphical, analytical, and numerical, respectively. Thus, modeling is a common component of all methods. In this chapter we introduce models of power system elements for transient analysis followed by solution methods. Subsequently, we study basic power system transients and mitigation methods. Finally, we discuss protection devices against transient overvoltages.

## 9.2 MODELS FOR TRANSIENT ANALYSIS

One of the key tasks in power system transient analysis is selection of the model by which the physical system will be represented. The mathematical model must accurately represent the physical phenomena to be studied. At the same time, to be practical, it should be as simple as possible. In this section we attempt to provide insights into the various models of power system elements for transient analysis and guidelines for selection of the appropriate model for specific applications.

### 9.2.1 Lumped-Parameter Models

The simplest representation of power system elements is by means of lumped parameters. In this way, a resistor is represented with an ideal resistance, an inductor with an ideal inductance, and a capacitor with an ideal capacitance. The mathematical models of ideal R, L, C elements are summarized in Fig. 9.2a.

### 9.2.2 Distributed-Parameter Models

For many applications, power system elements must be represented by distributed parameters. A classical example is the transmission line. It has been shown in Chapter 6 that a distributed-parameter line is represented mathematically by a set of partial differential equations. Specifically, consider a single-phase line with the following parameters:

- L: series inductance per unit length
- C: capacitance per unit length
- r: series resistance per unit length
- g: shunt conductance per unit length

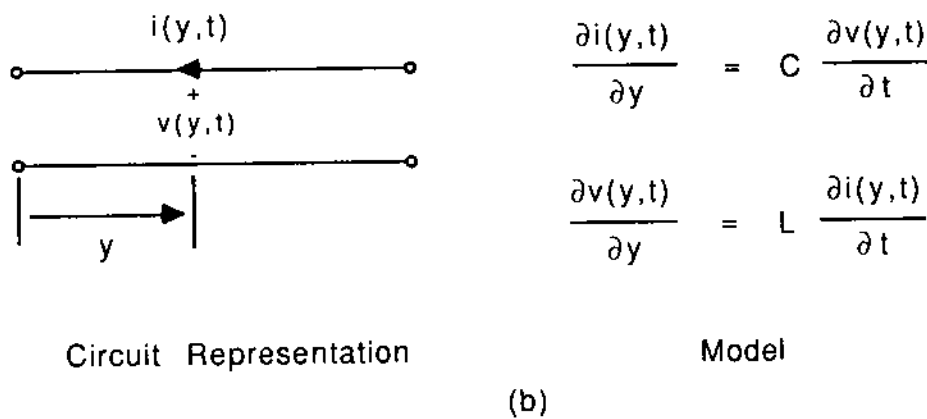
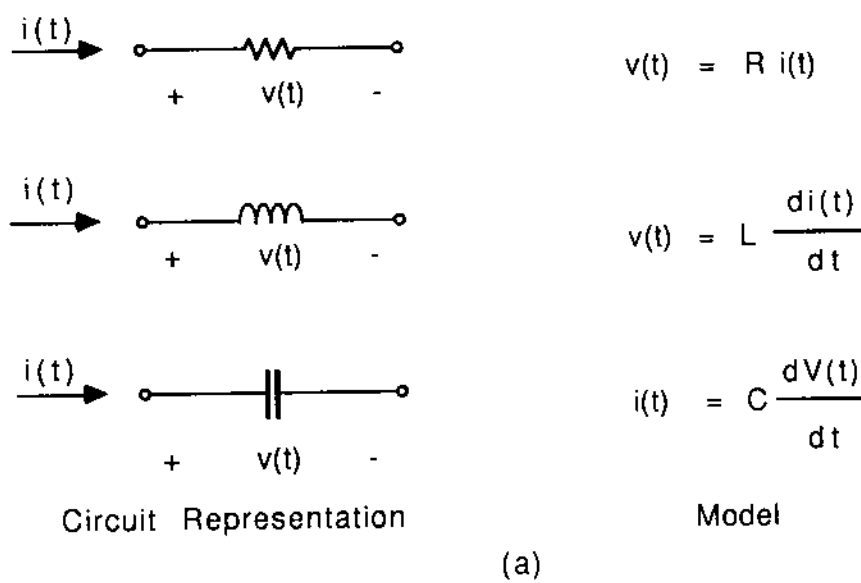


FIG. 9.2 Power system models for transient analysis. (a) Lumped parameter models, (b) distributed parameter models.

The mathematical model of this line was derived in Chapter 6:

$$\frac{\partial v(y, t)}{\partial y} = L \frac{\partial i(y, t)}{\partial t} + ri(y, t) \quad (9.1a)$$

$$\frac{\partial i(y, t)}{\partial y} = C \frac{\partial v(y, t)}{\partial t} + gv(y, t) \quad (9.1b)$$

For power lines, the shunt conductance is negligibly small and is always omitted. The series resistance is small and can be omitted as a first approximation. In addition, the parameters  $L$  and  $C$  are assumed to be constants, independent of frequency. These approximation

lead to the ideal distributed-parameter transmission line model illustrated in Fig. 9.2b.

In summary, models of power system elements for transient analysis are based on lumped parameters or distributed-parameter components. The selection of the model depends on the physical system and the transient phenomena to be studied. In later sections we discuss the basic concepts in selecting the appropriate model for the appropriate application.

### 9.3 THE IDEAL DISTRIBUTED-PARAMETER LINE

In this section we study the model of an ideal distributed-parameter transmission line. This model is obtained from Eqs. (9.1), assuming that the series resistance and shunt conductance are zero and the inductance and capacitance per unit length are constants independent of frequency. The equations of the ideal distributed-parameter transmission line are

$$\frac{\partial v(y,t)}{\partial y} = L \frac{\partial i(y,t)}{\partial t} \quad (9.2a)$$

$$\frac{\partial i(y,t)}{\partial y} = C \frac{\partial v(y,t)}{\partial t} \quad (9.2b)$$

where L and C are constants. The coupled partial differential equations are transformed into a set of uncoupled differential equations of higher order. For this purpose, the first equation is differentiated with respect to the variable y and the second equation with respect to the variable t.

$$\frac{\partial^2 v(y,t)}{\partial y^2} = L \frac{\partial^2 i(y,t)}{\partial y \partial t} \quad (9.3a)$$

$$\frac{\partial^2 i(y,t)}{\partial t \partial y} = C \frac{\partial^2 v(y,t)}{\partial t^2} \quad (9.3b)$$

Assuming that the function  $i(y,t)$  is twice differentiable, the order of differentiation can be interchanged, that is,

$$\frac{\partial^2 i(y,t)}{\partial y \partial t} = \frac{\partial^2 i(y,t)}{\partial t \partial y}$$

Upon elimination of  $\partial^2 i(y,t)/\partial t \partial y$  from Eqs. (9.3), we obtain

$$\frac{\partial^2 v(y,t)}{\partial y^2} = LC \frac{\partial^2 v(y,t)}{\partial t^2}$$

Note that  $L$  is measured in  $\text{H/m}$  (henries per meter),  $C$  is measured in  $\text{F/m}$  (farads per meter), and thus  $LC$  will be measured in  $\text{H} \cdot \text{F/m}^2$  (henries · farads per meter squared) =  $\text{s}^2/\text{m}^2$  or the quantity  $LC$  is the reciprocal of velocity squared. Thus we may write

$$LC = \frac{1}{c^2} \quad (9.4)$$

where  $c$  is velocity measured in meters per second.

The equation derived is a second-order partial differential equation in terms of the voltage  $v(y, t)$ . Assuming that the equation is solved for  $v(y, t)$ , the electric current can be found from Eq. (9.2a) or (9.2b). Thus the equations of the ideal transmission line are

$$\frac{\partial^2 v(y, t)}{\partial y^2} = \frac{1}{c^2} \frac{\partial^2 v(y, t)}{\partial t^2} \quad (9.5a)$$

$$\frac{\partial v(y, t)}{\partial y} = L \frac{\partial i(y, t)}{\partial t} \quad (9.5b)$$

Equations (9.5) are partial differential equations. Equation (9.5a) is of second order but uncoupled [in terms of the voltage variable  $v(y, t)$  only], while Eq. (9.5b) is of first order but coupled. Both spatial and time derivatives appear. In general, two boundary and two initial conditions are required to determine the solution of Eqs. (9.5) for a given transmission line. At this point the particular solution to a particular transmission line is not of interest, but rather, a general technique for solving Eqs. (9.5). For this reason we discuss the general solution of Eqs. (9.5).

The general solution of Eq. (9.5a) is well known. Specifically, the general solution  $v(y, t)$  is given in terms of two independent twice-differentiable functions  $f_1$  and  $f_2$ :

$$v(y, t) = v_1 f_1(y + ct) + v_2 f_2(y - ct)$$

where  $v_1$  and  $v_2$  are constants and  $c = 1/\sqrt{LC}$ .

The fact that the equation above is a general solution of Eq. (9.5a) is verified by direct substitution into Eq. (9.5a). Specifically, upon substitution of the general solution for  $v(y, t)$  into the right- and left-hand sides of Eq. (9.5a),

$$\frac{\partial^2 v(y, t)}{\partial y^2} = v_1 f''_1(y + ct) + v_2 f''_2(y - ct)$$

$$\frac{1}{c^2} \frac{\partial^2 v(y, t)}{\partial t^2} = \frac{v_1}{c^2} c^2 f_1''(y + ct) + \frac{v_2}{c^2} c^2 f_2''(y - ct)$$

$$= v_1 f_1''(y + ct) + v_2 f_2''(y - ct)$$

where " denotes second differentiation with respect to the argument of the function. Apparently, the right-hand side of Eq. (9.5a) is identical to the left-hand side of the same equation for any choice of the functions  $f_1$  and  $f_2$ .

The general solution for the electric current  $i(y, t)$  can be found from Eq. (9.5b). Upon substitution of the general solution  $v(y, t)$  into Eq. (9.5b), the equation becomes

$$v_1 f_1'(y + ct) + v_2 f_2'(y - ct) = L \frac{\partial i(y, t)}{\partial t}$$

Upon integration of the equation above with respect to time, we have

$$i(y, t) = i_1 f_1(y + ct) + i_2 f_2(y - ct) \quad (9.6)$$

where

$$i_1 = \frac{v_1}{Lc} \quad (9.7a)$$

$$i_2 = -\frac{v_2}{Lc} \quad (9.7b)$$

Note that

$$Lc = L \frac{1}{\sqrt{LC}} = \sqrt{\frac{L}{C}} = Z_0$$

The quantity  $Z_0$  has dimensions of impedance (ohms). It is the characteristic impedance of the line. Note that for the case of an ideal distributed-parameter line, the characteristic impedance is a real number (pure resistance).

Now Eqs. (9.7) become

$$i_1 = \frac{v_1}{Z_0} \quad (9.8a)$$

$$i_2 = -\frac{v_2}{Z_0} \quad (9.8b)$$

and the general solution to Eqs. (9.2) is

$$v(y, t) = v_1 f_1(y + ct) + v_2 f_2(y - ct) \quad (9.9a)$$

$$i(y, t) = \frac{v_1}{Z_0} f_1(y + ct) - \frac{v_2}{Z_0} f_2(y - ct) \quad (9.9b)$$

The general solution is given in terms of two constants,  $v_1$  and  $v_2$ , and two arbitrary twice differentiable functions,  $f_1$  and  $f_2$ . For a specific problem,  $v_1$ ,  $v_2$ ,  $f_1$ ,  $f_2$  will be determined from the boundary and initial conditions.

The general solution [Eqs. (9.9)] represents traveling waves along the transmission line. For example, observe that  $v_1 f_1(y + ct)$  represents a voltage wave traveling toward decreasing  $y$  and  $v_2 f_2(y - ct)$  represents an electric current wave traveling toward increasing  $y$ . Similarly,  $(v_1/Z_0)f_1(y + ct)$  represents an electric current wave traveling toward decreasing  $y$ , and  $(-v_2/Z_0)f_2(y - ct)$ , an electric current wave traveling toward increasing  $y$ . Figure 9.3 illustrates a traveling voltage wave on a single-phase line of the form

$$u_1(y, t) = v_1 f_1(y + ct)$$

At time  $t = t_1$ , the "front" of the wave  $u_1$  is at  $y = y_1$ . At time  $t_2$  the front of the wave  $u_1$  will be at  $y = y_2$ . The front of the wave  $u_1$  (or any other point of  $u_1$ ) is characterized by the fact that the argument of the function  $f_1$  remains constant. Thus

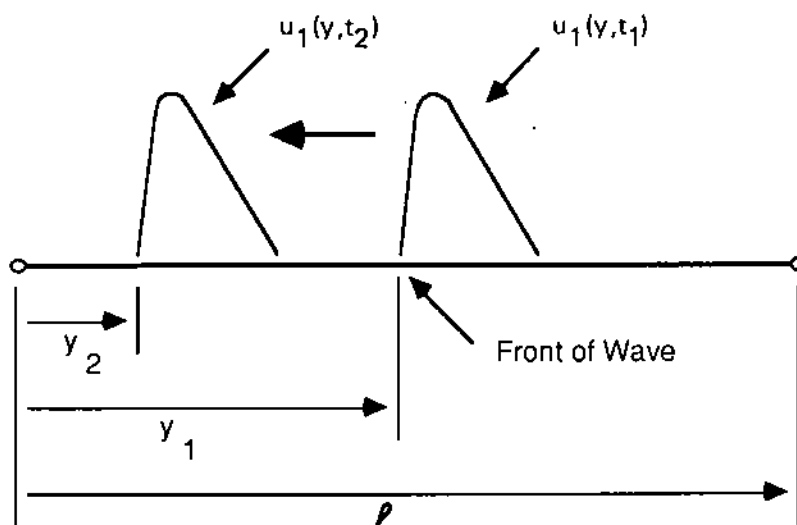


FIG. 9.3 A traveling wave on a single phase transmission line.

$$y_1 + ct_1 = y_2 + ct_2$$

or

$$y_2 - y_1 = -c(t_2 - t_1)$$

Since  $t_2 > t_1$ ,  $y_2 - y_1 < 0$  or  $y_2 < y_1$ . Thus the voltage wave moved with velocity  $c$  toward decreasing  $y$ . The shape of the voltage wave has not changed since

$$u_1(y, t) = v_1 f_1(y + ct)$$

where  $v_1$  is a constant. Similarly, the solution

$$u_2(y, t) = v_2 f_2(y - ct)$$

is interpreted as a voltage wave traveling toward increasing  $y$  with a velocity  $c$ . The shape of the voltage wave remains unchanged.

#### 9.4 GRAPHICAL TECHNIQUES

In Section 9.3 we discussed the fact that the general solution for the ideal distributed parameter transmission line is given in terms of two traveling waves. This simple solution is very useful in computing transient voltages in transmission systems. The basic concepts for such computations were developed by the French mathematician Bergeron and are discussed in this section.

Consider the general solution of an ideal distributed-parameter single-phase transmission line [Eqs. (9.9)] and compute the quantities  $v(y, t) + Z_0 i(y, t)$  and  $v(y, t) - Z_0 i(y, t)$ :

$$v(y, t) + Z_0 i(y, t) = 2v_1 f_1(y + ct) \quad (9.10a)$$

$$v(y, t) - Z_0 i(y, t) = 2v_2 f_2(y - ct) \quad (9.10b)$$

Now assume that an observer moves on the transmission line in such a way that  $y + ct = \text{constant}$ . In other words, he travels with speed  $c$  toward decreasing  $y$ . For this observer, the quantity  $[v(y, t) + Z_0 i(y, t)]$  remains constant equal to  $2v_1 f_1(y + ct)$ . Let  $2v_1 f_1(y + ct) = c_1$ . Similarly, consider an observer who moves on the transmission line in such a way that  $y - ct = \text{constant}$ . This observer travels with speed  $c$  toward increasing  $y$ . For this observer the quantity  $[v(y, t) - Z_0 i(y, t)]$  remains constant equal to  $2v_2 f_2(y - ct)$ . Let  $2v_2 f_2(y - ct) = c_2$ . Thus for the two observers above, the voltage and electric current on the line will obey the following relationships:

$$v(y,t) + Z_0 i(y,t) = c_1 \quad (9.11a)$$

$$v(y,t) - Z_0 i(y,t) = c_2 \quad (9.11b)$$

Bergeron's method is based on Eqs. (9.11). Observers are placed on the transmission line moving along with the same speed as the traveling waves. For these observers, Eqs. (9.11) hold. The constants  $c_1$  and  $c_2$  will change only when the observers meet discontinuities, such as a line termination or a load. If the location of these observers and the associated constants  $c_1$ ,  $c_2$ , and so on, are known at any instant of time, the voltage and current at any point of the system can be determined. Application of Bergeron's method leads to a simple graphical solution. The graphical solution, originally proposed by Bewley, is based on a systematic way of accounting for all traveling waves.

Bewley's basic idea was to keep track of all traveling waves on the transmission system by means of a simple diagram, which today is known as the Bewley diagram. Knowing the location of all traveling waves at any time, the voltage at any point is constructed as the superposition of all traveling voltage waves present at the point of interest. Similarly, the electric current at any point is constructed from the superposition of all traveling electric current waves present at the point of interest. Traveling waves change their course only when they encounter discontinuities such as a load or a different transmission line. In general, a traveling wave impeding on a discontinuity will be separated into two waves: one that will travel in the opposite direction, called the reflected wave, and another that will continue to travel past the discontinuity point, called the transmitted wave. The relationship of these waves with respect to the original wave, which is called the incident wave, is developed next.

Consider a discontinuity as illustrated in Fig. 4.9. Assume that at  $t = 0$ , a voltage wave arrives at point A. The duration of the wave will be some finite time. Consider time  $t$ ,  $t > 0$ .

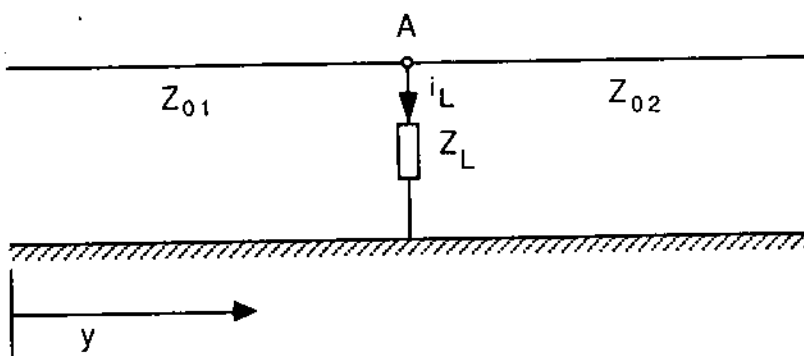


FIG. 9.4 A discontinuity in a transmission system.

Let  $v_i$  be the voltage of the incident wave at point A at time  $t$ ,  $v_r$  be the voltage of the reflected wave at point A at time  $t$ , and  $v_t$  be the voltage of the transmitted wave at point A at time  $t$ . The reflection and refraction coefficients  $\alpha$  and  $\delta$  are defined by

$$\alpha = \frac{v_r}{v_i} \quad (9.12)$$

$$\delta = \frac{v_t}{v_i} \quad (9.13)$$

The coefficients  $\alpha$  and  $\delta$  depend on the parameters of the discontinuity. As an example and with reference to Fig. 9.4, they depend on  $Z_{01}$ ,  $Z_{02}$ ,  $Z_L$ , where  $Z_{01}$ ,  $Z_{02}$  are the characteristic impedances of the transmission line to the left and to the right of point A, respectively, and  $Z_L$  is the lumped resistance connected to point A. The coefficients  $\alpha$  and  $\delta$  are computed as follows.

Associated with the incident, reflected, and transmitted voltage waves, there are electric current waves defined by

$$i_i = -\frac{v_i}{Z_{01}} \quad (9.14)$$

$$i_r = \frac{v_r}{Z_{01}} \quad (9.15)$$

$$i_t = -\frac{v_t}{Z_{02}} \quad (9.16)$$

On the other hand, the voltage at point A is  $v_A$ :

$$v_A = v_i + v_r = -Z_{01}i_i + Z_{01}i_r \quad (9.17)$$

$$v_A = v_t = -Z_{02}i_t \quad (9.18)$$

$$v_A = Z_L i_L \quad (9.19)$$

where  $i_L$  is the electric current through the resistance  $Z_L$ . The equations above result by considering a point just left of point A, just right of point A, and point A, respectively. Now at node A, Kirchhoff's current law yields

$$i_i + i_r = i_t - i_L \quad (9.20)$$

Upon elimination of the electric currents  $i_i$ ,  $i_r$ ,  $i_t$ , and  $i_L$  from Eqs. (9.17)–(9.20), subsequent solution for the voltages  $v_r$  and  $v_t$  in terms of the voltage  $v_i$  and substitution into Eqs. (9.12) and (9.13), the reflection and refraction coefficients  $\alpha$  and  $\delta$  for a wave impeding the discontinuity from left are obtained:

$$\alpha = \frac{Z_{eq} - Z_{01}}{Z_{eq} + Z_{01}} \quad (9.21)$$

$$\delta = \frac{2Z_{eq}}{Z_{eq} + Z_{01}} \quad (9.22)$$

where

$$Z_{eq} = \frac{Z_{02}Z_L}{Z_{02} + Z_L}$$

The electric current waves are computed from

$$i_r = \frac{v_r}{Z_{01}} = \alpha \frac{v_i}{Z_{01}} = -\alpha i_i \quad (9.23)$$

$$i_t = -\frac{v_t}{Z_{02}} = -\delta \frac{v_i}{Z_{02}} = -\delta \frac{Z_{01}}{Z_{02}} \frac{v_i}{Z_{01}} = \delta \frac{Z_{01}}{Z_{02}} i_i \quad (9.24)$$

Note that since  $Z_{01}$ ,  $Z_{02}$ , and  $Z_L$  are real numbers, the reflection and refraction coefficients  $\alpha$  and  $\delta$  are constant. This means that the reflected and transmitted waves will have the same waveform as the incident wave.

In summary, an incident wave arriving at a discontinuity point will be partially reflected and partially transmitted. The instantaneous values of the reflected and transmitted waves at the point of discontinuity are related to the instantaneous value of the incident wave with the following relationships:

Reflected wave:

$$v_r = \alpha v_i$$

$$i_r = -\alpha i_i$$

$$\alpha = \frac{Z_{eq} - Z_{01}}{Z_{eq} + Z_{01}} \quad \text{reflection coefficient}$$

Transmitted wave:

$$v_t = \delta v_i$$

$$i_t = \frac{Z_{01}}{Z_{02}} \delta i_i$$

$$\delta = \frac{2Z_{eq}}{Z_{eq} + Z_{01}} \quad \text{refraction coefficient}$$

A traveling voltage or current wave in a transmission system generates two more waves when it meets a discontinuity (line end, load, etc.). The waves multiply very fast. A systematic way of keeping track of all traveling waves has been proposed by Bewley and is known as the Bewley diagram. The diagram indicates where along a transmission system the wavefronts of the various traveling waves are located and in what direction they travel. The intensity of the waves is also denoted on the diagram. The x coordinate of the Bewley diagram is the adjusted distance of a point from a reference point. The adjusted distance is proportional to the travel time from the reference point to the point under consideration. Thus the adjustment accounts for different traveling speeds along different transmission lines. The x coordinate is symbolized by  $[(c_0/c)\ell]$ , where  $c_0$  is the speed of light in free space,  $c$  is the traveling speed of the waves along the line, and  $\ell$  is the actual distance of a point from the reference point. The adjusted distance equals the actual length of a transmission line on which traveling waves travel with the speed of light. The y coordinate is time measured from an arbitrarily selected time reference. Figure 9.5 illustrates a Bewley diagram. The application of the Bewley diagram for the computation of overvoltages will be illustrated with an example.

Example 9.1: Consider the simplified single-phase electric power transmission system of Fig. E9.1. It consists of a 300-m overhead line (section A-B) and a 300-m cable (section B-C). The characteristic impedance of the overhead and cable lines are 400 and 100  $\Omega$ , respectively. The speed of traveling waves along the overhead and the cable lines is 300 and 150 m/ $\mu$ s, respectively. Electric loads of resistance 600, 800, and 800  $\Omega$  are located at points A, B, and C, respectively. At time  $t = 0$ , lightning strikes at point A of the system. Assume the lightning to be an ideal electric current source of the waveform illustrated in Fig. E9.2. The crest of the electric current waveform is 5 kA. Compute the transient overvoltage at point B resulting from the lightning.

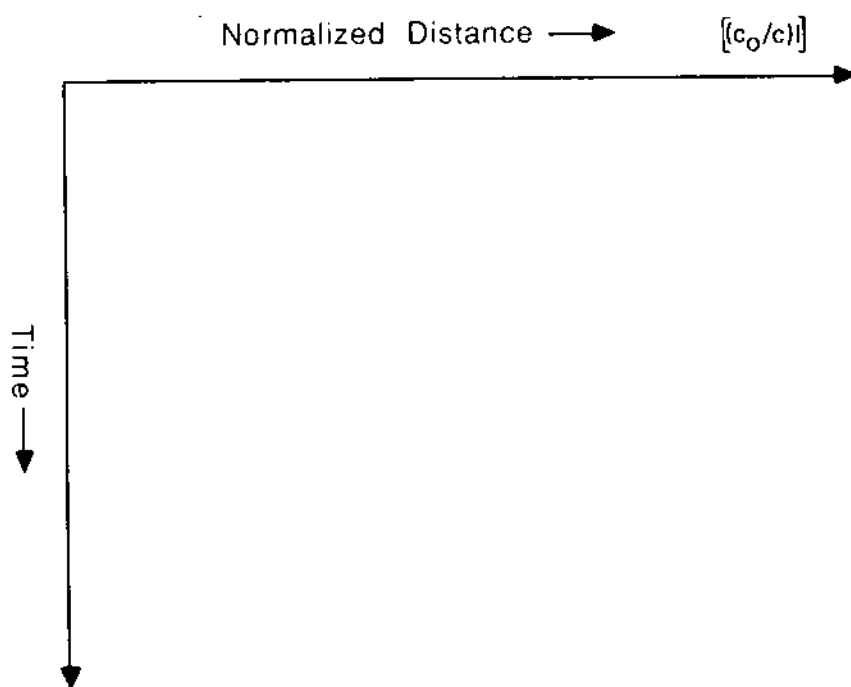


FIG. 9.5 The Bewley diagram.

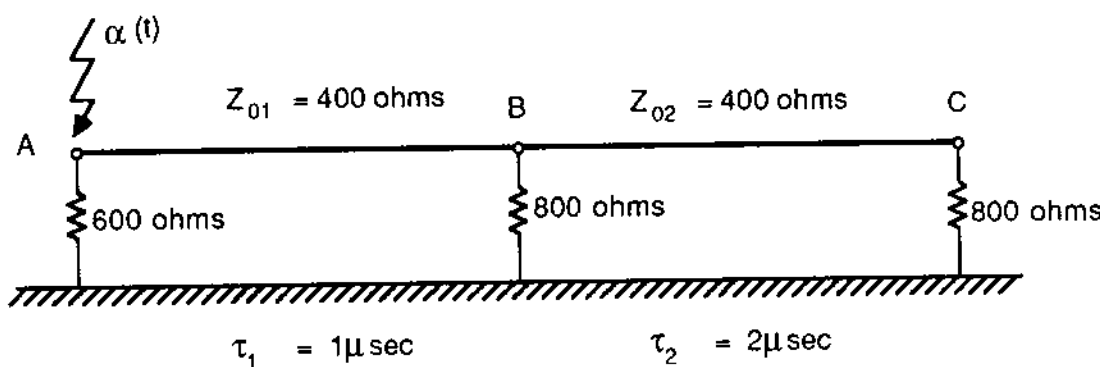


FIG. E9.1 Example transmission system.

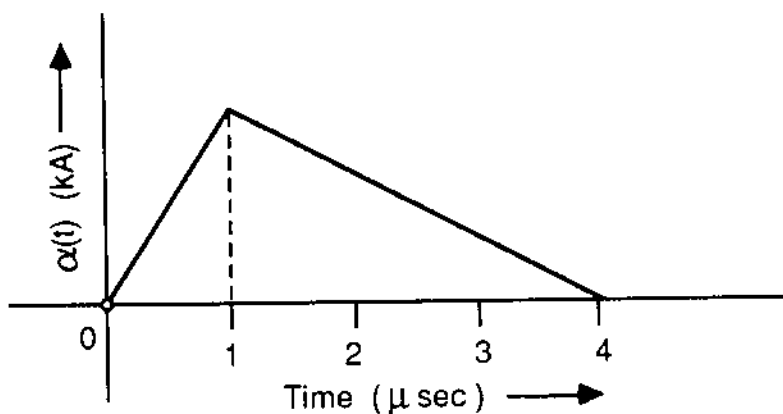


FIG. E9.2 Assumed lightning current waveform.

Solution: Application of the graphical method requires the computation of all possible reflection and refraction coefficients. These are illustrated in Fig. E9.3. Note that coefficients associated with waves impeding a discontinuity from the right are primed. The numerical values of the coefficients are

$$\alpha'_A = \frac{600 - 400}{600 + 400} = 0.20$$

$$\alpha_B = \frac{88.88 - 400}{88.88 + 400} = -0.64$$

$$\delta_B = \frac{(2)(88.88)}{88.88 + 400} = 0.36$$

$$\alpha'_B = \frac{266.66 - 100}{266.66 + 100} = 0.45$$

$$\delta'_B = \frac{(2)(266.66)}{266.66 + 100} = 1.45$$

$$\alpha_C = \frac{800 - 100}{800 + 100} = 0.78$$

The lightning wave, impeding point A, "sees" an equivalent resistance of  $R_{eq} = (600 \Omega \parallel 400 \Omega) = 240 \Omega$ . Since the lightning is represented as an ideal current source as in Fig. E9.2, it will generate a voltage wave  $u(t)$  equal to  $u(t) = (240 \Omega) \alpha(t)$ . This

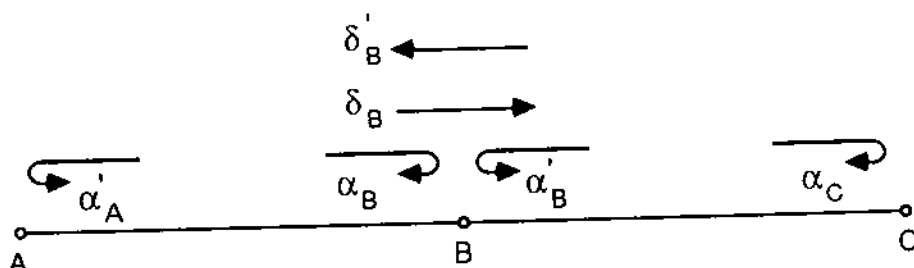


FIG. E9.3 Definition of all possible reflection and transmission coefficients for the system of Figure E9.1.

wave is illustrated in Fig. E9.4. As this voltage wave travels along the transmission system it will generate reflected and transmitted waves. The Bewley diagram of Fig. E9.5 indicates the position of the start of the waves as a function of time. The voltage at any point in the system can be constructed from the superposition of all waves present at the point. Assume, for example, that the voltage at point B is to be constructed as a function of time. This voltage will be the same as for a point just right of point B. At this point, the following voltage waves arrive:

- At time  $t = 1 \mu\text{s}$ , a voltage wave  $0.36u(t)$  arrives.
- At time  $t = 3 \mu\text{s}$ , a voltage wave  $-0.046u(t)$  arrives.
- At time  $t = 5 \mu\text{s}$ , a voltage wave  $0.28u(t)$  arrives.
- At time  $t = 5 \mu\text{s}$ , a voltage wave  $0.126u(t)$  arrives.
- At time  $t = 5 \mu\text{s}$ , a voltage wave  $0.005u(t)$  arrives.
- Etc.

Note that the waves attenuate fast. Thus, in order to determine the maximum overvoltages from the lightning, it is sufficient to retain only a few of the traveling waves. In the example, only four waves will be retained. Then the voltage at point B is constructed from the superposition of the four voltage waves. The procedure is illustrated in Fig. E9.6. Note that the maximum overvoltage at point B occurs  $6 \mu\text{s}$  after the incidence of lightning.

A similar procedure can be employed for the computation of the electric current at any point in the system.

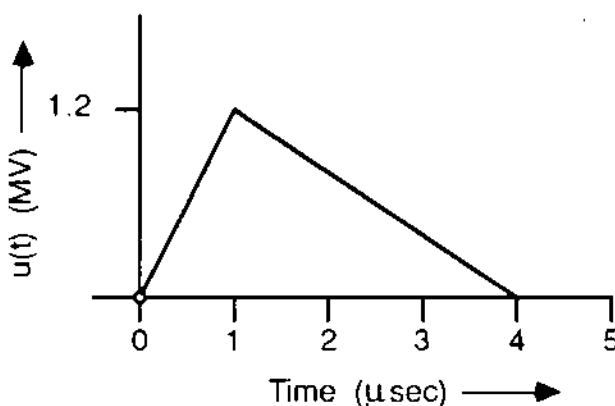


FIG. E9.4 Voltage waveform due to lightning current.

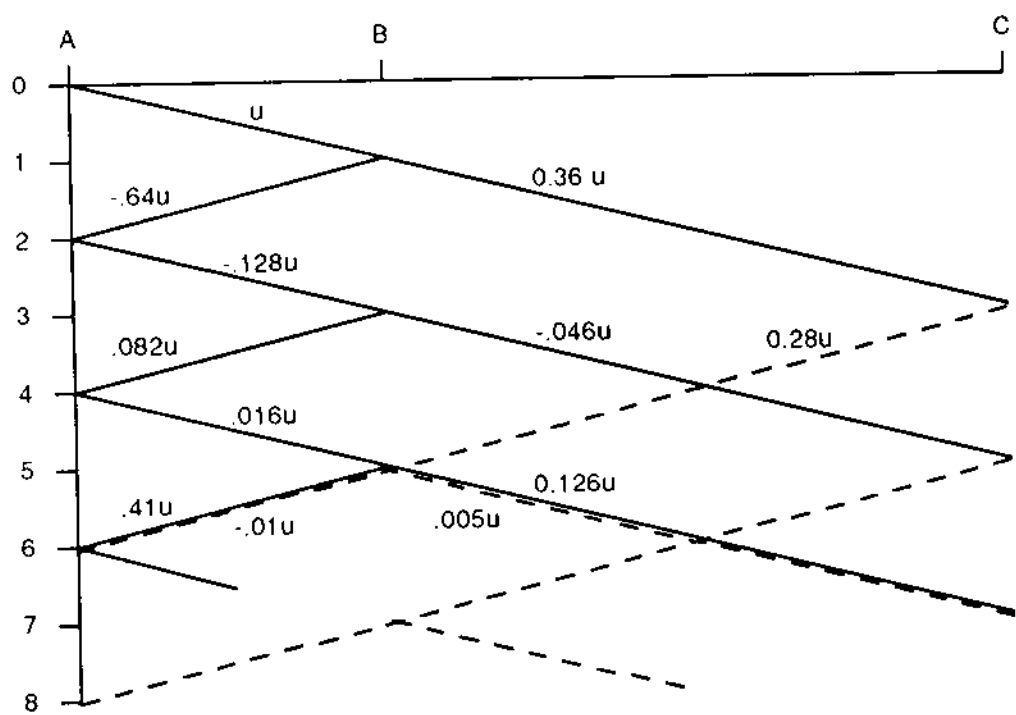


FIG. E9.5 Bewley diagram for the example system of Figure E9.1.

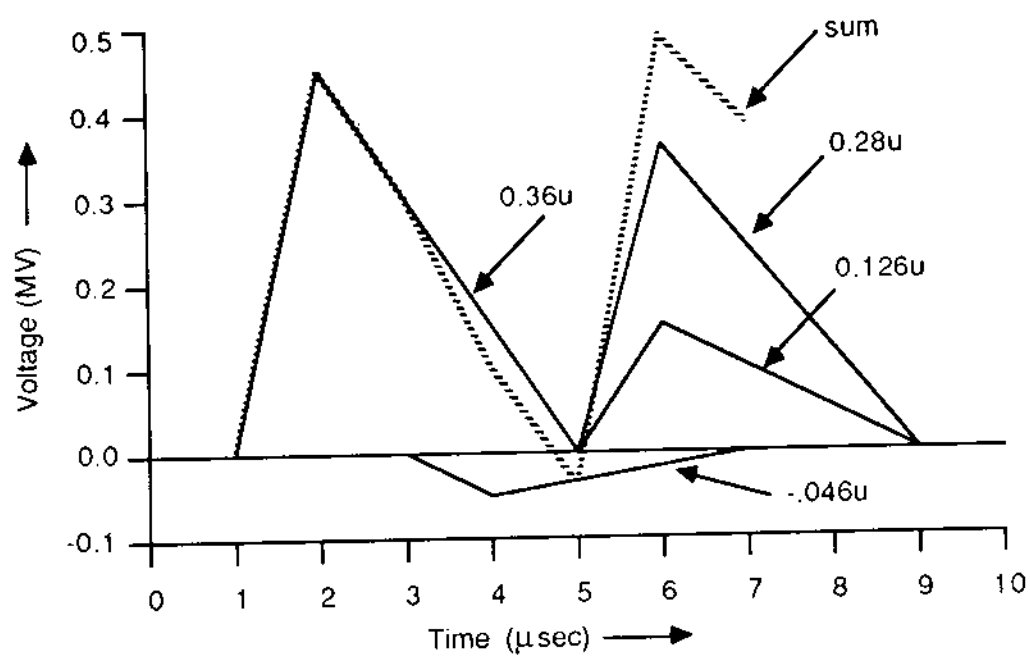


FIG. E9.6 Voltage waveform at point B.

## 9.5 ANALYTICAL TECHNIQUES

As we have discussed previously, the models of a physical system for transient analysis are represented with a set of ordinary differential equations or partial differential equations, or both. In addition, for a specific problem, a set of initial or boundary conditions will be known. The resulting mathematical problem can be solved by a number of analytical techniques. Laplace transforms provide a systematic way to obtain analytical solutions to the problem stated.

The Laplace transform,  $F(s)$  of a function  $f(t)$  is defined by the integral

$$F(s) = \int_0^{\infty} e^{-st} f(t) dt$$

Note that the Laplace transform transforms a function of time  $f(t)$  into another function of the variable  $s$ . The variable  $s$  is, in general, a complex variable. We shall denote the functions of time with lowercase letters and their Laplace transform with the corresponding uppercase letter. The most important properties of the Laplace transform are summarized in Table 9.1. A list of Laplace transforms for typical functions is given in Table 9.2.

For the purpose of solving a transient problem with the Laplace transform, the Laplace transform is applied to the differential equations and initial conditions that describe a specific problem. Subsequently, the resulting equations are solved yielding the quantity of interest in the Laplace domain (i.e., as a function of  $s$ ). Application of the inverse Laplace transform will provide the quantity of interest in the time domain. The use of Laplace transforms will be illustrated with an example.

Example 9.2: Consider the problem

$$\dot{x}(t) + ax(t) = 0$$

$$x(0) = c$$

Compute the solution  $x(t)$ .

Solution: Upon Laplace transformation

$$sX(s) - x(0) + aX(s) = 0$$

Upon solution of the equation above for  $X(s)$ , we have

$$X(s) = \frac{c}{s + a}$$

TABLE 9.1 Table of Operations for the Laplace Transformation

Time domain function	Laplace transform
1. $f(t)$	$F(s) = \int_0^{\infty} e^{-st} f(t) dt$
2. $af(t) + bg(t)$	$aF(s) + bG(s)$
3. $dt(t)/dt$	$sF(s) - f(0)$
4. $\int_0^t f(\tau) d\tau$	$(1/s)F(s)$
5. $\int_0^t f_1(t - \tau) f_2(\tau) d\tau$	$F_1(s)F_2(s)$
6. $tf(t)$	$-dF(s)/ds$
7. $e^{at}f(t)$	$F(s - a)$
8. $f(t - a)$ , $f(t - a) = 0$ for $t < a$	$e^{-as}F(s)$
9. $(1/c)f(t/c)$ , $c > 0$	$F(cs)$

TABLE 9.2 Table of Laplace Transforms

Time-domain function	Laplace transform
1. 1	$1/s$
2. $t$	$1/s^2$
3. $e^{at}$	$1/(s - a)$
4. $te^{at}$	$1/(s - a)^2$
5. $t^{n-1}e^{at}/(n - a)!$	$1/(s - a)^n$
6. $(1/a) \sin at$	$1/(s^2 + a^2)$
7. $\cos at$	$s/(s^2 + a^2)$

Taking the inverse Laplace transform of  $X(s)$  gives us

$$x(t) = ce^{-at}$$

The simple procedure above can be extended to the analysis of complex power system transients. A systematic way to solve power system transient problems with the aid of Laplace transforms is presented next. Consider the equations (differential) describing a specific power system element (an inductor, resistor, line, etc.). Application of the Laplace transform on these equations yields an equation in terms of the Laplace variable. The transformed equations represent equivalent circuits in the Laplace domain. This transformation is applied to all elements of the system under study. The result will be a network consisting of Laplace domain equivalent elements. Next, usual circuit analysis (nodal equations or loop equations) will provide the quantities of interest in the Laplace domain. Taking the Laplace inverse, the quantity of interest in time domain is obtained. In subsequent paragraphs we discuss the Laplace transformation of circuit elements and solution methods.

### 9.5.1 Laplace Domain Equivalents of Circuit Elements

The elementary models for transient analysis are (a) resistor, (b) inductor, (c) capacitor, and (d) distributed parameter line as it has been discussed in Section 9.2. In this section we derive the Laplace domain equivalents of these models.

#### Resistance

The constitutive relationship is

$$v(t) = Ri(t)$$

The Laplace transform is

$$V(s) = RI(s) \quad (9.25)$$

The Laplace domain equivalent of a resistance is illustrated in Fig. 9.6a2 and a3.

#### Inductance

The constitutive relationship of a lumped inductance is

$$v(t) = L \frac{di(t)}{dt}$$

Taking the Laplace transform of the equation above, we obtain

$$V(s) = sLI(s) - Li(0) \quad (9.26)$$

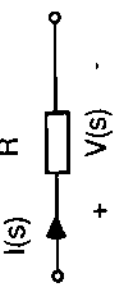
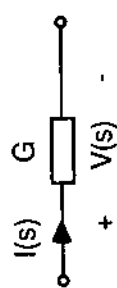
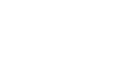
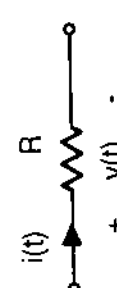
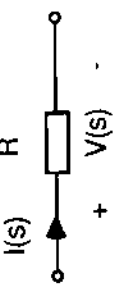
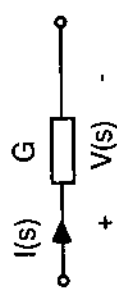
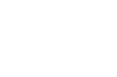
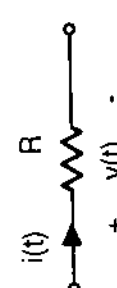
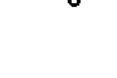
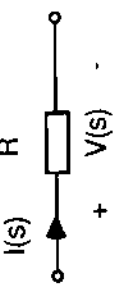
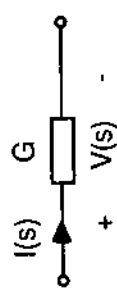
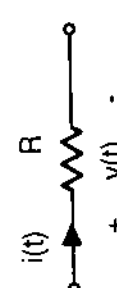
Network Element	Laplace Transform Element		
	Norton Form	Thevenin Form	
			a3
			a2
			b3
			b2
			c3
			c2
			d3
			d2
			d1

FIG. 9.6 Equivalent circuit representation in the Laplace domain.

where  $i(0)$  is the electric current through the inductor at time  $t = 0$ . Equation (9.26) represents an equivalent circuit in Thévenin form, that is, a voltage source  $Li(0)$  with internal "impedance"  $sL$  as illustrated in Fig. 9.6b3. Solution of Eq. (9.26) for the electric current  $I(s)$  yields

$$I(s) = \frac{1}{sL} V(s) + \frac{1}{s} i(0) \quad (9.27)$$

Equation (9.27) represents an equivalent circuit in Norton form, that is, a current source  $i(0)/s$  in parallel with an "admittance"  $1/sL$  as illustrated in Fig. 9.6b2.

### Capacitance

The constitutive relationship of a lumped capacitance is

$$i(t) = C \frac{dv(t)}{dt}$$

Taking the Laplace transform of the equation above gives us

$$I(s) = sCV(s) - Cv(0) \quad (9.28)$$

where  $v(0)$  is the voltage across the capacitor at time  $t = 0$ . Equation (9.28) represents an equivalent circuit in Norton form, that is, a current source of  $-Cv(0)$  in parallel with a conductance  $sC$  as illustrated in Fig. 9.6c2.

Solution of Eq. (9.28) for  $V(s)$  yields

$$V(s) = \frac{1}{sC} I(s) + \frac{1}{s} v(0) \quad (9.29)$$

Equation (9.29) represents an equivalent circuit in Thévenin form, that is, a voltage source of  $v(0)/s$  with an internal impedance of  $1/sC$ , as illustrated in Fig. 9.6c3.

### Single-Phase Lossless Transmission Line

The equivalent circuit of an ideal distributed-parameter single-phase transmission line in the Laplace domain is derived as follows: Consider Eqs. (9.5) of an ideal distributed-parameter line. Taking the Laplace transform of Eq. (9.5) assuming zero initial conditions:

$$\frac{\partial^2}{\partial y^2} V(y, s) = \frac{s^2}{c^2} V(y, s) \quad (9.30a)$$

$$\frac{\partial V(y, s)}{\partial y} = sLI(y, s) \quad (9.30b)$$

A general solution of Eq. (9.30a) is

$$V(y, s) = A(s)e^{s\sqrt{LC}y} + B(s)e^{-s\sqrt{LC}y} \quad (9.31)$$

In Eq. (9.31),  $A(s)$  and  $B(s)$  are "constants" to be determined by the boundary conditions of the problem. The electric current is derived from Eq. (9.30b) by direct substitution and subsequent manipulations:

$$I(y, s) = Y_0 A(s)e^{s\sqrt{LC}y} - Y_0 B(s)e^{-s\sqrt{LC}y} \quad (9.32)$$

where  $Y_0 = Z_0^{-1}$  and  $Z_0 = \sqrt{L/C}$  is the characteristic impedance of the line.

A useful form of the line equations is to express the current and voltage at one end as a linear combination of the current and voltage at the other end. Upon substitution of  $y = 0$  and  $y = \ell$  into Eqs. (9.31) and (9.32), we have

$$V(0, s) = A(s) + B(s)$$

$$I(0, s) = Y_0 A(s) - Y_0 B(s)$$

$$V(\ell, s) = A(s)e^{s\tau} + B(s)e^{-s\tau}$$

$$I(\ell, s) = Y_0 A(s)e^{s\tau} - Y_0 B(s)e^{-s\tau}$$

where  $\tau = \sqrt{LC} \ell$  and  $\ell$  is the length of the line. To simplify the notation, denote the terminal voltage and currents  $V(0, s)$ ,  $V(\ell, s)$ ,  $I(0, s)$ , and  $I(\ell, s)$  with

$$V_1(s) = V(0, s)$$

$$V_2(s) = V(\ell, s)$$

$$I_1(s) = -I(0, s)$$

$$I_2(s) = I(\ell, s)$$

Note that the currents  $I_1(s)$  and  $I_2(s)$  are both flowing into the line. The line terminal voltage and currents in the time domain will be denoted with  $v_1(t)$ ,  $v_2(t)$ ,  $i_1(t)$ , and  $i_2(t)$ . Now, upon elimination of the "constants"  $A(s)$  and  $B(s)$ , we have

$$V_1(s) = \cosh s\tau V_2(s) - Z_0 \sinh s\tau I_2(s) \quad (9.33a)$$

$$I_1(s) = Y_0 \sinh s\tau V_2(s) - \cosh s\tau I_2(s) \quad (9.33b)$$

Equations (9.33) provide the basis to develop an equivalent circuit in the Laplace domain. There are several alternative equivalent circuits corresponding to Eqs. (9.33). Here we discuss an equivalent circuit proposed by Snelson [47] which is suitable for transient analysis. For the purpose of deriving this equivalent circuit, Snelson [47] introduced four functions defined as follows:

$$f_1(t) = v_1(t) - Z i_1(t)$$

$$f_2(t) = v_2(t) + Z i_2(t)$$

$$b_1(t) = v_1(t) + Z i_1(t)$$

$$b_2(t) = v_2(t) - Z i_2(t)$$

where  $Z = Z_0$ . Taking the Laplace transform of the defining equations above yields

$$F_1(s) = V_1(s) + Z_0 I_1(s) \quad (9.34a)$$

$$F_2(s) = V_2(s) + Z_0 I_2(s) \quad (9.34b)$$

$$B_1(s) = V_1(s) - Z_0 I_1(s) \quad (9.35a)$$

$$B_2(s) = V_2(s) - Z_0 I_2(s) \quad (9.35b)$$

Now consider Eqs. (9.33), (9.34), and (9.35). It is possible to eliminate the voltage and electric currents from these equations in order to obtain a relationship between the functions  $B_1(s)$ ,  $B_2(s)$  and  $F_1(s)$ ,  $F_2(s)$ . For this purpose, substitute  $V_1(s)$  and  $I_1(s)$  from Eqs. (9.33) into Eqs. (9.34). The result is (after some manipulations)

$$\begin{bmatrix} F_1(s) \\ F_2(s) \end{bmatrix} = \begin{bmatrix} e^{+s\tau} & -Z_0 e^{+s\tau} \\ 1.0 & +Z_0 \end{bmatrix} \begin{bmatrix} V_2(s) \\ I_2(s) \end{bmatrix} \quad (9.36)$$

Similarly, upon substitution of  $V_1(s)$  and  $I_1(s)$  from Eqs. (9.33) into Eqs. (9.35) and subsequent manipulations, we have

$$\begin{bmatrix} B_1(s) \\ B_2(s) \end{bmatrix} = \begin{bmatrix} e^{-s\tau} & +Z_0 e^{-s\tau} \\ 1.0 & -Z_0 \end{bmatrix} \begin{bmatrix} V_2(s) \\ I_2(s) \end{bmatrix} \quad (9.37)$$

Solution of Eq. (9.36) for  $V_2(s)$ ,  $I_2(s)$  yields

$$\begin{bmatrix} V_2(s) \\ I_2(s) \end{bmatrix} = \frac{1}{2Z_0} \begin{bmatrix} Z_0 e^{-s\tau} & Z_0 \\ -e^{-s\tau} & +1 \end{bmatrix} \begin{bmatrix} F_1(s) \\ F_2(s) \end{bmatrix}$$

Substitution of the equations above into Eq. (9.37) and subsequent manipulations yields

$$B_1(s) = e^{-s\tau} F_2(s) \quad (9.38a)$$

$$B_2(s) = e^{-s\tau} F_1(s) \quad (9.38b)$$

Note that the expressions  $e^{-s\tau} F_2(s)$  and  $e^{-s\tau} F_1(s)$  in the time domain are  $f_2(t - \tau)$  and  $f_1(t - \tau)$ , respectively (see Table 9.1, line 8). Assuming that the conditions of the system in past times are known, the right-hand side of Eqs. (9.38) must be treated as known quantities. Now, upon substitution of  $B_1(s)$  and  $B_2(s)$  from Eqs. (9.35) into Eqs. (9.38) and subsequent solution for the electric currents  $I_1(s)$  and  $I_2(s)$ , we have

$$I_1(s) = Y_0 V_1(s) - Y_0 e^{-s\tau} F_2(s) \quad (9.39a)$$

$$I_2(s) = Y_0 V_2(s) - Y_0 e^{-s\tau} F_1(s) \quad (9.39b)$$

Equations (9.39) represent an equivalent circuit in Norton form which is illustrated in Fig. 9.6d2. Note that the known quantities  $Y_0 e^{-s\tau}$ ,  $F_2(s)$  and  $Y_0 e^{-s\tau} F_1(s)$  represent electric current sources.

An alternative equivalent circuit (Thévenin form) is obtained upon solution of Eqs. (9.39) for  $V_1(s)$  and  $V_2(s)$ :

$$V_1(s) = Z_0 I_1(s) + e^{-s\tau} F_2(s) \quad (9.40a)$$

$$V_2(s) = Z_0 I_2(s) + e^{-s\tau} F_1(s) \quad (9.40b)$$

Equations (9.40) represent the equivalent circuit illustrated in Fig. 9.6d3.

### 9.5.2 Transient Analysis Based on Laplace Transforms

Transient analysis of a specific system by means of the Laplace domain equivalent circuits is straightforward. Specifically, all the elements of the system under study are substituted with the Laplace domain equivalent circuits illustrated in Fig. 9.6. This procedure will generate an equivalent circuit of the system under study in the Laplace domain. Note that for each element there are two options:

Norton or Thévenin form. When the Norton form is selected, the resulting network will comprise admittance branches and current sources. Application of nodal analysis to this network will yield the node voltages in the Laplace domain. A subsequent inverse Laplace transformation will yield the node voltages in the time domain. When the Thévenin form is selected, the resulting network will comprise impedance branches and voltage sources. Application of loop analysis to this network will yield the branch currents in the Laplace domain. Again, a subsequent inverse Laplace transformation will yield the branch currents in the time domain.

The transient analysis based on Laplace transforms will be illustrated with two examples.

Example 9.3: Consider an impulse generator. The impulse generator is used to generate a double-exponential voltage waveform on power apparatus. The equivalent circuit of a single-stage impulse generator is illustrated in Fig. E9.7. The capacitor  $C_2$  represents the capacitance of the power apparatus (test subject). The capacitor  $C_1$  is charged and subsequently is discharged through the spark gap into the parallel combination of the resistor  $R_2$  and capacitor  $C_2$ . The parameters of the impulse generator of Fig. E9.7 are  $C_1 = 2 \mu\text{F}$ ,  $C_2 = 0.1 \mu\text{F}$ ,  $R_1 = 1.2 \Omega$ , and  $R_2 = 30 \Omega$ . Assume that the capacitor  $C_1$  is charged to 60 kV. Compute the voltage at point A following a spark in the indicated gap.

Solution: Each element of the circuit is replaced with its Laplace transformed in Norton form according to Fig. 9.6. The resulting equivalent circuit appears in Fig. E9.8. The nodal equations for this circuit are

$$\begin{bmatrix} G_1 + sC_1 & -G_1 \\ -G_1 & G_1 + G_2 + sC_2 \end{bmatrix} \begin{bmatrix} V_1(s) \\ V_2(s) \end{bmatrix} = \begin{bmatrix} C_1 v(0) \\ 0 \end{bmatrix}$$

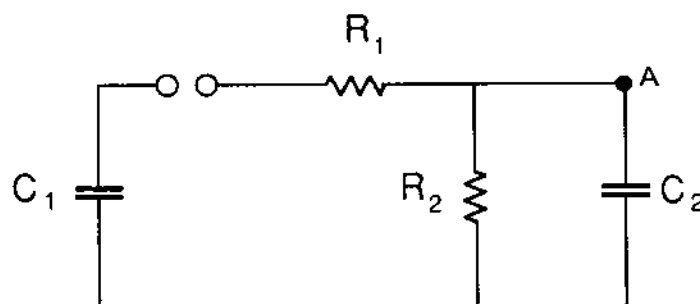


FIG. E9.7 Single stage impulse generator.

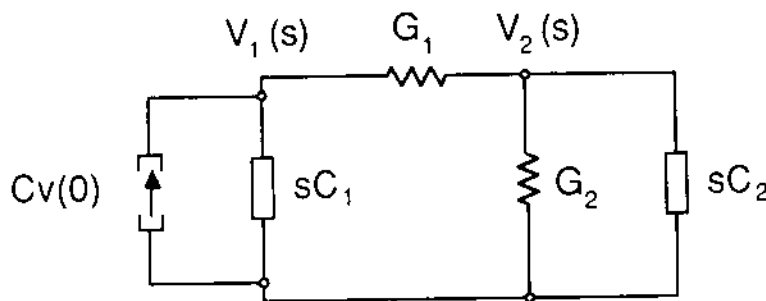


FIG. E9.8 Laplace domain equivalent circuit of the single stage impulse generator.

Solving for  $V_2(s)$  gives us

$$V_2(s) = \frac{G_1 C_1 v(0)}{s^2 C_1 C_2 + s[C_1(G_1 + G_2) + C_2 G_1] + G_1 G_2}$$

Upon substitution of numerical values, we obtain

$$V_2(s) = \frac{0.5 \times 10^{12}}{s^2 + 9.0833 \times 10^6 s + 0.13888 \times 10^{12}}$$

Now in order to compute the time-domain voltage  $V_2(t)$ , it is necessary to take the inverse Laplace transform of the function above. For this purpose it is expedient to analyze the foregoing function of  $s$  into simple fractions as follows:

$$V_2(s) = \frac{a}{s + \alpha_1} + \frac{b}{s + \alpha_2}$$

By equating the two expressions for  $V_2(s)$  and subsequent solution for  $\alpha_1$ ,  $\alpha_2$ ,  $a$ , and  $b$ , we get

$$\alpha_1 = -0.01531 \times 10^6$$

$$\alpha_2 = -9.068 \times 10^6$$

$$a = 0.0552 \times 10^6$$

$$b = -0.0552 \times 10^6$$

Thus

$$V_2(s) = \frac{55,200}{s + 0.01531 \times 10^6} - \frac{55,200}{s + 9.068 \times 10^6}$$

Now the inverse Laplace transform of the equation above is determined with the aid of Table 9.2:

$$V_2(t) = 55,200e^{-0.01531 \times 10^6 t} - 55,200e^{-9.068 \times 10^6 t} \text{ V}$$

Example 9.4: Consider a single-phase lossless transmission line. The parameters of the line are  $L$  (H/m) and  $C$  (F/m). The line has a length of  $\ell$  meters and is terminated at one end with a lumped resistor  $R$  as illustrated in Fig. E9.9. The line is not energized when at time  $t = 0$ , lightning strikes at the open end of the line. The lightning is to be represented with a double-exponential current waveform  $i(t) = I[\exp(-\alpha_1 t) - \exp(-\alpha_2 t)] = f(t)$ . Compute the transient voltage at the two ends of the line.

Solution: The equivalent circuit of the system in the Laplace domain is illustrated in Fig. E9.10. Note that lightning is represented as an ideal current source. Nodal analysis of the circuit yields the following equations:

$$(G + Y_0)V_1(s) = Y_0 e^{-s\tau} F_2(s)$$

$$Y_0 V_2(s) = F(s) + Y_0 e^{-s\tau} F_1(s)$$

where

$$F_1(s) = V_1(s) + Z_0 I_1(s)$$

$$F_2(s) = V_2(s) + Z_0 I_2(s)$$

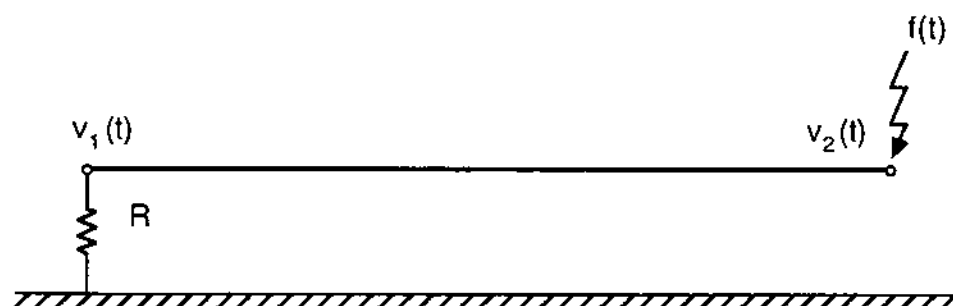


FIG. E9.9 A single phase transmission line.

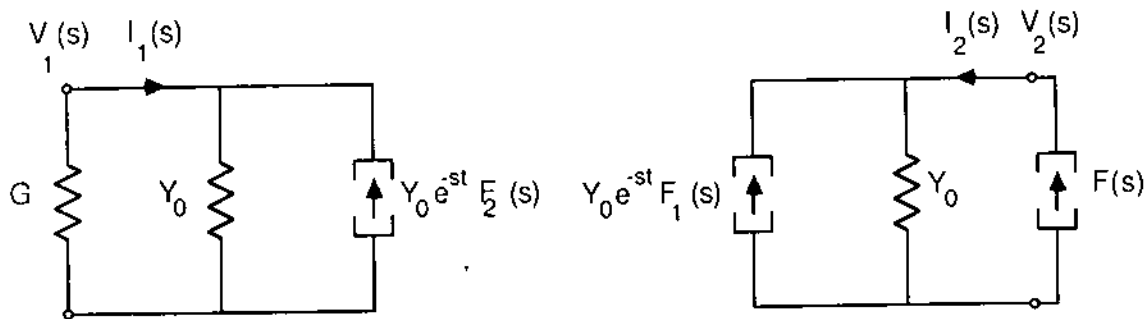


FIG. E9.10 Equivalent circuit in Laplace domain of the system of Figure E9.9.

Note also that

$$I_1(s) = -GV_1(s)$$

$$I_2(s) = F(s)$$

Upon substitution of  $I_1(s)$ ,  $I_2(s)$ ,  $F_1(s)$ ,  $F_2(s)$ :

$$(G + Y_0)V_1(s) = Y_0 e^{-s\tau}V_2(s) + e^{-s\tau}F(s)$$

$$Y_0V_2(s) = F(s) + Y_0 e^{-s\tau}V_1(s) - Ge^{-s\tau}V_1(s)$$

Solving for  $V_1(s)$  and  $V_2(s)$  gives us

$$V_1(s) = \frac{2}{G + Y_0} \frac{e^{-st}F(s)}{1 - \beta e^{-2st}}$$

$$V_2(s) = Z_0F(s) \frac{1 + \beta e^{-2s\tau}}{1 - \beta e^{-2s\tau}}$$

where

$$\beta = \frac{Y_0 - G}{Y_0 + G}$$

Recall the following identity:

$$\frac{1}{1 - \beta e^{-2s\tau}} = 1 + \beta e^{-2s\tau} + \beta^2 e^{-4s\tau} + \beta^3 e^{-6s\tau} + \dots \quad \text{for } |\beta e^{-2s\tau}| < 1$$

Also note that

$$\frac{2}{G + Y_0} = Z_0(1 + \beta)$$

Upon substitution into the equations for  $V_1(s)$  and  $V_2(s)$ , we obtain

$$V_1(s) = Z_0 F(s) e^{-s\tau} (1 + \beta)(1 + \beta e^{-2s\tau} + \beta^2 e^{-4s\tau} + \dots)$$

$$V_2(s) = Z_0 F(s) (1 + 2\beta e^{-2s\tau} + 2\beta^2 e^{-4s\tau} + 2\beta^3 e^{-6s\tau} + \dots)$$

Taking the inverse Laplace transform of the equations above gives us

$$v_1(t) = Z_0(1 + \beta)[f(t - \tau) + \beta f(t - 3\tau) + \beta^2 f(t - 5\tau) + \dots]$$

$$v_2(t) = Z_0[f(t) + 2\beta f(t - 2\tau) + 2\beta^2 f(t - 4\tau) + 2\beta^3 f(t - 6\tau) + \dots]$$

For a numerical example, consider the following parameters:

$$R = 200 \Omega$$

$$L = 1.32 \mu H/m$$

$$C = 8.5 \text{ pF/m}$$

and

$$f(t) = 10.537(e^{-0.15 \times 10^6 t} - e^{-1.65 \times 10^6 t}) \text{ kA}$$

Now

$$Z_0 = \sqrt{\frac{L}{C}} = 394 \Omega$$

$$c = \frac{1}{\sqrt{LC}} = 298.54 \times 10^6 \text{ m/s}$$

$$\tau = \sqrt{LC} = 26.95 \mu s$$

$$\beta = \frac{Y_0 - G}{Y_0 + G} = -0.3266$$

Upon substitution into the equations for the voltages  $v_1(t)$  and  $v_2(t)$ , we have

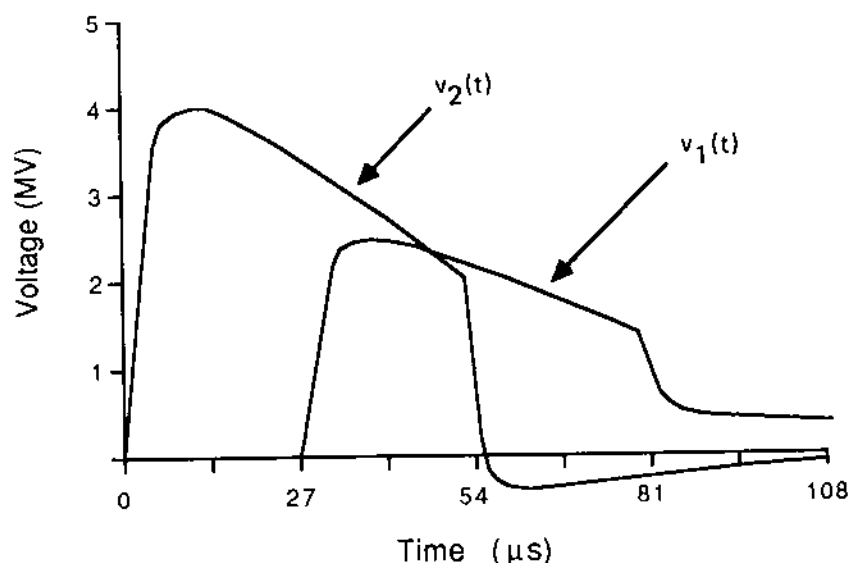


FIG. E9.11 Illustration of voltages  $v_1(t)$  and  $v_2(t)$ .

$$v_1(t) = 265.32f(t - \tau) - 86.64f(t - 3\tau) + 28.289f(t - 5\tau)$$

- ...

$$v_2(t) = 394f(t) - 257.36f(t - 2\tau) + 84.06f(t - 4\tau) + \dots$$

The waveform of the voltages  $v_1(t)$  and  $v_2(t)$  is illustrated in Fig. E9.11.

## 9.6 NUMERICAL TECHNIQUES

In this section we discuss numerical techniques for transient analysis. Numerical methods can be applied in the time domain or the frequency domain. In general, numerical techniques in the time domain are flexible because they allow modeling of nonlinear elements. Frequency-domain techniques are suitable for linear systems. In this book we examine time-domain numerical techniques only.

## 9.7 TIME-DOMAIN NUMERICAL TECHNIQUES

Time-domain numerical techniques are based on numerical integration of the differential equations describing a system. Many numerical integration techniques are known with various characteristics. Use of a numerical integration technique can transform any differential equation into a set of algebraic equations. These equations can be interpreted as representing a resistive network with appropriate sources. The circuits are in general called resistive companion network. The resistive companion networks can be solved with well-

established network techniques such as nodal or loop analysis. The application of this procedure for power system transient analysis was originally proposed by H. Dommel [43].

The most popular numerical integration method used for power system transients is the trapezoidal integration method. The method is simple to apply and it is numerically absolutely stable. The method is reviewed in Section 9.7.1. The derivation of the equivalent circuits and subsequent solution techniques is presented in Section 9.7.2.

### 9.7.1 Trapezoidal Integration Method

This method will be introduced with an example. Consider the first-order differential equation

$$\frac{dx(t)}{dt} = ax(t) \quad (9.41)$$

$$x(0) = c \quad (9.42)$$

Integration of the equation above from time  $t - h$  to  $t$  yields

$$x(t) - x(t - h) = a \int_{t-h}^t x(\tau) d\tau \quad (9.43)$$

The integral above cannot be computed unless the function  $x(t)$  in the interval  $(t - h, t)$  is known. This is generally not the case. However, if the time interval  $(t - h, t)$  is very small ( $h$  small), a reasonable approximation can be assumed for the function  $x(t)$  in the interval  $(t - h, t)$ . If it is assumed that the function  $x(t)$  varies linearly in the interval  $(t - h, t)$ , then

$$x(\tau) = \alpha(\tau - t + h) + \beta$$

where

$$\beta = x(t - h)$$

$$\alpha = \frac{x(t) - x(t - h)}{h}$$

Now the integral in Eq. (9.43) is evaluated to yield

$$\int_{t-h}^t x(\tau) d\tau = \frac{h}{2} [x(t) + x(t - h)] \quad (9.44)$$

Upon substitution into Eq. (9.43) and subsequent solution for  $x(t)$ , we have

$$x(t) = \left(1 - \frac{ha}{2}\right)^{-1} \left(1 + \frac{ha}{2}\right) x(t-h) \quad (9.45)$$

assuming that  $(1 - ha/2) \neq 0$ . Equation (9.45) provides the value of the function at time  $t$  when the value of the function at time  $t - h$  is known. Repeated application of Eq. (9.45) provides the value of the function  $x(t)$  at discrete times (i.e.,  $h$ ,  $2h$ ,  $3h$ , etc.). The time interval  $h$  will be called the integration time step.

If the system is stable,  $a < 0$ . In this case,  $1 - ha/2$  is always different from zero (greater than 1.0). Also, observe that the quantity  $(1 - ha/2)^{-1}(1 + ha/2)$  is always less than 1. Thus independently of the selected value of the time step  $h$ , the solution for  $x(t)$  will always be bounded by virtue of Eq. (9.45). Thus, for a physically stable problem, the numerical solution will also be stable. This property of the trapezoidal integration method is known as absolute numerical stability.

The name of the method has been coined from the graphical representation of Eq. (9.44), which is illustrated in Fig. 9.7. The value of the integral equals the area of the trapezoid defined with the points  $x(t)$  and  $x(t - h)$ .

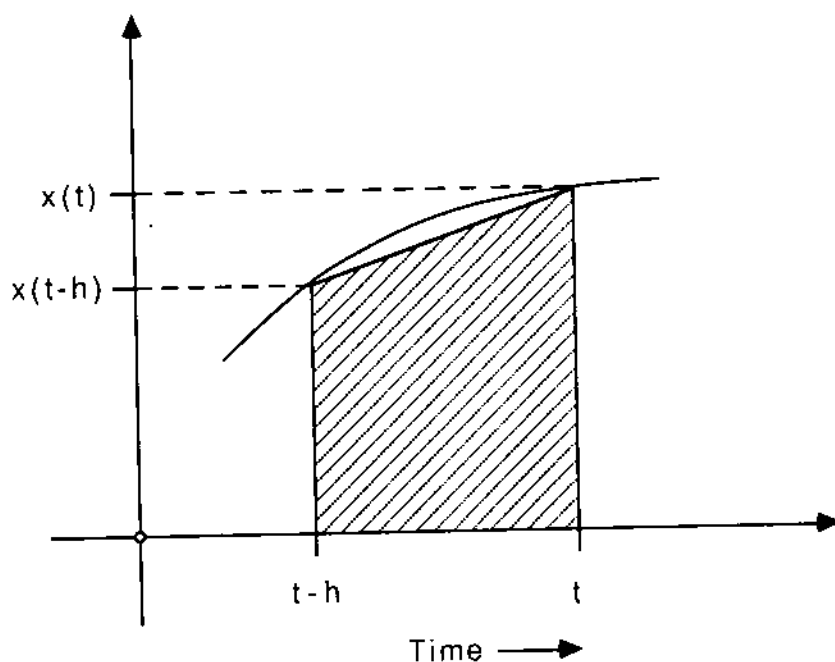


FIG. 9.7 Graphical representation of trapezoidal integration.

### 9.7.2 Equivalent Resistive Companion Circuits

In this section we discuss the derivation of resistive companion circuits. For this purpose the trapezoidal integration technique will be applied to the differential equations of individual circuit elements, such as resistors, inductors, capacitors, and transmission lines. The resulting equations will be interpreted as resistive circuits. The procedure will be applied to the four elementary models of Fig. 9.2.

#### Resistance

Consider a resistance that carries an electric current  $i(t)$  and voltage across  $v(t)$  as illustrated in Fig. 9.8a1. Since the equation describing this element is algebraic, there is no need for numerical integration. The equivalent resistive companion circuit of a resistance is the resistance itself as illustrated in Fig. 9.8a2 or a3.

#### Inductance

Consider an inductor of inductance  $L$ , carrying current  $i(t)$ , and voltage across  $v(t)$  as in Fig. 9.8b1. Two alternative resistive companion circuits of this inductor are illustrated in Fig. 9.8b2 and b3 and are derived as follows. The differential equation describing the inductor is

$$v(t) = L \frac{di(t)}{dt}$$

Application of the trapezoidal integration in the interval  $(t - h, t)$  yields

$$[v(t) - v(t - h)] \frac{h}{2} = L(i(t) - i(t - h))$$

Upon solution of the equation above for the electric current  $i(t)$  or the voltage  $v(t)$ , we have

$$i(t) = \frac{h}{2L} v(t) + I_L(t - h) \quad (9.46)$$

where

$$I_L(t - h) = i(t - h) + \frac{h}{2L} v(t - h)$$

and

$$v(t) = \frac{2L}{h} i(t) + E_L(t - h) \quad (9.47)$$

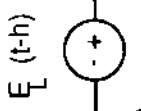
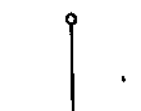
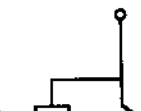
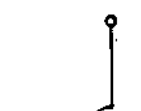
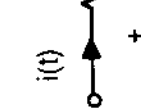
Network Element	Equivalent Resistive Companion Circuit		
	Norton Form	Thevenin Form	
$i(t)$ $R$			a3
$i(t)$ $L$			b3
$i(t)$ $C$			c3
$i_1(t)$ $i_2(t)$ $v_1(t)$ $v_2(t)$			d1
$i_1(t)$ $i_2(t)$ $v_1(t)$ $v_2(t)$			d2

FIG. 9.8 Equivalent resistive companion circuits.

where

$$E_L(t - h) = -\frac{2L}{h} i(t - h) - v(t - h)$$

Since  $I_L(t - h)$  and  $E_L(t - h)$  are defined in terms of voltages and currents at past time, they are known. Thus they can be treated as known current and voltage sources, respectively. This results in the equivalent resistive companion circuits of Fig. 9.8b2 and b3.

### Capacitance

Consider a capacitor of capacitance  $C$ , carrying current  $i(t)$ , and voltage across  $v(t)$  as illustrated in Fig. 9.8c1. Two alternative resistive companion circuits of this capacitor are illustrated in Fig. 9.8c2 and c3 and are derived as follows. The differential equation describing the capacitor is

$$i(t) = C \frac{dv(t)}{dt}$$

Application of the trapezoidal integration in the interval  $(t - h, t)$  yields

$$[i(t) + i(t - h)] \frac{h}{2} = C(v(t) - v(t - h))$$

Upon solution of this equation for the electric current  $i(t)$  or the voltage  $v(t)$ , we have

$$i(t) = \frac{2C}{h} v(t) + I_C(t - h) \quad (9.48)$$

where

$$I_C(t - h) = -i(t - h) - \frac{2C}{h} v(t - h)$$

and

$$v(t) = \frac{h}{2C} i(t) + E_C(t - h) \quad (9.49)$$

where

$$E_C(t - h) = \frac{h}{2C} i(t - h) + v(t - h)$$

Again, since  $I_C(t - h)$  and  $E_C(t - h)$  are defined in terms of voltages and currents at past time, they are known. Thus they can be treated as known current and voltage sources, respectively. This results in the equivalent resistive companion circuits of Fig. 9.8c2 and c3.

### Lossless Single-Phase Transmission Line

The resistive companion circuit of a lossless transmission line can be obtained directly from the equivalent circuit developed in Section 9.5.1. Specifically, consider Eqs. (9.39), which describe the equivalent circuit of the ideal transmission line in Laplace domain. Taking the inverse Laplace transform of these equations gives us

$$i_1(t) = Y_0 v_1(t) - Y_0 f_2(t - \tau)$$

$$i_2(t) = Y_0 v_2(t) - Y_0 f_1(t - \tau)$$

The quantities  $-Y_0 f_1(t - \tau)$  and  $-Y_0 f_2(t - \tau)$  are known since they depend on past time. They should be treated as known current sources. For simplicity, the equations above are written in the following form:

$$i_1(t) = Y_0 v_1(t) + I_2(t - \tau) \quad (9.50a)$$

$$i_2(t) = Y_0 v_2(t) + I_1(t - \tau) \quad (9.50b)$$

where

$$I_1(t - \tau) = -Y_0 f_1(t - \tau) = -Y_0 v_1(t - \tau) - i_1(t - \tau)$$

$$I_2(t - \tau) = -Y_0 f_2(t - \tau) = -Y_0 v_2(t - \tau) - i_2(t - \tau)$$

Equations (9.50) represent the equivalent resistive companion circuit of Fig. 9.8d2.

Upon solution of Eqs. (9.50) for the voltages  $v_1(t)$  and  $v_2(t)$ , we have

$$v_1(t) = Z_0 i_1(t) + f_2(t - \tau) \quad (9.51a)$$

$$v_2(t) = Z_0 i_2(t) + f_1(t - \tau) \quad (9.51b)$$

where

$$f_1(t - \tau) = v_1(t - \tau) + Z_0 i_1(t - \tau)$$

$$f_2(t - \tau) = v_2(t - \tau) + Z_0 i_2(t - \tau)$$

Equations (9.51) represent the equivalent resistive companion circuit of Fig. 9.8d3.

The equivalent resistive companion circuits of the single-phase transmission line can also be obtained with the help of the theory of traveling waves. For this purpose, consider a transmission line of characteristic admittance  $Y_0$ , terminating at nodes 1 and 2 as in Fig. 9.8d1. Let at time  $t$  the voltage at node 2 be  $v_2(t)$ . Also, let the electric current at node 2 be  $i_2(t)$  (directed from node 2 to node 1). Let  $\tau$  be the travel time of an electromagnetic wave from one end of the line to the other. If  $v_1(t - \tau)$  and  $i_1(t - \tau)$  are the corresponding voltage and electric current at node 1 at time  $t - \tau$ , it is obvious that this wave will arrive at node 2 at time  $t$ . With the voltage wave  $v_1(t - \tau)$ , there is an electric current wave equal to  $Y_0 v_1(t - \tau)$ . In addition, the voltage  $v_2(t)$  will generate electric current of  $Y_0 v_2(t)$  in the terminal 2 of the line. Thus the total current at node 2 at time  $t$  will be

$$i_2(t) = Y_0 v_2(t) - Y_0 v_1(t - \tau) - i_1(t - \tau)$$

Similarly, the electric current at node 1 is

$$i_1(t) = Y_0 v_1(t) - Y_0 v_2(t - \tau) - i_2(t - \tau)$$

These equations are exactly Eqs. (9.50).

### 9.7.3 Resistive Companion Network Analysis

Transient analysis problems can be solved with the aid of the resistive companion circuits in a simple algorithmic way. The basic idea of this algorithm is described as follows. Consider a system and assume that at some time,  $t - h$ , all the voltages and electric currents are known in the system. In this case the equivalent resistive companion circuits of all the circuit elements of the system are computed with an integration time step  $h$ . The procedure yields a resistive companion network for the system under study in which all the sources are known. Subsequent solution of the network problem will yield the voltage and electric current everywhere in the system. The procedure can start at any instant of time for which all voltages and currents are known. For example, assume that at time  $t = 0$  all the voltages and electric currents are known or they can be computed everywhere in the system of interest. These values represent the initial conditions. Then the procedure is repeated for times  $h$ ,  $2h$ ,  $3h$ , ...,  $t_{\max}$ , yielding the voltages and currents in the system at these discrete times.

In summary, the algorithm for transient analysis involves the following steps:

- Step 1. Set  $t = 0$ .
- Step 2. Determine the initial conditions.
- Step 3. Set  $t = t + h$ .
- Step 4. Assemble the equivalent resistive companion network (for nodal or loop analysis) for time  $t$ .
- Step 5. Solve the resistive companion network equations.
- Step 6. If  $t$  is less than  $t_{\max}$ , go to step 3. Otherwise, terminate the procedure.

The procedure will be illustrated with two examples. The first will use loop analysis, while the second will use nodal analysis.

Example 9.5: Consider the electric power system of Fig. E9.12. At time  $t = 0$ , an electric fault occurs at point A. Compute the fault current as a function of time.

Solution: Assume an integration time step of  $h = 0.8$  ms. Then each circuit element is substituted with the resistive companion circuit in Thévenin form, yielding the equivalent resistive companion network illustrated in Fig. E9.13. Note that

$$E_L(t - h) = -10i(t - h) - v_L(t - h)$$

The initial conditions are  $i(0) = 0$ ,  $v_L(0) = 0$ ,  $e(0) = 9.798$  kV. At each iteration, the assembly of the resistive companion network requires the computation of the following quantities in this order:

1. Compute  $e(t)$ :

$$e(t) = 9.798 \text{ kV} \cos \omega t$$

2. Compute  $v_L(t - h)$ ,  $E_L(t - h)$ :

$$v_L(t - h) = 10i(t - h) + E_L(t - 2h)$$

$$E_L(t - h) = -10i(t - h) - v_L(t - h)$$

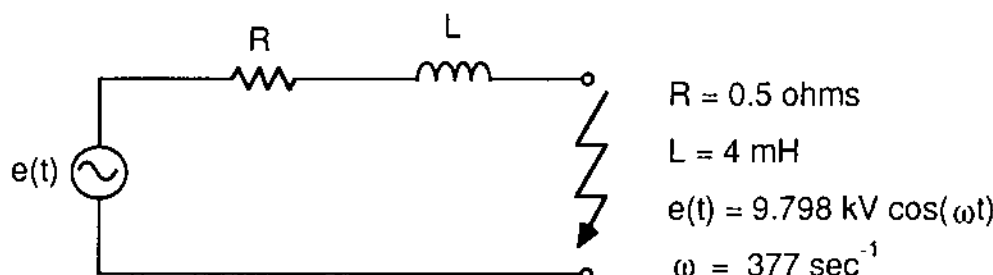


FIG. E9.12 A simple electric fault.

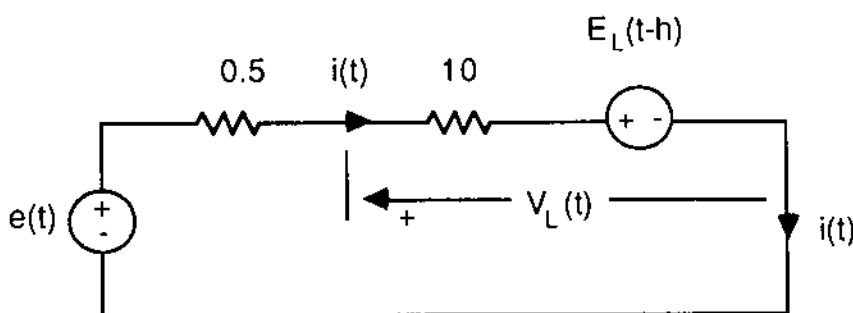


FIG. E9.13 Resistance companion network for the system of Figure E9.12.

$$3. \text{ Compute } i(t) = [e(t) - E_L(t - h)]/10.5.$$

Twelve iterations of the algorithm are illustrated in Table E9.1. The table provides the short-circuit current  $i(t)$  and the voltage across the inductor  $v_L(t)$ .

Example 9.6: Consider the electric power system of Example 9.1. Compute the transient overvoltage at point B for a period of 6  $\mu\text{s}$  using the numerical technique. Use a time step of 0.5  $\mu\text{s}$ .

Solutions: The equivalent resistive companion network is illustrated in Fig. E9.14. Note that the lightning is represented with the ideal current source  $a(t)$ . The following equations define the indicated electric currents and current sources illustrated in the figure:

$$i_{1,2}(t) = 0.0025v_1(t) + I_1(t - 1)$$

$$i_{2,1}(t) = 0.0025v_2(t) + I_2(t - 1)$$

$$i_{2,3}(t) = 0.01v_2(t) + I_3(t - 2)$$

$$i_{3,2}(t) = 0.01v_3(t) + I_4(t - 2)$$

where

$$I_1(t) = -i_{2,1}(t) - 0.0025v_2(t)$$

$$I_2(t) = -i_{1,2}(t) - 0.0025v_1(t)$$

$$I_3(t) = -i_{3,2}(t) - 0.01v_3(t)$$

$$I_4(t) = -i_{2,3}(t) - 0.01v_2(t)$$

Application of nodal analysis on the circuit of Fig. E9.14 yields

TABLE E9.1 Numerical Results for Example 9.5

Iteration number:	1	2	3	4	5	6	7	8	9	10	11	12
Time (ms):	0	0.8	1.6	2.4	3.2	4.0	4.8	5.6	6.4	7.2	8.0	8.8
$e(t)$	9.798	9.355	9.069	6.053	3.492	0.615	-2.317	-5.04	-7.308	-8.917	-9.721	-9.646
$i(t)$	0	0.8909	2.5607	3.757	4.308	4.288	3.718	2.663	1.233	-0.429	-2.163	-3.8013
$V_L(t - h)$	0	0	8.9095	7.7886	4.1751	1.3379	-1.5294	-4.1755	-6.3712	-7.9239	-8.7021	-8.638
$E_L(t - h)$	0	0	-17.819	-33.395	-41.745	-44.418	-41.358	-33.004	-20.258	-4.406	12.992	30.268

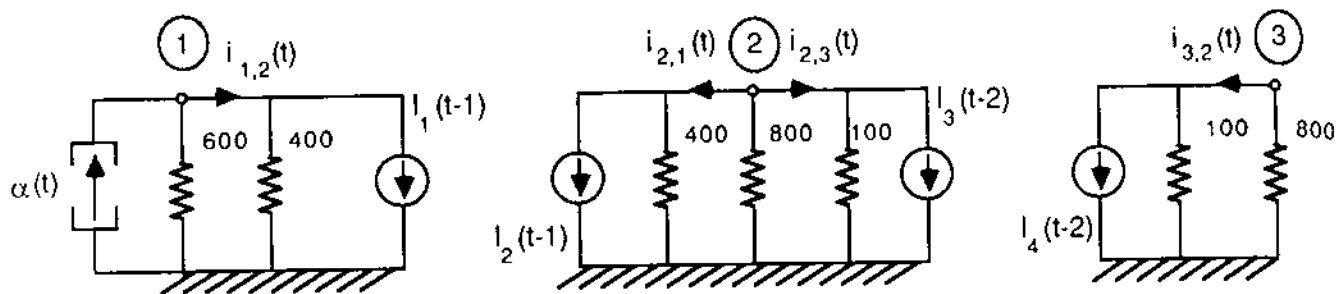


FIG. E9.14 Resistive companion network for the system of Figure E9.1.

$$v_1(t) = 240.0b_1(t)$$

$$v_2(t) = 72.72b_2(t)$$

$$v_3(t) = 88.88b_3(t)$$

where

$$b_1(t) = \alpha(t) - I_1(t - 1)$$

$$b_2(t) = -I_2(t - 1) - I_3(t - 2)$$

$$b_3(t) = -I_4(t - 2)$$

At each iteration, the network solution requires the following computations:

1.  $b_1(t) = \alpha(t) - I_1(t - 1.0)$   
 $b_2(t) = -I_2(t - 1.0) - I_3(t - 2.0)$   
 $b_3(t) = -I_4(t - 2.0)$
2.  $v_1(t) = 240.0b_1(t)$   
 $v_2(t) = 72.72b_2(t)$   
 $v_3(t) = 88.88b_3(t)$

The setup of the resistive companion network at each iteration requires the following computations:

1.  $\alpha(t)$  from Fig. E9.2
2.  $i_{1,2}(t) = 0.0025v_1(t) + I_1(t - 1.0)$   
 $i_{2,1}(t) = 0.0025v_2(t) + I_2(t - 1.0)$   
 $i_{2,3}(t) = 0.01v_2(t) + I_3(t - 2.0)$   
 $i_{3,2}(t) = 0.01v_3(t) + I_4(t - 2.0)$   
 where the time  $t$  is expressed in microseconds.
3.  $I_1(t) = -i_{2,1}(t) - 0.0025v_2(t)$   
 $I_2(t) = -i_{1,2}(t) - 0.0025v_1(t)$

$$\begin{aligned} I_3(t) &= -i_{3,2}(t) - 0.01v_3(t) \\ I_4(t) &= -i_{2,3}(t) - 0.01v_2(t) \end{aligned}$$

Twelve iterations of the algorithm are illustrated in Table E9.2. Compare the computed voltage  $v_2(t)$  with the same voltage computed with the graphical method in Example 9.1.

## 9.8 TRANSIENT ANALYSIS OF THREE-PHASE SYSTEMS

Transient analysis of multiphase transmission lines is rather complex. For all practical purposes, transient analysis of multiphase systems is performed with the aid of computers. In this section we present basic modeling techniques for transient analysis of multiphase lines. A very simple model will be presented first, which provides intuition into the transient behavior of three-phase systems. Subsequent paragraphs will elaborate on more accurate computer models.

The general approach for transient analysis of three-phase lines is as follows. As we have discussed in Chapter 6, a three-phase transmission line is described with a set of three coupled partial differential equations. To simplify the solution of these equations, an appropriate transformation is applied which transforms the coupled partial differential equations into a set of three uncoupled partial differential equations (modal decomposition). The new variables represent three uncoupled modes of wave propagation along the three-phase line. In this way the transient analysis of a three-phase line is reduced to the transient analysis of three single-phase transmission lines.

### 9.8.1 Three-Phase Transmission Line Models

To simplify the discussion, the modeling procedure for a three-phase transmission line will be confined to a line in which the shield or neutral conductor is neglected. The equations for a three-phase overhead transmission line without a shield or neutral conductor are

$$\frac{d^2v(y,t)}{dy^2} = LC \frac{d^2v(y,t)}{dt^2} + RC \frac{dv(y,t)}{dt} \quad (9.52a)$$

$$\frac{dv(y,t)}{dy} = Ri(y,t) + L \frac{di(y,t)}{dt} \quad (9.52b)$$

where

$$i(y,t) = \begin{bmatrix} i_a(y,t) \\ i_b(y,t) \\ i_c(y,t) \end{bmatrix}$$

TABLE E9.2

Iteration number:	1	2	3	4	5	6	7	8	9	10	11	12
$t$ ( $\mu s$ ):	0.5	1.0	1.5	2.0	2.5	3.0	3.5	4.0	4.5	5.0	5.5	6.0
$a(t)$	2.5	5.0	4.166	3.333	2.5	1.666	0.833	0	0	0	0	0
$b_1(t)$	2.5	5.0	4.166	3.333	0.5914	-2.1522	-2.349	-2.5456	-1.6662	-0.6144	-0.2312	0.3239
$b_2(t)$	0	0	3.0	6.0	5.0	4.0	2.6182	0.9656	0.3632	-0.5091	3.0594	6.6626
$b_3(t)$	0	0	0	0	0	0	4.363	8.726	7.272	5.8176	3.8078	0.4388
$v_1(t)$	600	1200	999.84	800	141.94	-516.53	-563.76	-610.944	-399.888	-147.456	-55.488	77.736
$v_2(t)$	0	0	218.16	436.32	363.60	290.88	190.39	70.21	26.41	-37.02	222.48	484.50
$v_3(t)$	0	0	0	0	0	0	387.78	755.56	646.33	517.07	338.44	39.00
$i_{1,2}(t)$	1.5	3.0	2.5	2.0	2.2634	2.5269	1.7726	1.0182	0.6665	0.2458	0.0925	-0.1295
$i_{2,1}(t)$	0	0	-2.454	-4.909	-4.091	-3.2728	-2.1422	-0.79	-0.2972	0.4165	0.8894	1.334
$i_{2,3}(t)$	0	0	2.1816	4.363	3.636	2.9088	1.9039	-0.2634	0.2641	-0.3702	-1.1678	-1.9404
$i_{3,2}(t)$	0	0	0	0	0	0	-0.4852	-0.9703	-0.8086	-0.6469	-0.4234	-0.0488
$I_1(t)$	0	0	1.9086	3.8182	3.182	2.5456	1.6662	0.6144	0.2312	-0.3239	-1.446	-2.545
$I_2(t)$	-3.0	-6.0	-5.0	-4.0	-2.6182	-0.9656	-0.3632	0.5091	0.3332	0.1228	0.0462	-0.0647
$I_3(t)$	0	0	0	0	0	0	-3.3926	-6.7854	5.6547	-4.5238	-2.961	-0.3412
$I_4(t)$	0	0	-4.363	-8.726	-7.272	-5.8176	-3.8078	-0.4388	-0.5282	0.7404	-1.057	-2.9046

$$v(y, t) = \begin{bmatrix} v_a(y, t) \\ v_b(y, t) \\ v_c(y, t) \end{bmatrix}$$

$$R = \begin{bmatrix} r_e + r_a & r_e & r_e \\ r_e & r_e + r_b & r_e \\ r_e & r_e & r_e + r_c \end{bmatrix}$$

$$L = \begin{bmatrix} L_{aae} & L_{abe} & L_{ace} \\ L_{bce} & L_{bbe} & L_{bce} \\ L_{cae} & L_{cbe} & L_{cce} \end{bmatrix}$$

$$C = \begin{bmatrix} C_{aa} & C_{ab} & C_{ac} \\ C_{ba} & C_{bb} & C_{bc} \\ C_{ca} & C_{cb} & C_{cc} \end{bmatrix}$$

In the equations above, the matrices R, L, and C are, in general, full matrices. Thus Eqs. (9.52) are second-order coupled differential equations. In addition, the elements of the matrices R, L, and C are frequency dependent. The numerical solution of these equations is, in general, very complex. For clarity of presentation, the analysis of this model is presented in steps. First, a number of simplifying assumptions are introduced which lead to the concept of a lossless continuously transposed line. This line model is examined in detail to present the basic concepts in overvoltage analysis of three-phase lines. Subsequently, modeling procedures to incorporate the exact line behavior will be examined.

### 9.8.2 The Concept of a Continuously Transposed Line

The concept of a continuously transposed transmission line is very useful for discussing the basic electromagnetic transient phenomena in three-phase transmission lines. It is based on the following assumptions:

1. The line inductance and capacitance (matrices L and C) are constant (independent of frequency).
2. The mutual parameters between any two phases (mutual inductance and capacitance) are equal.
3. The line resistance can be neglected (i.e.,  $R = 0$ ).

Mathematically, the continuously transposed line is obtained from Eqs. (9.52) by setting

$$L_{aae} = L_{bbe} = L_{cce} = L_s$$

$$L_{abe} = L_{bce} = L_{ace} = L_m$$

$$C_{aa} = C_{bb} = C_{cc} = C_s$$

$$C_{ab} = C_{bc} = C_{ac} = C_m$$

$$r_a + r_e = r_b + r_e = r_c + r_e = 0$$

$$r_e = 0$$

Naturally, there is no such thing as a continuously transposed three-phase line. However, any three-phase transmission line can be approximated with a continuously transposed three-phase line with the equations

$$L_s = \frac{1}{3} (L_{aae} + L_{bbe} + L_{cce}) \quad (9.53)$$

$$L_m = \frac{1}{3} (L_{ace} + L_{bce} + L_{cae}) \quad (9.54)$$

$$C_s = \frac{1}{3} (C_{aa} + C_{bb} + C_{cc}) \quad (9.55)$$

$$C_m = \frac{1}{3} (C_{ab} + C_{bc} + C_{ca}) \quad (9.56)$$

Based on these assumptions, the matrices L and C become

$$L = \begin{bmatrix} L_s & L_m & L_m \\ L_m & L_s & L_m \\ L_m & L_m & L_s \end{bmatrix}$$

$$C = \begin{bmatrix} C_s & C_m & C_m \\ C_m & C_s & C_m \\ C_m & C_m & C_s \end{bmatrix}$$

In this case, a constant transformation, known as the Karrenbauer's transformation, K, can be applied directly to decouple Eqs. (9.52). The phase voltage and currents are transformed to modal voltages and currents as follows:

$$v_p(y, t) = \begin{bmatrix} v_a(y, t) \\ v_b(y, t) \\ v_c(y, t) \end{bmatrix} = K \begin{bmatrix} v_g(y, t) \\ v_{\ell 1}(y, t) \\ v_{\ell 2}(y, t) \end{bmatrix} = Kv_m(y, t)$$

$$\mathbf{i}_p(y, t) = \begin{bmatrix} i_a(y, t) \\ i_b(y, t) \\ i_c(y, t) \end{bmatrix} = K \begin{bmatrix} i_g(y, t) \\ i_{\ell 1}(y, t) \\ i_{\ell 2}(y, t) \end{bmatrix} = K \mathbf{i}_m(y, t)$$

where

$$K = \begin{bmatrix} 1 & 1 & 1 \\ 1 & -2 & 1 \\ 1 & 1 & -2 \end{bmatrix} \quad K^{-1} = \frac{1}{3} \begin{bmatrix} 1 & 1 & 1 \\ 1 & -1 & 0 \\ 1 & 0 & -1 \end{bmatrix}$$

The vectors  $\mathbf{v}_p(y, t)$ ,  $\mathbf{i}_p(y, t)$  represent the phase voltage and currents at location  $y$ , time  $t$ , while the vectors  $\mathbf{v}_m(y, t)$  and  $\mathbf{i}_m(y, t)$  represent the modal voltages and currents at location  $y$  and time  $t$ . The modal voltages and currents are denoted with the subscripts  $g$  (for ground mode),  $\ell 1$  (for line mode 1), and  $\ell 2$  (for line mode 2). The selection of the names "ground mode" and "line mode" will be discussed later. Upon substitution of the phase voltages and currents with the modal voltages and currents, Eqs. (9.52) become

$$\frac{d^2 v_m(y, t)}{dy^2} = K^{-1} LCK \frac{d^2 v_m(y, t)}{dt^2} \quad (9.57a)$$

$$\frac{dv_m(y, t)}{dy} = K^{-1} LK \frac{di_m(y, t)}{dt} \quad (9.57b)$$

Upon evaluation of the matrix products  $K^{-1}LCK$ ,  $K^{-1}LK$ , and  $K^{-1}CK$ , we have

$$K^{-1}LK = \begin{bmatrix} L_s + 2L_m & 0 & 0 \\ 0 & L_s - L_m & 0 \\ 0 & 0 & L_s - L_m \end{bmatrix}$$

$$K^{-1}CK = \begin{bmatrix} C_s + 2C_m & 0 & 0 \\ 0 & C_s - C_m & 0 \\ 0 & 0 & C_s - C_m \end{bmatrix}$$

and

$$K^{-1}LCK = \begin{bmatrix} c_g^{-2} & 0 & 0 \\ 0 & c_{\ell}^{-2} & 0 \\ 0 & 0 & c_{\ell}^{-2} \end{bmatrix}$$

where

$$c_g = \frac{1}{[(L_s + 2L_m)(C_s + 2C_m)]^{1/2}}$$

$$c_\ell = \frac{1}{[(L_s - L_m)(C_s - C_m)]^{1/2}}$$

Equations (9.57) represent three sets of decoupled equations. From the three sets of equations, two sets have identical coefficients. The three sets of equations are

$$\frac{d^2 v_g(y, t)}{dy^2} = \frac{1}{c_g^2} \frac{d^2 v_g(y, t)}{dt^2} \quad (9.58a)$$

$$\frac{dv_g(y, t)}{dy} = (L_s + 2L_m) \frac{di_g(y, t)}{dt} \quad (9.58b)$$

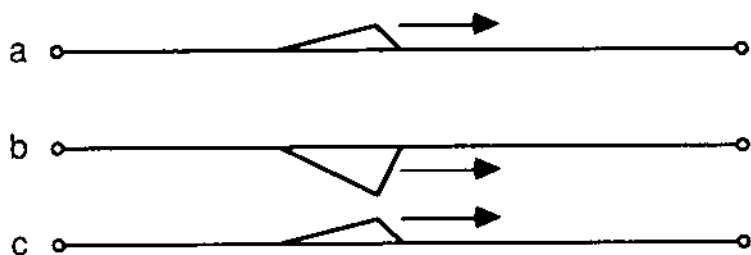
$$\frac{d^2 v_{\ell i}(y, t)}{dy^2} = \frac{1}{c_\ell^2} \frac{d^2 v_{\ell i}(y, t)}{dt^2} \quad (9.59a)$$

$$\frac{dv_{\ell i}(y, t)}{dy} = (L_s - L_m) \frac{di_{\ell i}(y, t)}{dt} \quad (9.59b)$$

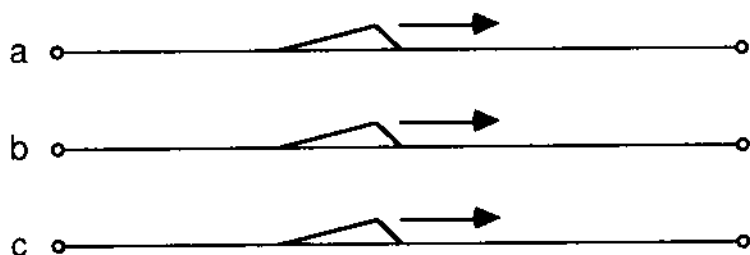
for  $i = 1, 2$ .

Note that Eqs. (9.58) are in terms of the ground-mode voltages and currents only. Equations (9.58) represent a single-phase ideal transmission line with inductance  $L_s + 2L_m$  (henries per meter) and speed of propagation of waves along the line  $c_g$ . They describe the propagation characteristics of the ground mode along the line. Similarly, Eqs. (9.59) are in terms of the line mode voltages and currents only (line mode 1 or line mode 2). They represent a single-phase ideal line with inductance  $L_s - L_m$  (henries per meter) and speed of propagation of waves along the line  $c_\ell$ . They describe the propagation characteristics of the two line modes along the line.

In order to gain some insight into the modal voltages and currents, consider a three-phase line energized with one mode only: for example, line mode 1. In this case,  $i_g = 0$ ,  $i_{\ell 1} \neq 0$ , and  $i_{\ell 2} = 0$ . The phase currents of the line can be computed with the transformation  $K$ . Specifically,  $i_a = i_{\ell 1}$ ,  $i_b = -2i_{\ell 1}$ , and  $i_c = i_{\ell 1}$ . In this case the earth current will be  $i_e = -i_a - i_b - i_c = 0$ . This condition is illustrated in Fig. 9.9a. Note that the line mode excites only the phase conductors; the earth path is not excited. Thus the



(a)



(b)

FIG. 9.9 Modes of propagation along a three phase line. (a) Line mode, (b) ground mode.

name line mode. Now assume that the line is excited with the ground mode only. In this case  $i_g \neq 0$ ,  $i_{\ell 1} = 0$ ,  $i_{\ell 2} = 0$ . Upon computation of the phase currents with the use of the transformation K,  $i_a = i_g$ ,  $i_b = i_g$ , and  $i_c = i_g$ . The earth current is  $i_e = -i_a - i_b - i_c = -3i_g$ . This condition is depicted in Fig. 9.9b. Note that the ground mode excites both the conductors and the earth (ground). Thus the name ground mode.

Equations (9.58) and (9.59) represent three ideal single-phase transmission lines. In Section 9.7.2 an equivalent circuit for an ideal single-phase transmission line has been developed. Utilizing the

results of Section 9.7.2, the equivalent-circuit model of a continuously transposed three-phase line is illustrated in Fig. 9.10. Specifically, the phase currents and voltages at the two terminals of the line are transformed into modal currents and voltages with the transformation K as follows:

Sending end of transmission line

$$\begin{bmatrix} v_{as}(t) \\ v_{bs}(t) \\ v_{cs}(t) \end{bmatrix} = K \begin{bmatrix} v_{gs}(t) \\ v_{\ell 1s}(t) \\ v_{\ell 2s}(t) \end{bmatrix} \quad (9.60)$$

$$\begin{bmatrix} i_{as}(t) \\ i_{bs}(t) \\ i_{cs}(t) \end{bmatrix} = K \begin{bmatrix} i_{gs}(t) \\ i_{\ell 1s}(t) \\ i_{\ell 2s}(t) \end{bmatrix} \quad (9.61)$$

Receiving end of transmission line

$$\begin{bmatrix} v_{aR}(t) \\ v_{bR}(t) \\ v_{cR}(t) \end{bmatrix} = K \begin{bmatrix} v_{gR}(t) \\ v_{\ell 1R}(t) \\ v_{\ell 2R}(t) \end{bmatrix} \quad (9.62)$$

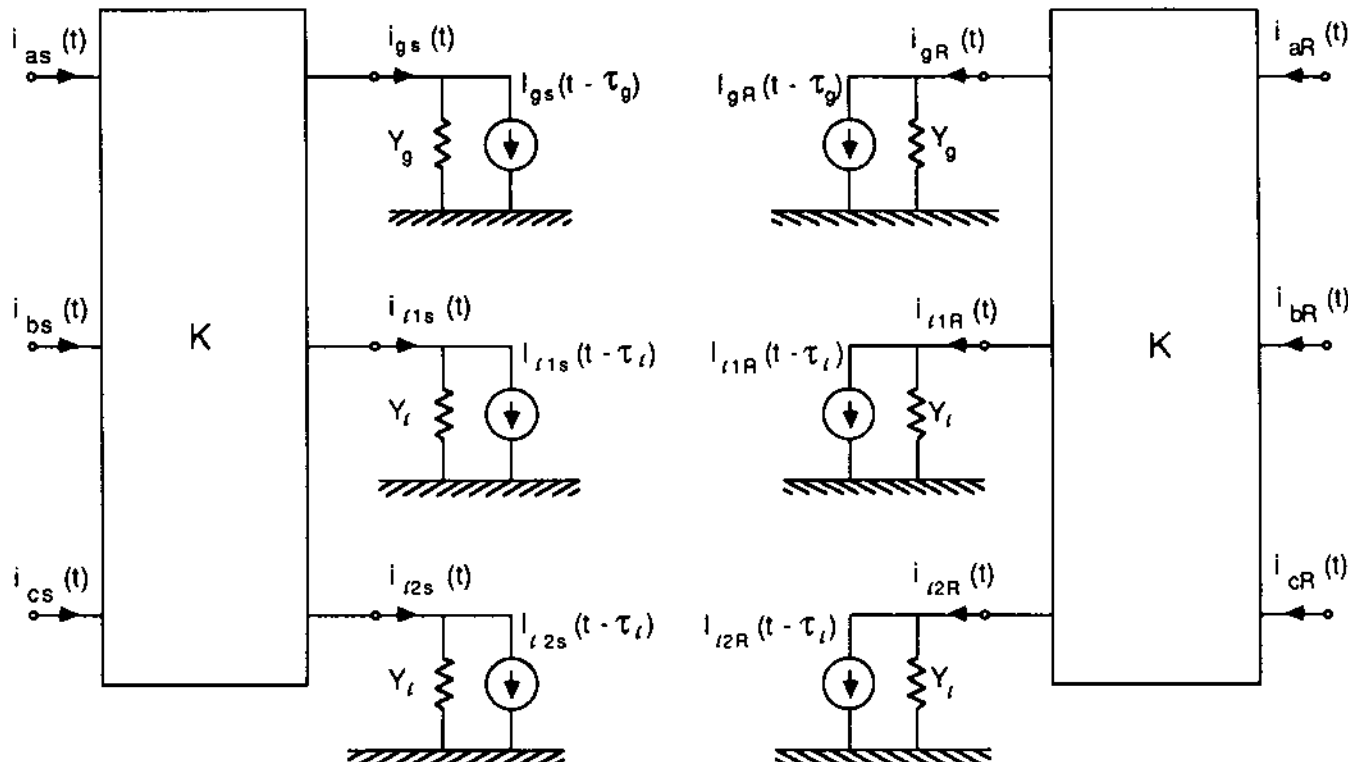


FIG. 9.10 Equivalent circuit of a continuously transposed line.

$$\begin{bmatrix} i_{aR}(t) \\ i_{bR}(t) \\ i_{cR}(t) \end{bmatrix} = K \begin{bmatrix} i_{gR}(t) \\ i_{\ell 1R}(t) \\ i_{\ell 2R}(t) \end{bmatrix} \quad (9.63)$$

The propagation parameters of the modal currents and voltages are defined as follows:

#### Ground mode

Speed of propagation:  $c_g = [(L_s + 2L_m)(C_s + 2C_m)]^{-1/2}$

Travel time along line:  $\tau_g = \frac{\ell}{c_g}$

Characteristic impedance:  $Z_g = Y_g^{-1} = \left( \frac{L_s + 2L_m}{C_s + 2C_m} \right)^{1/2}$

#### Line mode

Speed of propagation:  $c_\ell = [(L_s - L_m)(C_s - C_m)]^{-1/2}$

Travel time along line:  $\tau_\ell = \frac{\ell}{c_\ell}$

Characteristic impedance:  $Z_\ell = Y_\ell^{-1} = \left( \frac{L_s - L_m}{C_s - C_m} \right)^{1/2}$

The three equivalent circuits depicted in Fig. 9.10 are the equivalent circuits of the ground mode and the two line modes. The current sources illustrated in Fig. 9.10 are

$$I_{gs}(t - \tau_g) = -i_{gR}(t - \tau_g) - Y_g v_{gR}(t - \tau_g) \quad (9.64)$$

$$I_{gR}(t - \tau_g) = -i_{gs}(t - \tau_g) - Y_g v_{gs}(t - \tau_g) \quad (9.65)$$

$$I_{\ell 1s}(t - \tau_\ell) = -i_{\ell 1R}(t - \tau_\ell) - Y_\ell v_{\ell 1R}(t - \tau_\ell) \quad (9.66)$$

$$I_{\ell 1R}(t - \tau_\ell) = -i_{\ell 1s}(t - \tau_\ell) - Y_\ell v_{\ell 1s}(t - \tau_\ell) \quad (9.67)$$

$$I_{\ell 2s}(t - \tau_\ell) = -i_{\ell 2R}(t - \tau_\ell) - Y_\ell v_{\ell 2R}(t - \tau_\ell) \quad (9.68)$$

$$I_{\ell 2R}(t - \tau_\ell) = -i_{\ell 2s}(t - \tau_\ell) - Y_\ell v_{\ell 2s}(t - \tau_\ell) \quad (9.69)$$

The decomposition of a three-phase line into three uncoupled single-phase lines will be demonstrated with an example.

Example 9.7: Compute the ground and line modal equations of a 115-kV three-phase transmission line. The design of the transmission tower is illustrated in Fig. 1.6. Phase conductors are 336.4 kcm, ACSR. Neglect the shield wire. The resistivity of the soil is 150  $\Omega \cdot \text{m}$ . Use the equivalent depth of return method. Compute the line parameters at 60 Hz. Note that the line is identical to the one considered in Example 6.1.

Solution: The line inductance and capacitance matrices have been computed in Example 6.1. For convenience, they are repeated here:

$$\mathbf{L} = \begin{bmatrix} 2.361 & 1.1199 & 1.2071 \\ 1.1199 & 2.361 & 1.1186 \\ 1.2071 & 1.1186 & 2.361 \end{bmatrix} \mu\text{H/m}$$

$$\mathbf{C} = \begin{bmatrix} 7.8844 & -1.4954 & -2.0248 \\ -1.4954 & 7.7016 & -1.4097 \\ -2.0248 & -1.4097 & 8.0324 \end{bmatrix} \times 10^{-6} \mu\text{F/m}$$

Substitution into Eqs. (9.53)–(9.56) gives us

$$L_s = 2.361 \times 10^{-6} \text{ H/m}$$

$$L_m = 1.1485 \times 10^{-6} \text{ H/m}$$

$$C_s = 7.8728 \times 10^{-12} \text{ F/m}$$

$$C_m = -1.6433 \times 10^{-12} \text{ F/m}$$

The parameters of the ground and line modes are:

Ground mode

$$Z_g = \left( \frac{L_s + 2L_m}{C_s + 2C_m} \right)^{1/2} = 1008 \Omega$$

$$c_g = 2.163 \times 10^8 \text{ m/s}$$

Line mode

$$Z_\ell = \left( \frac{L_s - L_m}{C_s - C_m} \right)^{1/2} = 357 \Omega$$

$$c_\ell = 1/\sqrt{L_s - L_m}(C_s - C_m) = 2.944 \times 10^8 \text{ m/s}$$

Note that the speed of propagation of the line mode is near the speed of light, while the speed of propagation of the ground mode is about 72% of the speed of light. In addition, the characteristic impedance of the ground mode is about three times higher than that of the line mode.

### 9.8.3 Discussion on Three-Phase Line Models

The presented model of a three-phase transmission line is the simplest possible model for electromagnetic transient analysis. The model is characterized with three simplifying assumptions:

1. The transmission line is lossless.
2. The transmission line parameters are constant (frequency independent).
3. The transmission line is symmetric.

Despite the simplifying assumptions, the model provides a reasonable approximation for the purpose of obtaining ballpark values of transient overvoltages.

In many applications, however, it is necessary to use more accurate models. Such applications are: (a) computation of overvoltages due to lightning on shield wires, (b) computation of overvoltages due to switching of long transmission lines, and so on. In such cases the characteristics of the shield wire, the frequency dependence of the line parameters, and the tower grounding system play an important role and must be accounted for. The next section discusses the incorporation of frequency dependence in transient analysis.

## 9.9 SIMULATION OF FREQUENCY-DEPENDENT MODELS

The case of a lossless continuously transposed transmission line considered in the previous sections is characterized by two assumptions: (a) the line resistance is zero, and (b) the parameters L and C are constant (independent of frequency). Under these assumptions, transmission lines do not distort the waveform of traveling waves because their propagation constant and characteristic impedance are independent of frequency. However, the resistance of real power lines is nonzero. In addition, the parameters of real transmission lines are frequency dependent. In this case the propagation constant and the characteristic impedance are complex functions of frequency.

The effects of frequency on various parameters of transmission lines are substantial. Consider, for example, the typical variation of the ground-mode parameters of a 500-kV overhead line illustrated

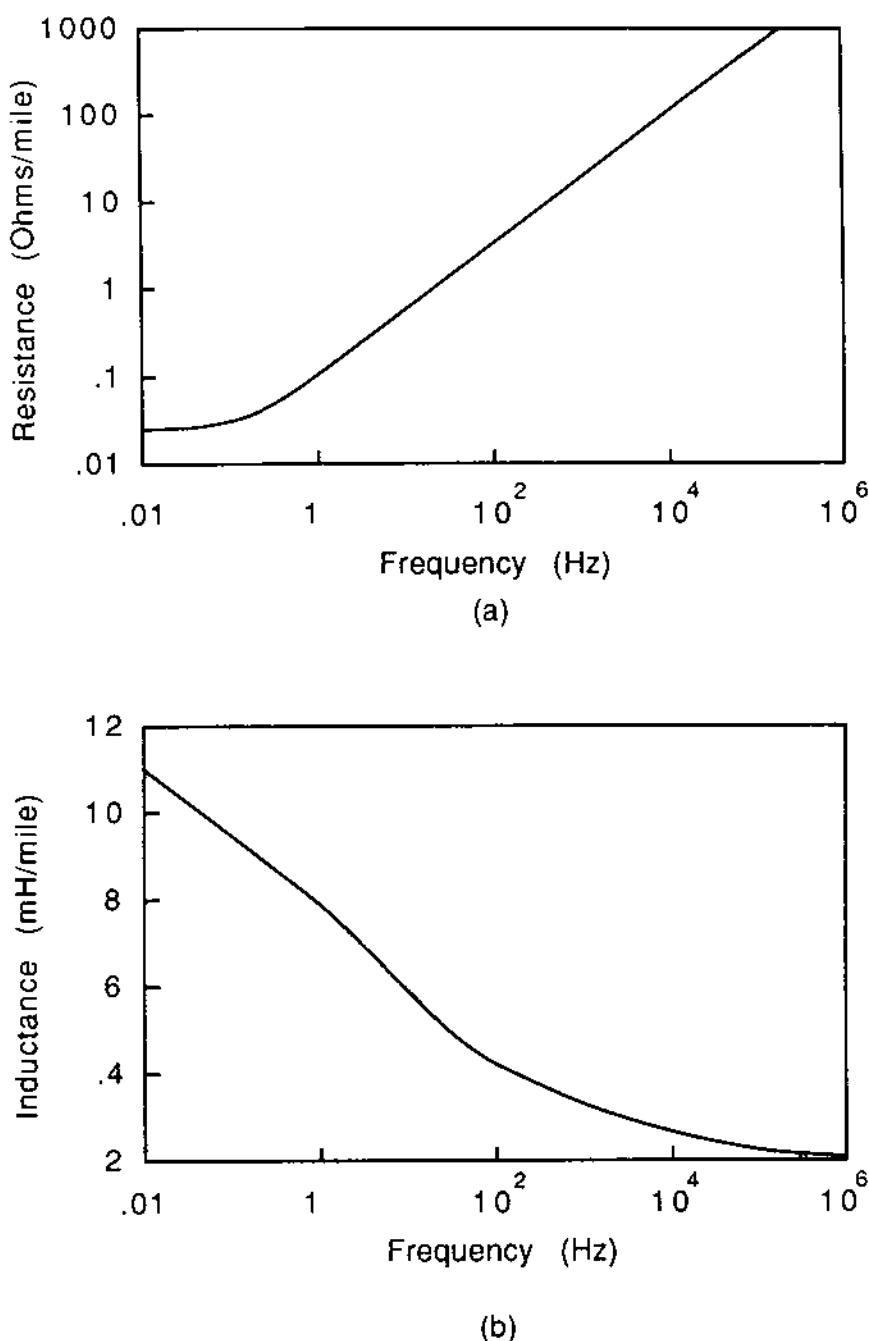


FIG. 9.11 Typical frequency dependence of the parameters of a 500 kV overhead transmission line. (a) Ground mode resistance, (b) ground mode inductance.

in Fig. 9.11. The ground-mode resistance (which equals  $r_a + 3r_e$ ) increases by a factor of more than 50,000 going from dc to 1 MHz. Similarly, the ground-mode inductance ( $L_s + 2L_m$ ) decreases by a factor of approximately 5 going from dc to 1 MHz. The dependence of cable parameters on frequency is even more complex. For accurate computation of electromagnetic transients on power lines, it is necessary to account for the frequency dependence of line parameters.

This section examines transient analysis techniques for transmission lines, including frequency-dependent phenomena. The discussion of this section will be confined to single-phase transmission lines.

We shall derive a transmission line model that incorporates the frequency-dependent characteristics of the line. The derivation of the model follows a procedure similar to the derivation of the ideal transmission line in Section 9.5. Recall that the model was developed in terms of four new variables defined by

$$f_1(t) = v_1(t) + Zi_1(t) \quad (9.70a)$$

$$f_2(t) = v_2(t) + Zi_2(t) \quad (9.70b)$$

$$b_1(t) = v_1(t) - Zi_1(t) \quad (9.71a)$$

$$b_2(t) = v_2(t) - Zi_2(t) \quad (9.71b)$$

The voltage and current variables are illustrated in Fig. 9.6d1. In the case of the ideal transmission line, the quantity  $Z$  was selected to be the characteristic impedance  $Z_0$ , which is purely resistive and frequency independent. In the case of a real transmission line with frequency-dependent parameters, the characteristic impedance is a complex number which is frequency dependent. Thus  $Z$  cannot be selected to be equal to the characteristic impedance. For the time being, assume that  $Z$  is an arbitrary real number. Now, taking the Laplace transform of Eqs. (9.70) and (9.71):

$$F_1(s) = V_1(s) + ZI_1(s) \quad (9.72a)$$

$$F_2(s) = V_2(s) + ZI_2(s) \quad (9.72b)$$

$$B_1(s) = V_1(s) - ZI_1(s) \quad (9.73a)$$

$$B_2(s) = V_2(s) - ZI_2(s) \quad (9.73b)$$

Next we shall derive the relationship between the functions  $f_1$ ,  $f_2$  and  $b_1$ ,  $b_2$ . Recall that Eqs. (9.33) express the voltage  $V_1(s)$  and current  $I_1(s)$  as a function of  $V_2(s)$  and  $I_2(s)$ . Upon substitution of  $V_1(s)$ ,  $I_1(s)$  of Eqs. (9.33) into Eqs. (9.72) and (9.73), we obtain

$$\begin{bmatrix} F_1(s) \\ F_2(s) \end{bmatrix} = M_1(s) \begin{bmatrix} V_2(s) \\ V_2(s) \end{bmatrix} \quad (9.74)$$

$$M_1(s) = \begin{bmatrix} \cosh s\tau + ZY_0 \sinh s\tau & -Z_0 \sinh s\tau - Z \cosh s\tau \\ 1 & Z \end{bmatrix}$$

$$\begin{bmatrix} B_1(s) \\ B_2(s) \end{bmatrix} = M_2(s) \begin{bmatrix} V_2(s) \\ I_2(s) \end{bmatrix} \quad (9.75)$$

$$M_2(s) = \begin{bmatrix} \cosh s\tau - ZY_0 \sinh s\tau & -Z_0 \sinh s\tau + Z \cosh s\tau \\ 1 & -Z \end{bmatrix}$$

Solution of Eq. (9.74) for  $V_2(s)$ ,  $I_2(s)$  yields

$$\begin{bmatrix} V_2(s) \\ I_2(s) \end{bmatrix} = \frac{1}{D(s)} \begin{bmatrix} Z & Z_0 \sinh s\tau + Z \cosh s\tau \\ -1 & \cosh s\tau + ZY_0 \sinh s\tau \end{bmatrix} \begin{bmatrix} F_1(s) \\ F_2(s) \end{bmatrix} \quad (9.76)$$

where  $D(s) = 2Z \cosh s\tau + (Z^2 Y_0 + Z_0) \sinh s\tau$ . Finally, substitution of Eq. (9.76) into Eq. (9.75) gives us

$$\begin{bmatrix} B_1(s) \\ B_2(s) \end{bmatrix} = M_3(s) \begin{bmatrix} F_1(s) \\ F_2(s) \end{bmatrix} \quad (9.77)$$

$$M_3(s) = \frac{1}{D(s)} \begin{bmatrix} (-Z^2 Y_0 + Z_0) \sinh s\tau & 2Z \\ 2Z & (-Z^2 Y_0 + Z_0) \sinh s\tau \end{bmatrix}$$

To cast Eq. (9.77) into a simpler form, define

$$A_2(s) = \frac{(-Z^2 Y_0 + Z_0) \sinh s\tau}{D(s)}$$

$$A_1(s) = \frac{2Z}{D(s)}$$

In terms of functions defined above, Eq. (9.77) becomes

$$B_1(s) = A_2(s)F_1(s) + A_1(s)F_2(s) \quad (9.78a)$$

$$B_2(s) = A_1(s)F_1(s) + A_2(s)F_2(s) \quad (9.78b)$$

$A_1(s)$  and  $A_2(s)$  are functions of the Laplace variable  $s$ . They depend on the parameters of the line and the constant  $Z$ . Thus they can be computed. The inverse Laplace transform of these functions will yield the time functions  $\alpha_1(t)$  and  $\alpha_2(t)$ . Now let's take the inverse Laplace transform of Eqs. (9.78):

$$b_1(t) = \alpha_2(t) * f_1(t) + \alpha_1(t) * f_2(t) \quad (9.79a)$$

$$b_2(t) = \alpha_1(t) * f_1(t) + \alpha_2(t) * f_2(t) \quad (9.79b)$$

where  $*$  denotes convolution defined by (see Table 9.2)

$$\begin{aligned} g_1(t) * g_2(t) &= \int_0^t g_1(t - \tau) g_2(\tau) d\tau \\ &= \int_0^t g_1(\tau) g_2(t - \tau) d\tau \end{aligned}$$

Now let's substitute the convolutions in Eqs. (9.79) explicitly and also the function  $b_1(t)$  and  $b_2(t)$  with the defining Eqs. (9.71). The results are

$$v_1(t) - Zi_1(t) = \int_0^t \alpha_2(\tau) f_1(t - \tau) d\tau + \int_0^t \alpha_1(\tau) f_2(t - \tau) d\tau \quad (9.80a)$$

$$v_2(t) - Zi_1(t) = \int_0^t \alpha_1(t) f_1(t - \tau) d\tau + \int_0^t \alpha_2(\tau) f_2(t - \tau) d\tau \quad (9.80b)$$

In Eqs. (9.80), note that the integrals depend on the functions  $\alpha_1(t)$  and  $\alpha_2(t)$  which are known and on values of the functions  $f_1$  and  $f_2$  for times less than time  $t$ . Assuming that the conditions of the line are known before time  $t$ , the integrals can be computed. Thus they can be treated as known quantities. Now upon solution of Eqs. (9.80) for the electric currents  $i_1(t)$  and  $i_2(t)$ , we have

$$\begin{aligned} i_1(t) &= Yv_1(t) - Y \int_0^t \alpha_2(\tau) f_1(t - \tau) d\tau - Y \int_0^t \alpha_1(\tau) f_2(t - \tau) d\tau \\ i_2(t) &= Yv_2(t) - Y \int_0^t \alpha_1(\tau) f_1(t - \tau) d\tau - Y \int_0^t \alpha_2(\tau) f_2(t - \tau) d\tau \end{aligned}$$

Define

$$\hat{i}_1(t) = -Y \int_0^t \alpha_2(\tau) f_1(t - \tau) d\tau - Y \int_0^t \alpha_1(\tau) f_2(t - \tau) d\tau$$

$$\hat{i}_2(t) = -Y \int_0^t \alpha_1(\tau) f_1(t - \tau) d\tau - Y \int_0^t \alpha_2(\tau) f_2(t - \tau) d\tau$$

Now the equations become

$$i_1(t) = Yv_1(t) + \hat{i}_1(t) \quad (9.81a)$$

$$i_2(t) = Yv_2(t) + \hat{i}_2(t) \quad (9.81b)$$

At time  $t$  the quantities  $\hat{i}_1(t)$  and  $\hat{i}_2(t)$  must be considered constants for the reasons mentioned. In this case Eqs. (9.81) represent the equivalent circuit illustrated in Fig. 9.12. The quantities  $\hat{i}_1(t)$  and  $\hat{i}_2(t)$  will be called past history current sources. Note that the form of the equivalent circuit is similar to the one of the lossless ideal line except for the fact that the past history current sources are computed with a convolution.

So far we have assumed that the selection of the constant  $Z$  is arbitrary. For the purpose of selecting the constant  $Z$  judiciously, we examine the physical meaning of the functions  $\alpha_1(t)$  and  $\alpha_2(t)$ , which depend on the transmission line parameters and selection of the constant  $Z$ . Consider a single-phase line which is terminated to a resistor of resistance  $Z$  at one end and to a source of internal resistance equal to  $Z$  at the other end. The system is illustrated in Fig. 9.13. Now assume that the source is an impulse voltage source [i.e.,  $e(t) = \delta(t)$ ]. Assume that at time  $t = 0$ , the switch closes. Prior to the closing of the switch, the line is not energized. Under the specified conditions, let's compute the voltages  $v_1(t)$  and  $v_2(t)$ . For this purpose observe that

$$i_1(t) = \frac{\delta(t) - v_1(t)}{Z} \quad (9.82a)$$

$$i_2(t) = -\frac{v_2(t)}{Z} \quad (9.82b)$$

Upon substitution of Eqs. (9.82) into Eqs. (9.81), subsequent multiplication by  $Z$  and solution for  $v_1(t)$  and  $v_2(t)$ :

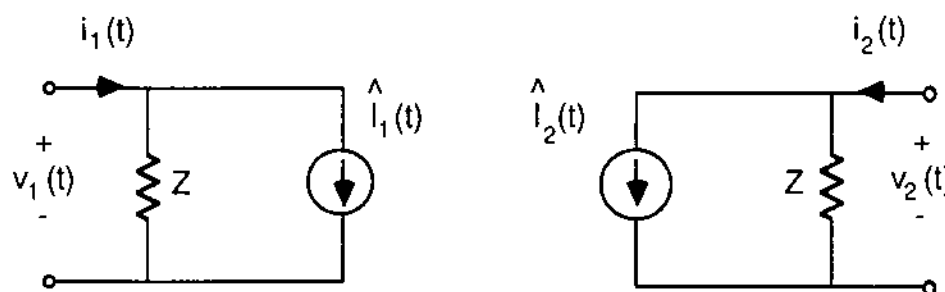


FIG. 9.12 Equivalent resistive network of a frequency dependant transmission line model.

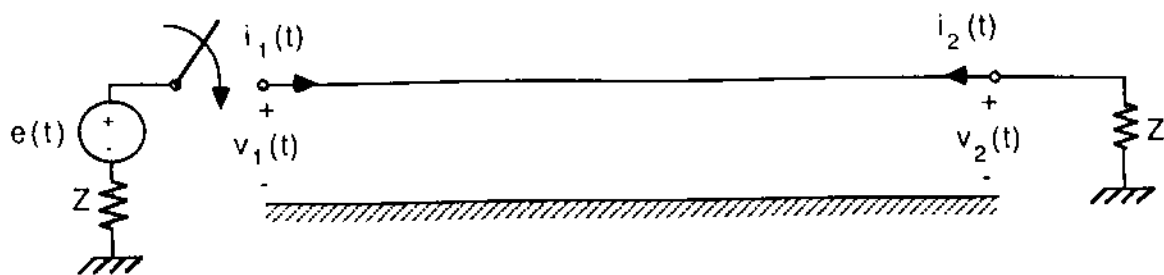


FIG. 9.13 Excitation of a single phase line terminated with impedance  $Z$ .

$$v_1(t) = \frac{1}{2} \delta(t) + \frac{1}{2} \int_0^t \alpha_2(\tau) f_1(t - \tau) d\tau + \frac{1}{2} \int_0^t \alpha_1(\tau) f_2(t - \tau) d\tau \quad (9.83a)$$

$$v_2(t) = \frac{1}{2} \int_0^t \alpha_1(\tau) f_1(t - \tau) d\tau + \frac{1}{2} \int_0^t \alpha_2(\tau) f_2(t - \tau) d\tau \quad (9.83b)$$

Now observe that Eqs. (9.82) can be cast into the form

$$\delta(t) = v_1(t) + Zi_1(t) = f_1(t)$$

$$0 = v_2(t) + Zi_2(t) = f_2(t)$$

Substitution of  $f_1(t)$  and  $f_2(t)$  into Eqs. (9.83) yields

$$v_1(t) = \frac{1}{2} \delta(t) + \frac{1}{2} \alpha_2(t)$$

$$v_2(t) = \frac{1}{2} \alpha_1(t)$$

The function  $\delta(t)$  assumes nonzero values only at  $t = 0$ . If  $t = 0$  is excluded, then

$$v_1(t) = \frac{1}{2} \alpha_2(t) \quad t \neq 0$$

$$v_2(t) = \frac{1}{2} \alpha_1(t) \quad t \neq 0$$

Therefore, the functions  $\alpha_1(t)$  and  $\alpha_2(t)$  represent the line terminal voltages when the line is terminated with the resistance  $Z$ , which has been used in the transformation (9.70), and excited with an impulse voltage source. Thus the functions  $\alpha_1(t)$  and  $\alpha_2(t)$  are the impulse response of the transmission line. This observation allows judicious

selection of the resistance  $Z$  of the transformation. Note that if the value of  $Z$  is selected to be close to the absolute value of the characteristic impedance  $Z_0$ , wave reflections at the terminals of the line are minimized and the duration of the functions  $\alpha_1(t)$  and  $\alpha_2(t)$  is minimized. In this case the effort for the computation of the integrals of Eqs. (9.81) is minimized. Since the characteristic impedance  $Z_0$  of a real transmission line is dependent on frequency, a judicious selection of  $Z$  is as follows:

$$Z = \lim_{f \rightarrow \infty} Z_0(f) = Z_1 \quad (9.84)$$

For this selection of  $Z$ , the typical variation of functions  $\alpha_1(t)$  and  $\alpha_2(t)$  is illustrated in Fig. 9.14.

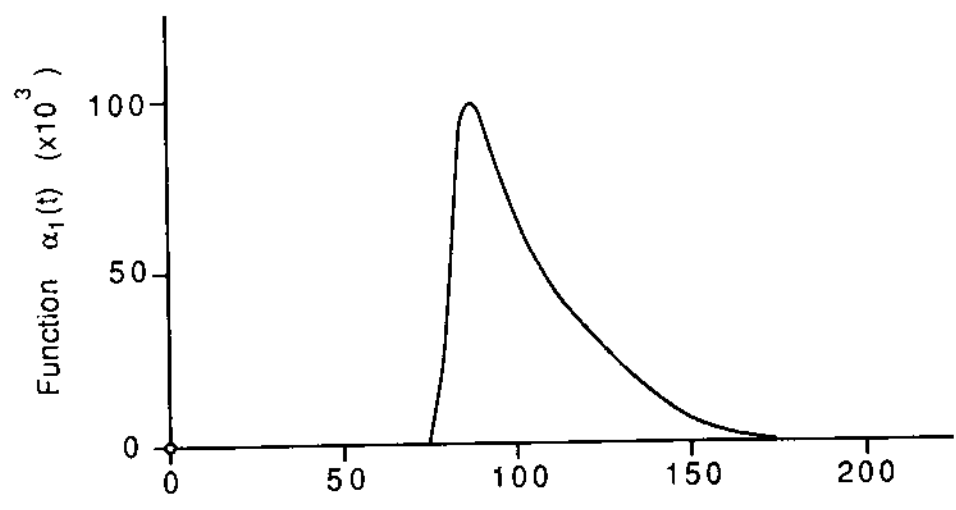
## 9.10 BASIC POWER SYSTEM SWITCHING TRANSIENTS

In this section we study typical power system transients resulting from switchings in electric power systems. There are several types of switchings with distinct transients. We examine transients resulting from (a) line switching, (b) electric faults, (c) capacitor switching, (d) transient recovery voltage, and (e) transformer energization. In our discussion, we emphasize the impact of the transients on system operation and protection.

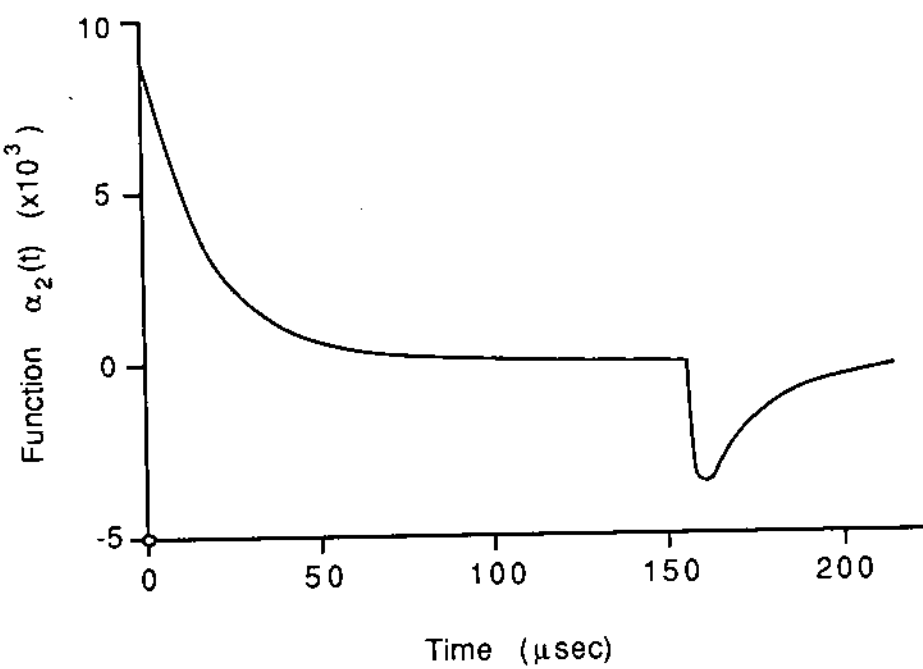
Transients during transformer energization involve nonlinear effects resulting from nonlinear magnetic cores. These transients are studied separately in Section 9.11.

### 9.10.1 Line Switching Transients

Closing of a switch or breaker to energize or deenergize a circuit results in voltage transients. A typical case is illustrated in Fig. 9.15a, which illustrates the energization of a 40-mi-long 115-kV line. The transient overvoltage of phase a is illustrated in Fig. 9.15b. Note that the voltage at point A exhibits a delay equal to the travel time of the surge along the line. When the surge arrives at point A, it doubles since the line is open. The surge will be reflected and travel toward the source. When it arrives there, it is reflected. The internal impedance of the source is typically inductive. Thus initially the coefficient of reflection will be 1.0 and as time progresses, it becomes -1.0. This means that the reflected wave initially will be positive and gradually will change to negative. This wave will travel along the line, arriving at point A at a time approximately  $3\tau$  after the closing of the breaker, where  $\tau$  is the travel time along the line. Note that there is an initial rise of the voltage followed by a rapid decrease. Theoretically, the peak voltage may reach the value of



(a)



(b)

FIG. 9.14 Typical functions  $\alpha_1(t)$  and  $\alpha_2(t)$  of the ground mode of a 15 mi. power line.

4.0 pu depending on the source characteristics. For transmission circuits, this value may be excessively high. As an example, for a 500-kV line, 4.0 pu overvoltage translates into a maximum phase voltage of 1633 kV! To mitigate the switching overvoltage in transmission circuits, it is customary to use resistor preinsertion breakers. The basic idea is very simple. Prior to the closing of the breaker, a

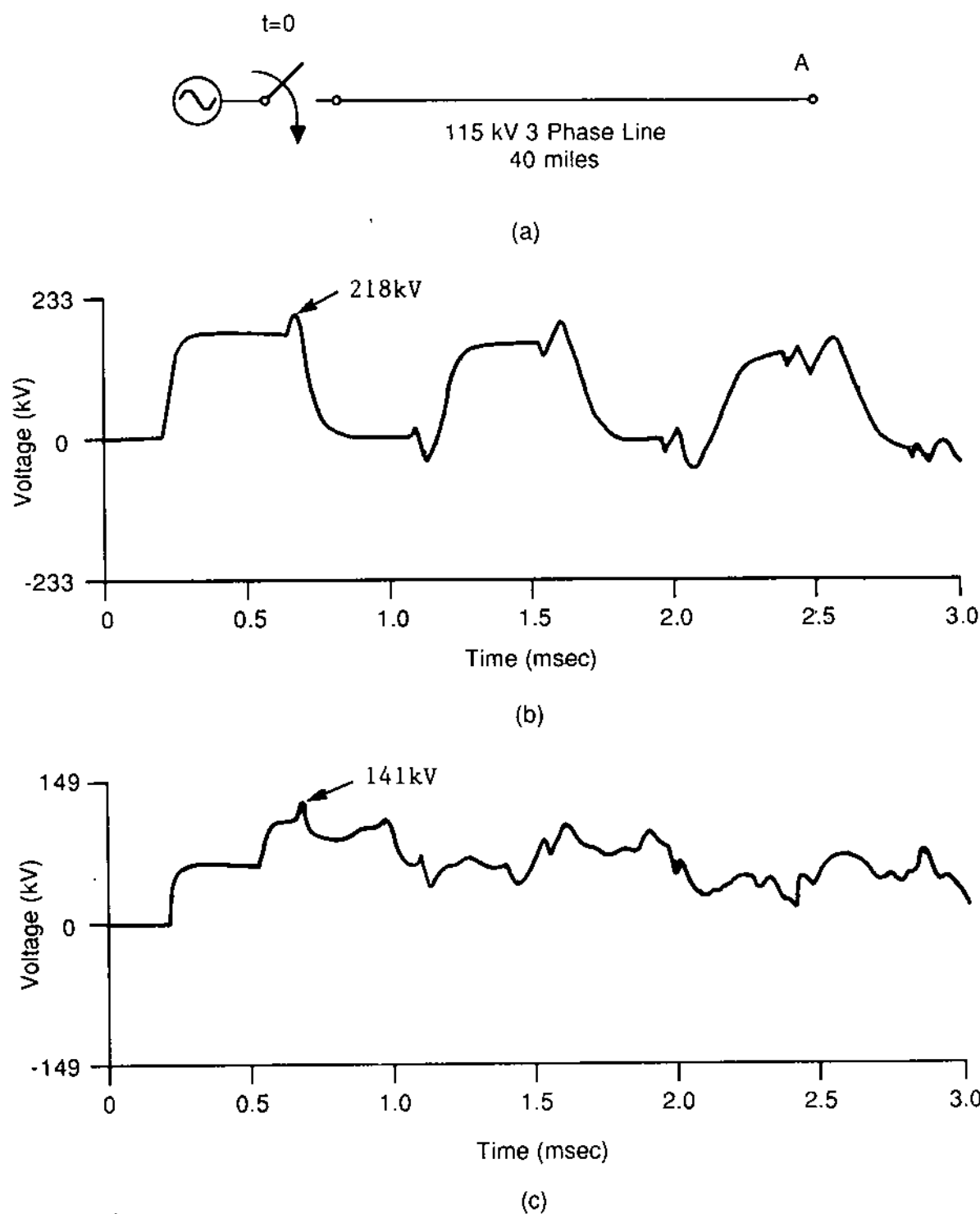


**FIG. 9.15** Typical line switching transients. (a) System configuration, (b) phase A transient voltage at point A without resistor preinsertion breaker, (c) phase A transient voltage at point A with a two stage resistor preinsertion breaker.

resistor is inserted between the source and the line for a specified period of time, typically 0.3 to 1.5 ms. There may be more than one stage of resistor preinsertion; at each stage a different resistor is utilized. The effect of the resistor preinsertion is illustrated in Fig. 9.15c. The figure illustrates the overvoltage of phase a at point A when the line is energized through a resistor preinsertion breaker. It is assumed that there are two stages: In the first stage, a  $600\text{-}\Omega$  resistor is preinserted for a period of 0.3 ms. In the second stage, a  $200\text{-}\Omega$  resistor is preinserted for another 0.3 ms. Finally, the breaker contacts close. The effect of the stages is clearly visible in Fig. 9.15c. Note that the resistor preinsertion breaker has reduced the maximum switching overvoltage from 218 kV to 141 kV.

The discussed switching transients are important for lines operating at extra-high voltages and of considerable length. These are the typical conditions of transmission lines. Distribution lines are typically of short lengths and operate at relatively low voltage (7 to 25 kV). In distribution lines, the switching overvoltages are typically below the insulation level of these lines.

#### 9.10.2 Fault Transients

Faults occur in a power system from a variety of causes. In Chapter 7 we examined analysis techniques of faulted power systems under steady-state conditions. Immediately after the fault initiation, transients occur that were neglected in Chapter 7. Here we examine these transients. Fault-initiated transients must be well understood to protect the system properly. The most important fault transients are (a) electric current transients, (b) undervoltage or overvoltages in the unfaulted phases, and (c) ground potential rise transients.

Consider the simple system illustrated in Fig. 9.16. The voltage of the indicated voltage source is

$$e(t) = \sqrt{2} V \cos(\omega t + \phi)$$

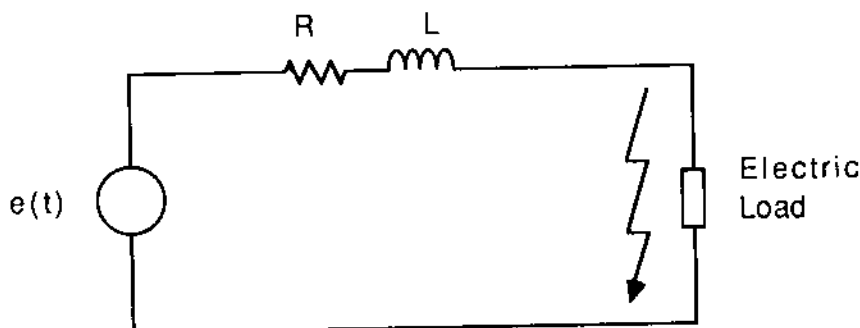


FIG. 9.16 Simplified model for studying fault transients.

Assume that at time  $t = 0$ , a fault occurs as indicated in the figure. Moments prior to the fault, the electric load current is  $i(0) = c$ . The faulted system of Fig. 9.16 is described with the following differential equation:

$$e(t) = Ri(t) + L \frac{di(t)}{dt} \quad (9.85)$$

Application of the Laplace transform on Eq. (9.85) and subsequent solution for  $I(s)$  yields

$$I(s) = \frac{\sqrt{2} V}{R + sL} N(s) + \frac{L}{R + sL} c \quad (9.86)$$

where  $N(s) = \text{Laplace transform of } \cos(\omega t + \phi)$ . Taking the inverse Laplace transform gives us

$$i(t) = c \exp\left(-\frac{R}{L}t\right) + \int_0^t \frac{\sqrt{2} V}{L} \exp\left(-\frac{R}{L}(t-\tau)\right) \cos(\omega\tau + \phi) d\tau \quad (9.87)$$

Upon evaluation of the integral,

$$\begin{aligned} i(t) &= \frac{\sqrt{2} V}{R^2 + \omega^2 L^2} [R \cos(\omega t + \phi) + \omega L \sin(\omega t + \phi)] \\ &\quad - \frac{\sqrt{2} V}{R^2 + \omega^2 L^2} \exp\left(-\frac{R}{L}t\right) (R \cos \phi + \omega L \sin \phi) \\ &\quad + c \exp\left(-\frac{R}{L}t\right) \end{aligned} \quad (9.88)$$

To simplify the expression above, define the variables  $\delta$  and  $I$ :

$$\tan \delta = -\frac{\omega L}{R}$$

$$I = \frac{V}{R^2 + \omega^2 L^2}$$

Then

$$i(t) = \sqrt{2} I \cos(\omega t + \phi + \delta) + [c - \sqrt{2} I \cos(\phi + \delta)] \exp\left(-\frac{R}{L}t\right) \quad (9.89)$$

A typical fault current waveform is illustrated in Fig. 9.17. It consists of an ac current component and an exponentially decaying dc component. Upon examination of Eq. (9.89), the two components are

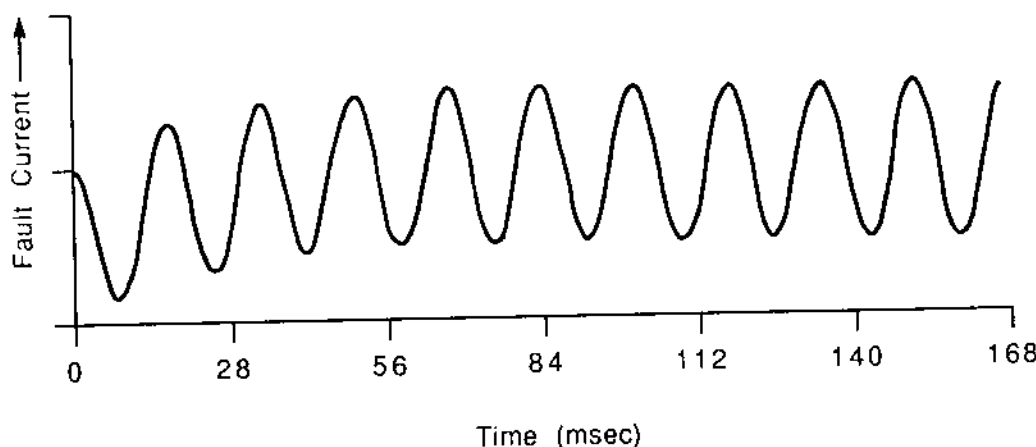


FIG. 9.17 Typical fault current transients.

$$\begin{aligned} \sqrt{2} I \cos(\omega t + \phi + \delta) & \quad \text{ac component} \\ [c - \sqrt{2} I \cos(\phi + \delta)] \exp\left(-\frac{R}{L} t\right) & \quad \text{dc component} \end{aligned}$$

Note that  $I$  is the rms value of the ac component. Since the dc component will vanish as time goes on,  $I$  is the steady state rms value of the fault current. Since the dc component is time dependent, the rms value of the electric current will be a function of time. Specifically, the rms value of the fault current is

$$I_{F_{rms}} = \{I^2 + [c - \sqrt{2} I \cos(\phi + \delta)]^2 \exp\left(-\frac{2R}{L} t\right)\}^{1/2} \quad (9.90)$$

If the initial current  $c$  is neglected, the worst case results when  $\phi + \delta = 0^\circ$ , yielding a maximum rms value at  $t = 0$ :

$$I_{F_{rms}, \max} = I\sqrt{3}$$

This value is 73% higher than the steady-state fault current.

The decaying dc component of the fault current is important for breaker applications. To make sure that the breaker will operate properly, it should be capable of interrupting the fault current. If the breaker operates at time  $t_1$  after fault initiation, the maximum rms value of the current to be interrupted is

$$I_{rms} = (I^2 + 2I^2 \exp\left(-\frac{2R}{L} t_1\right))^{1/2} \quad (9.91)$$

Other effects of a fault in a three-phase system are overvoltages or undervoltages in the unfaulted phases. The level of these abnormal voltages depends on the circuit parameters, the system grounding, and the fault impedance. A typical case is illustrated in Fig. 9.18a.

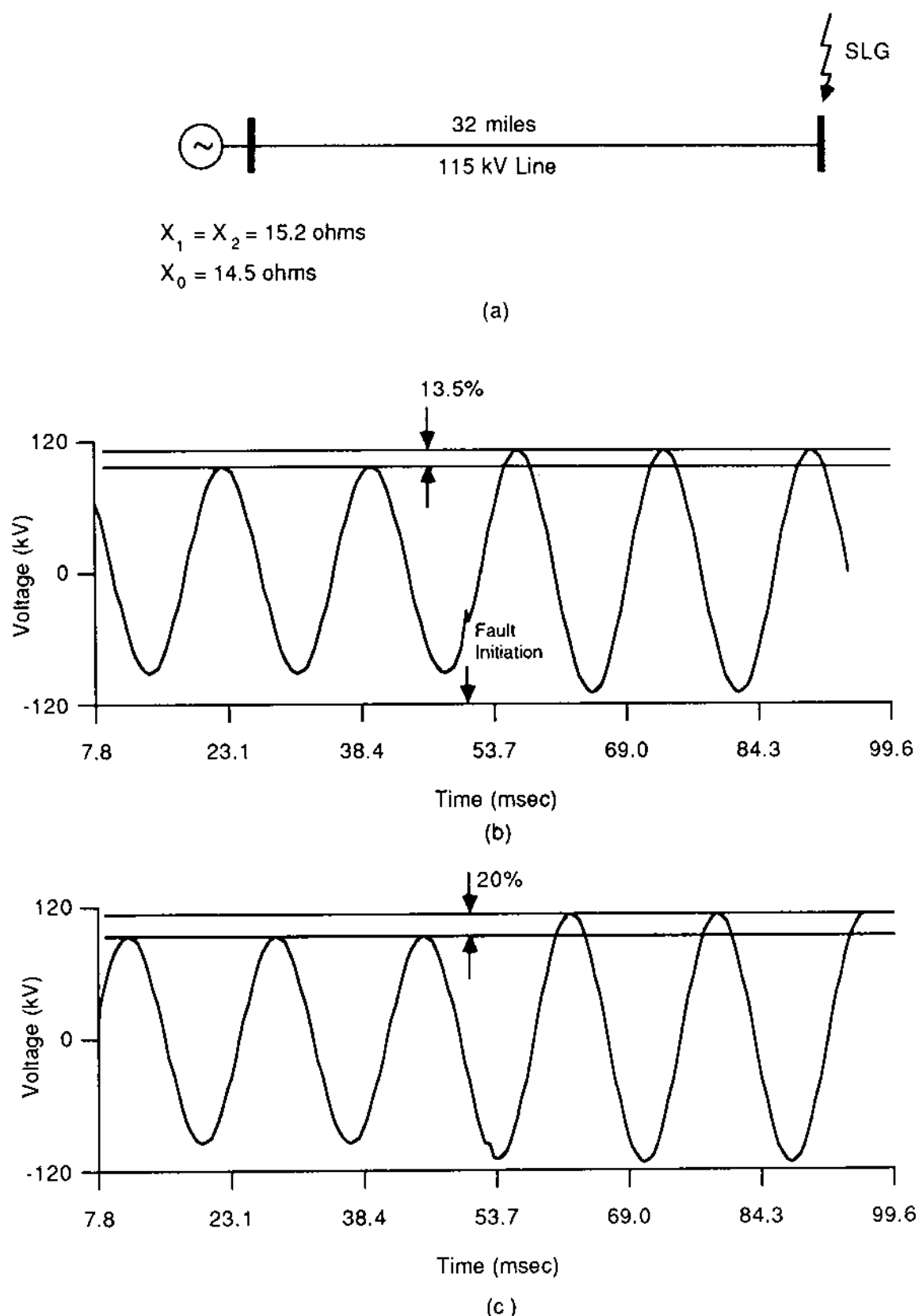


FIG. 9.18 Typical overvoltages due to faults. (a) System configuration, (b) unfaulted phase B voltage, (c) unfaulted phase C voltage.

A single line (phase A)-to-ground fault occurs at the end of a 32-mi 115-kV line. The line configuration is identical to the one illustrated in Fig. 1.6. The phase conductors are ACSR, 336 kcm, and the shield wire is  $\frac{5}{16}$ -in. steel. Figure 9.18b illustrates the voltage of phase B prior to and after the fault. Note a 13.5% overvoltage due to the fault on phase A. Similarly, Fig. 9.18c illustrates the voltage of Phase C. Note a 20% overvoltage due to the fault on phase A. Note that the overvoltages in phases b and c are different due to line asymmetries. Also note a short-duration transient voltage immediately after the fault.

Another effect of faults is ground potential rise and ground potential transients. A typical case is illustrated in Fig. 9.19. The

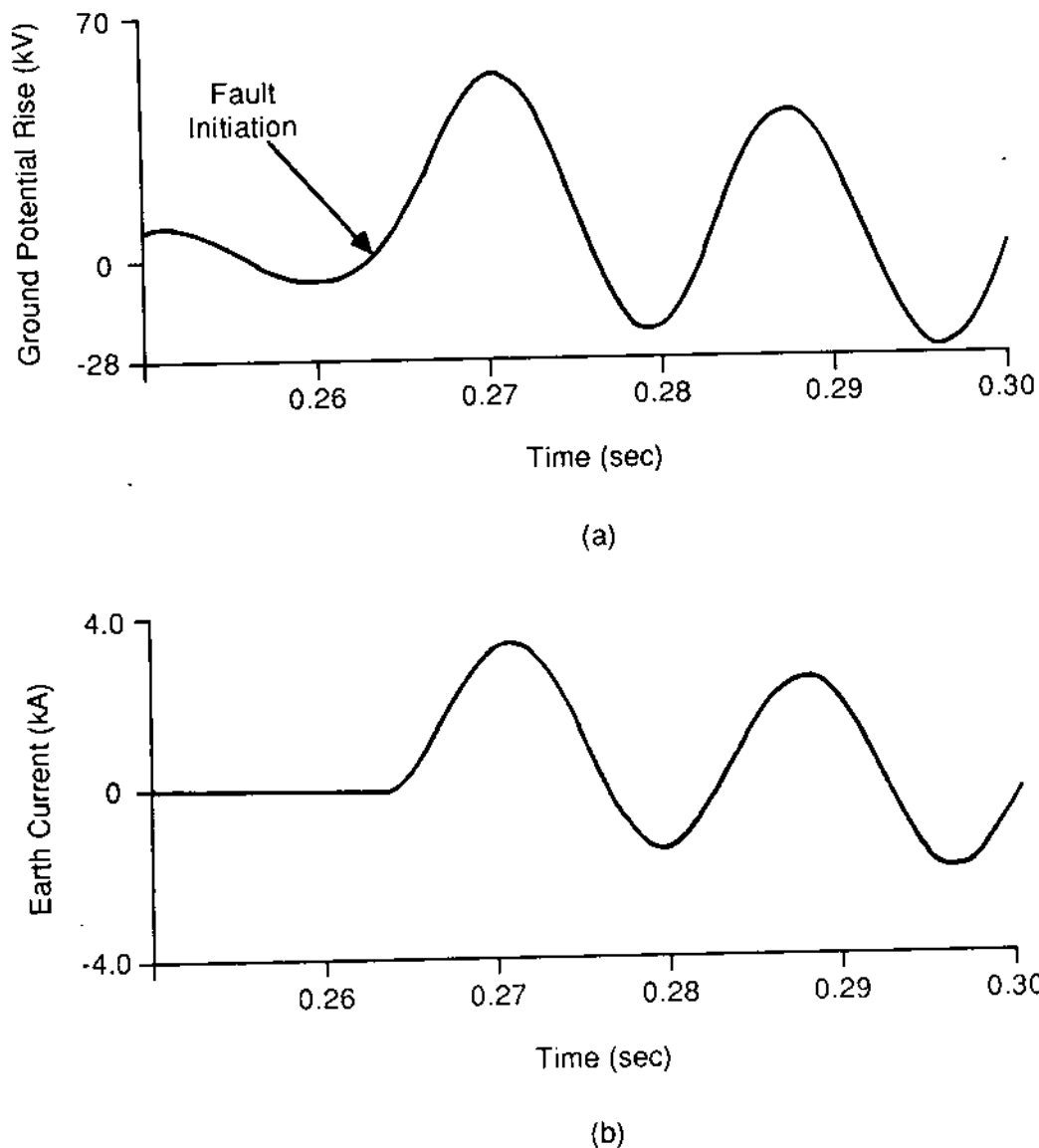


FIG. 9.19 Typical ground fault transients. (a) Ground potential rise transients, (b) earth current transients.

figure illustrates the transient ground potential rise and the transient earth current. Note that both the ground potential rise and the earth current exhibit similar dc offset transients as the fault current.

### 9.10.3 Capacitance Switching

Power systems utilize capacitors for voltage correction at both the transmission and distribution levels. The capacitors may regularly be switched in and out of the system during the day in response to changing load conditions. These switching operations may result in substantial overvoltages across the capacitor. As an example, consider the energization of a capacitor bank of the distribution system illustrated in Fig. 9.20a. The system does have another capacitor bank already energized. The resulting transients from the energization of the second capacitor bank are illustrated in Fig. 9.20b-d. Note that the maximum overvoltage across the capacitor in this case is 1.88 pu. This type of transient may be detrimental to the capacitor bank.

Another situation occurs from disconnecting a capacitor. The situation is depicted in Fig. 9.21. The capacitor bank B is disconnected from the circuit. When the breaker opens, it will not immediately interrupt the current of the capacitor. Specifically, an arc will develop across the plates of the breaker which will be interrupted only when the current becomes zero. Thus the current will be interrupted when it reaches a zero value as illustrated in Fig. 9.21d. Since the capacitor voltage lags the capacitor current by  $90^\circ$ , when the current equals zero, the capacitor voltage will be at maximum and thus the capacitor will be left fully charged as illustrated in Fig. 9.21b. As the voltage of the circuit varies sinusoidally, the voltage across the breaker will vary sinusoidally with a maximum value twice the rated voltage, as illustrated in Fig. 9.21c. In this case the breaker is subjected to a voltage twice the rated voltage, a condition that may lead to a restrike. To avoid this possibility, capacitor banks are equipped with internal resistors, which are supposed to discharge the capacitors in reasonable time. If restrike does happen, the effects may be severe. Figure 9.22 illustrates the effects of restrike. Note that restrike may cause severe overvoltages across the capacitor and severe transient capacitor current.

### 9.10.4 Transient Recovery Voltage

Circuit breakers provide the mechanisms to interrupt circuits during faults, and so on. The basic mechanism by which a circuit breaker operates is as follows: When the plates of the breaker open, the electric current is not interrupted instantaneously. Indeed, there is an electric arc between the plates which sustains itself as long as the

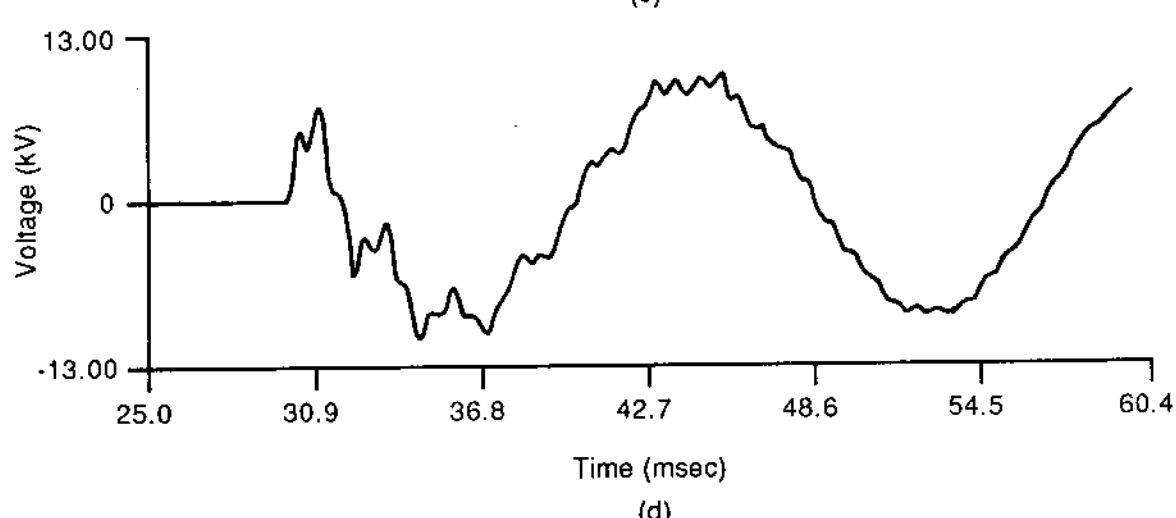
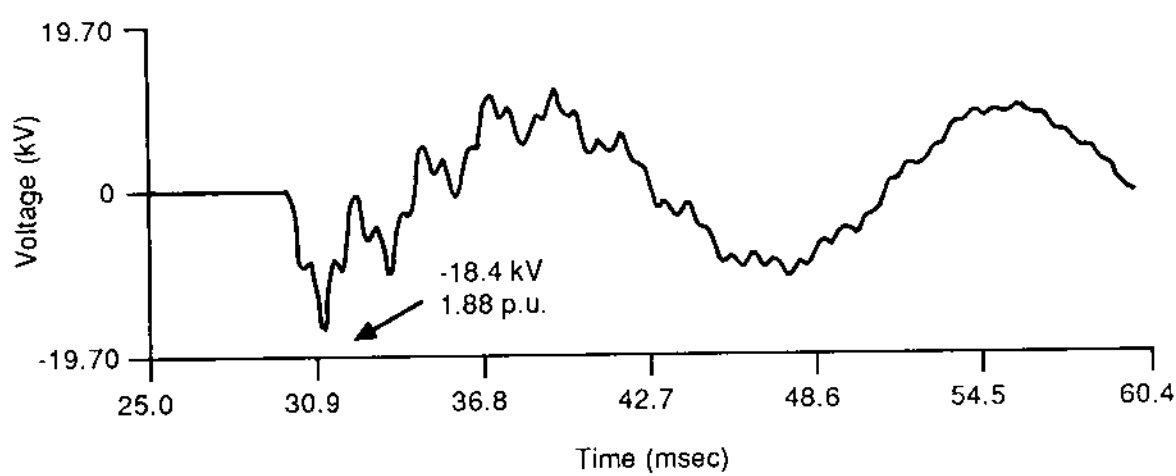
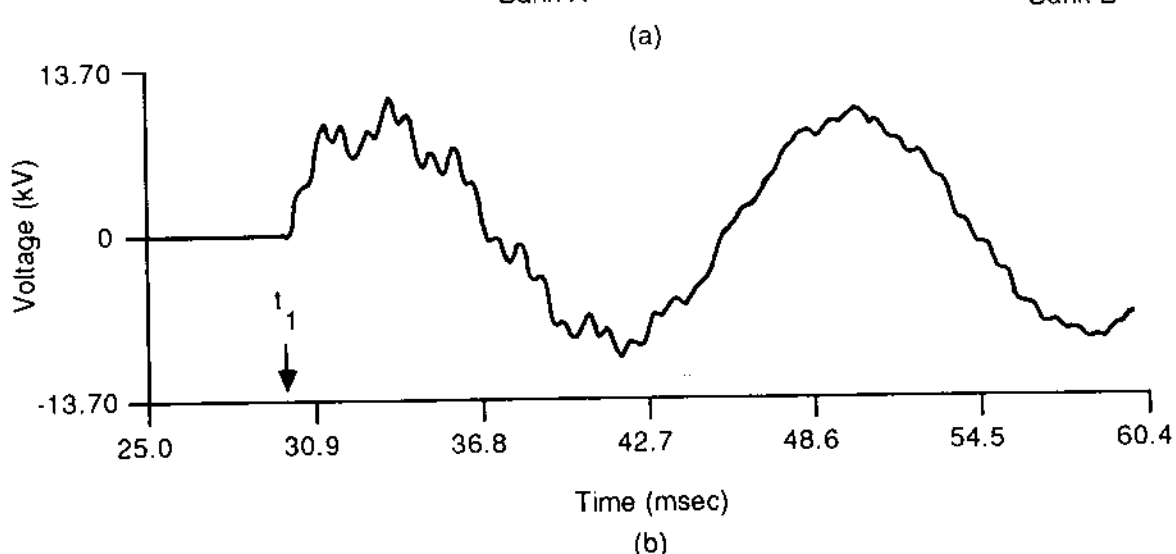
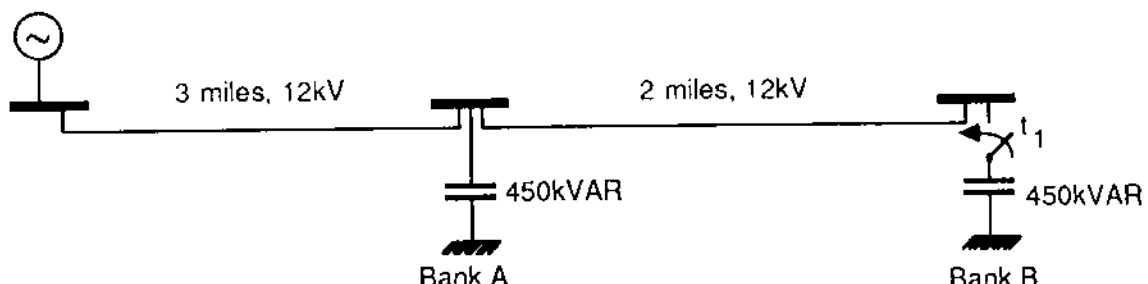


FIG. 9.20 Typical capacitor bank energization transients. (a) System configuration; (b) Phase A voltage, capacitor bank A; (c) Phase B voltage, capacitor bank B; (d) Phase C voltage, capacitor bank B.

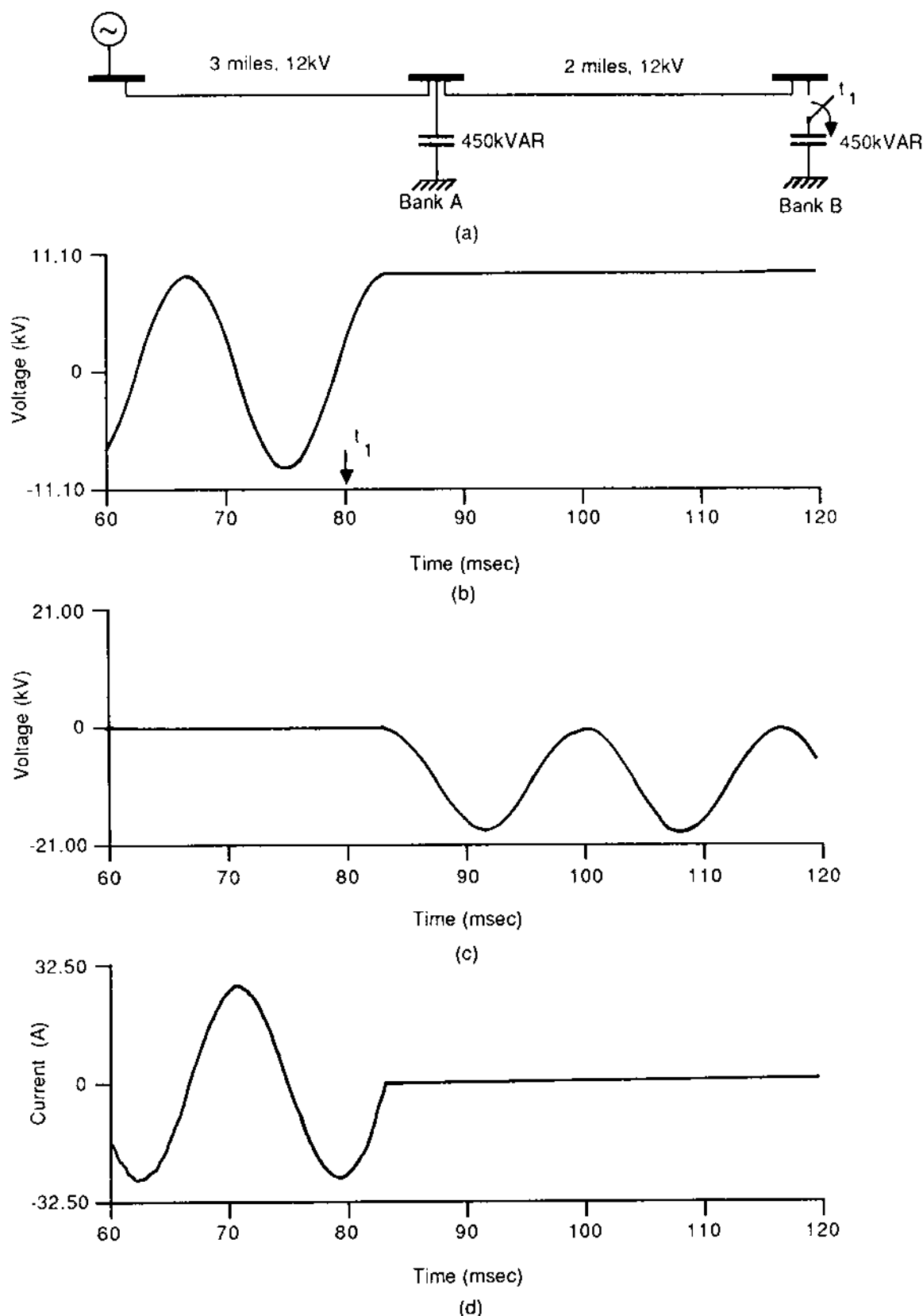


FIG. 9.21 Typical capacitor bank deenergization transients. (a) System configuration; (b) Phase A capacitor voltage: capacitor bank B; (c) Phase A breaker voltage: capacitor bank B; (d) Phase A capacitor current: capacitor bank B.

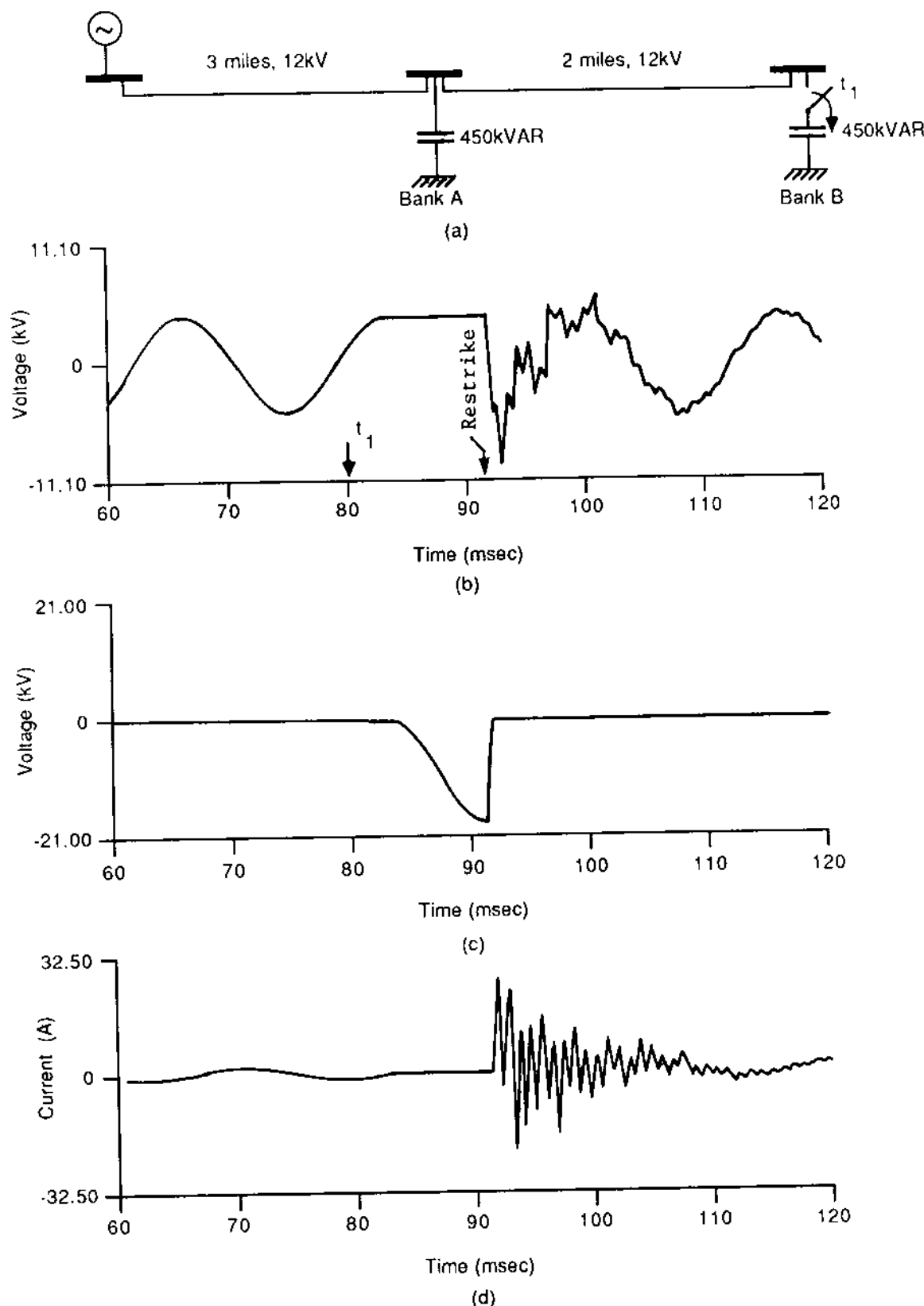


FIG. 9.22 Typical restrike transients following capacitor deenergization. (a) System configuration; (b) Phase A, capacitor voltage, capacitor bank B; (c) Phase A, breaker voltage, capacitor bank B; (d) Phase A, capacitor current, capacitor bank B.

electric current is substantial. Since the electric current varies sinusoidally with time, at a later time it will approach the value of zero. When the value of the electric current becomes very small, the electric arc is interrupted. At this instant of time there is an interruption in the electric circuit. At the location of the electric arc there are still hot ionized gases. If substantial voltage develops across the plates of the breaker immediately, it is possible that the electric arc will restart. For this reason, the rate by which voltage develops across the plates of the breaker after arc interruption should be slow. Enough time should be given that the hot gases between the plates cool off and the number of electricity carriers are minimized. Unfortunately, most power system circuits are mainly inductive. This means that the electric fault current is approximately  $90^\circ$  out of phase with the voltage. Thus, when the electric current is zero, the voltage is at its maximum. This means that immediately after the interruption of the arc, the voltage will start building up rapidly across the plates of the breaker. The rate by which the voltage across the breaker rises is determined by the inductance and the capacitance of the circuit. For analysis purposes, the circuit will be represented with the simplified equivalent of Fig. 9.23. The figure illustrates the fault, the location of the breaker, the equivalent inductance, and the equivalent capacitance. The voltage source is assumed to be sinusoidal as follows:

$$e(t) = \sqrt{2} V \cos \omega t \quad \omega = 2\pi f \quad f = 60 \text{ Hz}$$

Neglecting the initial fault transients, during steady-state conditions with the fault on, the electric fault current is

$$\tilde{I}_f = \frac{\tilde{V}}{j\omega L} \quad (9.92)$$

In the time domain the electric current is

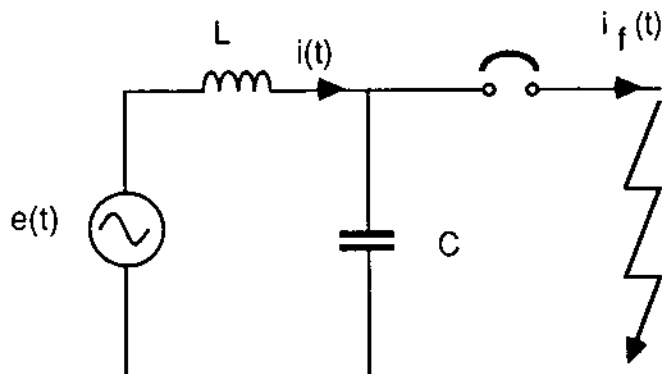


FIG. 9.23 Simplified circuit for TRV analysis.

$$i_f(t) = \frac{\sqrt{2} V}{\omega L} \cos(\omega t - 90^\circ)$$

Thus at time  $t = 0$ ,  $i_f(0) = 0$ . Assume that the breaker opens at time  $t < 0$  and that the first time the electric current crosses zero is  $t = 0$ . In this case the electric current through the breaker will be interrupted at time  $t = 0$ . The resulting circuit (source, inductor  $L$ , and capacitor  $C$ ) is a one-loop circuit. Let  $i(t)$  be the electric current through the inductor  $L$  for  $t > 0$ . Then

$$e(t) = L \frac{di(t)}{dt} + \frac{1}{C} \int_{-\infty}^t i(\tau) d\tau \quad (9.93)$$

$$i(0) = 0$$

Taking the Laplace transform, we have

$$E(s) = sLI(s) + \frac{1}{sC} I(s)$$

Solving for  $I(s)$  gives us

$$I(s) = \frac{sC}{s^2 LC + 1} E(s) = \frac{1}{L} \frac{s}{s^2 + \omega_1^2} E(s) \quad (9.94)$$

where  $\omega_1 = 1/\sqrt{LC}$ . Taking the inverse Laplace transform, we have

$$i(t) = \frac{1}{L} \int_0^t e(\tau) \cos[\omega(t - \tau)] d\tau$$

Upon evaluation of the integral, we have

$$i(t) = \frac{\sqrt{2} V}{\omega L} \frac{1}{1 - (\omega_1/\omega)^2} \left( \sin \omega t - \frac{\omega_1}{\omega} \sin \omega_1 t \right) \quad (9.95)$$

The voltage across the breaker is

$$\begin{aligned} v_b(t) &= e(t) - L \frac{di(t)}{dt} \\ &= \sqrt{2} V \left\{ \cos \omega t - \frac{1}{1 - (\omega_1/\omega)^2} \left[ \cos \omega t - \left( \frac{\omega_1}{\omega} \right)^2 \cos \omega_1 t \right] \right\} \end{aligned} \quad (9.96)$$

This equation provides the transient recovery voltage across the plates of the breaker. Two examples will illustrate the analysis of transient recovery voltage.

Example 9.8: Compute the transient recovery voltage for the system of Fig. 9.23 assuming that  $e(t) = 9.79 \text{ kV} \cos \omega t$ ,  $L = 8 \text{ mH}$ , and  $C = 0.5 \mu\text{F}$ . What is the maximum value and the rise time of the transient recovery voltage?

Solution: The angular frequency  $\omega_1$  is:

$$\omega_1 = \frac{1}{\sqrt{LC}} = 15,810 \text{ s}^{-1}$$

Upon substitution into Eq. (9.96), the voltage across the breaker is

$$v_b(t) = 9.79(\cos \omega t + 0.000569 \cos \omega t - \cos \omega_1 t) \text{ kV}$$

The voltage  $v_b(t)$  assumes its maximum value when  $t = 199 \mu\text{s}$ . The maximum voltage is approximately 19.58 kV. The rise time (zero to crest) is 199  $\mu\text{s}$ .

Example 9.9: Consider the plant auxiliary system of Fig. E9.15. Assume that a fault occurs at the indicated location. The breaker opens by relay action. It is desired to determine the transient recovery voltage across the breaker. Compute the transient recovery voltage for a period of 39  $\mu\text{s}$ . Use the numerical integration technique with a time step  $h = 3 \mu\text{s}$ . The indicated transformer and the power system connected to it can be represented by an ideal voltage source of  $13.8/\sqrt{3}$  kV behind an equivalent inductance of  $L = 0.50 \text{ mH}$ . Also, the cable can be represented as an ideal transmission line. The 60-Hz parameters of the cable are illustrated in Fig. E9.15.

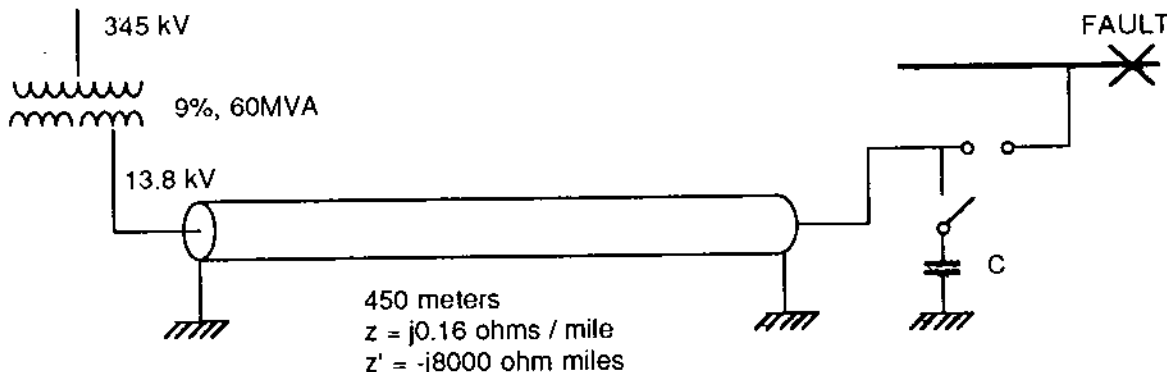


FIG. E9.15 A simplified plant auxiliary system.

Solution: For the analysis of this problem, we shall consider two time periods: (a) the period during the fault and prior to the fault current interruption, and (b) the period after the fault current interruption. We shall assume that in the period during the fault, steady-state conditions have been attained. In this period the model of the system is as illustrated in Fig. E9.16, where the capacitive (shunt) reactance of the cable has been omitted since it is very large compared to the inductive reactance (60-Hz steady-state conditions). The cable inductance is computed from

$$L_c = \frac{(0.16)(450)}{(1609)(2\pi 60)} = 0.119 \text{ mH}$$

The short-circuit current is determined by first computing the phasor of the fault current  $\tilde{I}_f$ :

$$\begin{aligned} \tilde{I}_f &= \frac{\tilde{E}}{j\omega L + j\omega L_c} \\ &= \frac{7.967}{j0.1885 + j0.0447} = -j34.164 \text{ kA} \end{aligned}$$

The fault current in the time domain is

$$i_f(t) = 48.31 \text{ kA} \cos(\omega t - 90^\circ)$$

Assume that the fault was initiated at  $t < 0$ . Also assume that the breaker plates opened at time  $t < 0$  and that the first time that the fault current becomes zero after the opening of the plates is  $t = 0$ . This means that the circuit is interrupted at time  $t = 0$ . At this time

$$i_f(0) = 0.0$$

$$v_2(0) = 0.0$$

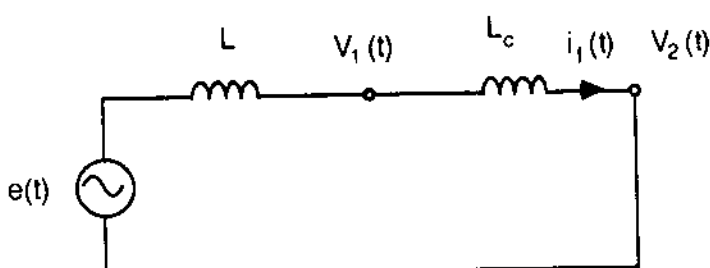


FIG. E9.16 Equivalent circuit during fault.

$$v_1(0) = L_c \frac{di_f(t)}{dt} \Big|_{t=0} = 2.16 \text{ kV}$$

The conditions above represent the initial conditions for the second time period after the fault interruption.

For the period after the fault interruption, the simplified equivalent circuit is illustrated in Fig. E9.17a. For numerical computations, the circuit of Fig. E9.17a is replaced with its resistive equivalent circuit of Fig. E9.17b, in which a time step of 3  $\mu\text{s}$  was used. The parameters of the resistive equivalent circuit are computed as follows:

Inductor:  $h/2L = 0.003 \text{ S}$ .

Cable line: The inductance and capacitance per unit length are

$$L_{cu} = \frac{Z}{\omega} = 0.2637 \text{ } \mu\text{H/m}$$

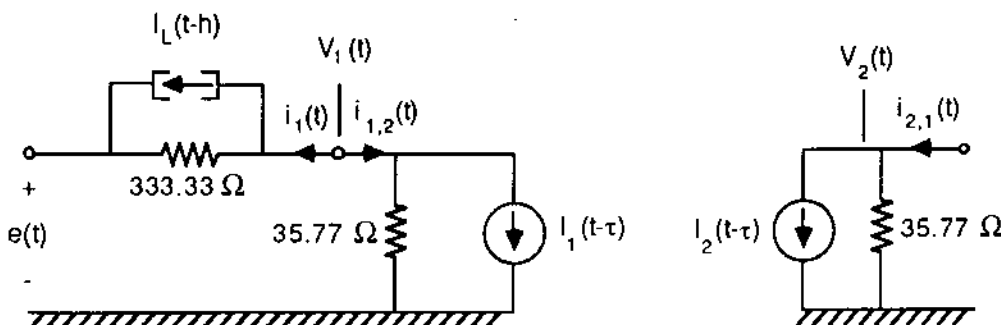
$$C_{cu} = \frac{1}{\omega Z'} = 0.206 \text{ pF/m}$$

The speed of propagation is

$$c = \frac{1}{\sqrt{L_{cu} C_{cu}}} = 150 \text{ m/}\mu\text{s}$$



(a)



(b)

FIG. E9.17 Circuit representation after fault interruption. (a) Equivalent circuit, (b) resistive companion circuit.

The characteristic impedance is

$$Z_0 = \sqrt{\frac{L_{cu}}{C_{cu}}} = 35.77 \Omega$$

Following these computations, each element of the circuit in Fig. E9.17a is replaced with its resistive companion circuit with the aid of Fig. 9.8. The computing equations for the resulting resistive network of Fig. E9.17b are

$$b_1(t) = 33.78 - I_L(t - h) - I_1(t - \tau)$$

$$b_2(t) = -I_2(t - \tau)$$

$$v_1(t) = 32.303b_1(t)$$

$$v_2(t) = 35.77b_2(t)$$

$$i_1(t) = 0.003e_1(t) - 33.78 + I_L(t - h)$$

$$i_{1,2}(t) = 0.0279e_1(t) + I_1(t - \tau)$$

$$i_{2,1}(t) = 0.0279e_2(t) + I_2(t - \tau)$$

$$I_L(t) = i_1(t) + 0.003e_1(t) - 33.78$$

$$I_1(t) = -0.0279e_2(t) - i_{2,1}(t)$$

$$I_2(t) = -0.0279e_1(t) - i_{1,2}(t)$$

Using the equations above, the transient recovery voltage can be computed with the algorithm illustrated on Table E9.3. The transient recovery voltage of the breaker is the voltage  $v_2(t)$  which is tabulated in Table E9.3 and plotted in Fig. E9.18 (curve a). Often, to decrease the rate of increase in the transient recovery voltage, a capacitor is inserted as in Fig. E9.15. Assuming that  $C = 100 \text{ nF}$ , the transient recovery voltage is as shown in Fig. E9.18 (curve b). Note that the rate of rise has decreased.

#### 9.10.5 Discussion of Basic Power System Transients

In this section we have examined the characteristics of typical electrical transients in power systems. We have discussed some techniques by which the transient overvoltage can be mitigated: for example, resistor preinsertion breakers for mitigating switching transients, and the use of capacitors for slowing the rate of rise of transient recovery voltage. In general, power equipment should be

TABLE E9.3

Iteration number:	1	2	3	4	5	6	7	8	9	10	11	12	13
$t$ ( $\mu s$ ):	0	3	6	9	12	15	18	21	24	27	30	33	36
$b_1$	-	61.08	177.2	260.3	426.7	511.8	631.4	629.9	640.2	527.6	446.6	280.3	193.4
$b_2$	-	60.38	110.3	259.6	359.8	511.1	564.5	629.3	573.3	526.9	379.7	279.6	126.6
$e_1(t)$	2,160.0	1,973	5,724	8,410	13,787	16,536	20,399	20,354	20,683	17,047	14,427	9,056	6,249
$e_2(t)$	0	2,160	3,946	9,288	12,875	18,286	20,197	22,513	20,510	18,852	13,584	10,003	4,528
$i_1(t)$	0	-55.1	-99.62	-124.7	-125.7	-102.3	-59.08	-4.38	51.17	96.80	123.6	126.5	104.9
$i_{1,2}(t)$	0	55.1	99.62	124.7	125.7	102.3	59.08	4.38	-51.17	-96.8	-123.6	-126.5	-104.9
$i_{2,1}(t)$	0	0	0	0	0	0	0	0	0	0	0	0	0
$I_L(t)$	-27.298	-83.01	-116.2	-133.3	-118.1	-86.5	-31.6	22.9	79.4	114.2	133.2	119.9	89.8
$I_1(t)$	0	-60.4	-110.3	-259.6	-359.8	-511.1	-564.5	-629.3	-573.3	-526.9	-379.7	-279.6	-126.6
$I_2(t)$	-60.38	-110.3	-259.6	-359.8	-511.1	-564.5	-629.3	-573.3	-526.9	-379.7	-279.6	-126.6	-69.7

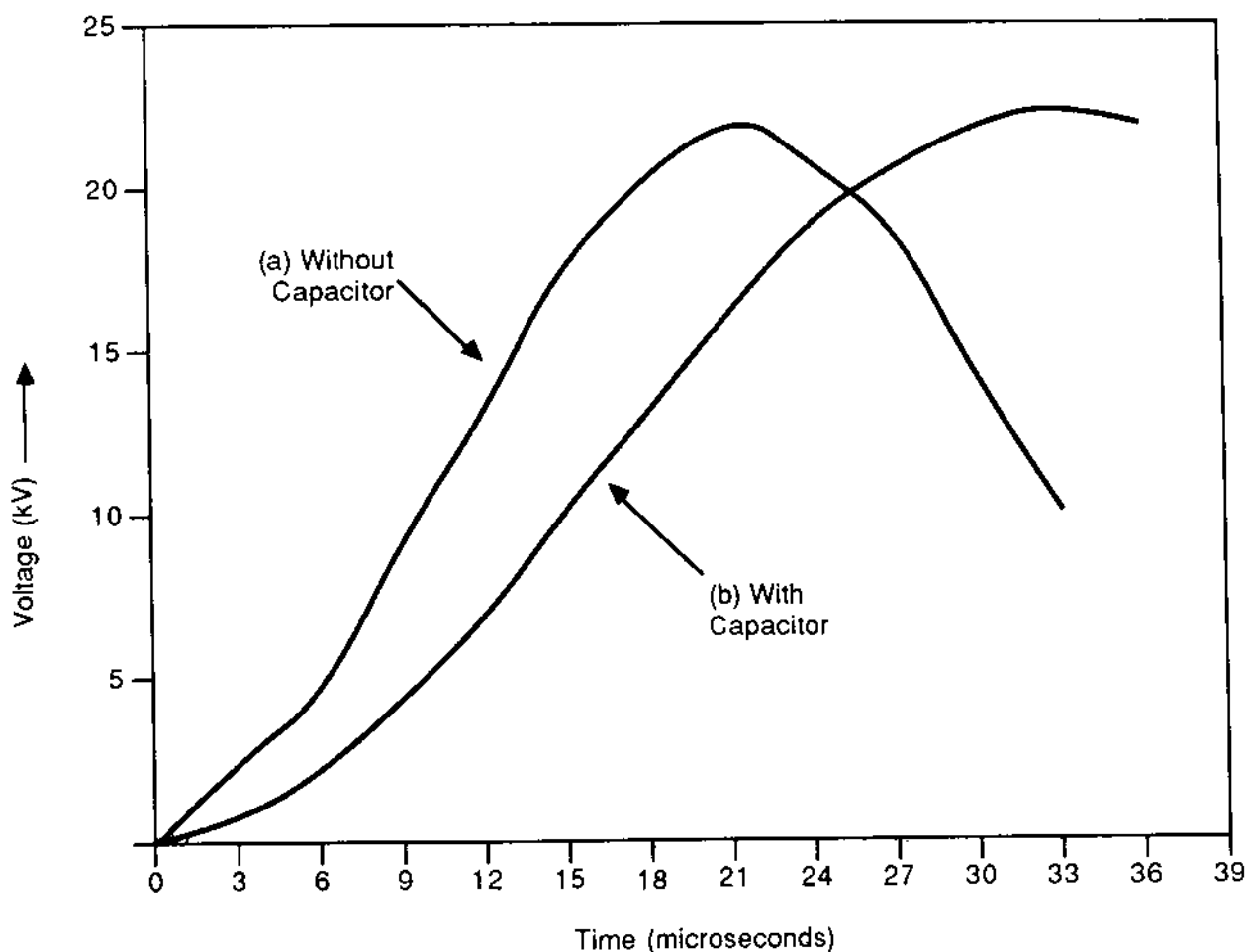


FIG. E9.18

designed as to withstand all possible transient overvoltages. Otherwise, insulation breakdown may occur.

### 9.11 TRANSFORMER INRUSH CURRENTS

A type of special transients can be generated during energization of magnetic core transformers. Specifically, during transformer energization, high-level electric currents known as inrush current may be absorbed. The cause of these transients is the nonlinear magnetization characteristics of iron core transformer. A typical iron core magnetization curve is illustrated in Fig. 9.24. In general, transformers are designed in such a way that the maximum operating magnetic flux is near the knee of the magnetization curve. During normal operating conditions, the flux oscillates between  $\lambda_{\max}$  and  $\lambda_{\min}$ . The magnetization current required is very small. During energization, however, transients are induced on the magnetic flux. It is possible that the flux may take as large values as twice the normal maximum operating flux. The magnetic flux transients are translated into magnetization current transients which are amplified by the nonlinear magnetization characteristics of the iron core.

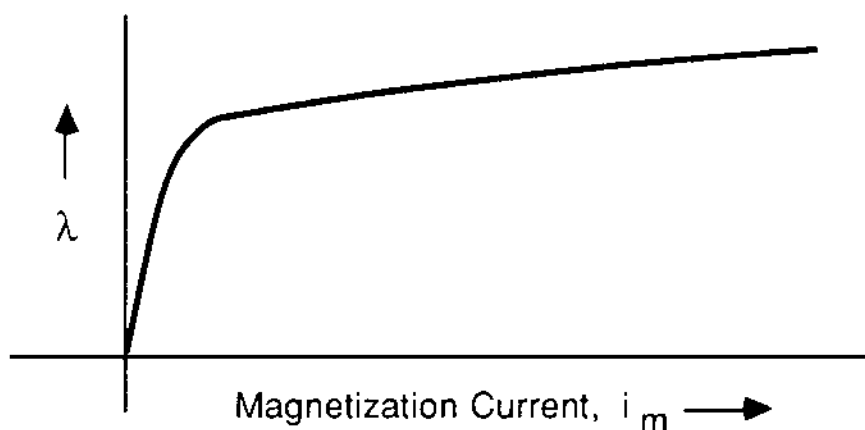


FIG. 9.24 Typical magnetization characteristic of an iron core transformer.

To study the phenomenon, consider a single-phase transformer energized at time zero by a source as illustrated in Fig. 9.25. For simplicity, assume that the source is an ideal voltage source. When the switch is closed, the transients in the transformer will be governed by the equation

$$e(t) = \frac{d\lambda(t)}{dt}$$

where  $e(t)$  is the voltage of the source and  $\lambda(t)$  is the magnetic flux linkage of the transformer. Assume that the initial condition of the flux is

$$\lambda(0) = \alpha$$

Also,

$$e(t) = V_m \cos(\omega t + \phi)$$

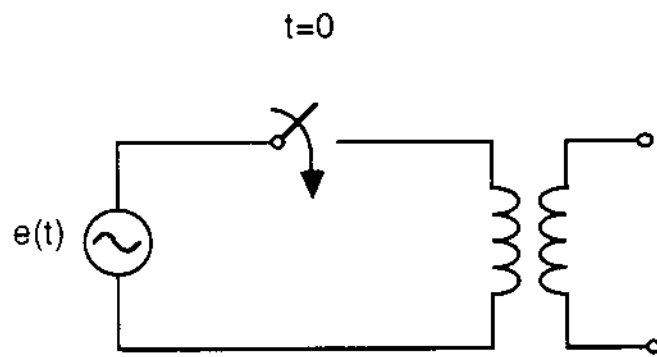


FIG. 9.25 Transformer energization with an ideal voltage source.

Upon solution of the problem above, we have

$$\lambda(t) = \left( \alpha - \frac{V_m}{\omega} \sin \phi \right) + \frac{V_m}{\omega} \sin(\omega t + \phi) \quad (9.97)$$

Equation (9.97) represents a sinusoidal curve with a dc bias. The dc bias is  $[\alpha - (V_m/\omega) \sin \phi]$ . It depends on the initial flux of the transformer  $\alpha$  and the time the switch was closed (or phase  $\phi$ ). Assuming that  $\alpha = 0$ , the flux may be fully offset when  $\phi = \pi/2$ . The magnetization current in this case is illustrated in Fig. 9.26. The figure also illustrates the magnetization current for one period. The magnetization current is constructed graphically as illustrated in the figure. Note that the magnetization current can assume extremely high values. The conditions illustrated in Fig. 9.26 ( $\phi = \pi/2$ ) represent the worst case. When  $\phi = 0$ , the magnetic flux is a pure sinusoidal. In this case the magnetization current is very small and typical of the steady-state operation of the transformer. Transients of different severity may occur for other values of  $\phi$ . Typically, the maximum magnetizing current for  $\phi = 0$  is 1% of rated current, while for  $\phi = \pi/2$  it may reach a peak of 800% of rated current.

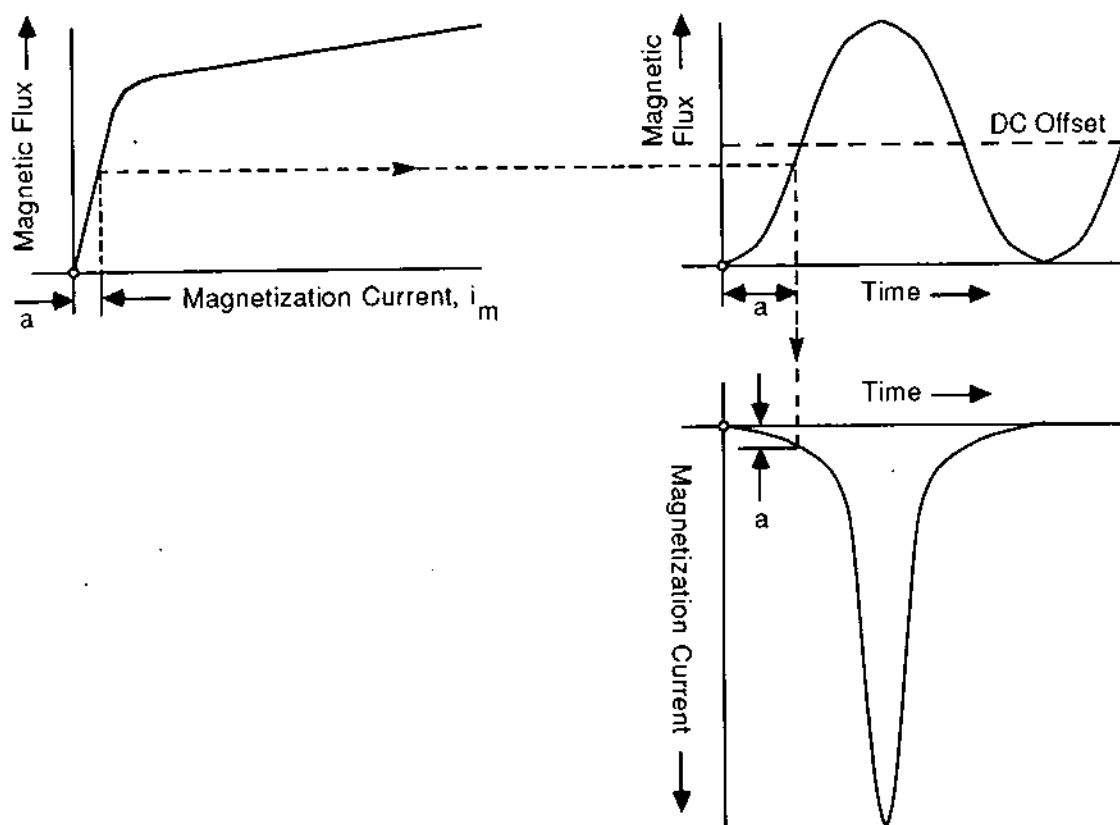


FIG. 9.26 Graphical determination of magnetization current from a fully offset magnetic flux linkage.

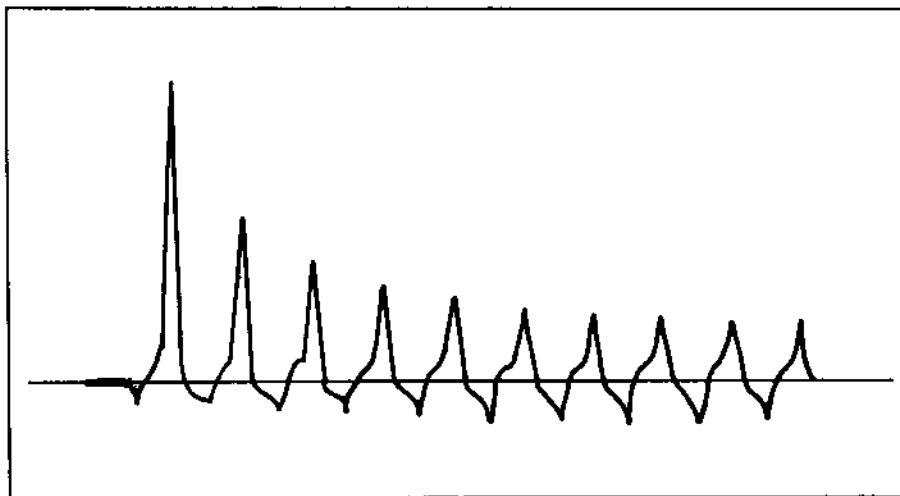


FIG. 9.27 Typical inrush current of an iron core transformer.

Because of the inherent resistance in a power system, the inrush currents decay slowly. Figure 9.27 illustrates a typical oscillosgram of inrush currents.

Example 9.10: Consider the saturable inductor of the Fig. E9.19a. At time  $t = 0$ , the switch closes. Compute the peak value of the inrush current. The magnetization curve of the inductor is illustrated in Fig. E9.19b. The voltage of the source is  $e(t) = (20.41 \text{ kV}) \cos(\omega t - 75^\circ)$ .

Solution: The magnetic flux linkage of the inductor following the closing of the switch is

$$\begin{aligned}\lambda(t) &= \frac{V_m}{\omega} \sin(\omega t + \phi) = \frac{V_m}{\omega} \sin \phi \\ &= 54.13 \sin(\omega t - 75^\circ) + 52.28 \text{ Wb} \\ \lambda_{\max} &= 106.42 \text{ Wb}\end{aligned}$$

The maximum magnetization current is obtained from Fig. E9.19b by reading the current value for  $\lambda_1 = \lambda_{\max}$ :

$$\begin{aligned}i_{\max} &= 0.04 + (27.0 - 0.04) \left( \frac{106.42 - 54.0}{108 - 54} \right) \\ &= 26.209 \text{ A}\end{aligned}$$

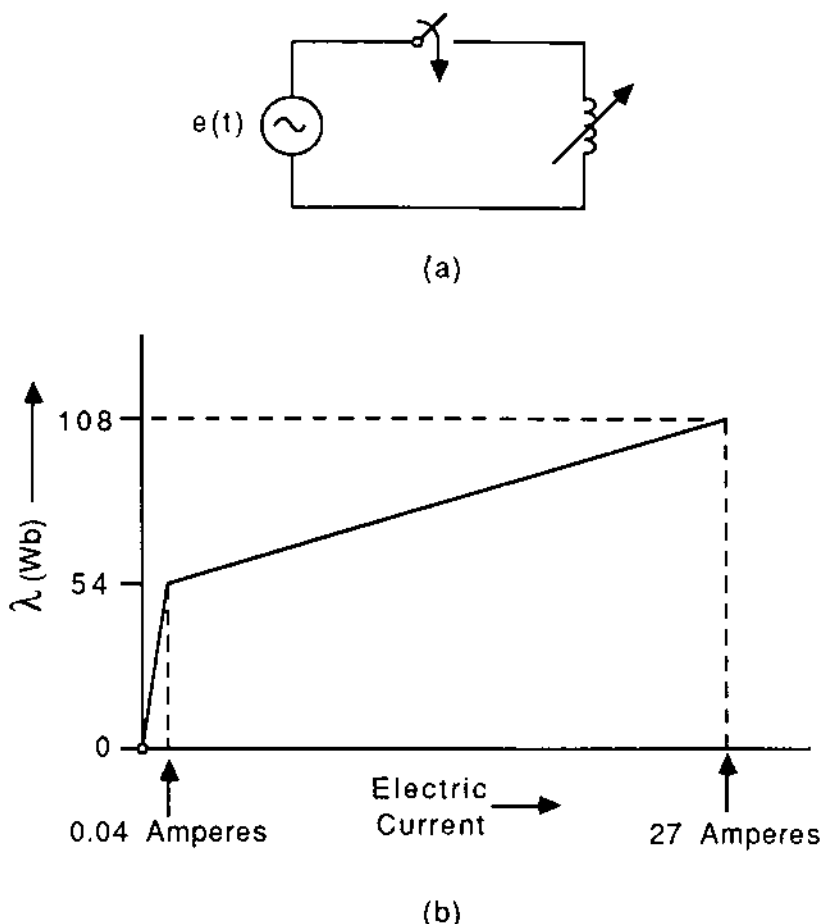


FIG. E9.19 A magnetic core inductor.

### 9.12 LIGHTNING OVERVOLTAGES

Transmission systems are exposed to weather conditions and therefore to lightning. In many respects, lightning can be considered as an ideal current source. Typical lightning waveforms exhibit a 0.2- to 1.5- $\mu$ s rise time and persist for 50 to 200  $\mu$ s. For testing and standardization purposes, a standard lightning wave has been established, the so-called 1.2/50- $\mu$ s waveform, which is illustrated in Fig. 9.28. Typical crest values of a lightning pulse range between 10 and 100 kA. When lightning hits a transmission line, it generates an electric current surge, which in turn causes an overvoltage. The overvoltage depends on the line characteristic impedance, the level of the lightning current wave, and the tower characteristics. As an example, Fig. 9.29 illustrates the lightning overvoltages developed on a 115-kV transmission line when the standard lightning stroke (1.2/50  $\mu$ s) hits the top of the transmission tower. The design of the transmission tower is illustrated in Fig. 1.6. The phase conductors are ACSR, 336 kcm, and the shield wire is  $\frac{5}{16}$ -in. steel. The tower footing resistance is 35  $\Omega$ . Figure 9.29a illustrates the transient voltage on the top of the transmission tower. Figure 9.29b illustrates the

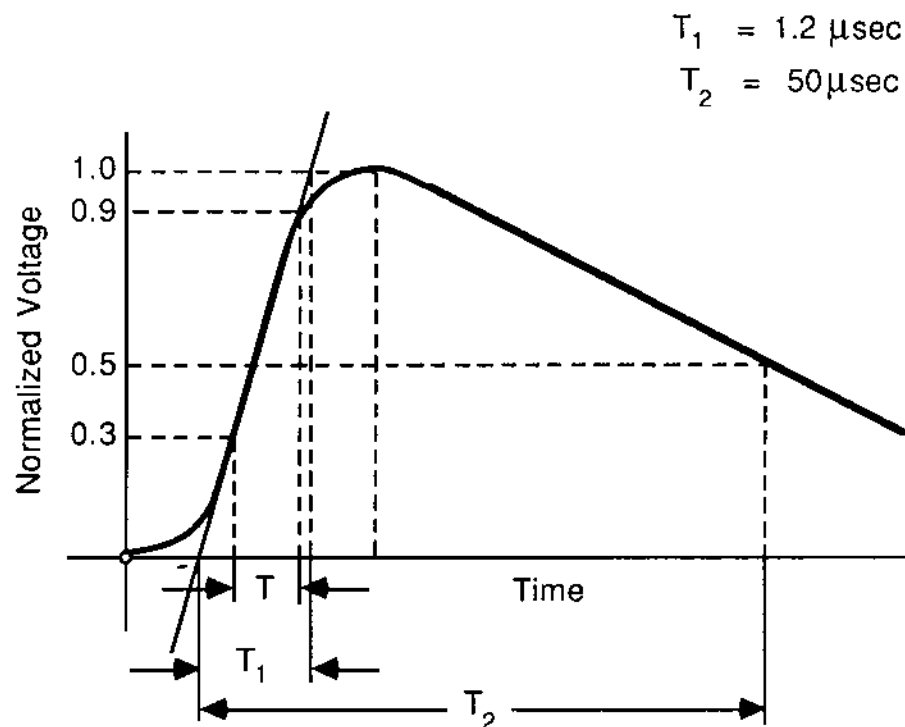


FIG. 9.28 The standard impulse test wave (1.2/50  $\mu\text{sec}$ ).

transient voltage developed across the insulator of phase A. Figure 9.29c illustrates the ground potential rise of the tower ground. Note that all voltages are normalized with respect to the lightning waveform crest (kV per kA of lightning current). Studies reveal that the tower footing resistance is one of the most important parameters affecting the maximum overvoltage resulting from lightning on the shield wire of a power line. Figure 9.30 illustrates the effect of the tower footing resistance on the maximum overvoltage for a 115-kV line. Note that for ground resistances below 50  $\Omega$ , the maximum overvoltage is not sensitive to the tower footing resistance.

### 9.13 OVERVOLTAGE PROTECTION DEVICES

Electric power systems must be protected against overvoltages to avoid insulation failure and subsequent fault. For this purpose overvoltage protection devices have been developed. Ideally, an overvoltage protection device must have a voltage-current characteristic as indicated in Fig. 9.31. This characteristic indicates that the device will never allow the voltage to exceed the value of  $V_p$ .  $V_p$  will be referred to as the protection level. Unfortunately, this ideal characteristic cannot be obtained in reality.

Historically, the first overvoltage protection device was a spark gap. The next generation of overvoltage protection devices were the

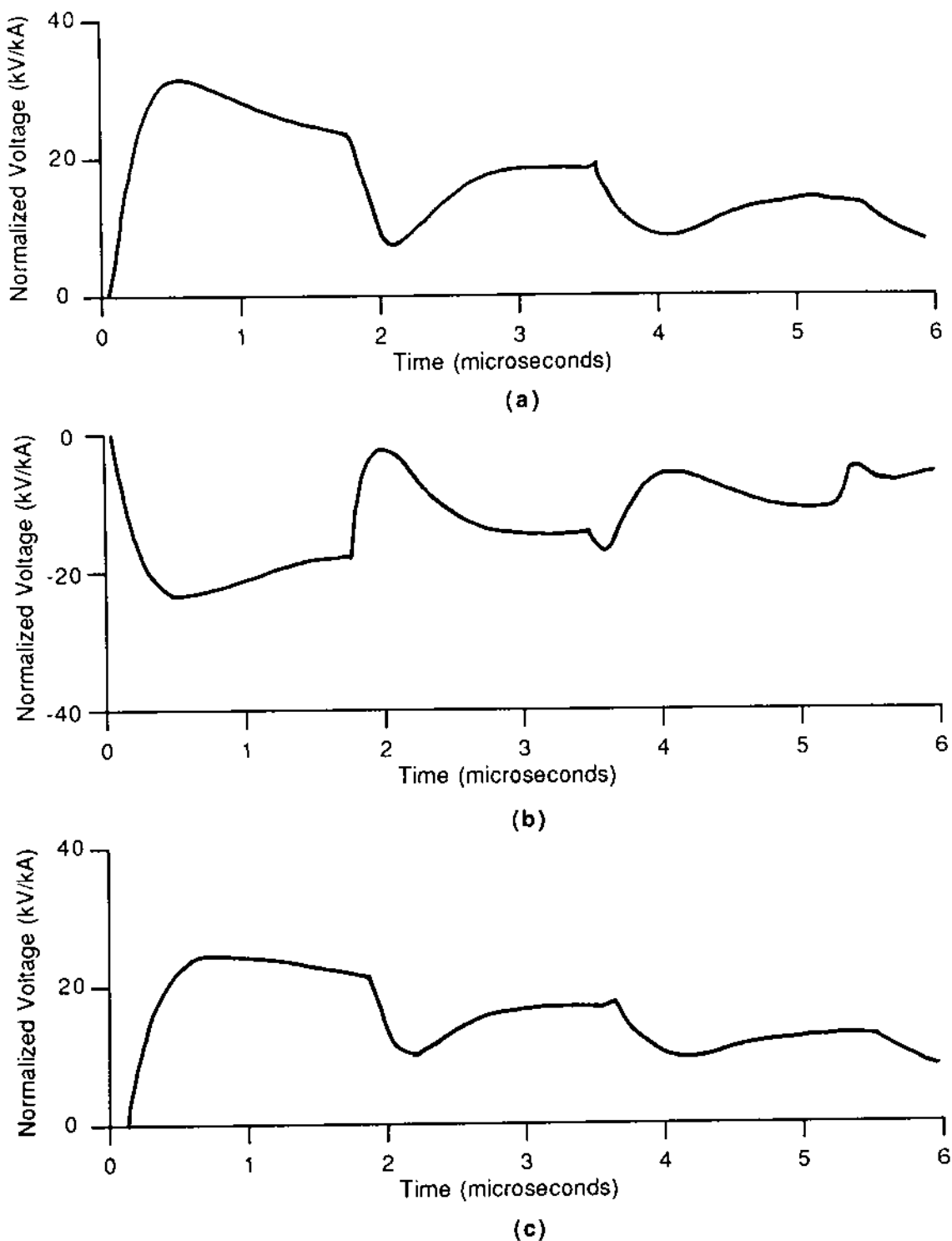


FIG. 9.29 Typical lightning overvoltages on a transmission line.  
(a) Top of tower voltage, (b) voltage across insulator: phase A,  
(c) tower ground potential rise.

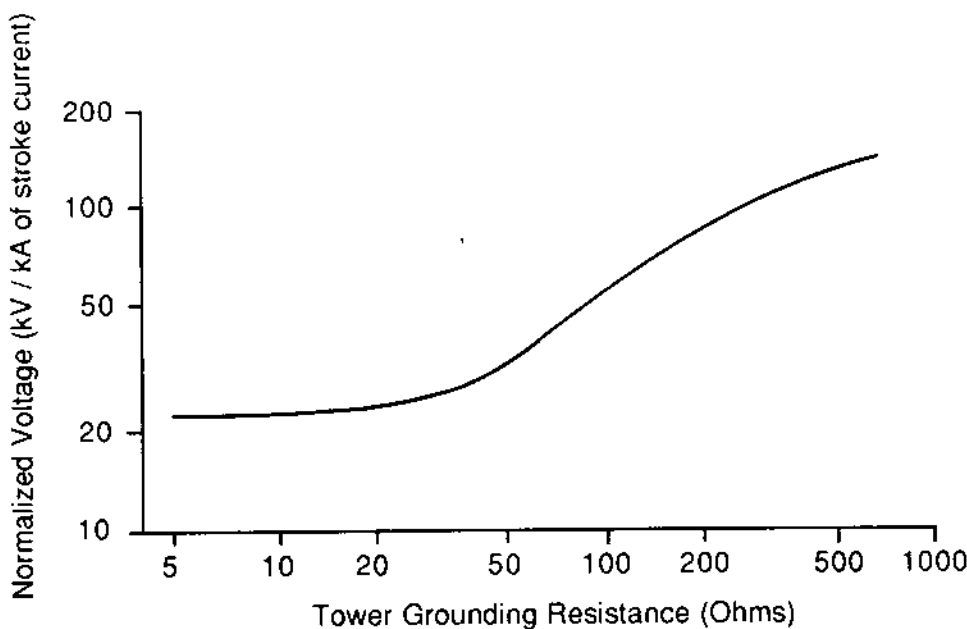


FIG. 9.30 Effects of tower footing resistance on a specific 115 kV transmission line. (Standard lightning wave = 1.2/50  $\mu$ sec).

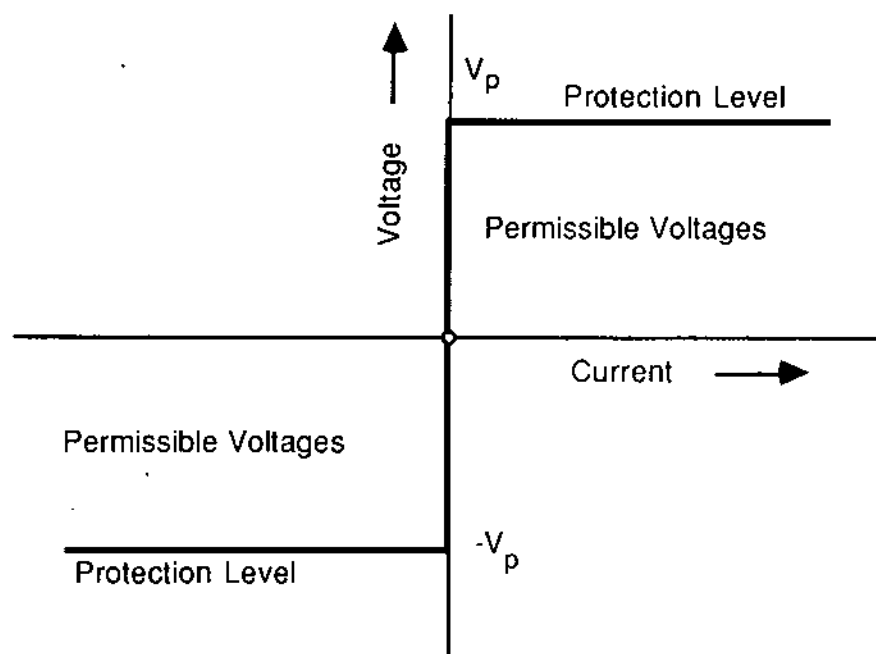


FIG. 9.31 Current-voltage characteristics of an ideal overvoltage protection device.

gapped surge arresters, without and with current-limiting blocks. Finally, metal oxide varistors (MOVs) were introduced. The characteristics of these protective devices will be described briefly. Today's technology has resulted in metal oxide varistors with characteristics very close to the ideal protection device of Fig. 9.31.

### 9.13.1 Spark Gaps

A spark gap is formed with two electrodes placed at a certain distance. The shape of the electrodes may be spherical, cylindrical, and so on. When voltage is applied across the spark gap, it is possible to initiate a spark whenever the voltage exceeds a value that will be called the sparkover voltage. Once the spark initiates, it develops, in time, into an arc. The voltage across the arc varies with time. In steady state, the voltage across the arc will have a constant value. When the electric current of the arc reduces to a certain value, the arc cannot sustain itself and is interrupted. Figure 9.32 illustrates a typical voltage-time characteristic of a long air gap. Note that the difference between the sparkover voltage and the steady-state voltage of the arc is very large. This characteristic severely limits the protection properties of spark gaps.

### 9.13.2 Gapped Surge Arresters

Gapped surge arresters comprise an arrangement of spark gaps. They employ a string of metal plates held apart by insulating material. During operation, arcs are formed between any two contingent plates. Thus the arc is broken into a number of short arcs. This basic arrangement decreases the difference between the sparkover

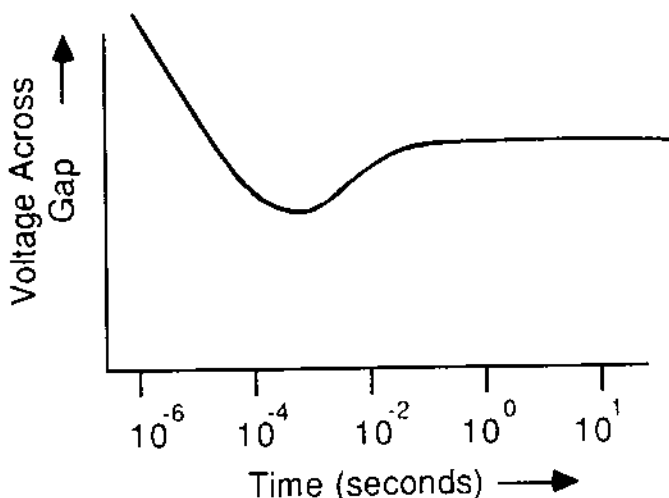


FIG. 9.32 Typical voltage-time characteristic of a long air gap.

voltage and the voltage of the arc since the sparkover voltage depends on the distance between two contingent plates, while the voltage of the arc is across the entire arrangement.

The protection characteristics of present-day gapped surge arresters have been improved with two basic innovations: (a) the arc voltage in an individual spark gap is increased by means of forming a chamber and increasing the length of the arc by means of magnetic induction, and (b) a current-limiting block is connected in series with the arrangements of spark gaps. This block is typically made of SiC, which has a nonlinear voltage-current characteristic. A typical current-voltage characteristic of a present-day arrester with spark gaps is illustrated in Fig. 9.33. Note that the difference between the sparkover voltage and reseal voltage is relatively low.

### 9.13.3 Solid-State Surge Arresters

It is possible to manufacture ZnO composite ceramic substances with nonlinear voltage-current characteristics close to the desirable (ideal) characteristics of an overvoltage protection device. As an example, Fig. 9.34 illustrates the characteristics of an arrester constructed with blocks of  $ZnO$  composite ceramic material. These characteristics come very close to the desirable ideal characteristics of a surge arrester. For this reason, solid-state surge arresters (MOVs) are rapidly becoming the preferred arrester.

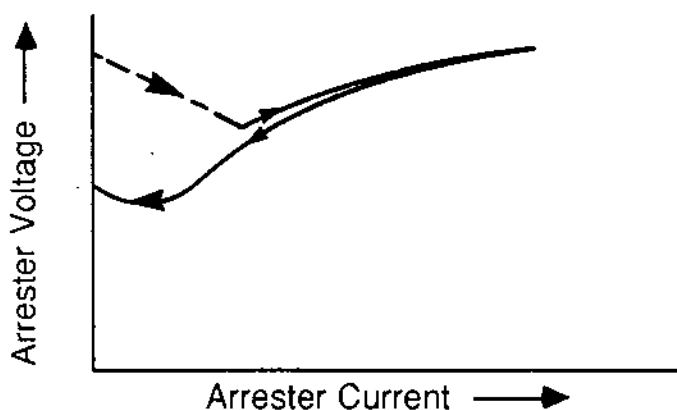


FIG. 9.33 Current-voltage characteristics of surge arresters with spark gaps.

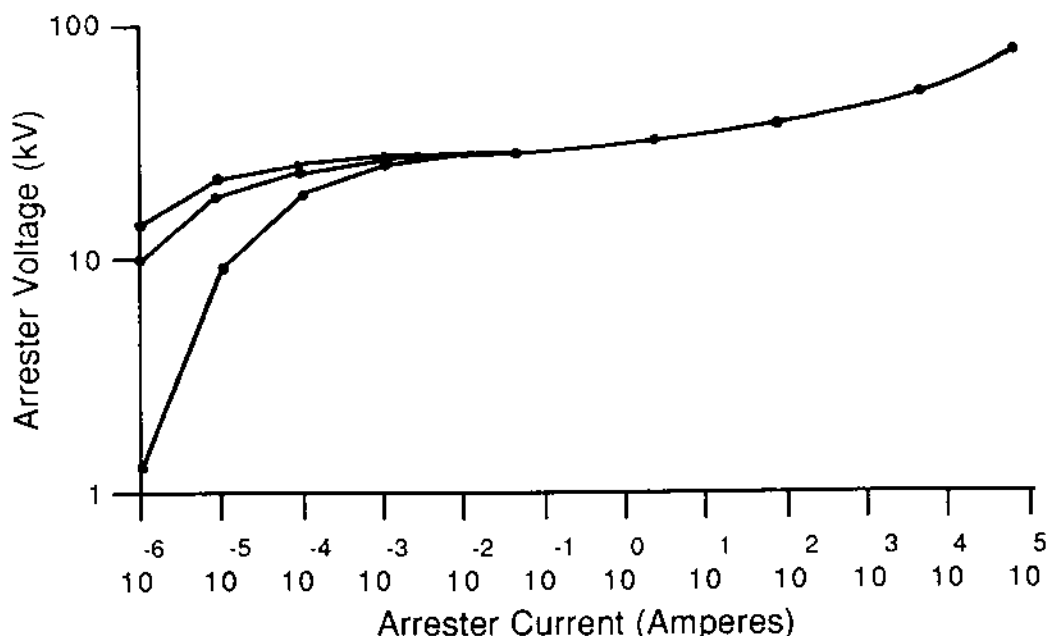


FIG. 9.34 Current-voltage characteristics of MOV arresters.

#### 9.14 SUMMARY AND DISCUSSION

In this chapter we have examined transient analysis techniques for power systems. Graphical, analytical, and numerical methods were studied. Typical electrical transients in power systems were studied with these techniques. The effects of specific electrical transients and mitigation procedures were discussed. Finally, we discussed the characteristics of overvoltage protection devices.

This chapter is by no means an exhaustive discussion of electrical transients in power systems. It provides comprehensive coverage of analysis methods and their typical application to power systems. These methods are the cornerstone for investigating specific problems or in the design of overvoltage protection of power systems. For additional reading, consult references 1, 44, 46, 55, 56, and others.

#### 9.15 PROBLEMS

Problem 9.1: Consider a 600-m-long single-phase cable, terminating in a  $150\text{-}\Omega$  resistor at one end and an open circuit at the other, as illustrated in Fig. P9.1. The cable is not energized [i.e.,  $v(t) = 0$ ,  $t < 0$  everywhere along the cable]. At time  $t = 0$ , lightning strikes the cable at point A. The lightning is to be represented as an ideal current source of electric current

$$i(t) = 1.0(e^{-0.2t} - e^{-1.4t}) \text{ kA}$$

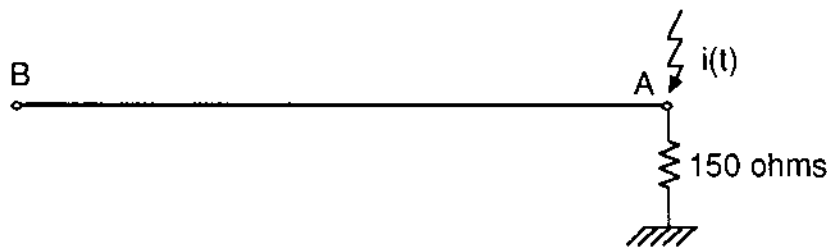


FIG. P9.1

where  $t$  is expressed in microseconds. Compute the transient voltage at point B (see Fig. P9.1) for the time interval  $0 \leq t \leq 20 \mu\text{s}$ . Give a rough plot of the transient voltage. The parameters of the cable are  $Z_0 = 50 \Omega$ ,  $c = 150 \text{ m}/\mu\text{s}$ .

- (a) Use the graphical method.
- (b) Use the Laplace transform method.

Problem 9.2: A 15-kV single-phase cable is charged to +20-kV dc voltage. At time  $t = 0$ , the switch, illustrated in Fig. P9.2, closes (restrike of a breaker). The source is an ideal (zero internal impedance) 60-Hz sinusoidal voltage source:

$$e(t) = 20(\text{kV}) \cos(\omega t + 180^\circ)$$

$$\omega = 377 \text{ s}^{-1}$$

The cable is 300 m long with the following parameters:  $Z_0 = 50 \Omega$ ,  $c = 150 \text{ m}/\mu\text{s}$ . Compute the transient voltage at point A for a period of 6  $\mu\text{s}$ . Use the numerical integration technique with a time step of 1  $\mu\text{s}$ .

Problem 9.3: Consider the electric power system of Fig. P9.3. It represents a Thévenin equivalent. Assume that the circuit is open when at time  $t = 0$  an electric fault occurs at point A. Compute the fault current using the numerical integration technique. Assume a time step of 0.8 ms. Show three iterations of the method. The voltage  $e(t)$  of the source is  $e(t) = (9.798 \text{ kV}) \cos \omega t$ ,  $\omega = 377 \text{ s}^{-1}$ . The other parameters are  $R = 0.5 \Omega$  and  $C = 500 \mu\text{F}$ .

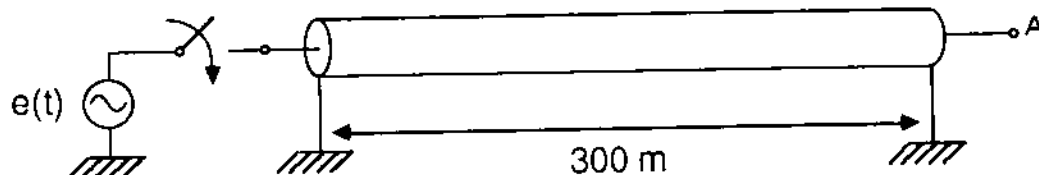


FIG. P9.2

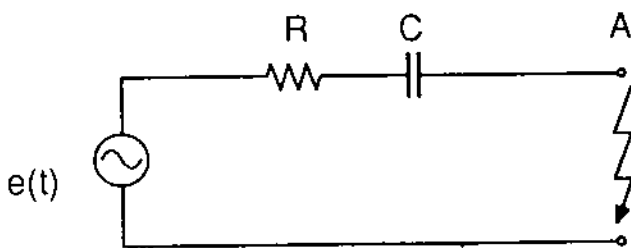


FIG. P9.3

Problem 9.4: Consider the single-stage impulse generator of Fig. P9.4. The parameters of the generator are  $C_1 = 1 \mu\text{F}$ ,  $R_1 = 1.0 \Omega$ , and  $R_2 = 50 \Omega$ . The capacitance of the test object is  $C_2 = 0.2 \mu\text{F}$ . Assume that the capacitor  $C_1$  is charged to 80 kV. Compute the voltage at point A following a spark in the indicated gap. Also, compute the electric current through the resistor  $R_1$ .

Problem 9.5: Consider a single-phase cable of length 1600 m and parameters

$$L = 0.3125 \mu\text{H/m}$$

$$C = 0.125 \text{nF/m}$$

The cable is terminated with lumped resistances of 100 and 85  $\Omega$ , respectively. At time  $t = 0$ , lightning hits the cable at the end terminated with the 85- $\Omega$  resistor. The lightning is to be represented as a current source with the waveform illustrated in Fig. P9.5b. Compute the transient voltage at point A of the cable. Use the Laplace method.

Problem 9.6: A power system is represented by the Thévenin equivalent. The Thévenin equivalent voltage source is  $e(t) = 15 \cos(377t + 30^\circ)$  and the equivalent resistance and inductance are  $R = 0.5 \Omega$ ,  $L = 5 \text{ mH}$ , respectively. At time  $t = 0$ , a short circuit occurs. Compute the rms value of the short-circuit current at  $t = 0.01 \text{ s}$ .

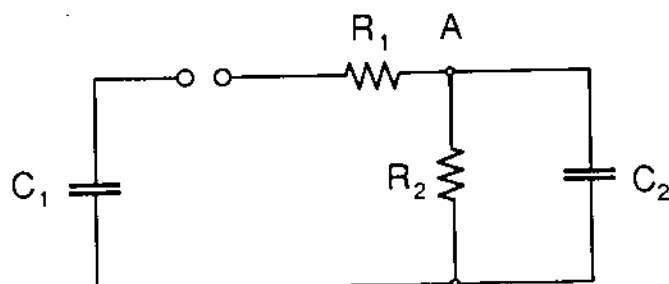


FIG. P9.4

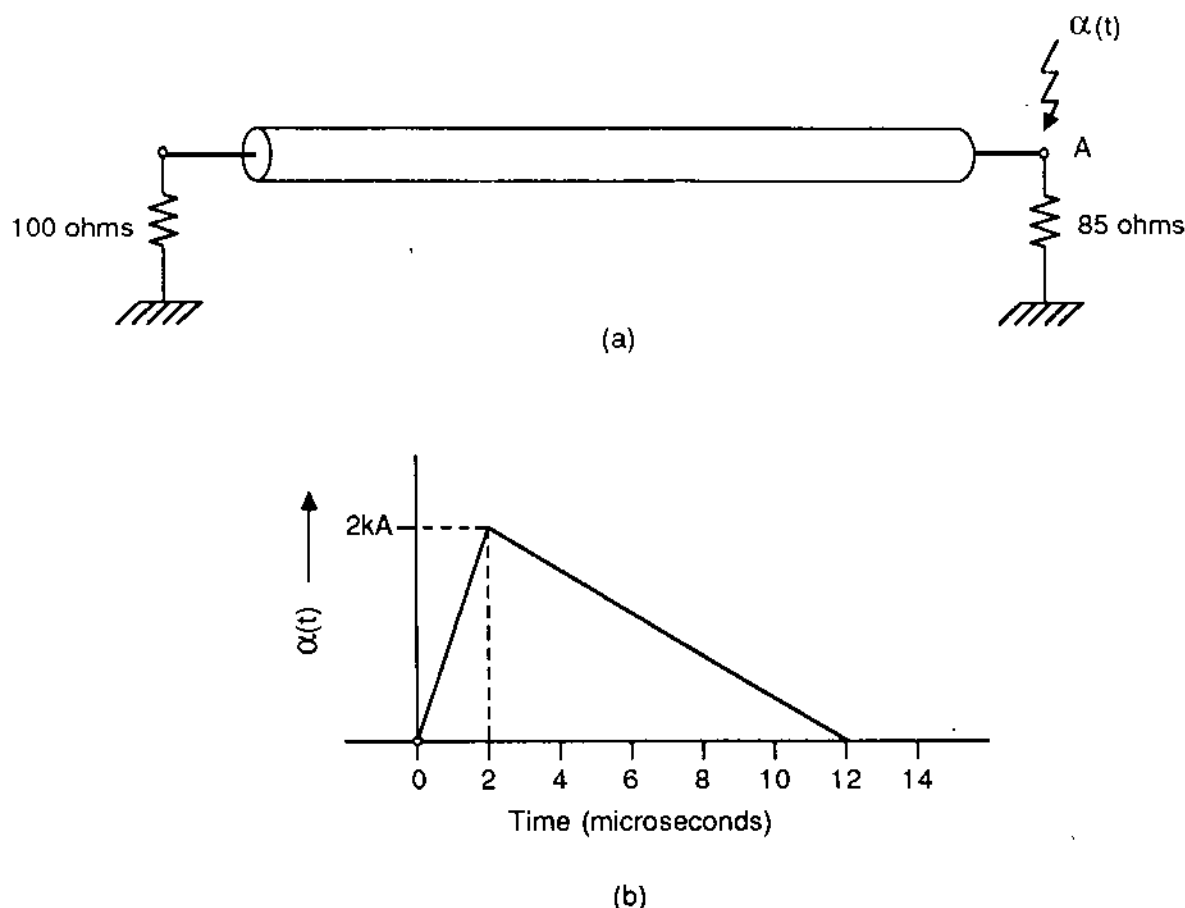


FIG. P9.5

**Problem 9.7:** Consider a single-phase cable terminated to a resistor  $R$  at one end and an inductor  $L$  at the other end, as in Fig. P9.6. The length of the cable is  $\ell$ , its characteristic impedance is  $Z_0$  and the travel time of waves along the cable is  $\tau$ . The cable is not energized [i.e.,  $v(t) = 0$ ,  $t < 0$  everywhere along the cable]. At time  $t = 0$ , lightning strikes the cable at point A. The lightning is to be represented as an ideal current source of electric current  $\alpha(t)$ . Compute the transient voltage at point B in the Laplace domain.

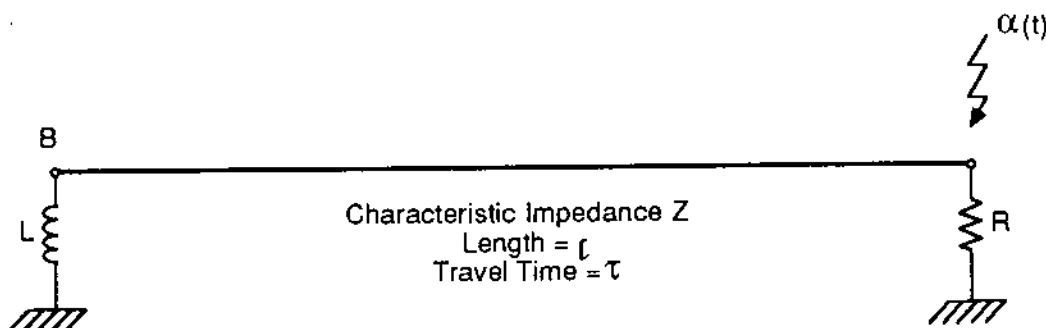


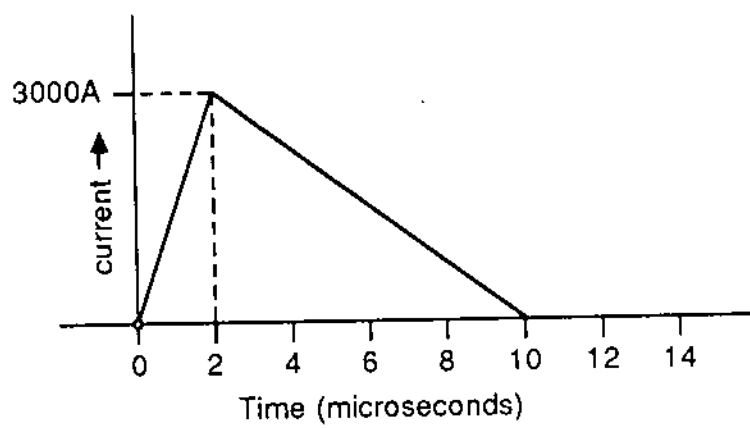
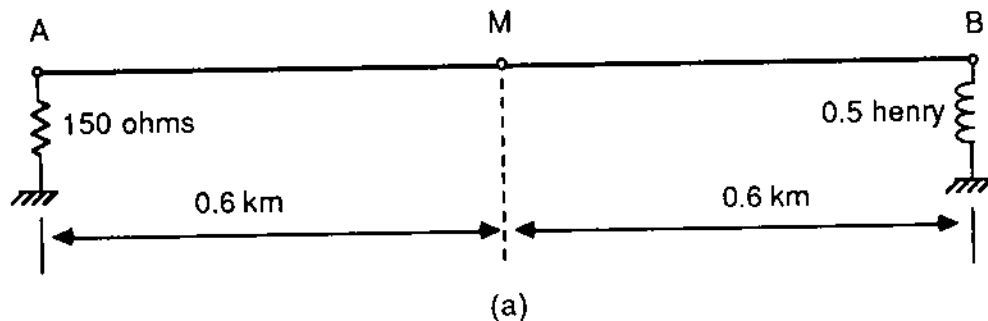
FIG. P9.6

Problem 9.8: A single-phase 69-kV overhead transmission line has the following parameters at 60 Hz:

$$Z = 0 + j3 \Omega \quad Z' = 0 - j40,000 \Omega$$

The line is terminated to a lumped resistance  $150 \Omega$  and a  $0.5\text{-H}$  inductor as indicated in Fig. P9.7a. At time  $t = 0$ , lightning strikes the line at point M, which is located in the middle of the line. The lightning may be approximated with the electric current waveform of Fig. P9.7b. Determine the voltages at points A, B, and M for a period of  $8 \mu\text{s}$  following the initiation of the stroke. Use the numerical method. The speed of traveling waves on the line is  $300 \text{ m}/\mu\text{s}$ . Write a computer program for the computation of voltages at points A, B, and M following the incidence of lightning.

Problem 9.9: An overhead single-phase transmission line has a total series impedance of  $Z = 50e^{j90^\circ} \Omega$  and a total shunt impedance of  $Z' = 2000e^{-j90^\circ} \Omega$  at 60 Hz. The speed of traveling waves on the line is  $3.10^8 \text{ m/s}$ .



(b)

FIG. P9.7

- (a) Compute the length of the line in meters.
- (b) Compute the characteristic impedance of the line in ohms.
- (c) Compute the propagation constant of the line in  $(\text{meter})^{-1}$ .

Problem 9.10: The 66-kV 1.2-km overhead single-phase transmission line of Fig. P9.8 is to be energized from a 60-Hz source with an equivalent internal impedance equal to  $j3.77 \Omega$ . The line terminates in a lumped inductance of 2 H. The characteristic impedance of the line is  $400 \Omega$ . The voltage source is

$$e(t) = (1.41)(66 \text{ kV}) \cos(377 \text{ s}^{-1}t)$$

Assume that the switch S closes at time  $t = 0$ .

- (a) Develop the resistive equivalent network for this system using a time step of  $2 \mu\text{s}$ .
- (b) Determine the initial conditions.
- (c) Compute the transient voltage at point A for the time period  $0 \leq t \leq 20 \mu\text{s}$ .
- (d) Write a computer program for the computation of the transient voltage at point A.

Problem 9.11: A three-phase transmission line has the following parameters:

Line mode:  $Z_L = 400 \Omega$   
 $c_L = 3 \times 10^8 \text{ m/s}$

Ground mode:  $Z_g = 910 \Omega$   
 $c_g = 2.0 \times 10^8 \text{ m/s}$

- (a) What is the inductance matrix of the line?
- (b) What is the capacitance matrix of the line?

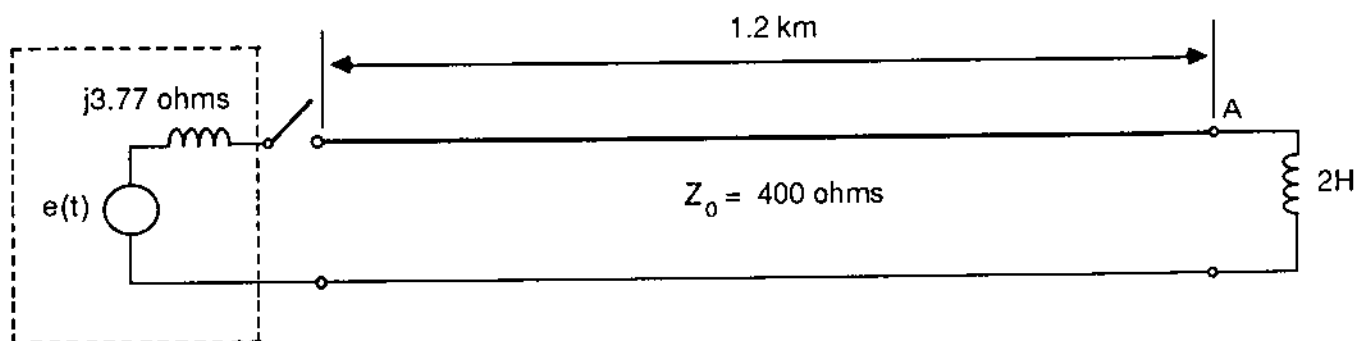


FIG. P9.8

# References

1. Electric Power Research Institute, Transmission Line Reference Book, 345 kV and Above, 2nd ed., EPRI, 1982.
2. J. R. Carson, "Wave Propagation in Overhead Wires with Ground Return," Bell System Technical Journal, pp. 539-554, 1929.
3. D. T. Paris and F. K. Hurd, Basic Electromagnetic Theory, McGraw-Hill Book Company, New York, 1969.
4. Electrical Transmission and Distribution Reference Book, 4th ed., Westinghouse, East Pittsburgh, Pa., 1964.
5. J. Zaborsky and J. W. Rittenhouse, Electric Power Transmission, The Rensselaer Bookstore, Troy, N. Y., 1969.
6. R. Rudenberg, "Fundamental Considerations on Ground Currents," Electrical Engineering, January 1945.
7. P. Anderson, Analysis of Faulted Power Systems, Iowa State University Press, Ames, Iowa, 1973.
8. E. D. Sunde, Earth Conduction Effects in Transmission System, D. Van Nostrand Company, Princeton, N. J., 1949.
9. N. N. Levedev, Special Functions and Their Applications, Dover Publications, Inc., New York, 1972.
10. F. Bowman, Introduction to Bessel Functions, Dover Publications, Inc., New York, 1958.
11. Handbook of Mathematical Functions, U. S. Department of Commerce, National Bureau of Standards, 1964.

12. A. Semlyen and A. Deri, "Time Domain Modeling of Frequency Dependent Three-Phase Transmission Line Impedance," IEEE Transactions on Power Apparatus and Systems, Vol. PAS104, No. 6, pp. 1549-1555, June 1985.
13. H. W. Dommel, "Overhead Line Parameters from Handbook Formulas and Computer Programs," IEEE Transactions on Power Apparatus and Systems, Vol. PAS104, No. 2, pp. 366-372, February 1985.
14. R. J. Heppe, "Computation of Potential at Surface Above an Energized Grid or Other Electrode, Allowing for Non-uniform Current Distribution," IEEE Transactions on Power Apparatus and Systems, Vol. PAS98, No. 6, pp. 1978-1989, November-December 1979.
15. A. P. Meliopoulos, R. P. Webb, and E. B. Joy, "Analysis of Grounding Systems," IEEE Transactions on Power Apparatus and Systems, Vol. PAS100, No. 3, pp. 1039-1048, March 1981.
16. A. P. Meliopoulos and M. G. Moharam, "Transient Analysis of Grounding Systems," IEEE Transactions on Power Apparatus and Systems, Vol. PAS102, No. 2, pp. 389-397.
17. R. Verma and D. Mukhedkar, "Fundamental Considerations and Impulse Impedance of Grounding Grids," IEEE Transactions on Power Apparatus and Systems, Vol. PAS100, No. 3, pp. 1023-1030, March 1981.
18. American National Standards Institute and Institute of Electrical and Electronics Engineers, ANSI/IEEE Standard 80, IEEE Guide for Safety in AC Substation Grounding, ANSI/IEEE, New York, 1986.
19. C. F. Dalziel, "Electric Shock Hazard," IEEE Spectrum, pp. 41-50, February 1972.
20. C. F. Dalziel and W. R. Lee, "Re-evaluation of Lethal Electric Currents," IEEE Transactions on Industry and General Applications, Vol. IGA4, pp. 467-476, 1968.
21. P. G. Biegelmeier and W. R. Lee, "New Considerations on the Threshold of Ventricular Fibrillation for AC Shocks at 50-60 Hz," IEEE Proceedings, Vol. 127, No. 2, Pt. A, March 1980.
22. A. P. Meliopoulos, "Computer Based Design of Grounding Systems," EEI Seminar, Pensacola, Fla., February 1983.
23. H. B. Dwight, "Calculation of Resistances to Ground," Electrical Engineering, Vol. 55, pp. 1319-1328, 1936.
24. D. Mukhedkar, Y. Gervais, and F. Dawalibi, "Modeling of Potential Distribution Around a Grounding Electrode," IEEE

- Transactions on Power Apparatus and Systems, Vol. PAS92, No. 5, pp. 1455-1459, 1973.
25. A. D. Papalexopoulos and A. P. Meliopoulos, "Frequency Characteristics of Grounding Systems," IEEE Transactions on Power Apparatus and Systems, Vol. PWRD-2, No. 4, pp. 1073-1081, October 1987.
26. W. Koch, "Grounding Methods of High Voltage Stations with Grounded Neutrals," Electrotechnische Zeitschrift, Vol. 71, No. 4, pp. 89-91, February 1950.
27. J. M. Nahman, "Zero-Sequence Representation of Overhead Lines," Archiv fuer Elektrotechnik, Vol. 65, pp. 209-217, 1982.
28. A. P. Meliopoulos, R. P. Webb, E. B. Joy, and S. Patel, "Computation of Maximum Earth Current in Substation Switchyards," IEEE Transactions on Power Apparatus and Systems, Vol. PAS-102, No. 9, pp. 3131-3139, September 1983.
29. C. A. Gross, Power System Analysis, John Wiley & Sons, Inc., New York, 1979.
30. C. F. Wagner and R. D. Evans, Symmetrical Components, McGraw-Hill Book Company, New York, 1933.
31. E. Clarke, Circuit Analysis of A-C Power Systems, John Wiley & Sons, Inc., New York, 1943.
32. G. O. Calabrese, Symmetrical Components, Ronand Press, New York, 1959.
33. W. D. Stevenson, Elements of Power System Analysis, 4th ed., McGraw-Hill Book Company, New York, 1982.
34. G. T. Heydt, Computer Analysis Methods for Power Systems, Macmillan Publishing Company, New York, 1986.
35. Institute of Electrical and Electronic Engineers, IEEE Brown Book, IEEE Standard 399-1980, Power System Analysis, IEEE, New York, 1980.
36. Institute of Electrical and Electronic Engineers, IEEE Standard 367, IEEE Guide for Determining the Maximum Electric Power Station Ground Potential Rise and Induced Voltage from a Power Fault, IEEE, New York, 1979.
37. E. B. Joy, A. P. Meliopoulos, and R. P. Webb, Analysis Techniques for Power Substation Grounding Systems, Vol. 1, Design Methodology and Tests, EPRI Report EL-2682, October 1982.
38. A. P. Meliopoulos, R. P. Webb, and E. B. Joy, "Computer Simulation of Faulted URD Cables: Analysis and Results," IEEE Transactions on Power Apparatus and Systems, Vol. PAS100, No. 4, pp. 1545-1552, April 1981.

39. A. P. Meliopoulos, A. D. Papalexopoulos, R. P. Webb, and C. Blattner, "Estimation of Soil Parameters from Driven Rod Measurements," IEEE Transactions on Power Apparatus and Systems, Vol. PAS103, No. 9, pp. 2579-2588, September 1984.
40. A. P. Meliopoulos and A. D. Papalexopoulos, "Interpretation of Soil Resistivity Measurements: Experience with the Model SOMIP," IEEE Transactions on Power Delivery, Vol. PWRD-4, No. 4, pp. 142-151, October 1986.
41. F. Dawalibi, Transmission Line Grounding, Vols. 1 and 2, EPRI Report EL-2699, October 1982.
42. Institute of Electrical and Electronic Engineers, IEEE Green Book, IEEE Standard 142-1982, IEEE Recommended Practice for Grounding of Industrial and Commercial Power Systems, IEEE, New York, 1982.
43. H. W. Dommel, "Digital Computer Solution of Electromagnetic Transients in Single and Multiphase Networks," IEEE Transactions on Power Apparatus and Systems, Vol. PAS88, No. 4, pp. 388-399, April 1969.
44. W. Diesendorf, Insulation Coordination in High Voltage Electric Power Systems, Butterworth & Company, Sevenoakes, Kent, England, 1974.
45. A. Greenwood, Electrical Transients in Power Systems, Wiley-Interscience, New York, 1971.
46. H. W. Dommel, "Nonlinear and Time-Varying Elements in Digital Simulation of Electromagnetic Transients," Proceedings of the 1971 Power Industry Computer Applications Conference, Boston, May 24-26, 1971.
47. J. K. Snelson, "Propagation of Traveling Waves on Transmission Lines—Frequency Dependent Parameters," IEEE Transactions on Power Apparatus and Systems, Vol. PAS91, No. 1, pp. 85-91, January-February 1972.
48. W. S. Meyer and H. W. Dommel, "Numerical Modeling of Frequency-Dependent Transmission-Line Parameters in an Electromagnetic Transients Program," IEEE Transactions on Power Apparatus and Systems, Vol. PAS93, No. 5, pp. 1401-1409, September-October 1974.
49. A. Ametani, "A Highly Efficient Method for Calculating Transmission Line Transients," IEEE Transactions on Power Apparatus and Systems, Vol. PAS95, No. 5, pp. 1545-1551, September-October 1976.
50. M. A. Sargent, "Monte Carlo Simulation of the Lightning Performance of Overhead Shielding Networks of High Voltage

- Stations," IEEE Transactions on Power Apparatus and Systems, Vol. PAS91, pp. 1651-1656, 1972.
51. J. G. Anderson, "Monte Carlo Computer Calculation of Transmission Line Lightning Performance," IEEE Transactions on Power Apparatus and Systems, Vol. PAS80, pp. 414-419, 1961.
  52. American National Standards Institute and Institute of Electrical and Electronics Engineers, ANSI/IEEE Standard 4-1978, IEEE Standard Techniques for High Voltage Testing, ANSI/IEEE, New York, 1978.
  53. IEEE Seminar/Report, Power Systems Transient Recovery Voltages, Publication 87 THO176-8-PWR.
  54. W. D. Humpage, z-Transform Electromagnetic Transient Analysis in High Voltage Networks, IEEE Power Engineering Series 3, Peter Peregrinus Ltd., Stevenage, Herts, England, 1982.
  55. K. Ragaller, Ed., Surges in High Voltage Networks, Plenum Press, New York, 1980.
  56. K. Ragaller, Ed., Current Interruption in High Voltage Networks, Plenum Press, New York, 1978.
  57. Institute of Electrical and Electronics Engineers, IEEE Standard 81-1962, IEEE Recommended Guide for Measuring Ground Resistance and Potential Gradients in the Earth, IEEE, New York, 1962.
  58. American National Standards Institute and Institute of Electrical and Electronics Engineers, ANSI/IEEE Standard 487-1980, IEEE Guide for the Protection of Wire-Line Communication Facilities Serving Electric Power Stations, ANSI/IEEE, New York, 1980.



# **Appendix**

Table A.1 Characteristics of Copper Conductors (97.3% Conductivity)

Size of conductor Circular mils	A.W.G. or B. & S. Number of strands	Outside diameter (in.)	Approx. current carrying capacity (A)	Geometric mean radius at 60 Hz (feet)	Resistance $r_a$ at 60 Hz ( $\Omega/\text{mi}$ )		Inductive reactance $X_a$ ( $\Omega/\text{mi}$ )	Shunt capacitive reactance $X_a'$ at 60 Hz ( $M\Omega \cdot \text{mi}$ )
					25°C (77°F)	50°C (122°F)		
1 000 000	-	37	1.151	1 300	0.0368	0.0634	0.0685	0.400
900 000	-	37	1.092	1 220	0.0349	0.0695	0.0752	0.406
800 000	-	37	1.029	1 130	0.0329	0.0772	0.0837	0.413
750 000	-	37	0.997	1 090	0.0319	0.0818	0.0888	0.417
700 000	-	37	0.963	1 040	0.0308	0.0871	0.0947	0.422
600 000	-	37	0.891	940	0.0285	0.1006	0.1095	0.432
500 000	-	37	0.814	840	0.0260	0.1196	0.1303	0.443
500 000	-	19	0.811	840	0.0256	0.1196	0.1303	0.445
450 000	-	19	0.770	780	0.0243	0.1323	0.1443	0.451
400 000	-	19	0.726	730	0.0229	0.1484	0.1619	0.458
350 000	-	19	0.679	670	0.0214	0.1690	0.1845	0.466
350 000	-	12	0.710	670	0.0225	0.1690	0.1845	0.460
300 000	-	19	0.629	610	0.01987	0.1966	0.2115	0.476
300 000	-	12	0.657	610	0.0208	0.1966	0.2115	0.470
250 000	-	19	0.574	540	0.01813	0.235	0.257	0.487
250 000	-	12	0.600	540	0.01902	0.235	0.257	0.481

211	600	4/0	19	0.528	480	0.01668	0.278	0.303	0.497	0.1132
211	600	4/0	12	0.552	490	0.01750	0.278	0.303	0.491	0.1119
211	600	4/0	7	0.522	480	0.01579	0.278	0.303	0.503	0.1136
167	800	3/0	12	0.492	420	0.01559	0.350	0.382	0.505	0.1153
167	800	3/0	7	0.464	420	0.01404	0.350	0.382	0.518	0.1171
133	100	2/0	7	0.414	360	0.01252	0.440	0.481	0.532	0.1205
105	500	1/0	7	0.368	310	0.01113	0.555	0.607	0.546	0.1240
83	690	1	7	0.328	270	0.00992	0.699	0.765	0.560	0.1275
83	690	1	3	0.360	270	0.01016	0.692	0.757	0.557	0.1246
66	370	2	7	0.292	230	0.00883	0.882	0.964	0.574	0.1308
66	370	2	3	0.320	240	0.00903	0.873	0.955	0.571	0.1281
66	370	2	1	0.258	220	0.00836	0.864	0.945	0.581	0.1345
52	630	3	7	0.260	200	0.00787	1.112	1.216	0.588	0.1343
52	630	3	3	0.285	200	0.00805	1.101	1.204	0.585	0.1315
52	630	3	1	0.229	190	0.00745	1.090	1.192	0.595	0.1380
41	740	4	3	0.254	180	0.00717	1.388	1.518	0.599	0.1349
41	740	4	1	0.204	170	0.00663	1.374	1.503	0.609	0.1415
33	100	5	3	0.226	150	0.00638	1.750	1.914	0.613	0.1384
33	100	5	1	0.1819	140	0.00590	1.733	1.895	0.623	0.1449
26	250	6	3	0.201	130	0.00568	2.21	2.41	0.628	0.1419
26	250	6	1	0.1620	120	0.00526	2.18	2.39	0.637	0.1483
20	820	7	1	0.1443	120	0.00468	2.75	3.01	0.651	0.1517
16	510	8	1	0.1285	90	0.00417	3.47	3.80	0.665	0.1552

Table A.2 Characteristics of Aluminum Cable Steel Reinforced Conductors

Circular mils or A.W.G. aluminum	Alumi- num	Steel	Geo- metric mean radius at 60 Hz (ft)	Outside diameter inches at 60 Hz	Strands lays	Strands lays	Resistance $r_a$ at 60 Hz ( $\Omega/\text{mi}$ )				Shunt capacitive reactance $X_S'$ at 60 Hz ( $M\Omega \cdot \text{mi}$ )
							50°C (122°F) Current approx. Small currents	25°C (77°F) Current approx. Small currents	50°C (122°F) Inductive reactance $X_a$ at 60 Hz ( $\Omega/\text{mi}$ )	25°C (77°F) Inductive reactance $X_a$ at 60 Hz ( $\Omega/\text{mi}$ )	
1 590 000	54	3	19	1.545	0.0520	1	380	0.0591	0.0684	0.359	0.0814
1 510 500	54	3	19	1.506	0.0507	1	340	0.0622	0.0720	0.362	0.0821
1 431 000	54	3	19	1.465	0.0493	1	300	0.0656	0.0760	0.365	0.0830
1 351 000	54	3	19	1.424	0.0479	1	250	0.0695	0.0803	0.369	0.0838
1 272 000	54	3	19	1.382	0.0465	1	200	0.0738	0.0851	0.372	0.0847
1 192 500	54	3	19	1.338	0.0450	1	160	0.0788	0.0906	0.376	0.0857
1 113 000	54	3	19	1.293	0.0435	1	110	0.0844	0.0969	0.380	0.0867
1 033 500	54	3	7	1.246	0.0420	1	60	0.0909	0.1035	0.385	0.0878
954 000	54	3	7	1.196	0.0403	1	10	0.0982	0.1128	0.390	0.0890
900 000	54	3	7	1.162	0.0391	970	0.104	0.1185	0.1393	0.393	0.0898
874 500	54	3	7	1.146	0.0386	950	0.108	0.1228	0.1395	0.395	0.0903
795 000	54	3	7	1.093	0.0368	900	0.119	0.1376	0.401	0.401	0.0917
795 000	26	2	7	1.108	0.0375	900	0.117	0.1288	0.399	0.399	0.0912
795 000	30	2	19	1.140	0.0393	910	0.117	0.1288	0.393	0.393	0.0904
715 000	54	3	7	1.036	0.0349	830	0.132	0.1482	0.407	0.407	0.0932
715 500	26	2	7	1.051	0.0355	840	0.131	0.1442	0.405	0.405	0.0928
715 500	30	2	19	1.081	0.0372	840	0.131	0.1442	0.399	0.399	0.0920
666 600	54	3	7	1.000	0.0337	800	0.141	0.1601	0.412	0.412	0.0943

636	000	54	3	7	7	7	0.977	0.0329	770	0.148	0.414	0.0950
636	000	26	2	7	0.990	0.0335	780	0.147	0.1618	0.412	0.0946	
636	000	30	2	19	1.019	0.0351	780	0.147	0.1618	0.406	0.0937	
605	000	54	3	7	0.953	0.0321	750	0.155	0.1775	0.417	0.0957	
605	000	26	2	7	0.966	0.0327	760	0.154	0.1720	0.415	0.0953	
556	500	26	2	7	0.927	0.0313	730	0.168	0.1859	0.420	0.0965	
556	500	30	2	7	0.953	0.0328	730	0.168	0.1589	0.415	0.0957	
500	000	30	2	7	0.904	0.0311	690	0.187	0.206	0.421	0.0973	
477	000	26	2	7	0.858	0.0290	670	0.196	0.216	0.430	0.0988	
477	000	30	2	7	0.883	0.0304	670	0.196	0.216	0.424	0.0980	
397	500	26	2	7	0.783	0.0265	590	0.235	0.259	0.441	0.1015	
397	500	30	2	7	0.806	0.0278	600	0.235	0.259	0.435	0.1006	
336	400	26	2	7	0.721	0.0244	530	0.278	0.306	0.451	0.1039	
336	400	30	2	7	0.741	0.0255	530	0.278	0.306	0.445	0.1032	
300	000	26	2	7	0.680	0.0230	490	0.311	0.342	0.458	0.1057	
300	000	30	2	7	0.700	0.0241	500	0.311	0.342	0.452	0.1049	
266	800	26	2	7	0.642	0.0217	460	0.350	0.385	0.465	0.1074	
266	800	6	1	7	0.633	0.00684	460	0.352	0.552	0.605	0.1079	
4/0	6	1	1	1	0.563	0.00814	340	0.445	0.592	0.581	0.1113	
3/0	6	1	1	1	0.502	0.00600	300	0.560	0.723	0.621	0.1147	
2/0	6	1	1	1	0.477	0.00510	270	0.706	0.895	0.641	0.1182	
1/0	6	1	1	1	0.398	0.00446	230	0.888	1.12	0.656	0.1216	
1	6	1	1	1	0.355	0.00418	200	1.12	1.38	0.665	0.1250	
2	6	1	1	1	0.316	0.00418	180	1.41	1.69	0.665	0.1285	
2	7	1	1	1	0.325	0.00504	180	1.41	1.65	0.642	0.1276	
3	6	1	1	1	0.281	0.00430	160	1.78	2.07	0.661	0.1320	
4	6	1	1	1	0.250	0.00437	140	2.24	2.57	0.659	0.1355	
4	7	1	1	1	0.257	0.00452	140	2.24	2.55	0.655	0.1346	
5	6	1	1	1	0.223	0.00416	120	2.82	3.18	0.665	0.1388	
6	6	1	1	1	0.198	0.00394	100	3.65	3.98	0.673	0.1423	

Table A.3 Characteristics of Copperweld Conductors (30% Conductivity)

Size	Number and size of wires	Outside diameter (in.)	Area of conductor (circular mils)	Geometric mean radius at 60 Hz (ft)	Approx. current carrying capacity at 60 Hz (A)	Resistance $r_a$ at 25°C (77°F)	Resistance $r_a$ at 75°C (167°F)	Resistance $r_a$ at 75°C (167°F)		
								Current approx.	75% of capacity at 60 Hz (Ω/mi)	Inductive reactance $X_a$ at 60 Hz (Ω/mi)
7/8"	19 No. 5	0.910	628 900	0.00758	620	0.331	0.499	0.592	0.0971	
13/16"	19 No. 6	0.810	498 800	0.00675	540	0.411	0.605	0.606	0.1005	
23/32"	19 No. 7	0.721	395 500	0.00601	470	0.511	0.737	0.621	0.1040	
21/32"	19 No. 8	0.642	313 700	0.00535	410	0.638	0.902	0.635	0.1074	
9/16"	19 No. 9	0.572	248 800	0.00477	360	0.798	1.106	0.649	0.1109	
5/8"	7 No. 4	0.613	292 200	0.00511	410	0.676	0.887	0.640	0.1088	
9/16"	7 No. 5	0.546	231 700	0.00455	360	0.847	1.099	0.654	0.1122	
1/2"	7 No. 6	0.486	183 800	0.00405	310	1.062	1.364	0.668	0.1157	
7/16"	7 No. 7	0.433	145 700	0.00361	270	1.335	1.697	0.683	0.1191	
3/8"	7 No. 8	0.385	115 600	0.00321	230	1.678	2.12	0.697	0.1226	
11/32"	7 No. 9	0.343	91 650	0.00286	200	2.11	2.64	0.711	0.1260	
5/16"	7 No. 10	0.306	72 680	0.00255	170	2.66	3.30	0.725	0.1294	
3 No. 5	3 No. 5	0.392	99 310	0.00457	220	1.938	2.35	0.654	0.1221	
3 No. 6	3 No. 6	0.349	78 750	0.00407	190	2.44	2.95	0.668	0.1255	
3 No. 7	3 No. 7	0.311	62 450	0.00363	160	3.07	3.71	0.682	0.1289	
3 No. 8	3 No. 8	0.277	49 530	0.00323	140	3.87	4.66	0.696	0.1324	
3 No. 9	3 No. 9	0.247	39 280	0.00288	120	4.88	5.86	0.710	0.1358	
3 No. 10	3 No. 10	0.220	31 150	0.00257	110	6.15	7.38	0.724	0.1392	

Table A.4 Electrical Characteristics of Alumoweld Ground Wires

Designation	Resistance ( $\Omega$ per conductor per mile)			Reactance per conductor per mile (1-ft spacing)			Geometric mean radius at 60 Hz (ft)	Approx. ampacity at 60 Hz <sup>b</sup> (A)
	$r_a$ At 25°C (77°F)	$r_a$ At 75°C (167°F)	Current approx. 75% of ampacity <sup>a</sup>	Inductive	Capacitive			
				$X_s$ at 60 Hz	$X_s'$ at 60 Hz (M $\Omega$ )			
19 No. 8 AWG	0.9038	1.280	0.9038	0.687	0.1074	0.003478	335	335
19 No. 9 AWG	1.140	1.554	1.140	0.701	0.1109	0.003098	295	295
7 No. 5 AWG	1.240	1.669	1.240	0.707	0.1122	0.002958	280	280
7 No. 6 AWG	1.536	2.01	1.536	0.721	0.1157	0.002633	250	250
7 No. 7 AWG	1.937	2.47	1.937	0.735	0.1191	0.002345	220	220
7 No. 8 AWG	2.44	3.06	2.44	0.749	0.1226	0.002085	190	190
7 No. 9 AWG	3.08	3.80	3.08	0.763	0.1260	0.001858	160	160
7 No. 10 AWG	3.88	4.73	3.88	0.777	0.1294	0.001658	140	140
3 No. 5 AWG	2.78	3.56	2.78	0.707	0.1221	0.002940	170	170
3 No. 6 AWG	3.51	4.41	3.51	0.721	0.1255	0.002618	150	150

<sup>a</sup>Resistance at 75°C total temperature, based on an ambient of 25°C plus 50°C rise due to heating effect of current. The approximate magnitude of current necessary to produce the 50°C rise is 75% of the approximate ampacity at 60 Hz.

<sup>b</sup>Based on a strand temperature of 125°C and an ambient of 25°C.

**Table A.5 Electrical Characteristics of Seven-wire Bethanized Steel Conductor**

Diameter (in.)	DC Resistance	Ohms per mile (at 60 Hz)			
		AC Resistance		Inductive Reactance <sup>a</sup>	
		10 A	20 A	10 A	20 A
1/4	11.88	11.93	11.98	1.029	1.066
5/16	7.65	7.71	7.81	1.045	1.082
3/8	5.54	5.54	5.65	1.072	1.108
7/16	3.96	4.01	4.06	1.098	1.140
1/2	3.16	3.27	3.38	1.135	1.188

<sup>a</sup> $x = j 0.2796 \log (1/d)$ , d is the geometric mean radius.

# Index

A, B, C line constants, 199  
Absolute numerical stability, 371  
Admittance matrix, 292  
    of transmission line, 226  
    of coupled lines, 233  
    of single phase transformer, 293  
    of single phase source, 295  
Ampere's law, 15, 16, 61  
Apparent soil resistivity, 315  
Asymmetry factor, 243  
Attenuation constant, 197

Balanced set, 3, 4  
Bergeron method, 347  
Bessel functions, 136  
    modified, 64, 72, 82  
Bewley's diagram, 348  
Bundled conductors, 37, 43  
    geometric mean radius of, 39

Capacitance, 99  
    of a transmission line, 100  
Capacitive current, 93  
    of single-phase line, 105

Capacitive reactance, 104  
conductor component of, 104  
effects of earth on, 110  
effects of neutral conductor on, 110  
separation component of, 104  
of three-phase line, 109  
Carson's formula, 47  
    infinite series, 79  
Characteristic impedance, 197, 199  
    positive/negative, 204  
    zero sequence, 204  
Charging current, 93  
Complex depth of return, 85, 241  
    Semlyen and Deri, 85  
Conductivity, 60  
Conductor  
    current density in, 63, 68  
    effective resistance of, 72  
    electric field around of, 94  
    heat dissipation in, 71  
    resistance of, 57  
    segments of ground, 160  
    total AC current, 70  
Counterpoise, 119  
Current density  
    in conductors, 63, 68

- [Current density]
  - in conductors, 63, 68
  - instantaneous value, 69
- Current limiting block, 425
  
- DC transmission, 6
- Delta connected, 2
- Depth of penetration, 75
- Direct axis, 262
- Direct phase analysis, 291
- Distribution system, 8
- Double-circuit transmission line, 40
- Driven rod method, 315
  
- Earth path
  - current distribution in, 78, 81
  - equivalent conductor of, 48, 84
  - reactance, 83
  - resistance, 83
- Earth voltage, 161
- Eddy currents, 55
- Effectively grounded, 217
- Electric body current, 120
  - due to touch and step voltage, 128
- Electric charge, 94
  - density, 95
  - distribution of, 97
  - exact solution of, 98
- Electric current
  - density in soil, 123
- Electric field, 94
  - around a conductor, 94
  - density, 95
  - intensity of, 94
  - of two parallel conductors, 96
- Equivalent circuit
  - of grounding systems, 171
  - resistive companion, 372
  - of transmission lines, 209
- Equivalent depth of return, 48, 81, 241
  
- Faraday's law, 60
- Fast transients, 187
- Fault analysis, 266
- Fault current distribution, 278
- Faults, 253
  - line-to-line, 269
  - line-to-line-to-ground, 270
  - single line-to-ground, 271
  - three-phase, 268
  
- Gapped surge arrester, 425
- Gauss' law, 94
- Geometric factors  $K_m$ ,  $K_s$ , 170
- Geometric mean distance, 37
- Geometric mean radius, 18, 73
- Grounded, 119
- Ground electrode
  - buried sphere, 125
  - buried strip, 128
  - buried wire, 128
  - disk, 128
  - ground rod, 128
  - hemispherical, 121
  - ring, 128
- Grounding system
  - impedance of, 119
  - resistance of, 161
- Ground mat, 119, 167
  - resistance, 170
- Ground mode, 385
- Ground potential rise, 120, 135, 142, 160, 175, 255, 310
  - analysis of, 277
  - maximum, 319
- Ground resistance
  - of one foot, 131
  - self, mutual, transfer, 142
- Ground rods, 119, 168
  
- Hyperbolic cosine, 198
- Hyperbolic sine, 198
  
- Ideal distributed-parameter line, 343

- Impulse generator, 364  
Incident wave, 348  
Induced voltage, 33  
    on communication lines, 300  
Inductive reactance, 23  
    conductor component of,  
    of the earth path, 47, 83  
    effects of skin, 73  
    of magnetic conductors, 76  
    separation component of,  
    use of tables, 26  
Inrush current, 417  
Insulation breakdown, 339  
Integration/matrix method, 143  
    of grounding system analysis,  
        143  
Integration time step, 371  
Isolation transformer, 303
- Karrenbauer transformation, 384  
Kelvin functions, 64  
    properties of, 72  
Kirchhoff's current law, 188, 192,  
    296  
Kirchhoff's voltage law, 188, 192
- Ladder network, 288  
Laplace domain equivalents, 358  
Laplace equation, 135  
Laplace transform, 356, 394  
Lightning, 339, 351  
Line inductance, 13  
Line mode, 385  
Loop analysis, 364
- Magnetic field, 14  
Magnetic flux linkage, 74  
Matrix method, 139  
    of grounding system analysis,  
        139  
Mesh  
    of ground mat, 178  
Mesh voltage, 179  
Metal oxide varistor, 425
- Modal currents, 201, 385  
Modal decomposition, 201  
Modal transformation matrix, 201  
Modal voltages, 201, 385  
Multiple grounds, 175  
    analysis of, 175  
    transmission line with, 227
- Neutral (conductor), 6, 32  
    effects of, 240, 244  
Neutralizing transformer, 303  
Nodal analysis, 296, 364  
Nonuniformity factor, 170  
Norton equivalent, 261, 296, 363  
Numerical integration, 369  
    trapezoidal, 370
- Ohm's law, 74, 122  
Overhead ground wire (OHGW),  
    5
- Parametric analysis  
    of ground mats, 178  
Past history sources,  
    396  
Permeability, 60  
Permittivity, 60, 96  
Phase constant, 197  
Phasor, 2  
Pi equivalent, 209  
    nominal, 212  
Potential difference, 97  
Power equations, 245  
    for A, B, C constants, 246  
    for pi-equivalent, 247  
    for tee-equivalent, 248  
Propagation constant, 197, 199  
    positive/negative, 204  
    zero sequence, 204  
protector blocks, 303  
Proximity effect, 55
- Quadrature axis, 263

- Reflected wave, 348  
 Reflection coefficient, 349  
 Refraction coefficient, 349  
 Resistance  
     of human body, 131, 134  
     of magnetic conductors, 76  
     of transmission line, 55  
 Resistive companion circuit, 372  
 Resistor preinsertion breaker, 399
- Safety assessment, 133, 330  
 Safety criteria, 312, 330  
 Sequence models, 201  
     negative sequence, 204  
     pi-equivalent of, 262  
     positive sequence, 204  
     tee-equivalent of, 209  
     zero sequence, 204  
 Series impedance, 215  
 SGSYS, 330  
 Shield conductor  
     effects of, 240, 244  
 Shunt admittance, 221  
 Sinusoidal steady state, 187  
     analysis of, 190  
     transmission line models for, 195  
 Skin effect, 55  
     of circular conductors, 58  
     effects on conductor reactance, 73  
     general solution for, 63  
 SMECC, 323  
 Snelson transformation, 362  
 SOMIP, 316  
 Spark gap, 422  
 Standard lightning wave, 421  
 Step voltage, 120, 167, 310, 324  
     maximum allowable, 134  
     mitigation of, 333  
 Subtransient reactance, 262  
 Superposition, 123  
 Symmetrical components, 204, 255  
     transformation, 237
- Symmetric three phase line, 31  
 Symmetric three phase system, 4  
 Synchronous reactance, 262
- Tee-equivalent, 209  
     nominal, 212  
 Theory of images, 111  
     application to overhead lines, 112  
 Thevenin equivalent, 129, 134, 262, 363  
     equivalent voltage, 129  
     equivalent resistance, 129  
 Touch voltage, 120, 167, 310, 324  
     maximum allowable, 134  
     mitigation of, 333  
 Tower footing resistance, 231  
 Transfer voltage, 327  
 Transient network analyzer, 340  
 Transient recovery voltage, 398  
 Transient reactance, 262  
 Transients  
     analysis of, 190  
 Transmission line  
     frequency dependent model, 391  
     model with grounds, 227  
     sequence parameters of, 236  
     series sequence impedance, 239  
     shunt sequence impedance, 239  
     single phase model, 187  
     three phase model, 190  
         comparison of, 240  
 Transmitted wave, 348  
 Transposition, 34  
 Trapezoidal integration, 370  
 Traveling waves, 346
- Voltage distribution factor, 142  
 Voltage profile, 167
- Wenner method, 312  
 Worst fault, 312, 319  
 Wye connected, 2